NATIONAL CENTER FOR EARTHQUAKE ENGINEERING RESEARCH

ISSN 1088-3800

Proceedings of the NCEER Workshop on Evaluation of Liquefaction Resistance of Soils

Edited by

T.L. Youd and I.M. Idriss

Technical Report NCEER-97-0022

December 31, 1997

This Workshop was conducted at the Inn at Temple Square, Salt Lake City, Utah and was supported by the Federal Highway Administration under contract number DTFH61-92-C-00112.

NOTICE

This report was prepared by the National Center for Earthquake Engineering Research (NCEER) through a contract from the Federal Highway Administration. Neither NCEER, associates of NCEER, its sponsors, nor any person acting on their behalf:

a. makes any warranty, express or implied, with respect to the use of any information, apparatus, method, or process disclosed in this report or that such use may not infringe upon privately owned rights; or

b. assumes any liabilities of whatsoever kind with respect to the use of, or the damage resulting from the use of, any information, apparatus, method, or process disclosed in this report.

Any opinions, findings, and conclusions or recommendations expressed in this publication are those of the author(s) and do not necessarily reflect the views of NCEER or the Federal Highway Administration.

NATIONAL CENTER FOR EARTHQUAKE ENGINEERING RESEARCH
Headquartered at the State University of New York at Buffalo

Proceedings of the NCEER Workshop on Evaluation of Liquefaction Resistance of Soils

held at
Inn at Temple Square
Salt Lake City, Utah
January 5-6, 1996

Edited by T. L. Youd[1] and I. M. Idriss[2]

Publication Date: December 31, 1997

Technical Report NCEER-97-0022

NCEER Highway Project Task Number 112-D-4.2

FHWA Contract Number DTFH61-92-C-00112

1 Professor and Chair, Department of Civil and Environmental Engineering, Brigham Young University
2 Professor, Department of Civil Engineering, University of California at Davis

NATIONAL CENTER FOR EARTHQUAKE ENGINEERING RESEARCH
State University of New York at Buffalo
Red Jacket Quadrangle, Buffalo, NY 14261

PREFACE

Over the past twenty-five years, a procedure termed the "simplified procedure" has evolved for evaluating the seismic liquefaction resistance of soils. This procedure has become the standard of practice in the U.S. and Canada and throughout much of the rest of the world. The development of the procedure has been incremental. Following the disastrous earthquakes in Alaska and in Niigata, Japan, in 1964, Seed and Idriss (1971) developed and published the basic "simplified procedure." The procedure has been revised and augmented periodically since that time, with landmark papers by Seed (1976), Seed and Idriss (1982), and Seed et al. (1985). In 1985, the Committee on Earthquake Engineering, National Research Council (NRC) organized a workshop with experts from the profession at large to evaluate and update the procedure. That workshop was convened by Prof. Robert V. Whitman, the Massachusetts Institute of Technology, with thirty-six experts and observers who thoroughly reviewed the state-of-knowledge and the state-of-the-art for assessing liquefaction hazard. That workshop produced a report (NRC, 1985) that has become a widely used reference. No additional general review or updating of procedures has been published since that time.

The purpose of the 1996 workshop, sponsored by the National Center for Earthquake Engineering Research (NCEER), was to convene a group of 21 experts to review recent developments and come to consensus on further improvements and augmentations to the simplified procedure. Emphasis was on developments that have been published in the ten-year period between the NRC and NCEER workshop. To keep the workshop focused and the content tractable, the scope was purposely restricted to a review of procedures for evaluating liquefaction resistance of soils as outlined in the simplified procedure. Thus, the workshop was primarily concerned with evaluation of triggering of liquefaction. Post liquefaction phenomena, such as soil deformation and ground failure, although equally or more important, were omitted from discussion.

The simplified procedure was originally developed for assessment of liquefaction resistance of shallow alluvial soils beneath level to gently sloping ground. Thus, by definition, valid application of the procedure should be limited to these terrain conditions. Although the procedure has been applied by some engineers to assess liquefaction hazard under steeply sloping terrain, constructed embankments, or deep soil layers, such extrapolations are beyond the range of empirical data upon which the original procedure was based. Such extrapolations should be made by experts with experience in such applications. Thus, deliberations at the workshop were largely restricted to shallow deposits beneath level or nearly level ground conditions. However, proposed revisions to the factors K_σ and K_α, respectively, used to correct the analyses for large static normal and shear stresses, respectively, were discussed and consensus gained on K_σ values to be used.

ACKNOWLEDGMENTS

Many hours of volunteer time were contributed by the participants in the workshop. This dedicated effort is gratefully acknowledged. Reviews of the workshop proceedings were provided by Thomas F. Blake, Fugro-West, Ventura, California, and Donald G. Anderson, CH2M-Hill, Bellevue, Washington. Steven F. Noble and Sam Gilstrap, graduate students at Brigham Young University, assisted with the workshop and preparation of the proceedings.

Table of Contents

Reports

Appendices

Summary Report

Workshop Participants

Chair: T. Leslie Youd, Brigham Young University, Provo, UT; **Co-chair: Izzat M. Idriss**, University of California at Davis, Davis, CA; **Ronald D. Andrus**, National Institute for Standards and Technology, Gaithersburg, MD; **Ignacio Arango**, Bechtel Corp., Oakland, CA; **Gonzalo Castro**, GEI Consultants, Inc., Winchester, MA; **John T. Christian**, Engineering Consultant, Boston, MA; **Ricardo Dobry**, Rensselaer Polytechnic Institute, Troy, NY; **W.D. Liam Finn**, University of British Columbia, Vancouver, BC; **Leslie F. Harder, Jr.**, California Department of Water Resources, Sacramento, CA; **Mary Ellen Hynes**,US Army Engineers Waterways Experiment Station, Vicksburg, MS; **Kenji Ishihara**, Science University of Tokyo, Tokyo, Japan; **Joseph P. Koester**, US Army Engineers Waterways Experiment Station, Vicksburg, MS; **Sam S.C. Liao**, Parsons Brinckerhoff, Boston, MA; **William F. Marcuson, III**, US Army Engineers Waterways Experiment Station, Vicksburg, MS; **Geoffrey R. Martin**, University of Southern California, Los Angeles, CA; **James K. Mitchell**, Virginia Tech, Blacksburg, VA; **Yoshiharu Moriwaki**, Woodward-Clyde Consultants, Santa Ana, CA; **Maurice S. Power**, Geomatrix Consultants, San Francisco, CA; **Peter K. Robertson**, University of Alberta, Edmonton, Alberta; **Raymond B. Seed**, University of California, Berkeley, CA; **Kenneth H. Stokoe, II**, University of Texas, Austin, TX

Abstract

Over the past twenty-five years, a procedure, termed the "simplified procedure," has evolved for evaluating liquefaction resistance of soils. This procedure has become the standard of practice in North America and throughout much of the world. Following disastrous earthquakes in Alaska and in Niigata, Japan in 1964, Professors H.B. Seed and I.M. Idriss developed and published the basic "simplified procedure." The procedure, which is largely empirical, evolved over the decades primarily through summary papers by H.B. Seed and his colleagues. In 1985, Professor Robert V. Whitman convened a workshop on behalf of the National Research Council (NRC) in which thirty-six experts reviewed the state-of-knowledge and the state-of-the-art for assessing liquefaction hazard. No general review or update of the simplified procedures has occurred since that time. The purpose of the 1996 workshop, sponsored by the National Center for Earthquake Engineering Research (NCEER), was to convene a group of experts to review developments and gain consensus for further augmentations to the procedure. To keep the workshop focused and the content tractable, the scope was limited to evaluation of liquefaction resistance. Post-liquefaction phenomena, such as soil deformation and ground failure, although equally or more important, were beyond the scope of this workshop. The participants developed consensus recommendations on the following topics: (1) use of the standard and cone penetration tests for evaluation of liquefaction resistance, (2) use of shear wave velocity measurements for evaluation of liquefaction resistance, (3) use of the Becker penetration test for gravelly soils, (4) magnitude scaling factors, (5) correction factors K_α and K_σ, and (6) evaluation of seismic factors required for the evaluation procedure. Probabilistic analysis and seismic energy considerations were also reviewed. Seismic energy concepts were judged to be insufficiently developed to make recommendations for engineering practice. Probabilistic methods have been used in some risk analyses, but are still outside the mainstream of standard practice.

Introduction

Over the past twenty-five years, a procedure, termed the "simplified procedure," has evolved for evaluating the seismic liquefaction resistance of soils. This procedure has become the standard of practice in North America and throughout much of the world. Following disastrous earthquakes in Alaska and Niigata, Japan in 1964, Seed and Idriss (1971) developed and published the basic "simplified procedure." The procedure has been corrected and augmented periodically since that time with landmark papers by Seed (1979), Seed and Idriss (1982), and Seed et al. (1985). In 1985, Professor Robert V. Whitman from the Massachusetts Institute of Technology convened a workshop on behalf of the National Research Council (NRC) in which thirty-six experts and observers thoroughly reviewed the state-of-knowledge and the state-of-the-art for assessing liquefaction hazard. That workshop produced a report (NRC, 1985) that has become a widely used standard and reference for liquefaction hazard assessment. No general review or update of the simplified procedures has occurred since that time.

The purpose of the 1996 workshop, sponsored by the National Center for Earthquake Engineering Research (NCEER), was to convene a group of experts to review recent developments and gain consensus on further corrections and augmentations to the procedure. Emphasis was placed on new developments since the NRC review. To keep the workshop focused and the content tractable, the scope was limited to procedures for evaluating liquefaction resistance of soils under level to gently sloping ground. In this context, liquefaction refers to the phenomena of seismic generation of large pore-water pressures and consequent severe softening of granular soils. Post-liquefaction phenomena, such as soil deformation and ground failure, although equally or more important than triggering, were beyond the scope of the workshop.

The simplified procedure was developed from evaluations of field observations and field and laboratory test data. Field evidence of liquefaction generally consisted of observed sand boils, ground fissures or lateral spreads. Data were collected mostly from sites on level to gently sloping terrain underlain by Holocene alluvial or fluvial sediment at shallow depths (less than 15 m). The original procedure was verified for and is applicable only to these site conditions. The primary focus of the workshop was to review and update procedures for evaluating soil liquefaction resistance for these general site conditions. Limited attention was given to liquefaction resistance evaluation for sediment layers at greater depths (high overburden pressures) and beneath steeply sloping terrain or embankments.

Cyclic Stress Ratio (CSR) and Cyclic Resistance Ratio (CRR)

Calculation or estimation of two variables is required for evaluation of liquefaction resistance of soils. These variables are the seismic demand placed on a soil layer, expressed in terms of cyclic stress ratio (CSR), and the capacity of the soil to resist liquefaction, expressed in terms of cyclic resistance ratio (CRR), hereafter referred to as liquefaction resistance or liquefaction resistance ratio. CRR is a symbol proposed by Robertson and Wride that was endorsed by the workshop. Previously, this factor had been called the cyclic stress ratio required to generate liquefaction, or the cyclic strength ratio, and had been given different symbols by different writers. For example, Seed and Harder (1990) used the symbol CSR_ℓ, Youd (1993) used the symbol CSRL, and Kramer (1996) used

the symbol CSR_L to denote this ratio. The workshop participants agreed that CRR conveys an appropriate meaning and generates less confusion than the use of CSR with or without a subscript to signify liquefaction resistance.

Seed and Idriss (1971) formulated the following equation for calculation of CSR:

$$CSR = (\tau_{av}/\sigma'_{vo}) = 0.65\ (a_{max}/g)(\sigma_{vo}/\sigma'_{vo})r_d \qquad (1)$$

where a_{max} is the peak horizontal acceleration at ground surface generated by the earthquake, g is the acceleration of gravity, σ_{vo} and σ'_{vo} are total and effective vertical overburden stresses, respectively, and r_d is a stress reduction coefficient. The latter coefficient provides an approximated correction for flexibility of the soil profile. The workshop participants recommend the following minor modification to the procedure for calculation of CSR. For noncritical projects, the following equations may be used to estimate average values of r_d.

$r_d = 1.0 - 0.00765\ z$ for $z \leq 9.15$ m (2a)

$r_d = 1.174 - 0.0267\ z$ for $9.15\ m < z \leq 23$ m (2b)

$r_d = 0.744 - 0.008\ z$ for $23 < z \leq 30$ m (2c)

$r_d = 0.50$ For $z > 30$ m (2d)

where z is depth below ground surface in meters. Parts a and b of this equation were proposed by Liao and Whitman (1986b), part c was added by Robertson and Wride (this report), and part d was suggested by William F. Marcuson (US Army Engineers, oral commun.) in post-workshop discussions. Mean values of r_d calculated from Equation 2 are plotted on Figure 1 along with the mean and range of values proposed by Seed and Idriss (1971). The workshop participants agreed that for convenience in programming spreadsheets and other electronic aids, and to be consistent with past practice, r_d values determined from Equation 2 are suitable for use in routine engineering practice. The user should understand, however, and take into account that r_d values calculated from Equations 2 or 3 give only the mean value from a range of possible r_d values and that the range of r_d values increases with depth. Thus the certainty with which CSR can be calculated decreases with depth when mean r_d values are used to simplify calculations. In addition to the uncertainty in r_d, the simplified procedure is not well verified for depths greater than about 15 m, as indicated on Figure 1. Thus the user should understand that results developed from the simplified procedure are quite uncertain at depths greater than 15 m.

As an alternative to Equation 2, Thomas F. Blake (Fugro-West, Inc., Ventura, Calif., written commun.) approximated the mean curve plotted on Figure 1 by the following equation:

$$r_d = \frac{(1.000 - 0.4113z^{0.5} + 0.04052z + 0.001753z^{1.5})}{(1.000 - 0.4177z^{0.5} + 0.05729z - 0.006205z^{1.5} + 0.001210z^{2})} \qquad (3)$$

where z is depth beneath ground surface in meters. Equation 3 yields essentially the same values for r_d as Equations 2a-d, but is easier to program for many applications and may be used in routine engineering practice.

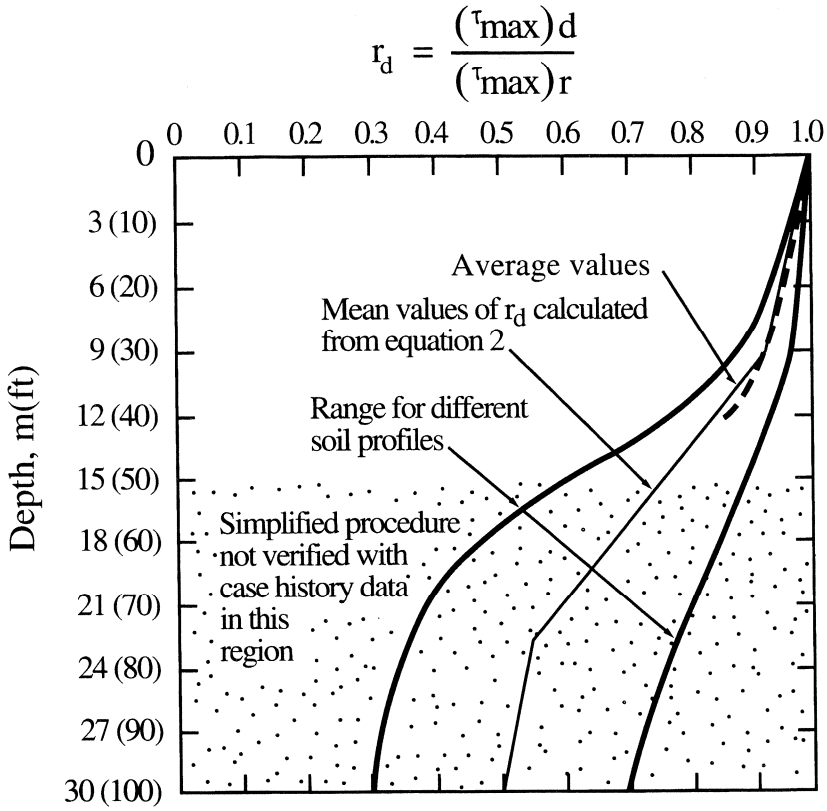

FIGURE 1 r_d Versus Depth Curves Developed by Seed and Idriss (1971) with Added Mean Value Lines from Equation 2

The primary focus of the workshop was to improve procedures for evaluating liquefaction resistance of soils, CRR. A plausible method for evaluating CRR is retrieving undisturbed soil specimens from field sites and testing those specimens in the laboratory using cyclic tests to model seismic loading conditions. Unfortunately, specimens of granular soils retrieved with typical drilling and sampling techniques are generally too disturbed to yield meaningful laboratory tests results. Only through use of specialized sampling techniques, such as ground freezing, can sufficiently undisturbed specimens be obtained. The cost of such procedures is generally prohibitive for all but the most critical projects. To avoid the difficulties associated with undisturbed sampling and testing, field tests have become the state-of-the-practice for routine liquefaction investigations.

Several field tests have gained common usage for evaluation of liquefaction resistance, including the cone penetration test (CPT), the standard penetration test (SPT), shear-wave velocity measurements (V_s), and the Becker penetration test (BPT). These tests were discussed at the workshop along with associated criteria for evaluating liquefaction resistance. Possible improvements to the state-of-the-art were reviewed and consensus recommendations developed for engineering practice. A conscientious attempt was made to correlate liquefaction resistance criteria from the various field tests to provide generally consistent results no matter which test is employed. Thus the choice of test should depend on availability of equipment, site conditions, cost, and preference. Primary advantages and disadvantages of each test are listed in Table 1.

Table 1. Comparison of Advantages and Disadvantages of Various Field Tests for Assessment of Liquefaction Resistance

Feature	Test Type			
	SPT	CPT	V_s	BPT
Number of test measurements at liquefaction sites	Abundant	Abundant	Limited	Sparse
Type of stress-strain behavior influencing test	Partially drained, large strain	Drained, large strain	Small strain	Partially drained, large strain
Quality control and repeatability	Poor to good	Very good	Good	Poor
Detection of variability of soil deposits	Good	Very good	Fair	Fair
Soil types in which test is recommended	Non-gravel	Non-gravel	All	Primarily gravel
Test provides sample of soil	Yes	No	No	No
Test measures index or engineering property	Index	Index	Engineering property	Index

Standard Penetration Test (SPT)

Criteria for evaluation of liquefaction resistance based on standard penetration test (SPT) blow counts have been rather robust over the years. Those criteria are largely embodied in the CSR versus $(N_1)_{60}$ plot reproduced in Figure 2. That plot shows calculated CSR and $(N_1)_{60}$ data from sites where liquefaction effects were or were not observed following past earthquakes along with CRR curves separating data indicative of liquefaction from data indicative of nonliquefaction for various fines contents. The CRR curve for a fines content less than five percent is the basic penetration criterion for the simplified procedure and is referred to hereafter as the "simplified base curve." The CRR curves in Figure 2 are valid only for magnitude 7.5 earthquakes.

Clean Sand Base Curve

Several changes to the SPT criteria were endorsed by workshop participants. The first change is to curve the trajectory of the simplified base curve at low $(N_1)_{60}$ to a projected CRR intercept of about 0.05 (Figure 2). This adjustment reshapes the base curve to achieve consistency with CRR curves

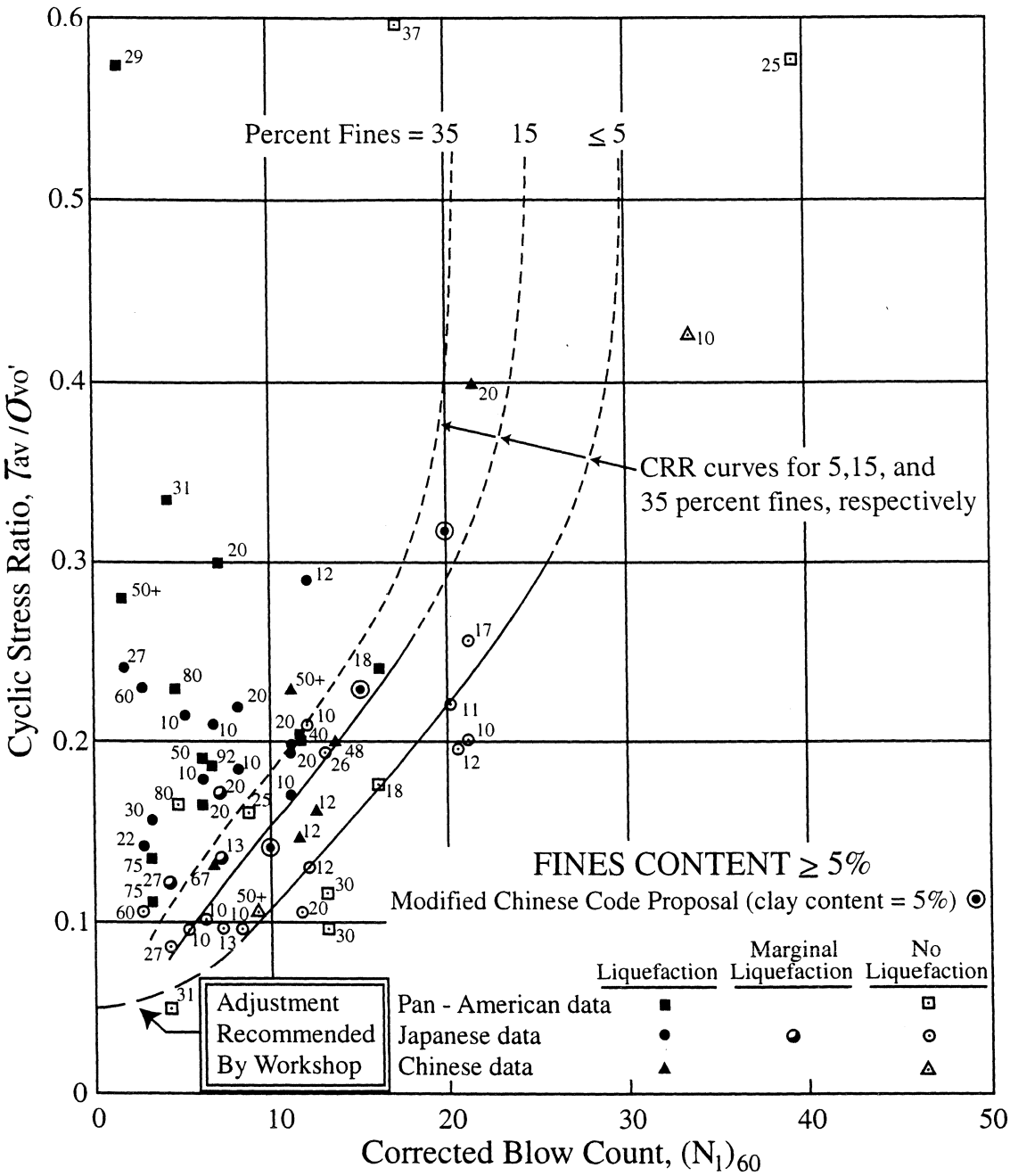

Figure 2 Simplified Base Curve Recommended for Calculation of CRR from SPT Data along with Empirical Liquefaction Data (modified From Seed et al., 1985)

developed from CPT data and probabilistic analyses by Liao et al. (1988) and Youd and Noble (Statistical and Probabilistic Analyses, this report). Seed and Idriss (1982) originally projected that curve through the origin, but there were few data to constrain the curve in the lower part of the plot. A better fit to the present empirical data is to bow the lower end of the base curve as indicated in Figure 2.

Thomas F. Blake (Fugro-West, Inc., Ventura, Calif., written commun.) approximated the simplified base curve plotted on Figure 2 by the following equation:

$$CRR_{7.5} = \frac{a + cx + ex^2 + gx^3}{1 + bx + dx^2 + fx^3 + hx^4} \quad (4)$$

where $CRR_{7.5}$ is the cyclic resistance ratio for magnitude 7.5 earthquakes; $x = (N_1)_{60}$; a = 0.048; b = -0.1248; c = -0.004721; d = 0.009578; e = 0.0006136; f = -0.0003285; g = -1.673E-05; and h = 3.714E-06. This equation is valid for $(N_1)_{60}$ less than 30 and may be used in spreadsheets and other analytical techniques to approximate the simplified base curve for engineering calculations. Robertson and Wride (this report) indicate that Equation 4 is not applicable for $(N_1)_{60}$ less than three, but the general consensus of workshop participants is that the curve defined by Equation 4 should be extended to intersect the intercept at a CRR value of about 0.05.

Correlations for Fines Content and Soil Plasticity

Another change was the quantification of the fines content correction to better fit the empirical data and to support computations with spreadsheets and other electronic computational aids. In the original development, Seed et al. (1985) found that for a given $(N_1)_{60}$, CRR increases with increased fines content. It is not clear, however, whether the CRR increase is because of greater liquefaction resistance or smaller penetration resistance as a consequence of the general increase of compressibility and decrease of permeability with increased fines content. Based on the empirical data available, Seed et al. developed CRR curves for various fines contents as shown on Figure 2.

After a lengthy review by the workshop participants, consensus was gained that the correction for fines content should be a function of penetration resistance as well as fines content. The participants also agreed that other grain characteristics, such as soil plasticity may affect liquefaction resistance; hence any correlation based solely on penetration resistance and fines content should be used with engineering judgement and caution. The following equations, developed by I.M. Idriss with assistance from R.B. Seed are recommended for correcting standard penetration resistance determined for silty sands to an equivalent clean sand penetration resistance:

$$(N_1)_{60cs} = \alpha + \beta(N_1)_{60} \quad (5)$$

where α and β are coefficients determined from the following equations:

$\alpha = 0$ for FC $\leq$ 5% (6a)

$\alpha = \exp[1.76 - (190/FC^2)]$ for 5% < FC < 35% (6b)

$\alpha = 5.0$ for FC $\geq$ 35% (6c)

$\beta = 1.0$ for FC $\leq$ 5% (7a)

$\beta = [0.99 + (FC^{1.5}/1000)]$ for 5% < FC < 35% (7b)

$\beta = 1.2$ for FC $\geq$ 35% (7c)

where FC is the fines content measured from laboratory gradation tests on retrieved soil samples.

These equations may be used for routine liquefaction resistance calculations. Back calculation of CRR curves as a function of fines content and $(N_1)_{60}$ for magnitude 7.5 earthquakes using Equations 5-7 yield curves that are essentially identical to the curves plotted on Figure 2.

Several workshop participants suggested that liquefaction resistance should also increase with soil plasticity. Agreement could not be reached, however, on formulation of a correction for plasticity. There is very little empirical data from which such a correction could be developed. Nevertheless, some practitioners have been increasing CRR by about 10 percent for soils with fines and plasticity indices greater than 15 percent. This increase seemed appropriate to several participants, but consensus was not attained. The participants did agree, however, that plasticity should be measured as part of liquefaction investigations with the goal of better defining the influence of plasticity on liquefaction resistance.

Although not endorsed by workshop participants, Robertson and Wride (this report) reviewed fines content data as part of their workshop assignment to review liquefaction resistance criteria based on SPT measurements. They suggest correcting the calculated $(N_1)_{60}$ to an equivalent $(N_1)_{60cs}$ using a correction factor, K_s, which is solely a factor of fines content as noted below:

$$(N_1)_{60cs} = K_s (N_1)_{60} \quad (8a)$$

where

$$K_s = 1 + [(0.75/30)(FC - 5)] \quad (8b)$$

This recommendation is for soils with nonplastic fines (PI $\leq$ 5 percent). For soil with plastic fines, the correction factor, K_s, would likely be larger, but the available empirical data are insufficient at present to define a plasticity adjustment. For fines contents less than about 15 percent, the CRR curves are not greatly different than the curves of Seed et al. (1985). However, for fines contents greater than 15 percent, the Robertson and Wride CRR curves are significantly less conservative and plot to the left of the curves of Seed and others. Although there are little empirical data to control the positioning of the curves for fines contents greater than 15 percent and $(N_1)_{60}$ greater than 10, the general consensus of workshop participants was that the CRR curves should not be shifted to a less conservative position, as proposed by Robertson and Wride, without additional supporting data.

Other Corrections

In addition to grain characteristics, several other factors affect SPT results. One of the more important of these factors is the energy delivered to the SPT sampler. An energy ratio, ER, of 60% has generally been accepted as the reference value. The ER delivered by a particular SPT setup depends primarily on the type of hammer and anvil in the drilling system and on the method of hammer release. Approximate correction factors (C_E = ER/60%) to modify the SPT results to a 60% energy ratio for various types of hammers and anvils are listed in Table 2. Because of variations in drilling and testing equipment and differences in procedures used, a rather wide range in the energy correction factor, C_E, has been observed as noted in the table. Even when procedures are carefully monitored to conform to established standards, such as ASTM D-1686, considerable variation in C_E may occur because of minor variations in equipment and procedures. Even within a given borehole, variations in energy ratio between hammer blows or between tests typically may vary by as much

Table 2. Corrections to SPT (Modified from Skempton, 1986) as Listed by Robertson and Wride (this report)

Factor	Equipment Variable	Term	Correction
Overburden Pressure		C_N	$(P_a/\sigma'_{vo})^{0.5}$ $C_N \leq 2$
Energy ratio	Donut Hammer Safety Hammer Automatic-Trip Donut-Type Hammer	C_E	0.5 to 1.0 0.7 to 1.2 0.8 to 1.3
Borehole diameter	65 mm to 115 mm 150 mm 200 mm	C_B	1.0 1.05 1.15
Rod length	3 m to 4 m 4 m to 6 m 6m to 10 m 10 to 30 m >30 m	C_R	0.75 0.85 0.95 1.0 <1.0
Sampling method	Standard sampler Sampler without liners	C_S	1.0 1.1 to 1.3

as ten percent. Thus, the recommended practice is to measure the energy ratio frequently at each site where the SPT is used. Where measurements can not be made, careful observation and notation of the equipment and procedures is required to estimate a C_E value for use in liquefaction resistance calculations. Use of good-quality testing equipment and carefully controlled testing procedures conforming to ASTM D-1686 will generally yield more consistent energy ratios and C_E values from the upper parts of the ranges listed in Table 2.

Additional correction factors are required for rod lengths less than 10 m and greater than 30 m, borehole diameters outside the recommended interval (65 mm to 125 mm), and sampling tubes without liners. Ranges of correction values for each of these variables are listed in Table 2. Careful documentation of drilling equipment and procedures, including measurement of ER, is required to select the most appropriate values for these correction factors. Even so, some uncertainty remains in the actual factors that should apply for any field operation.

Because the SPT N-value also varies with effective overburden stress, an overburden stress correction factor is also applied. This factor has commonly been calculated from the following equation (Liao and Whitman, 1968a):

$$C_N = (P_a/\sigma'_{vo})^{0.5} \qquad (9)$$

where C_N is a factor to correct measured penetration resistance for overburden pressure and P_a equals 100 kPa or approximately one atmosphere of pressure in the same units used for σ'_{vo}. The effective overburden pressure, σ'_{vo}, applied in this equation should be the overburden pressure that was effective at the time the SPT test was conducted. Even though the ground water level may have changed and a different water table level applied in the calculation of CSR (Equation 1), the correction of blow count requires use of the effective pressures that were effective at the time of drilling and testing.

The SPT N-value corrected for each of the above variables is given by the following equation:

$$(N_1)_{60} = N_m C_N C_E C_B C_R C_S \qquad (10)$$

where N_m is the measured standard penetration resistance, C_E is the correction for hammer energy ratio (ER), C_B is a correction factor for borehole diameter, C_R is the correction factor for rod length, and C_S is the correction for samplers with or without liners. Suggested ranges of values for each of these correction factors are listed in Table 2. Selection of appropriate factors from within these ranges requires specific information on equipment and drilling procedures and engineering judgement. The engineer should become familiar with details of the SPT procedure to avoid or at least minimize possible errors associated with SPT testing and to gain expertise in selecting appropriate correction factors.

A final change recommended by workshop participants is the use of revised magnitude scaling factors rather than the original Seed and Idriss (1982) factors to adjust $CRR_{7.5}$ to CRR for other earthquake magnitudes. Magnitude scaling factors are addressed later in this report.

Cone Penetration Test (CPT)

The workshop participants were unable to reach consensus on CPT criteria for evaluating liquefaction resistance. Robertson and Wride (this report) developed the techniques presented below with input from workshop attendees. Robertson and Wride verified these criteria against SPT and other data from sites they had investigated. T.L. Youd and his students compared liquefaction resistances calculated from CPT criteria against field performance at nineteen sites where surface effects of liquefaction were or were not observed. The CPT criteria yielded apparently correct prediction of liquefaction or nonliquefaction with greater than 90 percent reliability. Youd and his students also compared liquefaction resistances from CPT criteria with results from SPT criteria at 50 sites with parallel CPT soundings and SPT borings, with a conclusion that the CPT criteria listed below yield consistent and reasonably conservative results. G.R. Martin (oral commun., February 1998) and several colleagues from southern California also compared results developed from parallel CPT soundings and SPT boreholes. They determined that liquefaction resistances estimated from the CPT procedure are on average slightly smaller, and thus more conservative, than liquefaction resistances developed from the parallel SPT tests. The above investigators endorse the CPT criteria listed below, but strongly recommend that at least one parallel borehole near a CPT sounding be drilled at each site to verify soil types and liquefaction resistances estimated from the CPT. I.M. Idriss, on the other hand, reviewed the CPT criteria and concluded that inadequate development and verification has been made to presently recommend these criteria to the geotechnical profession. In

particular, Professor Idriss indicated that the correction for grain characteristics using I_c needs further consideration and verification. R.S. Olsen reviewed the CPT criteria listed below and concluded that the criteria are incorrectly developed and formulated. He recommends the criteria he has developed and presents in a paper submitted to the workshop (Olsen, this report).

A primary advantage of the CPT is that a nearly continuous profile of penetration resistance is developed for stratigraphic interpretation. The CPT results are generally more consistent and repeatable than results from other penetration tests listed in Table 1. The continuous profile also allows a more detailed interpretation of soil layers and soil types than the other tools listed in the Table. This stratigraphic capability makes the CPT particularly advantageous for reconnaissance investigations. In addition, CPT data can be used to estimate liquefaction resistance of penetrated soil layers. Thus the CPT can be used to develop preliminary soil and liquefaction resistance profiles for site investigations. These preliminary profiles should then be verified by other techniques, such as drilling and SPT testing.

In recent years, increased field performance data have become available at liquefaction sites investigated with CPT (Robertson and Wride, this report). These data have facilitated the development of CPT-based liquefaction resistance correlations. These correlations allow direct calculation of CRR, rather than through conversion of CPT measurements to equivalent SPT blow counts and then applying SPT criteria, a technique that was commonly applied in the past.

Figure 3 shows a chart developed by Robertson and Wride (this report) for determining cyclic resistance ratio ($CRR_{7.5}$) for clean sands (fines content, FC $\leq$ 5%) from CPT data. The chart, which is valid only for magnitude 7.5 earthquakes, shows calculated CRR plotted as a function of corrected and normalized CPT resistance, q_{c1N}, from sites where liquefaction effects were or were not observed following past earthquakes. A CRR curve separates regions of the plot with data indicative of liquefaction from regions indicative of nonliquefaction. Dashed curves showing approximate cyclic shear strain potential, γ, as a function of q_{c1N} are drawn on Figure 3 to emphasize that cyclic shear strain and ground deformation potential of liquefied soils decreases as penetration resistance increases.

The CRR curve in Figure 3 is approximated by the following simplified equation:

$$\text{If } (q_{c1N})_{cs} < 50 \qquad CRR_{7.5} = 0.833[(q_{c1N})_{cs}/1000] + 0.05 \qquad (11a)$$

$$\text{If } 50 \leq (q_{c1N})_{cs} < 160 \qquad CRR_{7.5} = 93\,[(q_{c1N})_{cs}/1000]^3 + 0.08 \qquad (11b)$$

where $(q_{c1N})_{cs}$ is the clean sand cone penetration resistance normalized to 100 kPa (approximately one atmosphere of pressure).

Normalization of Cone Penetration Resistance

Although cone penetration resistance is commonly corrected only for overburden stress, resulting in the term q_{c1}, truly normalized (i.e., dimensionless) cone penetration resistance corrected for overburden stress (q_{c1N}) is given by:

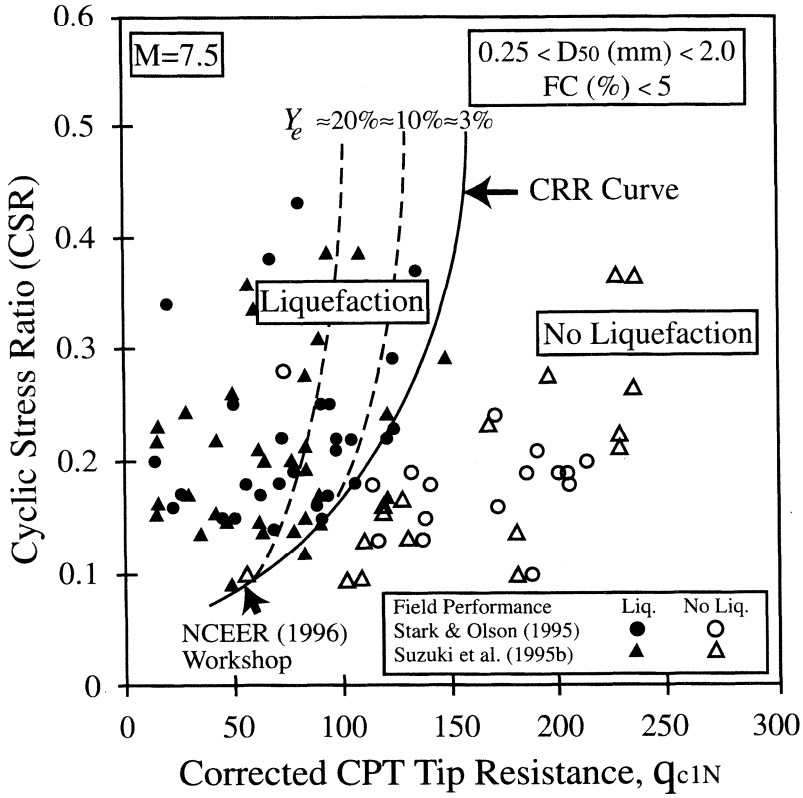

Figure 3 Curve Recommended for Calculation of CRR from CPT Data along with Empirical Liquefaction Data (After Robertson and Wride, this report)

$$q_{c1N} = C_Q(q_c / P_a) \quad (12)$$

where

$$C_Q = (P_a/\sigma'_{vo})^n \quad (13)$$

C_Q is a normalizing factor for cone penetration resistance, P_a is 100 kPa or approximately one atmosphere of pressure in the same units used for σ'_{vo}, and q_c is field cone penetration resistance measured at the tip. A maximum C_Q value of 2.0 is generally applied to CPT data at shallow depths. The value of the exponent, n, is dependent on grain characteristics of the soil and ranges from 0.5 for clean sands to 1.0 for clays (Olsen, this report). Selection of the value for use in liquefaction resistance calculations is discussed in the following paragraphs.

The CPT friction ratio (sleeve resistance, f_s, divided by cone tip resistance, q_c) generally increases with increasing fines content and soil plasticity. Robertson and Wride (this report) suggest that appropriate grain characteristics, such as approximate soil type and a rough estimate of fines content, termed apparent fines content herein, can be estimated directly from CPT data for sandy soils. Relationships recommended by Robertson and Wride are reproduced in Figures 4 and 5. The boundaries between soil types 2 through 7 on Figure 4 can be approximated as concentric circles (Jeffries and Davies, 1993). The radius of each circle, referred to as the soil behavior type index, I_c, is calculated from the following equation:

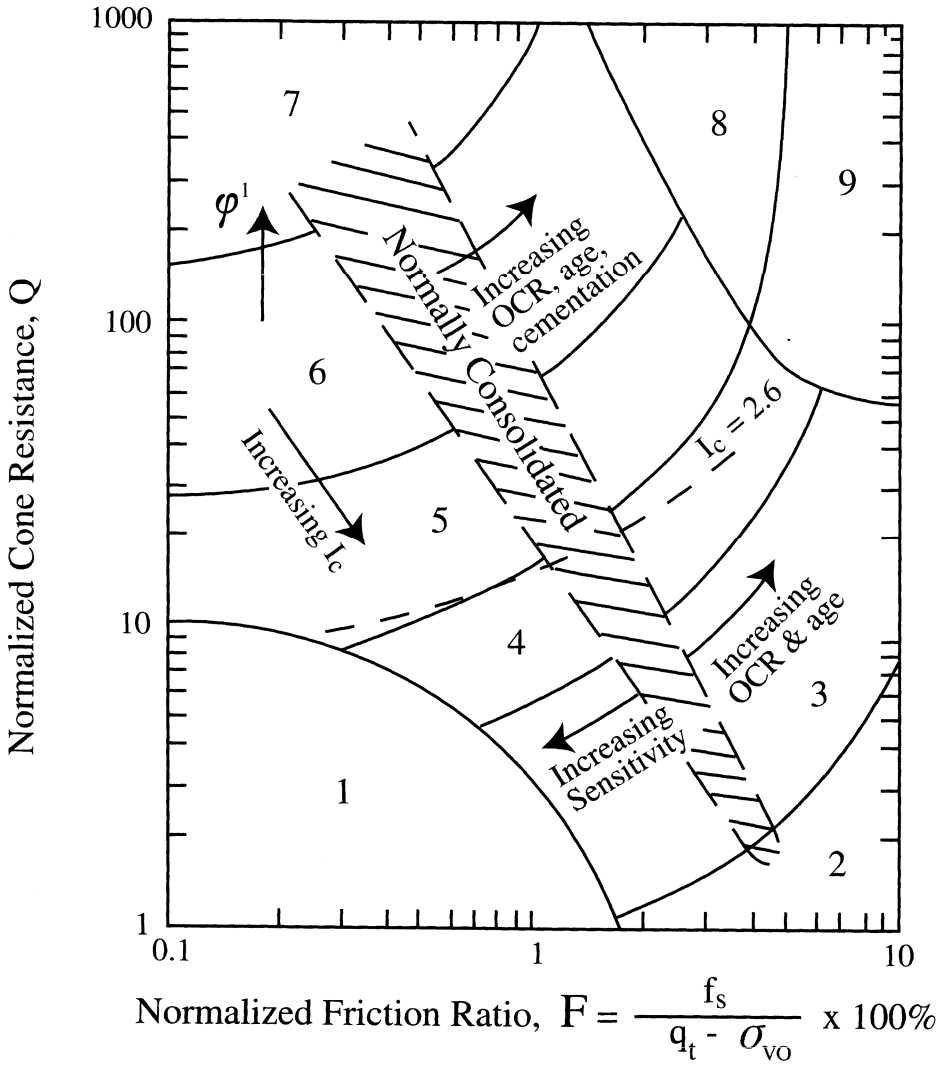

1. Sensitive, fine grained
2. Organic soils - peats
3. Clays - silty clay to clay
4. Silt mixtures - clayey silt to silty clay
5. Sand mixtures - silty sand to sandy silt
6. Sands - clean sand to silty sand
7. Gravelly sand to dense sand
8. Very stiff sand to clayey sand*
9. Very stiff, fine grained*

**Heavily overconsilidated or cemented*

Figure 4 CPT-Based Soil Behavior Type Chart Proposed by Robertson (1990)

$$I_c = [(3.47 - \log Q)^2 + (1.22 + \text{Log } F)^2]^{0.5} \quad (14)$$

where

$$Q = [(q_c - \sigma_{vo})/P_a][(P_a/\sigma'_{vo})^n] \quad (15)$$

and

$$F = [f_s/(q_c - \sigma_{vo})] \times 100\% \quad (16)$$

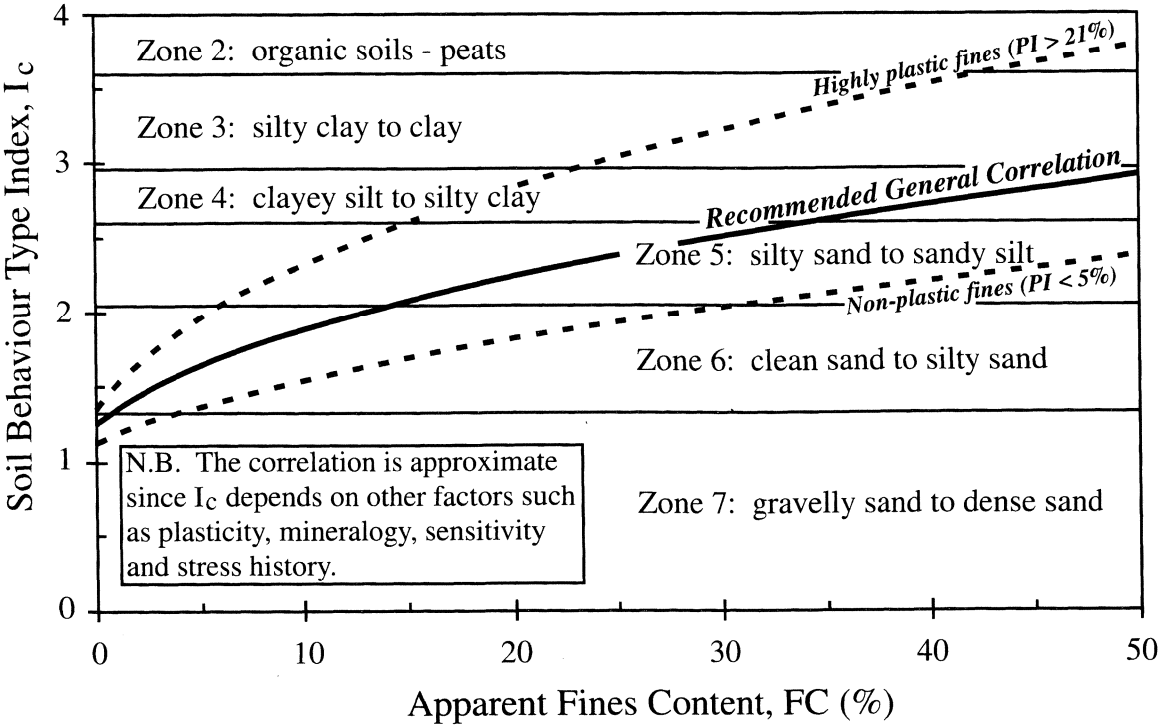

Figure 5 CPT Soil Behavior Type Index, I_c, Versus Apparent Fines Content for Normally Consolidated Soils (After Robertson and Wride, this report)

The soil behavior chart in Figure 4 was developed using an exponent, n, of 1.0, which is the appropriate value for clayey-type soils. For clean sands, however, an exponent value of 0.5 is more appropriate, and a value intermediate between 0.5 and 1.0 would be appropriate for silts and silty sands. Robertson and Wride recommend the following procedure for selecting an exponent and calculating the soil behavior type index, I_c.

The first step is to differentiate soil types characterized as clays from soil types characterized as sands and silts using Figure 4. This differentiation is performed by assuming an exponent, n, of 1.0 (characteristic of clays) and performing the following calculations. For clays, the dimensionless normalized CPT penetration resistance, Q, is defined as:

$$Q = [(q_c - \sigma_{vo})/P_a][P_a/\sigma'_{vo}]^{1.0} = [(q_c - \sigma_{vo})/\sigma'_{vo}] \qquad (17)$$

If the calculated I_c calculated with an exponent of 1.0 is greater than 2.6, the soil is classed as clayey and is considered too clay-rich to liquefy. Samples should be taken and tested, however, to confirm the soil type and liquefaction resistance. Criteria, such as the Chinese criteria, might be applied to confirm that the soil is nonliquefiable. The so-called Chinese criteria, as defined by Seed and Idriss (1982), stipulate that liquefaction can only occur if all three of the following conditions are met:

(1) The clay content (particles smaller than 5μ) is less than 15 percent, by weight.
(2) The liquid limit is less than 35% percent.
(3) The natural moisture content is less than 0.9 times the liquid limit.

If the calculated I_c is less than 2.6, the soil is most likely granular in nature and Q should be recalculated using an exponent, n, of 0.5. For this calculation, C_Q should also be calculated with an exponent, n, of 0.5 (Equation 13), and q_{c1N} (calculated from Equation 12) substituted for Q in Equation 14. I_c should then be recalculated using Equation 14. If the recalculated I_c is less than 2.6, the soil can be classed as nonplastic and granular, and this I_c can be used to estimate liquefaction resistance as noted below. If the recalculated I_c is greater than 2.6, however, the soil is likely to be very silty and possibly plastic. In this instance, q_{c1N} should be recalculated from Equation 12 using an intermediate exponent, n, of 0.7 in Equation 13 and I_c recalculated from Equation 14 using the recalculated value for q_{c1N}. This intermediate I_c is then used to calculate liquefaction resistance. In this instance, a soil sample should be retrieved and tested to verify the soil type and whether the soil is liquefiable by other criteria, such as the Chinese criteria.

Because the relationship between I_c and soil type is rather approximate, the consensus of the workshop was that all soils characterized by an I_c of 2.4 or greater should be sampled and tested to confirm the soil type and to test the liquefiability with other criteria. Also, soil layers characterized by an I_c greater than 2.6, but with a normalized friction ratio, F, less than 1.0 percent (Region 1 of Figure 4) can be very sensitive, and hence should also be sampled and tested. Although perhaps not technically liquefiable according to the Chinese criteria, such sensitive soils may suffer severe softening and even strength loss under earthquake loading conditions.

Calculation of Clean Sand Equivalent Normalized Cone Penetration Resistance, $(q_{c1N})_{cs}$

To correct the normalized penetration resistance, (q_{c1N}), of sands with fines to an equivalent clean sand value,$(q_{c1N})_{cs}$, for use in the calculation of liquefaction resistance, CRR, the following relationships are applied:

$$(q_{c1N})_{cs} = K_c q_{c1N} \qquad (18)$$

where the CPT correction factor for grain characteristics, K_c, is defined by the following equations (Robertson and Wride, this report):

$$\text{For } I_c \leq 1.64 \quad K_c = 1.0 \qquad (19a)$$

$$\text{For } I_c > 1.64 \quad K_c = -0.403\, I_c^4 + 5.581\, I_c^3 - 21.63\, I_c^2 + 33.75\, I_c - 17.88 \qquad (19b)$$

Although the measured fines content could be substituted for the apparent fines content in Figure 5 to determine an I_c, such a substitution will likely yield erroneous results and should not be done. As noted above, I_c is a function of plasticity and other factors as well as fines content. Thus when using CPT data, I_c must be calculated from Equation 14 rather than estimated from the measured fines content.

The K_c versus I_c curve defined by Equations 19a and 19b is plotted on Figure 6. For I_c greater than 2.6, the curve is shown as a dashed line, indicating that the soils are most likely too clay rich or plastic to liquefy.

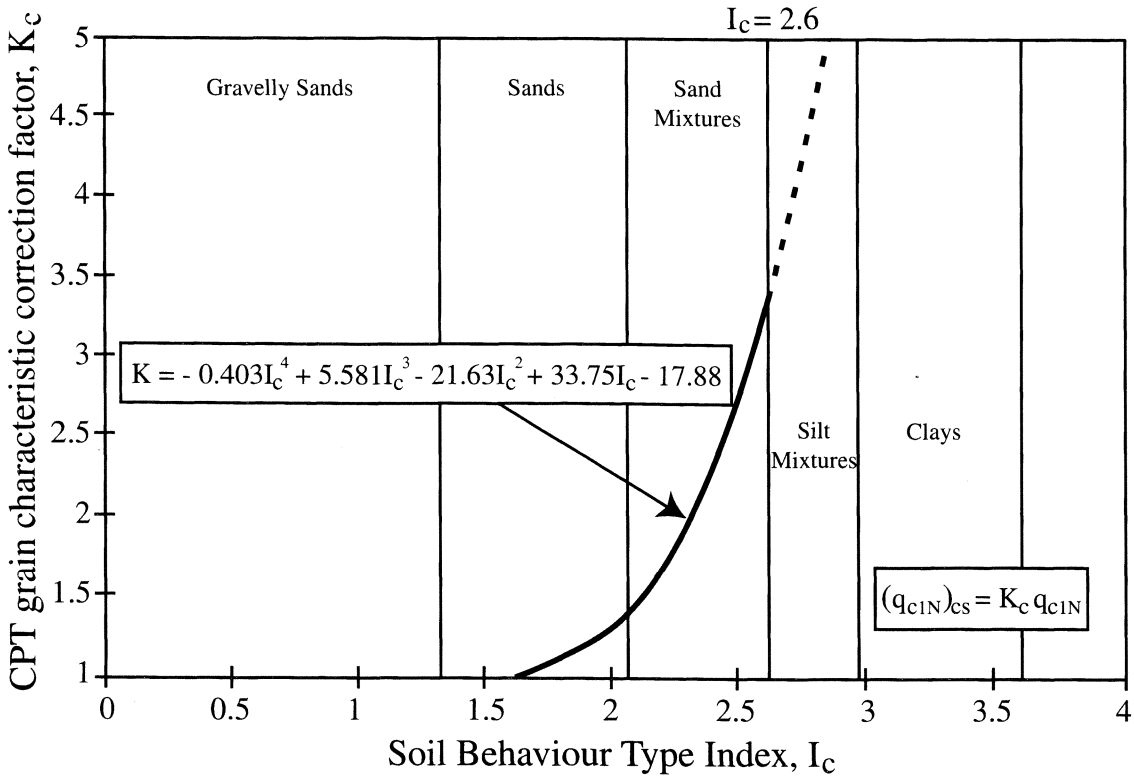

Figure 6 Grain-Characteristic Correction Factor, K_c, for Determination of Clean-Sand Equivalent CPT Resistance (After Robertson and Wride, this report)

With an appropriate I_c and K_c, Equations 11 and 19 can be used to calculate $CRR_{7.5}$. To adjust CRR to magnitudes smaller or larger than 7.5, the calculated $CRR_{7.5}$ is multiplied by an appropriate magnitude scaling factor. The same magnitude scaling factors are used with CPT data as with SPT or shear wave velocity data. Magnitude scaling factors are discussed in a later section of this report.

Although approached by a somewhat different route, the procedure for calculation of liquefaction resistance, CRR, given above is generally consistent and will generally give compatible results with the procedure proposed by Olsen (this report) for most level to gently sloping site conditions. As noted by Olsen, almost any CPT normalization technique, such as the procedure noted above, will give results consistent with his normalization procedure for shallow soil layers. For deep sites (σ'_{vo} > 150 kPa or depths greater than about 15 m), significant differences in results may develop between the two procedures. Those depths are deeper than most documented occurrences of liquefaction at natural sites and thus are deeper than the verified depth for the simplified procedure.

Correction of Cone Penetration Resistance for Thin Soil Layers

Theoretical as well as laboratory studies indicate that cone resistance is influenced by softer or stiffer soil layers above or below the cone tip. As a result, the CPT will not usually measure the full penetration resistance in thin sand layers sandwiched between layers of softer soils. The distance to which cone tip resistance is influenced by an approaching interface increases with stiffness of the

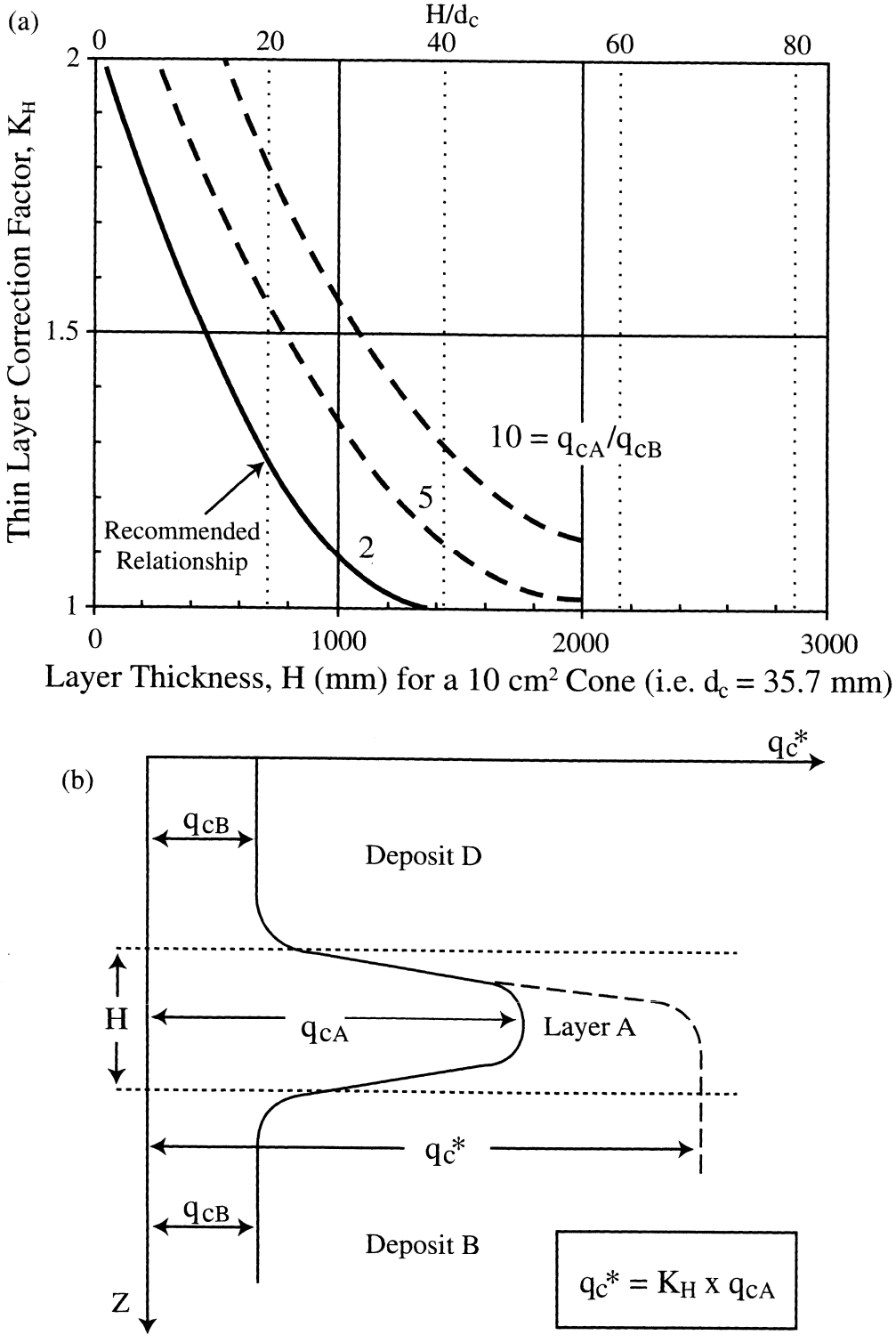

Figure 7 Thin-Layer Correction Factor, K_H, for Determination of Equivalent Thick-Layer CPT Resistance (After Robertson and Fear, 1995)

stiff layer. In soft clays or loose sands, the distance of influence can be as small as 2 to 3 cone diameters. In stiff clays or dense sands, the distance of influence may be as large as 20 cone diameters. (The diameter of the standard 10 cm^2 cone is 36 mm.) Thus care should be taken when interpreting cone resistance of sand layers sandwiched between silt or clay layers with lower penetration resistances. Based on a simplified elastic solution, Vreugdenhil et al. (1994) developed a procedure for estimating the full cone penetration resistance of thin stiff layers contained within softer strata. Based on this model, Robertson and Fear (1995) suggest a correction factor for cone resistance, K_H, as a function of layer thickness as shown in Figure 7. The correction applies only to thin stiff layers embedded within thick soft layers. Because the corrections have a reasonable trend, but appear rather large, Robertson and Fear (1995) recommend conservative corrections corresponding to $q_{cA}/q_{cB} = 2$ as shown on Figure 7. The equation for evaluating the correction factor, K_H, is

$$K_H = 0.5\ [(H/1{,}000) - 1.45]^2 + 1.0 \qquad (20)$$

where H is the thickness of the interbedded layer in mm, and q_{cA} and q_{cB} are cone resistances of the stiff and soft layers, respectively.

Shear Wave Velocity

During the past decade, several simplified procedures have been proposed for the use of field measurements of small-strain shear wave velocity, V_S, to assess liquefaction resistance of granular soils (Stokoe et al., 1988; Tokimatsu et al., 1991; Robertson et al., 1992; Kayen et al., 1992; Andrus, 1994; Lodge, 1994). The use of V_S as a field index of liquefaction resistance is justified because both V_S and CRR are similarly influenced by void ratio, effective confining stresses, stress history, and geologic age. The advantages of using V_S include the following: (1) V_S can be accurately measured in situ using a number of techniques such as crosshole and downhole seismic tests, the seismic cone penetration test, or spectral analysis of surface waves; (2) V_S measurements are possible in soils that are difficult to penetrate with CPT and SPT or to extract undisturbed samples, such as gravelly soils, and at sites where borings or soundings may not be permitted; (3) measurements can be performed in small laboratory specimens, allowing direct comparisons between measured laboratory and field behavior; and (4) V_S is directly related to small-strain shear modulus, a parameter required in analytical procedures for estimating dynamic soil response at small and intermediate shear strains.

Two significant limitations of using V_S in liquefaction hazard evaluations are that (1) seismic wave velocity measurements are made at small strains, whereas liquefaction is a large strain phenomenon; and (2) seismic testing does not provide samples for classification of soils and identification of nonliquefiable soft clay-rich soils. To compensate for the latter limitation, a limited number of borings should be drilled and samples taken to identify nonliquefiable clay-rich soils that might classify as liquefiable by V_S criteria and also to identify weakly cemented soils that might be liquefiable but classify as nonliquefiable because of their characteristically high V_S values.

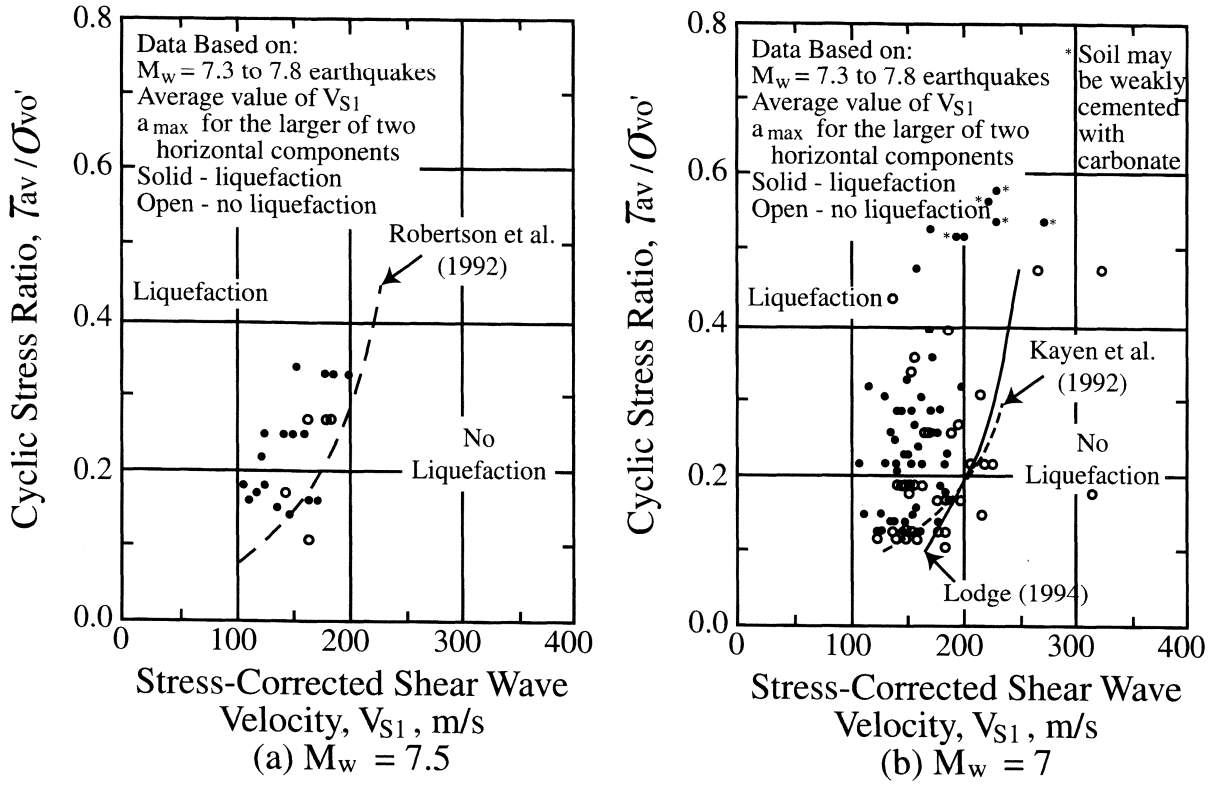

Figure 8 CSR Charts Based on Corrected Shear-Wave Velocities Suggested by (a) Robertson et al. (1992), and (b) Kayen et al. (1992) and Lodge (1994) (After Andrus and Stokoe, this report)

Criteria for Evaluating Liquefaction Resistance

Robertson et al. (1992) proposed a stress-based liquefaction assessment procedure using field performance data from sites in the Imperial Valley, California. These investigators normalized V_S by:

$$V_{S1} = V_S(P_a/\sigma'_{vo})^{0.25} \quad (21)$$

where P_a is a reference stress of 100 kPa, approximately atmospheric pressure, and σ'_{vo} is effective overburden pressure in kPa. Robertson et al. chose to modify V_S in terms of σ'_{vo} to follow the traditional procedures for modifying standard and cone penetration test resistances. The liquefaction resistance bound (CRR curve) determined by these investigators for magnitude 7.5 earthquakes is plotted on Figure 8a along with data calculated from several field sites where liquefaction did or did not occur. The cyclic stress ratios were calculated using estimates of a_{max} for the larger of two horizontal components of ground acceleration that would have occurred at the site in the absence of liquefaction.

Subsequent liquefaction resistance boundaries proposed by Kayen et al. (1992) and Lodge (1994) for magnitude 7 earthquakes are shown on Figure 8b. These curves are based on field performance

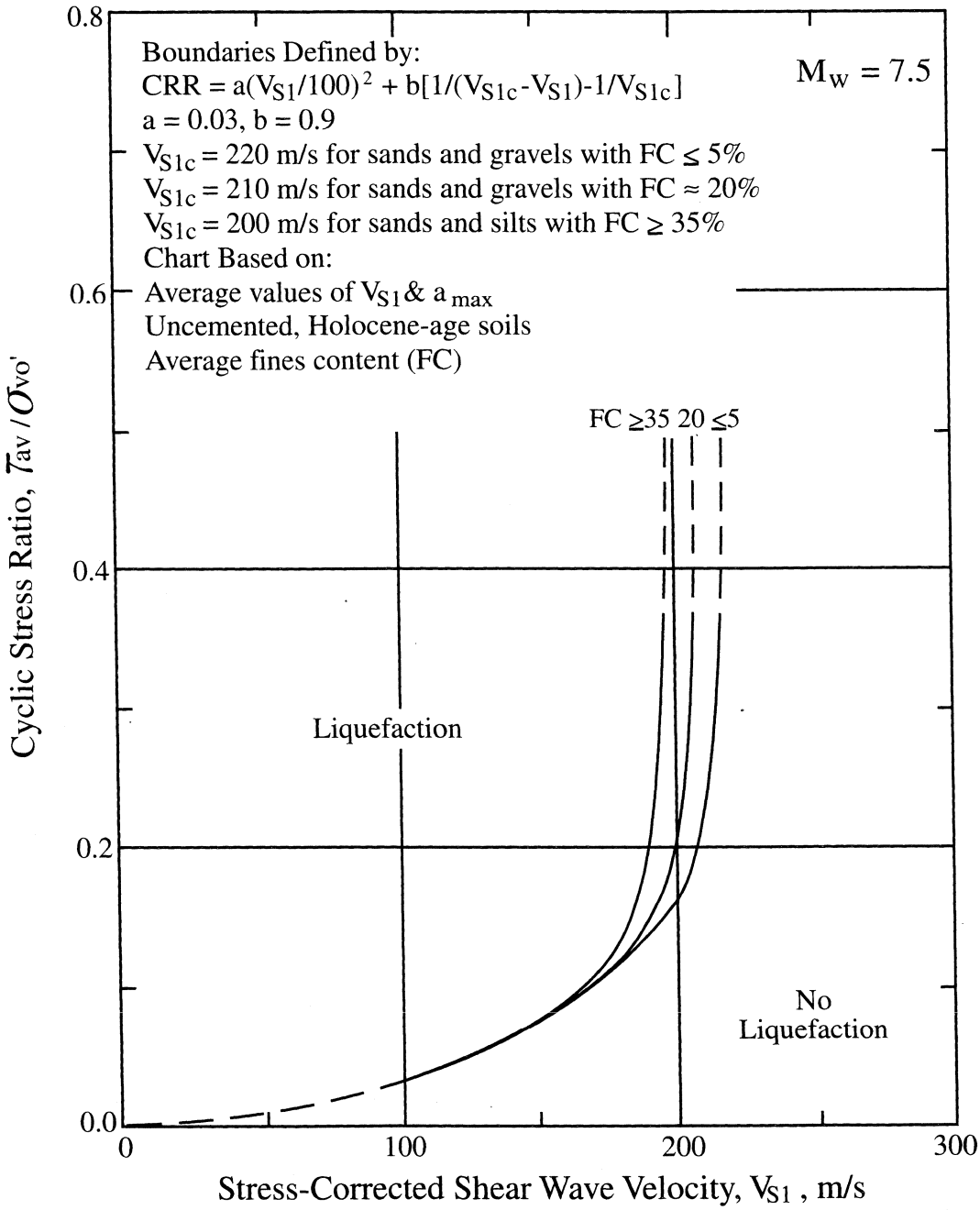

Figure 9 Curves Recommended by Workshop for Calculation of CRR from Corrected Shear Wave Velocity (After Andrus and Stokoe, this report)

data from the 1989 Loma Prieta earthquake. With few exceptions, the liquefaction case histories are bounded by the relationships proposed by these suggested bounds. The relationship proposed by Lodge (1994) provides a conservative lower boundary for liquefaction case histories with V_{S1} less than about 200 m/s. The relationship by Robertson et al. (1992) is the least conservative of the three.

Professor Ricardo Dobry suggested a relationship between cyclic resistance ratio and V_{S1} for constant average cyclic shear strain, γ_{av}, of the form:

$$CRR = \tau_{av}/\sigma'_{vo} = f(\gamma_{av})V_{S1}^2 \qquad (22)$$

where γ_{av} is constant average shear strain. This formula supports a CRR bound passing through the origin and provides a rational approach for extrapolating beyond the limits of the available field performance data, at least for lower values of V_{S1} ($V_{S1} \leq 125$ m/s).

For higher values of V_{S1}, Andrus and Stokoe (this report) reason that the CRR bound should become asymptotic to some limiting V_{S1} value. This limit is caused by the tendency of dense granular soils to exhibit dilative behavior at large strains. Thus Equation 22 is modified to:

$$\tau_{av}/\sigma'_{vo} = CRR = a(V_{S1}/100)^2 + b/(V_{S1c} - V_{S1}) - b/V_{S1c} \qquad (23)$$

where V_{S1c} is the critical value of V_{S1}, which separates contractive and dilative behavior, and a and b are curve fitting parameters.

Using the relationship between V_{S1} and CRR expressed by Equation 23, Andrus and Stokoe drew curves to separate data from sites where liquefaction effects were and were not observed. Best fit values for the constants a and b were 0.03 and 0.9, respectively, for magnitude 7.5 earthquakes. Andrus and Stokoe also determined the following best-fit values for V_{S1c}:

V_{S1c} = 220 m/s for sands and gravels with fines contents less than 5%
V_{S1c} = 210 m/s for sands and gravels with fines contents of about 20 %
V_{S1c} = 200 m/s for sands and gravels with fines contents greater than 35%

Figure 9 presents CRR boundaries recommended by Andrus and Stokoe for magnitude 7.5 earthquakes and uncemented Holocene-age soils with various fines contents. Although these boundaries pass through the origin, natural alluvial sandy soils with shallow water tables rarely have corrected shear wave velocities less than 100 m/s, even near ground surface. For a V_{S1} of 100 m/s and a magnitude 7.5 earthquake, the calculated CRR is 0.03. This minimal CRR value is generally consistent with intercept CRR values for the CPT and SPT procedures.

Equation 23 can be scaled to other magnitude values through use of magnitude scaling factors. These factors are discussed in a later section of this paper.

Becker Penetration Tests

Liquefaction resistance of non-gravelly soils has been evaluated primarily through CPT and SPT, with occasional V_S measurements. CPT and SPT measurements, however, are not generally reliable in gravelly soils. Large gravel particles may interfere with the normal deformation of soil materials around the penetrometer increasing penetration resistance. In an attempt to surmount these difficulties, several investigators have employed large-diameter penetrometers. The Becker penetration test (BPT) has become one of the more effective and widely used of these type of tools.

The BPT was developed in Canada in the late 1950s and consists of a 3-meter-long double-walled casing driven into the ground with a double-acting diesel-driven pile hammer. The hammer impacts are applied at the top of the casing and penetration is continuous. The Becker penetration resistance is defined as the number of blows required to drive the casing through an increment of 300 mm.

The BPT has not been standardized and several different types of equipment and procedures have been used. Also, only a few BPT blow counts have been measured at sites where liquefaction has occurred. Thus the BPT is not correlated directly with liquefaction resistance, but is used to estimate equivalent SPT blow counts though empirical correlation. The equivalent SPT blow count is then used to estimate liquefaction resistance.

To provide uniformity, Harder and Seed (1986) recommend employment of newer AP-1000 drill rigs equipped with supercharged diesel hammers, 168-mm O.D. casing , and a plugged bit. From several sites where both BPT and SPT tests were conducted in parallel soundings, Harder and Seed (1986) developed a preliminary correlation between Becker and standard penetration resistance (Figure 10a). Additional comparative data compiled since 1986 are plotted on Figure 10b. The original Harder and Seed correlation curve (solid line) is drawn on Figure 10b along with dashed curves representing 20% over- and under-predictions of SPT blow counts. These plots indicate that SPT blow counts can be roughly estimated from BPT measurements.

A major source of variation in BPT blow counts is deviations in hammer energy. Rather than measuring hammer energy directly, Harder and Seed (1986) monitored bounce-chamber pressures and found that uniform combustion conditions (e.g., full throttle with a supercharger) correlated rather well with variations in Becker blow count. From this information, Harder and Seed (this report) developed an energy correction procedure based on measured bounce-chamber pressure.

Direct measurement of transmitted hammer energy could provide a more theoretically rigorous correction for Becker hammer efficiency. Sy and Campanella (1994) and Sy et al. (1995) instrumented a small length of Becker casing with strain gages and accelerometers in an attempt to measure transferred energy. They analyzed the recorded data with a pile-driving analyzer to determine strain, force, acceleration, and velocity. The transferred energy was determined by time integration of force times velocity. They were able to verify many of the variations in hammer energy previously identified by Harder and Seed (1986), including effects of variable throttle settings and energy transmission efficiencies of various drill rigs. However, they were not able to reduce the scatter or uncertainty in converting BPT blow counts to SPT blow counts. Because the Sy and Campanella procedure requires considerably more effort than monitoring of bounce-chamber pressure without producing greatly improved results, the workshop participants agreed that the bounce-chamber technique appears adequate for routine practice.

Friction along the driven casing also influences penetration resistance. Harder and Seed (1986) did not evaluate the effect of casing friction; hence the correlation in Figure 10b intrinsically incorporates casing friction. Casing friction, however, remains a concern for depths greater than 30 m and for measurement of penetration resistance in soft soils underlying thick deposits of dense soil. Either of these circumstances could lead to greater casing friction than is intrinsically incorporated in the Seed and Harder correlation.

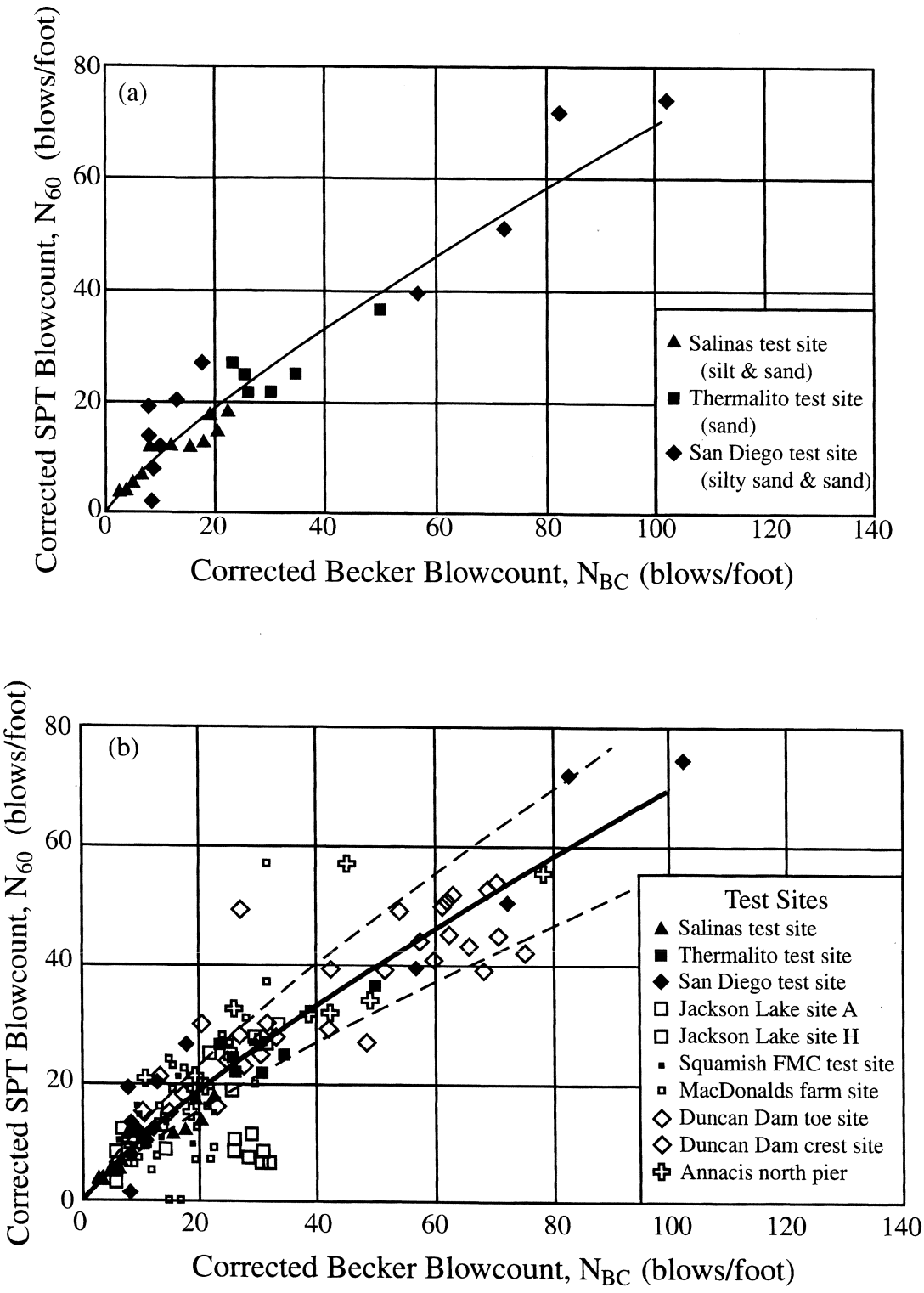

Figure 10 Correlation Between Corrected Becker Penetration Resistance, NBC, and Corrected SPT Resistance, N_{60}, (a) Harder and Seed (1986); (b) Data from Additional Sites (After Harder, this report)

The following procedures are recommended for routine practice: (1) The BPT should be conducted with newer AP-1000 drill rigs equipped with supercharged diesel hammers used to drive plugged 168-mm O.D. casing. (2) Bounce-chamber pressures should be used to adjust measured BPT blow counts to N_{bc} to account for variations in diesel hammer combustion efficiency. For most routine applications, correlations developed by Harder and Seed (1986) may be used for these adjustments. (3) The influence of casing friction is intrinsically accounted for in the Harder and Seed BPT-SPT correlation. This correlation, however, has not been verified and should not be used for depths greater than 30 meters or for sites with thick dense deposits overlying loose sands or gravels. For these conditions, mudded boreholes may be needed to reduce casing friction, or sophisticated wave-equation analyses may be applied to quantify frictional effects.

Magnitude Scaling Factors

In developing the simplified procedure, Seed and Idriss (1982) compiled a sizable data base from sites where liquefaction did or did not occur during earthquakes with magnitudes near 7.5. Analyses were made of these data to calculate cyclic stress ratios (CSR) and $(N_1)_{60}$ values for various sites where surface effects of liquefaction were or were not observed. Results from clean sand sites (fines content $\leq$ 5 percent) were plotted on a CSR versus $(N_1)_{60}$ plot. An updated version of that plot (Seed et al., 1985) is reproduced in Figure 2. A deterministic curve was drawn through the plot to separate regions with data indicative of liquefaction (solid symbols) from regions with data indicative of nonliquefaction (open symbols). Where there was a mixture of data, the curve was conservatively placed to ensure that data indicative of liquefaction plot above or to the left of the bounding curve. This curve, termed the simplified base curve or $CRR_{7.5}$ curve, is relatively well constrained by empirical data between CSR of 0.08 and 0.35 and is logically extrapolated to higher and lower values beyond that range. As shown in Figure 2, the workshop participants recommend bowing the lower part of the simplified base curve to intersect the ordinate of the plot at a CRR of about 0.05.

To adjust the simplified base curve to magnitudes smaller or larger than 7.5, Seed and Idriss (1982) introduced correction factors called "magnitude scaling factors." These factors are used to scale the simplified base curve upward or downward on the CSR versus $(N_1)_{60}$ plot. Conversely, magnitude weighting factors, which are the inverse of magnitude scaling factors, may be applied to correct CSR for magnitude. Either correcting CRR via magnitude scaling factors, or correcting CSR via magnitude weighting factors, leads to the same final result. Because the original papers by Seed and Idriss were written in terms of magnitude scaling factors, the use of magnitude scaling factors is continued in this report.

To illustrate the influence of magnitude scaling factors on calculated hazard, the equation for factor of safety (FS) against liquefaction can be written in terms of CRR, CSR, and MSF as follows:

$$FS = (CRR_{7.5}/CSR)MSF \qquad (24)$$

where $CRR_{7.5}$ is the cyclic resistance ratio determined for magnitude 7.5 earthquakes using Figure 2 or Equation 4 for SPT data, Figure 3 or Equation 11 for CPT data, or Figure 9 or Equation 23 for V_{S1} data. Equation 24 demonstrates that the factor of safety against development of liquefaction at a site is directly proportional to the magnitude scaling factor selected.

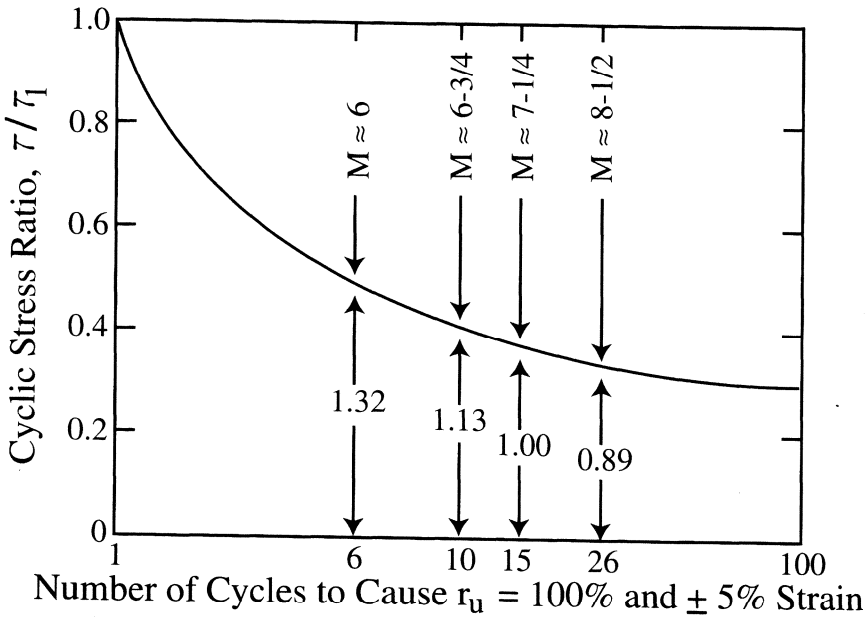

Figure 11 Representative Relationship Between CSR and Number of Cycles To Cause Liquefaction and (After Seed and Idriss, 1982)

Seed and Idriss (1982) Scaling Factors

Because of the limited empirical data available in the 1970s, Seed and Idriss (1982) were unable to narrowly constrain bounds between liquefaction and nonliquefaction regions on CRR plots for magnitudes other than 7.5. Consequently, they based their scaling factors on representative loading cycles and laboratory test results. From a study of strong-motion accelerograms, the number of representative loading cycles generated by an earthquake was correlated with earthquake magnitude. For example, magnitude 7.5 earthquakes were characterized by 15 loading cycles, whereas, magnitude 8.5 earthquakes were characterized by 26 loading cycles, and magnitude 6.5 earthquakes by 10 loading cycles. Second, laboratory tests were conducted to measure the number of loading cycles required to generate liquefaction and five percent cyclic strain. Laboratory tests were conducted using a variety of clean sands, void ratios, and ambient stress conditions. From these tests, a single representative curve was developed that relates cyclic stress ratio to the number of loading cycles required to generate liquefaction (Figure 11). By dividing CSR values from this curve for various numbers of cycles, representative of various earthquake magnitudes, by the CSR for 15 cycles (magnitude 7.5), the initial set of magnitude scaling factors was derived. These scaling factors are listed in Column 2 of Table 3 and are plotted on Figure 12. These magnitude scaling factors have been routinely applied in engineering practice since their introduction in 1982.

Idriss Scaling Factors

In preparing his H.B. Seed memorial lecture, I.M. Idriss reevaluated the data that he and the late Professor Seed had used to calculate the original (1982) magnitude scaling factors. In so doing, Idriss re-plotted the data on a log-log plot and found that the data plotted as a straight line. He further noted that one outlier point had strongly influenced the original analysis, causing the original

Table 3. Magnitude Scaling Factor Values Defined by Various Investigators (from Youd and Noble, Magnitude Scaling Factors, this report)

Mag-nitude, M (1)	Seed and Idriss (1982) (2)	Idriss (3)	Ambraseys (1988) (4)	Arango (1996) (5)	(6)	Andrus and Stokoe (in press) (7)	Youd and Noble (this report) P_L<20% (8)	P_L<32% (9)	P_L<50% (10)
5.5	1.43	2.20	2.86	3.00	2.20	2.8	2.86	3.42	4.44
6.0	1.32	1.76	2.20	2.00	1.65	2.1	1.93	2.35	2.92
6.5	1.19	1.44	1.69	1.60	1.40	1.6	1.34	1.66	1.99
7.0	1.08	1.19	1.30	1.25	1.10	1.25	1.00	1.20	1.39
7.5	1.00	1.00	1.00	1.00	1.00	1.00			1.00
8.0	0.94	0.84	0.67	0.75	0.85	0.8?			0.73?
8.5	0.89	0.72	0.44			0.65 ?			0.56?

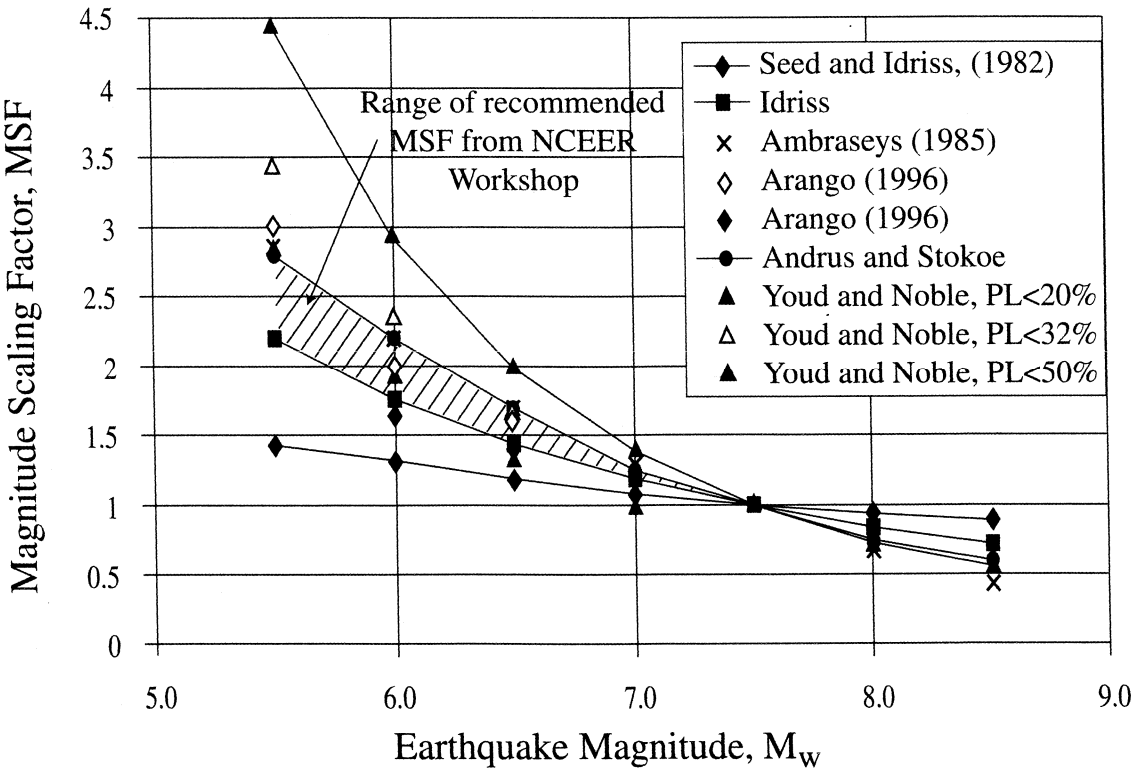

Figure 12 Magnitude Scaling Factors Derived by Various Investigators (After Youd and Noble, Magnitude Scaling Factors, this report)

plot to be nonlinear and characterized by unduly low values for magnitudes less than 7.5. Based on this reevaluation, Idriss defined a new set of magnitude scaling factors. These factors are listed in Column 3 of Table 3, plotted on Figure 12, and are defined by the following equation:

$$MSF = 10^{2.24}/M^{2.56} \quad (25)$$

Idriss recommends these revised scaling factors for use in engineering practice in place of the original factors.

The revised scaling factors are significantly larger than the original scaling factors for magnitudes less than 7.5 and somewhat smaller than the original factors for magnitudes greater than 7.5. Relative to the original scaling factors, the revised factors lead to a reduced calculated liquefaction hazard for magnitudes less than 7.5 and increased calculated hazard for magnitudes greater than 7.5.

Ambraseys Scaling Factors

Field performance data collected since the 1970s for magnitudes less than 7.5 indicate that the original Seed and Idriss (1982) scaling factors may be overly conservative. For example, Ambraseys (1988) analyzed liquefaction data compiled through the mid-1980s and plotted calculated cyclic stress ratios for sites that did or did not liquefy on CSR versus $(N_1)_{60}$ plots. From these plots, Ambraseys developed empirical exponential equations that define CRR as a function of $(N_1)_{60}$ and moment magnitude, M_w. By holding the value of $(N_1)_{60}$ constant in the equations and taking the ratio of CRR determined for various magnitudes of earthquakes to the CRR for a magnitude 7.5 earthquakes, Ambraseys derived the magnitude scaling factors listed in Column 4 of Table 3. These factors are also plotted on Figure 12. For magnitudes less than 7.5, the MSF suggested by Ambraseys are significantly greater than both the original factors developed by Seed and Idriss (Column 2, Table 3) and the revised factors by Idriss (Column 3). Because they are based on observational data, these factors have validity for estimating liquefaction hazard; however, they have not been widely used in engineering practice. Conversely, for magnitudes greater than 7.5, Ambraseys factors are significantly lower than the original (Seed and Idriss, 1982) and Idriss's revised scaling factors. Because there are little data to constrain Ambraseys' scaling factors for magnitudes greater than 7.5, these factors are uncertain, are likely overly conservative, and are not recommended for engineering practice.

Arango Scaling Factors

Arango (1996) developed two sets of magnitude scaling factors. The first set (Column 5, Table 3) is based on farthest observed liquefaction effects from the seismic energy source, the estimated average peak accelerations at those distant sites, and the absorbed seismic energy required to cause liquefaction. The second set (Column 6, Table 3) was developed from energy concepts and the relationship derived by Seed and Idriss (1982) between numbers of significant stress cycles and earthquake magnitude. The MSF listed in Column 5 are similar in value (within about 10%) to the MSF of Ambraseys (Column 4), and the MSF listed in Column 6 are similar in value (within 6%) to the revised MSF proposed by Idriss (Column 3).

Andrus and Stokoe Scaling Factors

From their studies of liquefaction resistance as a function of shear wave velocity, V_s, Andrus and Stokoe (this report) developed Equation 23 for calculating CRR from V_s for magnitude 7.5 earthquakes. Using this equation, Andrus and Stokoe drew curves on graphs with plotted values of CSR as a function of V_{S1} from sites where surface effects of liquefaction were or were not observed. Graphs were plotted for sites shaken by magnitude 6, 6.5, 7, and 7.5 earthquakes. The positions of the CRR curves were visually adjusted on each graph until a best fit bound was obtained. Magnitude scaling factors were then estimated by taking the ratio of CRR for a given magnitude to the CRR for magnitude 7.5 earthquakes. These MSF were then fitted to the following exponential function

$$MSF = (M_w/7.5)^{-3.3} \quad (26)$$

Values for magnitudes less than 6 and greater than 7.5 were extrapolated from this equation. MSF values from this analysis are listed in Column 7, Table 3, and plotted on Figure 12. For magnitudes less than 7.5, the MSF proposed by Andrus and Stokoe are rather close in value (within about 5 percent) to the MSF proposed by Ambraseys. For magnitudes greater than 7.5, the Andrus and Stokoe MSF are slightly smaller than the revised MSF proposed by Idriss.

Youd and Noble Scaling Factors

Youd and Noble (Magnitude Scaling Factors, this report) used a logistic analysis to analyze case history data from sites where effects of liquefaction were or were not reported following past earthquakes. This analysis yielded the following probabilistic equation:

$$\text{Logit}\,(P_L) = \ln(P_L/(1-P_L)) = -7.633 + 2.256\,M_w - 0.258\,(N_1)_{60cs} + 3.095\,\ln CRR \quad (27)$$

where P_L is the probability that liquefaction occurred, $1-P_L$ is the probability that liquefaction did not occur, and $(N_1)_{60cs}$ is the corrected blow count, including the correction for fines content. Youd and Noble recommend direct application of this equation to calculate the CRR for a given probability of liquefaction occurrence. In lieu of direct application, Youd and Noble define MSF for use with the simplified procedure. These MSF were developed by rotating the simplified base curve to near tangency with the probabilistic curves for P_L of 50%, 32%, and 20% and various earthquake magnitudes. These MSF are defined as the ratio of the ordinate of the rotated base curve at the point of near tangency to the ordinate of the unrotated simplified base curve at the same $(N_1)_{60cs}$. Because the rotated simplified base curves lie entirely below the given probability curve, CRR calculated with these MSF are characterized by smaller probability of liquefaction occurrence than the associated probabilistic curves. Thus the MSF listed in Columns 8, 9, and 10 (Table 3), are denoted by $P_L<50\%$, $P_L<32\%$, and $P_L<20\%$, respectively. Because the derived MSF are less than 1.0, Youd and Noble do not recommend use of MSF for $P_L<32\%$ and $P_L<20\%$ for earthquakes with magnitudes greater than 7.0. Equations for defining the Youd and Noble MSF are listed below:

Probability, $P_L < 20\%$	$MSF = 10^{3.81}/M^{4.53}$	For $M < 7$	(28)
Probability, $P_L < 32\%$	$MSF = 10^{3.74}/M^{4.33}$	For $M < 7$	(29)
Probability, $P_L < 50\%$	$MSF = 10^{4.21}/M^{4.81}$	For $M < 7.75$	(30)

Recommendations for Engineering Practice

The workshop participants reviewed the MSF listed in Table 3 and all but one (S.S.C. Liao) agree that the original factors were too conservative and that an increase is warranted for engineering practice for magnitudes less than 7.5. Rather than recommending a single set of factors, the workshop participants suggest a range of MSF with the engineer allowed to choose factors from within that range requisite with the conservatism required for the given application. For magnitudes less than 7.5, the lower bound for the recommended range is the revised set of magnitude scaling factors proposed by Idriss (Column 3, Table 3, or Equation 23). The upper bound for the suggested range is the MSF proposed by Andrus and Stokoe (Column 7, Table 3, or Equation 26). The upper bound values are consistent with MSF suggested by Ambraseys, Arango, and Youd and Noble for P_L<20% (generally within about 10 percent).

For magnitudes greater than 7.5, the factors recommended by Idriss (Column 3, Table 3; Equation 25) should be used for engineering practice. Above magnitude 7.5, these factors are smaller than the original Seed and Idriss (1982) factors, and hence application of the new factors leads to increased calculated liquefaction hazard compared to the original factors. The reasoning for this recommendation is that the original factors by Seed and Idriss (1982) may not have been sufficiently conservative for magnitudes greater than 7.5. There are insufficient case history data for earthquakes with magnitudes greater than 8 to support use of the lower MSF values listed in Table 3. These lower values were generally extrapolated from smaller magnitude earthquakes. Thus, these more conservative MSF are not recommended for engineering practice.

Corrections for High Overburden Pressures, Static Shear Stresses, and Age of Deposit

The correction factors K_σ and K_α were developed by Seed (1983) to adjust cyclic resistance ratios (CRR) to static overburden and shear stresses larger than those embodied in the development of the simplified procedure. As noted, the simplified procedure is only valid for level to gently sloping sites (low static shear stress) and depths less than about 15 m (low overburden pressures). The K_σ correction factor extends cyclic ratios to high overburden pressures, while the K_α correction factor allows extension of the simplified procedure to more steeply sloping ground conditions. Because there are virtually no case histories available to help define these correction factors, the results from laboratory test programs have been used to develop corrections for engineering practice.

K_σ Correction Factor

Cyclically loaded, isotropically consolidated triaxial compression tests show that while liquefaction resistance of a soil increases with increasing confining pressure, the resistance, as measured by the cyclic stress ratio, is a nonlinear function that decreases with increased normal stress. To incorporate the nonlinear effect of decreasing cyclic stress ratio with increasing confining pressure, Seed (1983) recommended incorporation of a correction factor, K_σ, for overburden pressures greater than 100 kPa. This factor allows correction of results obtained from the simplified procedure to overburden pressures that are greater than those generally extant in the observational data base from which the procedure was derived. Because of the lack of case history data, extrapolation of the simplified

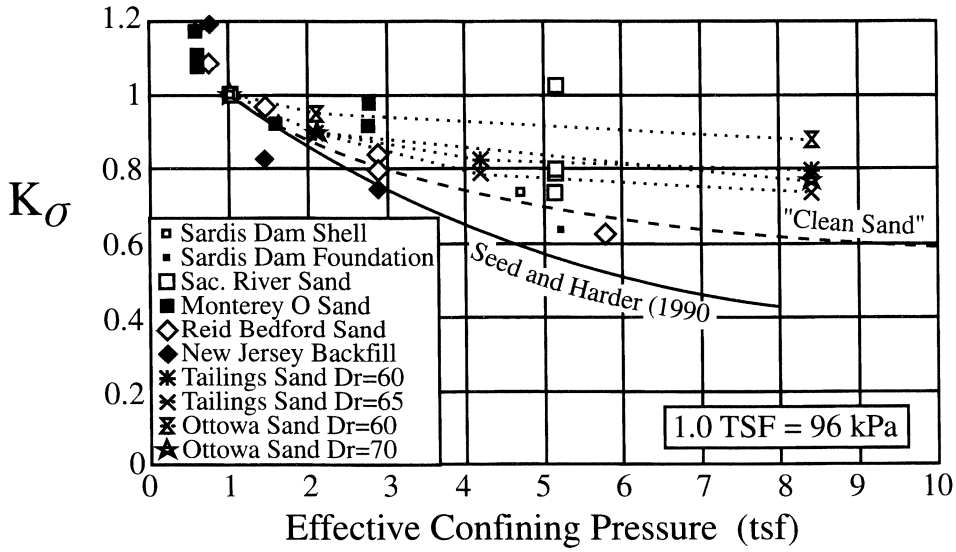

Figure 13 K_σ values determined by various investigators (After Seed and Harder, 1990)

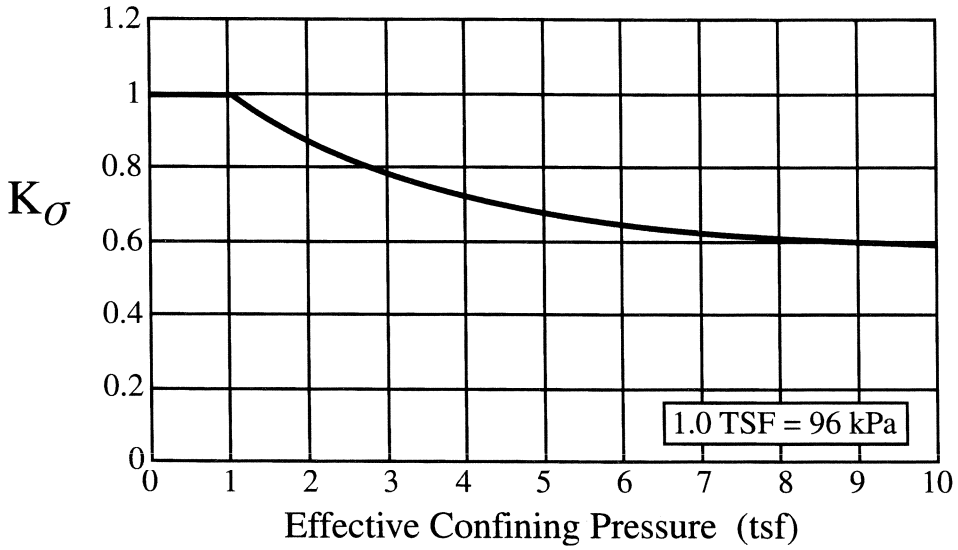

Figure 14. Minimum Values for K_σ Recommended for Clean and Silty Sands and Gravels (After Harder and Boulanger, this report)

procedure to depths greater than 15 m using K_σ factors yields results, such as factors of safety, that are less certain than at shallower depths.

The K_σ values developed by Seed (1983) were obtained by normalizing cyclic resistance ratios of isotropically consolidated cyclic triaxial compression tests to CRR values associated with an effective confining pressure of 100 kPa. For confining pressures greater than 100 kPa, the K_σ correction factor is less than one and decreases with increasing pressure. The original analyses by Seed (1983) yielded a band of suggested K_σ factors that decreased approximately linearly with effective overburden pressure from a value of 1.0 at 100 kPa to values ranging from about 0.40 to 0.65 at 800 kPa (Figure 13). Seed and Harder (1990) analyzed additional data and suggested

generally lower values that are defined by a single concave curve with a K_σ value of 0.44 at an effective confining pressure of 800 kPa. Vaid et al. (1985) and Vaid and Thomas (1994) performed constant-volume cyclic simple shear tests on clean sands and derived smaller decreases in K_σ. From tests on mine-tailing, Ottawa, and Frazer Delta sands (Figure 13), several investigators (Byrne and Harder, 1991; Pillai and Byrne, 1994; Arango, 1996) calculated values for K_σ ranging from about 0.75 to 0.90 for effective overburden pressures of 1,000 kPa to minimal values of 0.67 for effective overburden pressures as great as 2,600 kPa. These analyses indicate that lower relative densities generally produced higher K_σ values. The various analyses confirm the considerable variability in derived K_σ values, and that the factors developed by Seed and Harder were overly conservative.

Based on the above discussion and a review of test results presented by Harder and Boulanger (this report), the workshop participants gained consensus that the Seed and Harder K_σ values were too conservative and that an increase is recommended for general engineering practice. Based on this review, the workshop recommended K_σ values represented by the curve in Figure 14 as minimal values for engineering practice for both clean and silty sands and for gravels.

K_α Correction Factor for Sloping Ground

Sloping ground induces static shear within the body of a soil mass before the onset of earthquake shaking. The relative magnitude of the static shear, τ_{st}, on the horizontal plane can be assessed by normalizing it with respect to the effective vertical stress, σ'_{vo}. The resulting parameter is called the alpha ratio, where $\alpha = \tau_{st}/\sigma'_{vo}$. For level ground conditions, the alpha ratio is zero. Early researchers suggested that the presence of a static shear stress always improved the cyclic resistance of a soil because higher cyclic shear stresses were required to cause stress reversal. This conclusion is true for dense soils under relatively low confining pressures. However, loose soils and some soils under high confining pressures have lower liquefaction resistance under the influence of initial static shear stresses than in the absence of these stresses. This behavior is due to the potential strain softening nature of very loose soils.

To incorporate the effect of static shear stresses on liquefaction resistance of soils, Seed (1983) recommended use of a correction factor, K_α. This factor is used to correct results obtained from the simplified procedure for level ground to sloping ground sites with constant static shear stress.

For the workshop, Harder and Boulanger (this report) reviewed past publications, tests, and analyses relative to K_α. They concluded that the wide ranges in potential K_α values developed by past investigators indicate a lack of consensus and a need for continued research and field verification of the effects of static shear stress on liquefaction resistance. Different rates of pore pressure generation and different limiting values for excess pore pressure at different locations within a slope make liquefaction analyses for sloping ground conditions an extremely complicated endeavor.

The workshop participants agreed that the evaluation of liquefaction resistance beneath sloping ground or embankments (slopes greater than about six percent) is not well understood and that such evaluations are beyond routine application of the simplified procedure. Although curves relating K_α to α have been published (Harder and Boulanger, this report), the participants concluded that general recommendations for use of K_α by the engineering profession is not advisable at this time.

Influence of Age of Deposit

Several investigators have shown that liquefaction resistance of soils increases with age. For example, Seed (1979) observed significant increases in liquefaction resistance with age of reconstituted sand specimens tested in the laboratory. Cyclically loaded tests were conducted on freshly reconstituted sand specimens and on similar sand specimens at periods ranging up to one hundred days. Increases of as much as 25 percent in cyclic resistance ratio were noted between the freshly constituted and the 100-day-old specimens. Youd and Hoose (1977) and Youd and Perkins (1978) note that liquefaction resistance increases markedly with geologic age. Sediments deposited within the past few hundred years are generally much more susceptible to liquefaction than older Holocene sediments; Pleistocene sediments are even more resistant; and Pre-Pleistocene sediments are essentially insusceptible to liquefaction. Although qualitative increases in liquefaction resistance have been well documented, insufficient quantitative data have been assembled from which correction factors for age can be defined.

The age, and concomitantly the liquefaction resistance, of naturally sedimented deposits generally increases with depth. In natural soils, this increase may partially or wholly counteract the influence of the K_σ factor which generates an apparent decrease in liquefaction resistance with depth. In the absence of quantitative correction factors for age, engineering judgement is required in assessing liquefaction resistance of sediments older than a few hundred years. In some instances where deeper sediments have been dated as more than a few thousand years old, knowledgeable engineers have ignored the K_σ factor as partial compensation for unquantifiable, but known increases in liquefaction resistance with age. For man-made structures, such as thick fills and embankment dams, ageing effects are generally minimal and should be ignored in calculating liquefaction resistance.

Seismic Factors

Application of the simplified procedure for evaluating liquefaction resistance requires estimates of earthquake magnitude and peak horizontal ground acceleration. In the procedure, these factors characterize duration and intensity of ground shaking, respectively. The workshop addressed the following questions with respect to selection of magnitude and peak acceleration.

Earthquake Magnitude

Records from past earthquakes indicate that the relationship between duration and magnitude is rather uncertain and that factors other than magnitude influence duration. For example, unilateral faulting, in which rupture begins at one end of the fault and propagates to the other, usually produces longer shaking duration for a given magnitude than bilateral faulting, in which slip begins near the midpoint on the fault and propagates in both directions. Duration also generally increases with distance from the seismic energy source and may vary with site conditions and with bedrock topography (basin effects). The workshop addressed the following questions with respect to the use of magnitude as an index for shaking duration, and developed the following consensus answers.

Question: Should correlations or correction factors be developed to adjust duration of shaking to account for the influence of earthquake source mechanism and other factors?

Answer: Faulting characteristics and variations in shaking duration are difficult to predict in advance of an earthquake event. The influence of distance is generally of secondary importance within the range of distances to which potentially damaging effects of liquefaction commonly develop. Basin effects are not yet sufficiently predictable to be adequately accounted for in engineering practice. Thus workshop participants recommend continued use of conservative relationship between magnitude and duration embodied in the simplified procedure for routine evaluation of liquefaction resistance.

Question: An important difference between eastern US earthquakes and western US earthquakes is that eastern ground motions are generally richer in high frequency energy and thus could generate more significant stress cycles and equivalently longer durations than western earthquakes of the same magnitude. Should a correction be made to account for higher frequencies of ground motions generated by eastern US earthquakes?

Answer: The high-frequency motions of eastern earthquakes are generally limited to rock sites. High-frequency motions attenuate or are damped out rather quickly as they propagate through soil layers. This filtering action reduces the high-frequency energy at soil sites and should reduce differences in numbers of significant loading cycles between eastern and western earthquakes. Because liquefaction occurs only within soil strata, duration differences on soil sites between eastern and western earthquakes are not likely to be great. Without more instrumentally recorded data from which differences in ground motion characteristics can be quantified, there is little basis for the development of additional correction factors for eastern localities.

Another difference between eastern and western US earthquakes is that strong ground motions generally propagate to greater distances in the east than in the west. By applying present state-of-the-art procedures for estimating peak ground acceleration at eastern sites, differences in ground motion propagation between western and eastern earthquakes are properly accounted for.

Question: Which magnitude scale should be used by engineers in selecting a magnitude for use in liquefaction resistance analyses?

Answer: Seismologists commonly calculate earthquake magnitudes using five different scales: (1) local or Richter magnitude, M_L; (2) surface-wave magnitude, M_s; (3) short-period body-wave magnitude, m_b; (4) long-period body-wave magnitude, m_B; and (5) moment magnitude, M_w. Moment magnitude is the scale most commonly used for engineering applications and is the scale preferred for calculation of liquefaction resistance. As shown on Figure 15, magnitudes from other scales may be substituted directly for M_w within the following limits: $M_L < 6$, $m_B < 7.5$, and $6 < M_s < 8$. m_b, a scale commonly applied in the eastern US, may be used for magnitudes between 5 and 6, provided such magnitudes are corrected to M_w using the curves plotted in Figure 15 (Idriss, 1985).

Peak Acceleration

In the simplified procedure, peak horizontal acceleration (a_{max}) is used to characterize the intensity of ground shaking. To provide guidance for estimation of a_{max}, the workshop addressed the following questions.

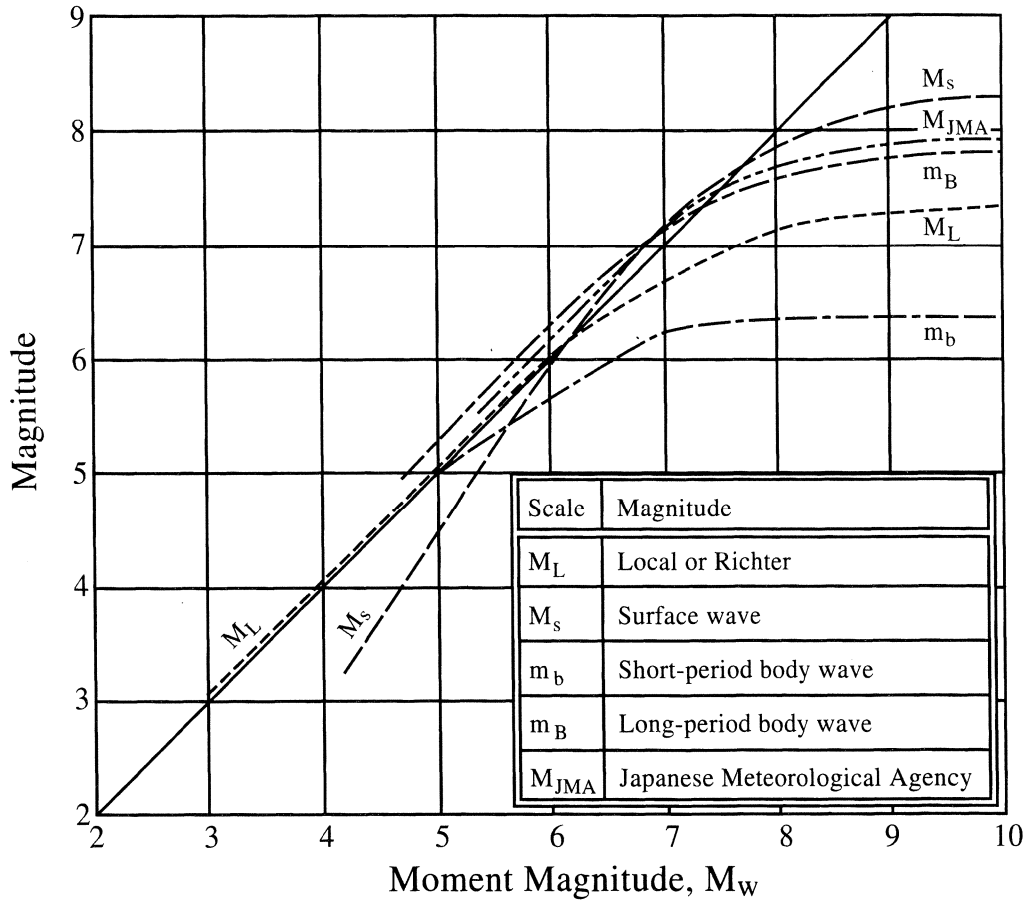

Figure 15 Relationship between Moment, M_w, and Other Magnitude Scales (After Heaton et al., 1982)

Question: What procedures are preferred for estimating a_{max} at potentially liquefiable sites?

Answer: The following three methods, in order of preference, may be used for estimating a_{max}:

(1) The preferred method for estimating a_{max} at a site is through application of empirical correlations for attenuation of a_{max} as a function of earthquake magnitude, distance from the seismic energy source, and local site conditions. Several correlations have been developed for estimating a_{max} for sites on bedrock or stiff to moderately stiff soils. Preliminary attenuation relationships have also been developed for soft soil sites (Idriss, 1991). Selection of an attenuation relationship should be based on factors such as region of the country, type of faulting, site condition, etc.

(2) For soft sites and other soil profiles that are not compatible with available attenuation relationships, a_{max} may be estimated from local site response analyses. Computer programs such as SHAKE, DESRA, etc., may be used for these calculations. Input ground motions

in the form of recorded accelerograms are preferable to synthetic records. Accelerograms derived from white noise should be avoided. A suite of plausible earthquake records should be used in the analysis, including as many records as feasible from earthquakes with similar magnitudes, source distances, etc.

(3) The third and least desirable method for estimating peak ground acceleration is through amplification ratios, such as those developed by Idriss (1990; 1991), Seed et al.(1994), and BSSC (1994). These factors use a multiplier or ratio by which bedrock outcrop motions are amplified to estimate motions at ground surface. Because amplification ratios are influenced by strain level, earthquake magnitude, and perhaps frequency content, caution and considerable engineering judgment are required in the application of these relationships.

Question: Which peak acceleration should be used? (a) the largest horizontal acceleration recorded on a three-component accelerogram; (b) the geometric mean (square root of the product) of the two maximum horizontal components; or (c) a vectorial combination of horizontal accelerations.

Answer: According to I.M. Idriss (oral communication at workshop), where recorded motions were available, the larger of the two horizontal peak components of acceleration were used in the original development of the simplified procedure. Where recorded values were not available, which was the circumstance for most sites in the data base, peak acceleration values were estimated from attenuation relationships based on the geometric mean of the two orthogonal peak horizontal accelerations. In nearly all instances where recorded motions were used, the peaks from the two horizontal records were approximately equal. Thus where a single peak was used that peak and the geometric mean of the two peaks were about the same value. Based on this information, the workshop participants concurred that use of the geometric mean is more consistent with the derivation of the procedure and is preferred for use in engineering practice. However, use of the larger of the two orthogonal peak accelerations would be conservative and is allowable. Vectorial accelerations are seldom calculated and should not be used. Peak vertical accelerations are ignored for calculation of liquefaction resistance.

Question: Liquefaction usually develops at soil sites where ground motion amplification may occur and where sediments may soften as excess pore pressures develop. How should investigators account for these factors in estimating peak acceleration?

Answer: The procedure recommended by the workshop is to calculate or estimate a peak acceleration that incorporates the influence of site amplification, but neglects the influence of excess pore-water pressure. Simply stated, the peak acceleration to be used in liquefaction resistance evaluations is the peak horizontal acceleration that would have occurred at ground surface at the site in the absence of increased pore-water pressure or the occurrence of liquefaction.

Question: Should high-frequency spikes (periods less than 0.1 sec) in acceleration records be considered or ignored?

Answer: In general, short-duration, high-frequency acceleration spikes should be ignored for liquefaction resistance evaluations. By using attenuation relationships for estimation of peak

acceleration, as noted above, high frequency spikes are essentially ignored because few high-frequency peaks are incorporated in data bases from which attenuation relationships have been derived. Similarly, ground response analyses programs such as SHAKE and DESRA generally attenuate or filter out high-frequency spikes, reducing their influence. Where amplification ratios are used engineering judgment should be used to determine which bedrock accelerations should be amplified.

Energy-Based Criteria and Probabilistic Analyses

The workshop considered two additional topics: liquefaction resistance criteria based on seismic energy passing through a liquefiable layer (Youd et al., this report) and probabilistic analyses of case history data (Youd and Noble, Statistical and Probabilistic Analyses, this report). Although risk analyses for several localities and facilities have been made using probabilistic criteria, the workshop attendees agreed that probabilistic procedures are still outside the mainstream of standard practice. Similarly, energy-based criteria need further development before recommendations can be made for general practice. The workshop participants did agree that research and development should continue on both of these potentially useful procedures.

Conclusions

The participants in the NCEER workshop reviewed the state-of-the-art for evaluation of liquefaction resistance and proposed several augmentations to that procedure that have been developed over the past ten years. Specific conclusions, including recommended procedures and equations, are listed within each section of this summary paper. General consensus recommendations from the workshop are as follows:

1. Four field tests are recommended for general use in evaluating liquefaction resistance--the cone penetration test (CPT), the standard penetration test (SPT), measurement of shear-wave velocity (V_s), and for gravelly sites, the Becker penetration test (BPT). The workshop reviewed and revised criteria for each test to incorporate recent developments and to maximize compatibilities between liquefaction resistances determined via the various tests. Each field test has its advantages and limitations. The CPT provides the most detailed soil stratigraphy and provides a preliminary estimate of liquefaction resistance. The SPT has been used more widely and provides disturbed soil samples from which fines content and other grain characteristics can be determined. V_s measurements provide fundamental information for evaluation of small-strain constitutive relations and can be applied at gravelly sites where CPT and SPT may not be reliable. The BPT test has been used primarily at gravelly sites and requires use of rough correlations between BPT and SPT. In many instances, two or more test procedures should be applied to assure that both adequate definition of soil stratigraphy and a consistent evaluation of liquefaction resistance is attained.

2. The magnitude scaling factors originally derived by Seed and Idriss (1982) have proven to be very conservative for earthquake magnitudes less than 7.5. The consensus of the workshop was that a range of scaling factors should be recommended for engineering

practice, with the lower end of the range being the revised MSF recommended by Idriss (Column 3, Table 3), and the upper end of the range being the MSF suggested by Andrus and Stokoe (Column 7, Table 3). These MSF are defined by Equations 25 and 26, respectively. For magnitudes greater than 7.5, the revised factors by Idriss (Column 3, Table 3) should be used. The latter factors are significantly more conservative than the original Seed and Idriss (1982) factors, but the consensus was that these more conservative factors should be applied.

3. The K_σ factors suggested by Seed and Harder (1990) are too conservative for recommended use in general engineering practice. The workshop participants recommend the K_σ values represented by the curve in Figure 14 as minimal values for engineering practice for clean and silty sands and for gravels.

4. The workshop participants agreed that the evaluation of liquefaction resistance beneath sloping ground or embankments (slopes greater than about six percent) is not well understood at this time and that such evaluations are beyond the applicability of the simplified procedure. Special expertise is required for evaluation of liquefaction resistance beneath sloping ground.

5. Moment magnitude, M_w, should be used as an estimate of earthquake size for liquefaction resistance calculations. No general corrections are recommended to adjust earthquake magnitude to account for differences in duration due to source mechanism or geographic region (eastern versus western US earthquakes).

6. The peak acceleration, a_{max}, recommended for calculation of cyclic stress ratio, CSR, is the a_{max} that would have occurred at the site in the absence of pore pressure increases or liquefaction generated by the earthquake. Application of attenuation relationships compatible with conditions at a given site is the preferred procedure for estimating a_{max}. Where site conditions are incompatible with existing attenuation relationships, site-specific response calculations, using programs such as SHAKE or DESRA, should be used. The least preferable technique is application of amplification factors.

References

Andrus, R.D., 1994, "In Situ Characterization of Gravelly Soils That Liquefied in the 1983 Borah Peak Earthquake," Ph.D. Dissertation, University of Texas at Austin, p. 533.

Ambraseys, N.N., 1988, "Engineering Seismology," *Earthquake Engineering and Structural Dynamics*, Vol. 17, p. 1-105.

Arango, I., 1996, "Magnitude Scaling Factors for Soil Liquefaction Evaluations," *Journal of Geotechnical Engineering*, ASCE, Vol. 122, No. 11, p. 929-936.

BSSC, 1994, *NEHRP Recommended Provisions for Seismic Regulations for New Buildings, Part 2--Commentary*, Federal Emergency Management Agency, 1994 Edition, Building Seismic Safety Council, Washington, D.C., 335 p.

Byrne, P.M. and Harder, L.F., jr., 1991, "Terzaghi Dam, Review of Deficiency Investigation, Report No. 3," prepared for B C Hydro, Vancouver, British Columbia.

Harder, L.F., Jr., and Seed, H.B., 1986, "Determination of Penetration Resistance for Coarse-Grained Soils using the Becker Hammer Drill," Earthquake Engineering Research Center, Report No. UCB/EERC-86/06, University of California, Berkeley.

Heaton, T.H., Tajima, F., and Mori, A.W., 1982, "Estimating Ground Motions Using Recorded Accelerograms," unpublished report by Dames and Moore to Exxon Production Res. Co., Houston, Texas.

Idriss, I.M., 1985, "Evaluating Seismic Risk in Engineering Practice," *Proceedings*, 11th Int. Conf. on Solid Mechanics and Foundation Engineering, San Francisco, Vol. 1, p. 255-320.

Idriss, I.M., 1990, "Response of Soft Soil Sites During Earthquakes," *Proceedings*, H. Bolton Seed Memorial Symposium, Vol. 2, BiTech Publishers, Ltd, Vancouver, B.C. Canada, p. 273-290.

Idriss, I.M., 1991, "Earthquake Ground Motions at Soft Soil Sites," *Proceedings*, 2nd Int. Conf. on Recent Advances in Geotechnical Earthquake Engineering and Soil Dynamics, Vol. 3, p. 2265-2271.

Kayen, R.E., Mitchell, J.K., Seed, R.B., Lodge, A., Nishio, S., and Coutinho, R., 1992, "Evaluation of SPT-, CPT-, and Shear Wave-Based Methods for Liquefaction Potential Assessment Using Loma Prieta Data," *Proceedings*, 4th Japan-US Workshop on Earthquake Resistant Design of Lifeline Facilities and Countermeasures for Soil Liquefaction, Honolulu, Hawaii, NCEER, Buffalo, NY, Technical Report NCEER-92-0019, Vol. 1, p. 177-204.

Kramer, S.L., 1996, *Geotechnical Earthquake Engineering*, Prentice Hall, Upper Saddle River, NJ, 653 p.

Liao, S.S.C. and Whitman, R. V., 1986a, "Overburden Correction Factors for SPT in Sand," *Journal of Geotechnical Engineering*, Vol. 112, No. 3, p. 373-377.

Liao, S.S.C., and Whitman, R.V., 1986b, *Catalogue of A Liquefaction and Non-Liquefaction Occurrences During Earthquakes*, Research Report, Dept. Of Civil Engineering, M.I.T., Cambridge, MA.

Liao, S.S.C., Veneziano, D., and Whitman, R.V., 1988, "Regression Models for Evaluating Liquefaction Probability," *Journ. of Geotechnical Engineering*, Vol. 114, No. 4, p. 389-411.

Lodge, A.L., 1994, "Shear Wave Velocity Measurements for Subsurface Characterization," Ph.D. Dissertation, University of California at Berkeley.

National Research Council (NRC), 1985, *Liquefaction of Soils During Earthquakes*, National Academy Press, Washington, D.C.

Robertson, P.K., and Campanella, R.G., 1985, "Liquefaction Potential of Sands Using the Cone Penetration Test," *Journal of the Geotechnical Division*, ASCE, Vol. 111, No. 3, p. 298-307.

Robertson, P.K., 1990, Soil Classification Using CPT, *Canadian Geotechnical Journal*, Vol 27, No. 1, p. 151-158.

Robertson P.K., and Fear, C.E., 1995, "Liquefaction of Sands and Its Evaluation," *Proceedings*, 1st Int. Conf. on Earthquake Geotechnical Engineering, Keynote Lecture, Tokyo, Japan.

Robertson, P.K., Woeler, D.J., and Finn, W.D.L, 1992, "Seismic Cone Penetration Test for Evaluating Liquefaction Potential Under Cyclic Loading," *Canadian Geotechnical Journal*, Vol. 29, p. 686-695.

Seed, H.B., 1979, "Soil Liquefaction and Cyclic Mobility Evaluation for Level Ground During Earthquakes," *Journal of Geotechnical Engineering*, ASCE, Vol. 105, No. GT2, p. 201-255.

Seed, H.B., 1983, "Earthquake Resistant Design of Earth Dams," *Symposium on Seismic Design of Earth Dams and Caverns*, ASCE, New York, p. 41-64.

Seed, H.B., and Idriss, I.M., 1971, "Simplified Procedure for Evaluating Soil Liquefaction Potential," *Journal of the Soil Mechanics and Foundations Division*, ASCE, Vol. 97, No. SM9, p. 1249-1273.

Seed, H.B., and Idriss, I.M., 1982, "Ground Motions and Soil Liquefaction During Earthquakes," Earthquake Engineering Research Institute Monograph.

Seed, H.B., Tokimatsu, K., and Harder, L.F., Jr., 1984, "The Influence of SPT Procedures in Evaluating Soil Liquefaction Resistance," *Report, UCB/EERC-84-15,* University of California at Berkeley, Berkeley, California.

Seed, H.B., Tokimatsu, K., Harder, L.F., and Chung, R.M., 1985, "The Influence of SPT Procedures in Soil Liquefaction Resistance Evaluations," *Journal of Geotechnical Engineering*, ASCE, Vol. 111, No. 12, p. 1425-1445.

Seed, R.B., Dickenson, S.E., Rau, G.A., White, R.K., and Mok, C.M., 1994, "Site Effects on Strong Shaking and Seismic Risk: Recent Developments and Their Impact on Seismic Design Codes and Practice," *Proceedings*, Structural Congress II, ASCE, Vol. 1, p. 573-578.

Seed, R.B., and Harder, L.F., Jr., 1990, "SPT-Based Analysis of Cyclic Pore Pressure Generation and Undrained Residual Strength,"*Proceedings*, H. Bolton Seed Memorial Symposium, May, 1990. BiTech Publishers, Ltd., p. 351-376.

Skempton, A.K., 1986, "Standard Penetration Test Procedures and the Effects in Sands of Overburden Pressure, Relative Density, Particle Size, Aging and Overconsolidation," *Geotechnique*, Vol 36, No. 3, p. 425-447.

Stark, T.D. and Olson, S.M., 1995, "Liquefaction Resistance Using CPT and Field Case Histories," *Journal of Geotechnical Engineering*, ASCE, Vol 121, No. 12, p. 856-869.

Stokoe, K.H., II, Roesset, J.M., Bierschwale, J.G., and Aoouad, M., 1988, "Liquefaction Potential of Sands From Shear Wave Velocity," *Proceedings*, 9th World Conf. on Earthquake Engineering, Tokyo, Japan, Vol III, p. 213-218.

Suzuki, Y., Tokimatsu, K., Koyamada, K., Taya, Y., and Kubota, Y., 1995, "Field Correlation of Soil Liquefaction Based on CPT Data," *Proceedings* of the International Symposium on Cone Penetration Testing, CPT'95, Linkoping, Sweden, Vol. 2, p. 583-588.

Sy, A. and Campanella, R.G., 1994, "Becker and Standard Penetration Tests (BPT-SPT) Correlations with Consideration of Casing Friction," *Canadian Geotechnical Journal*, Vol. 31, p. 343-356.

Sy, A., Campanella, R.G., and Stewart, R.A., 1995, "BPT-SPT Correlations for Evaluation of Liquefaction Resistance in Gravelly Soils," *Proceedings* of Specialty Session on Dynamic Properties of Gravelly Soil, ASCE Annual Convention, San Diego, California,

Tokimatsu, K., Kuwayama, S., and Tamura, S., 1991, "Liquefaction Potential Evaluation Based on Rayleigh Wave Investigation and Its Comparison with Field Behavior," *Proceedings*, 2nd Int. Conf. on Recent Advances in Geotechnical Earthquake Engineering and Soil Dynamics, held in St. Louis, Missouri, S. Prakash, Ed., University of Missouri-Rolla, Vol. 1, p. 357-364.

Vaid, Y.P., Chern, Jing C., and Tumi, Hadi, 1985, "Confining Pressure, Grain Angularity, and Liquefaction," *Journal of Geotechnical Engineering*, ASCE, Vol. 111, No. 10, October.

Vaid, Y.P., and Thomas, J., 1994, "Post Liquefaction Behaviour of Sand," *Proceedings* of the 13th Int. Conf. on Soil Mechanics and foundation Engineering, New Delhi, India.

Vreugdenhil, R., Davis, R. and Berrill, J., 1994, "Interpretation of Cone Penetration Results in Multilayered Soils," *Int. Journal for Numerical Methods in Geomechanics*, Vol. 18, p. 585-599.

Youd, T.L., 1993, *Liquefaction-Induced Lateral Spread Displacement*, US Navy, NCEL Technical Note N-1862, 44p.

Youd, T.L., and Hoose, S.N., 1977, "Liquefaction Susceptibility and Geologic Setting," Proceedings, 6th World Conference on Earthquake Engineering, Prentice-Hall, Inc., Vol 3, pp. 2189-2194.

Youd, T.L., and Perkins, D.M., 1978, "Mapping of Liquefaction-Induced Ground Failure Potential," Journal of the Geotechnical Engineering Division, ASCE, Vol. 104, No. GT4, pp. 433-446.

Cyclic Liquefaction and its Evaluation based on the SPT and CPT

P.K. Robertson and C.E. (Fear) Wride

Geotechnical Group, University of Alberta
Edmonton, Alberta, Canada

Abstract

Soil liquefaction is a major concern for structures constructed with or on sandy soils. This paper describes the phenomena of soil liquefaction, provides suitable definitions, and provides an update on methods to evaluate cyclic liquefaction using primarily the Standard Penetration Test and the Cone Penetration Test (CPT). A new method is described to estimate grain characteristics directly from the CPT and to incorporate this into one of the methods for evaluating resistance to cyclic loading. A method is also described for correcting the results of the CPT in thin layers. A worked example is also provided. This paper is the final submission from the authors to the proceedings of the 1996 NCEER workshop on soil liquefaction; a similar version has been submitted for review to the Canadian Geotechnical Journal.

Introduction

Soil liquefaction is a major concern for structures constructed with or on saturated sandy soils. The phenomenon of soil liquefaction has been recognized for many years. Terzaghi and Peck (1948) referred to 'spontaneous liquefaction' to describe the sudden loss of strength of very loose sands that caused flow slides due to a slight disturbance. Mogami and Kubo (1953) also used the term liquefaction to describe a similar phenomenon observed during earthquakes. The Niigata earthquake in 1964 is certainly the event that focused world attention on the phenomenon of soil liquefaction. Since 1964, much work has been carried out to explain and understand soil liquefaction. The progress of work on soil liquefaction has been described in detail in a series of state-of-the-art papers, such as Yoshimi et al. (1977), Seed (1979), Finn (1981), Ishihara (1993), and Robertson and Fear (1995). The major earthquakes of Niigata in 1964 and Kobe in 1995 have illustrated the significance and extent of damage caused by soil liquefaction. Liquefaction was the cause of much of the damage to the port facilities in Kobe in 1995. Soil liquefaction is also a major design problem for large sand structures, such as mine tailings impoundments and earth dams.

The state-of-the-art paper by Robertson and Fear (1995) provided a detailed description of soil liquefaction and its evaluation. In January 1996, the National Center for Earthquake Engineering (NCEER) in the U.S.A. arranged a workshop (chaired by T.L. Youd) in Salt Lake City, Utah, to discuss recent advances in the evaluation of cyclic liquefaction. This paper is the authors' final presentation to the proceedings of that workshop; a similar version has been submitted for review to the Canadian Geotechnical Journal. The objective of this paper is to provide an update on the evaluation of cyclic liquefaction using primarily the Standard Penetration Test (SPT) and the Cone Penetration Test (CPT). Several phenomena are described as soil liquefaction. In an effort to clarify the different phenomena, the mechanisms will be described and a set of definitions for soil liquefaction will be presented. Recent advances in the evaluation of cyclic liquefaction using laboratory testing are also briefly described.

Liquefaction definitions

Before describing methods to evaluate liquefaction potential, it is important to first define the terms used to explain the phenomena of soil liquefaction. Figure 1 shows the results from undrained triaxial compression tests on Toyoura sand presented by Ishihara (1993). These results present a clear picture of sand behaviour in undrained shear, since they show results at the same void ratio, but at different effective confining stresses. The results are presented in the form of deviator stress, q, versus axial strain and stress paths in q versus mean normal effective stress, p'. Very loose sand (density index = 16%), shows a marked strain softening response during undrained shear. The shear stress reaches a peak then strain softens, eventually reaching an ultimate condition referred to as critical or steady state. In this report, this ultimate condition will be referred to as 'ultimate state' (US), as recommended by Poorooshasb and Consoli (1991).

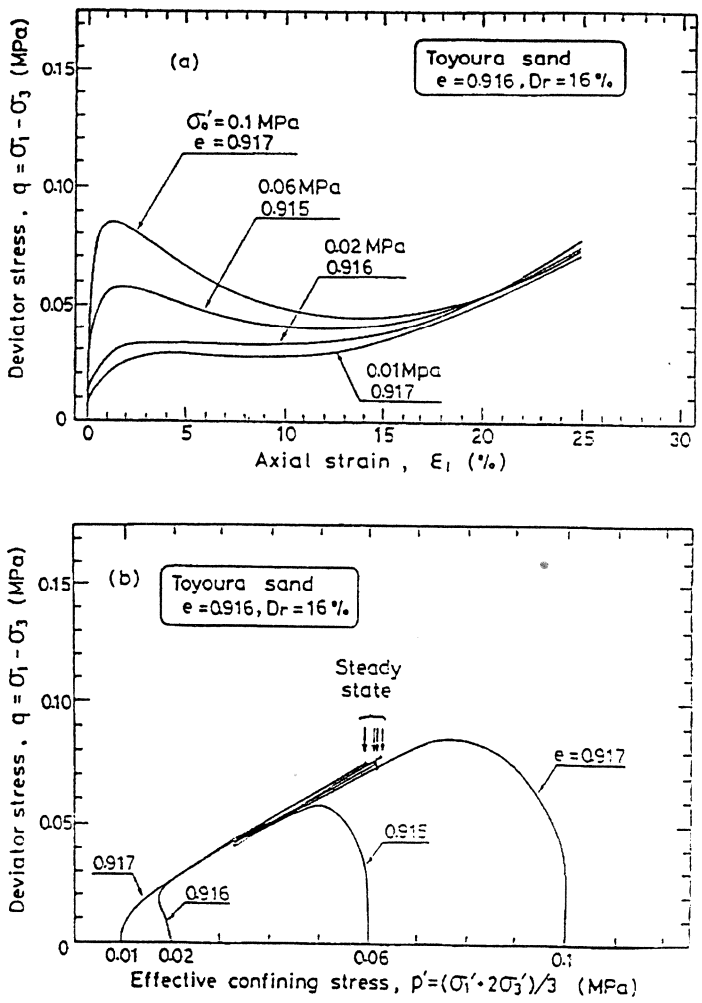

Figure 1 Undrained behaviour of Toyoura sand (after Ishihara, 1993).

The stress path during strain softening appears to follow a 'collapse surface', as suggested by Sladen et al. (1985). However, at a lower confining stress, sand at the same void ratio shows a strain hardening response before reaching ultimate state. For the same sand at a higher density, a similar behaviour is seen, except that the ultimate state condition is reached at a higher stress level (Ishihara, 1993). For dense sand, the response is predominately strain hardening since the ultimate state strength is very large. This confirms the basic behaviour suggested by Castro (1969) and that embodied in critical state soil mechanics (Roscoe et al., 1958). Been et al. (1991) showed that steady state and critical state are the same condition and in e-p' space are independent of the stress path followed to reach this ultimate state. The steady state or critical state represents an ultimate state that can be represented in e-p'-q space, where p' is the mean normal effective stress, q is the deviator stress and e is the void ratio.

Figure 2 shows a summary of the behaviour of a granular soil loaded in undrained triaxial compression. In e-p' space, a soil with an initial void ratio higher than the ultimate state line (USL) will strain soften (SS) at large strains, whereas a soil with an initial void ratio lower than

the USL will strain harden (SH) at large strains. It is possible to have a soil with an initial void ratio higher than but close to the USL. For this soil state, the response can show limited strain softening (LSS) to a quasi-steady state (QSS) (Ishihara, 1993), but eventually, at large strains, the response strain hardens to the ultimate state. For some sands, very large strains are required to reach the ultimate state, and in some cases, conventional triaxial equipment may not reach these large strains ($\varepsilon_a > 20\%$) (see Figure 1).

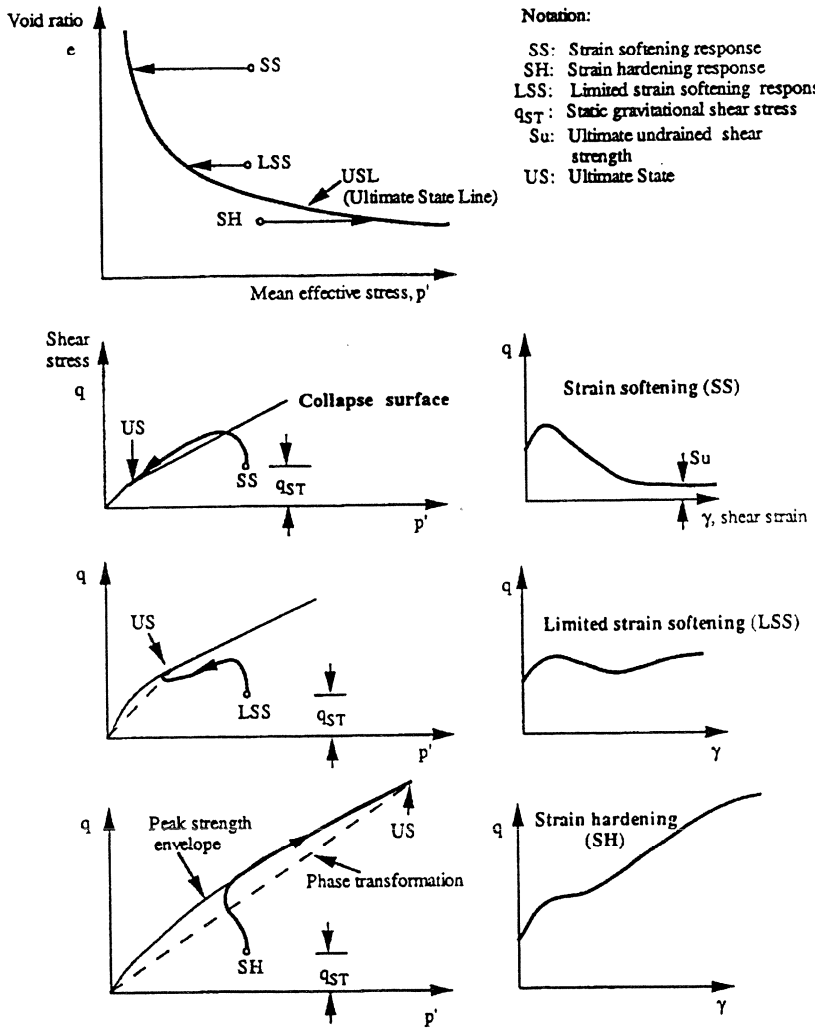

Figure 2 Schematic of undrained monotonic behaviour of sand in triaxial compression (after Robertson, 1994).

If a soil slope or structure, such as an earth dam or tailings dam, is composed entirely of a strain softening soil and the in-situ gravitational shear stresses are larger than the ultimate state strength (i.e. a relatively steep slope consisting of very loose sand), a catastrophic collapse and flow slide can occur if the soil is triggered to strain soften. Either cyclic or monotonic undrained loading can trigger the collapse. Sasitharan et al. (1994) have shown that certain types of drained monotonic loading (e.g. a slow rise in groundwater level) can trigger undrained collapse.

If a soil structure is composed entirely of strain hardening soil, undrained collapse can generally not occur unless the soil can become looser due to pore water redistribution. If a soil structure is composed of both strain softening (SS) and strain hardening (SH) zones and the SS soil is triggered to strain soften, a collapse and slide will occur only if, after stress redistribution due to softening of the SS soil, the SH soil cannot support the gravitational shear stresses. A flow slide will occur only if a kinematically admissible mechanism can develop. In general, a kinematically admissible mechanism cannot form under level ground conditions in the absence of driving loads. The trigger mechanism for a catastrophic flow slide can be cyclic, such as earthquake loading, or monotonic, such as a rise in groundwater level or a rapid undrained loading.

During cyclic undrained loading (e.g. earthquake loading), almost all saturated cohesionless soils develop positive pore pressures due to the contractive response of the soil at small strains. If there is shear stress reversal, the effective stress state can progress to the point of essentially zero effective stress (see Figure 3). For shear stress reversal to occur during earthquake loading, ground conditions must be generally level or gently sloping; however, shear stress reversal can occur in steeply sloping ground if the slope is of limited height (Pando and Robertson, 1995). When a soil element reaches the condition of essentially zero effective stress, the soil has very little stiffness and large deformations can occur during cyclic loading. However, when cyclic loading stops, the deformations essentially stop, except for those due to local pore pressure redistribution. If there is no shear stress reversal, such as in steeply sloping ground subjected to moderate cyclic loading, the stress state may not reach zero effective stress. As a result, only cyclic mobility with limited deformations will occur, provided that the initial void ratio of the sand is below the USL and the large strain response is dilative (i.e. the material is not susceptible to a catastrophic flow slide). However, shear stress reversal in the level ground area beyond the toe of a slope may lead to overall failure of the slope due to softening of the soil in the toe region.

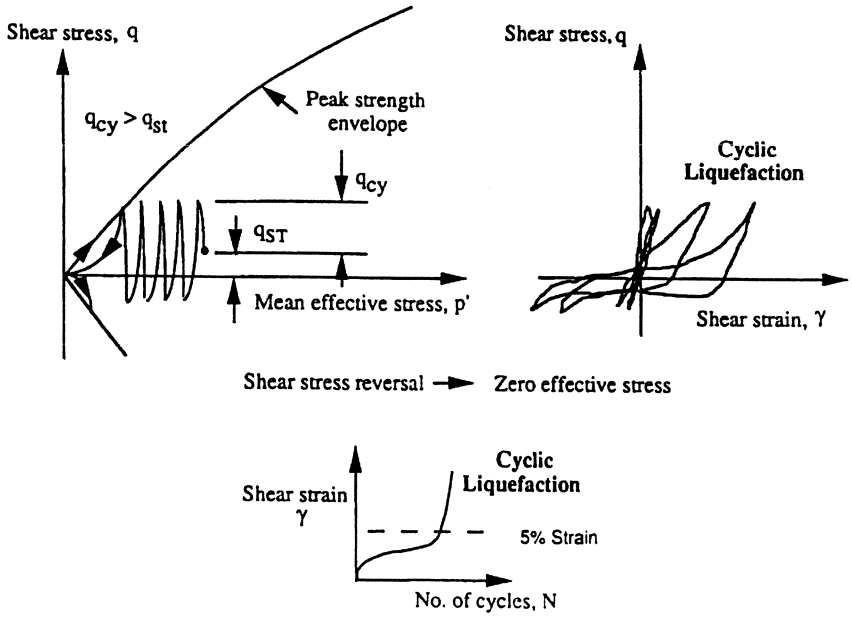

Figure 3 Schematic of undrained cyclic behaviour of sand illustrating cyclic liquefaction (after Robertson, 1994).

Based on the above descriptions of soil behaviour in undrained shear and following the work by Robertson (1994) and Robertson and Fear (1995), the following definitions are suggested:

Flow liquefaction

- Applies to strain softening soils only.
- Requires a strain softening response in undrained loading resulting in constant shear stress and effective stress, as illustrated in Figure 2.
- Requires in-situ shear stresses greater than the ultimate or minimum undrained shear strength.
- Either monotonic or cyclic loading can trigger flow liquefaction
- For failure of a soil structure to occur, such as a slope, a sufficient volume of material must strain soften. The resulting failure can be a slide or a flow depending on the material characteristics and ground geometry. The resulting movements are due to internal causes and can occur after the trigger mechanism occurs.
- Can occur in any metastable saturated soil, such as very loose granular deposits, very sensitive clays, and loess (silt) deposits.

Cyclic softening

- Applies to both strain softening and strain hardening soils.
- Two terms can be used: cyclic liquefaction and cyclic mobility.

Cyclic liquefaction

- Requires undrained cyclic loading during which shear stress reversal occurs or zero shear stress can develop (i.e. occurs when in-situ static shear stresses are low compared to cyclic shear stresses), as illustrated in Figure 3.
- Requires sufficient undrained cyclic loading to allow effective stresses to reach essentially zero.
- At the point of zero effective stress no shear stress exists. When shear stress is applied, pore pressure drops as the material tends to dilate, but a very soft initial stress strain response can develop resulting in large deformations.
- Deformations during cyclic loading can accumulate to large values, but generally stabilize when cyclic loading stops. The resulting movements are due to external causes and occur only during the cyclic loading.
- Can occur in almost all saturated sands provided that the cyclic loading is sufficiently large in magnitude and duration.
- Clayey soils can experience cyclic liquefaction but deformations are generally small due to the cohesive strength at zero effective stress. Rate effects (creep) often control deformations in cohesive soils.

Cyclic mobility

- Requires undrained cyclic loading during which shear stresses are always greater than zero; i.e. no shear stress reversal develops.

- Zero effective stress will not develop.
- Deformations during cyclic loading will stabilize, unless the soil is very loose and flow liquefaction is triggered. The resulting movements are due to external causes and occur only during the cyclic loading.
- Can occur in almost any saturated sand provided that the cyclic loading is sufficiently large in magnitude and duration, but no shear stress reversal occurs.
- Cohesive soils can experience cyclic mobility, but rate effects (creep) usually control deformations.

Note that strain softening soils can also experience cyclic softening (cyclic liquefaction or cyclic mobility) depending on the ground geometry.

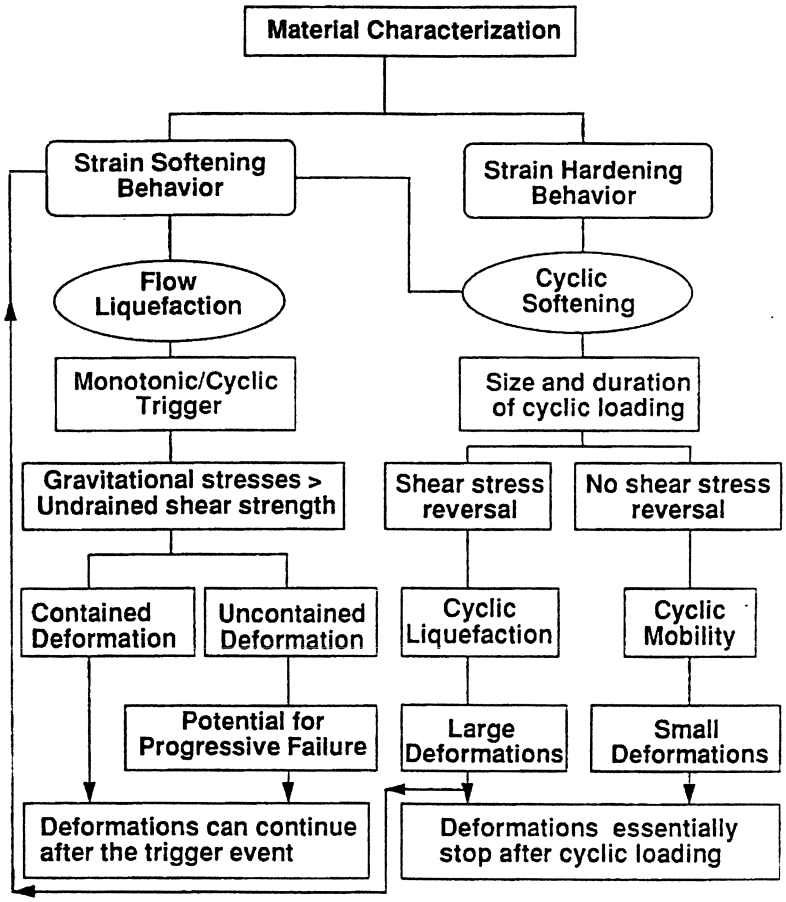

Figure 4 Suggested flow chart for evaluation of soil liquefaction (after Robertson, 1994).

Figure 4 presents a suggested flow chart (after Robertson, 1994) for the evaluation of liquefaction according to the above definitions. The first step is to evaluate the material characteristics in terms of a strain softening or strain hardening response. If the soil is strain softening, flow liquefaction is possible if the soil can be triggered to collapse and if the gravitational shear

stresses are larger than the ultimate or minimum strength. The trigger mechanism can be either monotonic or cyclic. Whether a slope or soil structure will fail and slide will depend on the amount of strain softening soil relative to strain hardening soil within the structure, the brittleness of the strain softening soil and the geometry of the ground. The resulting deformations of a soil structure with both strain softening and strain hardening soils will depend on many factors, such as distribution of soils, ground geometry, amount and type of trigger mechanism, brittleness of the strain softening soil and drainage conditions. Soils that are only temporarily strain-softening (i.e. experience a minimum strength before dilating to US) are not as dangerous as very loose soils that can strain-soften directly to ultimate state. Examples of flow liquefaction failures are Fort Peck Dam (Casagrande, 1965), Aberfan flowslide (Bishop, 1973), Zealand flowslide (Koppejan et al., 1948), and the Stava tailings dam. In general, flow liquefaction failures are not common; however, when they occur, they take place rapidly with little warning and are usually catastrophic. Hence, the design against flow liquefaction should be carried out cautiously.

If the soil is strain hardening, flow liquefaction will generally not occur. However, cyclic softening can occur due to cyclic undrained loading, such as earthquake loading. The amount and extent of deformations during cyclic loading will depend on the density of the soil, the magnitude and duration of the cyclic loading and the extent to which shear stress reversal occurs. If extensive shear stress reversal occurs, it is possible for the effective stresses to reach zero and, hence, cyclic liquefaction can take place. When the condition of essentially zero effective stress is achieved, large deformations can result. If cyclic loading continues, deformations can progressively increase. If shear stress reversal does not take place, it is generally not possible to reach the condition of zero effective stress and deformations will be smaller; i.e. cyclic mobility will occur. Examples of cyclic softening were common in the major earthquakes in Niigata in 1964 and Kobe in 1995 and manifested in the form of sand boils, damaged lifelines (pipelines, etc.), lateral spreads, slumping of small embankments, settlements, and ground surface cracks. If cyclic liquefaction occurs and drainage paths are restricted due to overlying less permeable layers, the sand immediately beneath the less permeable soil can loosen due to pore water redistribution, resulting in possible subsequent flow liquefaction, given the right geometry.

Both flow liquefaction and cyclic liquefaction can cause very large deformations. Hence, it can be very difficult to clearly identify the correct phenomenon based on observed deformations following earthquake loading. Earthquake-induced flow liquefaction movements tend to occur after the cyclic loading ceases due to the progressive nature of the load redistribution. However, if the soil is sufficiently loose and the static shear stresses are sufficiently large, the earthquake loading may trigger essentially 'spontaneous liquefaction' within the first few cycles of loading. Also, if the soil is sufficiently loose, the ultimate undrained strength may be close to zero with an associated effective confining stress very close to zero (Ishihara, 1993). Cyclic liquefaction movements, on the other hand, tend to occur during the cyclic loading since it is the inertial forces that drive the phenomenon. The post earthquake diagnosis can be further complicated by the possibility of pore water redistribution after the cyclic loading resulting in a change in soil density and possibly the subsequent triggering of flow liquefaction. Identifying the type of phenomenon after earthquake loading is difficult and, ideally, requires instrumentation during and after cyclic loading together with comprehensive site characterization.

The most common form of soil liquefaction observed in the field has been cyclic softening due to earthquake loading. Much of the existing research work on soil liquefaction has been related to cyclic softening, primarily cyclic liquefaction. Cyclic liquefaction applies to level or gently sloping ground where shear stress reversal occurs during earthquake loading. This paper is concerned primarily with cyclic liquefaction due to earthquake loading.

Cyclic resistance based on laboratory testing

Much of the early work related to earthquake-induced soil liquefaction resulted from laboratory testing of reconstituted samples subjected to cyclic loading by means of cyclic triaxial, cyclic simple shear, or cyclic torsional tests. The outcome of these studies generally confirmed that the resistance to cyclic loading is influenced primarily by the state of the soil (i.e. void ratio, effective confining stresses, and soil structure) and the intensity and duration of the cyclic loading (i.e. cyclic shear stress and number of cycles), as well as the grain characteristics of the soil. Soil structure incorporates features such as fabric, age and cementation. Grain characteristics incorporate features such as grain size distribution, grain shape, and mineralogy.

Resistance to cyclic loading is usually represented in terms of a cyclic stress ratio or cyclic resistance ratio (CRR). For cyclic simple shear tests, CRR is taken as the ratio of the cyclic shear stress to cause cyclic liquefaction to the initial vertical effective stress; i.e. $(CRR)_{ss} = \tau_{cyc}/\sigma'_{vo}$. For cyclic triaxial tests, CRR is taken as the ratio of the maximum cyclic shear stress to cause cyclic liquefaction to the initial effective confining stress; i.e. $(CRR)_{tx} = \sigma_{dc}/2\sigma'_{3c}$. The two tests impose different loading conditions and the CRR values are not equivalent. Cyclic simple shear tests are generally considered to be better than cyclic triaxial tests at closely representing earthquake loading for level ground conditions. However, experience has shown that the $(CRR)_{ss}$ can be estimated quite well from $(CRR)_{tx}$, and correction factors have been developed (Ishihara, 1993). The CRR is typically taken at about 15 cycles of uniform loading to represent an equivalent earthquake loading of Magnitude (M) 7.5; i.e. $CRR_{7.5}$.

The CRR for any other size earthquake can be estimated using the following equation:

$$CRR = (CRR_{7.5})(MSF) \quad (1)$$

where:
MSF = magnitude scaling factor (recommended values are provided in the report by Youd et al. (1997), which summarizes the results of the 1996 NCEER Workshop).

It is common practice to define the point of 'liquefaction' in a cyclic laboratory test as the time at which the sample achieves a strain level of either 5% double-amplitude axial strain in a cyclic triaxial test or 3 to 4% double-amplitude shear strain in a cyclic simple shear test. For loose sand

samples subjected to shear stress reversal, this often occurs close to the point at which the effective confining stress is essentially zero and deformations develop rapidly; hence, the definition is the same as that for cyclic liquefaction (see Figure 3). However, for denser sand samples, the 5% double-amplitude strain criteria can occur before sufficient pore pressure has developed to take the sample to the state of essentially zero effective stress. Hence, the criteria for liquefaction typically applied to laboratory results may well be unduly conservative, since deformations may actually be progressing rather slowly.

While void ratio (relative density) has been recognized as a dominant factor influencing the CRR of sands, studies by Ladd (1974), Mulilis et al. (1977), and Tatsuoka et al. (1986) have clearly shown that sample preparation (i.e. soil fabric) also plays an important role. This is consistent with the results of monotonic tests at small to intermediate strain levels. Hence, if results are to be directly applied with any confidence, it is important to conduct cyclic laboratory tests on reconstituted samples with a structure similar to that in-situ. Unfortunately, it is very difficult to determine the in-situ fabric of natural sands below the water table. As a result, there is often some uncertainty in the evaluation of CRR based on laboratory testing of reconstituted samples. Tokimatsu and Hosaka (1986) suggested that either the small strain shear modulus or shear wave velocity measurements could be used to improve the value of laboratory testing on reconstituted samples of sand.

Based on the above observations, there has been increasing interest in testing high quality undisturbed samples of sandy soils under conditions representative of those in-situ. Yoshimi et al. (1989) showed that aging and fabric had a significant influence on the CRR of clean sand from Niigata, as shown in Figure 5.

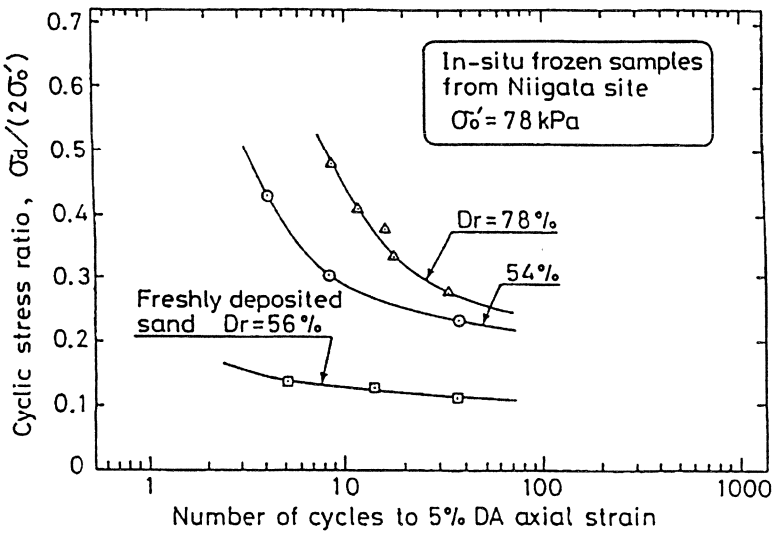

Figure 5 Comparison between triaxial cyclic resistance ratio (CRR) for a clean Niigata sand based on recently deposited and aged samples (after Yoshimi et al., 1989).

Yoshimi et al. (1994) also showed that sand samples obtained using conventional high quality fixed piston samplers produced different CRR values than undisturbed samples obtained using in-situ ground freezing, as summarized in Figure 6. Dense sand samples showed a decrease in CRR and loose sand samples showed an increase in CRR when obtained using a piston sampler, as compared to the results of testing in-situ frozen samples. The difference in CRR became more pronounced as the density of the sand increased.

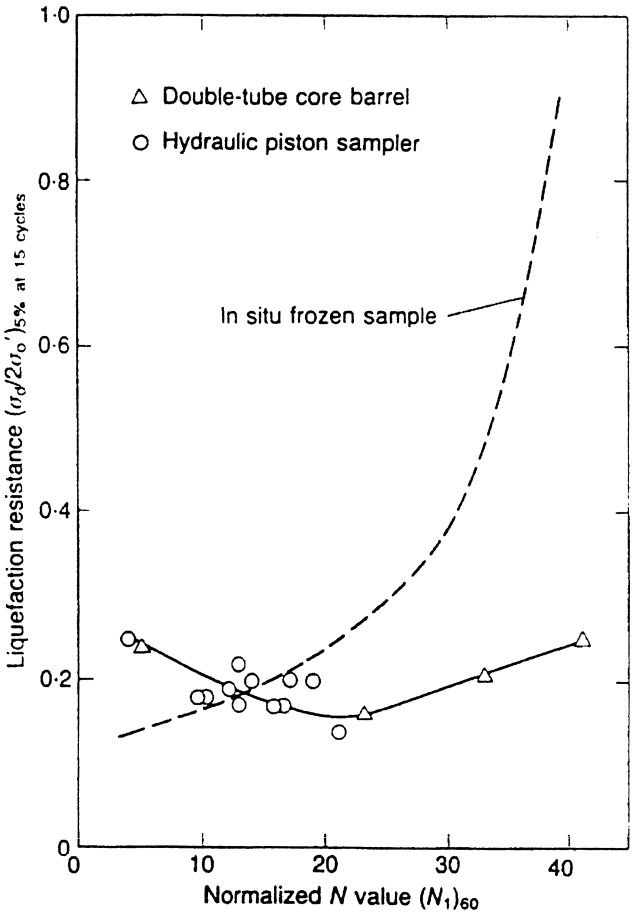

Figure 6 Comparison between triaxial cyclic resistance ratio (CRR) and SPT $(N_1)_{60}$ values for clean sands based on tube samples and undisturbed in-situ frozen samples (after Yoshimi et al., 1994).

The relationship, shown in Figure 6, (after Yoshimi et al., 1994) between $(CRR)_{tx}$ to cause 5% double-amplitude axial strain after 15 cycles and corrected SPT N value at 100 kPa effective overburden stress and 60% energy ($(N_1)_{60}$) obtained from adjacent soundings was based on undisturbed samples of sand obtained using ground freezing. It would appear that dense sand with a normalized SPT $(N_1)_{60}$ between 30 and 40 has a $(CRR)_{tx}$ less than 1.0. This is in conflict with field observation (Seed et al., 1985) and is almost certainly associated with the definition of 'liquefaction' based on a limiting double-amplitude axial strain of 5%. As explained earlier, dense sand samples can progressively develop 5% double-amplitude axial strain but may not

have achieved the condition of rapid deformation associated with essentially zero effective confining stress. Hence, it is important to clearly define the onset of 'liquefaction'. In general, for design purposes, cyclic liquefaction is the point at which the soil experiences large uncontrolled deformations.

Although the results shown in Figure 6 apply to a range of sands from Japan, it is likely that changes in grain characteristics will influence the correlation between CRR and SPT $(N_1)_{60}$. Based on the same laboratory test results on undisturbed in-situ frozen sand samples as those shown in Figure 6 plus one additional site, Suzuki et al. (1995a) suggested a correlation between CRR and corrected Cone Penetration Test (CPT) penetration resistance. To account for the variation due to differences in grain characteristics, Suzuki et al. (1995a) suggested a modification to the CPT corrected to incorporate the minimum void ratio (e_{min}), as a measure of the grain characteristics, as follows:

$$q_{tN} = \frac{q_c\left(\frac{Pa}{\sigma'_{vo}}\right)^{0.5}}{f(e_{min})} \qquad (2)$$

where q_{tN} is the cone tip resistance corrected for overburden stress and minimum void ratio; P_a is a reference pressure, usually equal to 100 kPa; σ'_{vo} is the vertical effective stress and $f(e_{min}) = (2.17 - e_{min})^2 / (1+ e_{min})$, is a factor to account for differences in grain characteristics. The resulting correlation is shown in Figure 7.

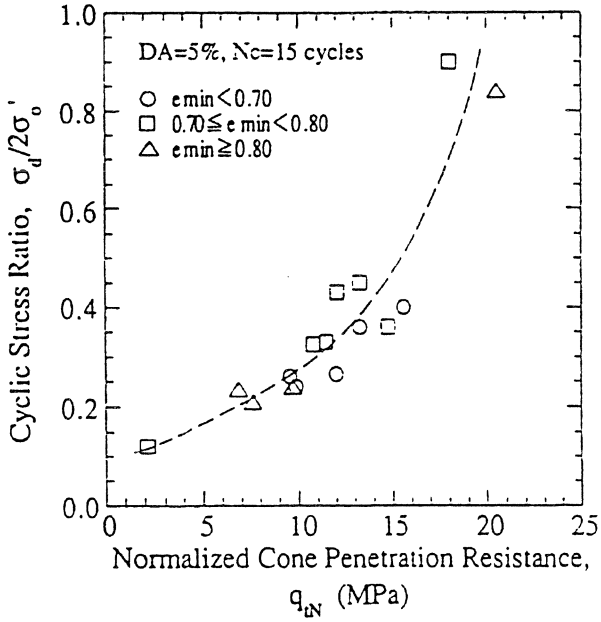

Figure 7 Correlation between triaxial cyclic resistance ratio (CRR) and modified normalized cone penetration resistance for a wide range of sands (after Suzuki et al., 1995a).

Suzuki et al. (1995a) suggested that the correlation in Figure 7 would be applicable to a wide range of sandy soils (i.e. sandy soils with various grain distributions, grain shapes and/or mineralogy). It is interesting to note that the modification using $f(e_{min})$ accounts for a correction to the traditional normalized cone penetration resistance by a factor of 0.65 to 0.96 when e_{min} varies from typical values of 0.6 to 0.8. However, the incorporation of e_{min} into the correlation is cumbersome, difficult to apply, and appears to have a relatively small influence for most sands.

When a soil is fine-grained or contains some amount of fines, some cohesion or adhesion can develop between the fine particles making the soil more resistant at essentially zero effective confining stress. Consequently, a greater resistance to cyclic liquefaction is generally exhibited by sandy soils containing some fines. However, this tendency depends on the nature of the fines contained in the sand (Ishihara, 1993). Laboratory testing has shown that one of the most important index properties influencing CRR is the plasticity index of the fines contained in the sand (Ishihara and Koseki, 1989). Figure 8 shows the results of cyclic triaxial tests versus plasticity index (I_p) for a variety of sandy soils (Ishihara, 1993) and illustrates that the $(CRR)_{tx}$ appears to increase with increasing plasticity index.

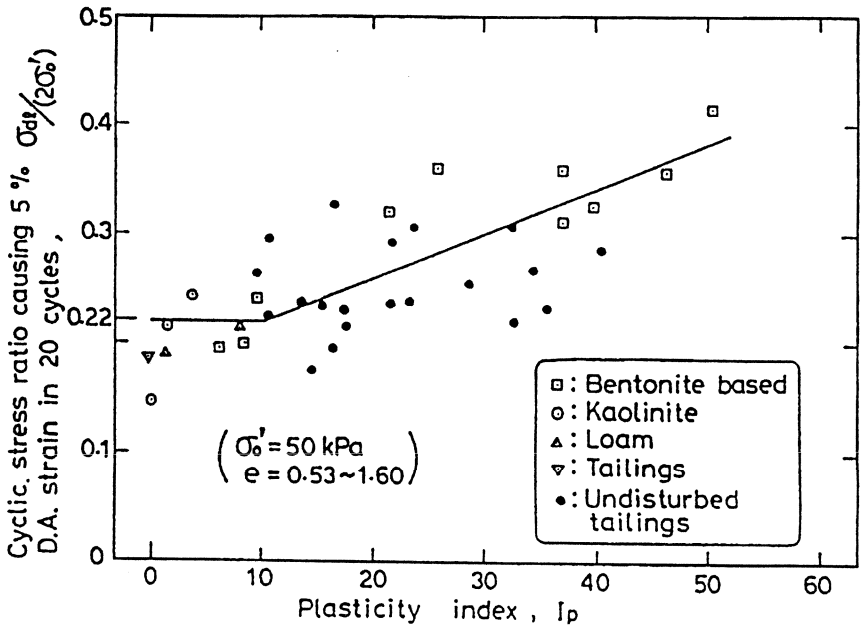

Figure 8 Effect of soil plasticity on cyclic resistance ratio (CRR) of fines-containing sands (after Ishihara, 1993).

Studies in China (Wang, 1979) suggest that the potential for cyclic liquefaction in silts and clays is controlled by grain size, liquid limit, and water content. The interpretation of this criterion as given by Marcuson et al. (1990) and shown in Figure 9 can be useful; however, it is important to note that it is based on limited data. Figure 9 suggests that when a soil has a liquid limit less than 35% combined with a water content greater than 90% of the liquid limit, it is unclear if the soil

can experience cyclic liquefaction and that the soil should be tested to clarify the expected response to undrained cyclic loading.

CRITERIA OF LIQUEFACTION ASSESSMENT OF CLAYEY SOILS FROM STUDIES IN CHINA (SEED ET AL. 1973 AND WANG 1979)

PERCENT FINER THAN 0.005 MM	<15%
LIQUID LIMIT	<35%
WATER CONTENT	>0.9 x LIQUID LIMIT

GRAPHICAL REPRESENTATION OF CRITERIA:

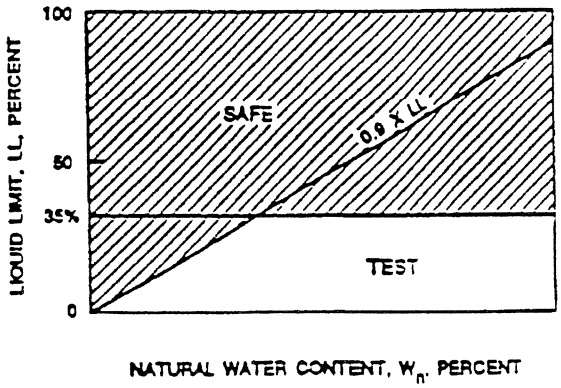

Figure 9 Liquefaction criteria for silts and clays (after Marcuson et al., 1990).

For high risk projects where the evaluation of the potential for soil liquefaction due to earthquake loading is very important, consideration should be given to a limited amount of appropriate laboratory testing on high quality undisturbed samples. Recently, in-situ ground freezing has been used to obtain undisturbed samples of sandy soils (Yoshimi et al., 1978; Yoshimi et al., 1989; Yoshimi et al., 1994; Sego et al., 1994; Hofmann et al. 1995; and Hofmann, 1997). Cyclic simple shear tests are generally the most appropriate tests although cyclic triaxial tests can also give reasonable results.

Cyclic resistance based on field testing

Standard penetration test (SPT)

The above comments have shown that testing high quality undisturbed samples will give better results than testing poor quality samples. However, obtaining high quality undisturbed samples of saturated sandy soils is very difficult and expensive and can only be carried out for large

projects for which the consequences of liquefaction may result in large costs. Therefore, there will always be a need for simple, economic procedures for estimating the CRR of sandy soils. Currently, the most popular simple method for estimating CRR makes use of the penetration resistance from the Standard Penetration Test (SPT) although, more recently, the Cone Penetration Test (CPT) has become very popular due to its greater repeatability and the continuous nature of its profile.

The late Professor H.B. Seed and his co-workers developed a comprehensive approach to estimate the potential for cyclic softening due to earthquake loading. The approach requires an estimate of the cyclic stress ratio (CSR) profile caused by a design earthquake. This is usually done based on a probability of occurrence for a given earthquake. A site specific seismicity analysis can be carried out to determine the design CSR profile with depth. A simplified method to estimate CSR was also developed by Seed and Idriss (1971) based on the maximum ground surface acceleration (a_{max}) at the site. This simplified approach can be summarized as follows:

$$CSR = \frac{\tau_{av}}{\sigma'_{vo}} = 0.65\left(\frac{a_{max}}{g}\right)\left(\frac{\sigma_{vo}}{\sigma'_{vo}}\right) r_d \qquad (3)$$

where τ_{av} is the average cyclic shear stress; a_{max} is the maximum horizontal acceleration at the ground surface; $g = 9.81 m/s^2$ is the acceleration due to gravity; σ_{vo} and σ'_{vo} are the total and effective vertical overburden stresses, respectively; and r_d is a stress reduction factor which is dependent on depth. The factor r_d can be estimating using the following tri-linear function, which provides a good fit to the average of the suggested range in r_d originally proposed by Seed and Idriss (1971):

$$\begin{aligned} r_d &= 1.0 - 0.00765\, z && \text{if } z < 9.15 \text{ m} \\ &= 1.174 - 0.0267\, z && \text{if } z = 9.15 \text{ to } 23 \text{ m} \\ &= 0.744 - 0.008\, z && \text{if } z = 23 \text{ to } 30 \text{ m} \\ &= 0.5 && \text{if } z > 30 \text{ m} \end{aligned} \qquad (4)$$

where z is the depth in metres. The first two formulae in Equation 4 (i.e. for depths less than 23 m) were recommended by Liao and Whitman (1986b). The third formula has been added here to provide a better match with the average of the range in r_d suggested by Seed and Idriss (1971) at depths between 23 m and 30 m. The fourth formula has been added as a conservative cutoff at large depths. These formulae are approximate, at best, and represent only average values since r_d shows considerable variation with increasing depth (Seed and Idriss, 1971). The CSR profile from the earthquake can be compared to the estimated CRR profile for the soil deposit, adjusted to the same magnitude using Equation 1. At any depth, if CSR is greater than CRR, cyclic softening (liquefaction) is possible. This approach is the most commonly used technique in most parts of the world for estimating soil liquefaction due to earthquake loading.

The approach based on the SPT has many problems, primarily due to the inconsistent nature of the SPT. The main factors affecting the SPT have been reviewed (e.g. Seed et al., 1985; Skempton, 1986; Robertson et al., 1983) and are summarized in Table 1. It is highly recommended that the engineer become familiar with the details of the SPT in order to avoid or at least minimize some of the major factors.

Table 1. Factors affecting the SPT (after Kulhawy and Mayne, 1990).

Cause	Effects	Influence on SPT N value
Inadequate cleaning of hole	SPT is not made in original in-situ soil, and therefore soil may become trapped in sampler and be compressed as sampler is driven, reducing recovery	Increases
Failure to maintain adequate head of water in borehole	Bottom of borehole may become quick	Decreases
Careless measure of hammer drop	Hammer energy varies (generally variations cluster on low side)	Increases
Hammer weight inaccurate	Hammer energy varies (driller supplies weight; variations of 5-7 % common)	Increases or decreases
Hammer strikes drill rod collar eccentrically	Hammer energy reduced	Increases
Lack of hammer free fall because of ungreased sheaves, new stiff rope on weight, more than two turns on cathead, incomplete release of rope each drop	Hammer energy reduced	Increases
Sampler driven above bottom of casing	Sampler driven in disturbed, artificially densified soil	Increases greatly
Careless blow count	Inaccurate results	Increases or decreases
Use of non-standard sampler	Corrections with standard sampler invalid	Increases or decreases
Coarse gravel or cobbles in soil	Sampler becomes clogged or impeded	Increases
Use of bent drill rods	Inhibited transfer of energy of sampler	Increases

One of the single most important factors affecting SPT results is the energy delivered to the SPT sampler. This is normally expressed in terms of the rod energy ratio (ER). An energy ratio of 60% has generally been accepted as the reference value, which represents the approximate historical average SPT energy. The value of ER (%) delivered by a particular SPT set-up

depends primarily on the type of hammer/anvil system and the method of hammer release. Values of the correction factor to modify the SPT results to 60% energy (ER/60) can vary from 0.3 to 1.6 corresponding to field values of ER of 20% to 100%. Additional correction factors are also required for rod lengths less than 10 m, borehole diameters outside the recommended interval (65 - 125 mm) and samplers without internal liners.

Since the SPT N value also varies with the effective overburden stress level, an overburden stress correction factor is usually also applied to provide a consistent reference (i.e. $(N_1)_{60}$). The SPT N value corrected for overburden stress, rod length, borehole diameter and sampling method is given by:

$$(N_1)_{60} = N\, C_N\, C_E\, C_B\, C_R\, C_S \tag{5}$$

where N is the measured SPT blowcount; $C_N = (P_a/\sigma'_{vo})^{0.5}$ (with a restriction that $C_N \leq 2$) is a correction for effective overburden stress; P_a is a reference pressure of 100 kPa; σ'_{vo} is the vertical effective stress; C_E = ER/60% is a correction to account for rod energy; ER is the actual energy ratio, in percent; C_B is a correction for borehole diameter; C_R is a correction for rod length; and C_S is a correction for the sampling method. The correction for overburden stress (C_N) is the same as that proposed by Liao and Whitman (1986a), except that, as noted above, a maximum value of C_N = 2 should be applied for SPT values at shallow depths. Correction factors for energy ratio, borehole diameter, rod length and sampling method were suggested by Skempton (1986) and are given in Table 2.

Table 2. Corrections to the SPT (modified from Skempton, 1986).

Factor	Equipment Variable	Term	Correction
Overburden Pressure		C_N	$(P_a/\sigma'_{vo})^{0.5}$ but ≤ 2
Energy Ratio	Donut Hammer Safety Hammer Automatic Hammer	C_E	0.5 to 1.0 0.7 to 1.2 0.8 to 1.5
Borehole diameter	65 to 115 mm (2.5 to 4.5 in) 150 mm (6 in) 200 mm (8 in)	C_B	1.0 1.05 1.15
Rod length	3 to 4 m (10 to 13 ft) 4 to 6 m (13 to 20 ft) 6 to 10 m (20 to 30 ft) 10 to 30 m (30 to 100 ft) >30 m (>100 ft)	C_R	0.75 0.85 0.95 1.0 <1.0
Sampling method	Standard sampler Sampler without liner	C_S	1.0 1.1 to 1.3

The ranges of correction values for ER (C_E) are given only as a guide. Actual values of C_E can vary significantly from the global averages. It is recommended that ER be measured during the actual site investigation to improve the level of reliability of the SPT.

A summary of the recommended procedure for performing the SPT is given in Table 3. The borehole should be made using mud rotary techniques using a side or upward discharge bit. Hollow stem auger techniques are not recommended in saturated sands and silts unless extreme care is taken, since disturbance and heave in the hole is common. There is a need for care when cleaning out the bottom of the borehole to avoid disturbance. The borehole should not exceed 115 mm (4.5 inches) in diameter, since the associated stress relief can reduce the measured N value in some sands. The energy delivered to the SPT sampler can also be very low for an SPT above a depth of about 10 m (30 ft.) due to rapid reflection of the compression wave in the rod. The energy reaching the sampler can also become reduced for an SPT below a depth of about 30 m (100 ft) due to energy losses and the large mass of the drill rods. If the SPT sampler has been designed to hold a liner, it is important to ensure that a liner is installed, since a correction of up to 30% may apply if a liner is not used (Schmertmann, 1979).

Table 3. Recommended SPT procedure (after Seed et al., 1985).

SPT Set-up	Recommended Procedure
Borehole size	66 mm < Diameter < 115 mm
Borehole support	Casing for full length and/or drilling mud
Drilling	Wash boring; side discharge bit Rotary boring; side or upward discharge bit Clean bottom of borehole*
Sampler	Standard 51 mm O.D. + 1 mm 35 mm I.D. + 1 mm > 457 mm length
Penetration Resistance	Record number of blows for each 150 mm N = number of blows from 150 to 450 mm penetration

* Maximum soil heave within casing < 70 mm

Seed (1979) developed a method to estimate the CRR for a sand under level ground conditions based on the SPT. This method was based on extensive field performance data for Holocene sands from essentially level ground sites which either had or had not experienced cyclic softening (liquefaction) due to earthquake loading. Liquefaction was assumed to have occurred based on the presence of observable surface features such as sand boils and ground cracks. A summary of the SPT based method to estimate CRR for clean sand is shown in Figure 10 (Seed et al., 1985).

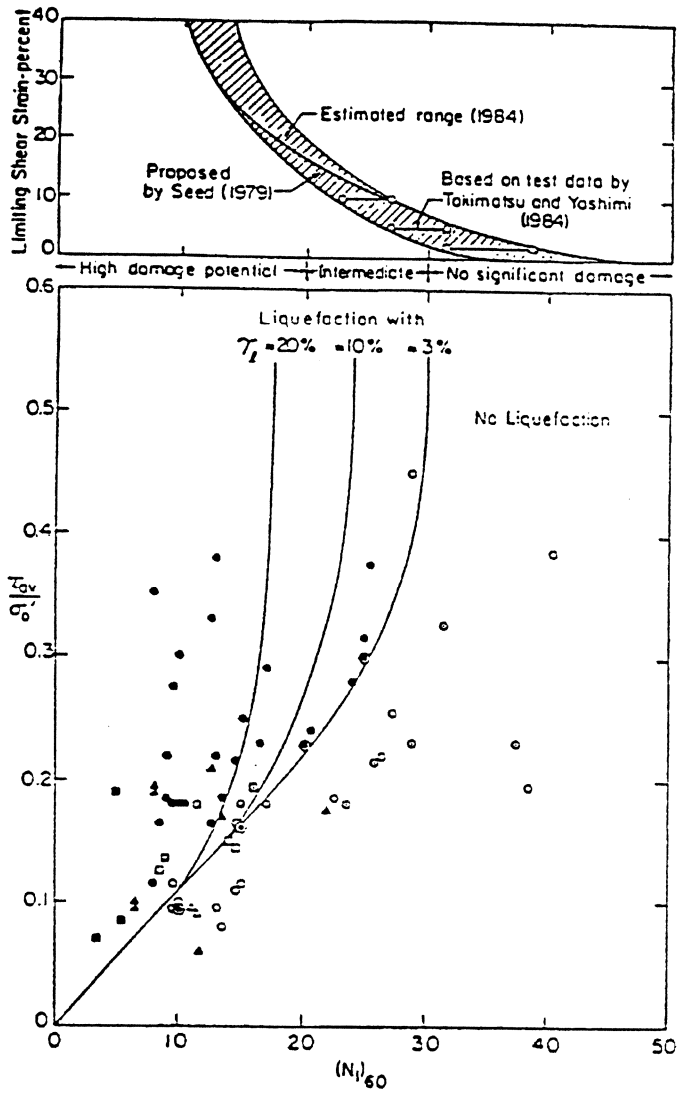

Figure 10 Cyclic resistance ratio (CRR) for clean sands under level ground conditions based on SPT and field performance data (after Seed et al., 1985).

Other SPT based methods have been developed (Tatsuoka et al., 1980; Shibata, 1981; Tokimatsu and Yoshimi, 1983; Kokusho et al., 1983; Ishihara, 1993; Fear and McRoberts, 1995), but the correlation by Seed et al. (1985) appears to maintain the most popularity, especially in North America. The correlation shown in Figure 10 includes the estimated limiting shear strain values associated with 'liquefaction'. Seed recognized that dense sands ($(N_1)_{60}$>15) generally experienced less deformation for a given cyclic loading (i.e. they experienced cyclic mobility) than loose sands (which experienced cyclic liquefaction). Hence, the definition of 'liquefaction' became flexible in that dense sand would not develop very large strains (i.e. would not reach the condition of essentially zero effective confining stress). This is supported by laboratory test results (Yoshimi et al., 1994) and field observations (Bartlett and Youd, 1995).

Based on discussions at the 1996 NCEER Workshop regarding the statistical analysis of the liquefaction database and physical considerations discussed in Liao et al. (1988) and the concept of a threshold strain (Dobry et al., 1982), the Seed et al. (1985) SPT curve was slightly modified to avoid the extrapolation to zero CRR at zero penetration resistance. The modified clean sand SPT curve is shown in Figure 11 and has an intercept of CRR=0.05. Occurrence of liquefaction is based on level ground observations of surface manifestations of cyclic liquefaction. For loose sand (i.e. $(N_1)_{60} < 15$) this could involve large deformations resulting from a condition of essentially zero effective stress being reached. For denser sand (i.e. $(N_1)_{60} > 15$), this could involve the development of large pore pressures, but the effective stress may not fully reduce to zero and deformations may not be as large as in loose sands. Hence, the consequences of 'liquefaction' will vary depending on the soil density as well as the size and duration of loading.

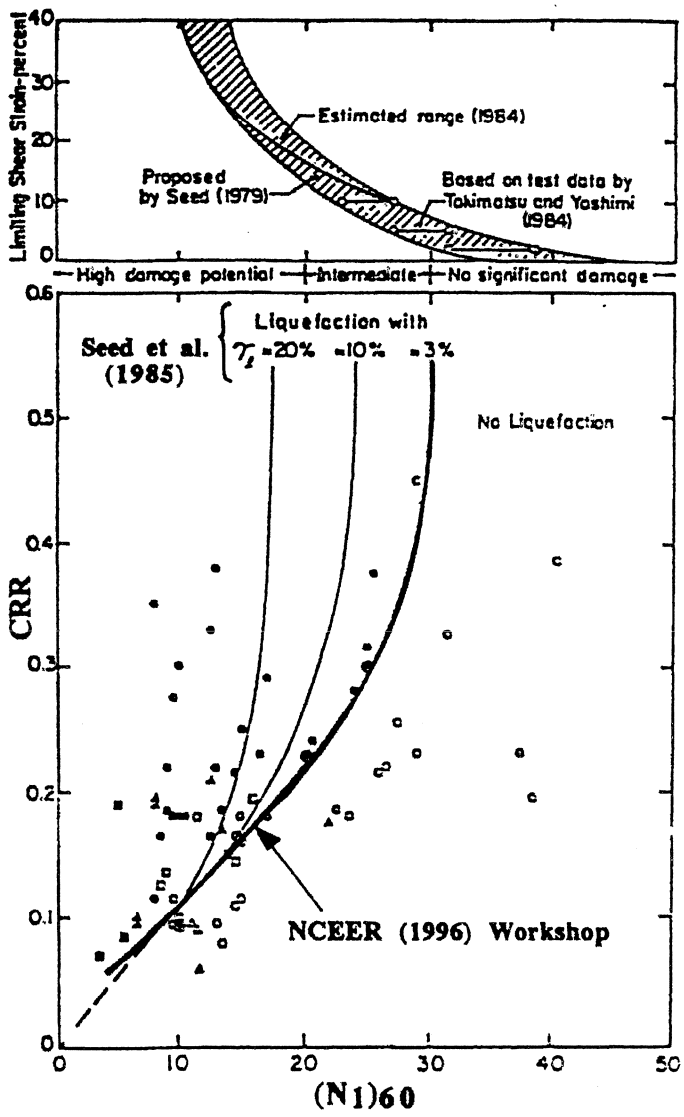

Figure 11 Recommended cyclic resistance ratio (CRR) for clean sands under level ground conditions based on SPT.

The recommended SPT clean sand curve can be approximated by the following equation proposed by Blake (1996):

$$CRR_{7.5} = \frac{a + cx + ex^2 + gx^3}{1 + bx + dx^2 + fx^3 + hx^4} \quad (6)$$

where: $x = (N_1)_{60cs}$ is the clean sand equivalent SPT blowcount corrected for overburden; and a = 4.844E-02, b = -1.248E-01, c = - 4.721E-03, d = 9.578E-03, e = 6.136E-04, f = - 3.285E-04, g = - 1.673E-05, and h = 3.714E-06 are all constants.

The field observation data used to compile the curves in Figure 10 and Figure 11 are apparently based on the following:

Holocene age, clean sand deposits
Level or gently sloping ground
Magnitude M = 7.5 earthquakes
Depth range from 1 to 14 m (3 to 47 ft)
(90% is for depths < 10 m, (32 ft))
Representative average SPT N values for the layer that was considered to have experienced cyclic liquefaction.

Hence, caution should be exercised when extrapolating the correlation to conditions outside of the above range. An important feature to recognize is that the correlation appears to be based on average values for the inferred liquefied layers. However, the correlation is often applied to all measured SPT values, which include low values below the average. Hence, the correlation can be conservative in variable deposits where a small part of the SPT data could indicate possible liquefaction.

Seed et al. (1985) showed that for a given CRR, a sand with fines has a lower SPT $(N_1)_{60}$ value and, based on this observation, developed the correlation further to include the influence of fines content, as shown in Figure 12. The correlation showed that, for the same CRR, the penetration resistance in silty sands was smaller. This is most likely due to the greater compressibility and decreased permeability of silty sands, which reduces penetration resistance and moves the penetration process toward an undrained penetration, respectively. Robertson and Fear (1995) recommended an average blowcount correction, which was dependent on fines content, but not on penetration resistance.

Although the original correlations shown in Figure 12 are based on fines content, it is clear that the CRR of a soil is a function of many factors, including type of fines; e.g. plasticity (Figure 8 and Figure 9), other grain characteristics (mineralogy, grain shape, etc), and fines content. Hence, any correction should be applied with caution.

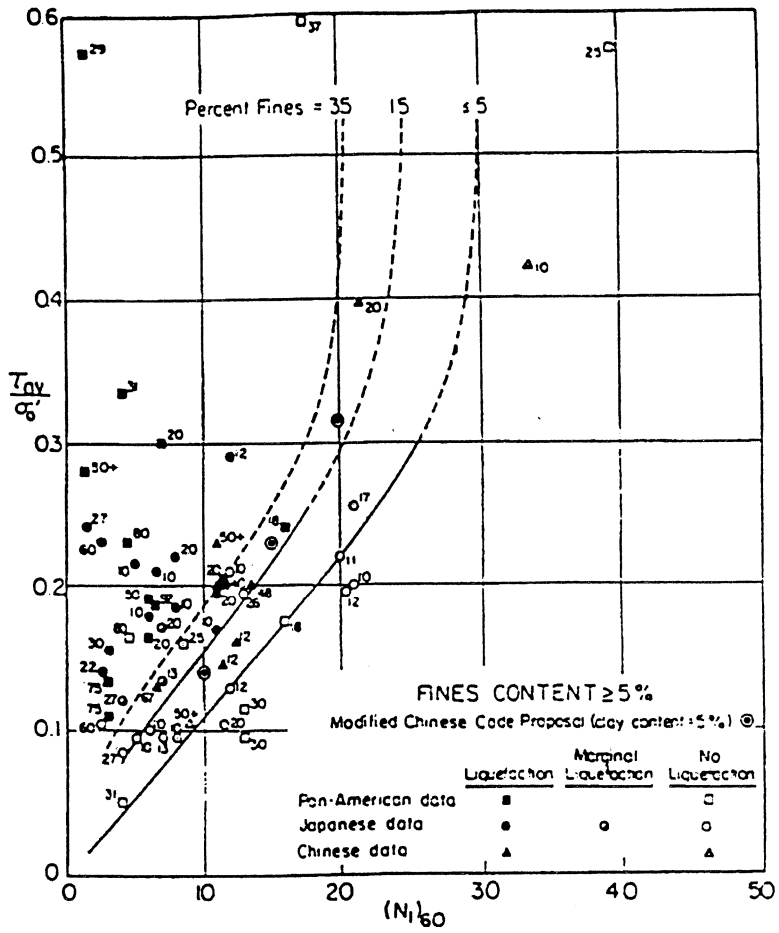

Figure 12 Relationship between cyclic resistance ratio (CRR) and SPT for sands and silty sands based on field performance data (after Seed et al., 1985).

Based on extensive discussions by the NCEER Workshop participants, it is recommended that a correction be applied to the measured $(N_1)_{60}$ to obtain the equivalent clean sand $(N_1)_{60cs}$ using the following equation:

$$(N_1)_{60cs} = K_s (N_1)_{60} \tag{7}$$

where K_s is a correction factor that is a function of fines content and plasticity of the fines. Based on observed field performance, the suggested correction factor K_s is shown in Figure 13. This basic recommendation is based on soils with non-plastic fines (PI ≤ 5%) for which K_s has a maximum value of 1.75 at a fines content of 35%. For soils with more plastic fines (PI > 5%), the correction factor is likely larger. However, the data are limited and contain much uncertainty (see Figure 8). For soils with a fines content greater than 35%, other criteria such as that shown in Figure 9 should be applied.

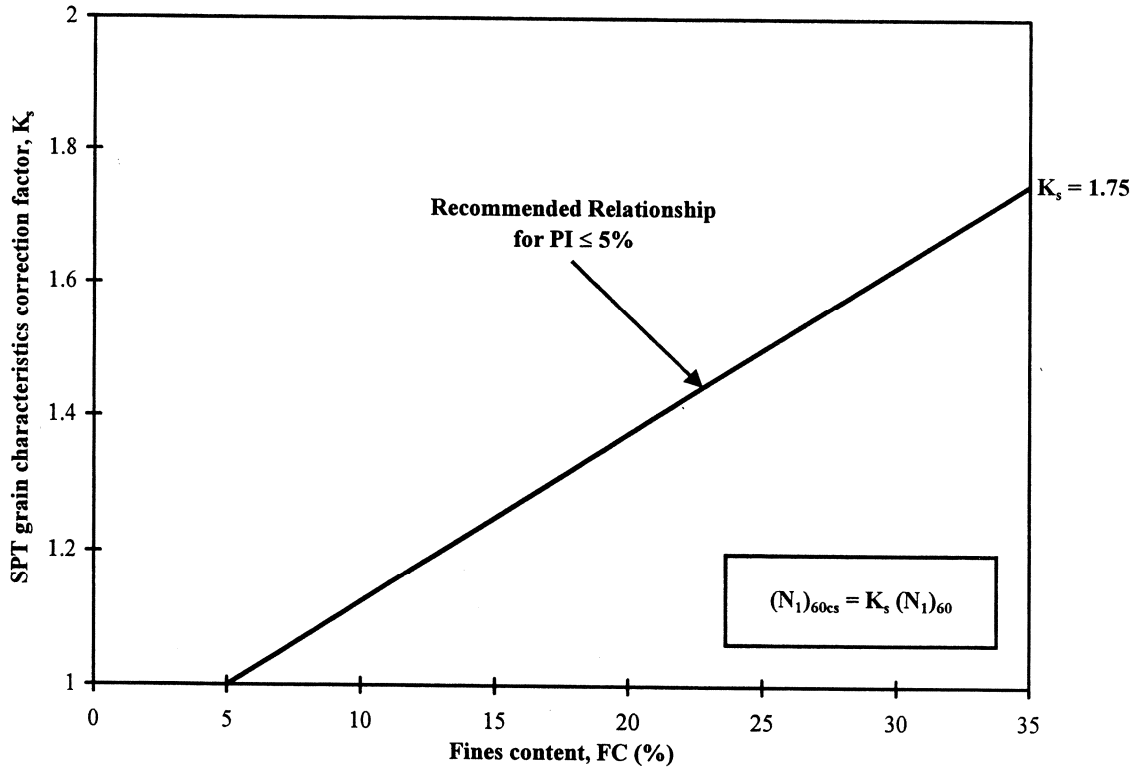

Figure 13 Recommended grain characteristic correction to obtain clean sand equivalent SPT penetration resistance in sandy soils with non-plastic fines.

The recommended procedure is to determine the fines content and plasticity of the fines and apply a correction to the measured SPT $(N_1)_{60}$ value using Figure 13 and Equation 7. The clean sand equivalent penetration resistance, $(N_1)_{60cs}$, can then be combined with the clean sand base curve shown in Figure 11 and approximated by Equation 6 to estimate $CRR_{7.5}$. However, for high fines content soils or soils with highly plastic fines, the criteria shown in Figure 9 should also be applied. Figure 14 shows the resulting equivalent CRR curves for fines contents of 15% and 35% for sandy soils with non-plastic fines (PI ≤ 5%).

Cone penetration test (CPT)

Due to the inherent difficulties and poor repeatability associated with the SPT, several correlations have been proposed to estimate CRR for clean sands and silty sands using corrected CPT penetration resistance (e.g. Robertson and Campanella, 1985; Seed and de Alba, 1986; Olsen, 1988; Olsen and Malone, 1988; Shibata and Teparaska, 1988; Mitchell and Tseng, 1990; Olsen and Koester, 1995; Suzuki et al., 1995a & 1995b; Stark and Olson, 1995; Robertson and Fear, 1995).

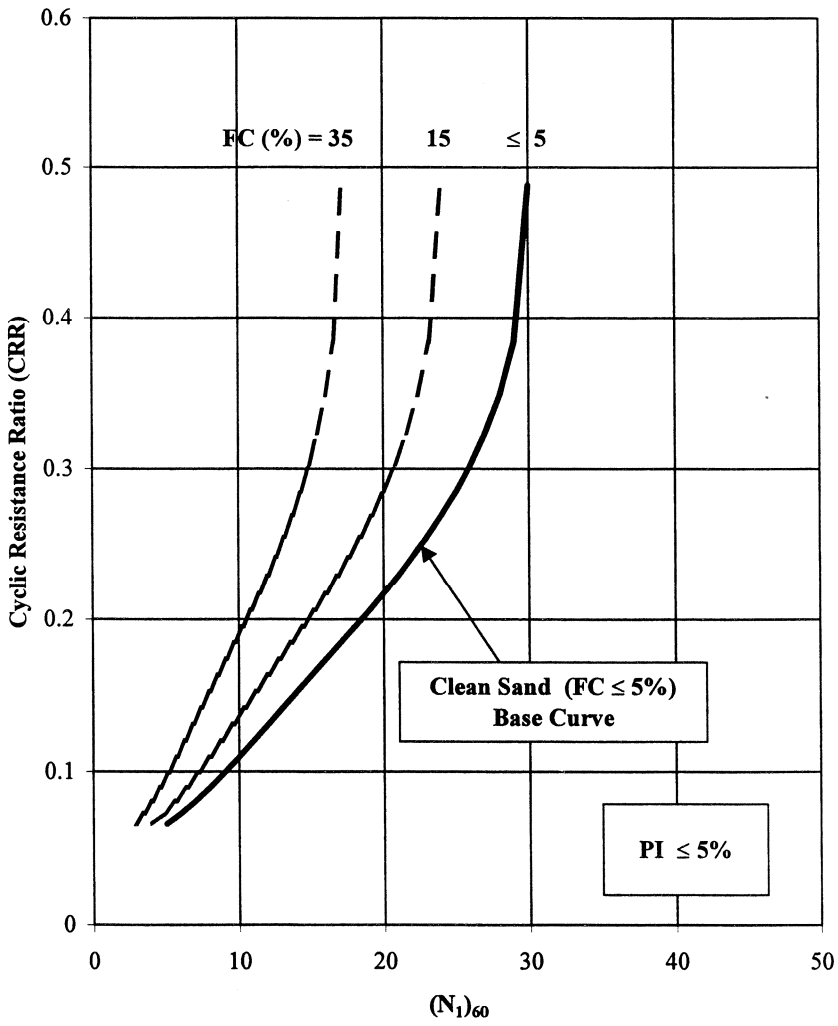

Figure 14 SPT base curves for various fines contents for non-plastic fines (PI ≤ 5%).

Although cone penetration resistance is often just corrected for overburden stress (resulting in the term q_{c1}), truly normalized (i.e. dimensionless) cone penetration resistance corrected for overburden stress (q_{c1N}) can be given by:

$$q_{c1N} = \left(\frac{q_c}{P_{a2}}\right) C_Q = \frac{q_{c1}}{P_{a2}} \tag{8}$$

where q_c is the measured cone tip penetration resistance; $C_Q = (P_a/\sigma'_{vo})^n$ is a correction for overburden stress; n = exponent, typically equal to 0.5; P_a is a reference pressure in the same units as σ'_{vo} (i.e. P_a=100 kPa if σ'_{vo} is in kPa); and P_{a2} is a reference pressure in the same units as q_c (i.e. P_{a2}=0.1 MPa if q_c is in MPa). A maximum value of C_Q=2 is generally applied to CPT data at shallow depths. The normalized cone penetration resistance, q_{c1N}, is dimensionless.

Robertson and Campanella (1985) developed a chart for estimating CRR from corrected CPT penetration resistance based on the Seed et al. (1985) SPT chart and SPT-CPT conversions. Other similar CPT-based charts were also developed by Seed and de Alba (1986), Shibata and Teparaska (1988), and Mitchell and Tseng (1990). A comparison between three of these CPT charts is shown in Figure 15.

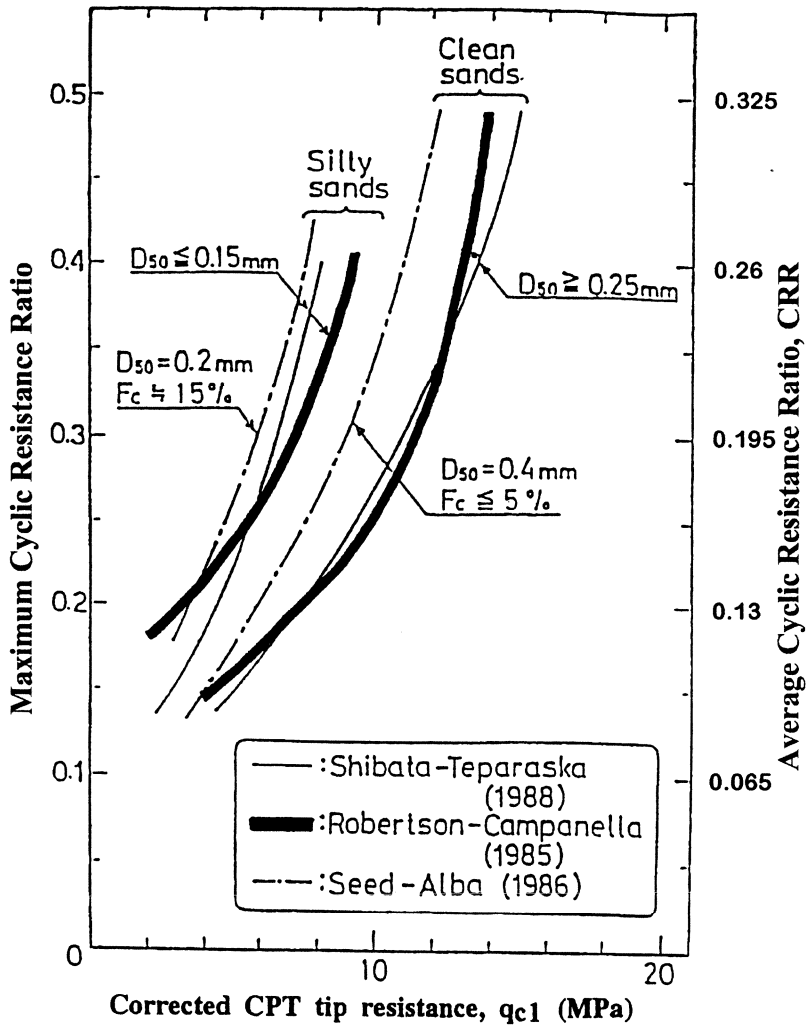

Figure 15 Comparison between three CPT based charts for estimating cyclic resistance ratio (CRR) for clean sands (after Ishihara, 1993).

In recent years, there has been an increase in available field performance data, especially for the CPT (Ishihara, 1993; Kayen et al., 1992; Stark and Olson, 1995; Suzuki et al., 1995b). The recent field performance data have shown that the existing CPT-based correlations to estimate CRR are generally good for clean sands. The recent field performance data show that the correlation between CRR and q_{c1N} by Robertson and Campanella (1985) for clean sands provides a reasonable estimate of CRR. Based on discussions at the 1996 NCEER Workshop,

the curve by Robertson and Campanella (1985) has been adjusted slightly at the lower end, in order to be more consistent with the SPT curve. The resulting recommended CPT correlation for clean sand is shown in Figure 16.

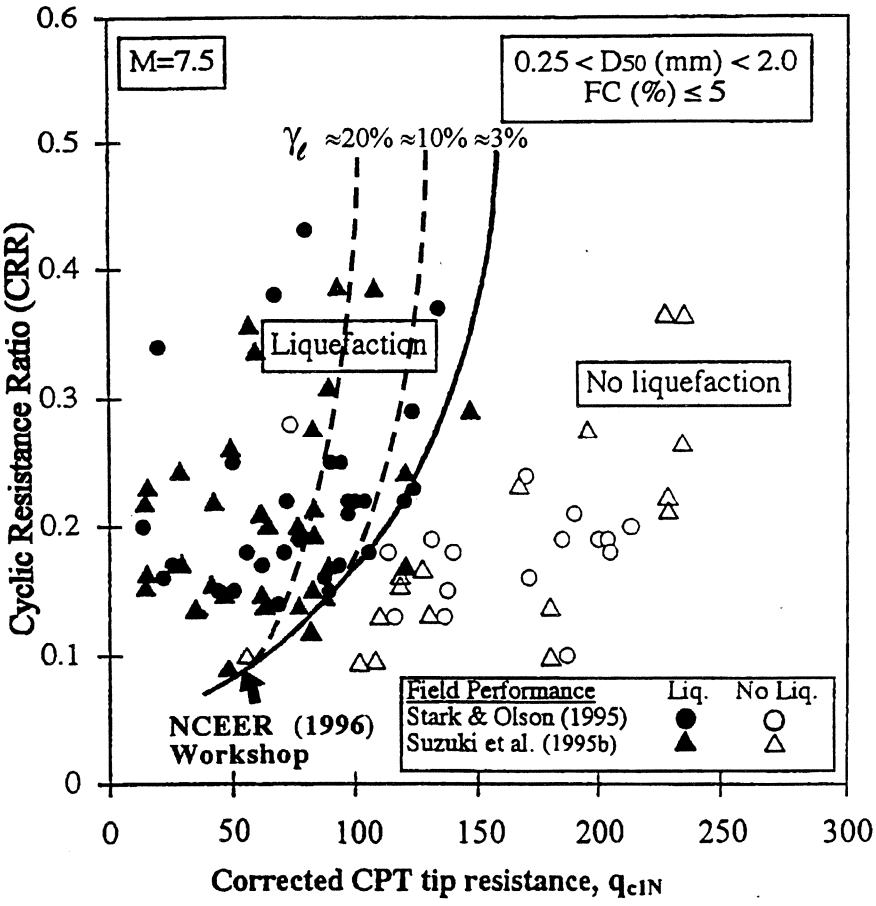

Figure 16 Recommended cyclic resistance ratio (CRR) for clean sands under level ground conditions based on CPT.

Included in Figure 16 are suggested curves of limiting shear strain, similar to those suggested by Seed et al. (1985) for the SPT. Occurrence of liquefaction is based on level ground observations of surface manifestations of cyclic liquefaction. For loose sand (i.e. $q_{c1N} < 75$) this could involve large deformations resulting from a condition of essentially zero effective stress being reached. For denser sand (i.e. $q_{c1N} > 75$) this could involve the development of large pore pressures, but the effective stress may not fully reduce to zero and deformations may not be as large as in loose sands. Hence, the consequences of 'liquefaction' will vary depending on the soil density as well as the size and duration of loading. An approximate equation for the clean sand CPT curve shown in Figure 16 is given later in this paper (Equation 14).

The field observation data used to compile the curve in Figure 16 are apparently based on the following conditions, similar in nature to those for the SPT based data:

Holocene age, clean sand deposits
Level or gently sloping ground
Magnitude M = 7.5 earthquakes
Depth range from 1 to 15 m (3 to 45 ft)
(84% is for depths < 10 m (30 ft))
Representative average CPT q_c values for the layer that was considered to have experienced cyclic liquefaction.

As for the SPT-based approach, caution should be exercised when extrapolating the CPT correlation to conditions outside of the above range. An important feature to recognize is that the correlation appears to be based on average values for the inferred liquefied layers. However, the correlation is often applied to all measured CPT values, which include low values below the average. Therefore, the correlation can be conservative in variable deposits where a small part of the CPT data could indicate possible liquefaction. Although some of the recorded case histories show liquefaction below the suggested curve in Figure 16, the data are based on average values and, hence, the authors consider the suggested curve to be consistent with field observations. The CPT curve in Figure 16 is also consistent with the SPT curve shown in Figure 11.

Based on data from 180 sites, Stark and Olson (1995) also developed a set of correlations between CRR and q_{c1} for various sandy soils based on fines content and mean grain size, as shown in Figure 17.

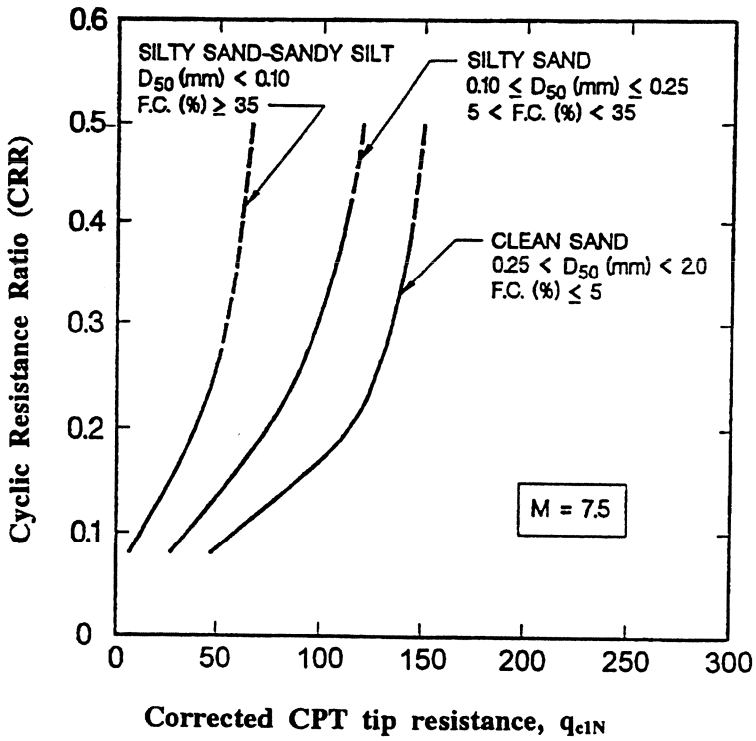

Figure 17 Summary of variation of cyclic resistance ratio (CRR) with fines content based on CPT field performance data (after Stark and Olson, 1995).

The CPT combined database is now larger than the original SPT-based database proposed by Seed et al. (1985). It is important to note that the simplified approach based on either the SPT or the CPT has many uncertainties. The correlations are empirical and there is some uncertainty over the degree of conservatism in the correlations as a result of the methods used to select representative values of penetration resistance within the layers assumed to have liquefied (Fear and McRoberts, 1995). A detailed review of the CPT data, similar to those carried out by Liao and Whitman (1986b) and Fear and McRoberts (1995) on SPT data, would be required to investigate the degree of conservatism contained in Figure 16 and Figure 17. The correlations are also sensitive to the amount and plasticity of the fines within the sand.

One reason for the continued use of the SPT has been the need to obtain a soil sample to determine the fines content of the soil. However, this has been offset by the poor repeatability of SPT data. With the increasing interest in the CPT due to its greater repeatability, several researchers (e.g. Robertson and Campanella, 1985; Olsen, 1988; Olsen and Malone, 1988; Olsen and Koester, 1995; Suzuki et al., 1995a & 1995b; Stark and Olson, 1995; Robertson and Fear, 1995) have developed a variety of approaches for evaluating cyclic liquefaction potential using CPT results. It is now possible to estimate grain characteristics such as apparent fines content and grain size from CPT data and incorporate this directly into the evaluation of liquefaction potential. The following is a modification and update of the CPT approach suggested by Robertson and Fear (1995).

As for the SPT, for the same CRR, the CPT penetration resistance in silty sands is smaller due to the greater compressibility and decreased permeability of silty sands. Robertson and Fear (1995) recommended an average correction, which was dependent on apparent fines content, but not on penetration resistance. Similar to the SPT, it is possible to correct the CPT penetration resistance based on grain characteristics, such as fines content, plasticity, etc. The proposed equation to obtain the equivalent clean sand normalized CPT penetration resistance, $(q_{c1N})_{cs}$, is a function of both the measured penetration resistance, q_{c1N}, and the grain characteristics of the soil, as follows:

$$(q_{c1N})_{cs} = K_c \; q_{c1N} \tag{9}$$

where K_c is a correction factor that is a function of the grain characteristics of the soil, as described later in this paper.

Grain characteristics from the CPT

In recent years, charts have been developed to estimate soil type from CPT data (Olsen and Malone, 1988; Olsen and Koester, 1995; Robertson and Campanella, 1988; Robertson, 1990). Experience has shown that the CPT friction ratio (ratio of the CPT sleeve friction to the cone tip resistance) increases with increasing fines content and soil plasticity. Hence, grain characteristics

such as apparent fines content of sandy soils can be estimated directly from CPT data using any of these soil behaviour charts, such as that by Robertson (1990) shown in Figure 18. As a result, the measured penetration resistance can be corrected to an equivalent clean sand value. The addition of pore pressure data can also provide valuable additional guidance in estimating fines content. Robertson et al. (1992) suggested a method for estimating fines content based on the rate of pore pressure dissipation (t_{50}) during a pause in the CPT.

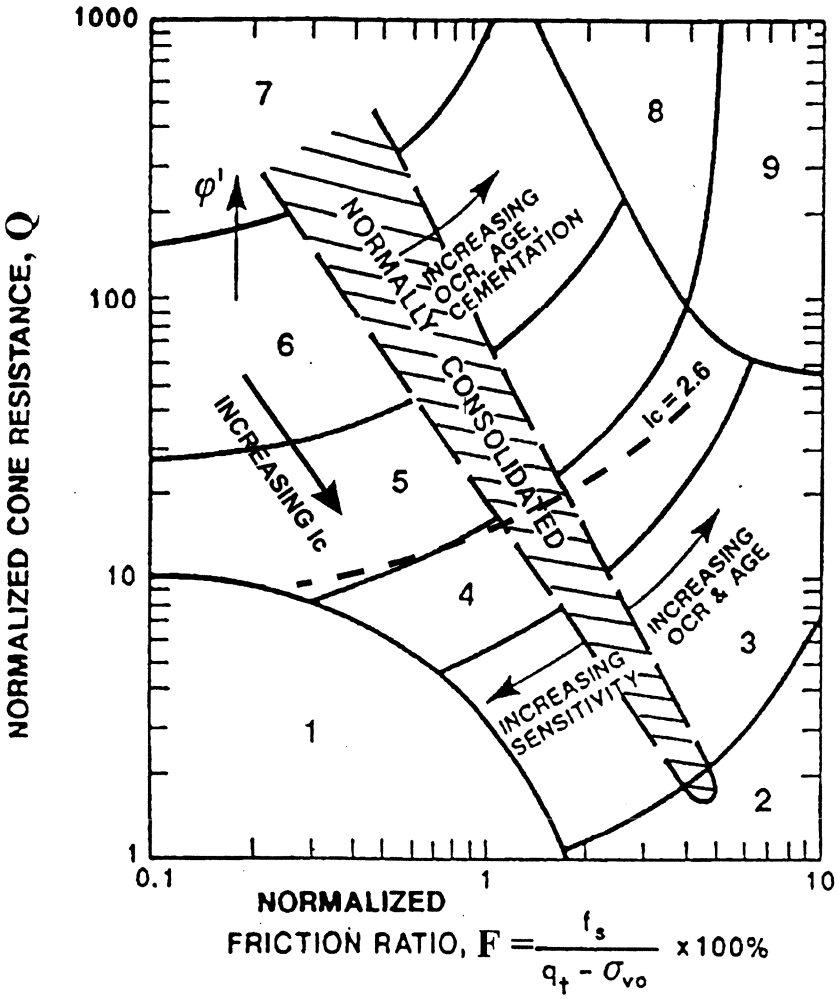

1. Sensitive, fine grained
2. Organic soils - peats
3. Clays - silty clay to clay
4. Silt Mixtures - clayey silt to silty clay
5. Sand Mixtures - silty sand to sandy silt
6. Sands - clean sand to silty sand
7. Gravelly sand to dense sand
8. Very stiff sand to clayey sand*
9. Very stiff, fine grained*

* *Heavily overconsolidated or cemented*

Figure 18 Normalized CPT soil behaviour type chart, as proposed by Robertson (1990).

Based on extensive field data and experience, it is possible to estimate grain characteristics directly from CPT results using the soil behaviour type chart shown in Figure 18. The boundaries between soil behaviour type Zones 2 to 7 can be approximated as concentric circles (Jefferies and Davies, 1993). The radius of each circle can then be used as a soil behaviour type index. Based on the CPT chart developed by Robertson (1990), the soil behaviour type index, I_c, can be defined as follows:

$$I_c = [(3.47 - \log Q)^2 + (\log F + 1.22)^2]^{0.5} \quad (10)$$

where $Q = \left(\frac{q_c - \sigma_{vo}}{P_{a2}} \right) \left(\frac{P_a}{\sigma'_{vo}} \right)^n$ is the normalized CPT penetration resistance, dimensionless; n = exponent, typically equal to 1.0; $F = [f_s / (q_c - \sigma_{vo})] \times 100\%$ is the normalized friction ratio, in percent; f_s is the CPT sleeve friction stress; σ_{vo} and σ'_{vo} are the total and effective overburden stresses, respectively; P_a is a reference pressure in the same units as σ'_{vo} (i.e. P_a=100 kPa if σ'_{vo} is in kPa); and P_{a2} is a reference pressure in the same units as q_c and σ_{vo} (i.e. P_{a2}=0.1 MPa if q_c and σ_{vo} are in MPa).

The soil behaviour type chart by Robertson (1990) uses a normalized cone penetration resistance (Q) based on a simple linear stress exponent of n = 1.0 (see above), whereas the chart recommended here for estimating CRR (see Figure 16) is essentially based on a normalized cone penetration resistance (q_{c1N}) based on a stress exponent n = 0.5 (see Equation 8). Olsen and Malone (1988) correctly suggested a normalization where the stress exponent (n) varies from around 0.5 in sands to 1.0 in clays. However, this normalization for soil type is somewhat complex and iterative.

The Robertson (1990) procedure using n=1.0 is recommended for soil classification in clay type soils when $I_c > 2.6$. However, in sandy soils when $I_c \leq 2.6$, it is recommended that data being plotted on the Robertson (1990) chart be modified by using n=0.5. Hence, the recommended procedure is to first use n = 1.0 to calculate Q and, therefore, an initial value of I_c for CPT data. If $I_c > 2.6$, the data should be plotted directly on the Robertson (1990) chart (and assume $q_{c1N} = Q$). However, if $I_c \leq 2.6$, the exponent to calculate Q should be changed to n = 0.5 (i.e. essentially calculate q_{c1N} using Equation 8 since $\sigma_{vo} << q_c$) and I_c should be recalculated based on q_{c1N} and F. If the recalculated I_c remains less than 2.6, the data should be plotted on the Robertson (1990) chart using q_{c1N} based on n = 0.5. If, however, I_c iterates above and below a value of 2.6, depending which value of n is used, a value of n = 0.75 should be selected to calculate q_{c1N} (using Equation 8) and plot data on the Robertson (1990) chart. Note that if the in-situ effective overburden stresses are in the order of 50 kPa to 150 kPa, the choice of normalization has little effect on the calculated normalized penetration resistance.

The boundaries of soil behaviour type are given in terms of the index, I_c, as shown in Table 4.

Table 4. Boundaries of soil behaviour type (after Robertson, 1990).

Soil Behaviour Type Index, I_c	Zone	Soil Behaviour Type (see Figure 18)
$I_c < 1.31$	7	Gravelly sand to dense sand
$1.31 < I_c < 2.05$	6	Sands: clean sand to silty sand
$2.05 < I_c < 2.60$	5	Sand Mixtures: silty sand to sandy silt
$2.60 < I_c < 2.95$	4	Silt Mixtures: clayey silt to silty clay
$2.95 < I_c < 3.60$	3	Clays: silty clay to clay
$I_c > 3.60$	2	Organic soils: peats

The soil behaviour type index does not apply to Zones 1, 8 or 9. Along the normally consolidated region in Figure 18, soil behaviour type index increases with increasing apparent fines content and soil plasticity, and the following simplified relationship is suggested:

if $I_c < 1.26$	Apparent fines content, FC (%) = 0	(11a)
if $1.26 \leq I_c \leq 3.5$	Apparent fines content, FC (%) = $1.75\ I_c^{3.25} - 3.7$	(11b)
if $I_c > 3.5$	Apparent fines content, FC (%) = 100	(11c)

The range of potential correlations is illustrated in Figure 19, which shows the variation of soil behaviour type index (I_c) with apparent fines content and the effect of the degree of plasticity of the fines. The recommended relationship given in Equation 11 is also shown in Figure 19. Note that this equation is slightly modified from the original work by Robertson and Fear (1995) in order to increase the prediction of apparent FC for a given value of I_c.

The proposed correlation between CPT soil behaviour index (I_c) and apparent fines content is approximate, since the CPT responds to many other factors affecting soil behaviour, such as soil plasticity, mineralogy, sensitivity and stress history. However, for small projects, the above correlation provides a useful guide. Caution must be taken in applying Equation 11 to sands that plot in the region defined by $1.64 < I_c < 2.36$ and $F < 0.5\%$ in Figure 18, so as not to confuse very loose clean sands with denser sands containing fines. In this zone, it is suggested that the apparent fines content is set equal to 5%, such that no correction will be applied to the measured CPT tip resistance when the CPT data plot in this zone. To evaluate the correlation shown in Figure 19 it is important to show the complete soil profile (CPT and samples; e.g. see Figure 24), since comparing soil samples with an adjacent CPT at the same elevation can be misleading due to soil stratigraphic changes and soil heterogeneity.

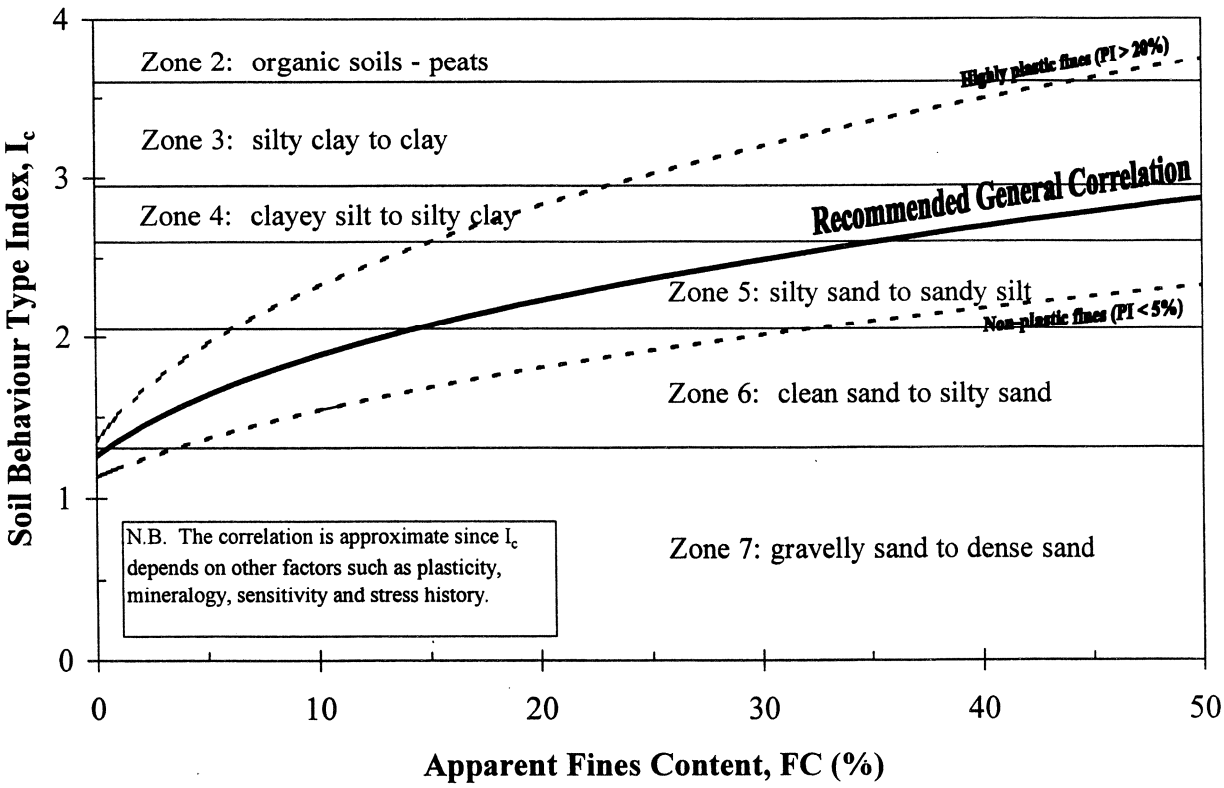

Figure 19 Variation of CPT soil behaviour type index (I_c) with apparent fines content in or close to the normally consolidated zone of the soil behaviour chart by Robertson (1990).

Based on the above method for estimating grain characteristics directly from the CPT using the soil behaviour index (I_c), the recommended relationship between I_c and the correction factor K_c is shown in Figure 20 and given by the following equations:

$$\text{if } I_c \leq 1.64 \qquad K_c = 1.0 \tag{12a}$$

$$\text{if } I_c > 1.64 \qquad K_c = -0.403\, I_c^4 + 5.581\, I_c^3 - 21.63\, I_c^2 + 33.75\, I_c - 17.88 \tag{12b}$$

The proposed correction factor, K_c, is approximate since the CPT responds to many factors, such as soil plasticity, fines content, mineralogy, soil sensitivity and stress history. However, for small projects or for initial screening on larger projects, the above correlation provides a useful guide. Caution must be taken in applying the relationship to sands that plot in the region defined by $1.64 < I_c < 2.36$ and $F \leq 0.5\%$ so as not to confuse very loose clean sands with sands containing fines. In this zone, it is suggested that the correction factor K_c be set to a value of 1.0 (i.e. assume that the sand is a clean sand).

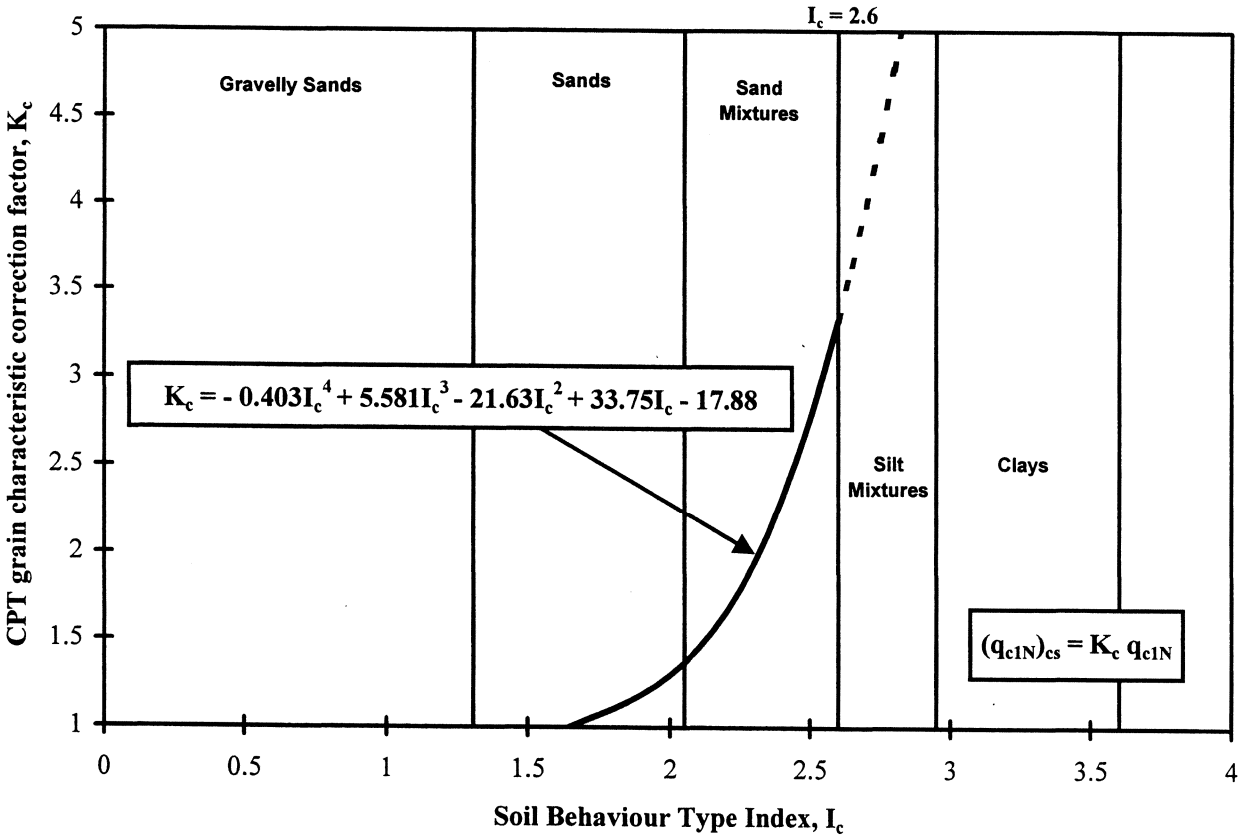

Figure 20 Recommended grain characteristic correction to obtain clean sand equivalent CPT penetration resistance in sandy soils.

Note that the relationship between the recommended correction factor, K_c, and soil behaviour type index, I_c, is shown dashed beyond an I_c of 2.6, which corresponds to an approximate apparent fines content of 35%. Soils with $I_c > 2.6$ fall into the clayey silt, silty clay and clay regions of the CPT soil behaviour chart (i.e. Zones 3 and 4). When the CPT indicates soils in these regions ($I_c > 2.6$), samples should be obtained and evaluated using the criteria shown in Figure 9. It is reasonable to assume, in general, that soils with $I_c > 2.6$ are non-liquefiable and that the correction K_c could be large. Soils that fall in the lower left region of the CPT soil behaviour chart (Figure 18), defined by $I_c > 2.6$ and $F \leq 1.0\%$, can be very sensitive and, hence, possibly susceptible to both cyclic and/or flow liquefaction. Soils in this region should be evaluated using criteria such as that shown in Figure 9 combined with additional testing.

Figure 21 shows the resulting equivalent CRR curves for I_c values of 1.64, 2.07 and 2.59 which represent approximate apparent fines contents of 5%, 15% and 35%, respectively.

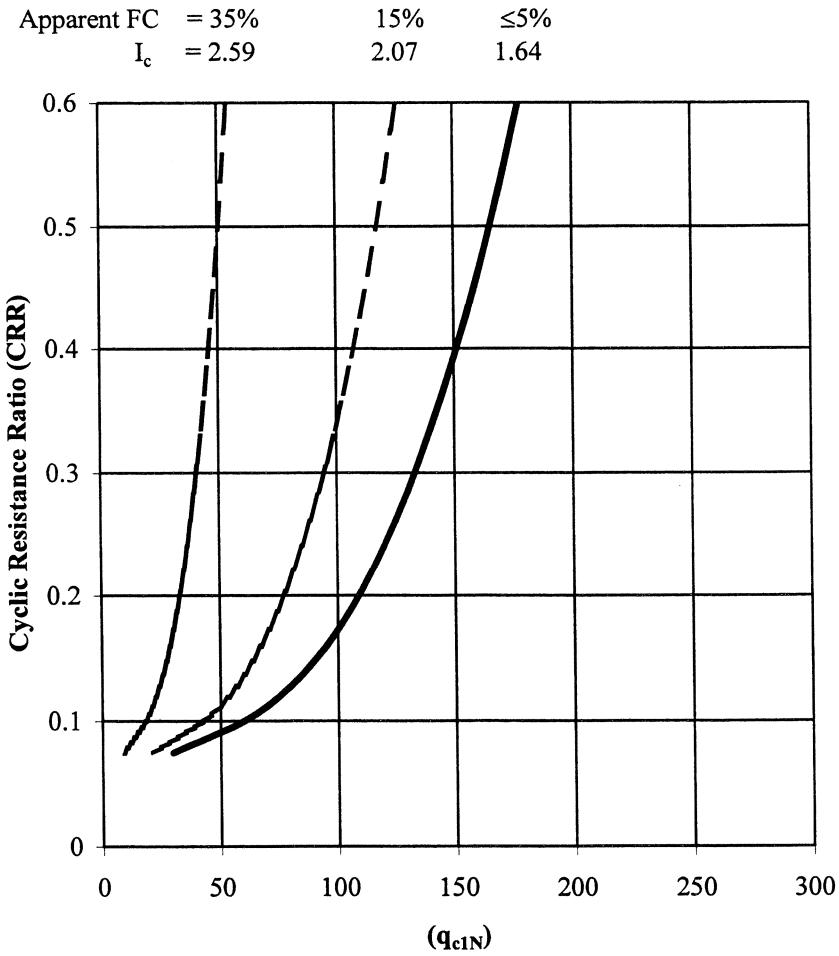

Figure 21 CPT base curves for various values of soil behaviour index, I_c (corresponding to various apparent fines contents, as indicated).

Influence of thin layers

A problem associated with the interpretation of penetration tests in interbedded soils occurs when thin sand layers are embedded in softer deposits. Theoretical as well as laboratory studies show that the cone resistance is influenced by the soil ahead of and behind the penetrating cone. The cone will start to sense a change in soil type before it reaches the new soil and will continue to sense the original soil even when it has entered a new soil. As a result, the CPT will not always measure the correct mechanical properties in thinly interbedded soils. The distance over which the cone tip senses an interface increases with increasing soil stiffness. In soft soils, the diameter of the sphere of influence can be as small as 2 to 3 cone diameters, whereas, in stiff soils, the sphere of influence can be up to 20 cone diameters. Hence, the cone resistance can fully respond (i.e. reach full value within the layer) in thin soft layers better than in thin stiff layers. Care should, therefore, be taken when interpreting cone resistance in thin sand layers located within soft clay or silt deposits. Based on a simplified elastic solution, Vreugdenhil et al. (1994) have

provided some insight as to how to correct cone data in thin layers. Vreugdenhil et al. (1994) have shown that the error in the measured cone resistance within thin stiff layers is a function of the thickness of the layer as well as the stiffness of the layer relative to that of the surrounding softer soil. The relative stiffness of the layers is reflected by the change in cone resistance from the soft surrounding soil to the stiff soil in the layer (q_{cA}/q_{cB}). Vreugdenhil et al. (1994) validated the model with laboratory and field data.

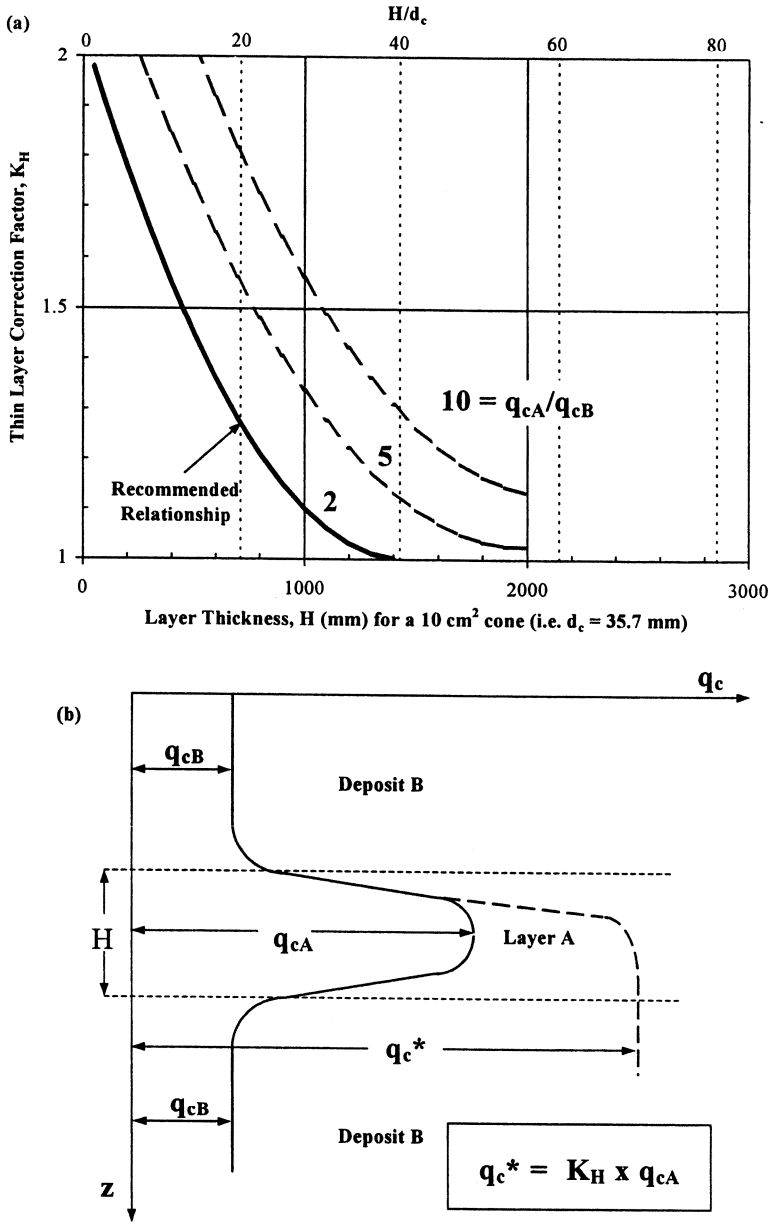

Figure 22 Suggested correction (K_H) to CPT penetration resistance in thin sand layers (based on results by Vreugdenhil et al., 1994) (after Robertson and Fear, 1995).

Based on this work, Robertson and Fear (1995) suggested a correction factor for cone resistance (originally termed K_c by Robertson and Fear (1995), but now termed K_H in order to prevent confusion with the correction outlined above for obtaining clean sand equivalent penetration resistance) as a function of layer thickness (H), as shown in Figure 22. The corrections apply only to thin sand layers embedded in thick fine-grained layers. The corrections appear to have a reasonable trend, but are rather large. Therefore, Robertson and Fear (1995) recommended a conservative correction (corresponding to $(q_{cA}/q_{cB}) = 2$) as is shown in Figure 22 and given by the following expression:

$$K_H = 0.5\left(\frac{H/d_c}{28} - 1.45\right)^2 + 1.0 \qquad (13)$$

where H is the layer thickness, in mm, for $H < 40.6\ d_c$; q_{cA} and q_{cB} are the tip resistances in the layer and in the soil surrounding the layer, respectively; and d_c is the cone diameter, in mm (e.g. for a 10 cm^2 cone, d_c=35.7 mm).

Thin sand layers embedded in soft clay deposits are often incorrectly classified as silty sands based on the CPT soil behaviour type charts. Hence, a slightly improved classification can be achieved if the cone resistance is first corrected for layer thickness before applying the classification charts.

Cyclic resistance from the CPT

In an earlier section, a method was suggested for estimating apparent fines content directly from CPT results, using Equation 11. Following the traditional SPT approach, the estimated apparent fines content could be used to estimate the correction necessary to obtain the clean sand equivalent penetration resistance. However, since other grain characteristics also influence the measured CPT penetration resistance, it is recommended that the necessary correction be estimated from the soil behaviour type index, as described above. Hence, Equations 9, 10 and 12 can be combined to estimate the equivalent clean sand normalized penetration resistance, $(q_{c1N})_{cs}$, directly from the measured CPT data. Then, using the equivalent clean sand normalized penetration resistance $(q_{c1N})_{cs}$, the CRR (for M = 7.5) can be estimated using the following simplified equation (which approximates the clean sand curve recommended in Figure 16):

$$\text{if } 50 \le (q_{c1N})_{cs} < 160 \qquad CRR = 93\left(\frac{(q_{c1N})_{cs}}{1000}\right)^3 + 0.08 \qquad (14a)$$

$$\text{if } (q_{c1N})_{cs} < 50 \qquad CRR = 0.833\left(\frac{(q_{c1N})_{cs}}{1000}\right) + 0.05 \qquad (14b)$$

In summary, Equations 9 to 12 and 14 (and Equation 13 if thin layers are present) can be combined to provide an integrated method for evaluating the cyclic resistance (M=7.5) of

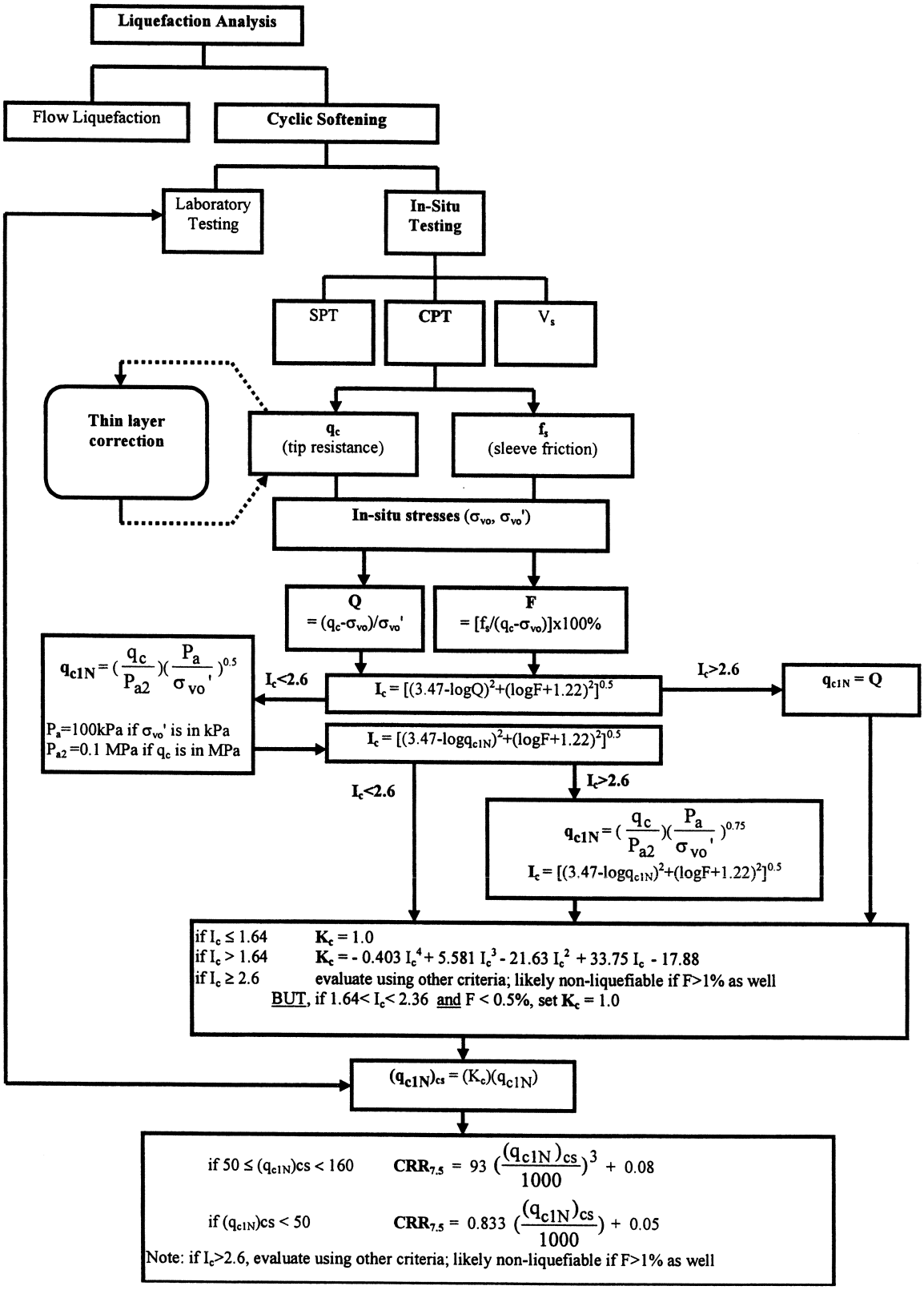

Figure 23 Flowchart illustrating the application of the integrated CPT method of evaluating cyclic resistance ratio (CRR) in sandy soils.

saturated sandy soils based on the CPT. The CPT-based method is an alternative to the SPT or shear wave velocity (V_s) based in-situ methods; however, using more than one method is useful in providing independent evaluations of liquefaction potential. The integrated CPT method is summarized in Figure 23 in the form of a flowchart. The flowchart clearly shows the step-by-step process involved in using the proposed integrated method based on the CPT for evaluating CRR and indicates the recommended equations for each step of the process.

An example of this proposed modified CPT-based method is shown in Figure 24 for the Moss Landing site that suffered cyclic liquefaction during the 1989 Loma Prieta earthquake in California (Boulanger et al., 1995 and 1997). The measured cone resistance is normalized and corrected for overburden stress to q_{c1N} and F and the soil behaviour type index (I_c) is calculated. The final continuous profile of CRR at N=15 cycles (M = 7.5) is calculated from the equivalent clean sand values of q_{c1N} (i.e. $(q_{c1N})_{cs} = K_c\ q_{c1N}$) and Equation 14. Included in Figure 24 are measured fines content values obtained from adjacent SPT samples. A good comparison is seen between the estimated apparent fines contents and the measured fines contents. Note that for $I_c > 2.6$ (i.e. FC > 35%; see Equation 11), the soil is considered to be non-liquefiable; however, this should be checked using other criteria (e.g. Marcuson et al., 1990; see Figure 9). The estimated zones of soil that are predicted to experience cyclic liquefaction are very similar to those observed and reported by Boulanger et al. (1995 and 1997).

Olsen (1988), Olsen and Koester (1995) and Suzuki et al. (1995b) have also suggested integrated methods to estimate the CRR of sandy soils directly from CPT results with the correlations presented in the form of soil behaviour charts. The Olsen and Koester (1995) method is based on SPT-CPT conversions plus some laboratory based CRR data. The method by Suzuki et al. (1995b) is based on limited field observations. The methods by Olsen and Koester (1995) and Suzuki et al. (1995b) are shown in Figure 25. The Olsen and Koester (1995) method uses a variable normalization technique, which requires an iterative process to determine the normalization. The method by Suzuki et al. (1995b) uses the q_{c1N} normalization suggested in this paper (Equation 8 with n=0.5). The Olsen and Koester (1995) method is very sensitive to small variations in measured friction ratio and the user is not able to adjust the correlations based on site specific experience. The friction sleeve measurement for the CPT can vary somewhat depending on specific CPT equipment and on tolerance details between the cone and the sleeve and hence, can be subject to some uncertainty. The method proposed in this paper is based on field observations and is essentially similar to those of Olsen and Koester (1995) and Suzuki et al. (1995b); however, the method described here is slightly more conservative and the process has been broken down into its individual components.

Built into each of the CPT methods for estimating CRR is the step of correcting the measured cone tip resistance to a clean sand equivalent value. It is the size of this correction that results in the largest differences between predicted values of CRR from the various methods. Figure 26 provides an approximate comparison between the methods by Stark and Olson (1995), Olsen and Koester (1995) and Suzuki et al. (1995b), in terms of K_c from soil behaviour type index, I_c. Also superimposed on Figure 26 is the recommended relationship, based on the equations given in this paper. The comparisons are approximate because the different authors

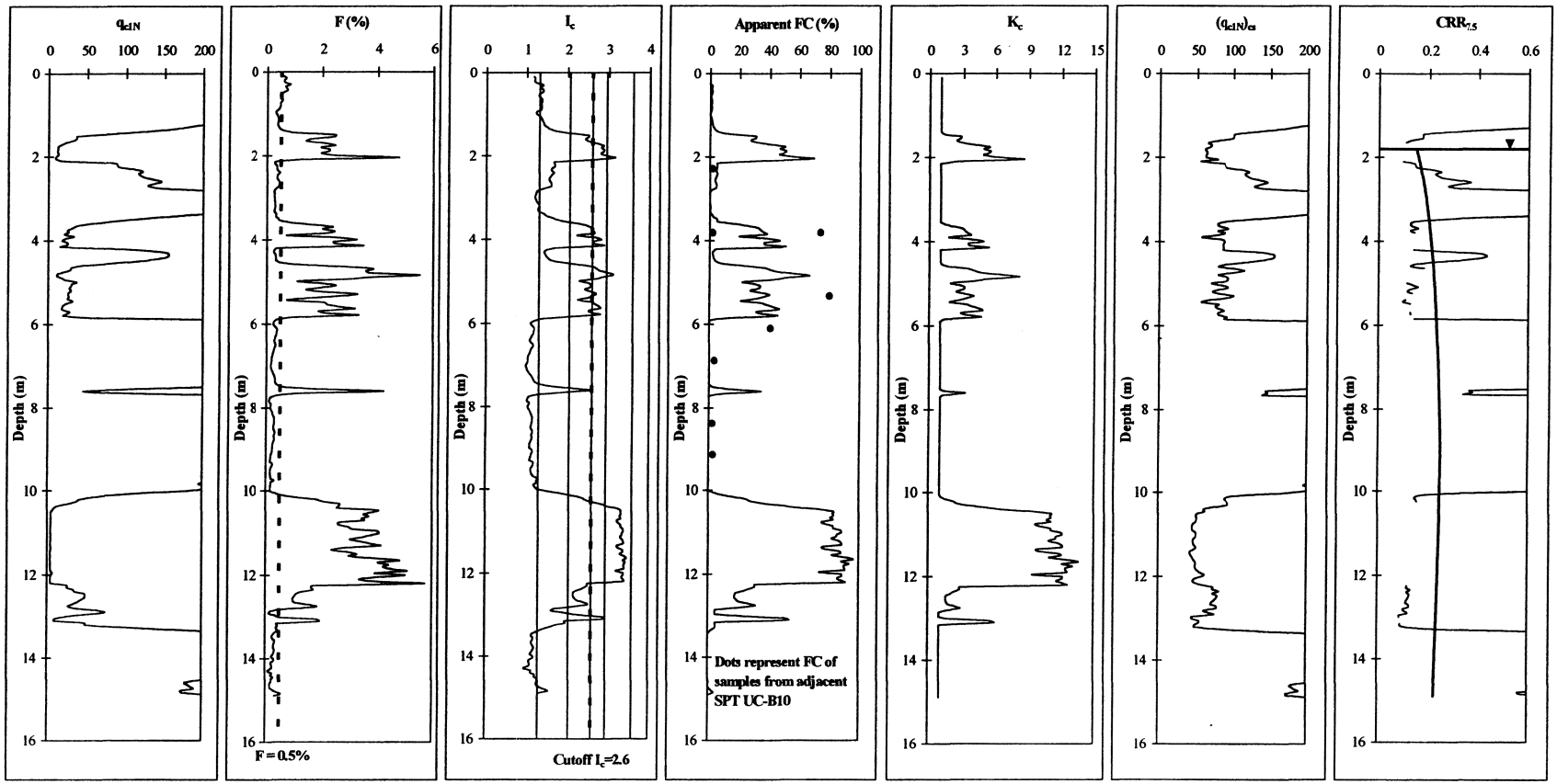

Figure 24 **Application of the integrated CPT method for estimating cyclic resistance ratio (CRR) to the State Beach site at Moss Landing, which suffered cyclic liquefaction during the 1989 Loma Prieta earthquake in California.**

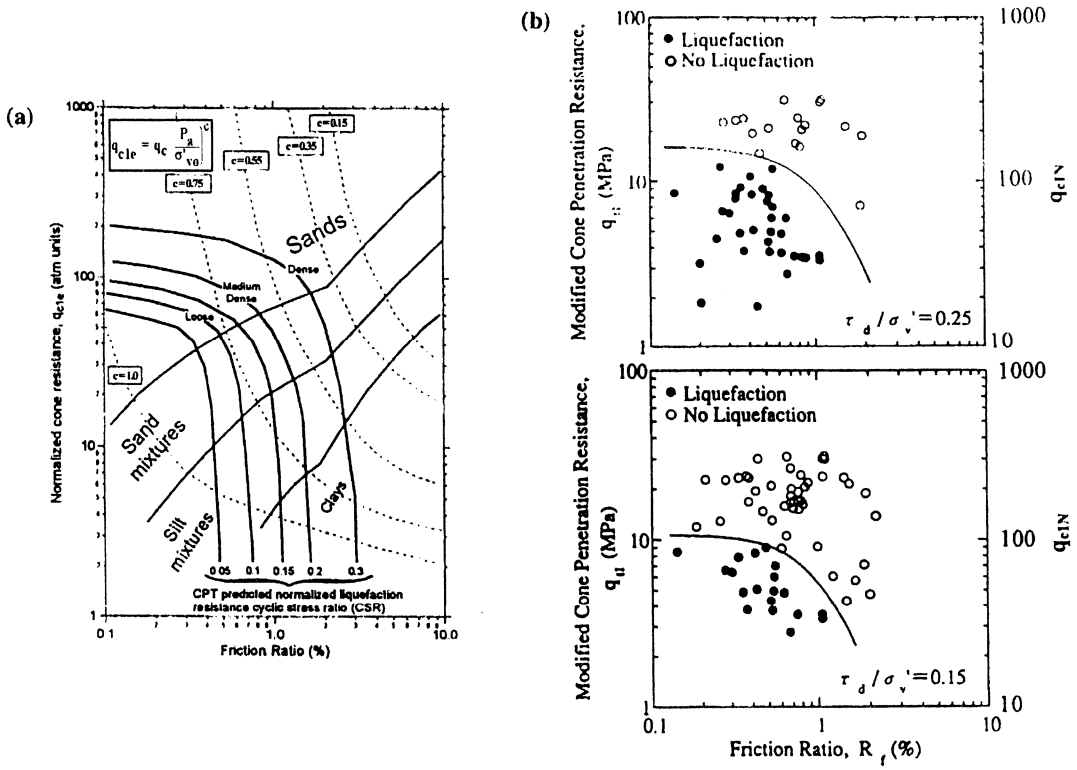

Figure 25 Comparison of estimating CRR from the CPT (a) CRR=0.05 to 0.3, after Olsen and Koester (1995); (b) CRR=0.15 and CRR=0.25, after Suzuki et al. (1995b).

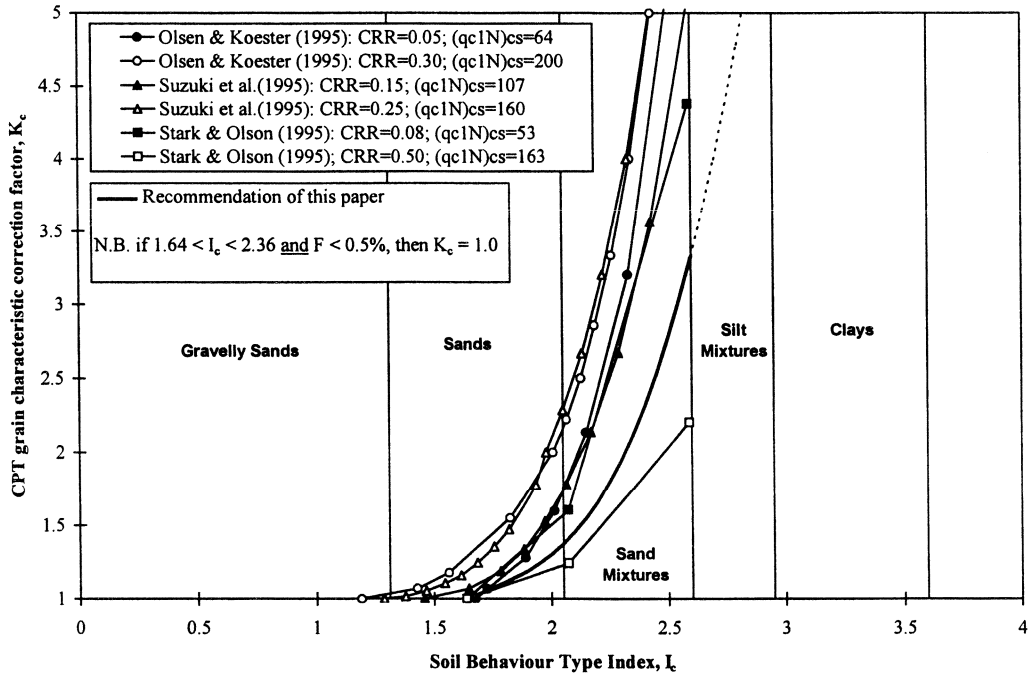

Figure 26 Approximate comparison of various methods for correcting CPT tip resistance to clean sand equivalent values, based on soil behaviour type.

use different normalizations when correcting CPT tip resistance for plotting data on a soil classification chart. However, for effective overburden stresses in the order of 100 kPa (≈ 1 tsf), all of the normalization methods should give similar values of normalized penetration resistance for the same value of measured penetration resistance. The boundaries between different soil behaviour types are also indicated on Figure 26, as a guide to the type of soil in which corrections of certain magnitudes are suggested by the various methods.

The methods by Suzuki et al. (1995b) and Olsen and Koester (1995) appear to be consistent with each other, indicating that K_c increases with increasing CRR. Very large corrections result especially in soils of high I_c. The method by Stark and Olson (1995) indicates that K_c decreases with increasing CRR for a given I_c and does not fit in with the trend of the combined Suzuki et al. (1995b) and Olsen and Koester (1995) lines. The magnitudes of the corrections suggested by Stark and Olson (1995) are generally smaller than the other methods.

Figure 26 indicates that the recommended correction is generally more conservative than the corrections proposed by the other authors. The other methods generally predict higher values of K_c and suggest that corrections should be applied beginning at lower values of I_c, particularly for higher values of CRR. Note that the recommended relationship between K_c and I_c is shown dashed beyond $I_c = 2.6$, which corresponds to an apparent FC of 35% (Equation 11). This shows that the integrated CPT method for evaluating CRR, as outlined here, does not apply to soils that would be classified as clayey silt, silty clay or clay. As explained earlier, when interpretation of the CPT indicates that these types of soils are present, samples should be obtained and evaluated using other criteria, such as that given in Figure 9 (Marcuson et al., 1990). It is logical that in non-liquefiable clay soils, the equivalent correction factor, K_c, could be very large for $I_c > 2.6$.

Recommendations

For low risk, small-scale projects, the potential for cyclic liquefaction can be estimated using penetration tests such as the SPT or CPT. The CPT is generally more repeatable than the SPT and is the preferred test, where possible. The CPT provides continuous profiles of penetration resistance, which are useful for identifying soil stratigraphy and for providing continuous profiles of estimated cyclic resistance ratio (CRR). When using the SPT, care should be taken to ensure that the test is carried out according to the above recommended procedures. Corrections are required for both the SPT and CPT for grain characteristics, such as fines content and plasticity. For the CPT, these corrections are best expressed as a function of soil behaviour type index, I_c, which is affected by a variety of grain characteristics.

For medium to high-risk projects, the SPT and CPT can be useful for providing a preliminary estimate of liquefaction potential in sandy soils. For higher risk projects, it is important to measure the rod energy during each SPT. For higher risk projects, it is also preferred practice to drill sufficient boreholes adjacent to CPT soundings to verify various soil types encountered and to perform index testing on disturbed samples. A procedure has been described to correct the

measured cone resistance for grain characteristics based on the CPT soil behaviour type index, I_c. The corrections are approximate, since the CPT responds to many factors affecting soil behaviour. Expressing the corrections in terms of soil behaviour index is the preferred method of incorporating the effects of various grain characteristics, in addition to fines content. When possible, it is recommended that the corrections be evaluated and modified to suit a specific site and project. However, for small-scale low risk projects and in the initial screening process for higher risk projects, the suggested general corrections provide a useful guide. A guide has also been given for correcting CPT results in thin sand layers embedded in softer fine-grained deposits. The SPT and CPT are generally limited to sandy soils with limited gravel contents. In soils with high gravel contents, penetration may be limited.

A summary of the CPT method is shown in Figure 27, which identifies the zones in which soils are susceptible to cyclic liquefaction (primarily Zone A). In general, soils with $I_c > 2.6$ and $F > 1.0\%$ (Zone B) are likely non-liquefiable. Soils that plot in the lower left portion of the chart (Zone C; $I_c > 2.6$ and $F < 1.0\%$) may be susceptible to cyclic and/or flow liquefaction due to the sensitive nature of these soils. Soils in this region should be evaluated using other criteria.

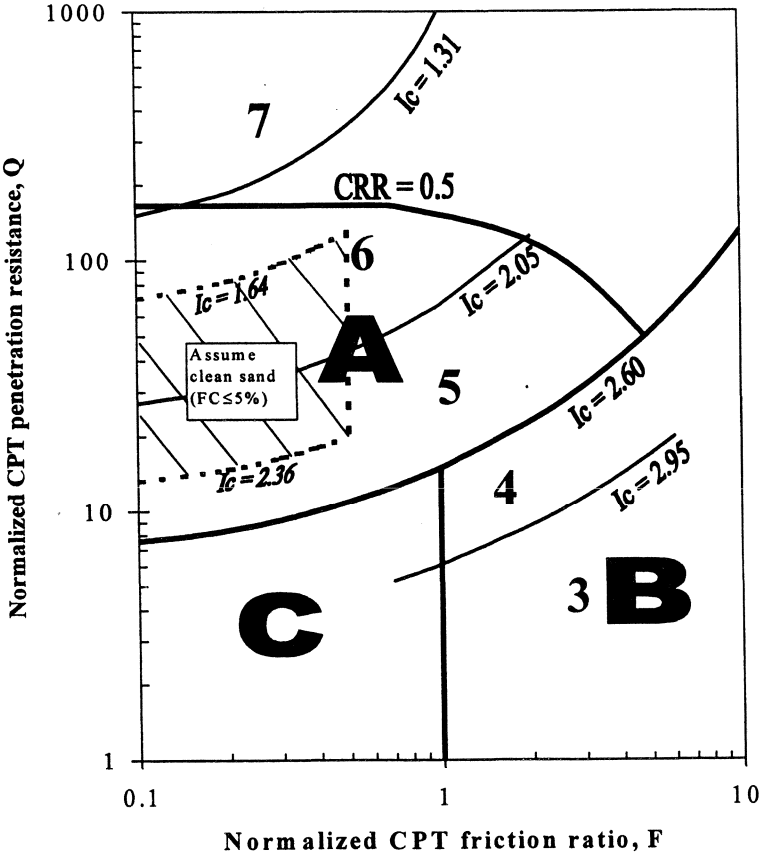

Zone A: Cyclic liquefaction possible – depends on size and duration of cyclic loading.
Zone B: Liquefaction unlikely – check other criteria.
Zone C: Flow/cyclic liquefaction possible – depends on soil plasticity and sensitivity as well as size and duration of cyclic loading.

Figure 27 Summary of liquefaction potential on soil behaviour chart by Robertson (1990).

Caution should be exercised when extrapolating the suggested SPT and CPT correlations to conditions outside of the range from which the field performance data were obtained. An important feature to recognize is that the correlations appear to be based on average values for the inferred liquefied layers. However, the correlations are often applied to all measured SPT and/or CPT values, which include low values below the average for a given sand deposit. Hence, the correlations could be conservative in variable stratified deposits where a small part of the penetration data could indicate possible liquefaction.

Finally, as mentioned earlier, it is clearly useful to evaluate CRR using more than one method. The seismic CPT provides a useful technique for independently evaluating liquefaction potential, since it measures both the usual CPT parameters and shear wave velocities within the same borehole. The CPT provides detailed profiles of cone tip resistance, but the penetration resistance is sensitive to grain characteristics, such as fines content and soil mineralogy and, hence, corrections are required. The seismic part of the CPT provides a shear wave velocity profile typically averaged over 1 m intervals and, therefore, contains less detail than the cone tip resistance profile. However, shear wave velocity is less influenced by grain characteristics and few or no corrections are required (Robertson et al, 1992; Andrus and Stokoe, 1996). Shear wave velocity should be measured with care in order to provide the most accurate results possible since the estimated CRR is sensitive to small changes in shear wave velocity. There should be consistency in the liquefaction evaluation using either method. If the two methods provide different predictions of CRR profiles, samples should be obtained to evaluate the grain characteristics of the soil.

Acknowledgements

The authors appreciate the contributions of the members of the 1996 NCEER Workshop on Evaluation of Liquefaction Resistance (T.L. Youd, Chair) that was held in Salt Lake City, Utah. Particular appreciation is extended to the following individuals: W.D.L. Finn, I.M. Idriss, J. Koester, S. Liao, W.F. Marcuson III, J.K. Mitchell, R. Olsen, R. Seed, and T.L. Youd.

References

Andrus, R.D., and Stokoe, K.H. 1996. Guidelines for evaluation of liquefaction resistance using shear wave velocity. Submission to the 1996 NCEER Workshop on Evaluation of Liquefaction Resistance (T.L. Youd, Chair), Salt Lake City, Utah.

Bartlett, S.F., and Youd, T.L. 1995. Empirical prediction of liquefaction induced lateral spread. Journal of Geotechnical Engineering, ASCE, **121**(3): 249-261.

Been, K., Jefferies, M. G., and Hachey, J. 1991. The critical state of sands. Géotechnique, **41**(3): 365-381.

Bishop, A.W. 1973. The stability of tips and spoil heaps. Quarterly Journal of Engineering. Geology, **6**: 335-376.

Blake, T.F. 1996. Personal communication from T.L. Youd, 1996.

Boulanger, R.W., Idriss, I.M., and Mejia, L.H. 1995. Investigation and evaluation of liquefaction related ground displacements at Moss Landing during the 1989 Loma Prieta earthquake. Center for Geotechnical Modeling, Department of Civil and Environmental Engineering, College of Engineering, University of California at Davis, Report No. UCD/CGM-95/02.

Boulanger, R.W., Mejia, L.H., and Idriss, I.M. 1997. Liquefaction at Moss Landing during Loma Prieta earthquake, Journal of Geotechnical and Geoenvironmental Engineering, **123**(5): 453-467.

Casagrande, A. 1965. The role of the "calculated risk" in earthwork and foundation engineering. The Terzaghi Lecture, Journal of Soil Mechanics and Foundation Division, ASCE, **91**(4): 1-40.

Castro, G. 1969. Liquefaction of sands. Harvard Soil Mechanics Series No. 81, Harvard University, Cambridge, MA.

Dobry, R., Ladd, R.S., Yokel, F.Y., Chung, R.M., and Powell, D. 1982. Prediction of pore water pressure buildup and liquefaction of sands during earthquakes by the cyclic strain method. NBS Building Science Series 138, U.S. Department of Commerce, National Bureau of Standards, Gaithersburg, MD, 152p.

Fear, C.E., and McRoberts, E.C. 1995. Reconsideration of initiation of liquefaction in sandy soils. Journal of Geotechnical Engineering, ASCE, **121**(3): 249-261.

Finn, W.D.L. 1981. Liquefaction potential: developments since 1976. Proceedings, 1st International Conference on Recent Advances in Geotechnical Earthquake Engineering and Soil Dynamics, St. Louis, Vol. 2, pp. 655-681.

Hofmann, B.A., Sego, D.C., and Robertson, P.K. 1995. Undisturbed sampling of a deep loose sand deposit using ground freezing. Proceedings of the 47th Canadian Geotechnical Conference, Halifax, Nova Scotia, pp. 287-296.

Hofmann, B.A., 1997. In-situ ground freezing to obtain undisturbed samples of loose sand for liquefaction assessment, Ph.D. Thesis, University of Alberta, Edmonton, Alberta, Canada.

Ishihara, K. 1993. Liquefaction and flow failure during earthquakes. The 33rd Rankine Lecture. Géotechnique **43**(3): 351-415.

Ishihara, K., and Koseki, J. 1989. Cyclic shear strength of fines-containing sands. Earthquake Geotechnical Engineering. Proceedings, Discussion Session on Influence of Local Conditions on Seismic Response, 12th International Conference on Soil Mechanics and Foundation Engineering, Rio de Janeiro, pp. 101-106.

Jefferies, M.G., and Davies, M.P. 1993. Use of CPTu to estimate equivalent SPT N_{60}. ASTM Geotechnical Testing Journal, **16**(4): 458-467.

Kayen, R.E., Mitchell, J.K., Lodge, A., Seed, R.B., Nishio, S., and Coutinho, R. 1992. Evaluation of SPT-, CPT-, and shear wave-based methods for liquefaction potential assessment using Loma Prieta data. Proceedings, 4th Japan-U.S. Workshop on Earthquake Resistant Design of Lifeline Facilities and Countermeasures for Soil Liquefaction, Technical Report NCEER-94-0019, *Edited by* M. Hamada and T.D. O-Rourke, Vol.1, pp. 177-204.

Kokusho, T., Yoshida, Y., and Eashi, Y. 1983. Evaluation of seismic stability of dense sand layer (Part 2) - Evaluation method by standard penetration test. Electric Power Central Research Institute, Japan, Report 383026(in Japanese).

Koppejan, A.W., Van Wamelen, B.M., and Weinberg, L.J.H. 1948. Coastal landslides in the Dutch province of Zealand. Proceedings, 2nd International Conference on Soil Mechanics and Foundation Engineering, Rotterdam, Holland, pp. 89-96.

Kulhawy, F.H., and Mayne, P.W. 1990. Manual on Estimating Soil Properties for Foundation Design. Cornell University, EL-6800, Research Project 1493-6, prepared for Electric Power Research Institute.

Ladd, R.S. 1974. Specimen preparation and liquefaction of sands. Journal of ASCE, **110**(GT10): 1180-1184.

Liao, S.S.C., and Whitman, R.V. 1986a. Overburden correction factors for SPT in sand, Journal of Geotechnical Engineering, ASCE, **112**(3): 373-377.

Liao, S.S.C., and Whitman R.V. 1986b. A catalog of liquefaction and non-liquefaction occurrences during earthquakes. Research Report, Department of Civil Eng., M.I.T., Cambridge, MA.

Liao, S.S.C., Veneziano, D., and Whitman, R.V. 1988. Regression models for evaluating liquefaction probability. Journal of Geotechnical Engineering, ASCE, **114**(4): 389-411.

Marcuson, III, W.F., Hynes, M.E., and Franklin, A.G. 1990. Evaluation and use of residual strength in seismic safety analysis of embankments. Earthquake Spectra, **6**(3): 529-572.

Mitchell, J.K., and Tseng, D.-J. 1990. Assessment of liquefaction potential by cone penetration resistance. Proceedings, H. Bolton Seed Memorial Symposium, Berkeley, California, *Edited by* J.M. Duncan, Vol. 2, pp. 335-350.

Mogami, and Kubo 1953. The behaviour of soil during vibration. Proceedings, 3rd International Conference on Soil Mechanics and Foundation Engineering, Vol. 1, pp. 152-153.

Mulilis, J.P., Seed, H.B., Chan, C.K., Mitchell, J.K., and Arulanandan, K. 1977. Effects of sample preparation on sand liquefaction. Journal of ASCE, **103**(GT2): 99-108.

Olsen, R.S. 1988. Using the CPT for dynamic response characterization. Proceedings, Earthquake Engineering and Soil Dynamics II Conference, ASCE.

Olsen R.S., and Koester J.P. 1995. Prediction of liquefaction resistance using the CPT. Proceedings, International Symposium on Cone Penetration Testing, CPT'95. Linkoping, Sweden, Vol. 2, pp. 251-256.

Olsen, R.S., and Malone, P.G. 1988. Soil classification and site characterization using the cone penetrometer test. Penetration Testing 1988, ISOPT-1, *Edited by* De Ruiter, Balkema, Rotterdam, Vol. 2, pp. 887-893.

Pando, M., and Robertson, P.K. 1995. Evaluation of shear stress reversal due to earthquake loading for sloping ground. Proceedings, 48th Canadian Geotechnical Conference, Vancouver, B.C., Vol. 2, pp. 955-962.

Poorooshasb, H.B., and Consoli, N.C. 1991. The ultimate state. Proceedings, IX Pan-American Conference, pp. 1083-1090.

Robertson, P.K. 1990. Soil classification using the CPT. Canadian Geotechnical Journal, **27**(1): 151-158.

Robertson, P.K. 1994. Suggested terminology for liquefaction. Proceedings, 47th Canadian Geotechnical Conference, Halifax, Nova Scotia, pp. 277-286.

Robertson, P.K., and Campanella, R.G. 1985. Liquefaction potential of sands using the cone penetration test. Journal of Geotechnical Division of ASCE, March 1985, **22**(3): 298-307.

Robertson, P.K., and Campanella, R.G. 1988. Design manual for use of CPT and CPTu. Pennsylvania Department of Transportation, (Penn Dot), 200 p.

Robertson, P.K., and Fear, C.E. 1995. Liquefaction of sands and its evaluation. Proceedings, IS Tokyo '95, 1st International Conference on Earthquake Geotechnical Eng., Keynote Lecture.

Robertson, P.K., Campanella, R.G., and Wightman, A. 1983. SPT-CPT correlations. Journal. of Geotechnical Division of ASCE, **109**: 1449-1459.

Robertson, P.K., Woeller, D.J., and Finn, W.D.L. 1992. Seismic cone penetration test for evaluating liquefaction potential under cyclic loading. Canadian Geotechnical Journal, **29**: 686-695.

Roscoe, K.H., Schofield, A.N., and Wroth, C.P. 1958. On the yielding of soils. Géotechnique, **8**: 22-53.

Sasitharan, S., Robertson, P.K., Sego, D.C., and Morgenstern, N.R. 1994. State boundary surface for very loose sand and its practical implications. Canadian Geotechnical Journal, **31**(3): 321-334.

Schmertmann, J.H. 1979. Statics of SPT. Journal of the Geotechnical Engineering Division, ASCE, **105**(GT5): 655-670.

Seed, H.B. 1979. Soil liquefaction and cyclic mobility evaluation for level ground during earthquakes. Journal of the Geotechnical Engineering Division, ASCE, **105**(GT2): 201-255.

Seed, H.B., and de Alba, P. 1986. Use of SPT and CPT tests for evaluating the liquefaction resistance of sands. Use of In-situ Tests in Geotechnical Engineering, ASCE, Geotechnical Special Publication, **6**: 281-302.

Seed H.B., and Idriss, I.M. 1971. Simplified procedure for evaluating soil liquefaction potential. Journal of the Soil Mechanics and Foundation Division, ASCE, **97**(SM9): 1249-1273.

Seed, H.B., Tokimatsu, K., Harder, L.F., and Chung, R. 1985. Influence of SPT procedures in soil liquefaction resistance evaluations. Journal of Geotechnical Engineering, ASCE **111**(12): 1425-1445.

Sego, D.C., Robertson, P.K., Sasitharan, S., Kilpatrick, B.L., and Pillai, V.S. 1994. Ground freezing and sampling of foundation soils at Duncan Dam. Canadian Geotechnical Journal, **31**(6): 939-950.

Shibata, T. 1981. Relations between N-value and liquefaction potential of sand deposits. Proceedings, 16th Annual Convention of Japanese Society of Soil Mechanics and Foundation Engineering, pp. 621-624 (in Japanese).

Shibata, T., and Teparaska, W. 1988. Evaluation of liquefaction potentials of soils using cone penetration tests. Soils and Foundations, **28**(2): 49-60.

Skempton, A.W. 1986. Standard penetration test procedures and the effects in sands of overburden pressure, relative density, particle size, aging and overconsolidation. Géotechnique **36**(3): 425-447.

Sladen, J.A., D'Hollander, R.D., and Krahn, J. 1985. The liquefaction of sands, a collapse surface approach. Canadian Geotechnical Journal, **22**: 564-578.

Stark, T.D., and Olson, S.M. 1995. Liquefaction resistance using CPT and field case histories. Journal of Geotechnical Engineering, ASCE **121**(12), 856-869.

Suzuki, Y., Tokimatsu, K., Taye, Y., and Kubota, Y. 1995a. Correlation between CPT data and dynamic properties of in-situ frozen samples. Proceedings, 3rd International Conference on Recent Advances in Geotechnical Earthquake Engineering and Soil Dynamics, St. Louis, U.S.A., Vol.1.

Suzuki, Y., Tokimatsu, K., Koyamada, K., Taya, Y., and Kubota, Y. 1995b. Field correlation of soil liquefaction based on CPT data. Proceedings, International Symposium on Cone Penetration Testing, CPT'95. Linkoping, Sweden, Vol. 2, pp. 583-588.

Tatsuoka, F., Iwasaki, T., Touida, K., Yasuda, S., Hirose, M., Imai, T., and Kon-no, M. 1980. Standard penetration tests and soil liquefaction potential evaluation. Soils and Foundations, **20**(4): 95-111.

Tatsuoka, F., Ochi, K., Fujii, S., and Okamoto, M. 1986. Cyclic undrained triaxial and torsional shear strength of sands for different sample preparation methods. Soil and Foundations, **26**(3): 23-41.

Terzaghi, K. and Peck, R.B. 1948. Soil mechanics in engineering practice. John Wiley and Sons, Inc., 2nd edition.

Tokimatsu, K., and Hosaka, Y. 1986. Effects of sample disturbance on dynamic properties of sand. Soils and Foundations, **26**(1): 53-64.

Tokimatsu, K., and Yoshimi, Y. 1983. Empirical correlation of soil liquefaction based on SPT N-value and fines content. Soils and Foundations, **23**(4): 56-74.

Vreugdenhil, R., Davis, R., and Berrill, J. 1994. Interpretation of cone penetration results in multilayered soils. International Journal for Numerical Methods in Geomechanics, **18**: 585-599.

Wang, W. 1979. Some findings in soil liquefaction. Water Conservancy and Hydroelectric Power Scientific Research Institute, Beijing, China.

Yoshimi, Y., Richart, F.E., Prakash, S., Balkan, D.D., and Ilyichev 1977. Soil dynamics and its application to foundation engineering. Proceedings, 9th International Conference on Soil Mechanics and Foundation Engineering, Tokyo, Vol. 2, pp. 605-650.

Yoshimi, Y., Hatanaka, M., and Oh-Oka, H. 1978. Undisturbed sampling of saturated sands by freezing. Soils and Foundations, **18**(3): 105-111.

Yoshimi, Y., Tokimatsu, K., and Hosaka, Y. 1989. Evaluation of liquefaction resistance of clean sands based on high-quality undisturbed samples. Soils and Foundations, **29**(1): 93-104.

Yoshimi, Y., Tokimatsu, K., and Ohara, J. 1994. In situ liquefaction resistance of clean sands over a wide density range. Géotechnique, **44**(3): 479-494.

Youd, T.L., Idriss, I.M., Andrus, R.D., Arango, I., Castro, G., Christian, J.T., Dobry, R., Finn, W.D.L., Harder, L.F., Hynes, M.E., Ishihara, K., Koester, J., Liao, S., Marcuson III, W.F., Martin, G.R., Mitchell, J.K., Moriwaki, Y., Power, M.S., Robertson, P.K., Seed, R., and Stokoe, K.H. 1997. Summary report of the 1996 NCEER Workshop on Evaluation of Liquefaction Resistance, Salt Lake City, Utah.

Liquefaction Resistance Based on Shear Wave Velocity

By Ronald D. Andrus[1] and Kenneth H. Stokoe, II[2]

[1]Research Civil Engineer
National Institute of Standards and Technology

[2]Professor of Civil Engineering
The University of Texas at Austin

Abstract

This report reviews the current simplified procedures for evaluating the liquefaction resistance of granular soil deposits using small-strain shear wave velocity. These procedures were developed from analytical studies, laboratory studies, or very limited field performance data. Their accuracy is evaluated through field performance data from 20 earthquakes and in situ shear wave velocity measurements at over 50 different sites (124 test arrays) in soils ranging from sandy gravel with cobbles to profiles including silty clay layers, resulting in a total of 193 liquefaction and non-liquefaction case histories. The current procedures correctly predict high liquefaction potential at many sites where surface manifestations of liquefaction were observed. Revisions and enhancements to the current procedures are proposed using the compiled case history data. The recommended procedure follows the general format of the SPT- and CPT-based procedures. Liquefaction potential boundaries are established by applying a modified relationship between shear wave velocity and cyclic stress ratio for constant average cyclic shear strain suggested by Dobry. These new boundaries, which are simply defined mathematically and easy to implement, correctly predict moderate to high liquefaction potential for more than 95% of the liquefaction case histories. Additional case histories are needed of all types of soils that have and have not liquefied during earthquakes, particularly from deeper deposits (depth > 8 m) and from denser soils (V_S > 200 m/s) shaken by stronger ground motions (a_{max} > 0.4 g), to further validate the proposed procedures.

Introduction

During the past decade, several simplified procedures using small-strain shear wave velocity, V_S, have been proposed for assessing the liquefaction resistance of granular soils (Stokoe et al. 1988b; Tokimatsu et al. 1991a; Robertson et al. 1992; Kayen et al. 1992; Andrus 1994; Lodge 1994). The use of V_S as an index of liquefaction resistance is justified since both V_S and liquefaction resistance are influenced by many of the same factors (e.g. void ratio, effective confining pressure, stress history, and geologic age).

The in situ V_S can be measured by a number of techniques such as the crosshole seismic test, the Seismic Cone Penetration Test (SCPT), or the Spectral-Analysis-of-Surface-Wave (SASW) test. The accuracy of these techniques can be sensitive to procedural details, soil conditions, and interpretation methods. Some advantages of using V_S are:

- Measurements are possible in soils that are hard to sample, such as gravelly soils, and at sites where borings or soundings may not be permitted, such as capped landfills;

- Measurements can be performed in small laboratory specimens, allowing direct comparisons between measured laboratory and field behavior;

- V_S is directly related to small-strain shear modulus, G_{max}, a parameter required in analytical procedures for estimating dynamic shearing strain in soils; and

- For large earthquake magnitudes and long durations of shaking, the cyclic shear strain needed for liquefaction decreases and approaches the threshold strain in sand ($\approx 0.02\%$), thus making it possible to conduct analytical evaluations of liquefaction using V_S and G_{max} as basic parameters (Dobry et al. 1981; Seed et al. 1983).

Two limitations of using V_S to evaluate liquefaction resistance are: (1) Field seismic measurements are made with small strains, whereas liquefaction is a large-strain phenomenon (Roy et al. 1996). This limitation can be significant for cemented soils, since V_S is highly sensitive to weak interparticle bonding which is eliminated at large strains. (2) Seismic testing does not provide samples for classification of soils and identification of non-liquefiable soft clay-rich soils. Non-liquefiable soils by the so-called Chinese criteria have clay contents (particles smaller than 5 μm) greater than 15%, liquid limits greater than 35%, or moisture contents less than 90% of the liquid limit (Seed and Idriss 1982). To compensate for these limitations, a limited number of borings should be drilled and samples taken to identify weakly cemented soils that might be liquefiable but classed as non-liquefiable by V_S criteria and also to identify non-liquefiable clay-rich soils that otherwise might be classed as liquefiable.

The purpose of this report is to recommend guidelines for evaluating liquefaction resistance using in situ measurements of V_S. To accomplish this purpose, current procedures are reviewed and their accuracy is evaluated using V_S measurements at over 50 different sites (124 test arrays) and field performance data from 20 earthquakes, resulting in a total of 193 liquefaction and non-liquefaction case histories.

Earthquake and site characteristics used in the evaluations are summarized in Table 1. In Column 2 of Table 1, test array refers to the two boreholes used for crosshole measurements, the borehole (or cone sounding) and source used for downhole measurements, or the line of receivers used for SASW measurements. The occurrence of liquefaction is based on the appearance of sand boils, ground cracks and fissures, or ground settlement. The shear wave velocities used in the subsequent evaluations are either the average or minimum of values reported by the investigator(s) for the most vulnerable layer at the test array. Shown in Fig. 1 are the relationships between shear wave velocity and depth. Some of the velocities are from measurements made before the earthquake, and others are from measurements made following the earthquake. The values of total vertical stress, σ_v, and effective vertical stress, σ'_v, listed in Columns 8 and 9 of Table 1 are averages for the depth range of the measurements, estimated using total unit weights reported by the investigator(s). When no values are reported, total unit weights of 17.3 kN/m^3 for soils above the water table and 18.9 kN/m^3 for soils below the water table are assumed. The materials comprising the most vulnerable layer at all sites are Holocene to latest Pleistocene age (< 15,000 years). The peak horizontal ground surface accelerations, a_{max}, used in subsequent evaluations are either the peak value for the larger of the x and y ground motion records or the average of peak values for the x and y ground motion records that would have occurred at the site in the absence of liquefaction. Values of a_{max} are determined by averaging estimates reported by the investigator(s) and estimates made as part of this study using attenuation relationships developed from published ground surface acceleration data.

The proposed liquefaction assessment procedures can be divided into three general categories: (1) procedures developed from analytical studies; (2) procedures developed from laboratory studies; and (3) procedures developed from field performance studies.

Procedures Developed From Analytical Studies

Stokoe et al. (1988b) applied the cyclic strain approach developed by Dobry and his colleagues (1982) in a parametric study of the liquefaction potential of sandy soils in the Imperial Valley, California. In the cyclic strain approach, the peak cyclic shearing strain at which the cyclic pore water pressure equals the confining pressure is used as the criterion for liquefaction occurrence.

Two generalized soil profiles were used in the parametric study. The first generalized soil profile contained a shallow (≤ 12 m) liquefiable sand layer. The three parameters of the sand layer which were varied are: soil stiffness in terms of V_S (or small-strain shear modulus), depth, and thickness. Depicted in Fig. 2a are three variations of the first generalized soil profile. The second generalized soil profile is presented in Fig. 2b, and was simply a 61-m thick clay deposit representative of a soil site in the Imperial Valley upon which strong-motion accelerographs

Table 1 - V_S-based Liquefaction and Non-liquefaction Case Histories

Site (1)	Test array (2)	Measure-ment type (3)	Lique-faction observed ? (4)	Water table depth (m) (5)	Top of layer depth (m) (6)	Layer thick-ness (m) (7)	σ_v (kPa) (8)	σ'_v (kPa) (9)	Soil type (10)	Aver-age V_S (m/s) (11)	Aver-age V_{S1} (m/s) (12)	Aver-age a_{max} (g) (13)	Cyclic stress ratio (14)	Reference (15)
(a) 1906 San Francisco, California Earthquake (M_W = 7.7)														
Coyote Creek	SR1	crosshole	yes	2.4	3.5	2.5	83.6	62.1	sand &	136	153	0.36	0.30	Youd and
	R1R2	crosshole	yes	2.4	3.5	2.5	75.4	58.2	gravel	154	177	0.36	0.29	Hoose
	R1R3	crosshole	yes	2.4	3.5	2.5	75.4	58.2		161	185	0.36	0.29	(1978);
	R2R3	crosshole	yes	2.4	3.5	2.5	75.4	58.2		173	198	0.36	0.29	Barrow (1983);
Salinas River, north	SR1	crosshole	no	6.0	9.1	1.5	178.2	140.8	sandy silt	177	162	0.32	0.24	Bennett and
	R1R2	crosshole	no	6.0	9.1	1.5	178.2	140.8		195	179	0.32	0.24	Tinsley
	R1R3	crosshole	no	6.0	9.1	1.5	178.2	140.8		200	184	0.32	0.24	(1995)
	R2R3	crosshole	no	6.0	9.1	1.5	178.2	140.8		199	183	0.32	0.24	
Salinas River, south	SR1	crosshole	yes	6.0	6.5	4.5	142.2	123.5	sand &	131	124	0.32	0.22	
	R1R2	crosshole	yes	6.0	6.5	4.5	142.2	123.5	silty sand	149	141	0.32	0.22	
	R1R3	crosshole	yes	6.0	6.5	4.5	142.2	123.5		158	150	0.32	0.22	
	R2R3	crosshole	yes	6.0	6.5	4.5	142.2	123.5		168	159	0.32	0.22	
(b) 1964 Niigata, Japan Earthquake (M_W = 7.5)														
Niigata City	A1	SASW	no	5.0	5.0	2.5	110.9	97.7	sand	163	164	0.16	0.11	Tokimatsu et
	C1	SASW	yes	1.2	1.6	6.5	90.0	54.7	sand	115	136	0.16	0.16	al. (1991a)
	C2	SASW	yes	1.2	1.2	4.8	67.8	44.5	sand	118	148	0.16	0.14	
(c) 1975 Haicheng, PRC Earthquake (M_W = 7.1)														
Paper Mill		downhole	yes	1.0	3.0	2.0	54.7	35.3	clayey silt	122	158	0.12	0.12	Arulanandan et al. (1986)
Glass Fiber		downhole	yes	0.8	3.0	3.5	90.0	50.1	sandy silt to clayey silt	98	117	0.12	0.14	
Construction Building		downhole	yes	1.5	5.0	4.5	124.9	73.7	clayey silt	103	111	0.12	0.13	
Fishery & Shipbuilding		downhole	yes	0.5	2.5	4.0	81.7	43.6	silty sand to clayey silt	101	124	0.12	0.14	
Middle School		downhole	no	1.0	9.0	2.5	191.8	101.2	clayey silt	143	142	0.12	0.13	
Chemical Fiber		downhole	marginal	1.5	6.0	5.5	159.4	90.1	sand to clayey silt	147	152	0.12	0.13	
(d) 1979 Imperial Valley, California Earthquake (M_W = 6.5)														
Wildlife	1	crosshole	no	1.5	2.5	4.3	83.8	53.9	silty sand	127	148	0.13	0.13	Bennett et al.
	2	crosshole	no	1.5	2.5	4.3	83.8	53.9	to sandy	124	145	0.13	0.13	(1981,
		SASW	no	1.5	2.5	4.3	91.8	57.8	silt	115	132	0.13	0.13	1984);
Radio Tower		SASW	yes	2.0	2.7	3.4	79.2	55.8	silty sand to sandy silt	90	104	0.21	0.18	Sykora and Stokoe (1982); Youd and Bennett
McKim		SASW	yes	1.4	1.4	3.5	54.3	38.1	silty sand	126	161	0.51	0.45	(1983);
Vail Canal		SASW	no	2.7	2.7	2.8	70.4	58.4	sand to silty sand	101	116	0.12	0.10	Bierschwale and Stokoe (1984);
Kornbloom		SASW	no	2.5	2.5	3.5	74.7	57.8	sandy silt	105	120	0.12	0.09	Stokoe and Nazarian (1984);
Heber Road, channel fill	SR1	crosshole	yes	2.0	2.0	3.3	63.0	48.0	silty sand	131	158	0.50	0.41	Dobry et al.
	R1R2	crosshole	yes	2.0	2.0	3.3	63.0	48.0		133	160	0.50	0.41	(1992)
Heber Road, point bar	SR1	crosshole	no	2.0	2.0	2.3	60.1	46.6	sand	164	200	0.50	0.40	
	R1R2	crosshole	no	2.0	2.0	2.3	60.1	46.6		173	210	0.50	0.40	

Table 1 (cont.) - Vs-based Liquefaction and Non-liquefaction Case Histories

(1)	(2)	(3)	(4)	(5)	(6)	(7)	(8)	(9)	(10)	(11)	(12)	(13)	(14)	(15)
(e) 1980 Mid-Chiba, Japan Earthquake (M_w = 5.9)														
Owi Island No. 1	C2, upper C2, lower	downhole downhole	no no	1.35 1.35	4.5 13.0	3.3 3.6	105.4 251.6	59.2 120.2	silty sand	155 195	178 186	0.08 0.08	0.09 0.08	Ishihara et al. (1981; 1987)
(f) 1981 Westmorland, California Earthquake (M_w = 5.9)														
Wildlife	1 2	crosshole crosshole SASW	yes yes yes	1.5 1.5 1.5	2.5 2.5 2.5	4.3 4.3 4.3	83.8 83.8 91.8	53.9 53.9 57.8	silty sand to sandy silt	127 124 115	148 145 132	0.27 0.27 0.27	0.26 0.26 0.27	Bennett et al. (1981, 1984);
Radio Tower		SASW	yes	2.0	2.7	3.4	79.2	55.8	silty sand to sandy silt	90	104	0.20	0.18	Sykora and Stokoe (1982);
McKim		SASW	no	1.4	1.4	3.5	54.3	38.1	silty sand	126	161	0.06	0.05	Youd and Bennett (1983);
Vail Canal		SASW	yes	2.7	2.7	2.8	70.4	58.4	sand to silty sand	101	116	0.30	0.23	Bierschwale and Stokoe (1984);
Kornbloom		SASW	yes	2.5	2.5	3.5	74.7	57.8	sandy silt	105	120	0.36	0.29	Stokoe and Nazarian (1984);
Heber Road, channel fill	SR1 R1R2	crosshole crosshole	no no	2.0 2.0	2.0 2.0	3.3 3.3	63.0 63.0	48.0 48.0	silty sand	131 133	158 160	0.02 0.02	0.02 0.02	Dobry et al. (1992)
Heber Road, point bar	SR1 R1R2	crosshole crosshole	no no	2.0 2.0	2.0 2.0	2.3 2.3	60.1 60.1	46.6 46.6	sand	164 173	200 210	0.02 0.02	0.02 0.02	
(g) 1983 Borah Peak, Idaho Earthquake (M_w = 6.9)														
Pence Ranch	SA1 SA2 SA3 SA4 SA5 SAA SAB SAC SAD SAE XDXE	SASW SASW SASW SASW SASW SASW SASW SASW SASW SASW crosshole	yes yes yes yes yes yes yes yes yes yes yes	1.7 1.5 1.4 1.8 1.5 2.0 1.5 1.5 1.5 1.7 1.5	1.8 1.5 1.4 1.8 1.5 2.0 1.5 1.5 1.5 1.7 1.5	1.9 2.8 1.8 2.8 1.9 1.7 1.7 1.9 1.7 1.5 2.3	57.2 52.7 44.5 62.1 60.5 57.5 38.8 38.4 39.4 43.3 48.5	46.2 40.5 36.0 49.4 45.6 46.3 32.9 32.4 33.8 38.3 38.1	gravelly sand to sandy gravel	107 94 102 109 122 134 128 107 131 122 154	131 118 132 131 151 164 170 142 173 155 198	0.36 0.36 0.36 0.36 0.36 0.36 0.36 0.36 0.36 0.36 0.36	0.28 0.29 0.28 0.28 0.29 0.28 0.26 0.27 0.26 0.26 0.29	Andrus and Youd (1987); Stokoe et al. (1988a); Andrus et al. (1992); Andrus (1994)
Goddard Ranch	SA2 SA4	SASW SASW	yes yes	1.2 1.2	1.2 1.2	2.0 2.0	47.3 41.1	36.0 32.7	sandy gravel	122 105	158 137	0.30 0.30	0.24 0.23	
Andersen Bar	X1X2 SA1	crosshole SASW	yes yes	0.8 0.8	0.8 0.8	2.4 2.4	40.6 39.0	28.7 27.8	sandy gravel	106 105	146 145	0.29 0.29	0.26 0.25	
Larter Ranch	X3X4 SA1,85 SA1,90	crosshole SASW SASW	yes yes yes	0.8 0.8 0.8	2.2 2.2 2.2	1.3 1.3 1.3	59.9 55.4 59.9	39.0 38.4 40.5	silty sandy gravel	176 153 183	223 194 230	0.50 0.50 0.50	0.49 0.46 0.47	
Whiskey Springs	WS1a SA5	crosshole SASW	yes yes	0.8 0.8	1.8 1.8	2.2 2.2	59.1 45.6	38.2 31.7	sandy silty gravel	181 210	230 271	0.50 0.50	0.49 0.46	
North Gravel Bar	SA1 SA2	SASW SASW	no no	1.0 3.0	1.8 3.0	1.2 1.3	51.0 75.2	36.0 53.5	sandy gravel	206 274	266 322	0.46 0.46	0.41 0.42	
Mackay Dam, downstream toe	SA2	SASW	no	2.3	2.3	2.7	66.6	57.4	silty sandy gravel	271	313	0.23	0.17	
(h) 1985 Chiba-Ibaragi-Kenkyo, Japan Earthquake (M_w = 6.0)														
Owi Island No. 1	C2, upper C2, lower	downhole downhole	no no	1.35 1.35	4.5 13.0	3.3 3.6	105.4 251.6	59.2 120.2	silty sand	155 195	178 186	0.06 0.06	0.07 0.06	Ishihara et al. (1987)
(i) 1/16/86 Taiwan Earthquake (M_w = 6.6; Event LSST4)														
Lotung LSST Facility	L8L3 L8L4 L2L5L6 L2L7	crosshole crosshole crosshole crosshole	no no no no	0.5 0.5 0.5 0.5	2.0 2.0 2.0 2.0	5.0 5.0 5.0 5.0	85.4 85.4 85.4 85.4	35.4 35.4 35.4 35.4	silty sand to sandy silt	146 133 127 130	190 173 166 171	0.22 0.22 0.22 0.22	0.33 0.33 0.33 0.33	Shen et al. (1991); EPRI (1992)
(j) 5/20/86 Taiwan Earthquake (M_w = 6.6; Event LSST7)														
Lotung LSST Facility	L8L3 L8L4 L2L5L6 L2L7	crosshole crosshole crosshole crosshole	no no no no	0.5 0.5 0.5 0.5	2.0 2.0 2.0 2.0	5.0 5.0 5.0 5.0	85.4 85.4 85.4 85.4	35.4 35.4 35.4 35.4	silty sand to sandy silt	146 133 127 130	190 173 166 171	0.18 0.18 0.18 0.18	0.27 0.27 0.27 0.27	Shen et al. (1991); EPRI (1992)

Table 1 (cont.) - V_S-based Liquefaction and Non-liquefaction Case Histories

(1)	(2)	(3)	(4)	(5)	(6)	(7)	(8)	(9)	(10)	(11)	(12)	(13)	(14)	(15)
(k) 5/20/86 Taiwan Earthquake (M_w = 6.2; Event LSST8)														
Lotung LSST Facility	L8L3	crosshole	no	0.5	2.0	5.0	85.4	35.4	silty sand	146	190	0.04	0.06	Shen et al.
	L8L4	crosshole	no	0.5	2.0	5.0	85.4	35.4	to sandy	133	173	0.04	0.06	(1991); EPRI
	L2L5L6	crosshole	no	0.5	2.0	5.0	85.4	35.4	silt	127	166	0.04	0.06	(1992)
	L2L7	crosshole	no	0.5	2.0	5.0	85.4	35.4		130	171	0.04	0.06	
(l) 7/30/86 Taiwan Earthquake (M_w = 6.2; Event LSST12)														
Lotung LSST Facility	L8L3	crosshole	no	0.5	2.0	5.0	85.4	35.4	silty sand	146	190	0.18	0.27	Shen et al.
	L8L4	crosshole	no	0.5	2.0	5.0	85.4	35.4	to sandy	133	173	0.18	0.27	(1991); EPRI
	L2L5L6	crosshole	no	0.5	2.0	5.0	85.4	35.4	silt	127	166	0.18	0.27	(1992)
	L2L7	crosshole	no	0.5	2.0	5.0	85.4	35.4		130	171	0.18	0.27	
(m) 7/30/86 Taiwan Earthquake (M_w = 6.2; Event LSST13)														
Lotung LSST Facility	L8L3	crosshole	no	0.5	2.0	5.0	85.4	35.4	silty sand	146	190	0.05	0.08	Shen et al.
	L8L4	crosshole	no	0.5	2.0	5.0	85.4	35.4	to sandy	133	173	0.05	0.08	(1991); EPRI
	L2L5L6	crosshole	no	0.5	2.0	5.0	85.4	35.4	silt	127	166	0.05	0.08	(1992)
	L2L7	crosshole	no	0.5	2.0	5.0	85.4	35.4		130	171	0.05	0.08	
(n) 11/4/86 Taiwan Earthquake (M_w = 6.2; Event LSST16)														
Lotung LSST Facility	L8L3	crosshole	no	0.5	2.0	5.0	85.4	35.4	silty sand	146	190	0.16	0.24	Shen et al.
	L8L4	crosshole	no	0.5	2.0	5.0	85.4	35.4	to sandy	133	173	0.16	0.24	(1991); EPRI
	L2L5L6	crosshole	no	0.5	2.0	5.0	85.4	35.4	silt	127	166	0.16	0.24	(1992)
	L2L7	crosshole	no	0.5	2.0	5.0	85.4	35.4		130	171	0.16	0.24	
(o) 1987 Chiba-Toho-Oki, Japan Earthquake (M_w = 6.5)														
Sunamachi		downhole	no	6.2	6.2	5.8	168.2	140.2	sand with silt to silty sand	150	138	0.10	0.07	Ishihara et al. (1989)
(p) 1987 Elmore Ranch, California Earthquake (M_w = 5.9)														
Wildlife	1	crosshole	no	1.5	2.5	4.3	83.8	53.9	silty sand	127	148	0.12	0.12	Bennett et al.
	2	crosshole	no	1.5	2.5	4.3	83.8	53.9	to sandy	124	145	0.12	0.12	(1981,
		SASW	no	1.5	2.5	4.3	91.8	57.8	silt	115	132	0.12	0.12	1984);
Radio Tower		SASW	no	2.0	2.7	3.4	79.2	55.8	silty sand to sandy silt	90	104	0.11	0.10	Sykora and Stokoe (1982); Youd and Bennett
McKim		SASW	no	1.4	1.4	3.5	54.3	38.1	silty sand	126	161	0.06	0.05	(1983);
Vail Canal		SASW	no	2.7	2.7	2.8	70.4	58.4	sand to silty sand	101	116	0.13	0.10	Bierschwale and Stokoe (1984);
Kornbloom		SASW	no	2.5	2.5	3.5	74.7	57.8	sandy silt	105	120	0.24	0.19	Stokoe and Nazarian (1984);
Heber Road, channel fill	SR1	crosshole	no	2.0	2.0	3.3	63.0	48.0	silty sand	131	158	0.03	0.02	Dobry et al.
	R1R2	crosshole	no	2.0	2.0	3.3	63.0	48.0		133	160	0.03	0.02	(1992)
Heber Road, point bar	SR1	crosshole	no	2.0	2.0	2.3	60.1	46.6	sand	164	200	0.03	0.02	
	R1R2	crosshole	no	2.0	2.0	2.3	60.1	46.6		173	210	0.03	0.02	
(q) 1987 Superstition Hills, California Earthquake (M_w = 6.5)														
Wildlife	1	crosshole	yes	1.5	2.5	4.3	83.8	53.9	silty sand	127	148	0.20	0.19	Bennett et al.
	2	crosshole	yes	1.5	2.5	4.3	83.8	53.9	to sandy	124	145	0.20	0.19	(1981,
		SASW	yes	1.5	2.5	4.3	91.8	57.8	silt	115	132	0.20	0.20	1984);
Radio Tower		SASW	no	2.0	2.7	3.4	79.2	55.8	silty sand to sandy silt	90	104	0.20	0.18	Sykora and Stokoe (1982); Youd and Bennett
McKim		SASW	no	1.4	1.4	3.5	54.3	38.1	silty sand	126	161	0.19	0.17	(1983);
Vail Canal		SASW	no	2.7	2.7	2.8	70.4	58.4	sand to silty sand	101	116	0.20	0.15	Bierschwale and Stokoe (1984);
Kornbloom		SASW	no	2.5	2.5	3.5	74.7	57.8	sandy silt	105	120	0.21	0.17	Stokoe and Nazarian (1984);
Heber Road, channel fill	SR1	crosshole	no	2.0	2.0	3.3	63.0	48.0	silty sand	131	158	0.18	0.15	Dobry et al.
	R1R2	crosshole	no	2.0	2.0	3.3	63.0	48.0		133	160	0.18	0.15	(1992)
Heber Road, point bar	SR1	crosshole	no	2.0	2.0	2.3	60.1	46.6	sand	164	200	0.18	0.15	
	R1R2	crosshole	no	2.0	2.0	2.3	60.1	46.6		173	210	0.18	0.15	

Table 1 (cont.) - Vs-based Liquefaction and Non-liquefaction Case Histories

(1)	(2)	(3)	(4)	(5)	(6)	(7)	(8)	(9)	(10)	(11)	(12)	(13)	(14)	(15)
(r) 1989 Loma Prieta, California Earthquake (M_w = 7.0)														
Treasure Island, fire station	X1X2	crosshole	marginal	1.4	4.2	7.3	106.6	63.5	silty sand	130	145	0.14	0.15	Furhriman (1993);
	B2B3	crosshole	marginal	1.4	4.5	7.7	148.7	83.7	to clayey	157	164	0.14	0.15	
	B1B4	crosshole	marginal	1.4	4.5	7.7	147.2	83.0	silty sand	157	165	0.14	0.15	Andrus (1994);
	B4B5	crosshole	marginal	1.4	4.5	7.7	101.3	60.9		131	148	0.14	0.15	
	B2B4	crosshole	marginal	1.4	4.5	7.7	118.5	69.2		136	150	0.14	0.15	Redpath (1991);
		SASW	marginal	1.4	4.5	7.7	139.9	78.6		148	145	0.14	0.15	
		downhole	marginal	1.4	4.5	7.7	163.0	90.6		137	142	0.14	0.15	Gibbs et al. (1992);
		downhole	marginal	1.4	4.5	7.7	154.4	86.4		152	158	0.14	0.15	
		SCPT	marginal	1.4	4.5	7.7	146.3	82.5		146	154	0.14	0.15	Hryciw et al. (1991); Rollins et al. (1994)
Treasure Island, perimeter	UM03	SCPT	no	1.5	4.4	5.6	133.1	77.5	sand to	178	190	0.14	0.15	Hryciw (1991);
	UM05	SCPT	yes	2.4	3.5	4.5	102.6	71.0	silty sand	163	178	0.15	0.14	
	UM06	SCPT	yes	1.4	2.0	4.0	75.4	48.8		154	185	0.14	0.14	Hryciw et al. (1991);
	UM09	SCPT	yes	2.7	2.7	3.7	82.1	63.9		143	160	0.15	0.12	
	UM11	SCPT	yes	1.4	4.0	3.0	101.2	61.2		160	181	0.14	0.15	Geomatrix (1990)
Port of Richmond	SR1	crosshole	yes	3.5	4.0	4.0	110.1	84.7	silt to	143	149	0.16	0.13	Stokoe et al. (1992);
	R1R2	crosshole	yes	3.5	4.0	4.0	110.1	84.7	silty sand	135	140	0.16	0.13	
		SASW	yes	3.5	4.0	4.0	97.0	78.8		117	124	0.16	0.12	Mitchell et al. (1994)
	POR2	SCPT	yes	3.5	4.0	4.0	98.9	79.4		152	161	0.16	0.12	
	POR3	SCPT	yes	3.5	5.0	2.0	98.9	79.4		121	128	0.16	0.12	
	POR4	SCPT	yes	3.5	5.0	2.0	98.9	79.4		138	147	0.16	0.12	
Port of Richmond, Hall Ave.	SR1	crosshole	no	3.5	3.5	5.0	104.4	82.0	silty to	148	155	0.16	0.12	
	R1R2	crosshole	no	3.5	3.5	5.0	104.4	82.0	silty sand	145	152	0.16	0.12	
		SASW	no	3.5	3.5	5.0	109.2	84.3		133	139	0.16	0.12	
Bay Bridge Toll Plaza	SR1	crosshole	yes	3.0	5.5	1.5	115.9	82.4	sand to	134	141	0.24	0.21	
	R1R2	crosshole	yes	3.0	5.5	1.5	115.9	82.4	silty sand	134	141	0.24	0.21	
	SFOBB1	SCPT	yes	3.0	5.5	1.5	108.3	78.8		146	155	0.24	0.21	
	SFOBB2	SCPT	yes	3.0	6.0	3.0	136.6	92.4		148	151	0.24	0.22	
Port of Oakland	SR1	crosshole	yes	3.0	5.5	2.5	121.6	85.8	sand	145	151	0.24	0.21	
	R1R2	crosshole	yes	3.0	5.5	2.5	121.6	85.8		179	186	0.24	0.21	
		SASW	yes	3.0	5.5	2.5	115.8	83.1		157	165	0.24	0.21	
	POO71	SCPT	yes	3.0	5.5	2.5	122.5	86.2		142	148	0.24	0.21	
	POO72	SCPT	yes	3.0	5.5	2.5	122.5	86.2		145	150	0.24	0.21	
	POO73	SCPT	yes	3.0	5.5	1.5	113.1	81.7		176	185	0.24	0.21	
Bay Farm Island, dike	SR1	crosshole	no	3.6	3.6	2.8	87.1	75.2	sand	193	207	0.27	0.20	
	R1R2	crosshole	no	3.6	3.6	2.8	87.1	75.2		212	227	0.27	0.20	
		SASW	no	3.6	3.6	2.8	91.9	77.0		204	219	0.27	0.20	
Bay Farm Island, So. Loop Road	SR1	crosshole	yes	3.0	3.0	1.7	69.9	60.9	sand	97	109	0.27	0.20	
	R1R2	crosshole	yes	3.0	3.0	1.7	69.9	60.9		116	131	0.27	0.20	
		SASW	yes	3.0	3.0	1.7	67.0	59.6		125	143	0.27	0.19	
Marina District	school	downhole	yes	2.7	2.7	1.6	61.9	54.4	sand to	153	177	0.15	0.11	Kayen et al. (1990);
	2	SASW	yes	2.9	2.9	7.1	117.0	82.2	silty sand	120	129	0.15	0.12	
	3	SASW	yes	2.9	2.9	7.1	117.0	82.2		105	113	0.15	0.12	Tokimatsu et al. (1991b)
	4	SASW	yes	2.9	2.9	2.1	69.9	59.6		120	137	0.15	0.11	
	5	SASW	no	5.9	5.9	4.1	140.6	105.7		220	217	0.15	0.12	
Coyote Creek	SR1	crosshole	no	2.4	3.5	2.5	83.6	62.1	sand &	136	153	0.19	0.16	Barrow (1983);
	R1R2	crosshole	no	2.4	3.5	2.5	75.4	58.2	gravel	154	177	0.19	0.16	
	R1R3	crosshole	no	2.4	3.5	2.5	75.4	58.2		161	185	0.19	0.16	Bennett (1995);
	R2R3	crosshole	no	2.4	3.5	2.5	75.4	58.2		173	198	0.19	0.16	
Salinas River, north	SR1	crosshole	no	6.0	9.1	1.5	178.2	140.8	silty sand	177	162	0.15	0.11	Bennett and Tinsley (1995)
	R1R2	crosshole	no	6.0	9.1	1.5	178.2	140.8		195	179	0.15	0.11	
	R1R3	crosshole	no	6.0	9.1	1.5	178.2	140.8		200	184	0.15	0.11	
	R2R3	crosshole	no	6.0	9.1	1.5	178.2	140.8		199	183	0.15	0.11	
Salinas River, south	SR1	crosshole	no	6.0	6.5	4.5	142.2	123.5	sand &	131	124	0.15	0.11	
	R1R2	crosshole	no	6.0	6.5	4.5	142.2	123.5	silty	149	141	0.15	0.11	
	R1R3	crosshole	no	6.0	6.5	4.5	142.2	123.5	sand	158	150	0.15	0.11	
	R2R3	crosshole	no	6.0	6.5	4.5	142.2	123.5		168	159	0.15	0.11	

Table 1 (cont.) - V_S-based Liquefaction and Non-liquefaction Case Histories

(1)	(2)	(3)	(4)	(5)	(6)	(7)	(8)	(9)	(10)	(11)	(12)	(13)	(14)	(15)
Santa Cruz	SC02	SCPT	yes	0.6	1.3	2.6	48.1	28.7	sand to	116	160	0.42	0.44	Hryciw
	SC03	SCPT	yes	2.1	2.1	2.3	60.1	48.1	sandy silt	145	174	0.42	0.33	(1991)
	SC04	SCPT	no	1.8	1.8	2.2	51.0	41.0		126	158	0.42	0.33	
	SC05	SCPT	no	2.8	3.0	1.6	67.7	57.8		135	155	0.42	0.31	
	SC13	SCPT	no	1.8	2.0	4.0	69.2	49.8		158	188	0.42	0.36	
	SC14	SCPT	yes	1.2	1.4	1.6	41.0	30.5		126	170	0.42	0.37	
Moss Landing, State Beach	UC-15	SCPT	yes	1.8	1.8	2.8	63.6	46.9	Sand	116	140	0.25	0.21	Boulanger et al. (1995); Boulanger et al. (1997)
	UC-16	SCPT	yes	2.3	2.3	7.1	101.3	69.8		162	178	0.25	0.22	
Moss Landing, Sandholt Rd.	UC-4	SCPT	yes	1.8	2.1	1.5	54.2	42.4	Sand	130	161	0.25	0.20	
	UC-4	SCPT	no	1.8	5.9	4.1	148.5	87.7		209	216	0.25	0.26	
	UC-6	SCPT	marginal	1.7	3.0	4.3	85.6	59.5		171	196	0.25	0.22	
Moss Landing, Harbor Office	UC-12	SCPT	yes	1.9	3.0	1.6	74.8	53.1	Silty sand	150	175	0.25	0.22	
Moss Landing, Woodward Marine	UC-9	SCPT	yes	1.2	2.6	1.4	60.3	39.6	Sand	143	180	0.25	0.24	
(s) 1993 Hokkaido-nansei-oki, Japan Earthquake (M_W = 8.3)														
Pension House	BH1	downhole	yes	1.0	1.0	2.5	45.5	33.4	sandy	79	105	0.19	0.16	Kokusho et al. (1995a, 1995b)
	BH2	downhole	marginal	0.7	3.7	4.8	122.9	70.0	gravel	144	159	0.19	0.21	
(t) 1995 Hyogo-ken Nanbu, Japan Earthquake (M_W = 6.9)														
Port Island, instrumented array	1991	downhole	yes	2.4	2.4	12.6	160.8	98.8	sandy	197	202	0.50	0.43	Sato et al. (1996); Shibata et al. (1996); Sugito et al. (1996)
	1995	downhole	yes	2.4	2.4	12.6	185.9	110.9	gravel with silt	174	172	0.50	0.44	
SGK (TRC)		downhole	no	7.0	7.0	4.0	158.5	139.1	sand, silt	149	138	0.48	0.32	
TKS (TPS)		downhole	yes	2.5	2.5	4.6	73.8	57.9	gravel, sand, silt	135	157	0.20	0.15	
KNK (KPS)		downhole	no	2.0	3.8	13.2	193.6	111.0	sand, silt	179	184	0.12	0.10	

Test array refers to the two boreholes used for crosshole measurements, the borehole (or cone sounding) and source used for downhole measurements, or the line of receivers used for SASW measurements.

V_S is shear wave velocity and V_{S1} is shear wave velocity modified to an overburden pressure of 100 kPa using $V_{S1} = V_S$ (100 kPa / $\sigma'_v)^{0.25}$ (Robertson et al. 1992). Averages for the Treasure Island and Santa Cruz SCPT data are of the unfiltered data. One high velocity measurement is omitted from the average for Santa Cruz test array SC04. Refracted wave velocities measured at 5.5 m are omitted from the averages for Coyote Creek (test arrays R1R2, R1R3 and R2R3).

Average a_{max} is the average of two peak ground surface accelerations obtained from the x and y ground motion records that would have occurred at the site in the absence of liquefaction.

M_W is moment magnitude.

At Owi Island No. 1, Lotung LSST Faculity, Sunamachi, Wildlife (1987 earthquakes), and Port Island sites the assessment of liquefaction or no liquefaction is supported by pore water pressure measurements.

At Larter Ranch and Whiskey Springs, soil may be weakly cemented by carbonate.

At Lotung LSST Facility, the artesian pressure is assumed to vary linearly from a pressure head of 8.1 m at a depth of 7 m to a pressure head of 1.9 m at a depth of 2 m.

At Treasure Island Fire Station, Moss Landing Sandholt Road UC-6, and Pension House BH2 no sand boils or damaged observed, although some liquefaction observed in adjacent areas. Thus, liquefaction behavior is listed as marginal for these sites.

At Moss Landing Sandholt Road UC-4 no lateral displacement occurred below 5.9 m based on slope inclinometer data.

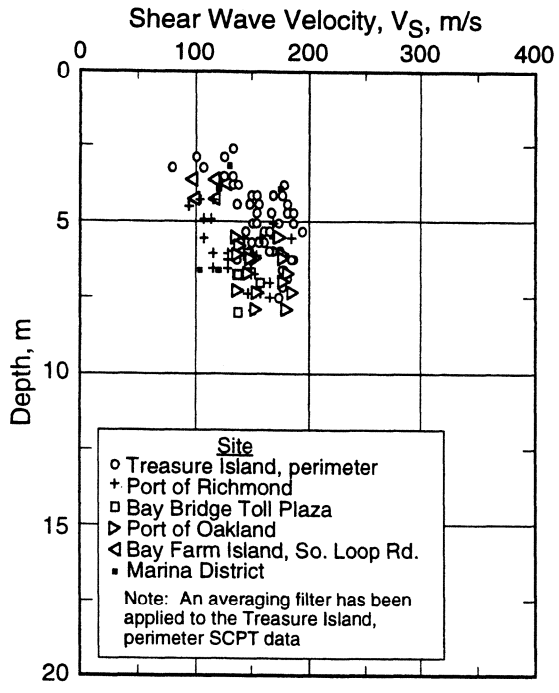

(a) Northern California Fill Sites Exhibiting Surface Manifestations of Liquefaction

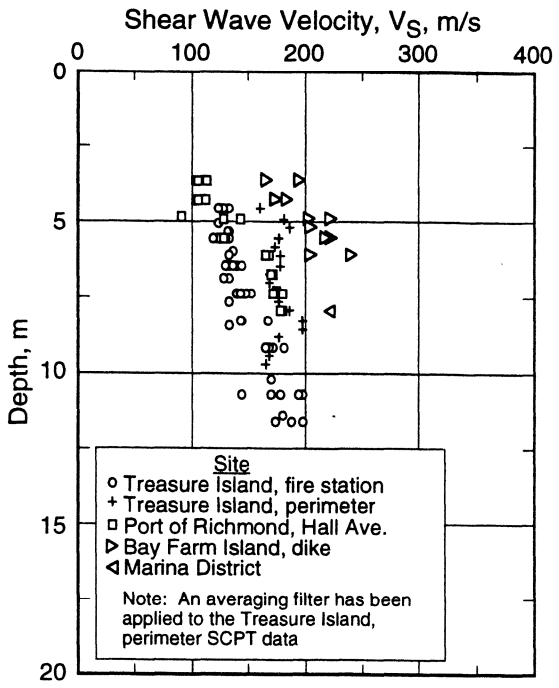

(b) Northern California Fill Sites Not Exhibiting Surface Manifestations of Liquefaction

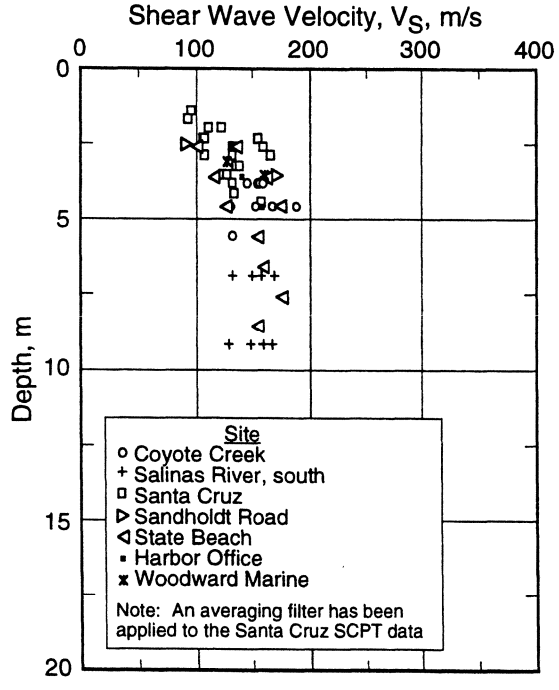

(c) Northern California Natural Soil Sites Exhibiting Surface Manifestations of Liquefaction

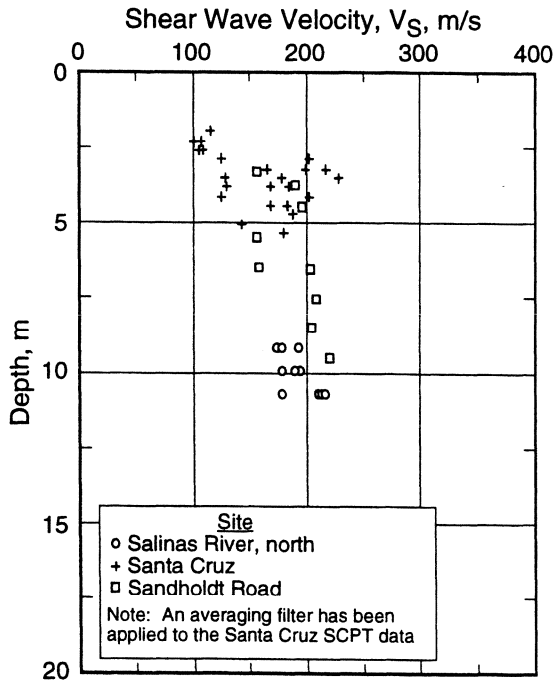

(d) Northern California Natural Soil Sites Not Exhibiting Surface Manifestations of Liquefaction

Fig. 1 - The Distribution of Shear Wave Velocity with Depth for the Most Vulnerable Layer at the Sites Listed in Table 1.

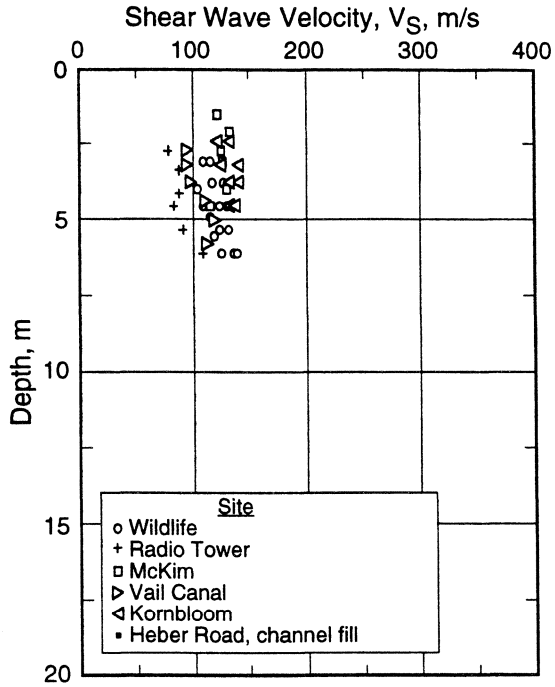

(e) Imperial Valley, California Sandy Soil Sites Exhibiting Surface Manifestations of Liquefaction

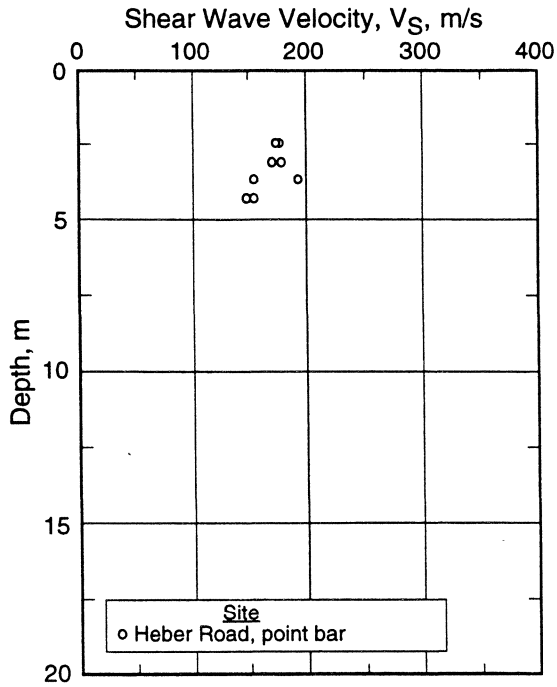

(f) Imperial Valley, California Sandy Sites Not Exhibiting Surface Manifestations of Liquefaction

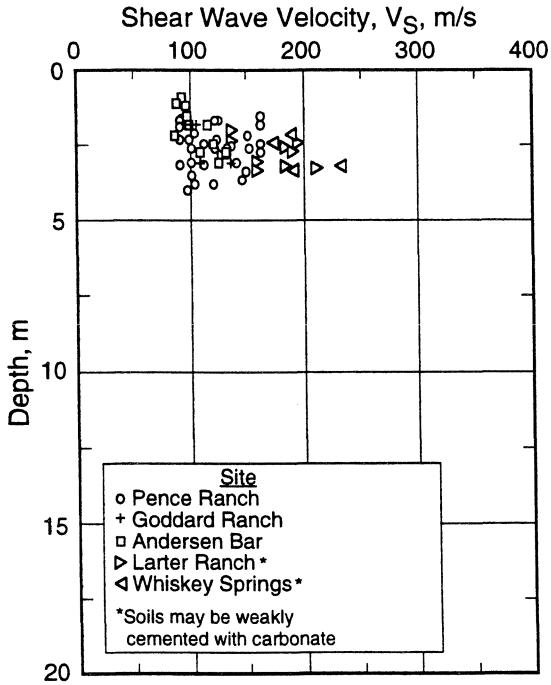

(g) Idaho Gravelly Soil Sites Exhibiting Surface Manifestations of Liquefaction

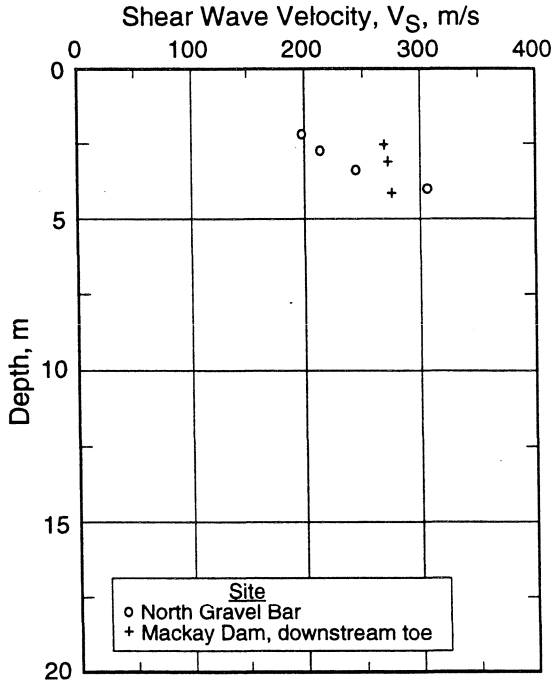

(h) Idaho Gravelly Soil Sites Not Exhibiting Surface Manifestations of Liquefaction

Fig. 1 (cont.) - The Distribution of Shear Wave Velocity with Depth for the Most Vulnerable Layer at the Sites Listed in Table 1.

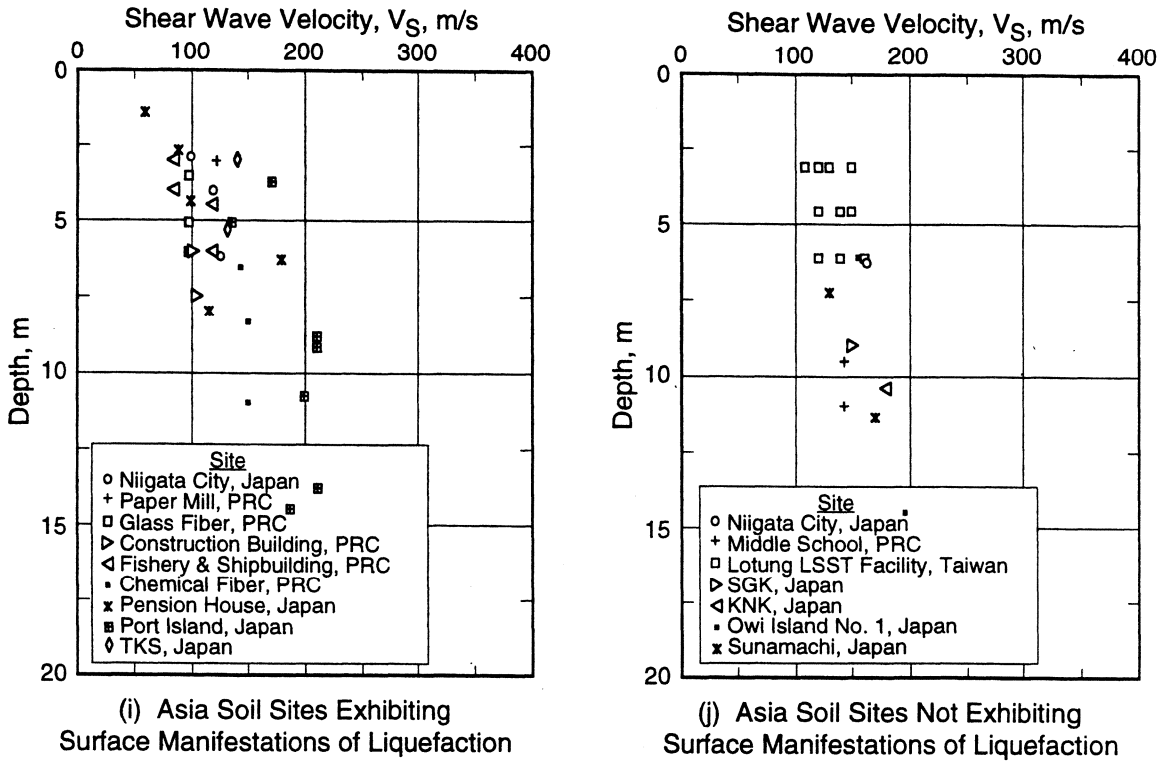

(i) Asia Soil Sites Exhibiting Surface Manifestations of Liquefaction

(j) Asia Soil Sites Not Exhibiting Surface Manifestations of Liquefaction

Fig. 1 (cont.) - The Distribution of Shear Wave Velocity with Depth for the Most Vulnerable Layer at the Sites Listed in Table 1.

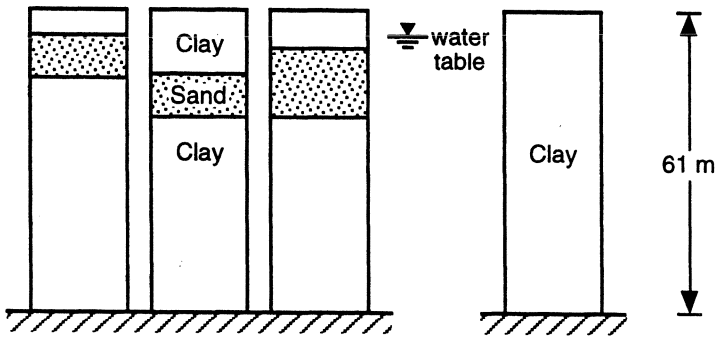

(a) Sand Liquefaction Site

(b) "Reference" Site

Fig. 2 - Soil Model Used in the Parametric Study by Stokoe et al (1988b).

were placed. The variations in shear modulus and material damping ratio with shearing strain assumed for the sand and clay layers were based on resonant column and cyclic triaxial tests on specimens from the Imperial Valley (Ladd 1982; Turner and Stokoe 1982).

Most of the analyses were performed (Bierschwale and Stokoe 1984; Aouad 1986) with the strong-motion acceleration time history which was recorded at the Salton Sea station during the 1981 Westmorland earthquake (moment magnitude, M_w = 5.9). This strong-motion record exhibited a peak horizontal ground surface acceleration, a_{max}, of 0.20 g and an equivalent number of cycles, N_c, of about 10. Records of larger magnitude were fabricated by simply multiplying the Salton Sea record by a pre-selected factor. Records with N_c of about 20 cycles and 30 cycles were generated by doubling and tripling the strong-motion portion of the Salton Sea record.

Stresses and strains within each soil profile were computed with program SHAKE (Schnabel et al. 1972), an equivalent linear analysis. These calculations were repeated with either a larger or smaller magnitude record until the estimated shearing strain within the liquefiable sand layer equaled the cyclic strain required for initial liquefaction. Initial liquefaction was assumed to occur at shearing strains of about 2%, 1% and 0.5% for 10 cycles, 20 cycles and 30 cycles of loading, respectively, based on undrained, strain-controlled cyclic triaxial tests on two Imperial Valley sands (Ladd 1982). The sand layer had been divided into 1.5-m thick sublayers, each having the same stiffness. The computed strain within the bottom sublayer was always greater than the computed strain in the other sublayers. Thus, criterion for initial liquefaction was first satisfied in the bottom sublayer. Next, the scaled record that generated initial liquefaction was applied at bedrock beneath the second profile, shown in Fig. 2b, to determine a_{max} at the ground surface of the non-liquefiable or "reference" soil site. These procedures were followed for each set of parameters characterizing the liquefiable sand layer (V_S, depth, and thickness). A total of 46 velocity profiles was considered.

Since it seemed more likely engineers would estimate a_{max} at the ground surface of non-liquefiable soil sites than at liquefiable sites, Stokoe et al. (1988b) correlated V_S of the liquefiable sand layer with a_{max} estimated for a "reference" soil site at the candidate-site location. The data from their parametric study are summarized in Figs. 3a, 3b and 3c for N_c of 10 cycles, 20 cycles and 30 cycles, respectively. As noted by Stokoe et al., the plotted data exhibit the following general trends: (1) the higher the V_S, the less likely the site is to liquefy for a given a_{max}; (2) the greater the thickness of the liquefiable sand layer, the less likely the site is to liquefy for a given V_S; and (3) the greater the depth to the bottom of the liquefiable sand layer, the slightly more likely the site is to liquefy at a given V_S. These findings suggest that liquefaction potential is dependent on layer thickness and depth, and indicate that a separating band (to allow for variations in thickness and depth) is more appropriate than a separating line to distinguish between liquefaction and non-liquefaction.

Stokoe et al. (1988b) created liquefaction assessment charts by dividing Figs. 3a, 3b and 3c each into three regions: the region left of the plotted data, the region of the plotted data, and the region right of the plotted data. Liquefaction is predicted to not occur left of the plotted data

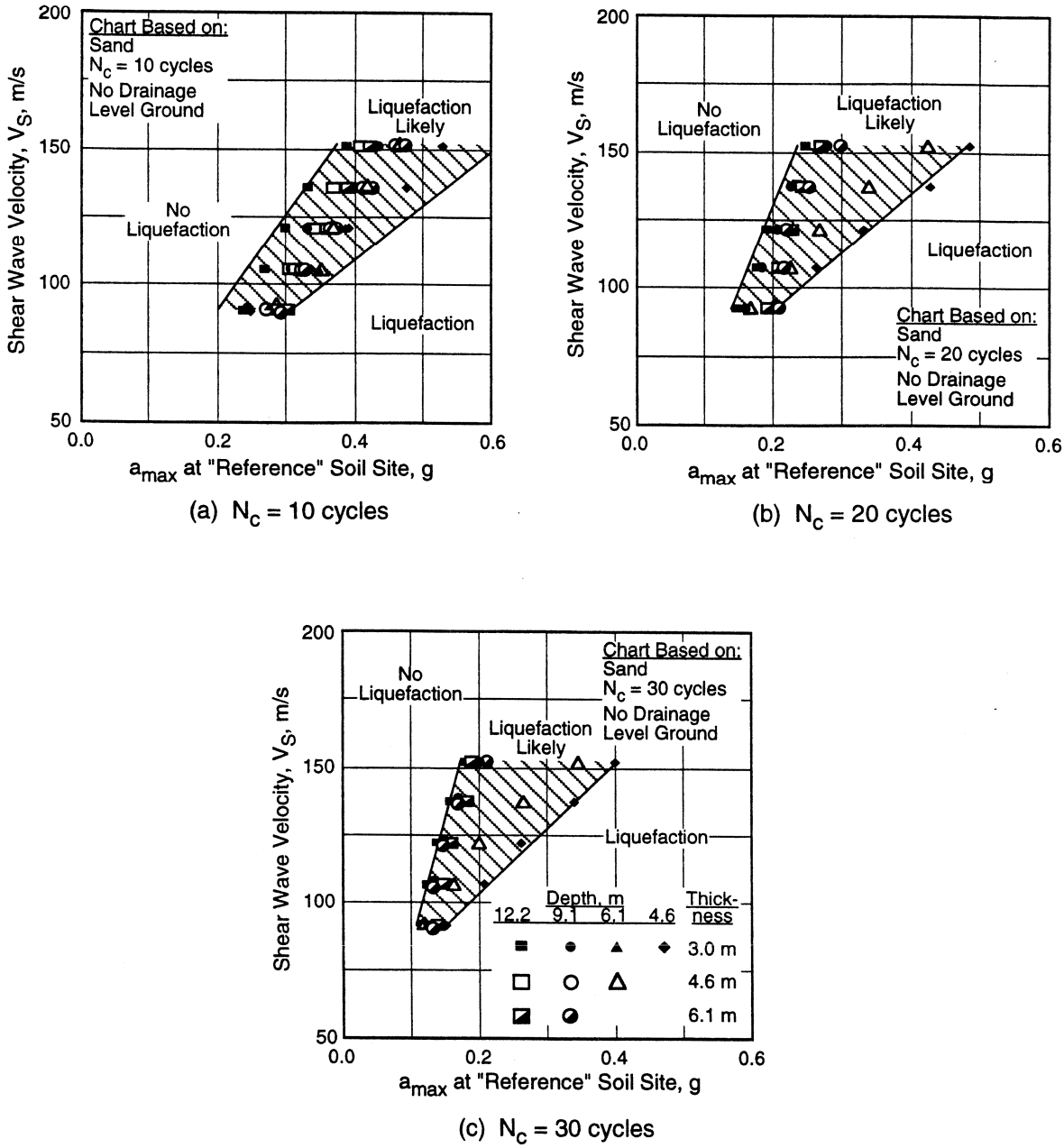

Fig. 3 - Comparison of Liquefaction Assessment Charts Proposed by Stokoe et al. (1988b) with Relationship Between V_S of Liquefiable Sand Layer and a_{max} for 10, 20 and 30 Cycles of Shaking as Determined Analytically by Bierschwale and Stokoe (1984) and Aouad (1986).

because the sand is too stiff to liquefy. Within the region of the plotted data, liquefaction would likely occur, but depends on layer thickness and depth. Right of the plotted data, liquefaction is predicted to occur.

To test the accuracy of these liquefaction assessment charts, field performance data for the magnitude 5.9 to 6.6 earthquakes listed in Table 1 are plotted on the chart for N_c of 10 cycles shown in Fig. 4a. The chart for N_c of 10 cycles is used since it was developed using a strong motion record from the magnitude 5.9 Westmorland earthquake. The field performance data for the magnitude 6.9 to 7.1 earthquakes are plotted on the chart for N_c of 15 cycles shown in Fig. 4b. For each case history, the shear wave velocity shown is the minimum measurement made within the most vulnerable layer. The value of a_{max} is for the larger of the x and y records of ground acceleration that would have occurred at the site in the absence of liquefaction. With several exceptions, the liquefaction (solid symbols) and non-liquefaction (open symbols) case histories are distinctly separated by the likely liquefaction region. Marginal liquefaction (half open symbols) is shown for the Chemical Fiber, Treasure Island Fire Station, and Sandholt Road UC-6 sites. Liquefaction behavior predicted by the procedure by Stokoe et al. (1988b) is nonconservative for lower levels of shaking ($a_{max} < 0.3$ g) and lower values of V_S ($V_S < 180$ m/s). A similar conclusion was reached by Arulanandan et al. (1986) based on the six sites shaken by the 1975 Haicheng earthquake listed in Table 1.

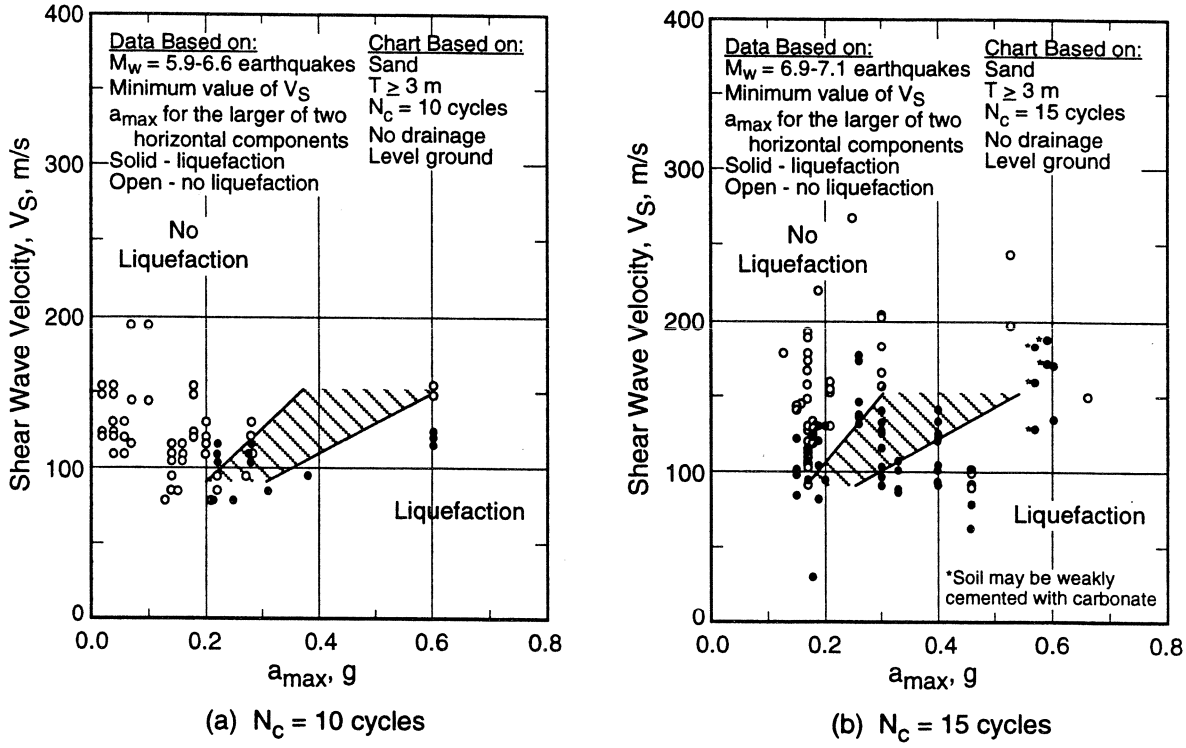

Fig. 4 - Comparison of Liquefaction Assessment Charts Proposed by Stokoe et al. (1988b) Based on V_S and a_{max} with Case Histories of Sites Shaken by Earthquakes with Magnitude of 5.9 to 7.1 (after Stokoe et al. 1988b; Andrus 1994).

While it has been suggested (Andrus 1994; after Robertson et al. 1992) that V_S be modified to a reference overburden stress, this modification alone does not improve the distribution of the performance data shown in Fig. 4. More work is needed to quantify the effects of layer thickness and depth.

Procedures Developed from Laboratory Studies

Tokimatsu et al. (1991a) proposed a procedure for evaluating liquefaction resistance using the stress approach developed by Seed and his colleagues (1971, 1983, and 1985) and results from laboratory cyclic triaxial tests on reconstituted sand specimens. In the stress approach, cyclic loading is represented by the ratio of cyclic shear stress to initial vertical effective stress acting on a horizontal plane, called cyclic stress ratio. The cyclic stress ratio, CSR, at a particular depth in a level soil deposit can be expressed as (Seed and Idriss 1971):

$$CSR = \tau_{av}/\sigma'_v = 0.65\ (a_{max}/g)\ (\sigma_v/\sigma'_v)\ r_d \qquad (1)$$

where τ_{av} is average cyclic shear stress generated by the earthquake, σ'_v is initial effective vertical (overburden) stress, σ_v is total overburden stress, g is acceleration of gravity, and r_d is a shear stress reduction factor with a value less than 1.

Resistance to liquefaction in a soil deposit is represented by a cyclic stress ratio or cyclic resistance ratio, CRR. Tokimatsu et al. (1991a) defined the cyclic resistance ratio for cyclic triaxial tests, CRR_{tx}, as the ratio of cyclic deviator stress to initial effective confining stress, $\sigma_d/2\sigma'_o$, at the time the double-amplitude axial strain, DA, reaches 5%. Their correlations between CRR_{tx} at different number of cycles and stress corrected shear wave velocity, V_{S1}, are shown in Fig. 5. They used the assumption that V_S is a function of the cube root of the mean normal effective stress, σ'_m, and corrected V_S by:

$$V_{S1} = V_S\ (1/\sigma'_m)^{0.33} \qquad (2)$$

where σ'_m is in kgf/cm^2 (1 kgf/cm^2 = 98.07 kPa). Tokimatsu et al. selected an exponent of 0.33 rather than 0.25, as determined by Hardin and Drnevich (1972), because it seemed that a slightly better correlation could be obtained.

For converting CRR_{tx} to an equivalent field cyclic resistance ratio, Tokimatsu et al. (1991a) suggested the following expression (after Seed 1979):

$$CRR = \tau_l/\sigma'_v = 1/3\ (1+2K_o)\ r_c\ (CRR_{tx}) \qquad (3)$$

where τ_l is average cyclic shear stress resisting liquefaction, K_o is the coefficient of earth pressure at rest, and r_c is a constant to account for the effects of multidirectional shaking with a value between 0.9 and 1.0. As noted by Tokimatsu et al., any value of K_o between 0.5 and 1 can be assumed for all practical purposes since the effects involved in Eqs. 2 and 3 almost cancel each other out.

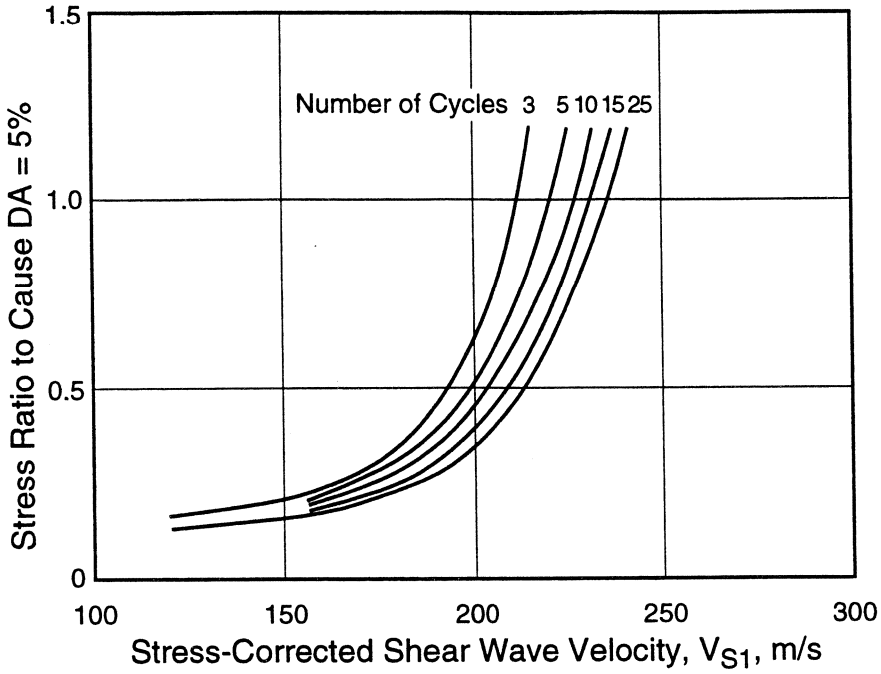

(a) Clean Sand

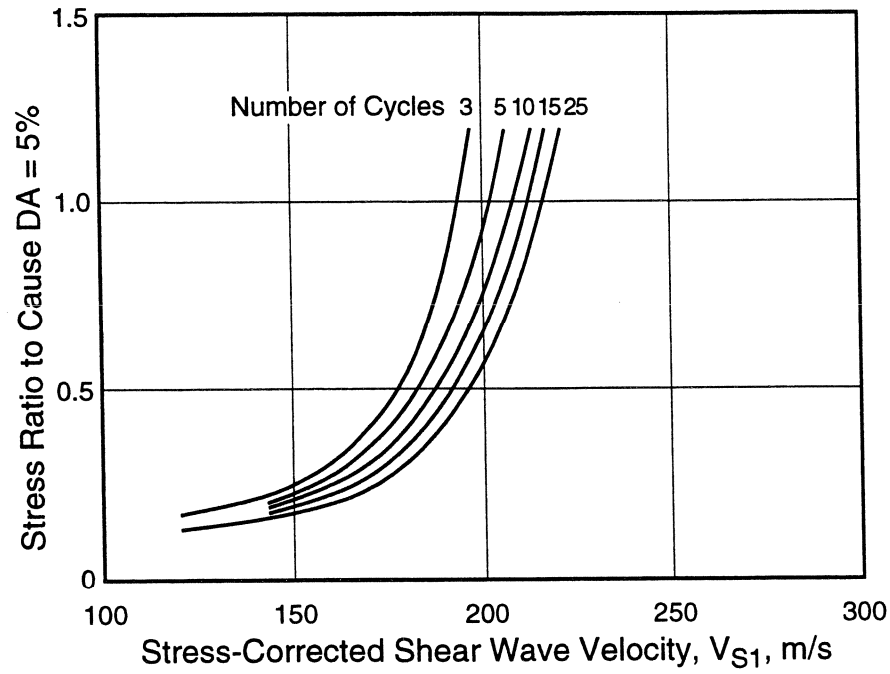

(b) Silty Sand

Fig. 5 - Liquefaction Assessment Charts Based on V_{S1} Proposed by Tokimatsu et al. (1991a).

The field performance data for 20 earthquakes are plotted in Fig. 6. The plotted data are based on the procedure of Tokimatsu et al. (1991a) outlined above using minimum values of V_{S1} from the most vulnerable layer and estimates of a_{max} for the larger of the x and y records of ground acceleration that would have occurred at the site in the absence of liquefaction. Included in Fig. 6 are the liquefaction potential boundaries by Tokimatsu et al. The boundaries are constructed from the relationships shown in Fig. 5 using Eq. 3 and assuming K_o of 0.6 and r_c of 0.95. Liquefaction behavior predicted by these boundaries is nonconservative for N_c greater than about 10 cycles and V_{S1} greater than about 150 m/s (see Figs. 6c and 6d).

Procedures Developed from Field Performance Studies

Robertson et al. (1992) proposed another stress-based liquefaction assessment procedure using field performance data from primarily the Imperial Valley, California sites. They corrected V_S by:

$$V_{S1} = V_S (P_a/\sigma'_v)^{0.25} \quad (4)$$

where P_a is a reference stress, 100 kPa or approximately atmospheric pressure, and σ'_v is in kPa. Robertson et al. chose to correct V_S in terms of σ'_v to follow the traditional procedures for correcting standard and cone penetration resistances. It is implied by Eq. 4 that K_o equals 1, since V_S is a function of mean effective stress (Hardin and Drnevich 1972). Their liquefaction potential boundary for earthquakes with magnitude of 7.5 is shown in Fig. 7a.

Two subsequent liquefaction potential boundaries proposed by Kayen et al. (1992) and Lodge (1994) for earthquakes with magnitude of about 7 are shown in Fig. 7b. These later curves are based on field performance data from primarily the 1989 Loma Prieta, California earthquake. Kayen et al. used field performance data from the Port of Richmond, Bay Bridge Toll Plaza, Port of Oakland, and Bay Farm Island sites. They assumed average values of V_{S1} and a_{max} for the larger component of acceleration time histories recorded at neighboring seismograph stations.

Lodge (1994) considered the same sites that Kayen et al. (1992) evaluated as well as several additional sites that had been shaken by the Loma Prieta earthquake. The boundary by Lodge was developed as follows. First, cyclic stress ratios for the entire soil profile at each site were calculated using Eq. 1 and a_{max} for the larger component of acceleration time histories recorded at neighboring seismograph stations. Second, soil layers with a high and a low liquefaction potential were identified with the simplified procedure of Seed et al. (1985) and SPT blow counts. Soil layers where the modified blow count fell within 3 blows per 0.3 m of the SPT-based liquefaction potential boundary of Seed et al. were eliminated due to uncertainties in the correlation. Third, shear wave velocity measured by the SCPT and crosshole methods were normalized using Eq. 4. Fourth, on a "meter by meter" basis values of V_{S1} and cyclic stress ratio were plotted for both layer types, those which were predicted liquefiable and those which were predicted non-liquefiable. Finally, a curve was drawn to include all data for liquefiable layers.

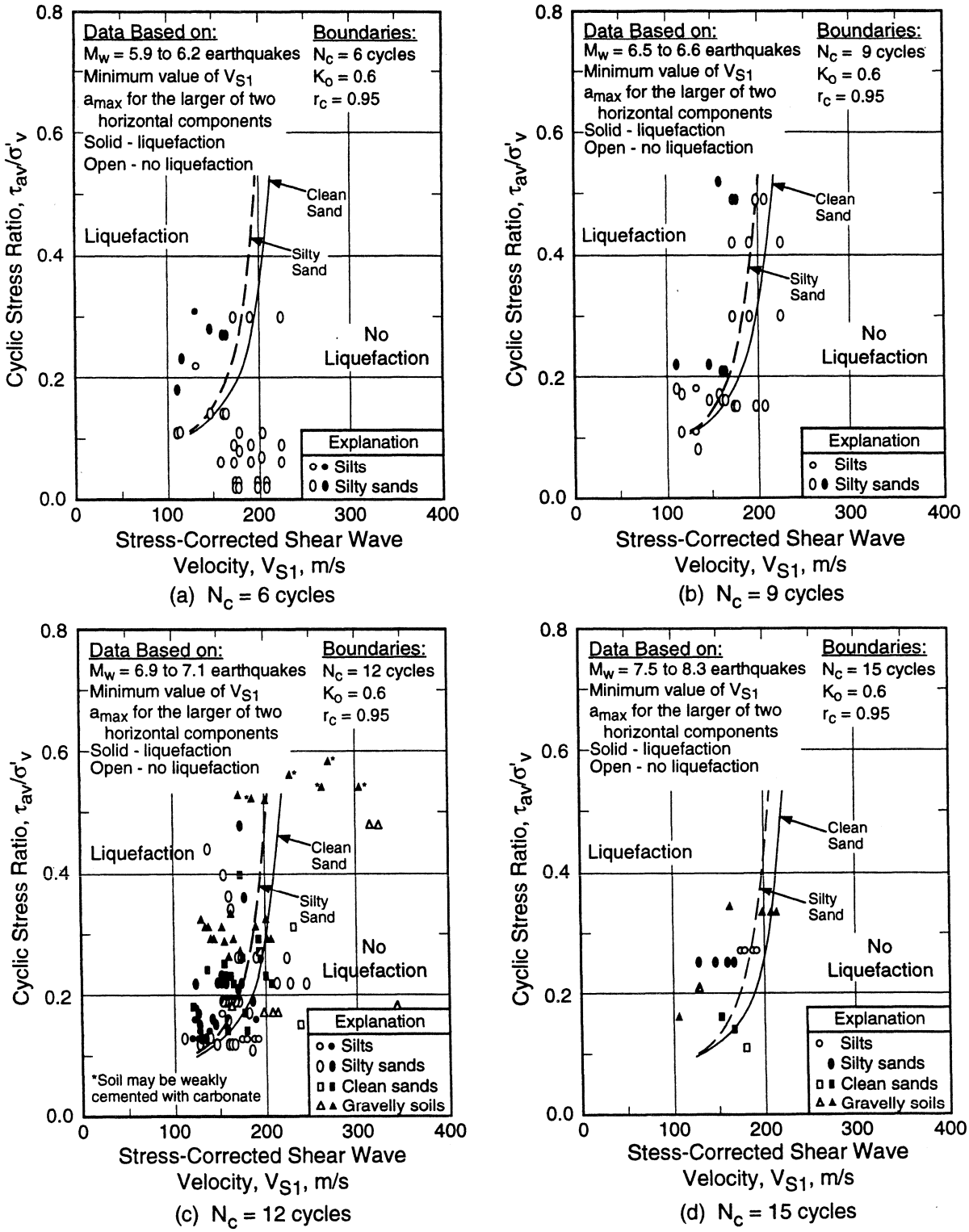

Fig. 6 - Comparison of Liquefaction Assessment Charts Based on V_{S1} and CSR Proposed by Tokimatsu et al. (1991a) with Case Histories from 20 Earthquake

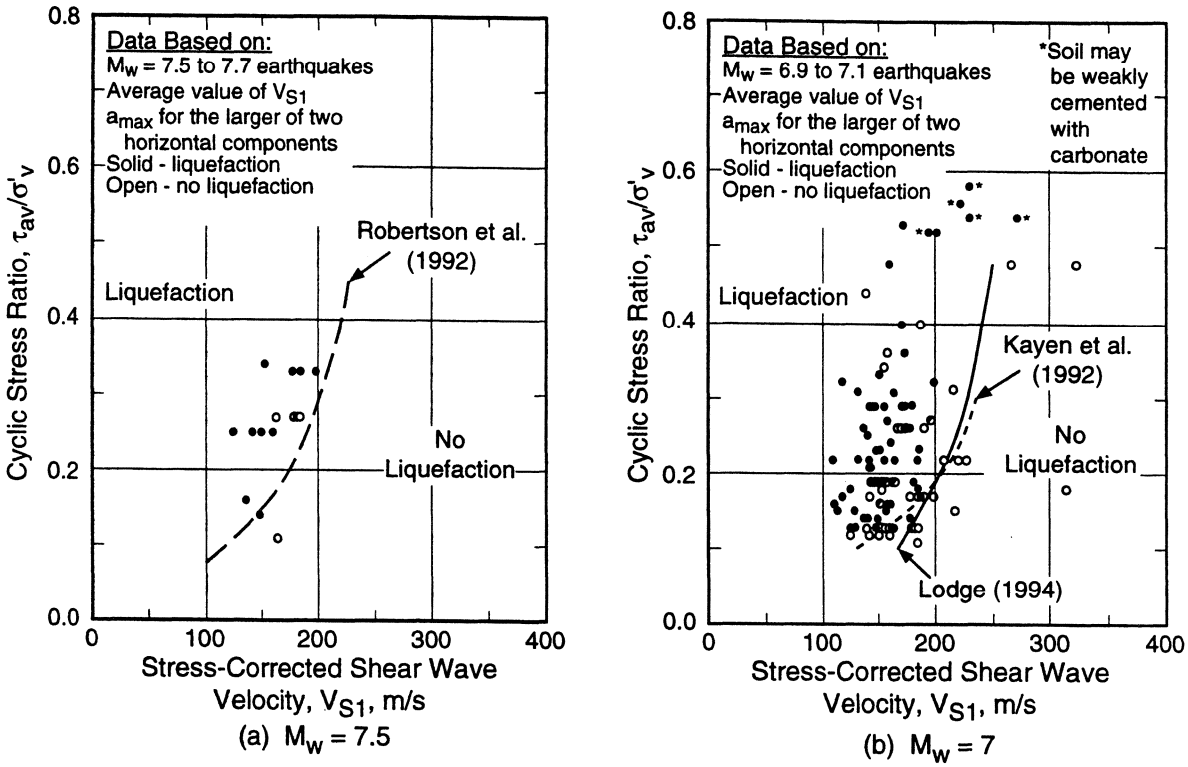

Fig. 7 - Comparison of Liquefaction Assessment Charts Based on V_{S1} and CSR Proposed by (a) Robertson et al. (1992) and (b) Kayen et al. (1992) and Lodge (1994) with Case Histories from Earthquakes with Magnitude of 6.9 to 7.7.

Field performance data from earthquakes with magnitude of 6.9 to 7.7 are also plotted in Fig. 7. The plotted data are based on average values of V_{S1} from the most vulnerable layer at the investigated sites. The cyclic stress ratios are calculated using estimates of a_{max} for the larger of two horizontal components of ground acceleration that would have occurred at the site in the absence of liquefaction. With a few exceptions, the liquefaction case histories are bounded by the relationships by Kayen et al. (1992) and Lodge (1994). The relationship by Robertson et al. (1992) is the least conservative of the three relationships.

Recommended Liquefaction Potential Boundaries Based on V_{S1} and CRR

After reviewing the proposed procedures outlined above, this workshop agreed that a careful review of the case histories should be conducted. It was suggested that the recommended V_S-based procedure follow the general format of the CPT- and SPT-based procedures.

The compiled case histories for magnitude 5.9 to 7.7 earthquakes are shown in Figs. 8, 9 and 10. The plotted data have been separated into three categories: (1) sands and gravels with average fines (particles smaller than 75 μm) content less than or equal to 5%, Fig. 8; (2) sands and gravels with average fines content of 6% to 34%, Fig. 9; and (3) sands and silts with average fines content greater than or equal to 35%, Fig. 10. Where possible, the fines content is noted next to the data point corresponding to soils with over 5% fines. The data for the Larter Ranch and Whiskey Springs sites are not shown, since the soils at these two sites may be weakly cemented with carbonate. Following the recommendation of this workshop, the plotted data are based on representative values of V_{S1} and a_{max} for the average of peak values for the x and y ground acceleration time histories that would have occurred at the site in the absence of liquefaction. Values of V_{S1} are calculated using Eq. 4. Values of r_d are estimated using the relationship by Seed and Idriss (1971).

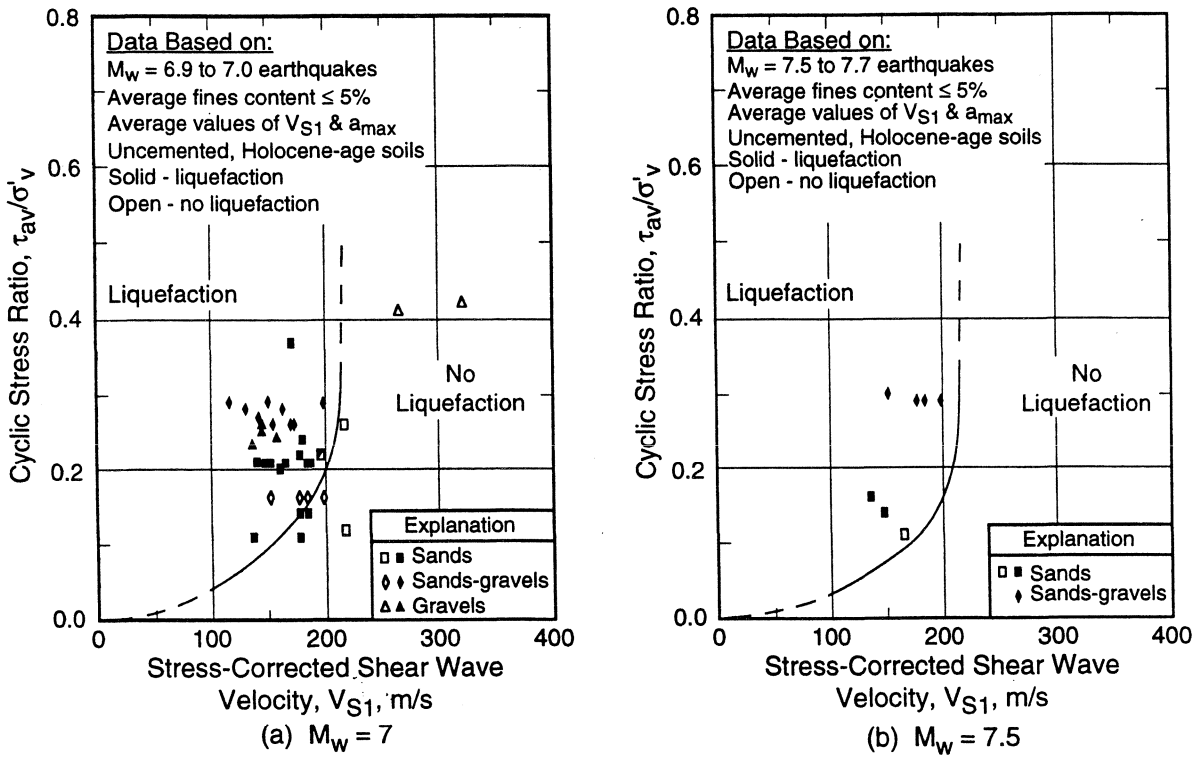

Fig. 8 - Comparison of Liquefaction Assessment Charts Based on V_{S1} and CSR from Analysis for this Report with Case Histories of Uncemented Soils with Fines Content Less than or Equal to 5%.

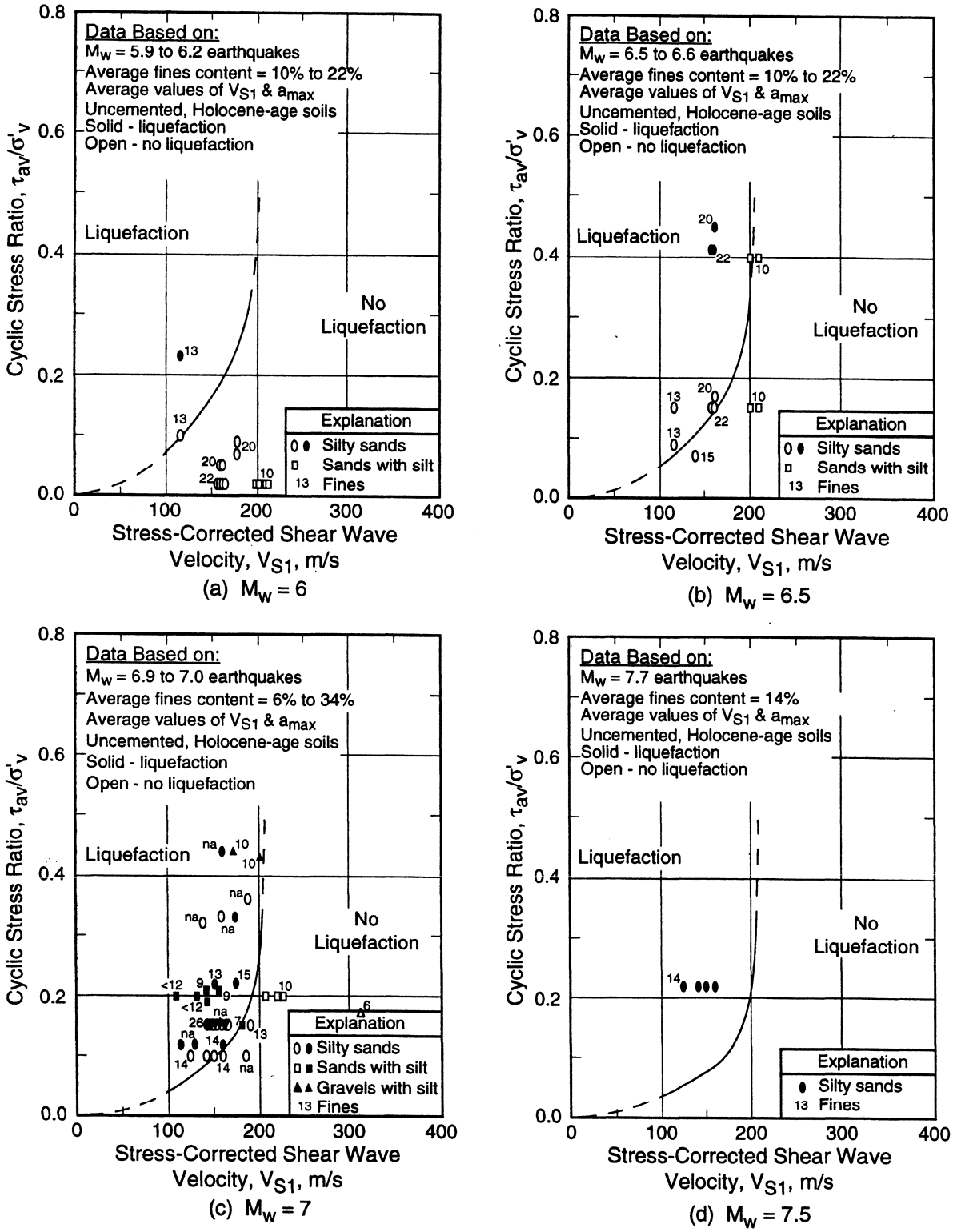

Fig. 9 - Comparison of Liquefaction Assessment Charts Based on V_{S1} and CSR from Analysis for this Report with Case Histories of Uncemented Soils with Fines Content of 6% to 34%.

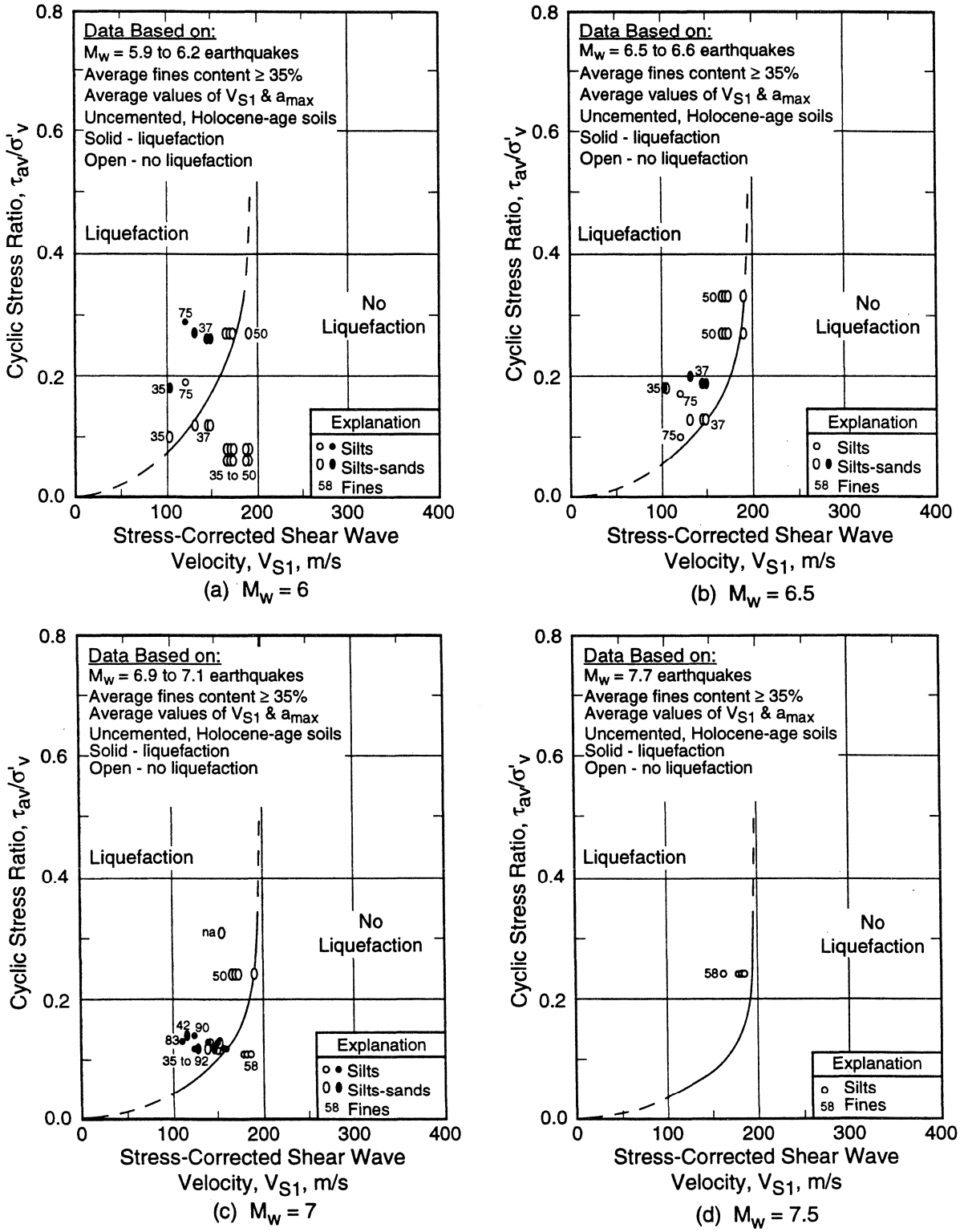

Fig. 10 - Comparison of Liquefaction Assessment Charts Based on V_{S1} and CSR from Analysis for this Report with Case Histories of Uncemented Soils with Fines Content Greater than or Equal to 35%.

Dobry (1996) derived a relationship between cyclic stress ratio and V_{S1} for constant average cyclic strain, γ_{av}, using the equations:

$$\gamma_{av} = \tau_{av}/(G)_{\gamma_{av}} \quad (5)$$

and

$$G_{max} = \rho\, V_S^2 \quad (6)$$

where $(G)_{\gamma_{av}}$ is shear modulus at γ_{av}, G_{max} is small-strain shear modulus, and ρ is mass density. Combining Eqs. 5 and 6, and dividing both sides by σ'_v leads to:

$$\tau_{av}/\sigma'_v = (\rho/\sigma'_v)\, \gamma_{av}\, (G/G_{max})_{\gamma_{av}}\, V_S^2 \quad (7)$$

If everything is done at a reference stress, P_a, then $V_S = V_{S1}$ and a line of constant average cyclic strain is of the form:

$$\tau_{av}/\sigma'_v = f(\gamma_{av})\, V_{S1}^2 \quad (8)$$

where $f(\gamma_{av}) = (\rho/P_a)\, \gamma_{av}\, (G/G_{max})_{\gamma_{av}}$. This formulation assumes the modulus reduction factor, $(G/G_{max})_{\gamma_{av}}$, is independent of confining pressure and pore water pressure buildup. Equation 8 is strong evidence for extending the liquefaction potential boundaries to the origin, and provides a rational approach for establishing the boundaries at low values of V_{S1} (say $V_{S1} \leq 125$ m/s).

For higher values of V_{S1}, it seems reasonable that the boundary separating liquefiable and non-liquefiable soils would become asymptotic to some limiting value of V_{S1}. This limit is caused by the tendency of dense granular soils to exhibit dilative behavior at large strains. Thus, Eq. 8 is modified to:

$$CRR = \tau_l/\sigma'_v = a\, (V_{S1}/100)^2 + b\, [1/(V_{S1c} - V_{S1}) - 1/V_{S1c}] \quad (9)$$

where V_{S1c} is the critical value of V_{S1} that separates contractive and dilative behavior, and "a" and "b" are curve fitting parameters.

Using the relationship between CRR and V_{S1} expressed by Eq. 9, curves have been drawn to separate the liquefaction and non-liquefaction case histories plotted in Figs. 8, 9 and 10. The curves are drawn assuming a = 0.03 and b = 0.9 for earthquakes with magnitude of 7.5. Depending on fines content (FC), the following values of V_{S1c} are also assumed:

$V_{S1c} = 220$ m/s for sands and gravels with FC $\leq 5\%$ (10a)
$V_{S1c} = 210$ m/s for sands and gravels with FC $\approx 20\%$ (10b)
$V_{S1c} = 200$ m/s for sands and silts with FC $\geq 35\%$ (10c)

For earthquakes with magnitude of 6, 6.5 and 7, scaling factors of 2.1, 1.6 and 1.25, respectively, are applied to the curves for magnitude 7.5 earthquakes. The curves shown in Figs. 8, 9 and 10 correctly predict more than 95% of the occurrences of liquefaction.

The three liquefaction case histories that lie slightly below the boundary curves shown in Figs. 8a and 9c are for the Treasure Island UM06 and UM11, and Marina District School sites. The data point for Treasure Island UM11 (see Fig. 9c) would lie on the boundary for 7% fines content, the average fines content of the most vulnerable layer for this site. In addition, the Treasure Island sites are located along the perimeter of the island where liquefaction was moderate during the 1989 Loma Prieta earthquake and where sloping ground may have been a factor. The Marina District School site is located on the margin of mapped artificial fill and liquefaction damage caused by the Loma Prieta earthquake. Hence, there are only two cases of liquefaction that incorrectly lie outside the region of predicted liquefaction as defined by these procedures, and they are cases of marginal to moderate liquefaction.

Figure 11 presents the recommended liquefaction potential boundaries for magnitude 7.5 earthquakes and uncemented Holocene-age soils with various fines content. Although these boundaries pass through the origin, natural alluvial sandy soils with shallow water tables rarely have stress corrected shear wave velocities less than 100 m/s, as shown by the in situ measurements presented in Figs. 8, 9 and 10. For a V_{S1}-value of 100 m/s and a magnitude 7.5 earthquake, the calculated CRR is 0.03. This minimal CRR value is consistent with intercept CRR values of 0.03 to 0.05 suggested by the CPT and SPT procedures. The recommended boundary for uncemented soils with fines content $\leq$ 5% and earthquakes with magnitude of 7, shown in Fig. 8a, is similar to the boundaries of Kayen et al. (1992) and Lodge (1994), shown in Fig. 7b, at lower values of V_{S1} ($V_{S1} < 200$ m/s).

Values of V_{S1c} between 200 m/s and 220 m/s are consistent with values determined using the relationship between SPT blow count and shear wave velocity by Ohta and Goto (1976) modified to blow count with theoretical free-fall energy of 60% (Seed et al. 1985). Assuming a corrected blow count of 30 and a depth of 10 m, approximate values of V_{S1} range from 190 m/s for clays to 220 m/s for sandy gravels of Holocene-age. More work is needed to further validate and refine the values of V_{S1c}.

The magnitudes scaling factors of 2.1, 1.6 and 1.25 for earthquakes with magnitude of 6, 6.5 and 7, respectively, compare well with SPT-based factors developed in recent years by several investigators (Youd and Noble in press), as noted in Columns 3 through 7 of Table 2. They form the upper bound of scaling factors recommended by this workshop (Section 1, workshop report) for earthquakes with magnitude less than 7.5. The lower bound of the range of recommended scaling factors is defined by the scaling factors developed by Idriss (1996), as listed in Column 3 of Table 2.

The relationship between earthquake magnitude and magnitude scaling factor, MSF, can be expressed by (modified from Idriss 1996):

$$MSF = (M_w/7.5)^n \qquad (11)$$

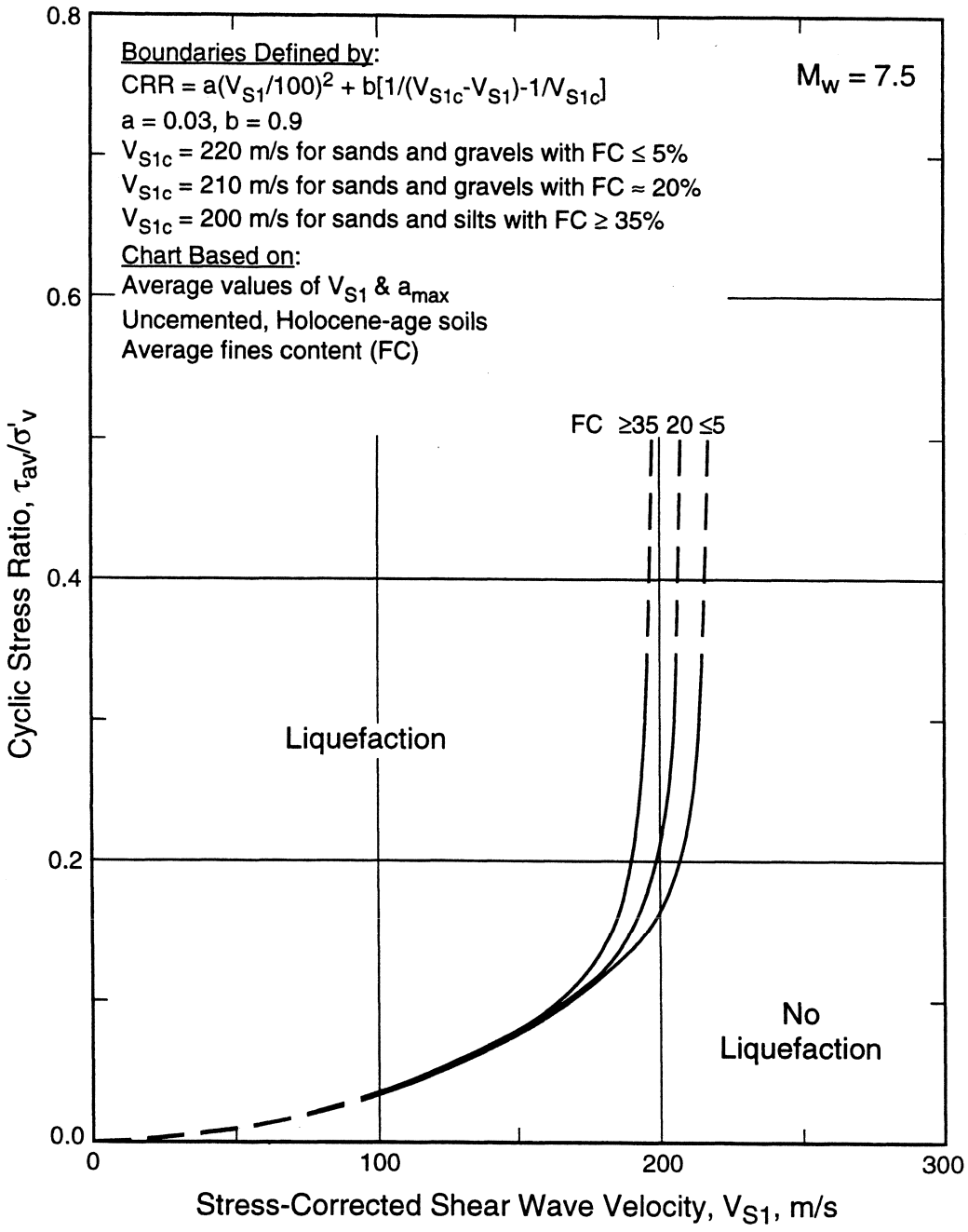

Fig. 11 - Recommended Liquefaction Assessment Chart Based on V_{S1} and CSR for Magnitude 7.5 Earthquakes and Uncemented Soils of Holocene Age.

where "n" is a curve fitting parameter. The scaling factors developed by Prof. Idriss as listed in Column 3 of Table 2 are defined by Eq. 11 with n = -2.56. For the scaling factors used to construct the V_S-based liquefaction potential boundaries shown in Figs. 8, 9 and 10 (MSF = 2.1, 1.6, 1.25, and 1.0 for M_W = 6, 6.5, 7 and 7.5, respectively), the value of "n" is -3.3.

While only the scaling factors determined by Idriss (1996) for earthquakes with magnitude greater than 7.5 have been recommended by this workshop, the scaling factors determined using n = -3.3 are slightly more conservative. For example, Eq. 11 with n = -3.3 provides scaling factors of 0.81 and 0.66 for earthquakes with magnitude of 8 and 8.5, respectively. These scaling factors are slightly less than the scaling factors of 0.84 and 0.72 for earthquakes with magnitude of 8 and 8.5, respectively, determined by Prof. Idriss.

Using Eq. 11 with n = -3.3 and the boundary for uncemented clean sands and gravels shown in Fig. 11, leads to the family of curves shown in Fig. 12. The curves shown in Fig. 12 imply that liquefaction will never occur in any earthquake if V_{S1} exceeds 220 m/s and the soils are uncemented and of Holocene age.

In areas with cemented soils, local correlations between shear wave velocity and penetration resistance should be developed to determine the effects of cementation. The boundaries shown in Fig. 11 could then be modified by increasing the abscissas by some factor. For example, measurements from the Larter Ranch and Whiskey Springs sites which liquefied during the 1983 Borah Peak, Idaho earthquake suggest a correction factor of about 1.3 to 1.4 (Andrus 1994) for those distal alluvial fan sediments.

Table 2. Magnitude Scaling Factors Obtained by Various Investigators (modified from Youd and Noble in press).

Moment Magnitude, M_W	Magnitude Scaling Factor (MSF)						
	Seed and Idriss (1982)	Idriss (1996)	Ambraseys (1988)	Youd and Noble, p<32% (in press)	Arango (1996)		This Report
(1)	(2)	(3)	(4)	(5)	(6)	(7)	(8)
5.5	1.43	2.20	2.86	3.42	3.00	2.20	2.8*
6.0	1.32	1.76	2.20	2.35	2.00	1.65	2.1
6.5	1.19	1.44	1.69	1.66	1.60	1.40	1.6
7.0	1.08	1.19	1.30	1.20	1.25	1.10	1.25
7.5	1.00	1.00	1.00		1.00	1.00	1.0
8.0	0.94	0.84	0.67		0.75	0.85	0.8*
8.5	0.89	0.72	0.44				0.65*

*Extrapolated from scaling factors for M_W = 6, 6.5, 7 and 7.5 using MSF = $(M_W/7.5)^{-3.3}$.

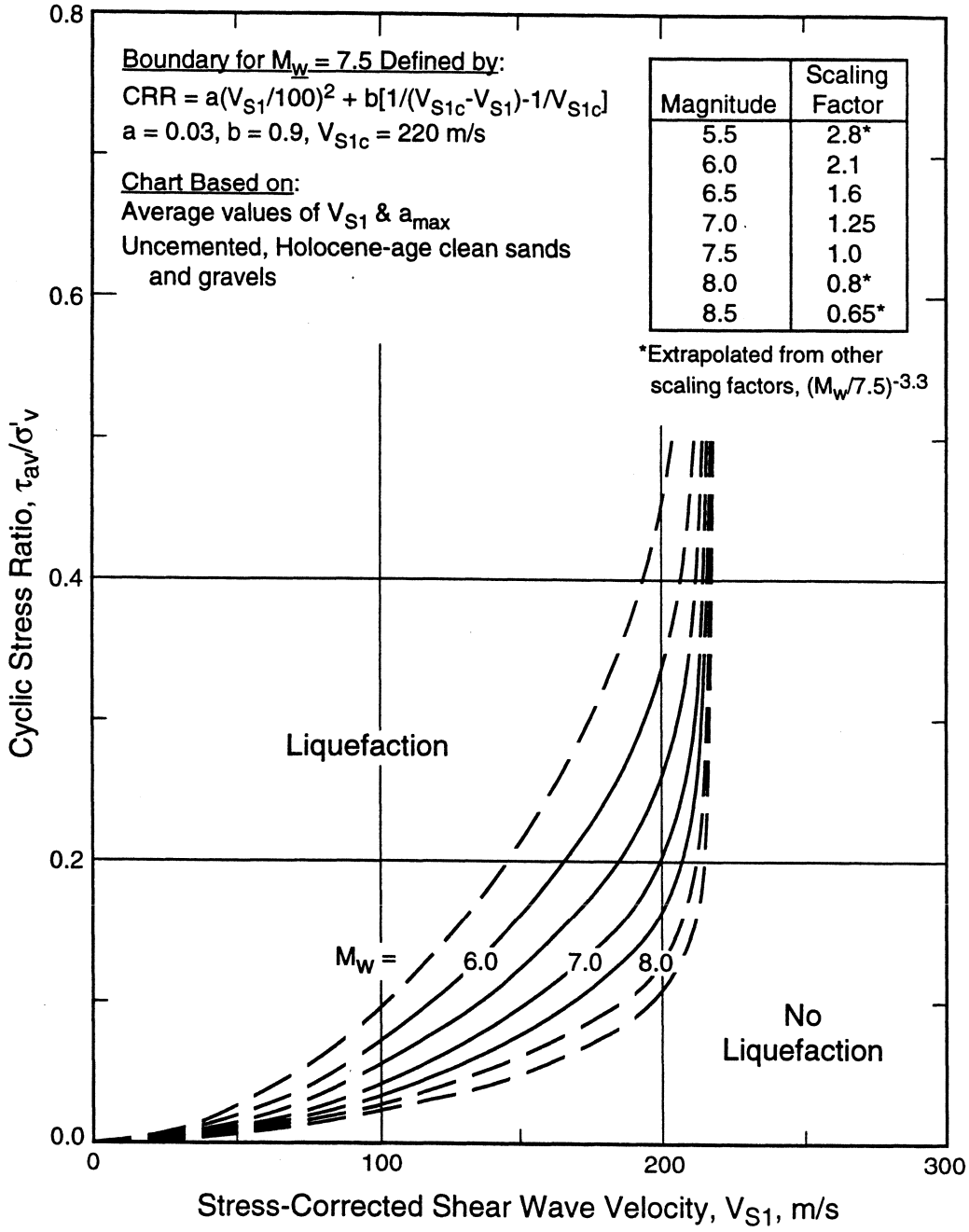

Fig. 12 - Recommended Chart Based on V_{S1} and CSR for Evaluation of Liquefaction Potential of Uncemented Clean Sands and Gravels of Holocene Age.

Recommended Liquefaction Potential Boundaries Based on V_S and a_{max}

By combining Eqs. 1, 4 and 9, a relationship based on V_S and a_{max} is obtained in the form of:

$$a_{max}/g = f_1 \{a (f_2 V_S/100)^2 + b [1/(V_{S1c} - f_2 V_S) - 1/V_{S1c}]\} \quad (12)$$

where $f_1 = \sigma'_v/(0.65\ \sigma_v\ r_d)$ and $f_2 = (P_a/\sigma'_v)^{0.25}$. Assuming (1) the water table is located midway between the ground surface and the center of the most vulnerable layer and (2) the total unit weight of soil is 17.3 kN/m^3 above the water table and 18.9 kN/m^3 below the water table, then f_1 and f_2 can be approximated by:

$$f_1 \approx 1.1/r_d \quad (13)$$

and

$$f_2 \approx (7.3/z)^{0.25} \quad (14)$$

where z is depth to center of the most vulnerable layer in meters. For noncritical projects, this workshop suggests the following equations to estimate average values of r_d (Liao and Whitman):

$$r_d = 1.0 - 0.00765\ z \qquad \text{for } z \le 9.15 \text{ m} \quad (15a)$$
$$r_d = 1.174 - 0.0267\ z \qquad \text{for } 9.15 \text{ m} < z \le 23 \text{ m} \quad (15b)$$

Equations 12 through 15 provide a simple relationship between V_S and a_{max} that depends on depth. A relationship that depends on depth agrees with the analytical study by Stokoe et al. (1988b). For example, the critical values of V_S shown in Fig. 3c at a_{max} equal to 0.2 g and layer thickness of 3.0 m are about 110 m/s for a depth of 4.6 m and 170 m/s for a depth 12.2 m.

Liquefaction potential boundaries defined by Eqs. 12 through 15 are shown in Figs. 13, 14 and 15. Also shown are the case history data. Liquefaction behavior predicted by these boundaries is similar to behavior predicted by the boundaries based on V_{S1} and CRR. The three liquefaction case histories that lie slightly below the boundaries shown in Figs. 13a and 14c are the same three that lie slightly below the boundaries shown in Figs. 8a and 9c (Treasure Island UM06 and UM11, and Marina District School sites). Thus, the procedure based on V_S, a_{max} and depth is a good approximation to the recommended procedure based on V_{S1} and CRR.

The application of Eqs. 12 through 15 should be limited to sites with characteristics similar to the database (i.e., level ground, depth of most vulnerable layer less than 12 m, depth of water table 0.5-7.6 m, and uncemented soils of Holocene age).

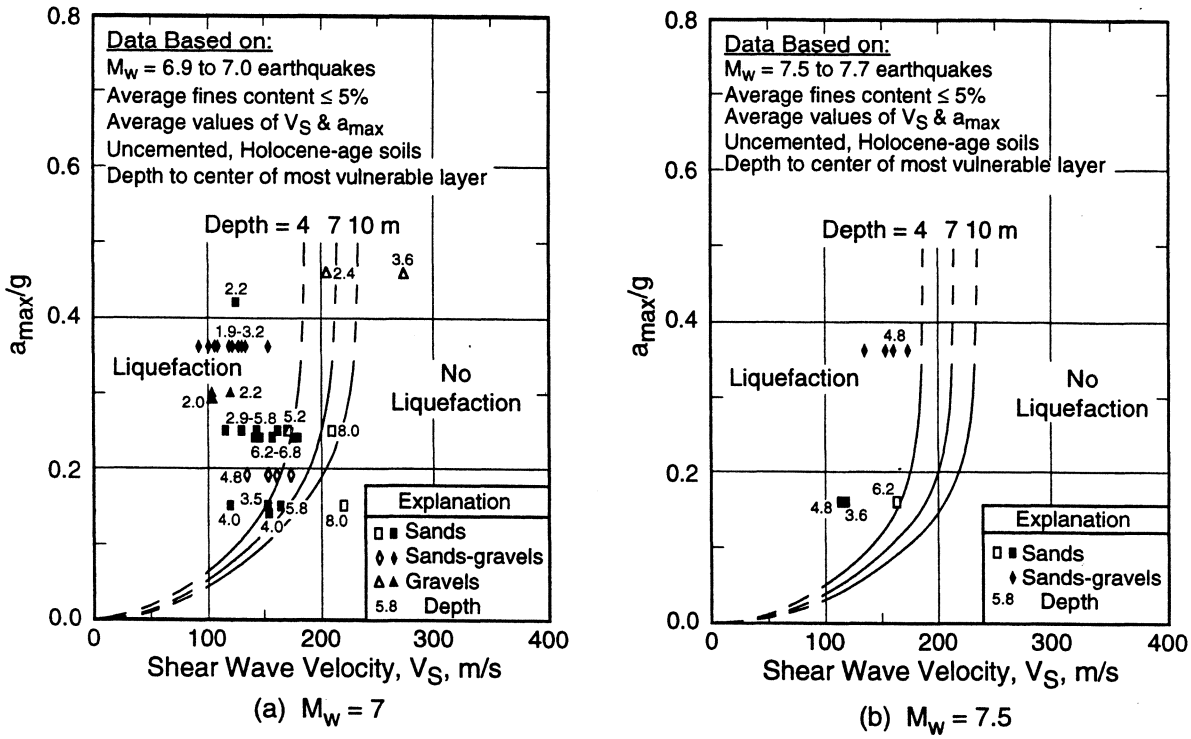

Fig. 13 - Comparison of Liquefaction Assessment Charts Based on V_S and Average a_{max} from Analysis for this Report with Case Histories of Uncemented Soils with Fines Content Less than or Equal to 5%.

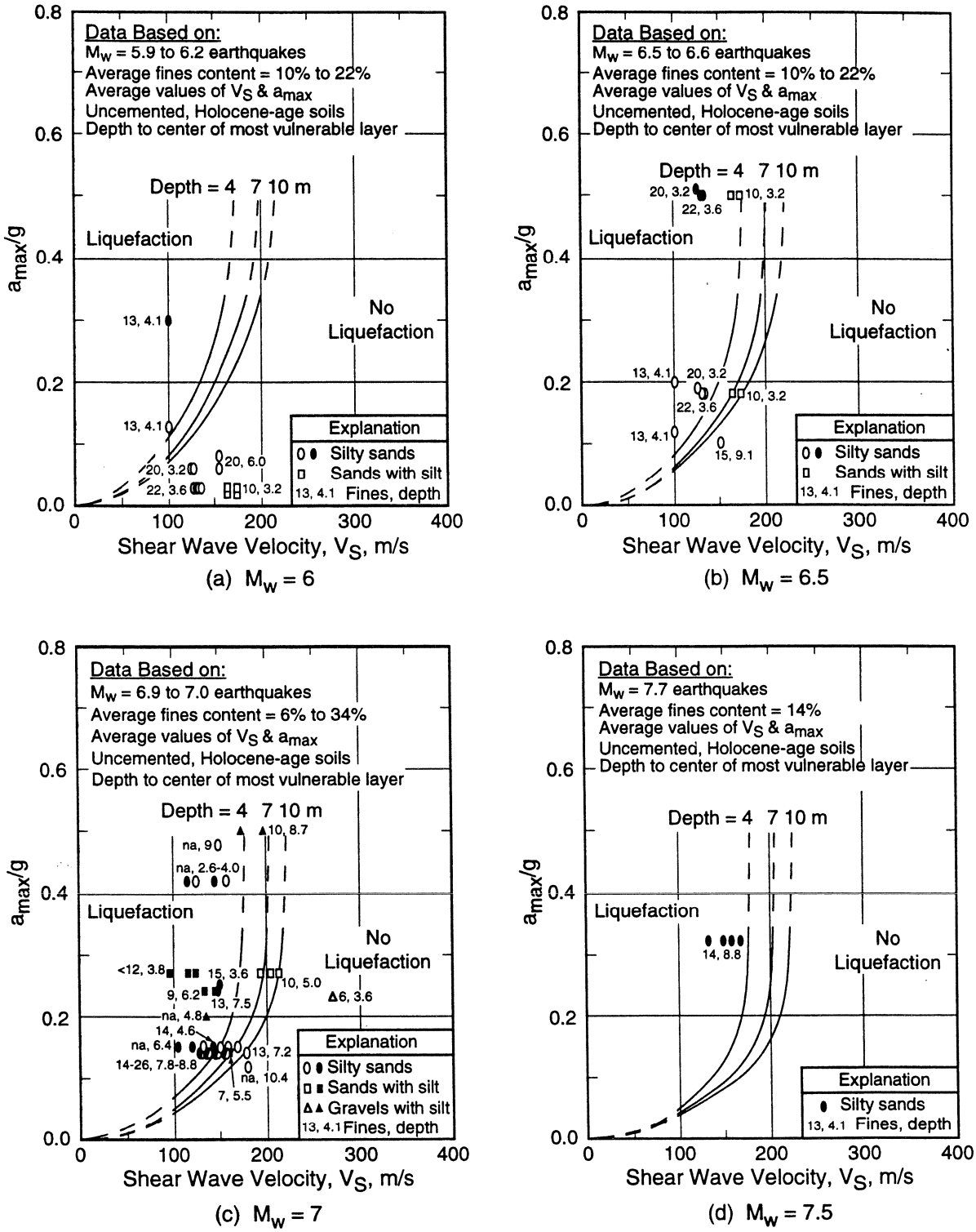

Fig. 14 - Comparison of Liquefaction Assessment Charts Based on V_S and Average a_{max} from Analysis for this Report with Case Histories of Uncemented Soils with Fines Content of 6% to 34%.

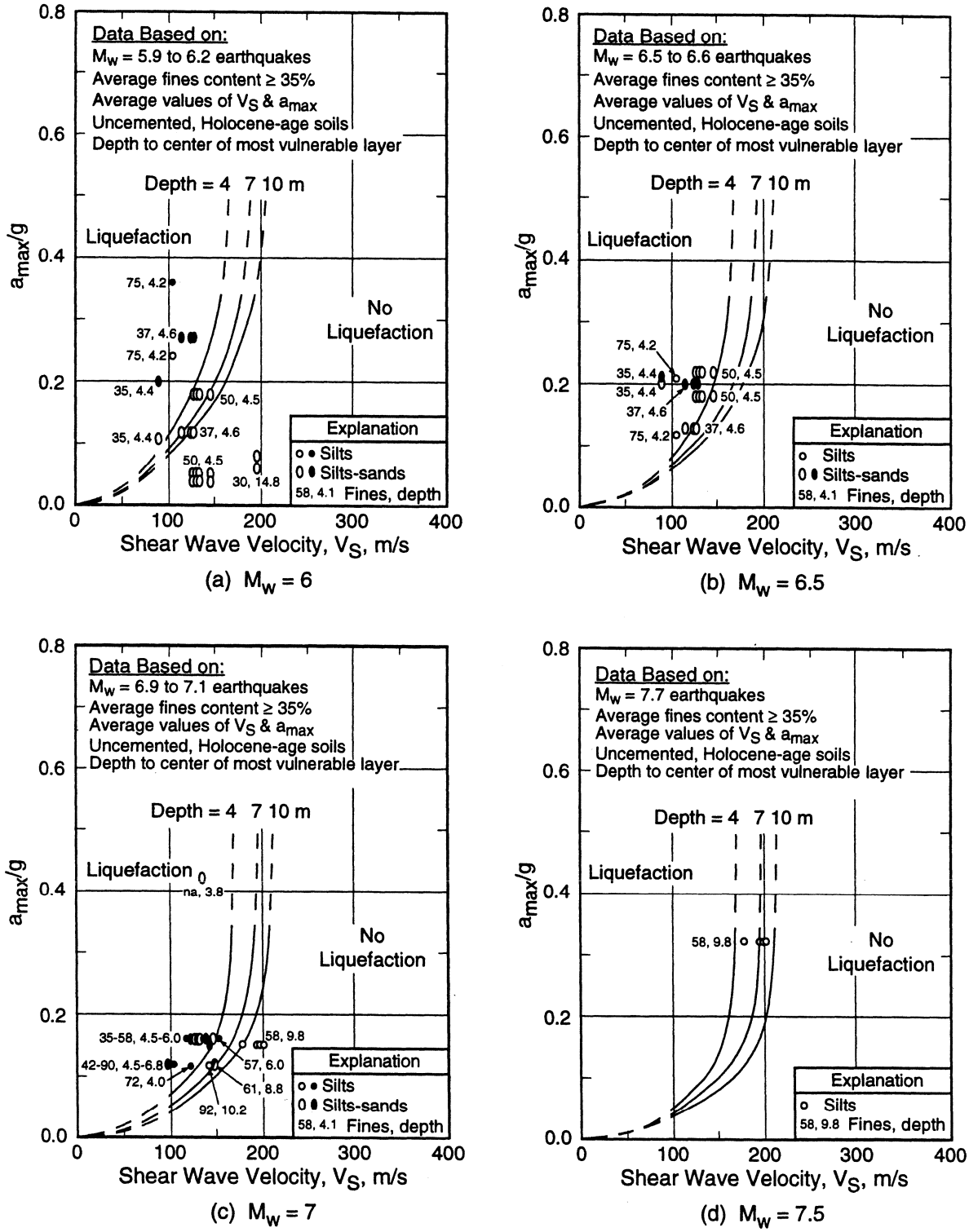

Fig. 15 - Comparison of Liquefaction Assessment Charts Based on V_S and Average a_{max} from Analysis for this Report with Case Histories of Uncemented Soils with Fines Content Greater than or Equal to 35%.

Conclusions and Recommendations

This report summarizes liquefaction and non-liquefaction case histories from 20 earthquakes and over 50 sites in soils ranging from sandy gravel with cobbles to profiles including silty clay layers. The data are limited to relatively level ground sites with the following characteristics: (1) depth of most vulnerable layer less than 12 m; (2) uncemented soils of Holocene age, with a few exceptions; and (3) depth of water table between 0.5 m and 7.6 m.

The compiled case histories are used to evaluate current liquefaction assessment procedures based on small-strain shear wave velocity. Most sites where surface manifestations of liquefaction were observed are correctly predicted by the current procedures. However, the boundaries by Stokoe et al. (1988b) are nonconservative at values of V_S less than about 180 m/s. The boundaries by Tokimatsu et al. (1991a) for earthquakes with greater than about 10 cycles of loading are nonconservative at values of V_{S1} greater than about 150 m/s. The boundary by Robertson et al. (1992) for earthquakes with magnitude of 7.5 is nonconservative at values of V_{S1} less than about 200 m/s. With few exceptions, the liquefaction case histories for earthquakes with magnitude of 7 are bounded by the relationships by Kayen et al. (1992) and Lodge (1994).

This workshop agreed that a careful review of the compiled case histories should be conducted. It was suggested that the recommended V_S-based procedure follow the general format of the CPT- and SPT-based procedures.

To develop the recommended liquefaction potential boundaries, the compiled case histories are separated into three categories: (1) sands and gravels with average fines content less than or equal to 5%; (2) sands and gravels with average fines content of 6% to 34%; and (3) sands and silts with average fines content greater than or equal to 35%. The data for two sites are not considered, since soils at these sites may be weakly cemented with carbonate. Representative values of V_{S1} for the most vulnerable layer and average values of a_{max} that would have occurred at the site in the absence of liquefaction are used. Values of V_{S1} are calculated using Eq. 4. Values of r_d are estimated using the relationship by Seed and Idriss (1971).

The recommended liquefaction potential boundaries are established by applying a modified relationship between V_{S1} and cyclic stress ratio for constant average cyclic shear strain suggested by Dobry (1996). The relationship by Dobry provides strong evidence for extending the boundaries to the origin. It is modified to become asymptotic to some limiting value of V_{S1}. This limit is caused by the tendency of dense granular soils to exhibit dilative behavior at large strains.

Figure 11 presents the recommended liquefaction potential boundaries for magnitude 7.5 earthquakes and uncemented Holocene-age soils. These boundaries are defined by Eq. 9 with a = 0.03, b = 0.9, and V_{S1c} = 200 m/s to 220 m/s depending on fines content.

Using scaling factors of 2.1, 1.6, 1.25 and 1.0 for earthquakes with magnitude of 6, 6.5, 7 and 7.5, respectively, provide boundaries that included more than 95% of the liquefaction case histories. These magnitude scaling factors lie within the range of scaling factors recommended by this workshop.

Caution should be exercised when applying the liquefaction potential boundaries to sites where conditions are different from the database. More work is needed to further validate and refine the values of V_{S1c}. Additional well-documented case histories of all types of soil that have and have not liquefied during earthquakes should be compiled, particularly from deeper deposits (depth > 8 m) and from denser soils (V_S > 200 m/s) shaken by stronger ground motions (a_{max} > 0.4 g), to further validate these boundaries.

Liquefaction potential boundaries based on V_S, a_{max} and depth defined by Eqs. 12 through 15 provide a good approximation to the recommended procedure based on V_{S1} and CRR. These simpler boundaries are suggested for initial site screening, and should be limited to sites with characteristics similar to the database.

Two limitations of using shear wave velocity are its high sensitivity to weak interparticle bonding, and the lack of a sample for identifying non-liquefiable clayey soils. Therefore, the preferred practice is to drill sufficient boreholes and take samples to verify or develop local correlations for soil types encountered, to identify non-liquefiable clay-rich soils, and to detect liquefiable weakly cemented soils. A combination of techniques may provide the most cost-effective approach for evaluating sites of large areal extent. In some cases, such as many landfills where borings are not permitted, evaluation based on shear wave velocity may be the only feasible approach.

Acknowledgments

The reporters thank the participants of this workshop for their constructive review, which greatly enhanced the quality of this report. Workshop participants included T. L. Youd (Chair), I. M. Idriss (Co-chair), I. Arango, G. Castro, J. T. Christian, R. Dobry, W. D. L. Finn, L. F. Harder, Jr., M. E. Hynes, K. Ishihara, J. P. Koester, S. S. C. Liao, W. F. Marcuson, III, G. R. Martin, J. K. Mitchell, Y. Moriwaki, M. S. Power, P. K. Robertson, and R. B. Seed. The review comments and encouragement of R. M. Chung are also greatly appreciated.

References

Ambraseys, N. N. (1988). "Engineering Seismology," Earthquake Engineering and Structural Dynamics, Vol. 17, p. 1-105.

Andrus, R. D., Stokoe, K. H., II, Bay, J. A., and Youd, T. L. (1992). "In Situ V_S of Gravelly Soils Which Liquefied," Proceedings, Tenth World Conference on Earthquake Engineering, held in Madrid, Spain, A.A. Balkema, Rotterdam, The Netherlands, pp. 1447-1452.

Andrus, R. D. (1994). "In Situ Characterization of Gravelly Soils That Liquefied in the 1983 Borah Peak Earthquake," Ph.D. Dissertation, University of Texas at Austin, 533 p.

Andrus, R. D., and Youd, T. L. (1987). "Subsurface Investigation of a Liquefaction-Induced Lateral Spread, Thousand Springs Valley, Idaho," Geotechnical Laboratory Miscellaneous Paper GL-87-8, U.S. Army Engineer Waterways Experiment Station, Vicksburg, MS, 131 p.

Aouad, M. F. (1986). "Analytical Investigations of the Relationship between Shear Wave Velocity and the Liquefaction Potential of Sands," M.S. Report, Geotechnical Engineering Center, Department of Civil Engineering, University of Texas at Austin, 87 p.

Arango, I. (1996). "Magnitude Scaling Factors for Soil Liquefaction Evaluations," Journal of Geotechnical Engineering, ASCE, Vol. 122, No. 11, pp. 929-936.

Arulanandan, K., Yogachandran, C., Meegoda, N. J., Ying, L., and Zhauji, S. (1986). "Comparison of the SPT, CPT, SV and Electrical Methods of Evaluating Earthquake Induced Liquefaction Susceptibility in Ying Kou City During the Haicheng Earthquake," Proceedings, Use of In Situ Tests in Geotechnical Engineering, Geotechnical Special Publication No. 6, held in Blacksburg, Virginia, S. P. Clemence, Ed., ASCE, New York, NY, pp. 389-415.

Barrow, B. L. (1983). "Field Investigation of Liquefaction Sites in Northern California," Geotechnical Engineering Thesis GT83-1, University of Texas at Austin, 213 p.

Bennett, M. J. (1995). Personal communication to R. D. Andrus.

Bennett, M. J., Youd, T. L., Harp, E. L., and Wieczorek, G. F. (1981). "Subsurface Investigation of Liquefaction, Imperial Valley Earthquake, California, October 15, 1979," Open-File Report 81-502, U.S. Geological Survey, 83 p.

Bennett, M. J., McLaughlin, P. V., Sarmiento, J. S., and Youd, T. L. (1984). "Geotechnical Investigation of Liquefaction Sites, Imperial Valley, California," Open-File Report 84-252, U.S. Geological Survey, 103 p.

Bennett, M. J., and Tinsley, J. C. (1995). "Geotechnical Data from Surface and Subsurface Samples Outside of and within Liquefaction-Related Ground Failures Caused by the October 17, 1989, Loma Prieta Earthquake, Santa Cruz and Monterey Counties, California," Open-File Report 95-663, U.S. Geological Survey.

Bierschwale, J. G., and Stokoe, K. H., II (1984). "Analytical Evaluation of Liquefaction Potential of Sands Subjected to the 1981 Westmorland Earthquake," Geotechnical Engineering Report GR-84-15, University of Texas at Austin, 231 p.

Boulanger, R. W., Idriss, I. M., and Mejia, L. H. (1995). "Investigation and Evaluation of Liquefaction Related Ground Displacements at Moss Landing During the 1989 Loma Prieta Earthquake," Report No. UCD/CGM-95/02, University of California at Davis.

Boulanger, R. W., Mejia, L. H., and Idriss, I. M. (1997). "Liquefaction at Moss Landing During Loma Prieta Earthquake," Journal of Geotechnical and Geoenviromental Engineering, ASCE, Vol. 123, No. 5, pp. 453-467.

Dobry, R. (1996). Personal communication to R. D. Andrus.

Dobry, R., Stokoe, K. H., II, Ladd, R. S., and Youd, T. L. (1981). "Liquefaction Susceptibility from S-Wave Velocity, " Proc., In Situ Testing to Evaluate Liquefaction Susceptibility, ASCE National Convention, held in St. Louis, MO.

Dobry, R., Baziar, M. H., O'Rourke, T. D., Roth, B. L., and Youd, T. L. (1992). "Liquefaction and Ground Failure in the Imperial Valley, Southern California During the 1979, 1981 and 1987 Earthquakes," Case Studies of Liquefaction and Lifeline Performance During Past Earthquakes, Technical Report NCEER-92-0002, T. O'Rourke and M. Hamada, Eds., National Center for Earthquake Engineering Research, Buffalo, NY, Vol. 2.

Dobry, R., Ladd, R. S., Yokel, F. Y., Chung, R. M., and Powell, D. (1982). "Prediction of Pore Water Pressure Buildup and Liquefaction of Sands During Earthquakes by the Cyclic Strain Method," NBS Building Science Series 138, U.S. Department of Commerce, National Bureau of Standards, Gaithersburg, MD, 152 p.

EPRI (1992). Lotung Large-Scale Seismic Test Strong Motion Records, EPRI NP-7496L, Electric Power Research Institute, Palo Alto, California, Vols. 1-7.

Fuhriman, M. D. (1993). "Crosshole Seismic Tests at Two Northern California Sites Affected by the 1989 Loma Prieta Earthquake," M.S. Thesis, University of Texas at Austin, 516 p.

Geomatrix (1990). "Results of Field Exploration and Laboratory Testing Program for Perimeter Dike Stability Evaluation Naval Station Treasure Island San Francisco, California, Project No. 1539.05, Vol. 2.

Gibbs, J. F., Fumal, T. E., Boore, D. M., and Joyner, W. B. (1992). "Seismic Velocities and Geologic Logs from Borehole Measurements at Seven Strong-Motion Stations that Recorded the Loma Prieta Earthquake," Open-File Report 92-287, U.S. Geological Survey, 139 p.

Hardin, B. O., and Drnevich, V. P. (1972). "Shear Modulus and Damping in Soils: Design Equations and Curves," Journal of the Soil Mechanics and Foundation Division, ASCE, New York, NY, Vol. 98, SM7, pp. 667-692.

Hryciw, R. D. (1991). "Post Loma Prieta Earthquake CPT, DMT and Shear Wave Velocity Investigations of Liquefaction Sites in Santa Cruz and on Treasure Island," Final Report to the U.S. Geological Survey, Award No. 14-08-0001-G1865, University of Michigan, 68 p.

Hryciw, R. D., Rollins, K. M., Homolka, M., Shewbridge, S. E., and McHood, M. (1991). "Soil Amplification at Treasure Island During the Loma Prieta Earthquake," Proceedings, Second International Conference on Recent Advances in Geotechnical Earthquake Engineering and Soil Dynamics, held in St. Louis, Missouri, S. Prakash, Ed., University of Missouri-Rolla, Vol. II, pp. 1679-1685.

Idriss, I. M. (1996). Personal communication to T. L. Youd.

Ishihara, K., Shimizu, K., and Yamada, Y. (1981). "Pore Water Pressures Measured in Sand Deposits During an Earthquake," Soils and Foundations, Japanese Society of Soil Mechanics and Foundation Engineering, Vol. 21, No. 4, pp. 85-100.

Ishihara, K., Anazawa, Y., and Kuwano, J. (1987). "Pore Water Pressures and Ground Motions Monitored During the 1985 Chiba-Ibaragi Earthquake," Soils and Foundations, Japanese Society of Soil Mechanics and Foundation Engineering, Vol. 27, No. 3, pp. 13-30.

Ishihara, K., Muroi, T., and Towhata, I. (1989). "In-situ Pore Water Pressures and Ground Motions Monitored During the 1985 Chiba-Ibaragi Earthquake," Soils and Foundations, Japanese Society of Soil Mechanics and Foundation Engineering, Vol. 29, No. 4, pp. 75-90.

Kayen, R. E., Liu, H. -P., Fumal, T. E., Westerland, R. E., Warrick, R. E., Gibbs, J. F., and Lee, H. J. (1990). "Engineering and Seismic Properties of the Soil Column at Winfield Scott School, San Francisco," Effects of the Loma Prieta Earthquake on the Marina District San Francisco, California, Open-file Report 90-253, U.S. Geological Survey, pp. 112-129.

Kayen, R. E., Mitchell, J. K., Seed, R. B., Lodge, A., Nishio, S., and Coutinho, R. (1992). "Evaluation of SPT-, CPT-, and Shear Wave-Based Methods for Liquefaction Potential Assessment Using Loma Prieta Data," Proceedings, Fourth Japan-U.S. Workshop on Earthquake Resistant Design of Lifeline Facilities and Countermeasures for Soil Liquefaction, Technical Report NCEER-92-0019, held in Honolulu, Hawaii, M. Hamada and T. D. O'Rourke, Eds., National Center for Earthquake Engineering Research, Buffalo, NY, Vol. 1, pp. 177-204.

Kokusho, T., Sato, K., and Matsumoto, M. (1995a). "Nonlinear Seismic Amplification of Soil Ground During 1995 Hyogoken-Nanbu Earthquake," Proceedings, Fifth International Conference on Seismic Zonation, held in Nice, France, Presses Académiqes, Vol. II, pp. 1603-1610.

Kokusho, T., Tanaka, Y., Kudo, K., and Kawai, T. (1995b). "Liquefaction Case Study of Volcanic Gravel Layer during 1993 Hokkaido-Nansei-Oki Earthquake," Proceedings, Third International Conference on Recent Advances in Geotechnical Earthquake Engineering and Soil Dynamics, held in St. Louis, Missouri, S. Prakash, Ed., University of Missouri-Rolla, Vol. I, pp. 235-242.

Kokusho, T., Yoshida, Y., and Tanaka, Y. (1995c). "Shear Wave Velocity in Gravelly Soils with Different Particle Gradings," Proceedings, Static and Dynamic Properties of Gravelly Soils, Geotechnical Special Publication No. 56, M. D. Evans and R. J. Fragaszy, Eds., ASCE, pp. 92-106.

Liao, S. S. C., and Whitman, R. V. (1986). "A Catalogue of Liquefaction and Non-liquefaction Occurrences During Earthquakes," Research Report, Dept. of Civil Engineering, M.I.T., Cambridge, MA.

Ladd, R. S. (1982). "Geotechnical Laboratory Testing Program for Study and Evaluation of Liquefaction Ground Failure Using Stress and Strain Approaches: Heber Road Site, October 15, 1979 Imperial Valley Earthquake," Woodward-Clyde Consultants, Wayne, New Jersey, February.

Lodge, A. L. (1994). "Shear Wave Velocity Measurements for Subsurface Characterization," Ph.D. Dissertation, University of California at Berkeley.

Mitchell, J. K., Lodge, A. L., Coutinho, R. Q., Kayen, R. E., Seed, R. B., Nishio, S., and Stokoe, K. H., II (1994). "Insitu Test Results from Four Loma Prieta Earthquake Liquefaction Sites: SPT, CPT, DMT, and Shear Wave Velocity," Report No. UCB/EERC-94/04, Earthquake Engineering Research Center, University of California at Berkeley, 171 p.

Ohta, Y., and Goto, N. (1976). "Estimation of S-Wave Velocity in Terms of Characteristic Indices of Soil," Butsuri-Tanko (Geophysical Exploration), Vol. 24, No. 4, pp. 34-41 (in Japanese).

Redpath, B. B. (1991). "Seismic Velocity Logging in the San Francisco Bay Area," Report to the Electric Power Research Institute, Palo Alto, California, 34 p.

Robertson, P. K., Woeller, D. J., and Finn, W. D. L. (1992). "Seismic Cone Penetration Test for Evaluating Liquefaction Potential Under Cyclic Loading," Canadian Geotechnical Journal, Ottawa, Canada, Vol. 29, pp. 686-695.

Rollins, K. M., McHood, M. D., Hryciw, R. D., Homolka, M., and Shewbridge, S. E. (1994). "Ground Response on Treasure Island," The Loma Prieta, California, Earthquake of October 17, 1989--Strong Ground Motion, U.S. Geological Survey Professional Paper 1551-A, R. D. Borcherdt, Ed., United States Government Printing Office, Washington, pp. A109-A121.

Roy, D., Campanella, R. G., Byrne, P. M., and Hughes, J. M. O. (1996). "Strain Level and Uncertainty of Liquefaction Related Index Tests," Proceedings, Uncertainty in the Geologic Environment: From Theory to Practice, Geotechnical Special Publication No. 58, held in Madison, Wisconsin, C. D. Shackelford, P. P. Nelson, and M. J. S. Roth, Eds., ASCE, Vol. 2, pp. 1149-1162.

Sato, K., Kokusho, T., Matsumoto, M., and Yamada, E. (1996). "Nonlinear Seismic Response and Soil Property During Strong Motion," Soils and Foundations, Special Issue on the 1995 Hyogoken-Nambu Earthquake, Japanese Geotechnical Society, January, pp. 41-52.

Schnabel, P. B., Lysmer, J., and Seed, H. B. (1972). "SHAKE: A Computer Program for Earthquake Response Analysis of Horizontally Layered Sites," Earthquake Engineering Research Center Report No. UCB/EERC-72-12, University of California, Berkeley.

Seed, H. B. (1979). "Soil Liquefaction and Cyclic Mobility Evaluation for Level Ground During Earthquakes," Journal of the Geotechnical Engineering Division, ASCE, New York, NY, Vol. 105, GT2, pp. 201-255.

Seed, H. B., and Idriss, I. M. (1971). "Simplified Procedure for Evaluating Soil Liquefaction Potential," Journal of the Soil Mechanics and Foundation Division, ASCE, New York, NY, Vol. 97, SM9, pp. 1249-1273.

Seed, H. B., and Idriss, I. M. (1982). Ground Motions and Soil Liquefaction During Earthquakes, monograph series, Earthquake Engineering Research Institute, Berkeley, California, 134 p.

Seed, H. B., Idriss, I. M., and Arango, I. (1983). "Evaluation of Liquefaction Potential Using Field Performance Data," Journal of Geotechnical Engineering Division, ASCE, New York, NY, Vol. 109, No. 3, pp. 458-482.

Seed, H. B., Tokimatsu, K., Harder, L. F., and Chung, R. M. (1985). "Influence of SPT Procedures in Soil Liquefaction Resistance Evaluations," Journal of Geotechnical Engineering Division, ASCE, Vol. 111, No. 12, pp. 1425-1445.

Shen, C. K., Li, X. S., and Wang, Z. (1991). "Pore Pressure Response During 1986 Lotung Earthquakes," Proceedings, Second International Conference on Recent Advances in Geotechnical Earthquake Engineering and Soil Dynamics, held in St. Louis, Missouri, S. Prakash, Ed., University of Missouri-Rolla, Rolla, Mo., Vol. I, pp. 557-563.

Shibata, T., Oka, F., and Ozawa, Y. (1996). "Characteristics of Ground Deformation Due to Liquefaction," Soils and Foundations, Special Issue on the 1995 Hyogoken-Nambu Earthquake, Japanese Geotechnical Society, January, pp. 65-79.

Stokoe, K. H., II, Andrus, R. D., Bay, J. A., Fuhriman, M. D., Lee, N. J., and Yang, Y. (1992). "SASW and Crosshole Seismic Test Results from Sites that Did and Did not Liquefy During the 1989 Loma Prieta, California Earthquake," Geotechnical Engineering Center, Department of Civil Engineering, University of Texas at Austin.

Stokoe, K. H., II, and Nazarian, S. (1985). "Use of Rayleigh Waves in Liquefaction Studies," Proceedings, Measurement and Use of Shear Wave Velocity for Evaluating Dynamic Soil Properties, held in Denver, Colorado, R. D. Woods, Ed., ASCE, New York, NY, pp. 1-17.

Stokoe, K. H., II, Andrus, R. D., Rix, G. J., Sanchez-Salinero, I., Sheu, J. C., and Mok, Y. J. (1988a). "Field Investigation of Gravelly Soils Which Did and Did Not Liquefy During the 1983 Borah Peak, Idaho, Earthquake," Geotechnical Engineering Center Report GR 87-1, University of Texas at Austin, 206 p.

Stokoe, K. H., II, Roesset, J. M., Bierschwale, J. G., and Aouad, M. (1988b). "Liquefaction Potential of Sands from Shear Wave Velocity," Proceedings, Ninth World Conference on Earthquake Engineering, held in Tokyo, Japan, Vol. III, pp. 213-218.

Sugito, M., Sekiguchi, K., Oka, F., and Yashima, A. (1996). "Analysis of Borehole Array Records from the South Hyogo Earthquake of Jan. 17, 1995," Proceedings of the International Workshop on Site Response Subjected to Strong Earthquake Motions, held in Yokosuka, Japan on January 15-17, Port and Harbor Research Institute, Yokosuka, Japan, Vol. 2, pp. 343-357.

Sykora, D. W., and Stokoe, K. H., (1982), "Seismic Investigation of Three Heber Road Sites After the Oct. 15, 1979 Imperial Valley Earthquake," Geotechnical Engineering Report GR82-24, University of Texas at Austin.

Tokimatsu, K., Kuwayama, S., and Tamura, S. (1991a). "Liquefaction Potential Evaluation Based on Rayleigh Wave Investigation and Its Comparison with Field Behavior," Proceedings, Second International Conference on Recent Advances in Geotechnical Earthquake Engineering and Soil Dynamics, held in St. Louis, Missouri, S. Prakash, Ed., University of Missouri-Rolla, Rolla, Mo., Vol. I, pp. 357-364.

Tokimatsu, K., Kuwayma, S., Abe, A., Nomura, S., and Tamura, S. (1991b). "Considerations to Damage Patterns in the Marina District During Loma Prieta Earthquake Based on Rayleigh Wave Investigation," Proceedings, Second International Conference on Recent Advances in Geotechnical Earthquake Engineering and Soil Dynamics, held in St. Louis, Missouri, S. Prakash, Ed., University of Missouri-Rolla, Vol. II, pp. 1649-1654.

Turner, E. and Stokoe, K. H., II (1992). "Static and Dynamic Properties of Clayey Soils Subjected to the 1979 Imperial Valley Earthquake," Geotechnical Engineering Report GR82-26, University of Texas at Austin, 208 p.

Youd, T. L., and Noble, S. K. (in press). "Magnitude Scaling Factors," Proceedings, NCEER Workshop on Evaluation of Liquefaction Resistance, held in Salt Lake City, Utah, T. L. Youd and I. M. Idriss, Eds., National Center for Earthquake Engineering Research, Buffalo, NY.

Youd, T. L., and Bennett, M. J. (1983). "Liquefaction Sites, Imperial Valley, California," Journal of Geotechnical Engineering Division, ASCE, Vol. 109, No. 3, pp. 440-457.

Youd, T. L., and Hoose, S. N. (1978). "Historic Ground Failures in Northern California Triggered by Earthquakes," U.S. Geological Survey Professional Paper 993, 177 p.

Application of the Becker Penetration Test for Evaluating the Liquefaction Potential of Gravelly Soils

Leslie F. Harder, Jr.

Chief, Division of Engineering
California Department of Water Resources
Sacramento, California 94236-0001

Abstract

The Becker Penetration Test has seen increased use in North America as an in situ technique for measuring the liquefaction potential of gravelly soils. This test involves the use of a large dynamic penetrometer and incorporates elements of both pile driving and the Standard Penetration Test. Despite its increasing use, it remains a non-standard test with many uncertainties involving driving energy and casing friction. This paper describes the development of the test, its application, and recommendation for its use in the assessment of liquefaction potential.

INTRODUCTION

The liquefaction potential of sandy and silty soils in situ is generally evaluated with the use of either the Standard Penetration Test (SPT) or the Cone Penetrometer Test (CPT). However, soils with substantial gravel contents cannot be reliably evaluated with these tools because the gravel particles are large relative to the effective size of the penetrometers. The inevitable result is that these tools will give erroneously high penetration resistances because the gravel particles disrupt the normal displacement of the soil by the penetrometer. Further, the drive shoe of a SPT sampler may become blocked by a gravel particle and driven as a solid penetrometer rather than as a hollow penetrometer.

The difficulties associated with drilling and testing gravelly soils with conventional penetrometers has led to the use of larger penetrometers. Large dynamic penetrometers have been used both in Italy and Japan (Jamiolkowski, et al.; Tokimatsu, 1988). In North America, the Becker Penetration Test has seen increased use for the evaluation of gravelly deposits. The Becker Penetration Test was developed in Canada in the late 1950's and is now widely used for exploring the characteristics of deposits containing gravel and cobble-size particles. The test consists of driving a double-walled casing into the ground with a double-acting diesel pile hammer. The general approach is to count the number of diesel hammer blows per 30 centimeters of penetration. Although similar in nature to the SPT, the Becker Penetration Test is a continuous sounding method. Typically, a 3-meter length of casing is driven into the ground and the blowcounts are recorded. After the initial casing length is driven into the ground, another section of casing is threaded onto the end of the previous casing, and driving is resumed. The process is continued until the desired depth is reached and the casing is jacked out of the ground.

In recent years, the test has been used by several investigators to evaluate the equivalent relative density and/or the liquefaction potential of gravelly soils. The general approach is to determine Becker Penetration resistance in the field and then convert it into an equivalent SPT resistance to evaluate future performance of the gravelly soil. Although the Becker Penetration Test has been used successfully in this manner for many projects, it remains a non-standard test that is used with a multitude of different types of equipment and procedures. The test continues to need improved standardization and interpretation in the following main areas:

- Elimination of the use of open-bit Becker soundings for evaluation of penetration resistance.
- Standardization of driving and penetration equipment.
- Determination/Interpretation of diesel hammer driving energy.
- Evaluation/Interpretation of the effect of casing friction on penetration resistance.

These subjects are described further in the following sections.

OPEN-BIT BECKER SOUNDINGS

The original intent of the Becker apparatus was to rapidly obtain samples of gravelly material. This is accomplished by driving with an open bit and using reverse air circulation in the annular space between the double-walled casing. During driving, air is forced down the annulus of the casing system to the drive bit. Soil particles entering the bit are then transported up the inner casing to the surface by the air flow and are then collected in a cyclone for examination or testing (see Figure 1).

Company literature from Becker Drills, Inc. and others have recommended that reliable penetration resistance should be obtained with a plugged drive bit, and that sampling should be obtained with a separate sounding with an open-bit and reverse air circulation. However, this approach requires additional soundings, and many firms have in the past opted to use **only** open-bit soundings to obtain both penetration resistance and sampling information. This latter approach is likely to result in excessively low (overly conservative) values of penetration resistance. Harder and Seed (1986) documented the fact that the air recirculation process commonly loosens and removes material ahead of the bit, particularly in saturated sandy material. This then results in unreasonably low blowcount data, even for very dense soils.

The study by Harder and Seed (1986) also recommended that penetration and sampling information be obtained in separate plugged-bit and open-bit soundings. Although this recommendation currently appears to be generally followed, some investigators still try to obtain both types of data with open-bit soundings alone. In addition, some investigators will stop the driving of an open-bit sounding and then complete SPT tests through the Becker casing within sandy layers that have been encountered. As documented by Harder and Seed (1986), this also commonly results in unreasonably low blowcount data because the soil ahead of the Becker bit has been disturbed by the air recirculation sampling process performed earlier. The only way this SPT sampling approach would work successfully is if the disturbed material ahead of the bit was removed by mud rotary drilling performed through the Becker casing. This would probably require drilling and removing material for a distance of at least 2 to 3 meters ahead of the bit before performing the SPT test.

STANDARDIZATION OF DRIVING AND PENETRATION EQUIPMENT

Becker Penetration Tests continue to be performed with a variety of different types of driving and penetration equipment:

- Drill rigs: Older HAV-180 or B-180 rigs
  Newer AP-1000 rigs*

- Superchargers: Some diesel hammers have superchargers*
  Some diesel hammers do not have superchargers

- Casing sizes: 140-mm (5.5-inch) O.D.
  168-mm (6.6-inch) O.D.*
  229-mm (9.0-inch) O.D.

- Drive bit: Crowd-in open bit
  Crowd-out open bit
  Crowd-in plugged bit
  Crowd-out plugged bit*

* Recommended by Harder and Seed (1986)

Local correlations can generally be made between Becker and SPT blowcounts with most of the above equipment combinations, except with open bits as noted previously. However, different sets of equipment types will result in different penetration resistances being determined for the same deposit. The correlation between Becker and SPT blowcounts published by Harder and Seed (1986) is intended for a plugged, crowd-out bit, 168-mm O.D. casing, and driven with an AP-1000 drill rig. The original Harder and Seed (1986) correlation has been supplemented with data from other projects and appears to remain the most practical correlation available (see Figure 2). It is also the only correlation that has been used to evaluate actual gravel deposits which have liquefied during earthquake shaking. Consequently, even with the use of local correlations it is desirable to use the Harder and Seed (1986) correlation as a check on the information being gathered. Therefore, the above recommended set of equipment types should be used essentially as a standard to perform most investigations if the Harder and Seed (1986) correlation is to be used.

A second choice would be to use the same set of equipment, but with a HAV-180 drill rig. Several comparison tests have been performed to show that this older style of drill rig is significantly more efficient in allowing the hammer energy to be transmitted to the drive casing. This difference is thought to result from the different manner by which the diesel hammer is mounted to the mast of the different types of drill rigs. Comparison tests generally indicate that corrected Becker blowcounts obtained using a HAV-180 drill rig should be multiplied by a 1.5 correction factor to be converted into equivalent AP-1000 drill rig blowcounts. Several investigations have been successfully conducted with HAV-180 drill rigs using this 1.5 correction factor.

DETERMINATION/EVALUATION OF DIESEL HAMMER DRIVING ENERGY

Constant energy conditions are not a feature of the double-acting diesel hammers used in the Becker Penetration Test. One reason for this is that the energy is dependent upon combustion conditions. Thus, anything that affects combustion, such as fuel quantity, fuel quality, air mixture and pressure all have a significant effect on the energy produced. Combustion efficiency is also operator-dependent because the operator controls a variable throttle which affects how much fuel is injected for combustion. On some rigs, the operator also controls a rotary blower, or supercharger, which adds additional air to the combustion cylinder during each stroke. This additional air is thought to

better scavenge the cylinder of burnt combustion gases and has been found to produce higher energies.

To monitor the level of energy produced by the diesel hammer during driving, use has been made of the bounce chamber pressure. For the ICE Model 180 diesel hammers used on the Becker drill rigs, the top of the hammer is closed off to allow a smaller stroke and a faster driving rate. At the top, air trapped in the compression cylinder and a connected bounce chamber acts as a spring. The amount of potential energy within the ram at the top of its stroke can be estimated by measuring the peak pressure induced in the bounce chamber.

The studies by Harder and Seed (1986) made use of the bounce chamber to monitor combustion efficiencies. They did not attempt to directly measure the actual energy transferred to the casing during driving. Rather, they found that constant combustion conditions (e.g. full throttle with a supercharger) resulted in a relatively unique relationship between bounce chamber pressure and Becker blowcount. This relationship took the form of a curve and was designated a constant combustion rating curve. The Harder and Seed (1986) studies showed that different combustion conditions (e.g. reduced fuel or no supercharger) resulted in different Becker blowcounts and different constant combustion curves. Presented in schematic form in Figure 3 are typical results obtained for different combustion efficiencies. In the upper plot, three combustion rating curves representing three different combustion efficiencies are shown. With different combustion conditions, the resulting blowcounts from tests performed in the same materials can be radically different. Consequently, tests in the same material at a depth of 40 feet can give a Becker blowcount of 14 when the hammer is operated at high combustion efficiency, but give blowcounts of 26 and 50 at succeeding reductions of combustion energy.

To account for variable combustion effects, Harder and Seed (1986) adopted a standard constant combustion rating curve designated Curve AA (see Figure 4). They also developed correction curves for correcting data with low combustion efficiencies to this standard rating curve. Becker penetration resistance corrected to the standard rating curve was designated as the corrected Becker blowcount, N_{BC}. To use the correction curves, it is simply necessary to locate each uncorrected test result on the chart using both the uncorrected blowcount and the bounce chamber pressure, and then follow the correction curves down to the standard rating curve AA, to obtain the corrected Becker blowcount. For example, if the uncorrected Becker blowcount was 43 and it was obtained at sea level with a bounce chamber pressure of 18 psig, then the corrected Becker blowcount would be 30 (see Figure 4). Harder and Seed (1986) developed their SPT-Becker correlation by comparing corrected SPT blowcounts, N_{60}, in sandy and silty soils to the corrected Becker blowcount, N_{BC}, in adjacent borings and soundings (see Figure 2).

The standard constant combustion curve in Figure 4 is for sea level atmospheric pressures. To obtain equivalent sea level bounce chamber pressures, it is necessary to increase the measured bounce chamber pressures. Bounce chamber pressures measured at approximately 2,000 feet above sea level must be increased typically about 1.5 to 2 psi. Bounce chamber pressures measured at approximately 6,000 feet above sea level must be increased typically about 4 to 6 psi.

Several researchers have advocated the use of instrumentation and wave equation techniques developed for pile driving in an effort to better quantify the effects of variable hammer energy. Such an approach is very attractive as it would theoretically capture variations in both hammer energy and energy transmission through the hammer anvil to the casing. To date, the most notable of these efforts are those by Sy and Campanella (1994, 1995). In their studies, Sy and Campanella employed a small length of Becker casing fitted with strain gages and accelerometers together with a "Pile-Driving Analyzer" to determine strain, force, acceleration, and velocity. The transferred energy is determined by time integration of force times velocity. Measured blowcounts were corrected by Sy and Campanella to a reference energy value equal to 30 percent of the theoretical rated energy of the ICE 180 hammer. The energy corrected blowcount was designated as N_{b30}.

In their studies, Sy and Campanella were able to verify many of the variations in hammer energy previously identified by Harder and Seed (1986). These include the effect of variable throttle settings and the different energy transmission efficiencies of the HAV-180 and AP-1000 drill rigs. However, they were unable to improve or reduce the scatter associated with correlating corrected Becker and SPT blowcounts. Shown in Figure 5 is a comparison between Becker and SPT blowcounts using data obtained from the Richmond and Annacis Test Sites (after Sy and Campanella, 1994). In both cases the level of scatter is comparable. However, it should be noted that, as observed by these researchers, the Harder and Seed (1986) correlation developed for other sites fit well through the middle of the data when applied with the bounce chamber pressure correlation. This was true for SPT data obtained at depths extending down as far as 24 and 42 meters (Richmond and Annacis, respectively).

It is believed that such instrumentation and wave equation techniques will eventually be used with established correlations on a routine basis. However, this approach currently has had limited verification in the field and it requires significantly more time, cost, effort, and interpretation than the bounce chamber technique. For most investigations, therefore, there appears to be little benefit for the increased effort over the proper application of the Harder and Seed (1986) bounce pressure approach. However, both approaches point to the critical need to evaluate the hammer energy in at least some form during the evaluation of penetration resistance.

EVALUATION/INTERPRETATION OF THE EFFECT OF CASING FRICTION

The studies by Harder and Seed (1986) did not specifically address the effect of casing friction on the determined Becker blowcount. However, it is an important consideration because, unlike the SPT, the Becker penetration resistance is determined by both the tip resistance and any friction acting on the casing along the entire depth for which testing is being performed. During the studies performed by Harder and Seed, there was concern that casing friction would mask any loose, or low blowcount, gravelly soil layers. However, the initial studies found that low blowcount sand and gravel layers could be identified at depth by the Becker Penetration Test. Consequently, the initial concerns were somewhat abated and casing friction was considered to have an almost negligible impact for routine investigations to depths of about 30 meters.

During the last ten years, various investigations using the Harder and Seed approach have been able to identify loose sand and/or gravel layers both at depth and below layers of denser material. This has given continued support for the approach. However, casing friction still remains a concern in special circumstances, particularly involving great depths and/or the investigation of very soft soils underlying very thick deposits of very dense material. Recent investigations have identified some important results involving Becker casing friction:

1. A certain amount of casing friction is built into the Harder and Seed approach. Recent studies have shown that:

   a. There are now several test sites (e.g. Seymour Falls Dam, Duncan Dam, and Mormon Island Auxiliary Dam) where Becker Penetration Tests have been performed through pre-drilled and cased borings. When a significant portion of the depth is pre-drilled and cased, the cased Becker penetration resistance is significantly less than the uncased penetration resistance. In addition, the cased Becker penetration resistance used with the Harder and Seed approach generally under predicts measured values of SPT resistance of sandy soils at depth. Accordingly, the use of pre-drilled holes and casing to remove excessive friction is overly conservative and counter productive.

   b. Recent studies by Yan and Wightman (1992) have involved a mudded Becker sounding where bentonite drill mud is injected out of the casing just above the drive bit during driving. This technique also uses a modified drive bit that has a larger diameter than the casing to further reduce friction. The resulting Becker penetration resistance yields substantially lower blowcounts, commonly only 30 percent of the penetration resistance developed using conventional driving techniques (see Figure 6). This type of modified equipment may have great potential for sounding deep deposits. However, it would require a different correlation than those developed by Harder and Seed (1986). It may also have a depth limitation in that mudded Becker soundings may relieve too much of the casing friction and lead to conservatively low blowcounts at depth. As shown in the right plot in Figure 6, a traditional Becker sounding tends to give higher ratios of Becker blowcounts to SPT blowcounts with depth, indicating that casing friction may be significant. For the mudded Becker sounding, however, the ratio of Becker blowcount to SPT blowcount is approximately constant until about a 30-meter depth, and then it decreases significantly. It may be that the unsupported weight of the casing lengths and the diesel hammer significantly reduces penetration resistance when not supported by casing friction.

2. Several investigations have shown the ability of the Becker Penetration Test to identify loose sandy and/or gravelly deposits at depth. However, there are three sites (Jackson Lake Dam - Site A, McDonald's Farm, and Annacis) where the Becker Penetration Test used with the Harder and Seed approach missed the presence of soft silt deposits at depth. In all three cases the soft silt had SPT blowcounts of less than 5 and the silt

layer was at a depth of between 10 and 45 meters underlying moderately dense sand. Corrected Becker blowcounts were typically three to eight times higher at these particular depth intervals.

Recent studies by Sy and Campanella (1994, 1995) have attempted to directly address the effect of casing friction. In addition to correcting for energy content, Sy and Campanella perform CAPWAP analyses to separately estimate casing friction, Rs, and tip resistance. CAPWAP is a computer program which uses the force and velocity traces obtained with the Pile Driving Analyzer to estimate loading conditions and resistances through a trial and error process. As described by Lum and Yan (1994), this process can be time consuming and expensive. Consequently, CAPWAP analyses have generally been performed only at three or four depths for any Becker sounding. The casing friction determined at these depths is then interpolated and extrapolated for the rest of the sounding profile. Sy and Campanella produced a correlation between Becker and SPT blowcounts which uses both the energy corrected Becker blowcount and the estimated shaft resistance (see Figure 7). This correlation was developed using CAPWAP analyses of data obtained at the Annacis Test Site.

The Sy and Campanella correlation has been compared to the Harder and Seed correlation at a few projects. Figure 8 presents comparisons developed by Lum and Yan (1994) for three soundings performed within gravelly soil at Keenlyside Dam. As may be observed in the figure, the two correlations give similar equivalent SPT blowcounts for much of each profile. However, as noted by Lum and Yan (1994), the Sy and Campanella correlation yields much more variability. In addition, it may be seen that the Sy and Campanella correlation predicts extremely high penetration resistance at some depth intervals. To provide support for their correlation, Sy and Campanella compared equivalent Becker and actual SPT N_{60} values for one of their correlation sites, Annacis. As shown in Figure 9, the Sy and Campanella correlation compared reasonably well for the Annacis site down to depths of about 42 meters, not surprising since this was the site used to develop the correlation. Also shown in Figure 9 is a comparison for the same site, only using the Harder and Seed approach to interpret the Becker soundings. As may be observed, the Harder and Seed correlation produced predicted SPT blowcounts that correlated with measured SPT resistance just as well as the Sy and Campanella correlation. The Sy and Campanella work published to date does not appear to attempt to predict the presence of soft silt layers at depth.

As noted previously, the "mudded" casing approach may provide a way to eliminate the effects of casing friction. In this approach, it may not be necessary to account for friction effects, either by explicit or implicit means, as the casing friction is nearly eliminated (see Figure 6). The effects of drill rig type and hammer energy might be determined with a few site specific calibrations between bounce chamber pressure and a limited number of measurements of hammer energy delivered to the casing. However, the time consuming and expensive CAPWAP analyses would not be necessary as friction is essentially eliminated. In this way, a simple and inexpensive approach might be very successful in determining equivalent SPT blowcounts at large depths beneath even very dense material. More research and correlations need to be developed and published for practitioners to evaluate the potential of this approach. One concern is that the weight of the casing and hammer will result in conservatively low penetration resistance at depth in a mudded sounding due to the

elimination of casing friction. As shown in Figure 6, the ratio of mudded Becker blowcounts to SPT blowcounts decreases with depth. This issue needs to be addressed in future developments of this approach. Nevertheless, it is a very promising direction for future improvements in the Becker Penetration Test.

RECOMMENDATIONS

The Becker Penetration Test remains a non-standard test with results subject to interpretation. Many uncertainties will eventually be cleared up with the use of new equipment and approaches. However, for current use, the following procedures are recommended:

1. The use of the Becker Penetration Test should be carried out with plugged-bit soundings in order to avoid an overly conservative evaluation of subsurface deposits.

2. In order to avoid the use of several correction factors, it is recommended that the Becker Penetration Test be performed with the following set of equipment:

   - AP-1000 Drill Rig
   - Plugged 168-mm O.D. Drive Bit and Casing

3. It is necessary to monitor the efficiency/performance of the diesel hammer during driving. This can be done using the bounce chamber pressure with the Harder and Seed method, or may be performed using more sophisticated instrumentation similar to that used by Sy and Campanella. The Sy and Campanella approach provides insight on the tip and casing friction elements of Becker penetration resistance. However, for most investigations where depths are less than about 30 meters, the simpler Harder and Seed approach is probably warranted because of the greater data base together with its ease of implementation and lower cost.

4. Casing friction will remain a concern until either different equipment or approaches are developed to make the determined penetration resistance independent of casing length. For most investigations, the Harder and Seed approach with friction effects implicitly incorporated will probably be adequate. However, for depths greater than 30 meters and/or for sites with thick deposits of very dense material overlying much looser material, more sophisticated approaches involving wave equation techniques may be necessary. Unreasonably low penetration resistance will be determined with the Harder and Seed approach if Becker soundings are performed through cased boreholes to reduce friction effects.

5. The Sy and Campanella studies have shown that wave equation techniques were able to confirm results previously produced by Harder and Seed (1986) using less sophisticated methods. This research has shown that the wave equation approach may

eventually produce better correlations for predicting the performance of gravelly materials. Hopefully, such methods will accurately account for casing friction in all cases, including conditions where soft silt layers are present at depth below much denser sand and gravel deposits. However, the Sy and Campanella approach can predict extremely high equivalent SPT blowcounts when the Becker blowcounts are only moderately high. This trend needs to be examined further and confirmed with comparisons of actual SPT blowcounts. The Sy and Campanella work, however, shows that this approach is promising and that it should be pursued further.

6. Additional research into the use of mudded Becker soundings with and without wave equation techniques should be performed with the goal of developing a sounding tool that could be efficiently used for all conditions regardless of friction concerns. There may be a concern that the use of the mudded technique relieves too much friction and that excessively low (overly conservative) penetration resistance may be predicted at large depths.

7. For all projects involving the Becker Penetration Test to investigate gravelly deposits, it is recommended that a local correlation or check be performed either at the project site or nearby. This local check would consist of performing Becker soundings in sandy material near the depth of interest and to also perform high quality SPT tests in the same layer. In this way, a check on the applicability of the Becker equipment and correlations may be made.

8. Several investigations have indicated that the Becker Penetration Test may not detect the presence of a very soft silt layer at depth. If such layers are thought to be present and of concern for the project, it is recommended that other investigative techniques (e.g. SPT) be carried out to explore and characterize such materials.

ACKNOWLEDGEMENTS

The investigations performed for the Harder and Seed (1986) studies were carried out under the direction of the late H. Bolton Seed. Dr. Seed's leadership, review, and guidance during the phases of these studies were instrumental in their successful completion. Many of the recent investigations associated with the Becker Penetration Test were sponsored by the British Columbia Hydroelectric Power Authority (B C Hydro). Permission to publish this data and sponsorship of these studies is gratefully acknowledged. In this regard, the assistance of Mr. Al Imrie is particularly appreciated.

REFERENCES

1. British Columbia Hydroelectric Power Authority (BC Hydro), Uncorrected Becker Data obtained at FMC, McDonald Farm, and Duncan Dam Test Sites.

2. Harder, L. F. (1988) "Use of Penetration Tests to Determine the Cyclic Load Resistance of Gravelly Soils," Dissertation submitted as partial satisfaction for the degree of Doctor of Philosophy, University of California, Berkeley.

3. Harder, L. F. Jr. and Seed, H. Bolton (1986), "Determination of Penetration Resistance for Coarse-Grained Soils using the Becker Hammer Drill," Earthquake Engineering Research Center, Report No. UCB/EERC-86/06, University of California, Berkeley.

4. Lum, Ken K. Y. and Yan, Li (1994) "In-situ Measurements of Dynamic Soil Properties and Liquefaction Resistances of Gravelly Soils at Keenleyside Dam," Proceedings of Specialty Session on Ground Failures under Seismic Conditions, ASCE Annual Convention, Atlanta, GA, October 9-13, 1994.

5. Sy, A. and Campanella, R.G. (1994) "Becker and standard penetration tests (BPT-SPT) correlations with consideration of casing friction," Canadian Geotechnical Journal, Vol. 31, pp. 343-356.

6. Sy, Alex, Campanella, R. G., and Stewart, Raymond A. (1995) "BPT-SPT Correlations for Evaluation of Liquefaction Resistance in Gravelly Soils," Proceedings of Specialty Session on Dynamic Properties of Gravelly Soil, ASCE Annual Convention, San Diego, California, October, 1995.

7. Tokimatsu, Kohji (1988) "Penetration Tests for Dynamic Problems," Proceedings of the first International Symposium on Penetration Testing, ISOPT-1, Orlando, March 20-24, 1988, A.A. Balkema.

8. Yan, L. and Wightman, A. (1992) "A Testing Technique for Earthquake Liquefaction Prediction in Gravelly Soils," Report by Foundex Explorations Ltd. and Klohn Leonoff Ltd. to National Research Council of Canada, Contract No. IRAP-M 40401W.

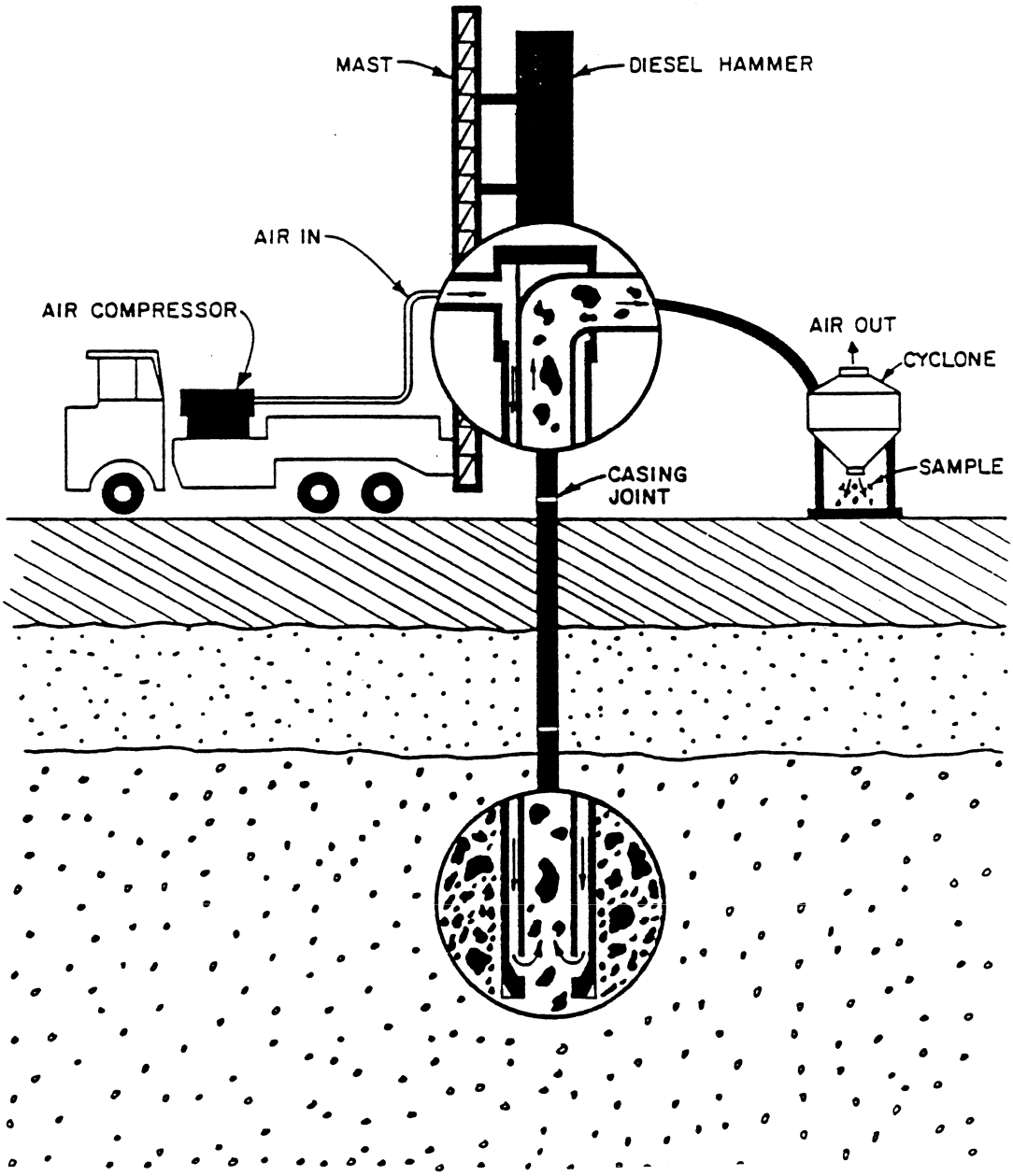

Figure 1: Schematic Diagram of Becker Sampling Operation

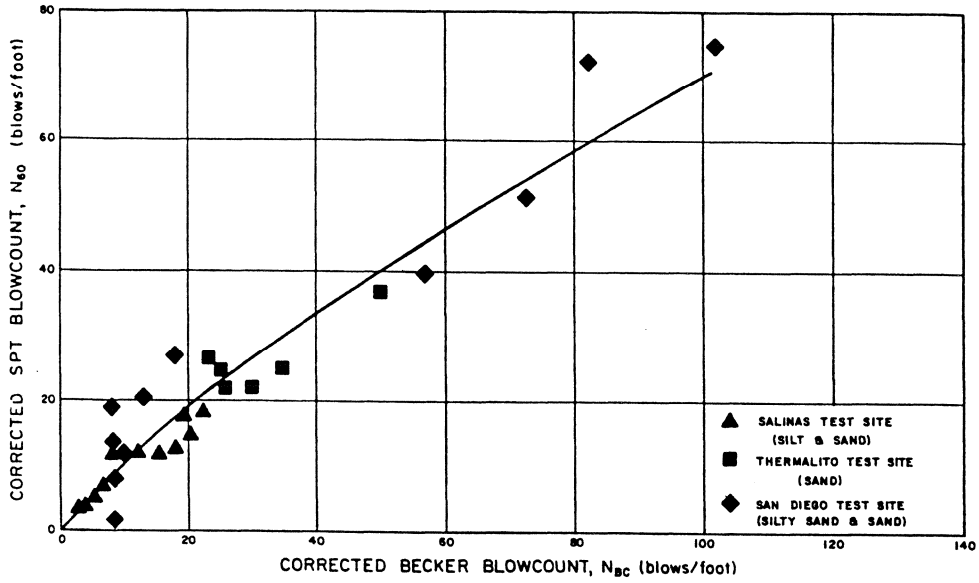

a. Original Harder and Seed (1986) Correlation

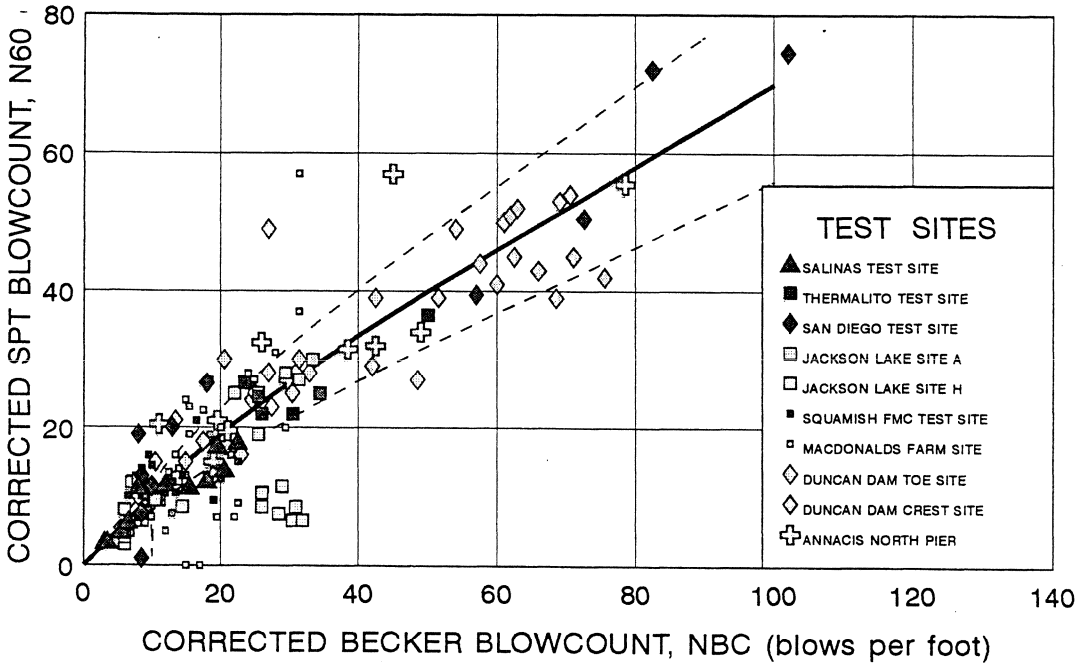

b. Harder and Seed (1986) Correlation Supplemented with Data from Additional Test Sites

Figure 2: Correlation Between Corrected Becker and SPT Blowcounts (from Harder and Seed, 1986)

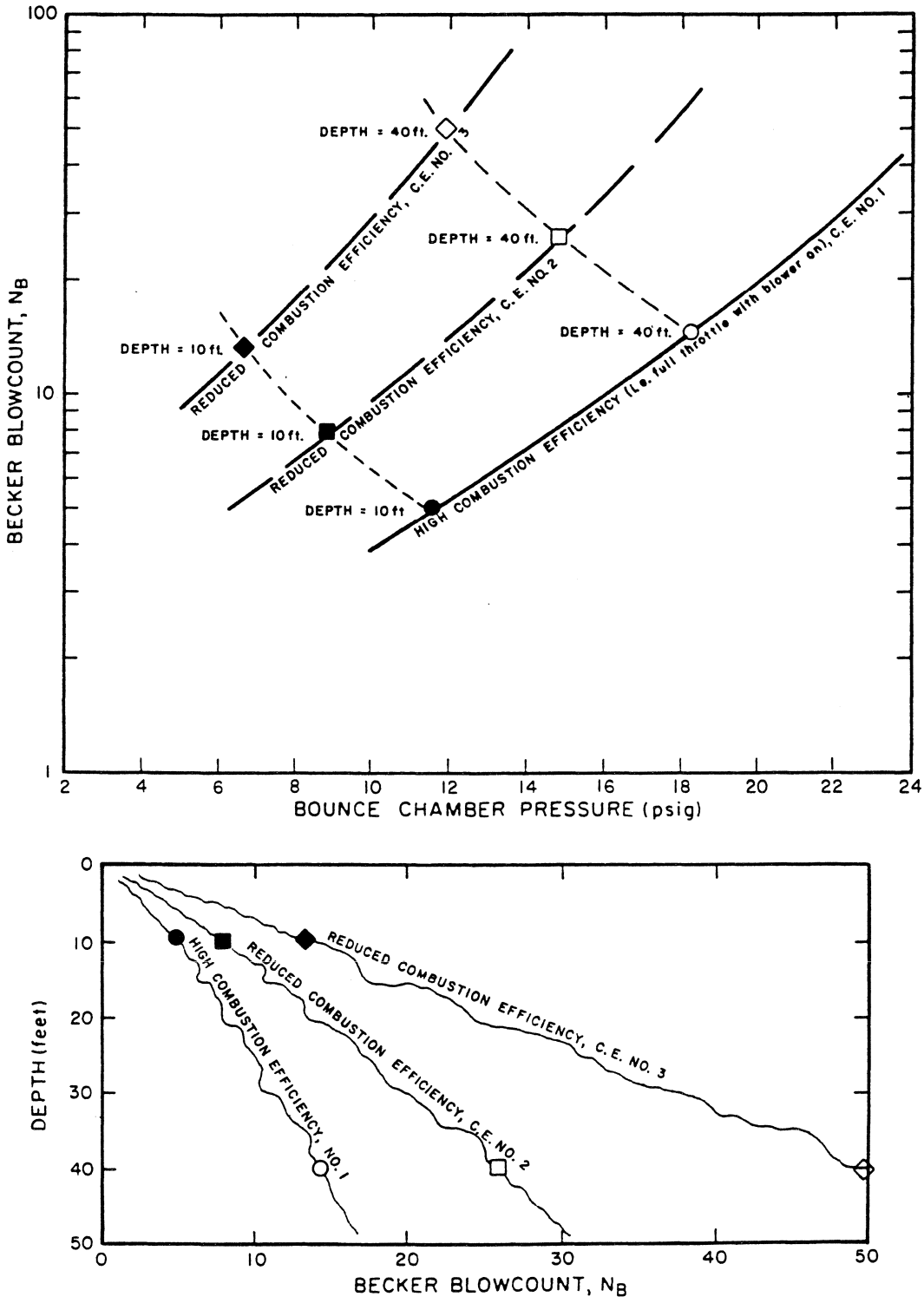

Figure 3: Effect of Diesel Hammer Combustion Efficiency on Becker Blowcount (after Harder and Seed, 1986)

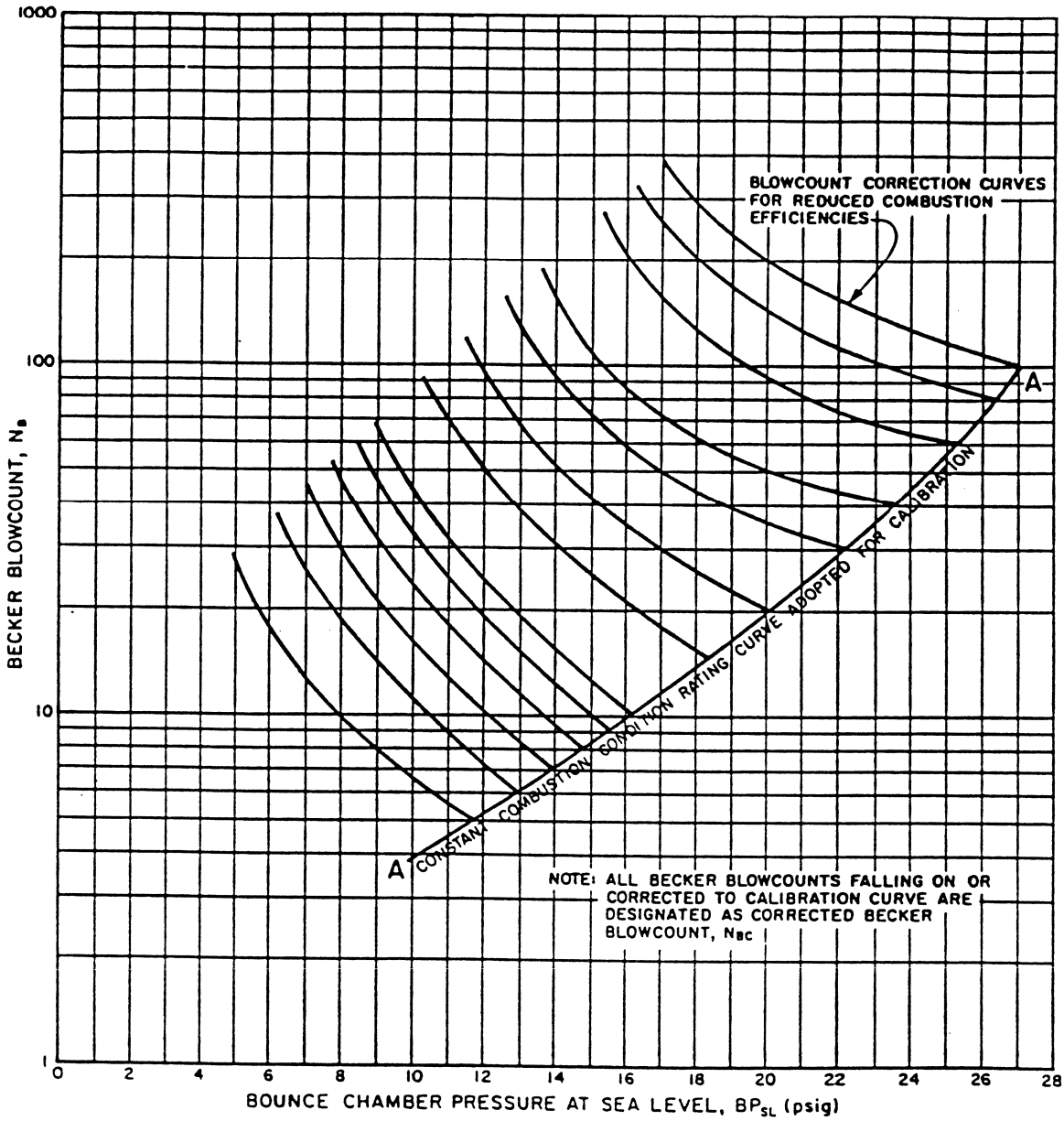

Figure 4: Correction Curves Adopted to Correct Becker Blowcounts to Constant Combustion Curve Adopted for Correlation (from Harder and Seed, 1986)

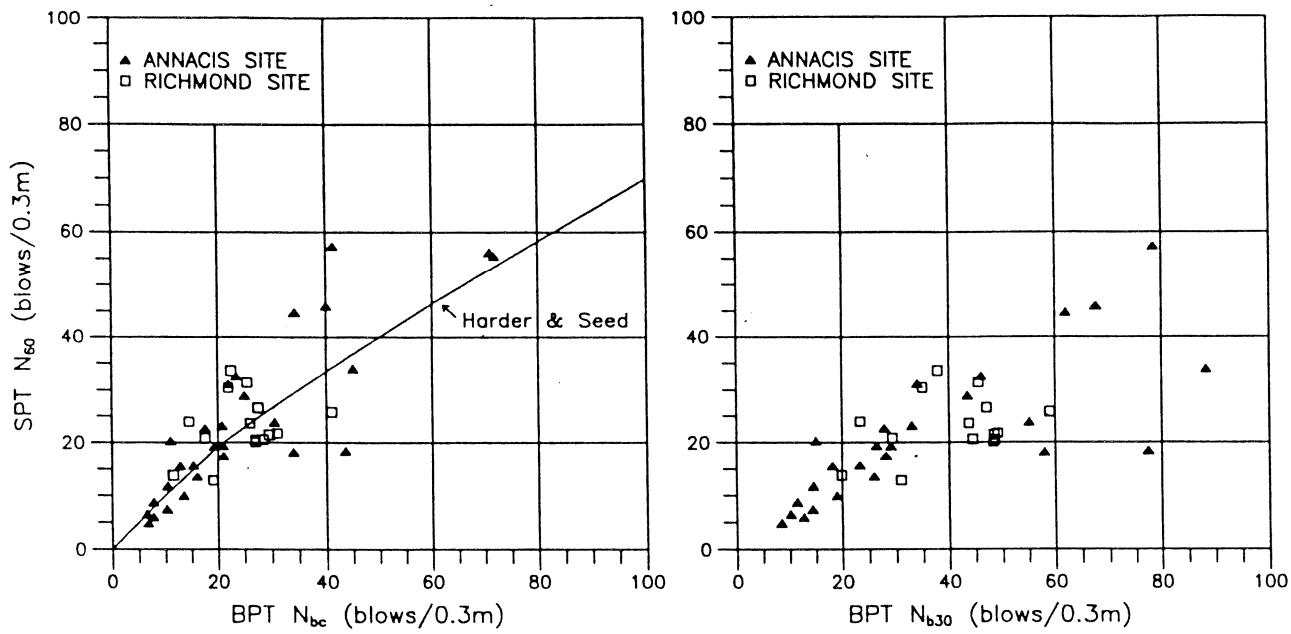

Figure 5: SPT N_{60} vs. Becker N_{BC} and N_{b30} for Annacis and Richmond Test Sties (from Sy and Campanella, 1993)

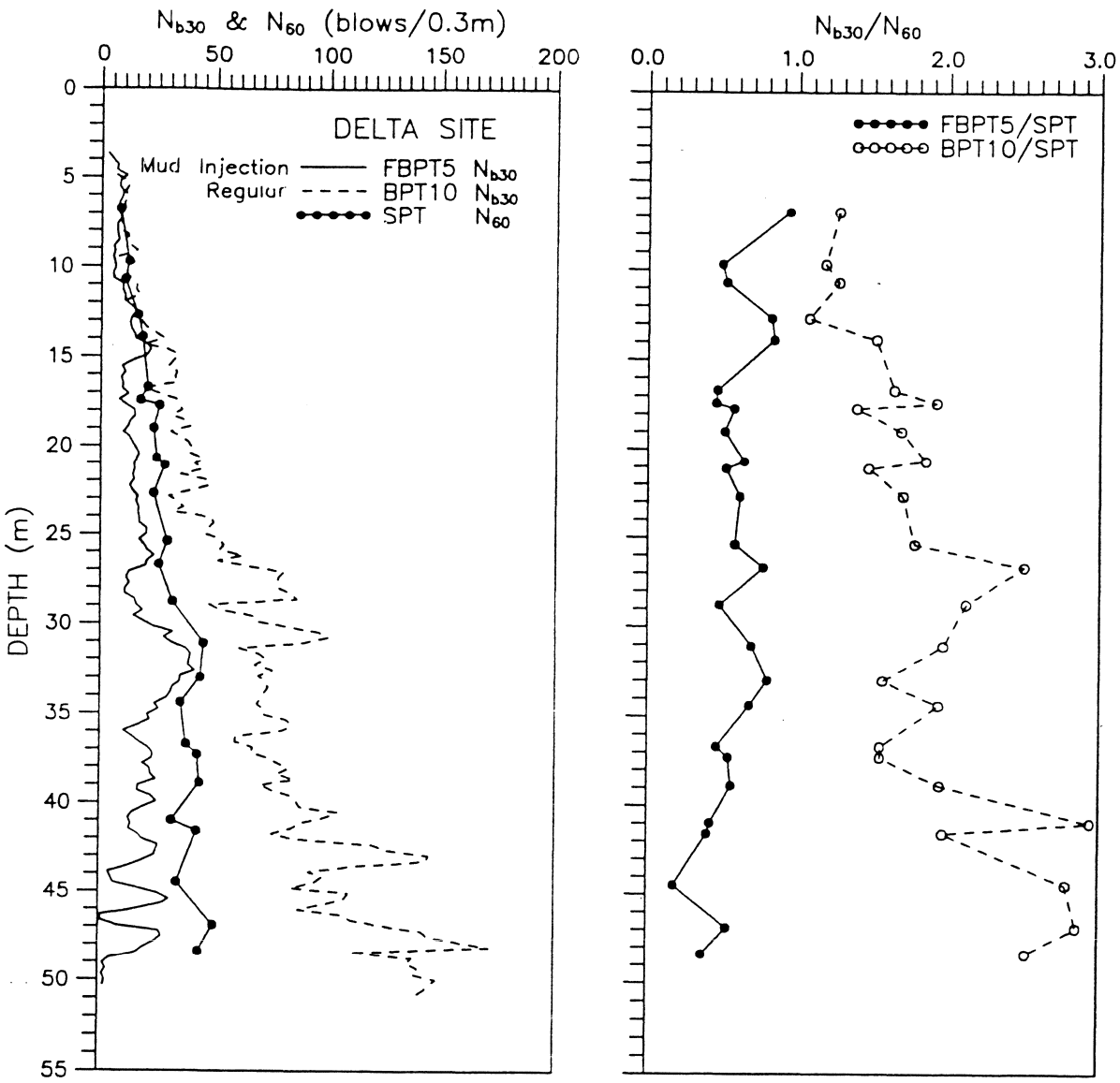

Figure 6: Effect of "Mudded" Becker Casing on Determined Becker Blowcounts (after Sy and Campanella, 1994)

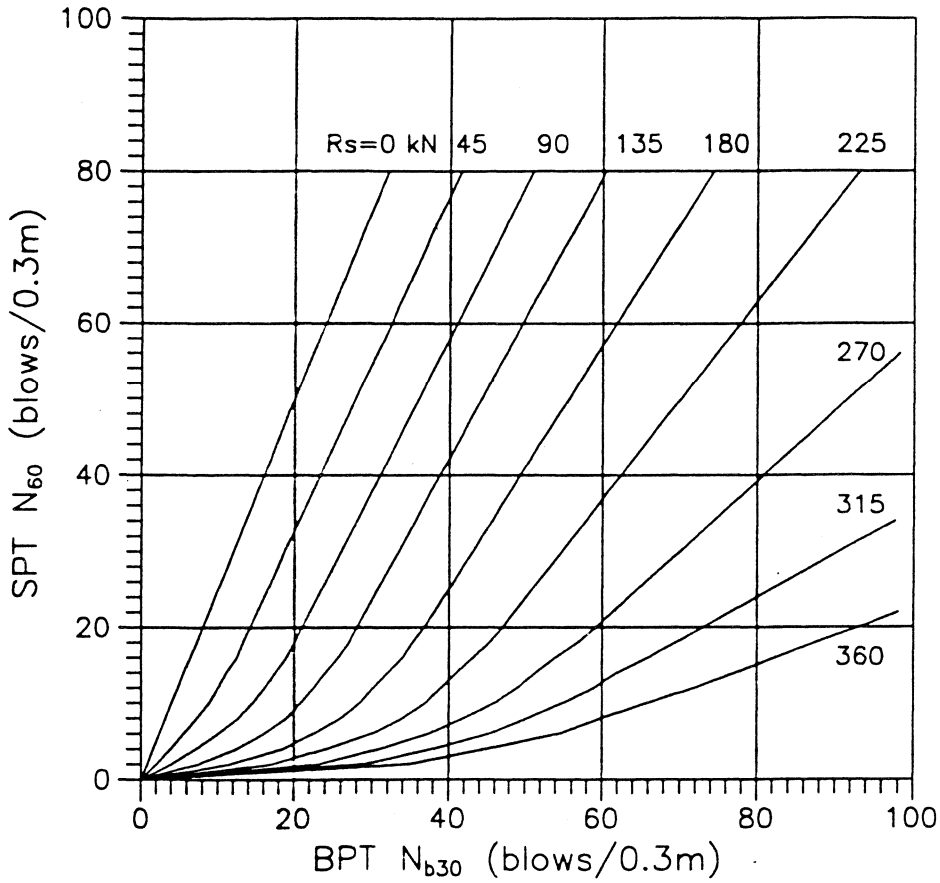

Figure 7: Computed BPT vs. SPT Correlation for Different BPT Casing Shaft Resistance (from Sy and Campanella, 1994)

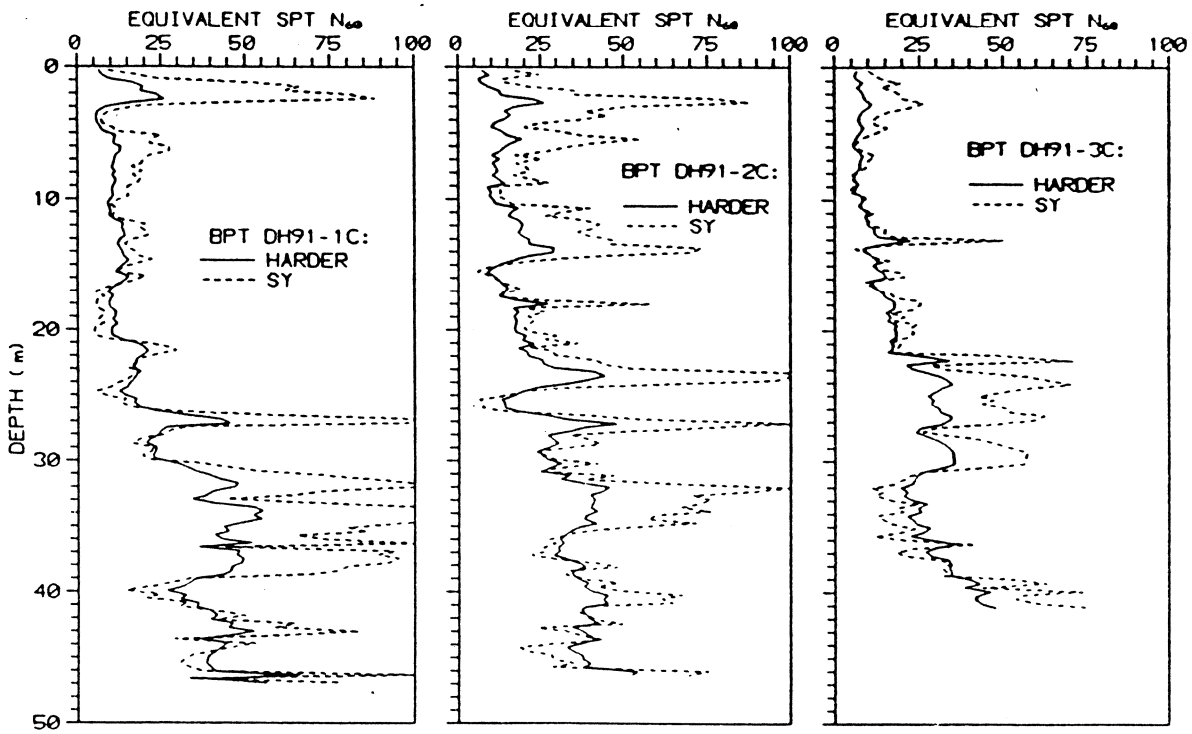

Figure 8: Comparison of the Equivalent SPT N_{60} Values from Becker Soundings using Correlations Developed by Harder and Seed (1986) and Sy and Campanella (1994) - (from Lum and Yan, 1994)

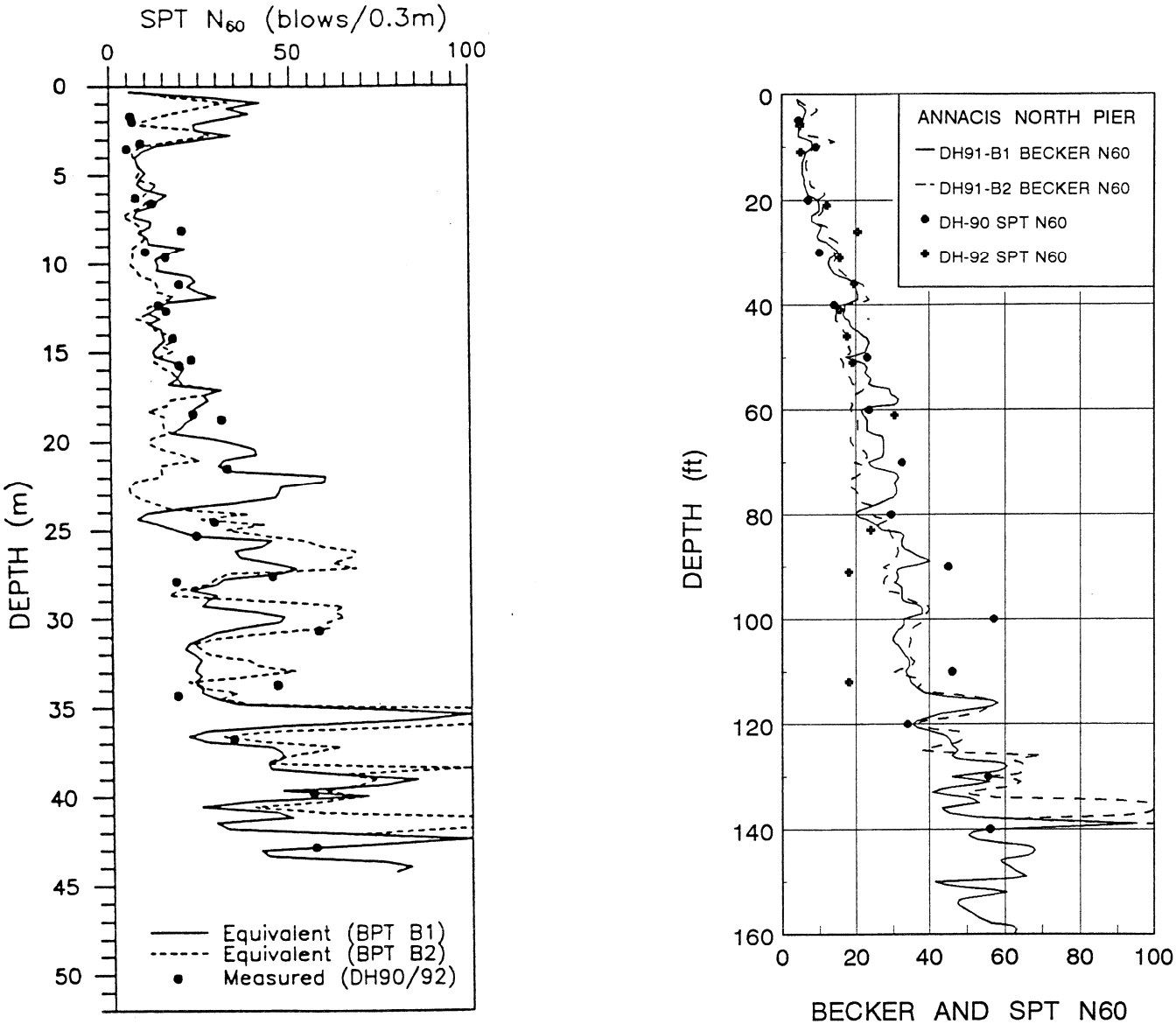

a. Sy and Campanella

b. Harder and Seed

Figure 9: Comparisons of Predicted and Actual SPT N_{60} Values at Annacis Test Site using Harder and Seed (1986) and Sy and Campanella (1994) Methods

Magnitude Scaling Factors

T. Leslie Youd

Professor of Civil Engineering
Brigham Young University
Provo, Utah, 84602-4081

Steven K. Noble

Project Engineer
DOWL Engineers, Inc.
Anchorage, Alaska, 99503-5999

Abstract

In developing the "simplified procedure" for evaluating liquefaction resistance, Seed and Idriss (1982) compiled a sizable database from sites where liquefaction did or did not occur during earthquakes with magnitudes near 7.5. From this database, these investigators defined a conservative deterministic bound separating data indicative of liquefaction from data indicative of nonliquefaction. They then scaled this bound to other earthquake magnitudes using magnitude scaling factors (MSF). Because insufficient observational data were available for magnitudes other than 7.5, Seed and Idriss (1982) analyzed recorded ground motions and laboratory test data to define the original set of scaling factors. As more field performance data were collected, the observed occurrences and nonoccurrences of liquefaction for smaller earthquakes (magnitudes less than 7) indicated that the original Seed and Idriss (1982) MSF may have been overly conservative for smaller magnitudes. In response to this apparent overconservatism, Idriss reevaluated the original seismic and laboratory data, made corrections, linearized the data on a logarithmic plot, and developed a revised set of MSF. Ambraseys (1988), Arango (1996), Andrus and Stokoe (this report) and Youd and Noble (herein) defined alternative sets of MSF based on empirical field observations. These MSF lie within a narrow range for $M_w \leq 7.5$. The workshop gained consensus that a range of MSF values should be suggested for engineering practice. Practitioners could then select MSF from within this range, depending on the degree of risk they or their clients are willing to accept for various applications. The lower bound for that recommended range is the MSF proposed by Idriss (Column 3, Table 1) and the upper bound for the range is the factors proposed by Andrus and Stokoe (Column 7, Table 1). For magnitudes greater than 7.5, the revised factors of Idriss should be used. These factors are smaller than the original Seed and Idriss (1982) factors, and hence lead to an increase of calculated liquefaction hazard compared to the old factors. The workshop participants agreed, however, that the original factors by Seed and Idriss (1982) may not have been adequately conservative for large magnitude earthquakes.

Introduction

In developing the "simplified procedure" for evaluating liquefaction resistance, Seed and Idriss (1982) compiled a sizable database from sites where liquefaction did or did not occur during earthquakes with magnitudes of near 7.5. Data from the following earthquakes were compiled: 1964 Niigata, Japan (M = 7.5), 1974 Haicheng, China (M = 7.3), 1976 Tangshan, China (M = 7.6), 1976 Guatemala (M = 7.6), 1977 western Argentina (M = 7.4), and 1978 Miyagiken-Oki, Japan (M = 7.4). Cyclic stress ratios were calculated for sites where surface effects of liquefaction were or were not observed, and results from Holocene clean sand (fines contents ≤ 5 percent) were plotted on a cyclic stress ratio versus $(N_1)_{60}$ plot. An updated version of that plot by Seed et al. (1984) is reproduced in Figure 1. A deterministic CRR curve was drawn on the plot to separate regions with data indicative of liquefaction occurrence (solid symbols) from regions indicative of nonoccurrence.

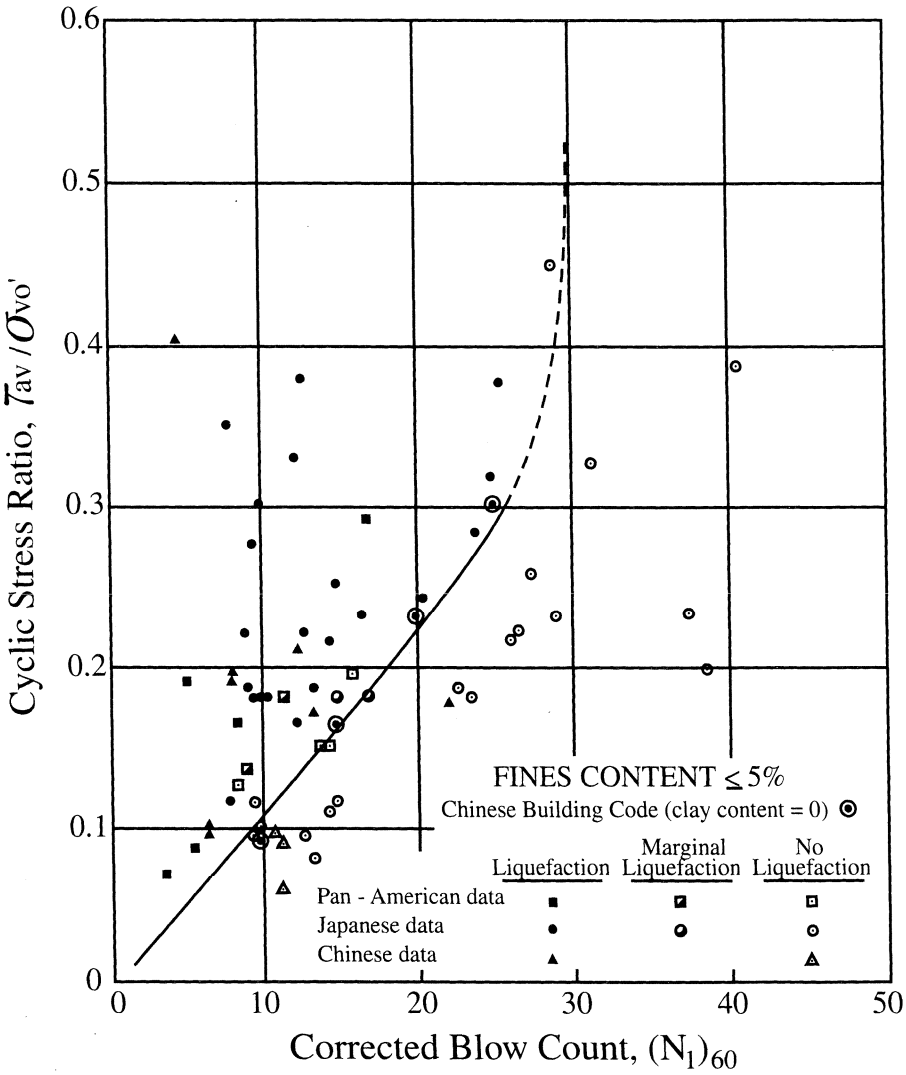

Figure 1 Cyclic Stress Ratio Versus $(N_1)_{60}$ for Magnitude 7.5 Earthquakes with Simplified Base Curve Drawn to Separate Data Indicative of Liquefaction from that Indicative on Nonliquefaction (modified from Seed 1984)

In areas where a mixture of both types of data populated the chart, the curve was conservatively positioned to assure that nearly all of the points from sites where liquefaction had occurred plotted above the bounding curve. The position of the curve is well constrained by observational data between cyclic stress ratios of 0.08 and 0.35, and was logically extrapolated to higher and lower values beyond that range. This curve, hereafter called the "simplified base curve," provides the fundamental SPT-based criterion for assessing liquefaction resistance of clean granular soils for magnitude 7.5 earthquakes. As noted in the Summary Report, the workshop participants agreed that the lower limb of the curve should be bowed to intersect the ordinate of the plot at a CRR of about 0.05.

To adjust the simplified base curve for magnitudes other than 7.5, correction factors called "magnitude scaling factors (MSF)" were applied to scale the base curve upward or downward on a cyclic resistance ratio (CRR) plot as required. Conversely, magnitude weighting factors (MWF), which are the inverse of magnitude scaling factors (MWF = 1/MSF), may be applied to correct the stress ratio generated by the earthquake (CSR) to incorporate the influence of magnitude. Correcting either CRR via magnitude scaling factors or CSR via magnitude weighting factors leads to the same final result. Because the original papers by Seed and Idriss were written in terms of magnitude scaling factors, use of magnitude scaling factors will be continued through this report.

The influence of magnitude scaling factors on calculated liquefaction resistance is illustrated by the equation for factor of safety (FS) against liquefaction:

$$FS = (CRR_{7.5}/CSR)*MSF \qquad (1)$$

where $CRR_{7.5}$ is the cyclic liquefaction resistance ratio for a magnitude 7.5 earthquake as determined from the simplified base curve. This equation indicates that the factor of safety against liquefaction is directly proportional to the selected magnitude scaling factor.

Original Seed and Idriss Scaling Factors

Because sufficient empirical data were not available in the 1970s to constrain bounds between liquefaction and nonliquefaction regions on CSR plots for magnitudes other than 7.5, Seed and Idriss (1982) developed magnitude scaling factors based on strong motion records and laboratory test data as follows: From a study of strong motion accelerograms, Seed and Idriss correlated the number of representative loading cycles generated by an earthquake with earthquake magnitude. For example, a magnitude 7.5 earthquake was characterized by 15 loading cycles, whereas a magnitude 8.5 earthquake was characterized by 26 loading cycles, and a magnitude 6.5 earthquake by 10 loading cycles. Laboratory test data were then used to assess the number of loading cycles required to generate liquefaction and 5 percent cyclic strain as a function of cyclic stress ratio. Tests were conducted on several different clean sands at various void ratios or relative densities and ambient stress conditions. From these tests, a single representative curve was developed that relates cyclic stress ratio to the number of loading cycles required to generate liquefaction (Figure 2). Earthquake magnitudes were then assigned to various points on the curve based on the equivalent number of representative loading cycles. By dividing ordinates on the representative curve for various earthquake magnitudes by the ordinate for magnitude 7.5, the original set of magnitude scaling

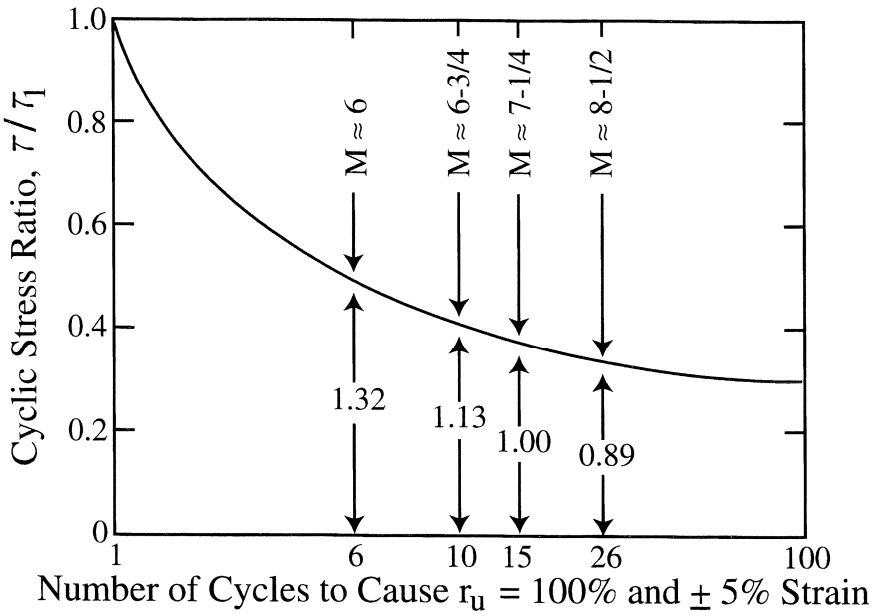

Figure 2 Representative Relationship between τ/τ_1 and Number of Cycles Required to Cause Liquefaction (modified from Seed and Idriss, 1982)

factors was derived (Seed and Idriss, 1982). These scaling factors are listed in Column 2 of Table 1, and plotted on Figure 3. These scaling factors have been widely applied as the standard of practice since their initial introduction into the simplified procedure.

Idriss Revised Magnitude Scaling Factors

In preparing his H.B. Seed memorial lecture, I.M. Idriss (written commun.) reevaluated the data he and the late Prof. H.B. Seed had used to calculate the original (1982) magnitude scaling factors. In so doing, Idriss re-plotted the data on a logarithmic plot and determined that the scaling factors should plot as a straight line. He further noted that one outlier point had unduly influenced the original analysis, causing the original plot to be nonlinear on the logarithmic plot and characterized by much lower values than those on the revised linear plot. Based on this reevaluation, Idriss defined the revised set of magnitude scaling factors listed in Column 3 of Table 1, and plotted on Figure 3. Idriss recommends the revised scaling factors for use in engineering practice. These revised magnitude scaling factors are defined by the following equation:

$$MSF = 173(M)^{-2.56} \quad (2)$$

or in terms of magnitude weighting factors (MWF):

$$MWF = M^{2.56}/173 \quad (3)$$

The revised scaling factors are significantly larger than the original scaling factors for magnitudes less than 7 and significantly smaller than the original factors for magnitudes greater than 8. Relative to the original scaling factors, the revised factors lead to reduced calculated liquefaction hazard for

Table 1. Magnitude Scaling Factor Values Defined by Various Investigators

Mw	Seed and Idriss (1982)	Idriss revised	Ambraseys (1988)	Arango (1996)		Andrus and Stokoe (this report)	Youd and Noble (herein)		
							P_L<20%	P_L<32%	P_L<50%
(1)	(2)	(3)	(4)	(5)	(6)	(7)	(8)	(9)	(10)
5.5	1.43	2.20	2.86	3.00		2.8	2.86	3.45	4.44
6.0	1.32	1.76	2.20	2.00	1.65	2.1	1.93	2.35	2.92
6.5	1.19	1.44	1.69			1.6	1.34	1.65	1.99
7.0	1.08	1.19	1.30	1.25		1.25	0.96	1.19	1.39
7.5	1.00	1.00	1.00	1.00	1.00	1.0	0.70?	0.88?	1.00
8.0	0.94	0.84	0.67	0.75		0.8			0.73?
8.5	0.89	0.72	0.44		0.76	0.65			0.56?

Table 2. Equations for Calculation of Magnitude Scaling Factors

Idriss (written commun.)	$MSF = 10^{2.24}/M^{2.56} = (M_w/7.5)^{-2.56}$		(3)
Andrus and Stokoe (this report)	$MSF = (M_w/7.5)^{-3.3}$		(7)
Youd and Noble (herein)			
Probability, $P_L < 20\%$,	$MSF = 10^{3.81}/M^{4.53}$	For M<7	(11)
Probability, $P_L < 32\%$,	$MSF = 10^{3.81}/M^{4.42}$	For M<7	(12)
Probability, $P_L < 50\%$,	$MSF = 10^{4.21}/M^{4.81}$	For M<7.75	(13)

magnitudes less than 7.5, but increased calculated hazard for magnitudes greater than 7.5. Because there have been few large earthquakes (M > 8.0) causing widespread liquefaction since the 1960s, there is little high-quality field data with which to verify or constrain magnitude scaling factors for earthquakes greater than magnitude 8. To be conservative, the revised factors should be used, even though they may lead to reclassification of some areas as liquefiable that were previously considered to be nonliquefiable.

Ambrayses Magnitude Scaling Factors

As more field performance data were collected, the observed occurrences and nonoccurrences of liquefaction for smaller earthquakes (magnitudes less than 7) indicated that the original Seed and Idriss (1982) scaling factors were overly conservative. Consequently, Ambraseys (1988) analyzed liquefaction data compiled through the mid-1980s and plotted calculated cyclic stress ratios for sites that did or did not liquefy on CSR versus $(N_1)_{60}$ plots. Ambraseys segregated the data into magnitude ranges (6.0 to 6.6, 6.7 to 7.2, 7.3 to 7.5, and 7.6 to 8.2) and fit a deterministic bound through the data

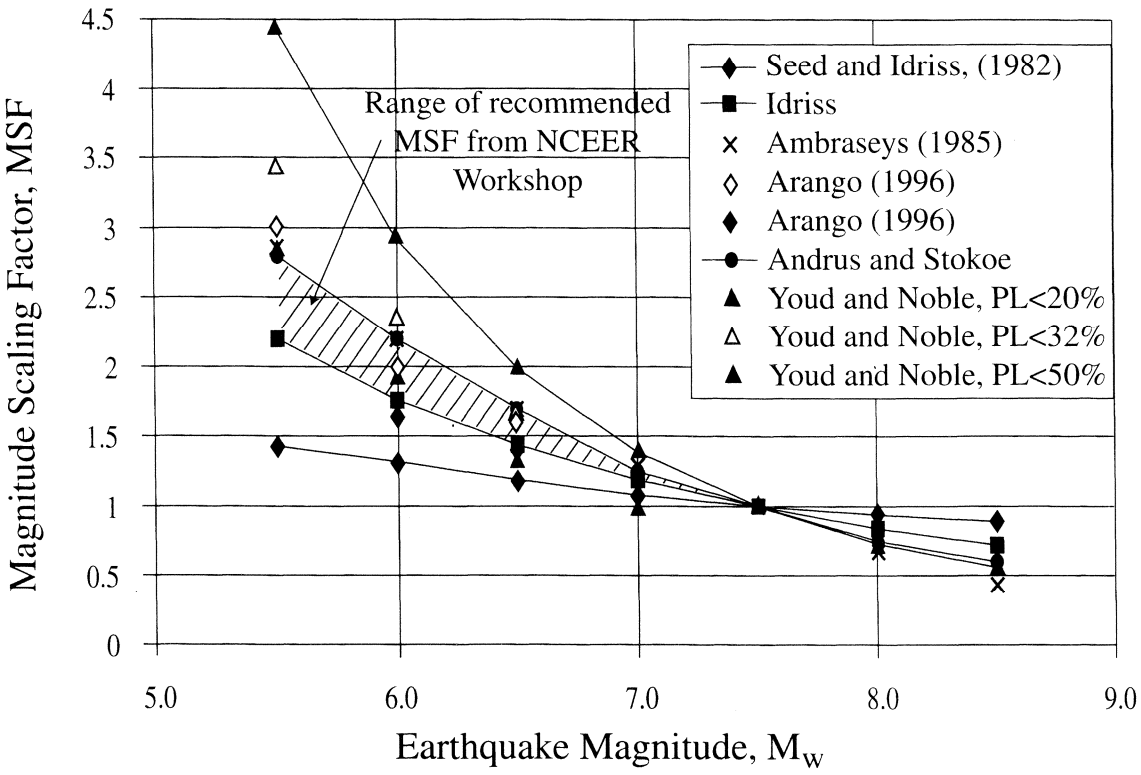

Figure 3 Magnitude Scaling Factors Proposed by Various Investigators

on each plot using an exponential form for the bounding equation. The equation Ambraseys developed using the compiled data (all magnitude ranges and all soil gradations) is:

$$Q = 3.29 \exp[0.06(N_1)_{60}][(N_1)_{60}]^{0.755}[\exp(-0.81M_w)] \quad (4)$$

where Q is equivalent to cyclic resistance ratio (CRR) as used in this report, M_w is moment magnitude, and $(N_1)_{60}$ is corrected standard penetration resistance. Ambraseys developed a second equation using only data from earthquakes with magnitudes less than 7.5 and data from sites underlain by clean sands (fines contents less than 5 percent):

$$Q = 0.40 \exp[0.06(N_1)_{60}][(N_1)_{60}]^{0.755}[\exp(-0.525M_w)] \quad (5)$$

The exponential form of these equations is consistent with the exponential form used with many attenuation relationships for peak acceleration as a function of distance. One criticism raised at the workshop was that the derived scaling factors are strongly influenced by the functional form of the equation. The equation may be appropriate for attenuation of peak acceleration, but may not be adequate for occurrence of liquefaction, which is a function of shaking duration or magnitude, as well as peak acceleration.

By holding the value of $(N_1)_{60}$ constant in Equations 4 and 5 and taking the ratio of Q determined for various magnitudes of earthquakes to the Q for magnitude 7.5 earthquakes, Ambraseys derived the

set of magnitude scaling factors listed in Column 4 of Table 1 and plotted on Figure 3. For magnitudes less than 7.5, the scaling factors suggested by Ambraseys are significantly greater than the original factors developed by Seed and Idriss (1982) and the revised factors by Idriss. Use of these larger factors leads to greater calculated liquefaction resistances and less calculated hazard for earthquakes with magnitudes less than 7.5. Conversely, for magnitudes greater than 7.5, use of Ambraseys' factors leads to significantly less calculated liquefaction resistance and much greater hazard than any of the prior factors.

Procedures used to develop the original factors by Seed and Idriss and the revised factors by Idriss are considerably different from procedures used by Ambraseys. Seed and Idriss used laboratory tests and strong motion records to develop their scaling factors; whereas, Ambraseys used field observations of liquefaction and nonliquefaction effects. The different scaling factors determined by these different investigators may be partly due to differences in developmental procedures.

Arango Magnitude Scaling Factors

Arango (1996) developed two sets of magnitude scaling factors: The first set (Column 5, Table 1) is based on the farthest observed liquefaction effects past earthquakes of various magnitudes and estimated average peak accelerations at those distant sites. The second set (Column 6, Table 2) is based on absorbed seismic energy required to generate liquefaction and the relationship derived by Seed and Idriss (1982) between number of significant stress cycles and earthquake magnitude. Arango's scaling factors listed in Column 5 generally have values similar (within 10%) to those derived by Ambraseys (1988). The MSF listed in Column 6 are rather close in value (within 6%) to the revised MSF of Idriss (Column 3).

Andrus and Stokoe Magnitude Scaling Factors

From their studies of liquefaction resistance as a function of shear wave velocity, V_s, Andrus and Stokoe (this report) developed the following equation for calculating CRR from V_s for magnitude 7.5 earthquakes:

$$CRR_{7.5} = a(V_{S1}/100)^2 + b[1/(V_{S1c} - V_{s1}) - 1/V_{S1c}] \quad (6)$$

where V_{S1} is the corrected shear wave velocity; V_{S1c} is acritical value of V_{S1}, which separates contractive and dilative behavior; and a and b are curve-fitting parameters. Values of a and b recommended by Andrus and Stokoe for magnitude 7.5 earthquakes are 0.03 and 0.9, respectively. The value of V_{S1c} depends on the fines content of the soil, but ranges from 220 m/s for clean sands to 200 m/s for silty sands with fines contents greater than 35%.

Using Equation 6, Andrus and Stokoe drew curves on graphs with plotted values of CSR as a function of calculated V_{S1} from sites where surface effects of liquefaction were or were not observed. Graphs were plotted for sites shaken by magnitude 6, 6.5, 7, and 7.5 earthquakes. The positions of the curves were visually adjusted on each of these graphs until a best-fit bound was obtained, separating data indicative of liquefaction from data indicative of nonliquefaction. Magnitude scaling factors were then estimated by taking the ratio of CRR ordinates for a given V_{S1} from plots or

magnitude 6, 6.5 and 7 earthquakes to CRR at the same V_{S1} for magnitude 7.5 earthquakes. These MSF values were then fitted to an exponential equation and values extrapolated for magnitudes less than 6 and greater than 7.5. That equation is

$$MSF = (M_w/7.5)^{-3.3} \quad (7)$$

MSF values calculated from this equation are listed in Column 7, Table 1, and plotted on Figure 3. For magnitudes less than 7.5, the MSF proposed by Andrus and Stokoe are rather close in value to the MSF proposed by Ambraseys. For magnitudes greater than 7.5, the Andrus and Stokoe MSF are rather close in value to the MSF proposed by Idriss.

Youd and Noble Magnitude Scaling Factors

In a study for this workshop, the authors reanalyzed case history data using logistic regression (Youd and Noble, Probabilistic Analysis, this report). The data analyzed were from sites for which subsurface soil information is available and for which surface effects of liquefaction were or were not observed. From that regression, Youd and Noble developed the following empirical equation:

$$Q_L=\text{Logit}(P_L)=\ln[P_L/(1-P_L)] = -7.633 + 2.256\, M_w - 0.258\, (N_1)_{60cs} + 3.095 \ln CRR \quad (8)$$

where P_L is the probability that liquefaction will occur, $1-P_L$ is the probability that liquefaction will not occur, M_w is moment magnitude, and $(N_1)_{60cs}$ is the corrected blow count, including a correction for fines content. This equation allows cyclic resistance ratios, CRR, to be calculated as a function of $(N_1)_{60cs}$, earthquake magnitude, and a given probability of liquefaction occurrence. Figure 4 shows CRR curves plotted from Equation 6 for magnitude 7.5 earthquakes and P_L of 20%, 32%, and 50%, respectively. For reference, the simplified base curve for clean sands is also plotted on that figure as well as calculated CSR from sites in the case history database where effects of liquefaction were or were not observed. The plotted data are from earthquakes with magnitudes between 7.25 and 7.75. For $(N_1)_{60}$ between 3 and 30, the simplified base curve is enveloped between probabilistic CRR curves with P_L between 20% and 50%.

P_L<50% Magnitude Scaling Factors

Although Youd and Noble (Statistical and Probabilistic Analyses, this report) recommend direct use of Equation 8 for evaluating liquefaction resistance, an alternative method is to calculate magnitude scaling factors using Equation 8, and then apply those factors with the simplified procedure. The development of magnitude scaling factors for a probabilities of liquefaction of 50% or less ($P_L \leq 50\%$) is rather simple and straightforward. The following text and examples illustrate this procedure. Setting P_L equal to 50% in Equation 8, and solving for CRR yields the following equation:

$$CRR_{PL=50\%} = e^{(2.466 - 0.7289M + 0.0834(N1)60cs)} \quad (9)$$

Holding $(N_1)_{60cs}$ constant at any value and taking the ratio of CRR for any magnitude to the CRR for magnitude 7.5 earthquakes yields the following equation for calculating magnitude scaling factors with P_L=50%:

$$MSF_{PL=50\%} = CRR/CRR_{7.5} = e^{-0.7289M}/e^{-0.7289(7.5)} \quad (10)$$

For example, solving this equation for magnitude 6.5 earthquakes yields a calculated $MSF_{PL=50\%}$ of 2.07. Scaling factors for earthquake magnitudes ranging from 5.5 to 8.5 were calculated from this equation and are plotted with a plus symbol on Figure 5. These values are very close in value to the MSF based on a probability of 32% previously published by Loertscher and Youd (1994). Using these scaling factors, one can calculate the 50% probability curve for any magnitude simply by multiplying the CRR ordinates of the magnitude 7.5 curve by the appropriate MSF. For example, the 50% probability curve for magnitude 6.5 earthquakes can be generated by multiplying the $CRR_{7.5}$ for each $(N_1)_{60cs}$ by 2.07.

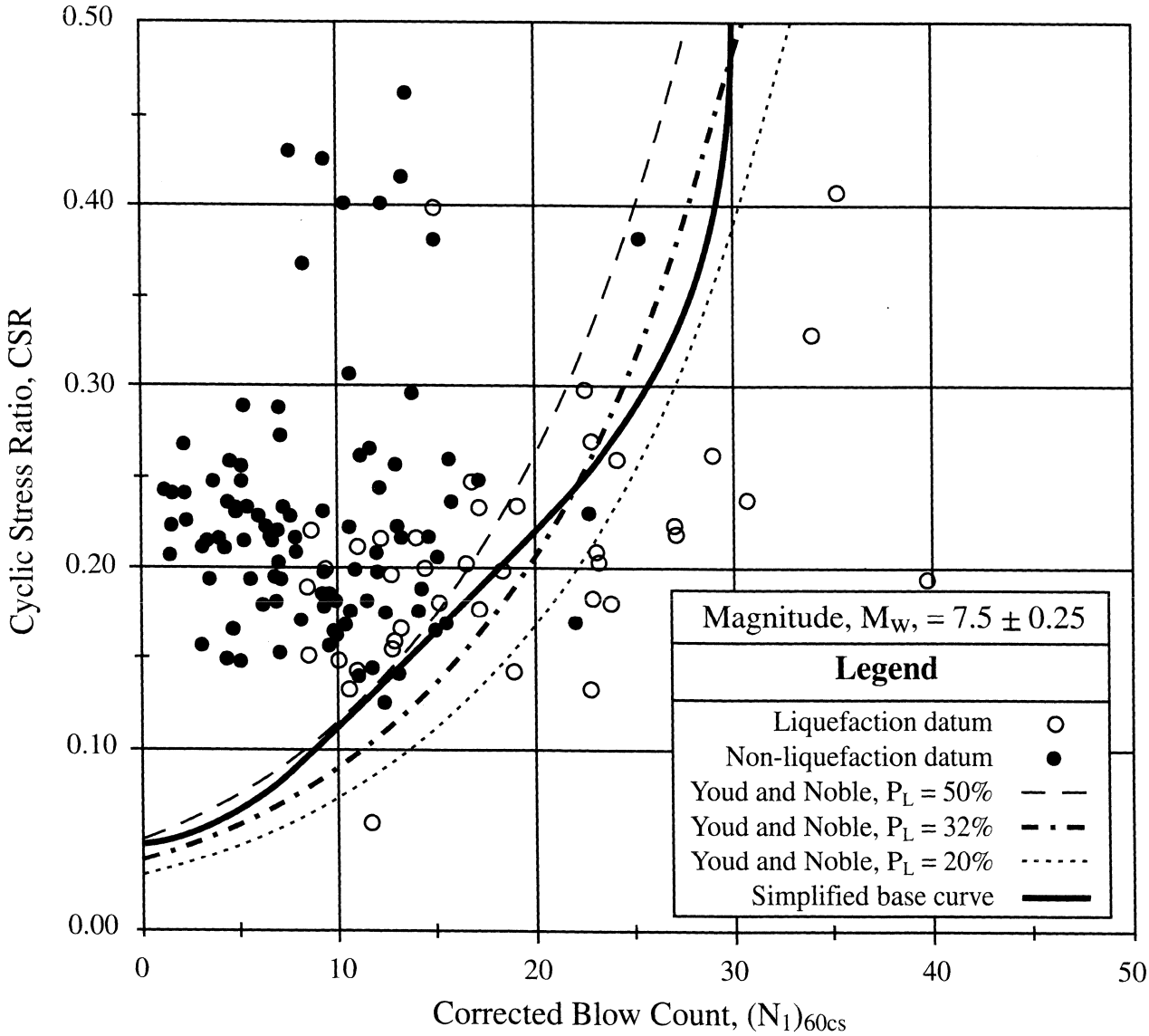

Figure 4 Probabilistic CRR Curves for P_L = 20%, 32% and 50% from Youd and Noble (Probabilistic Analysis, this report) with Simplified Base Curve and Empirical Liquefaction Data for Magnitude 7.25 to 7.75 earthquakes

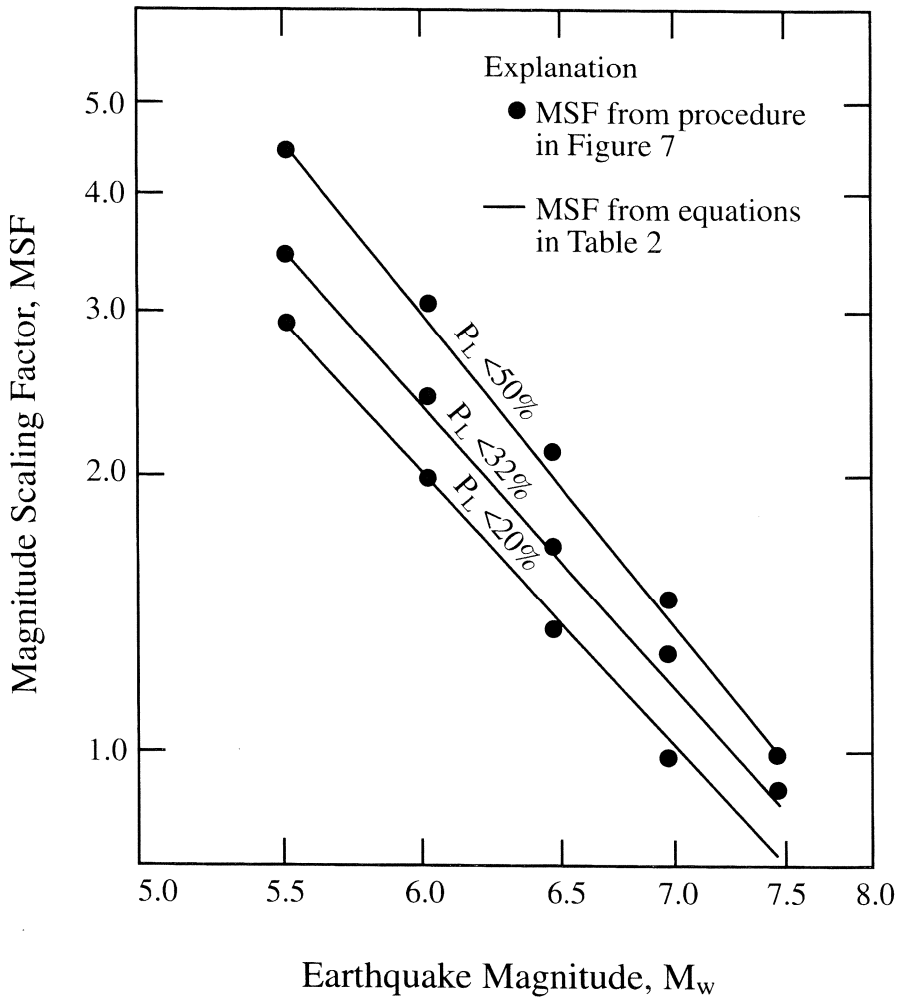

Figure 5 Logarithmic Plot of Probabilistically Determined Magnitude Scaling Factors Versus Earthquake Magnitude

The simplified base curve is nearly tangent with, but lies slightly below, the 50% probability curve at an $(N_1)_{60cs}$ of about 12, and lies below that curve for all other $(N_1)_{60cs}$ up to an $(N_1)_{60cs}$ of 30 (Figure 4). Thus multiplying the simplified base curve by $MSF_{PL=50\%}$ calculated from Equation 8 yields scaled base curves that lie below the 50% probability curve for all earthquake magnitudes. These scaled curves, however, would be nearly tangent with, but lie slightly below the 50% probability curves at an $(N_1)_{60cs}$ of approximately 12. Scaling the simplified base curve in this manner yields predicted CRR that are always characterized by a probability of liquefaction less than 50%, or P_L<50%. For illustration, the scaled simplified base curve for magnitude 6.5 earthquakes is plotted on Figure 6. Thus the P_L=50% magnitude scaling factors can be used as scaling factors for use with the simplified procedure and will give estimates of CRR that are characterized by probabilities of liquefaction occurrence of less than 50%.

Rather than using the P_L = 50% scaling factors directly, the authors followed the model of Idriss and plotted the derived magnitude scaling factors on a log-log plot (Figure 5) and developed a straight-line fit to those MSF. To develop the straight-line fit, magnitude scaling factors calculated from

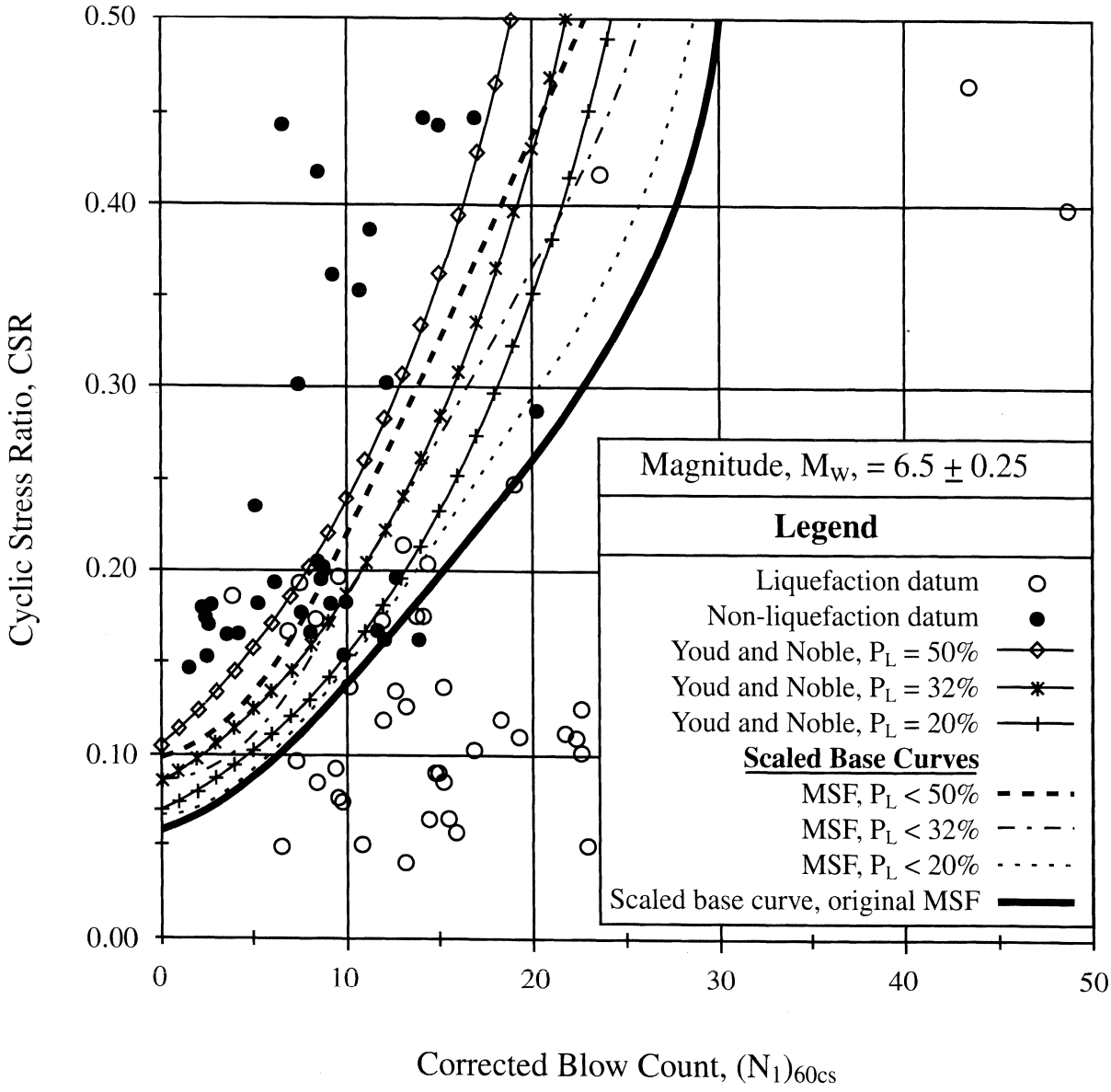

Figure 6 Probabilistic CRR Curves with Scaled Simplified Base Curve for Magnitude 6.5 Earthquakes

equation 8 were plotted on Figure 5 as noted above for earthquakes with magnitudes between 5.5 and 8.5. The straight line was drawn conservatively (slightly below the plotted data for magnitudes less than 7.5) to assure that all CRR calculated using these magnitude scaling factors indeed are characterized by a probability of liquefaction occurrence of less than fifty percent. The straight line approximation for MSF with P_L<50% is defined by the following equation:

$$MSF = 10^{4.21}/M^{4.81} \qquad \text{For } P_L<50\% \text{ and } M_w<7.75 \qquad (11)$$

This equation is also listed in Table 2, and MSF values calculated from this equation are listed in Table 1, Column 10, and plotted on Figure 3. For clarity, these MSF are marked with the designator P_L<50%, indicating that CRR calculated using these MSF yielded values characterized by less than 50% probability of liquefaction occurrence. These MSF may be used for engineering applications where up to 50% probability of liquefaction occurrence is acceptable, but are restricted to earthquakes with magnitudes less than 7.75.

As noted by Youd and Noble (Statistical and Probabilistic Analyses, this report), the case history data are sufficient to adequately constrain the probabilistic analysis for magnitudes between 5.5 and 7.75. Above magnitude 7.75, the data are too sparse and scattered to adequately constrain the probabilistic analysis. Thus the validity of MSF determined by this procedure is questionable for magnitudes greater than 7.75. Although MSF values for P_L<50% are listed for reference for magnitudes 8 and 8.5 in Table 1, Column 10, these values are marked with a question mark indicating they are uncertain. MSF in this tabulation marked with a question marks are not recommended for use in engineering practice.

P_L<32% and P_L<20% Magnitude Scaling Factors

Most engineering applications require a more conservative likelihood of liquefaction than a probability of 50%, thus magnitude scaling factors are also derived for probabilities less than 32% and less than 20%, respectively. Because the simplified base curve for magnitude 7.5 earthquakes lies above both the 32% and 20% probability curves for magnitude 7.5 earthquakes over part of its trajectory, the technique used for P_L<50% can not be used directly for these lower probability values. That is, because the probabilistic CRR curves intersect the base curve, scaling these curves directly would also produce curves that intersect and hence do not lie entirely below the given probabilistic curve. The magnitude 7.5 simplified base curve, however, lies entirely below the 32% and 20 % probability curves for magnitudes less than 7. For these magnitudes, scaling the simplified base curve upward to near tangency with the probabilistic CRR curves is a pragmatic procedure for defining magnitude scaling factors. In essence, this is the procedure that was used in developing the P_L<50% MSF. In that instance, the simplified base curve was effectively scaled upward to near tangency with the 50% probabilistic curve for earthquake magnitudes less than 7.5.

The development of MSF using this technique is illustrated by the following example. Figure 7 shows the simplified base curve and the P_L=32% probabilistic curve for magnitude 6.5 earthquakes. The simplified base curve was rotated upward about the origin until the curves become tangent at some point. In this instance, the point of tangency occurs at an $(N_1)_{60cs}$ of about 12, as shown by the dashed curve. The CRR from the P_L=32% curve for an $(N_1)_{60cs}$ of 12 is 0.224. The CRR from the simplified base curve for an $(N_1)_{60cs}$ of 12 is 0.134 . By taking the ratio of these two CRR, MSF are defined for a probability of liquefaction occurrence equal to less than 32% ($P_L \leq 32\%$). For magnitude 6.5 earthquakes, that value is:

$$MSF_{M=6.5,PL<32\%} = 0.224/0.134 = 1.67$$

Similarly, upwardly scaling of the simplified base curve to a point of tangency with P_L=32% probability curves for other earthquake magnitudes, and then taking the ratio of the CRR at the point

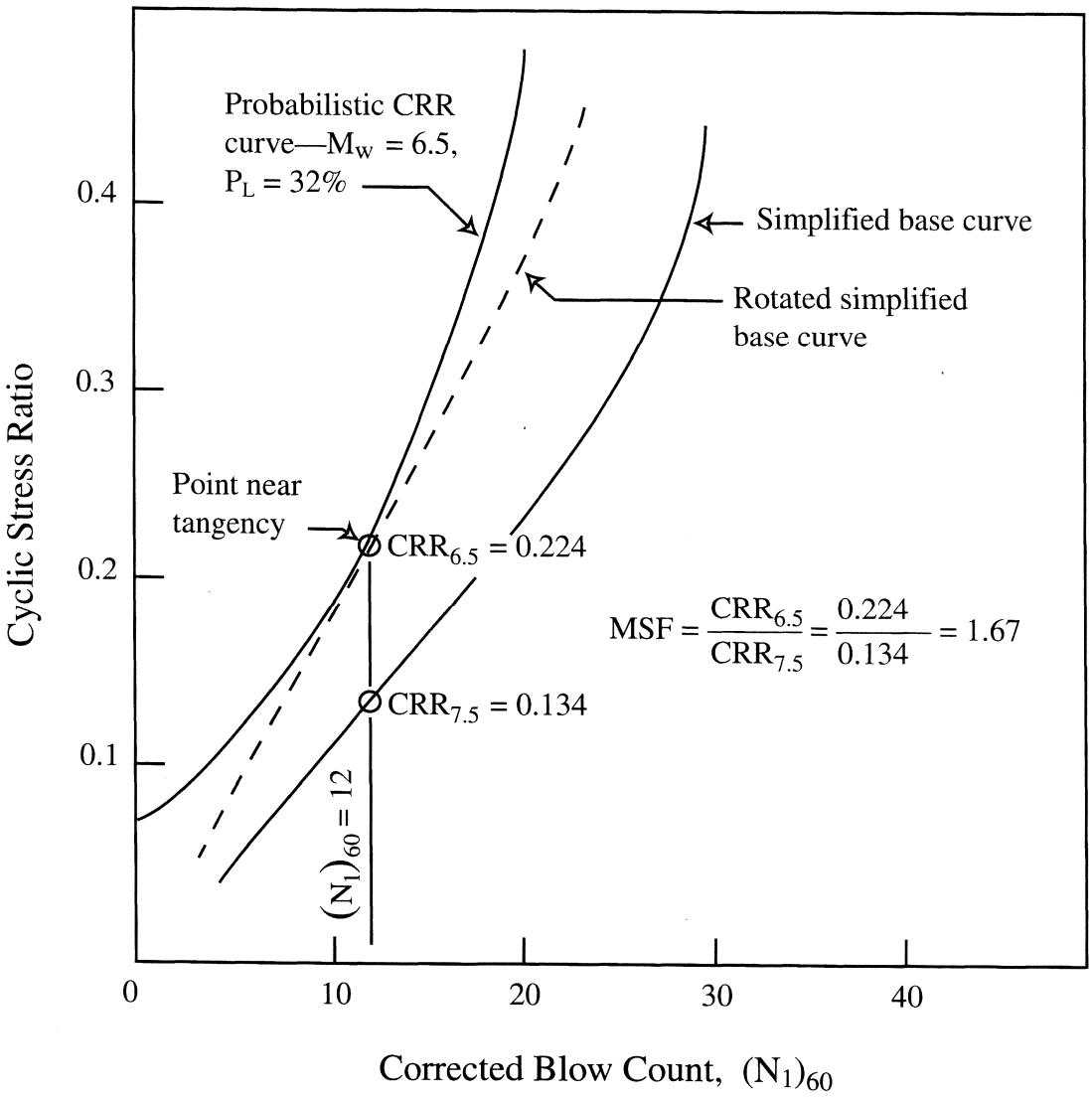

Figure 7 Diagram Showing Calculation of P_L=32% Magnitude Scaling Factor

of tangency to the CRR from the simplified base curve at the same $(N_1)_{60cs}$, would create a set of MSF with $P_L \leq 32\%$. These MSF were calculated and are plotted on the logarithmic chart in Figure 5. A straight line was then drawn slightly below the $P_L \leq 32\%$ MSF yielding the following equation:

$$MSF = 10^{3.81}/M_w^{4.42} \quad \text{for } P_L<32\% \text{ and } M_w<7 \qquad (12)$$

Values of MSF listed in Column 9, Table 1, were calculated from this equation. Because the straight-line fit was drawn conservatively (slightly below) the plotted values, CRR calculated using these MSF will always be characterized by $P_L<32\%$, and this designation is used as a descriptor for these MSF. A simplified base curve scaled by these MSF for magnitude 6.5 earthquakes is plotted on Figure 6. The MSF listed in Column 9, Table 1, and plotted on Figure 3 are valid for use in engineering applications where up to 32% probability of liquefaction occurrence is acceptable. Extrapolation of Equation 12 to a magnitude of 7.5 yields MSF less than 1.0. This lower value

occurs because Equation 12 scales the base curve to a point of near tangency with the probabilistic curves. Because the P_L=32% curve lies below the simplified base curve at magnitude 7.5, the scaling factor has to be less than 1.0.

The procedure used to develop P_L<20% MSF was the same as that used for P_L<32% MSF, except that the simplified base curve was scaled up to tangency with the 20% probability curves rather than the 32% probability curves. The MSF determined by that procedure are plotted on Figure 5. A slightly conservative straight line fitted to those calculated MSF is quantified by the following equation:

$$MSF = 10^{3.81}/M_w^{4.53} \quad \text{for } P_L<20\% \text{ and } M_w<7 \qquad (13)$$

MSF calculated from Equation 13 are listed in Column 8, Table 1, and plotted on Figure 3. These MSF are valid for use in engineering applications where up to 20% probability of liquefaction occurrence is acceptable. Again, probabilistic curves for M_w equal to or less than 7 lie below the simplified base curve. As with MSF for P_L<32%, extrapolation of Equation 13 to magnitude of 7 or less yields MSF that are less than 1.0.

Magnitude Scaling Factors For Engineering Practice

Magnitudes Equal to or Less than 7.5

Magnitude scaling factors from the various investigators noted herein are plotted on Figure 3. This plot shows considerable consistency between values developed by the various investigators, each of whom used distinctly different methodologies to develop their scaling factors. This consistency adds confidence that the derived MSF are generally correct and appropriate for use in engineering practice. For magnitudes less than 7.5, the MSF suggested by Ambraseys, Arango, and Andrus and Stokoe (Columns 4 through 7, Table 1) lie within a narrow grouping. The P_L<20% MSF of Youd and Noble (Column 8, Table 1), also lie within this grouping for magnitudes less than 6.5. The MSF recommended by Idriss (Column 3, Table 1) generally lie below and are about 20% smaller than the average values within the above grouping. The P_L<32% MSF of Youd and Noble (Column 9, Table 1) lie above and are roughly 20% larger than the values within the group for magnitudes less than 6.5. The P_L<50% MSF developed by Youd and Noble (Column 10, Table 1) are significantly higher than all of the other factors. The original MSF of Seed and Idriss (Column 2, Table 1) plot well below the MSF of all the more recent investigators and appear to be overly conservative. As noted by Idriss, some errors and extra-onservative interpretations influenced the original derivation. Thus the original Seed and Idriss (1982) scaling factors should no longer be used in engineering practice, but should be superseded by more recently generated MSF as recommended below.

After evaluation of the various proposed MSF, the workshop gained consensus (with S.S.C. Liao dissenting) that a range of values should be suggested for engineering practice for earthquakes with magnitudes less than 7.75. This range is marked by a stippled pattern on Figure 3. Practitioners could then select MSF from within that range, depending on the degree of risk they or their clients are willing to accept for a given application. The lower bound for this recommended range is the MSF proposed by Idriss (Column 3, Table 1) and the upper bound of the range is the MSF proposed

by Andrus and Stokoe (Column 7, Table 1). Based on the probabilistic analysis of Youd and Noble, the upper values in this range are characterized by a probability of liquefaction occurrence of 20% or less. The MSF proposed by Idriss, which form the lower bound of the range, are characterized by a probability of liquefaction much less than 20%. These MSF are valid for use with liquefaction resistance criteria based on SPT, CPT, shear-wave velocity, or Becker penetration resistance.

Magnitudes greater than 7.5

For magnitudes greater than 7.75, the MSF developed by Idriss (Column 3, Table 1; and Equation 3) are up to 20% smaller than the original Seed and Idriss MSF, but are still greater than those suggested by other investigators as listed in Table 1. The values by Ambraseys, Andrus and Stokoe, and Youd and Noble (Columns 4 and 7-10, respectively, Table 1), are extrapolated from smaller magnitude earthquakes and thus are uncertain for magnitudes greater than 7.75. The MSF by Arango are derived from distance and energy relationships, but still generally yield values much smaller than the Idriss values. The workshop participants agreed that there is insufficient evidence and verification to recommend MSF lower than those proposed by Idriss for use in engineering practice. Even so, the MSF proposed by Idriss still lead to greater calculated liquefaction hazard than was predicted by the original Seed and Idriss MSF, which have been the standard of practice. Thus some areas that have been determined to be safe against liquefaction using the original MSF may be predicted to liquefy using the Idriss MSF. Use of MSF proposed by all of the other investigators would lead to an even greater calculated hazard, but as noted above, there is little verification for this greater hazard for earthquakes with magnitudes greater than 7.75.

The MSF by Idriss for magnitudes greater than 7.75 were derived from a reanalysis of the original Seed and Idriss (1982) data and thus not extrapolated from smaller magnitude earthquakes. The case history data provide some verification if the MSF proposed by Idriss for magnitudes greater than 7.75. For example, Figure 8 shows a plot of liquefaction data from the compiled case histories for earthquakes with magnitudes between 7.75 and 8.25. Scaled simplified base curves, using the various MSF for magnitude 8 earthquakes listed in Table 1, are also plotted on this chart. The case history data are rather sparse on this plot and nearly all of the data are from three pre-1925 earthquakes, primarily the 1991 Mino-Owari, Japan (M = 7.8), 1906 San Francisco, California (M_w = 7.9), and 1923 Kwanto, Japan (M_w = 7.9). Also, there is insufficient case history data over much of the trajectories to adequately constrain the positioning of the curves. The data do indicate, however, that the simplified base curve scaled by the Idriss scaling factor for a magnitude of 8 generates a slightly conservative bound for the plotted data. The data is even more sparse for larger magnitude earthquakes. Little data have been collected for magnitude 8.25 to 8.75 earthquakes, and essentially the only data from earthquakes with magnitudes greater than 8.75 are from sites observed to have liquefied during the 1964 Alaska earthquake (M_w = 9.2). These data are insufficient to constrain empirical analyses of magnitude scaling factors for these larger magnitudes.

Although these data are insufficient to fully verify that the MSF by Idriss are conservative, they also do not provide evidence that the Idriss factors are unconservative. The data are insufficient to justify MSF smaller than those proposed by Idriss, as is indicated by nearly all of the factors in columns 4-10 of Table 1. Thus the consensus of workshop participants is that the MSF by Idriss are the best estimates available for large earthquakes for use in engineering practice.

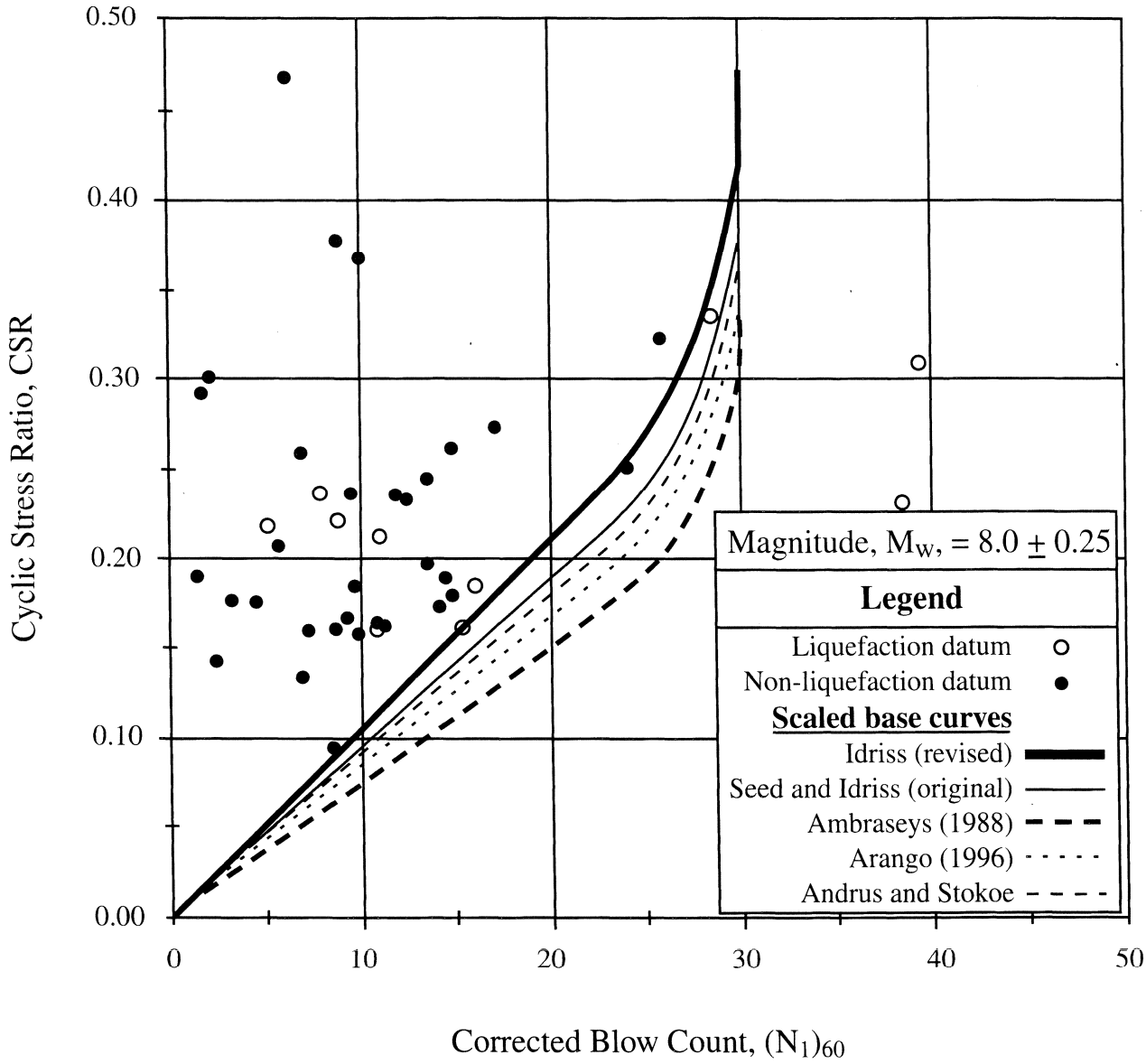

Figure 8 Empirical Liquefaction Data from Magnitude 8 Earthquakes with Scaled Simplified Base Curves Using Various MSF from Table 1

References

Ambraseys, N.N., 1988, Engineering Seismology: Earthquake Engineering and Structural Dynamics, Vol. 17, p. 1-105.

Arango, I., 1996, Magnitude Scaling Factors for Soil Liquefaction Evaluations: Journal of Geotechnical Engineering, ASCE, Vol. 122, No. 11, p. 929-36.

Loertscher, T.W. and Youd, T.L., 1994, Magnitude Scaling Factors for Analysis of Liquefaction: Proceedings from the Fifth U.S.-Japan Workshop on Earthquake Resistant Design of Lifeline Facilities and Countermeasures Against Soil Liquefaction, National Center of Earthquake Engineering Research Technical Report NCEER-94-0026, p. 703-15.

Seed, H.B., and Idriss, I.M., 1982, Ground Motions and Soil Liquefaction During Earthquakes: Earthquake Engineering Research Institute Monograph.

Seed, H.B., Tokimatsu, K, Harder, L.F., and Chung, R.F., 1984, "The Influence of SPT Procedures in Soil Liquefaction Resistance Evaluations, Report No. UBC/EERC-84/15, Earthquake Engineering Research Center, University of California, Berkeley, California.

Application of K_σ and K_α Correction Factors

Leslie F. Harder, Jr.

Chief, Division of Engineering
California Department of Water Resources
Sacramento, California 94236-0001

Ross Boulanger

Assistant Professor
Department of Civil and Environmental Engineering
University of California, Davis
Davis, California 95616

Abstract

The K_σ and K_α correction factors were originally developed by Seed (1983) to adjust cyclic resistance ratios obtained from empirical SPT and CPT correlations to different static stress conditions. The K_σ correction factor extends cyclic resistance ratios to high confining stresses, while the K_α correction factor adjusts cyclic resistance ratios to sloping ground conditions. Because there are virtually no case histories available to help define these correction factors, the results from laboratory test programs have been used to develop these factors. This section describes the development of these correction factors, describes the results of recent laboratory programs, and recommends modified correction factors for use in liquefaction evaluations.

INTRODUCTION

Liquefaction evaluations generally employ correlations between liquefaction resistance and corrected SPT blowcount or CPT tip resistance. One of the most commonly used SPT correlations is the one developed by Seed et al. (1985). In this correlation, the performance of over one hundred sites following earthquake loading was evaluated. For the critical layer at each site, the estimated cyclic stress ratio induced by the earthquake (τ_{av}/σ_{vo}') was determined and plotted as a function of the corrected SPT blowcount, $(N_1)_{60}$ (see Figure 1). Sites which had liquefied (solid symbols) plotted in areas with low SPT resistance and/or high cyclic stress ratio. Sites which showed no evidence of liquefaction (hollow points) plotted in areas with high SPT resistance and/or low cyclic stress ratio. Three dividing lines between areas of liquefaction and no liquefaction were drawn for fines contents of 5, 15, and 35 percent fines. These dividing lines are curved and have been used with corrected SPT blowcounts to predict the liquefaction resistance of sandy and silty soils.

This liquefaction resistance is expressed in a normalized form as a cyclic stress ratio causing liquefaction. As pointed out by Peter Byrne, use of the Seed et al. (1985) SPT correlation gives a cyclic resistance ratio (CRR) and should properly be noted as such. Although this and similar correlations are invaluable for the evaluations of liquefaction resistance, the database for the correlations are limited to flat ground under relatively low levels of confining stress. To extend the correlations for use with soils under sloping ground or high confining stresses, correction factors must be used. Because SPT and CPT correlations are used in conjunction with the Seed-Lee-Idriss approach, the correction factors are based on the pre-earthquake static stress conditions on the horizontal plane. The use of correction factors to extend the existing correlations to different stress conditions is performed as follows:

$$CRR = (CRR)_1 \times K_\sigma \times K_\alpha \qquad (1)$$

where:

CRR = the cyclic resistance ratio (τ_{av}/σ_{vo}') at the current stress state (σ_{vo}', τ_s).

$(CRR)_1$ = the cyclic resistance ratio at the reference state:
(SPT correlation; $\sigma_{vo}' = 1$ tsf, $\tau_s = 0$).

K_σ = a correction factor for the level of vertical effective confining stress, σ_{vo}'.

K_α = a correction for the level of static horizontal shear stress, ($\alpha=\tau_s/\sigma_{vo}'$).

σ_{vo}' = initial vertical effective confining stress.

τ_s = static shear stress on the horizontal plane.

The K_σ and K_α correction factors have generally been based on the normalized results of cyclic triaxial and cyclic simple shear tests. Several studies (e.g. Seed, 1983, and Seed and Harder, 1990) have offered suggested ranges for the factors based on available laboratory test results. The magnitudes of these corrections can be extremely large for deep soil layers under either flat or sloping ground. However, there is a wide range and scatter in the available data and, because the correction factors often have a controlling influence on the final evaluation of liquefaction resistance, their use has been questioned for particular projects.

K_σ CORRECTION FACTOR FOR CONFINING STRESS

General

In early liquefaction evaluations, liquefaction resistance was determined by performing cyclic laboratory tests (e.g. cyclic triaxial) on "undisturbed" soil specimens. The tests were performed for a range of static stress conditions. To represent level ground conditions, isotropically-consolidated cyclic triaxial tests were commonly performed. To correct for the incorrect boundary conditions inherent in the cyclic triaxial test, a C_r correction factor was used.

The results of tests performed on "undisturbed" isotropically-consolidated specimens of several different soils are shown in Figure 2. The results show that, while the cyclic resistance of a soil increases with increasing confinement, the cyclic resistance ratio decreases. This is because the cyclic resistance curves for the different soils are not straight lines passing through the origin, but rather are curves that flatten out at increasing consolidation stresses. As illustrated in Figure 3, the cyclic resistance ratio is simply the secant line intersecting the cyclic resistance curve at the consolidation stress of interest. At higher and higher levels of confinement, Figures 2 and 3 show that the slope of the secant line will flatten and that the cyclic resistance ratio will decrease.

Studies by Seed (1983)

In recent years, the use of cyclic laboratory tests for direct evaluations of liquefaction resistance has dramatically decreased because of concerns regarding sample disturbance and other factors. Such evaluations now generally employ empirical correlations such as the Seed et al. (1985) SPT-liquefaction correlation. The Seed SPT correlation and others generally define the cyclic resistance of soils to liquefaction in the form of a cyclic resistance ratio (τ_{av}/σ_{vo}'). This normalized cyclic resistance is based on the performance of soils which were under relatively low effective confining stresses, typically less than 1 tsf (~100 kPa). However, many liquefaction evaluations require the determination of cyclic resistance for significantly higher confining stresses. To extend SPT liquefaction correlations to higher confinement, Seed (1983) developed the K_σ correction factor. The approach used by Seed is illustrated in Figure 3 and the range of K_σ values recommended by Seed (1983) is shown in Figure 4.

The K_σ values developed by Seed (1983) were the result of normalizing cyclic resistance ratios of isotropically-consolidated cyclic triaxial tests to the CRR values associated with an effective confining stress of 1 tsf. For confining stresses greater than 1 tsf, the K_σ correction factor is less than one and decreases with increasing confining stress. Using this suggested range for K_σ, the CRR value at 8 tsf becomes only about 40 to 60 percent of the CRR value at 1 tsf.

Studies by Seed and Harder (1990)

Later studies by Harder (1988) and Seed and Harder (1990) employed the same approach and used the results of available cyclic triaxial testing programs. The Seed and Harder (1990) K_σ values are shown in Figure 5 and show a suggested curve for the K_σ correction factor. This later curve gives a K_σ value of 0.44 at a confining stress of 8 tsf and is generally somewhat lower than the range suggested by Seed (1983). For confining stresses above 8 tsf, the Seed (1983) curve suggests a continuing linear decrease in K_σ whereas the later Seed and Harder (1990) curve is concave up, suggesting a limiting K_σ value of about 0.4 for very high confining stresses.

The Seed and Harder (1990) K_σ curve is based on laboratory tests performed on both "undisturbed" and reconstituted sand specimens. The "undisturbed" specimens generally consisted of silty sands typically recovered in thin-walled tubes with Piston samplers as part of dam safety investigations. The reconstituted specimens generally consisted of clean sands prepared by pluviation or moist tamping as part of university research studies. Failure criteria generally consisted of 5 percent axial strain within either 10 or 15 cycles of loading.

There is considerable scatter in the Seed and Harder K_σ database and this is partly due to the different sources of the data. For the "undisturbed" specimens, there was often a wide range in densities and materials due to the heterogeneity of both natural deposits and fills. In addition, there was generally no attempt to compensate for the increased densities of "undisturbed" specimens that would be expected to occur with higher confining stresses. Compensating for the higher densities would be expected to result in even lower K_σ values. On the other hand, consolidation of "undisturbed" specimens in the laboratory to confining stresses greater than their in situ values may have adversely affected their particle fabrics (including the beneficial effects of aging and prior seismic history), and possibly resulted in an unrepresentative decrease in both cyclic resistance ratio and K_σ. Reconstituted specimens prepared in the laboratory, however, can be constructed to maintain similar relative densities and particle fabric over the full range of confining stresses.

Studies by Vaid et al. (1985) and Vaid and Thomas (1994)

Research performed in recent years by Y. Vaid and his colleagues on clean sands have indicated relatively little decrease in CRR values for even very high confining pressures. This corresponds to relatively high K_σ values. Data developed by Dr. Vaid at the University of British Columbia has

been obtained using a constant volume cyclic simple shear device to test dry sand specimens prepared by pluviation. The results have been reported in the studies by Vaid et al. (1985) and Vaid and Thomas (1994). Shown in Figure 6 are the UBC K_σ results for Tailings, Ottawa, and Fraser sands for confining stresses of up to 26 tsf (2500 kPa). This data has been developed for specimens with the same relative densities after consolidation (i.e. the increase in density produced by increasing the confining stress has been compensated for). For confining stresses of up to 26 tsf, the UBC K_σ values are above 0.67. For confining stresses of only about 10 tsf, the UBC K_σ values are generally between 0.75 and 0.9. The results also showed that lower relative densities produced higher K_σ values.

The UBC K_σ values are significantly higher than those suggested by either Seed (1983) or Seed and Harder (1990). This suggests that use of the Seed and Harder (1990) K_σ curve could be very conservative for some soils, particularly clean sands.

Discussion

The available results from cyclic laboratory tests show a wide potential range for K_σ values. At confining stresses of about 8 tsf, the Seed (1983) and the Seed and Harder (1990) curves (see Figures 4 and 5) give K_σ values that are only half of those indicated by recent UBC testing (see Figure 6). In 1991, portions of the Seed and Harder (1990) database were reexamined and the results for clean sands were found to be significantly higher than those for "undisturbed" silty sand specimens. Shown in Figure 7 are the clean sand data from Seed and Harder (1990) compared with some of the UBC data. The clean sand data points from the Seed and Harder database show far better agreement with the UBC results than did the silty sand data.

As a result of this comparison, Byrne and Harder (1991) recommended a clean sand K_σ curve for use in evaluating liquefaction resistance of clean sands and gravels at Terzaghi Dam. This clean sand curve gave a K_σ value about 45 percent higher than the Seed and Harder (1990) curve at a confining stress of 8 tsf. However, due to the lack of new data for silty soils, it was recommended at that time that liquefaction evaluations employ the original Seed and Harder K_σ curve for soils with significant fines contents.

The large range in potential K_σ values may require that critical projects such as large dams employ site specific corrections developed using laboratory tests performed on project soils. Pillai and Byrne (1994) presented the results of a site specific investigation of confining stress effects for the fine sand beneath Duncan Dam. In this investigation, frozen samples were obtained near the downstream toe of the dam, taken to the laboratory, and tested in cyclic triaxial and cyclic simple shear devices after thawing. The test results showed that the CRR values determined in both sets of tests were independent of confining stress. This was because of compensating factors that essentially balanced each other:

- Increasing confining stress decreased the CRR (i.e. the K_σ effect).
- Increasing confining stress also increased the consolidated density of the specimens before cyclic loading and this increased the CRR.

Pillai and Byrne used SPT test results to estimate the effect of the increased density on CRR and were able to back calculate a set of site-specific K_σ values for the Duncan Dam fine sand (see Figure 8). By comparing Figures 7 and 8, it may be observed that the Duncan Dam K_σ values were just slightly less than the "clean sand" K_σ values previously recommended by Bryne and Harder (1991). In addition to this, Arango (1996) describes recent K_σ data obtained from cyclic tests of silty and clayey sands that plot between the Duncan Dam and UBC curves.

Recommendations

Recent laboratory test programs on a range of potentially liquefiable soil types have provided a basis for refining the relationship between K_σ and effective confining stress. The available information indicates that the curve shown in Figure 9 will provide a reasonably conservative estimate of K_σ for use in evaluations of liquefaction resistance. This curve is considered appropriate for both clean and silty sands and gravels.

For any given value of confining stress, K_σ generally decreases with increasing relative density. However, the decrease in K_σ with increasing relative density is likely to be offset by the decrease in post-liquefaction deformability that accompanies increases in relative density. For high risk and critical projects where there are potentially liquefiable layers under high effective confining stresses, site-specific laboratory testing may be necessary to develop reliable corrections. Samples of the highest possible quality should be obtained for this purpose.

K_α CORRECTION FACTOR FOR SLOPING GROUND

General

The K_α correction factor was suggested by Seed (1983) to extend SPT and CPT correlations to sloping ground conditions. Sloping ground induces static shear stresses on horizontal planes within a soil mass prior to the onset of earthquake shaking (see Figure 10). The relative magnitude of the static shear stress (τ_s) on the horizontal plane can be assessed by normalizing it with respect to the vertical effective confining stress. The resulting parameter is called the alpha value ($\alpha=\tau_s/\sigma_{vo}'$). For level ground conditions, the alpha value is zero. Early research suggested that the presence of a static shear stress always improved the cyclic resistance of a soil because higher cyclic shear stresses were required to cause shear stress reversal. This conclusion still appears to hold for moderately

dense and dense cohesionless soils under relatively low confining pressures (say < 3 tsf). However, the presence of a static shear stress has since been shown to decrease the cyclic resistance of loose sandy soils and/or some moderately dense soils under very high confining stresses.

Studies by Seed (1983)

Seed and his colleagues at the University of California, Berkeley performed both cyclic simple shear and anisotropically-consolidated cyclic triaxial tests to investigate the effect of static shear stresses on cyclic resistance. Shown in Figure 11 are typical results from cyclic simple shear tests showing increases in cyclic resistance for increasing levels of static shear. This result was considered typical for soils with relative densities of 50 percent or higher.

The results of early research led Seed (1983) to develop the K_α correction for the presence of static shear. The K_α correction factor is used to extend the SPT and CPT correlations developed for level ground to conditions where sloping ground would induce static shear stresses on horizontal planes. Presented in Figure 12 is the K_α range suggested by Seed (1983) for relative densities equal to 50 percent or higher. As may be noted, the K_α correction factors lead to very large increases in cyclic resistance. For an alpha value of about 0.2, comparable to a soil layer beneath a moderate slope, the K_α correction factor would increase the cyclic resistance by approximately 70 percent.

Studies by Vaid et al., Yoshimi et al., Szerdy, Jong and Seed

Continued research performed at various universities showed that the effect of the static shear stress on cyclic resistance was very complicated. Several of these studies were completed in the 1970's and 1980's, including those performed by Yoshimi and Oh-Oka (1975), Vaid and Finn (1979), Tatsuoka et al. (1982), Vaid and Chern (1983, 1985), Szerdy (1986), and Jong and Seed (1989). These research programs involved the use of cyclic simple shear, cyclic ring torsional shear, and cyclic triaxial equipment. All of these research programs resulted in very consistent results regardless of the type of test equipment employed:

- The presence of a static shear stress increased the cyclic resistance (i.e. $K_\alpha>1$) of moderately dense or dense sandy soils for confining stresses less than about 3 tsf.
- The presence of a static shear stress decreased the cyclic resistance of loose, sandy soils (i.e. $K_\alpha<1$).
- The effect of static shear stresses on cyclic resistance was significantly dependent on the failure criterion used to define failure during testing.
- The effect of static shear stresses on cyclic resistance was significantly dependent on the confining stresses used during testing.

Figure 13 presents results obtained by Vaid and Finn (1979) and Vaid and Chern (1983), which illustrate the trends observed at confining stresses less than about 3 tsf. Figure 14 presents results by Vaid and Chern (1985) that illustrate how very high confining stresses can result in K_α values less than 1 for a dense sand. This effect is attributed to the sandy soils becoming more contractive with increasing confining stress.

Studies by Seed and Harder (1990)

The studies by Seed and Harder (1990) compiled much of the available laboratory research and developed a set of K_α correction factors for a range of relative densities (see Figure 15). The derivation of these K_α factors used a failure criterion of 7.5 percent shear strain (5 percent axial strain) in 10 or 15 cycles. This criterion was chosen because it was in common use in the late 1980's. The Seed and Harder (1990) K_α values shown in Figure 15 reflect the large range in laboratory results available at the time and show the effect of relative density. The Seed and Harder K_α values were based on data obtained for effective confining stresses of 3 tsf or less. Higher confinement makes soils more contractive and could lead to lower K_α factors, as illustrated by the Vaid and Chern (1985) data shown in Figure 14.

Studies by Boulanger et al. (1991) and Boulanger and Seed (1995)

Boulanger and Seed (1995) presented the results of bi-directional cyclic simple shear tests performed to investigate the effects of static shear stresses both parallel and perpendicular to the direction of cyclic loading. Their work verified many of the results previously developed by other researchers (e.g. Vaid and Finn, 1979) regarding the effects of density and failure criteria on the determined cyclic resistance. Their studies also showed the following results regarding the direction of shaking relative to the direction of the static shear (i.e. the direction of sloping ground):

- For cyclic loading perpendicular to the direction of the static shear stress, the effect of static shear was to reduce the cyclic shear resistance of sand specimens with relative densities of 35 and 45 percent, regardless of failure criterion. Reduced cyclic shear resistance was also found in the perpendicular direction for a relative density of 55 percent for failure criteria of less than 3 percent shear strain.

- Cyclic shear resistance in the direction perpendicular to the static shear stress was up to 30 percent less than the cyclic resistance parallel to the static shear stress. This difference increased with higher alpha values, and did not appear to be dependent on either relative density or number of loading cycles (see Figure 16).

The studies by Boulanger and Seed (1995) noted that, as for similar studies, the residual pore pressure ratios were limited to values far less than unity with increasing levels of static shear stress. Residual pore pressures for alpha values of about 0.1 never exceeded about 80 percent of the initial

vertical effective stresses, and residual pore pressures for alpha values of about 0.3 never exceeded about 40 percent of the initial vertical effective stresses (It should be noted that residual pore pressure refers to the pore pressure value after cyclic loading has ended, and that higher peak pore pressures often temporarily occur during cyclic loading).

Boulanger et al. (1991) also found that specimens tested with static shear stresses developed most of their limiting excess pore pressure ratios relatively early within individual tests. For this reason, Boulanger et al. (1991) tentatively recommended the use of revised K_α values. These revised K_α values are somewhat lower than those developed by Seed and Harder (1990), and are generally based on a failure criterion of 3 percent shear strain rather than 7.5 percent. Use of the 3 percent shear strain failure criterion is believed to better capture the onset of large pore pressure generation. The revised K_α values of Boulanger et al. (1991) were also weighted more heavily towards the data from simple shear or torsional simple shear tests rather than those from triaxial tests. This was because the former allow continuous rotation of principal stress directions, and thus a better representation of how static shear stresses affect shear stress reversal on all possible planes.

Figure 17 presents a slightly modified version of the K_α values previously recommended by Boulanger et al. (1991). In general, the new K_α values shown in Figure 17 for relative densities of about 35 percent are about the same as those suggested by Seed and Harder (1990). However, the K_α values for higher relative densities are up to 40 percent lower than comparable values suggested by Seed and Harder (1990). However, there is some overlap in the ranges suggested by both sets of studies. Also shown in Figure 17 are SPT $(N_1)_{60}$ values that are considered to approximately correspond to the different ranges in relative density.

Discussion

The wide ranges in potential K_α values show the need for continued research and field verification of the effects of static shear stresses on liquefiable soils. The different rates of pore pressure generation and different limiting values of potential excess pore pressure for different locations within a slope show that the evaluation of liquefaction resistance of sloping ground is an extremely complicated endeavor. Considerable research is needed into what constitutes liquefaction under sloping ground conditions and how to determine the potential for triggering liquefaction in a practical manner. It is essential that case histories illustrating the liquefaction performance of sloping ground and soil beneath and adjacent to foundations be studied to enable assessment of K_α factors under field conditions.

Recommendations

Recent laboratory studies have yielded a wide range of K_α correction factors. After evaluating the results from recent test programs, it is recommended that the K_α vs. alpha relationships shown in

Figure 17 be used for liquefaction evaluations of soils. The values shown in Figure 17 are appropriate for effective confining stresses of less than 3 tsf. Significantly higher confining stresses will cause sandy soils to behave more contractive, and thus lower values of K_α may be appropriate for such conditions (see Figure 14).

For high risk and critical projects on sloping ground or where there are high initial static shear stresses, site-specific laboratory testing should be considered using high quality samples in order to develop reliable values of K_α.

CONCLUSIONS/RECOMMENDATIONS

1. The empirical data available for use in predicting liquefaction resistance is generally limited to relatively flat ground under relatively small levels of confining stress. There remains considerable uncertainty regarding the appropriateness of various correction factors to extend the available SPT and CPT empirical correlations to conditions with sloping ground or high confining stresses.

2. It is essential that case histories regarding the seismic performance of earth structures with liquefiable soils under high confining stresses and sloping ground be investigated and documented.

3. Laboratory test programs have shown a large range of potential K_σ and K_α correction factors. Some of the available data is relatively old and of lesser quality than more recent studies. Additional research examining the effect of fines content and higher confinement on both corrections would be of great benefit.

4. The K_σ curve shown in Figure 9 is considered to provide a reasonably conservative estimate of K_σ values for use in liquefaction analyses of clean or silty sands and gravels.

5. The K_α relationships shown in Figure 17 are recommended for effective confining stresses less than 3 tsf. For significantly higher confining stresses, lower K_α values may be appropriate.

6. For critical projects, site specific laboratory testing may be necessary to develop corrections for <u>both</u> sloping ground and high confining stresses. Samples of the highest possible quality should be obtained for this purpose. For soils with low fines contents, in situ freezing of samples for laboratory testing may be the best approach. Alternatively, considerable insight may still be gained from tests performed on reconstituted specimens.

REFERENCES

1. Arango, Ignacio (1996) "Correction Factor K_σ - Derivation of Site-Specific K_σ for an Old Clayey Sand Deposit," working paper prepared for Workshop on Evaluation of Liquefaction Resistance, Salt Lake City, Utah, January 4-5, 1996.

2. Boulanger, Ross W. and Seed, Raymond B. (1995) "Liquefaction of Sand under Bidirectional Monotonic and Cyclic Loading," ASCE Journal of Geotechnical Engineering, Vol. 121, No. 12, December.

3. Boulanger, Ross W., Seed, R. B., Chan, C. K., Seed, H. B., and Sousa, J. (1991) "Liquefaction Behavior of Saturated Sands under Uni-directional and Bi-Directional Monotonic and Cyclic Simple Shear Loading," Geotechnical Engineering Report No. UCB/GT/91-08, University of California, Berkeley.

4. Byrne, Peter M. and Harder, Leslie F., (1991) "Terzaghi Dam, Review of Deficiency Investigation, Report No. 3," prepared for B C Hydro, Vancouver, British Columbia.

5. Harder, L. F., Jr. (1988) "Use of Penetration Tests to Determine the Cyclic Load Resistance of Gravelly Soils," Dissertation submitted as partial satisfaction for the degree of Doctor of Philosophy, University of California, Berkeley.

6. Harder, L. F., Jr. and Seed, H. Bolton (1986), "Determination of Penetration Resistance for Coarse-Grained Soils using the Becker Hammer Drill," Earthquake Engineering Research Center, Report No. UCB/EERC-86/06, University of California, Berkeley.

7. Hynes, M. E. (1988) "Pore Pressure Generation Characteristics of Gravel under Undrained Cyclic Loading," Dissertation submitted as partial satisfaction for the degree of Doctor of Philosophy, University of California, Berkeley.

8. Pillai, V. S. and Byrne, P. M. (1994) "Effect of Overburden Pressure on Liquefaction Resistance of Sand," Canadian Geotechnical Journal, Vol. 31, pp. 53-60.

9. Seed, H. Bolton (1983) "Earthquake-Resistant Design of Earth Dams," Proceedings of a Symposium on Seismic Design of Embankments and Caverns, ASCE, Philadelphia, Pennsylvania, May 6-10, 1983.

10. Seed, H. B., Tokimatsu, K., Harder, L. F., and Chung, R. (1985) "Influence of SPT Procedures in Soil Liquefaction Resistance Evaluations," ASCE Journal of Geotechnical Engineering, Vol. 111, No. 12, December.

11. Seed, R. B., and Harder, L. F., Jr. (1990) "SPT-based analysis of Cyclic Pore Pressure Generation and Undrained Residual Strength," Proceedings of the H. Bolton Seed Memorial Symposium, May, 1990.

12. Vaid, Y. P. and Chern, J. C. (1983) "Effect of Static Shear on Resistance to Liquefaction," Soils and Foundations, JSSMFE, Vol. 23, No. 1, March.

13. Vaid, Y. P. and Chern, J. C. (1985) "Cyclic and Monotonic Undrained Response of Saturated Sands," Advances in the Art of Testing Soils under Cyclic Conditions, ASCE Convention, Detroit.

14. Vaid, Yoginder P., Chern, Jing C., and Tumi, Hadi (1985) "Confining Pressure, Grain Angularity, and Liquefaction," ASCE Journal of Geotechnical Engineering, Vol. 111, No. 10, October.

15. Vaid, Y. P. and Finn, W. D. L. (1979) "Static Shear and Liquefaction Potential," ASCE Journal of the Geotechnical Division, Vol. 105, No. GT10, October.

16. Vaid, Y. P. and Thomas, J. (1994) "Post Liquefaction Behaviour of Sand," Proceedings of the 13th International Conference on Soil Mechanics and Foundation Engineering, New Delhi, India.

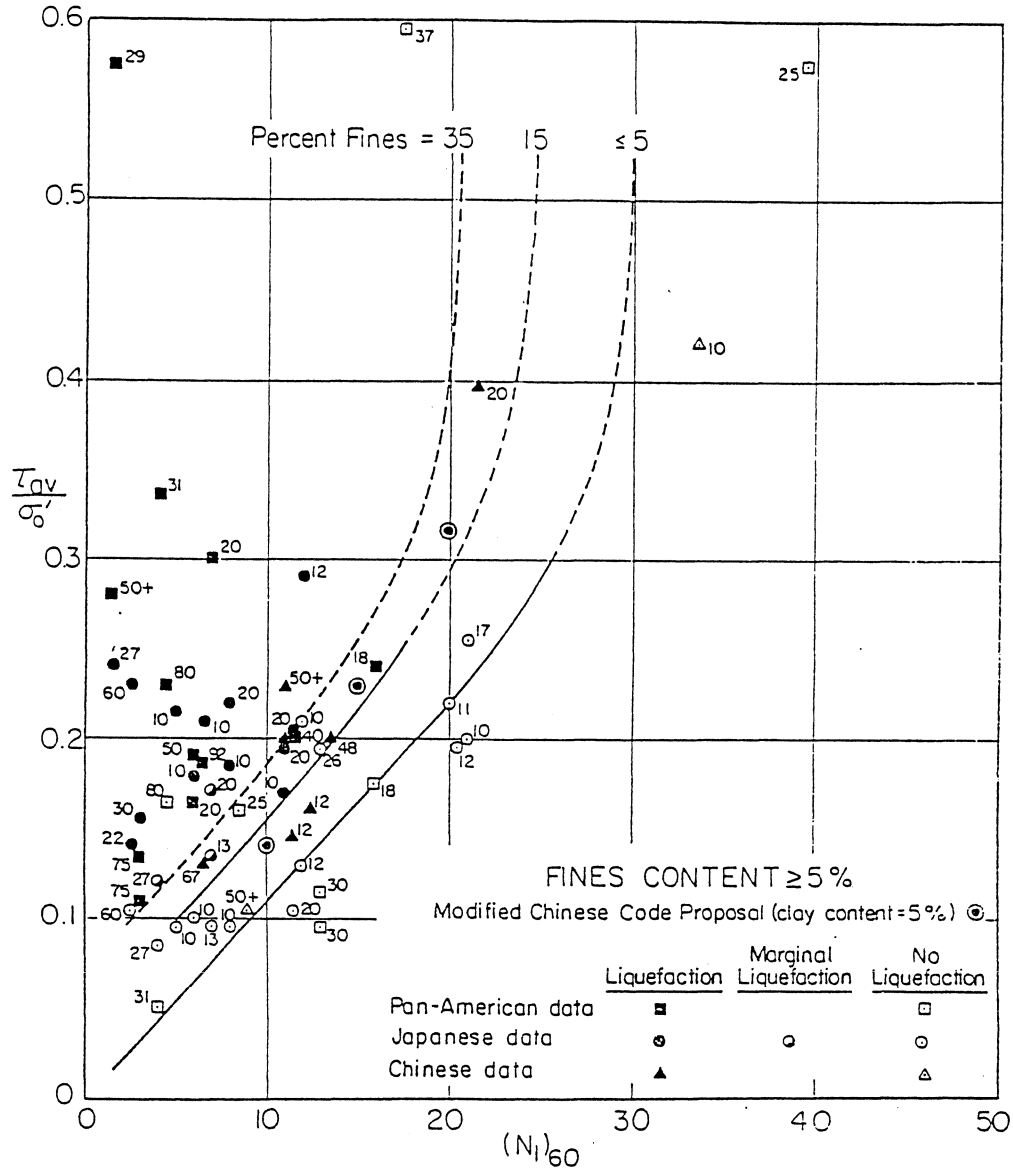

Figure 1: Relationship Between Cyclic Stress Ratios Causing Liquefaction During M=7.5 Earthquakes and Corrected SPT Blowcounts in Silty Sands (after Seed et al., 1985)

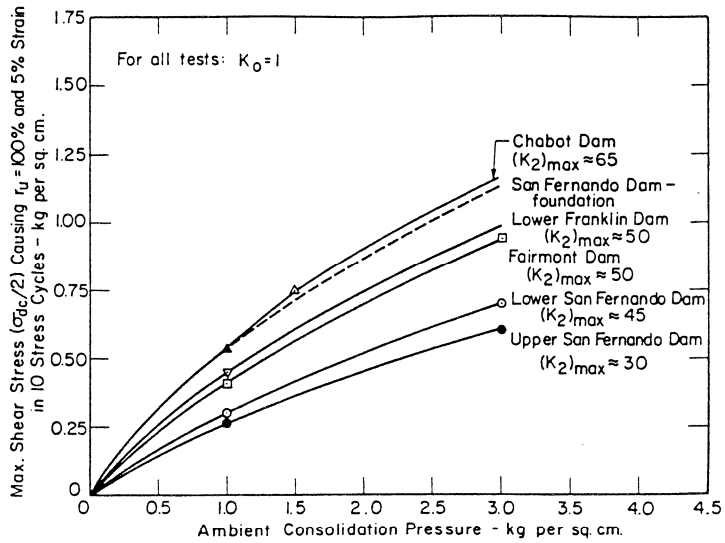

Cyclic Loading Resistance of Shell Materials for Selected Dams (see Table 2)

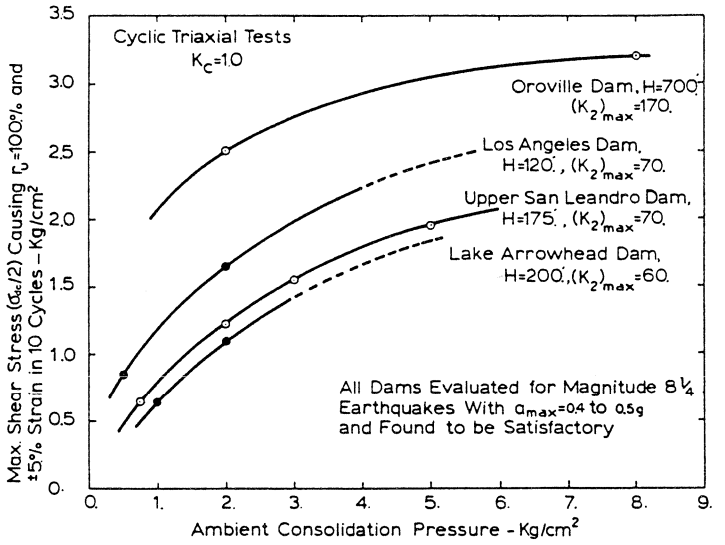

Cyclic Loading Characteristics of Shell Materials for Several Dams Shown by Analyses to be Capable of withstanding Strong Earthquake Shaking

Figure 2: Cyclic Loading Resistance of Selected Soils as Determined by Isotropically-Consolidated Cyclic Triaxial Tests (from Seed, 1983)

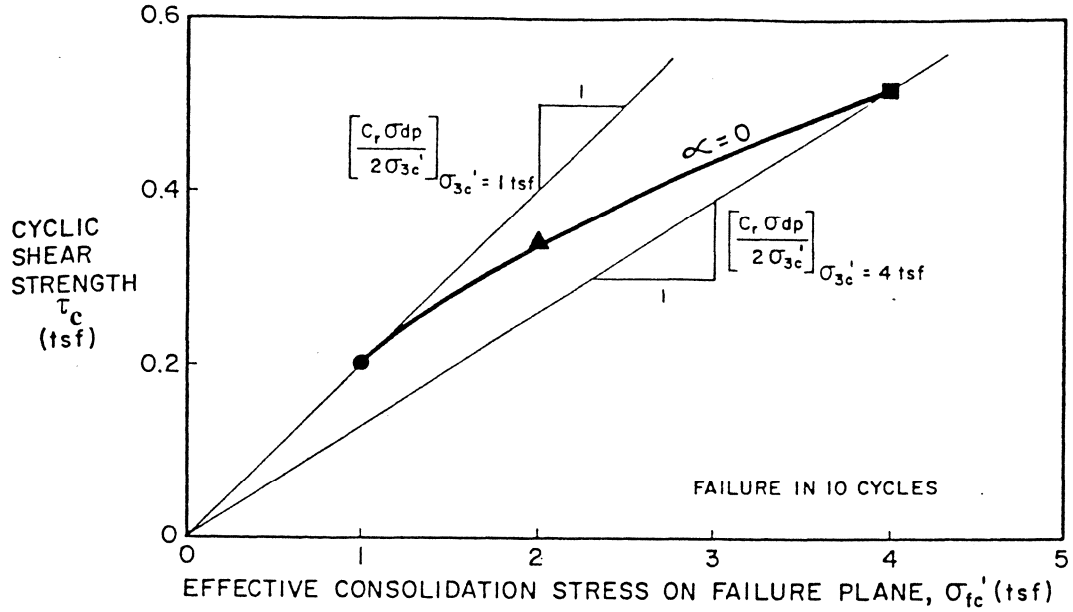

NOTE: $\sigma_{fc}' = \sigma_{3c}'$ for ISOTROPICALLY – CONSOLIDATED CYCLIC TRIAXIAL TESTS

$$\tau_s = C_r \frac{\sigma dp}{2}$$

$$\text{CYCLIC STRESS RATIO} = \frac{\tau_s}{\sigma_{fc}'} = \frac{C_r \sigma dp}{2\sigma_{3c}'}$$

$$\left[\frac{C_r \sigma dp}{2\sigma_{3c}'}\right]_{\sigma_{3c}' = 1\ tsf} > \left[\frac{C_r \sigma dp}{2\sigma_{3c}'}\right]_{\sigma_{3c}' > 1\ tsf}$$

$$K_\sigma = \left[\frac{C_r \sigma dp}{2\sigma_{3c}'}\right]_{\sigma_{3c}'} \Big/ \left[\frac{C_r \sigma dp}{2}\right]_{\sigma_{3c}' = 1\ tsf}$$

Figure 3: Typical Cyclic Resistance Determined from Isotropically-Consolidated Cyclic Triaxial Tests

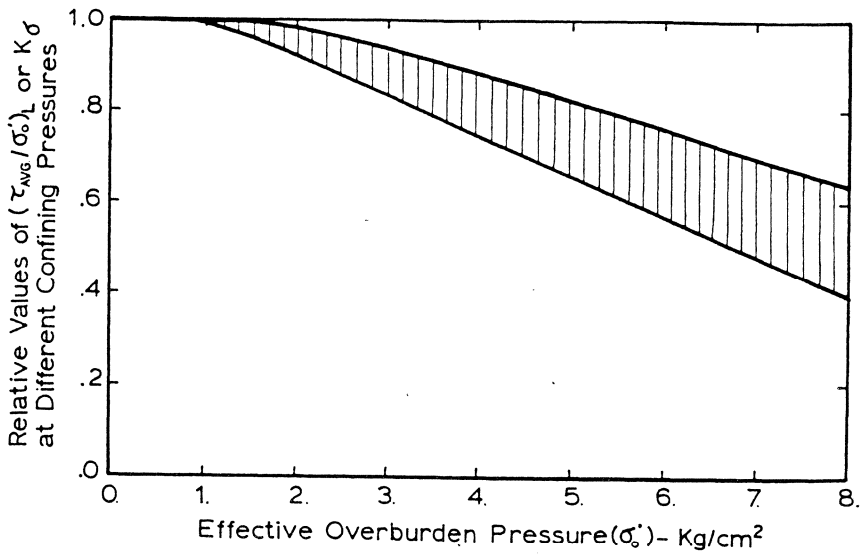

Figure 4: Relationship between Effective Confining Pressure and Kσ Suggested by Seed (1983)

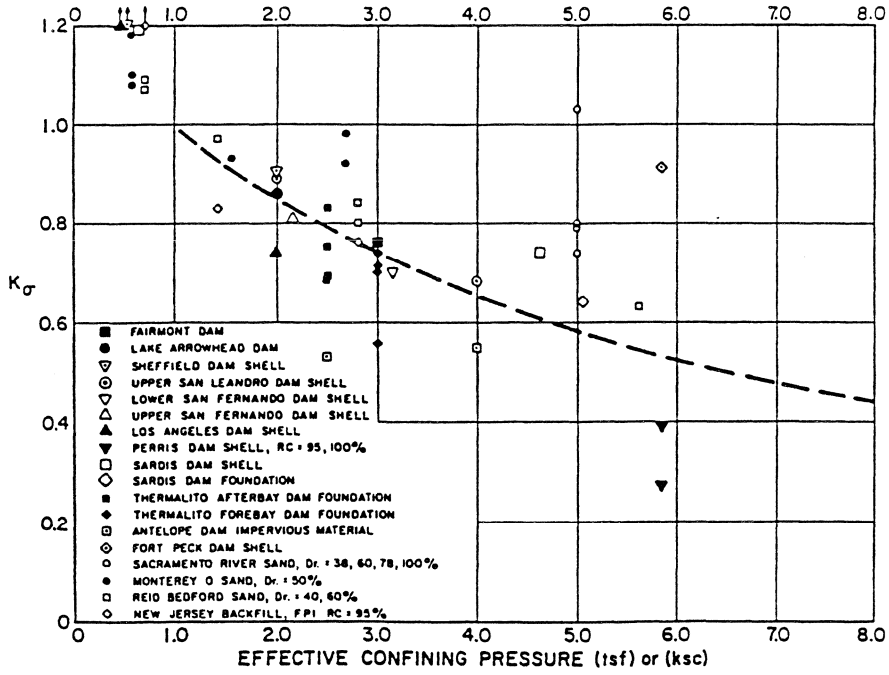

Figure 5: Relationshiop between Effective Confining Pressure and Kσ Suggested by Seed and Harder (1990)

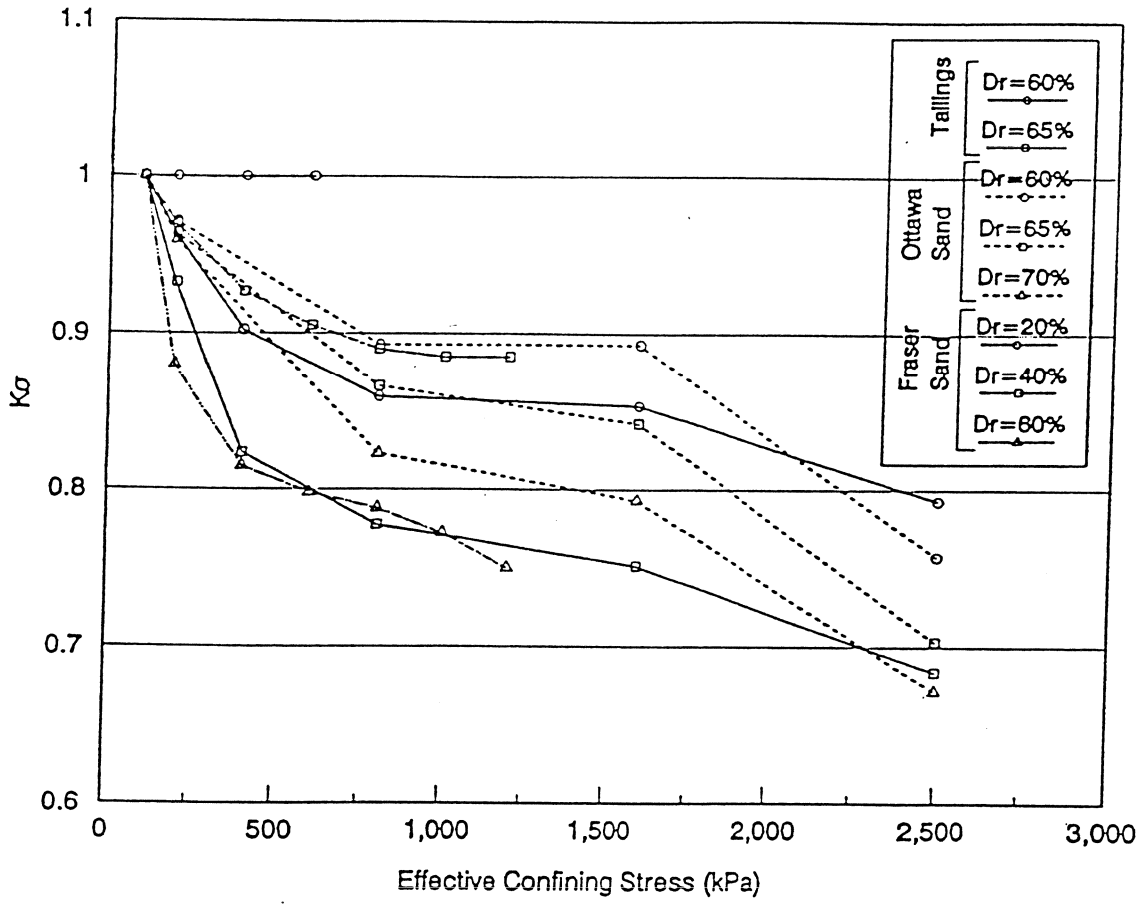

Figure 6: Relationship between Effective Overburden Pressure and Kσ (UBC data from Vaid et al., 1985 and Vaid and Thomas, 1994)

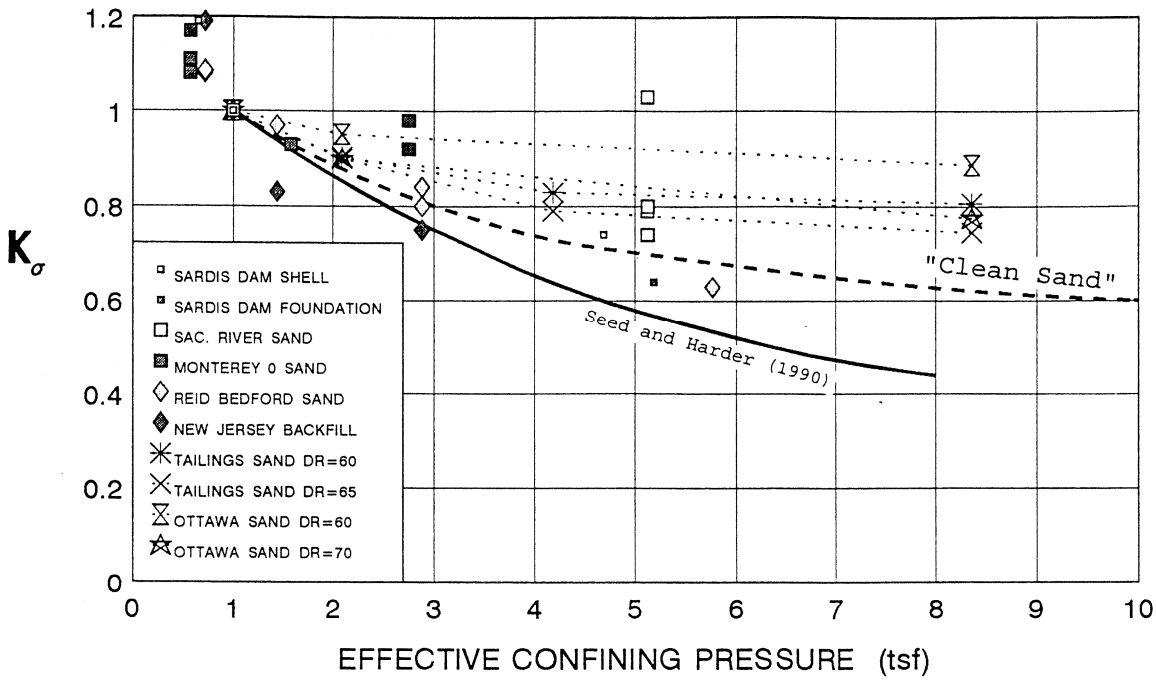

Figure 7: Comparison of UBC Kσ Values with Clean Sand Data from Seed and Harder (1990)

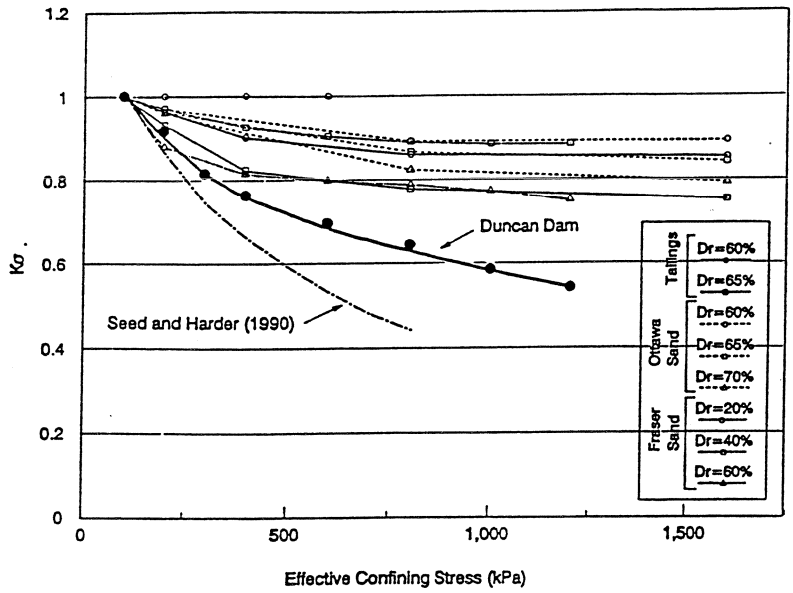

Figure 8: Comparison of Duncan Dam Kσ Values with other Kσ Data (after Pillai and Byrne, 1994)

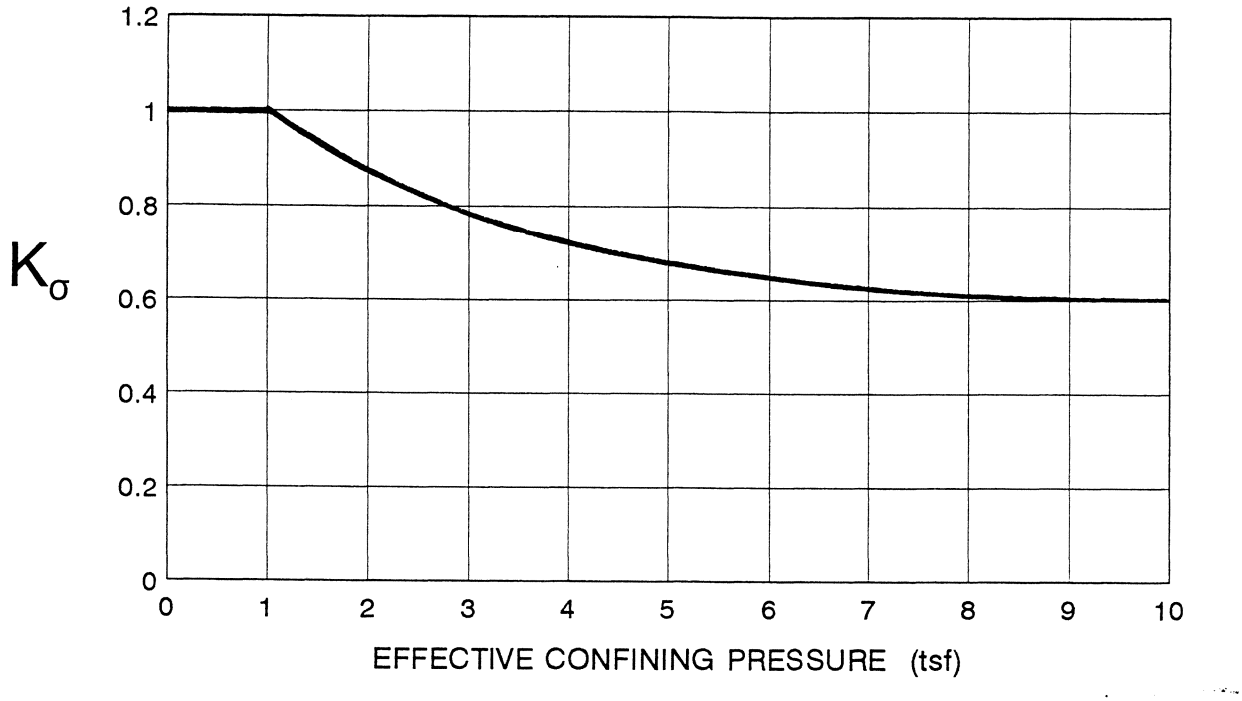

Figure 9: Recommended Kσ Values for Clean and Silty Sands and Gravels

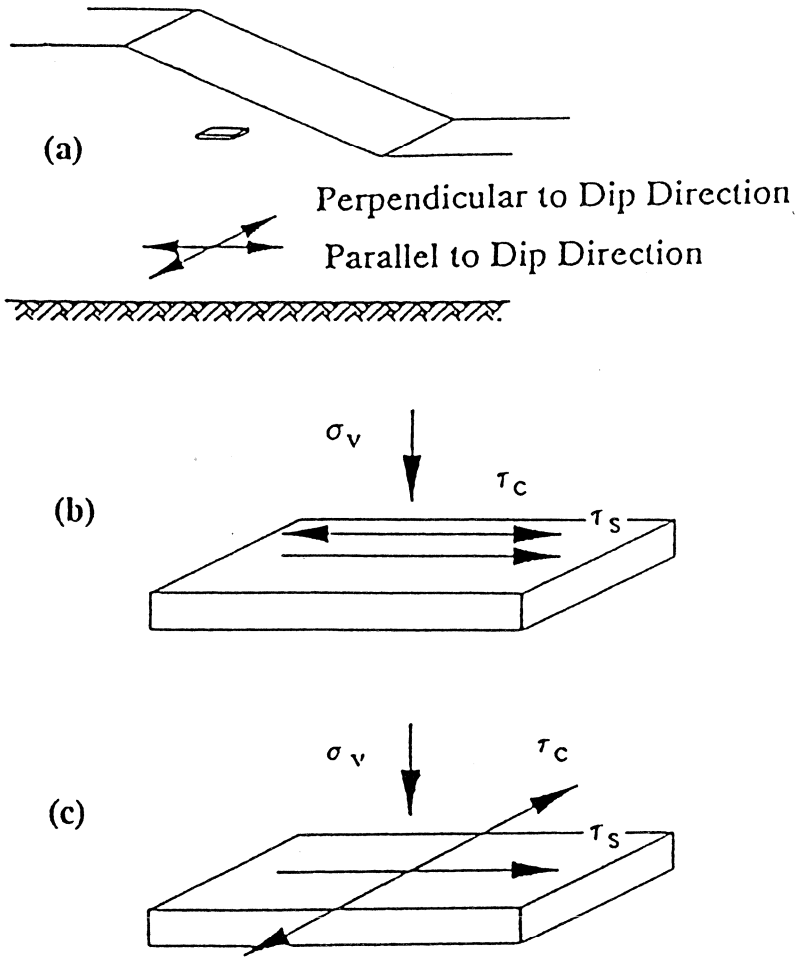

Figure 10: Static and Cyclic Stress Conditions on Horizontal Planes Beneath Sloping Ground (from Boulanger and Seed, 1995)

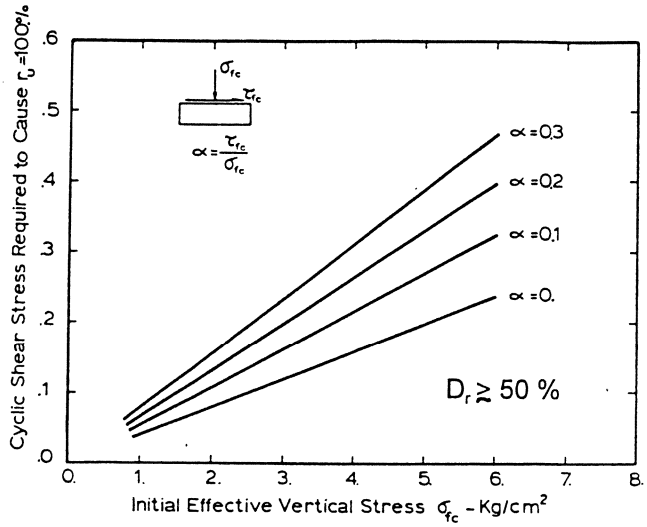

Figure 11: Typical Effects of Initial Static Shear Stresses on the Cyclic Resistance of Sands (after Seed, 1983)

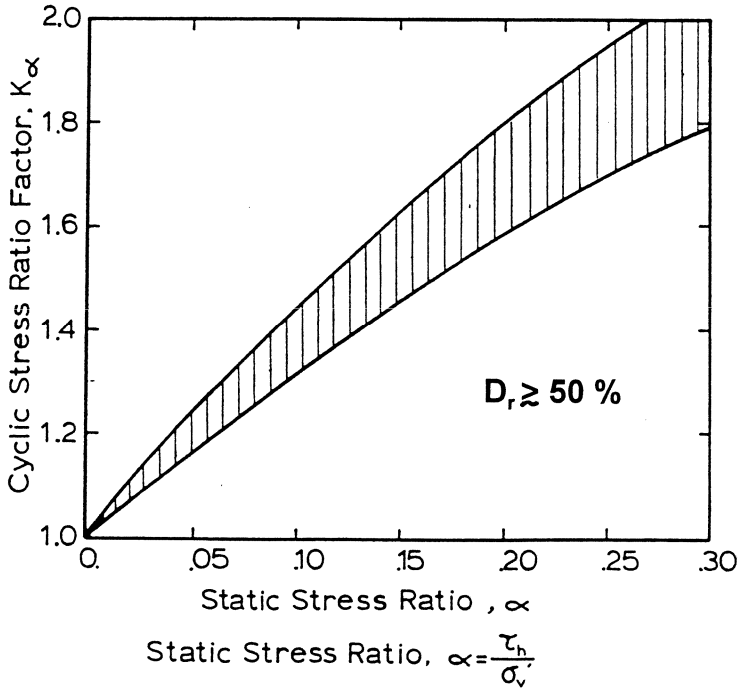

Figure 12: Kα Correction Factors Suggested by Seed (1983)

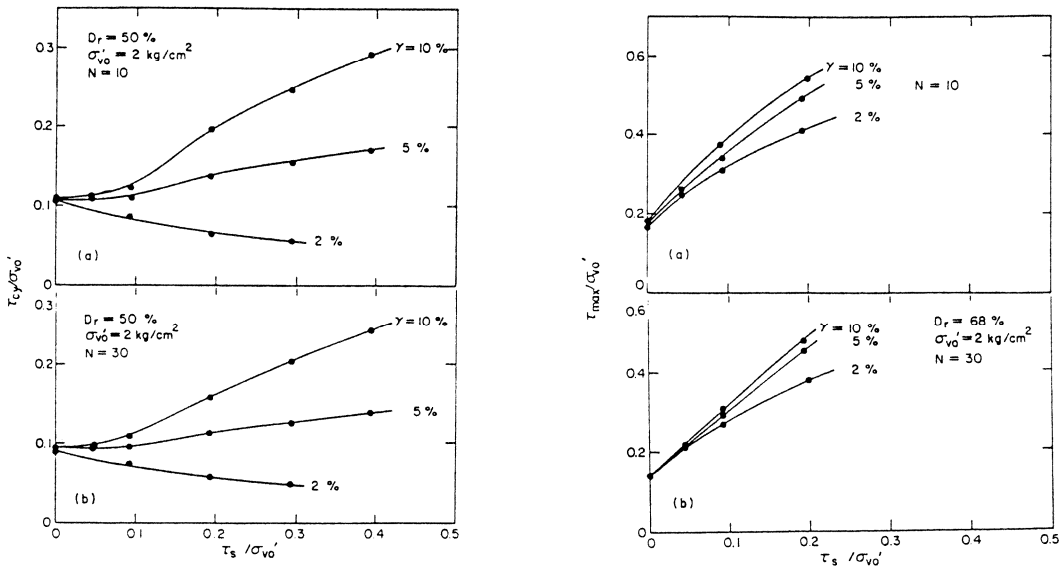

a. **Effect of Static Shear on Cyclic Resistance Determined in Constant Volume Cyclic Shear Tests (After Vaid and Finn, 1979)**

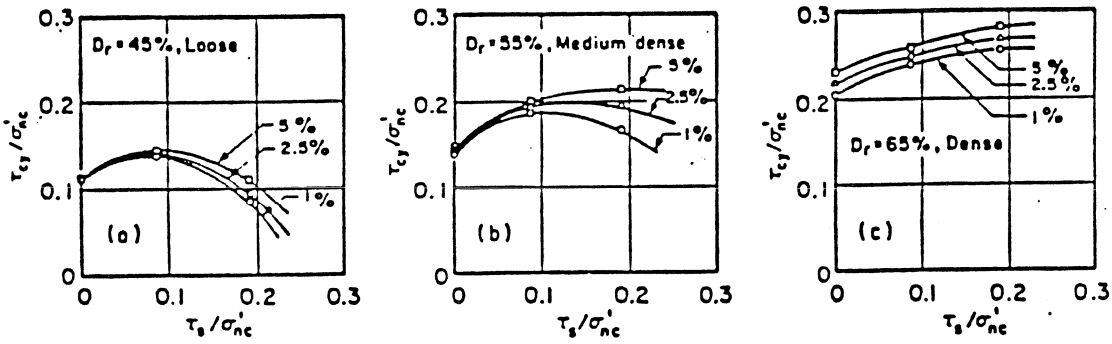

b. **Effect of Static Shear on Cyclic Resistance Determined in Cyclic Triaxial Tests (after Vaid and Chern, 1983)**

Figure 13: Typical Effects of Static Shear on Cyclic Resistance

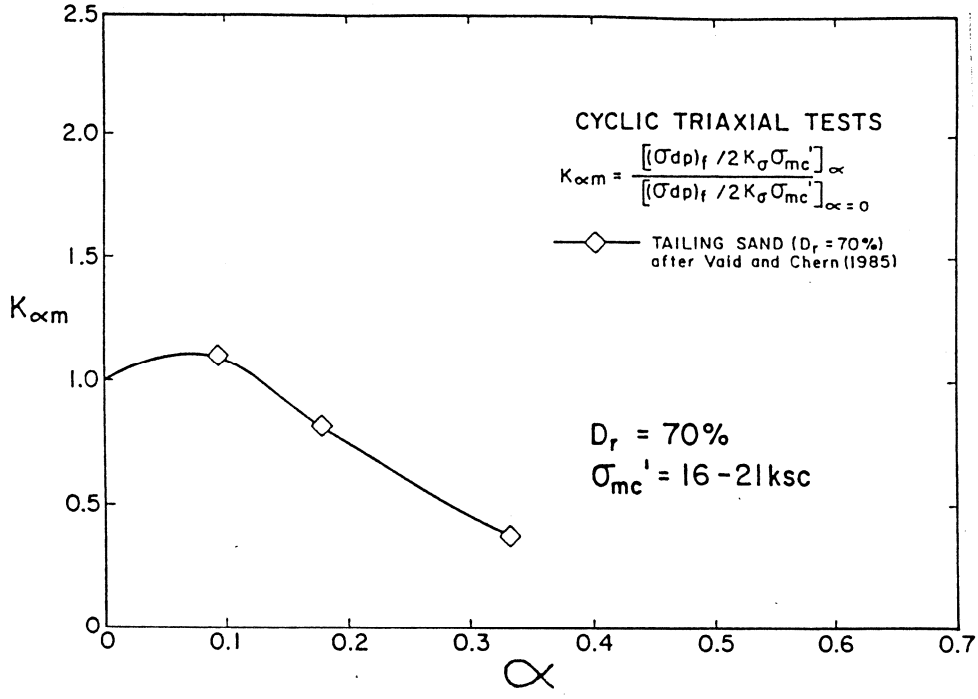

Figure 14: Effect of Static Shear on Cyclic Resistance for Moderately Dense Sand (Dr = 70 %) at High Confinement (adapted from Vaid and Chern, 1985)

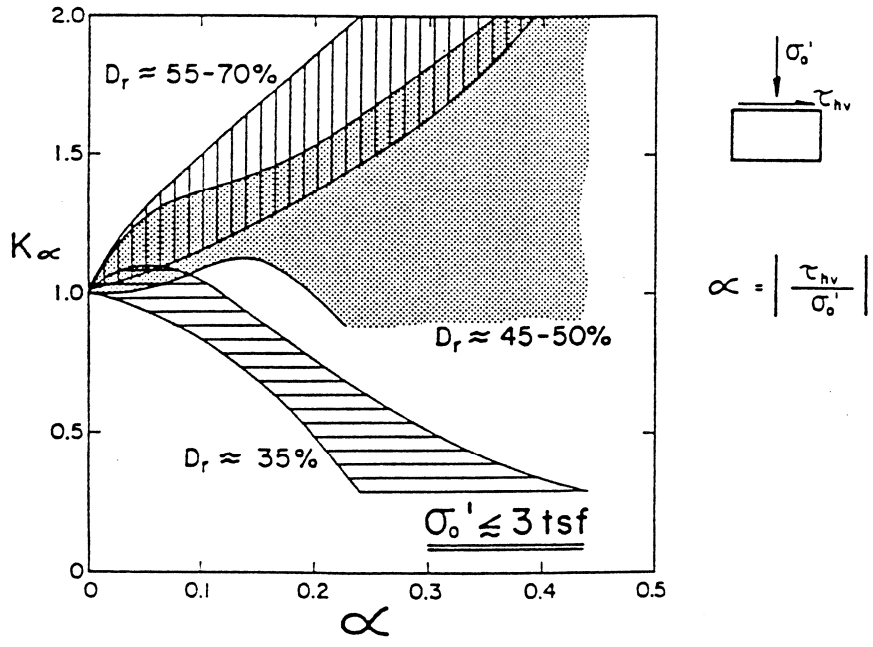

Figure 15: Kα Correction Factors Suggested by Seed and Harder (1990)

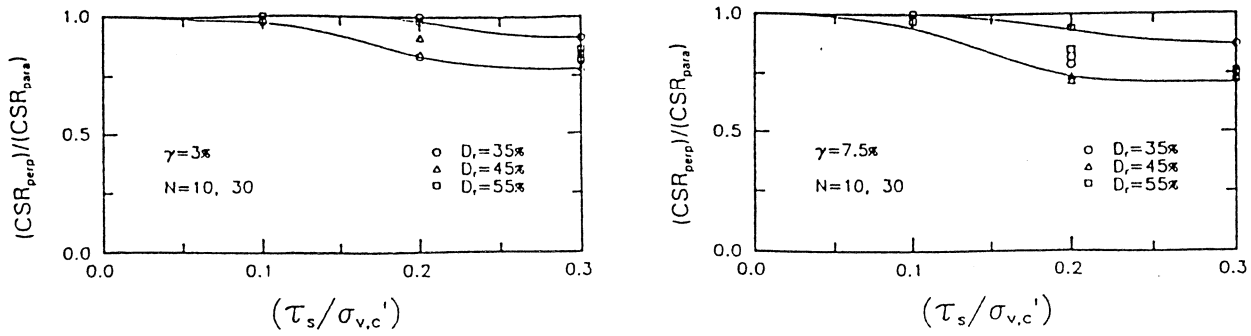

Figure 16: Ratio of "Perpendicular" to "Parallel" Cyclic Loading Resistance for Failure Criteria of 3% and 7.5% Shear Strain (from Boulanger and Seed, 1995)

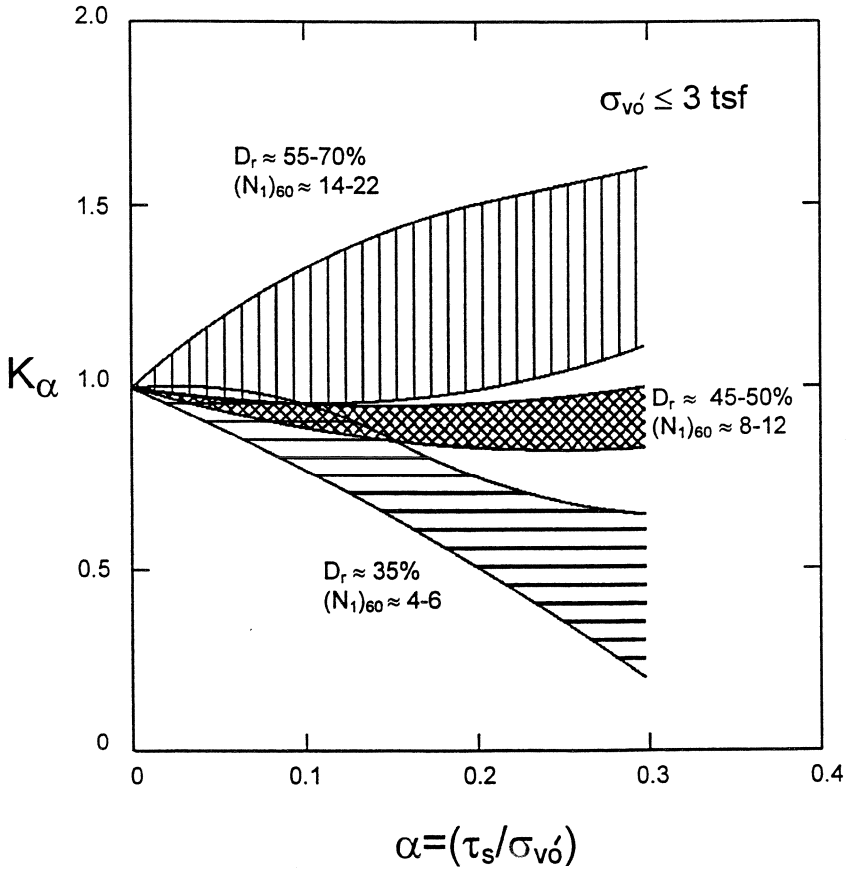

Figure 17: Recommended Kα Values for Effective Confining Pressures Less than 3 tsf

Seismic Factors for Use in Evaluating Liquefaction Resistance

T. Leslie Youd

Professor of Civil Engineering
Brigham Young University
Provo, Utah, 84602-4081

Abstract

Application of the simplified procedure for evaluation of liquefaction resistance requires estimates of earthquake magnitude and peak acceleration as input seismic parameters. These factors characterize duration and intensity, respectively, of earthquake shaking at a site. The following comments summarize consensus statements developed at the workshop for determining these seismic factors.

- The simple correlation between magnitude and duration incorporated within the simplified procedure is adequate and conservative for typical liquefaction hazard analyses. This relationship is adequate for application in the eastern U.S. as well as the western U.S.

- Magnitudes based on the moment magnitude scale, M_w, are the preferred for calculation of liquefaction resistance. Where estimates of M_w are not available, magnitudes from other scales may be substituted within the following limits: $M_L < 6$, $m_B < 7.5$, and $6 < M_s < 8$.

- The preferred procedure for estimating peak accelerations for use in liquefaction resistance analyses is through application of empirical attenuation relationships specifically developed for soil conditions representative of the site. For sites with soft soils or other soils not characterized in attenuation relationships, local site response calculations using programs such as SHAKE or DESRA may be used. The least desirable procedure is application of amplification factors or transfer functions.

- Use of attenuation relationships based on the geometric mean of two orthogonal peak horizontal components is consistent with development of the simplified procedure and should be used in liquefaction resistance evaluations. Peak accelerations estimated from attenuation relationships incorporating the larger of the two peaks, however, are conservative and allowable.
- High-frequency acceleration spikes that occur in some strong motion records may be safely ignored for calculation of liquefaction resistance.

Introduction

Application of the simplified procedure for evaluating liquefaction resistance of soil layers requires estimates of earthquake magnitude, peak acceleration, and a magnitude scaling factor as seismic input factors for the analysis. These factors characterize duration and intensity of earthquake shaking at a site. Magnitude and peak acceleration are discussed in this section. Magnitude scaling factors are discussed in a separate section entitled "Magnitude Scaling Factors" (Youd and Noble, this report).

Earthquake Magnitude

In the development of the simplified procedure, Seed and Idriss (1982) used magnitude as a measure of duration of strong seismic shaking. To incorporate duration, they introduced the concept of an equivalent number of significant stress cycles contained in a strong motion accelerogram (Seed et al., 1975; Seed and Idriss, 1982). From an evaluation of the number of significant stress cycles contained in accelerograms recorded at free field sites, Seed et al. (1975) developed the generalized relationship between earthquake magnitude and number of equivalent stress cycles listed in Table 1. Thus magnitude is effectively a measure of shaking duration as used in the simplified procedure.

Records from past earthquakes indicate that the relationship between duration and magnitude is rather uncertain and that several factors other than magnitude influence duration. For example, recorded durations have varied by a factor of two or more for earthquakes of a given magnitude. This variation is partially dependent on the mechanism of faulting. Unilateral faulting with rupture beginning at one end of the fault and propagating to the other end usually produces much longer durations than bilateral faulting in which slip begins near the midpoint on the fault and propagates in both directions. Duration also generally increases with distance from the seismic energy source and may vary with topography of subsurface bedrock (basin effect) and with site conditions. To compensate for uncertainty in duration and other factors, Seed and Idriss (1982) drew a rather conservative bound on the standard CRR plot for magnitude 7.5 earthquakes to separate data indicative of liquefaction from data indicative of nonliquefaction (Figure 1). The conservative placement of this bound assures that liquefaction will seldom occur at sites where nonliquefaction is predicted, even where longer than normal durations of shaking occur. Conversely, in some instances liquefaction may not occur because of shorter than normal duration even though liquefaction is predicted by the conservative bound plotted on Figure 1.

Because of uncertainty between magnitude and duration, the workshop addressed the following questions with respect to magnitude as an index of shaking duration and developed the following consensus answers:

Question A: Is magnitude a sufficient parameter or should additional correction factors or adjustments be developed to account for unusually long or short durations?

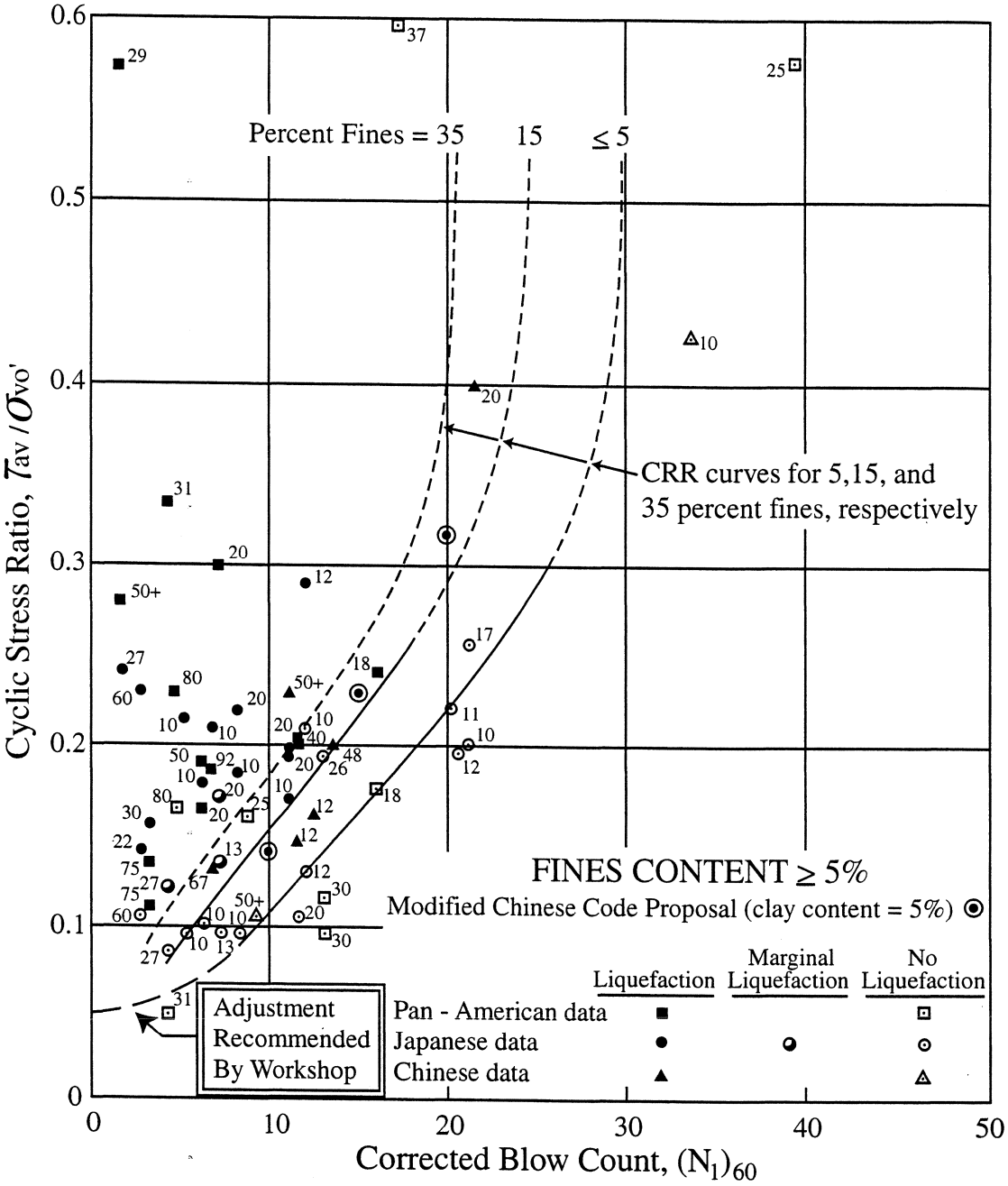

Figure 1. Base Curve and Liquefaction Data from the Simplified Procedure (modified from Seed et al., 1984).

Answer A: Variations of shaking duration for a given magnitude are commonly a function of the mechanics and style of faulting. For example, bilateral faulting associated with the 1989 Loma Prieta ($M_w = 6.9$) and 1995 Hyogoken-Nanbu (Kobe) ($M_w = 6.8$) earthquakes generated durations (7 to 10 seconds) that were less than half of durations normally expected for those magnitudes of earthquakes. Conversely, the 1988 Armenian earthquake ($M_w = 6.8$) was characterized by a very long duration of about 50 seconds, which is more than twice the duration normally expected.

Table 1. Number of Equivalent Stress Cycles as a Function of Earthquake Magnitude (after Seed and Idriss, 1982)

Earthquake Magnitude	Number of Equivalent Stress Cycles
5 1/2	2-3
6	5
6 3/4	10
7 1/2	15
8 1/2	26

Faulting characteristics and variations in shaking duration for a given magnitude of earthquake, however, are difficult to predict in advance of the event. Thus use of a conservative simplified relationship between magnitude and duration is an acceptable approach for routine evaluations of liquefaction resistance.

Question B: A primary difference between eastern U.S. earthquakes and western U.S. earthquakes is that strong ground motions generated by eastern earthquakes are generally richer in high-frequency components. Consequently, eastern earthquakes of the same magnitude and duration may generate more significant stress cycles than western events. Because of the likely larger number of loading cycles in the east, should an additional correction factor be introduced for eastern U.S. earthquakes?

Answer B: Although higher frequencies of motion and greater numbers of loading cycles may occur at bedrock outcrops in the eastern U.S., their influence on the development of liquefaction may not be significant. High-frequency motions generally attenuate or damp out rather quickly as they propagate through soil layers. This filtering action would reduce differences in numbers of significant loading cycles between eastern and western earthquakes at soil sites. Because liquefaction occurs only within soil strata, differences in numbers of loading cycles between eastern and western earthquakes are not likely to be great. Without more recorded strong motion data from soil sites in the eastern U.S. from which numbers of significant loading cycles can be quantified, there is little basis for development of additional correction factors for eastern localities.

Another difference between eastern and western U.S. earthquakes is that strong ground motions generally propagate to greater distances in the east. By applying state-of-the-art procedures for the eastern U.S. for estimating peak ground accelerations, differences in ground motion propagation between western and eastern earthquakes are properly accounted for. Thus use of standard criteria developed largely for western U.S. earthquakes is acceptable for routine application in the eastern U.S., provided peak accelerations are estimated using attenuation functions specifically developed for eastern U.S. earthquakes.

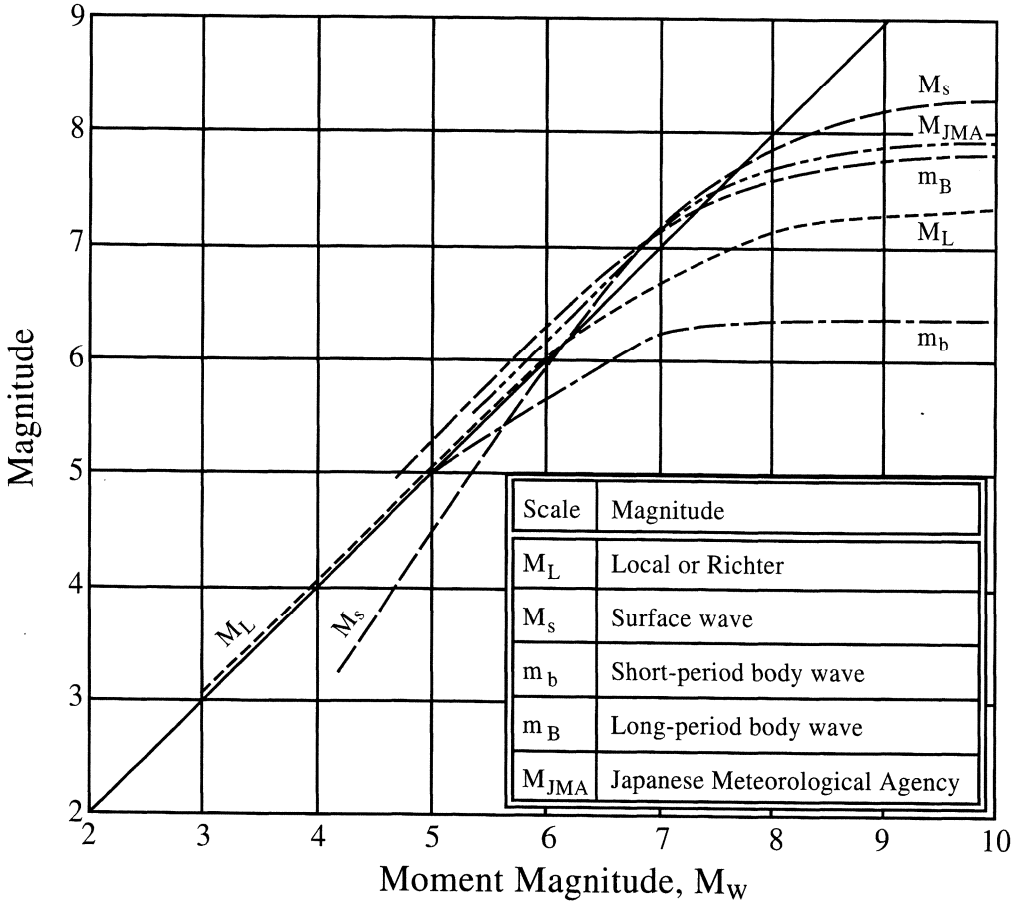

Figure 2. Relationships Between Moment Magnitude and Various Magnitude Scales (after Heaton et al., 1986)

Question C: Which magnitude scale should be used by engineers in selecting a magnitude parameter for liquefaction resistance analyses?

Answer C: Seismologists commonly calculate earthquake magnitudes using five different scales: (1) local or Richter magnitude, M_L; (2) surface-wave magnitude, M_s; (3) short-period body-wave magnitude, m_b; (4) long-period body-wave magnitude, m_B; and (5) moment magnitude, M_w. Moment magnitude, M_w, is the scale most commonly used for engineering applications and is the scale preferred for calculation of liquefaction resistance. For example, engineering seismologists have found that M_w generally correlates better than other scales with attenuation of peak ground motions and spectral ordinates, and, consequently, with earthquake damage. Moment magnitude is calculated from the amount of seismic energy released in earthquakes rather than peak displacement of an accelerogram trace. Thus M_w is a more theoretically correct measure of earthquake strength and duration than other magnitude estimates for engineering purposes.

Where estimates of moment magnitude are not available, magnitudes from other scales may be substituted directly for M_w within the following limits: $M_L < 6$, $m_B < 7.5$, and $6 < M_s < 8$ (Figure 2).

The short-period body-wave magnitude, m_b, a scale commonly used in the eastern U.S., may be used for magnitudes between 5 and 6 provided such magnitudes are corrected to M_w using the curves plotted in Figure 2. Because all magnitude scales, except M_w, saturate at some level (do not increase in magnitude with increased seismic energy), substitutions, as listed above, should not be applied beyond the given limits (Idriss, 1985).

Peak Acceleration

For calculation of liquefaction resistance using the simplified procedure, peak horizontal acceleration at ground surface is used to characterize the intensity of ground shaking at a site. Specific guidance was not given in the original procedure for defining this parameter. To provide some guidance on estimating peak acceleration for evaluation of liquefaction resistance, the workshop participants addressed the following questions and developed the accompanying consensus answers.

Question D: What procedures are preferred for estimating peak horizontal ground acceleration at potentially liquefiable sites?

Answer D: In practice, peak accelerations for use in analysis of liquefaction resistance are generally evaluated from ground motion attenuation relationships. Estimates of peak acceleration may be either deterministic or probabilistic. Deterministic estimates are based on magnitude and the distance between the site and the seismic source zone for the design earthquake. Probabilistic estimates are based on the largest acceleration likely to excite a site in a given exposure time (usually 50 years with two to ten percent probability of exceedance). Because the associated earthquake magnitude is not generally known, a separate estimate of magnitude is generally required. Future probabilistic hazard maps will likely include information on earthquake magnitude as well as peak ground motion parameters.

The following three methods, in order of preference, may be used for estimating peak acceleration.

(1) The preferred method for estimating peak acceleration at a site is through direct application of correlations between peak horizontal acceleration, earthquake magnitude, and distance from the seismic energy source. Several investigators have developed and routinely apply correlations for bedrock and stiff to moderately stiff soil sites. Which of these relationships should be used for liquefaction hazard assessment requires consideration of such factors as region of the country, type of faulting, local preference, etc. Some preliminary attenuation relationships have also been developed for soft soil sites. For example, Idriss (1991) developed the attenuation relationships plotted on Figure 3b from response of soft soil sites during the 1989 Loma Prieta earthquake. Also shown in the figure (3a) are attenuation relationships developed by Idriss for rock sites.

In summary, the preferred procedure for estimating peak acceleration is through statistically reliable attenuation relationships that were developed for site conditions similar to those at the site in question.

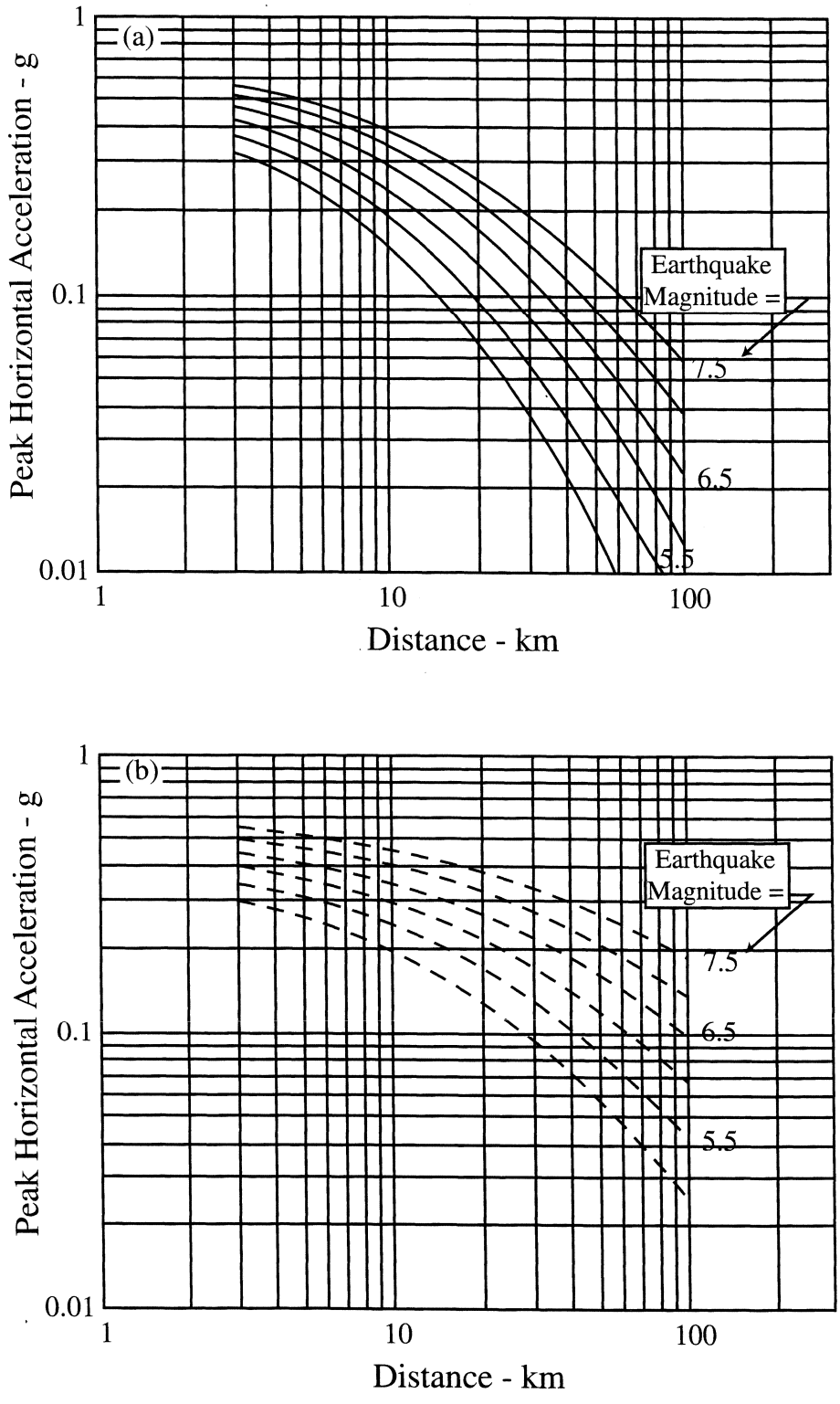

Figure 3. Mean Peak Horizontal Accelerations at (a) Rock Sites and (b) Soft Soil Sites (After Idriss, 1991)

(2) For site conditions that are not compatible with those specified for available attenuation relationships, peak acceleration should be estimated from local site response analyses. Computer programs such as SHAKE, DESRA, etc., may be used for these calculations. Input information required for these analyses include well-documented soil profiles, measured or estimated shear-wave velocity profiles, and time histories of acceleration (accelerograms). The time histories should approximate anticipated future ground shaking either on a bedrock outcrop near the site or in stiff soil layers or bedrock beneath the site. Recorded accelerograms are preferable to synthetic records. Accelerograms derived from white noise should be avoided because of unnatural characteristics commonly assimilated into these records. A suite of plausible earthquake records should be used in the analysis, including as many records as feasible from earthquakes with similar magnitudes recorded at similar distances from the seismic source as the site in question.

(3) A third and least desirable method for estimating peak ground acceleration is through amplification ratios, such as those developed by Idriss (1990; 1991) and Seed et al.(1994). These factors, commonly incorporated in building code provisions, use a multiplier or ratio by which bedrock outcrop or stiff-site motions are amplified to estimate ground motions on soft sites. Because amplification ratios are magnitude and perhaps frequency dependent, caution and considerable engineering judgment are required in their application. Amplification ratios by Idriss (1991) for soft soil sites are plotted on Figure 4. This plot shows ratios for magnitude 5.5 and 7 earthquakes that are appropriate for sites underlain by several meters or more of soft soil similar in consistency to San Francisco Bay mud.

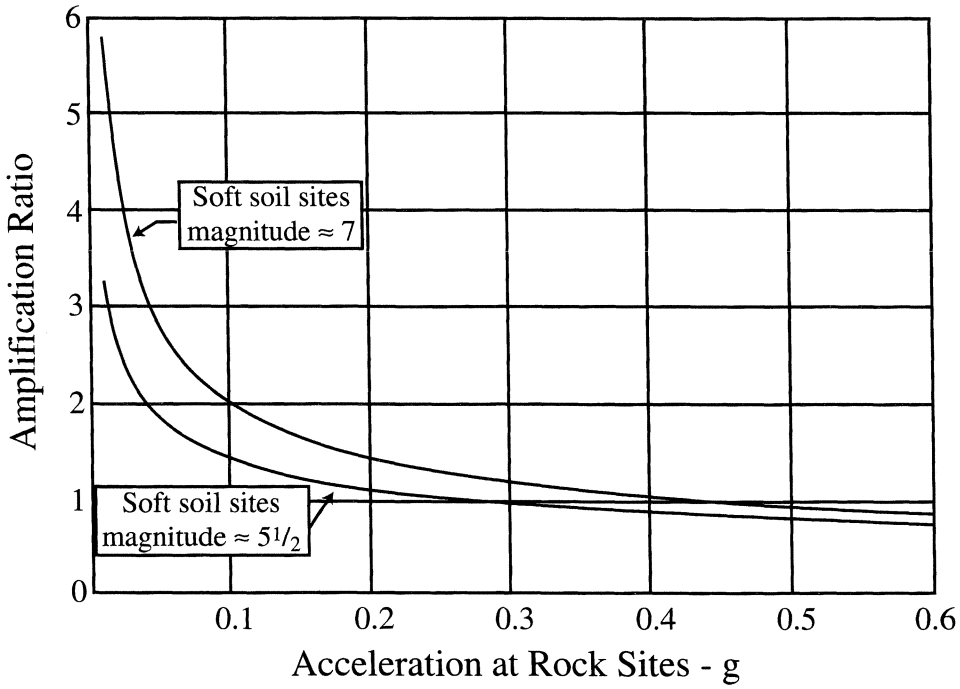

Figure 4. Magnitude-Dependence variations of Amplification of Peak Horizontal Accelerations at Soft Soil Sites (After Idriss, 1991)

Question E: Which peak acceleration should be used? (a) the largest horizontal acceleration recorded on a three-component accelerogram; (b) the geometric mean of the peaks from the horizontal records; or (c) a vectorial combination of horizontal accelerations.

Answer E: According to I.M. Idriss (oral report at workshop), the larger of the two horizontal peak components of acceleration were used in the original development of the simplified procedure, where recorded values were available. Where recorded values were not available, which was the circumstance for most sites in the data base, peak acceleration values were estimated from attenuation relationships incorporating the geometric mean of the two orthogonal peak horizontal accelerations. The geometric mean is defined as the square root of the product of the two orthogonal peaks. In nearly all instances where recorded motions were used, the peaks from the two horizontal records were approximately equal. Thus where a single peak was used, that peak and the geometric mean of the two peaks were near the same value. Based on this information, the workshop concurred that the geometric mean is more consistent with the derivation of the procedure, and recommended use of the peak accelerations derived from attenuation relationships incorporating the geometric mean. The larger of the two peaks, however, is always equal to or larger than the geometric mean; thus use of the larger peak, a common procedure in engineering practice, is conservative and allowable. Vectorial accelerations are seldom calculated and should not be used.

Question F: Liquefaction usually develops at soil sites where ground motion amplification may occur, but also at localities where sediments may soften as excess pore pressures develop, reducing peak acceleration. How should investigators account for both amplification and softening in estimations of peak acceleration?

Answer F: With respect to site amplification and increased pore-water pressure, the recommended procedure is to calculate or estimate a peak acceleration that incorporates the influence of site amplification, but neglects the influence of excess pore pressure. Simply stated, the peak acceleration to be used in liquefaction resistance evaluations is the peak horizontal acceleration that would have occurred at ground surface in the absence of increased pore water pressure or liquefaction.

Question G: Should high-frequency spikes in acceleration records be considered or ignored?

Answer G: In general, short duration, high-frequency acceleration spikes should be ignored for liquefaction resistance evaluations. By using attenuation relationships for estimation of peak acceleration, as noted above, high-frequency spikes are essentially neglected because few high-frequency peaks occur in data bases from which attenuation relationships were derived. Similarly, ground response analyses using programs such as SHAKE or DESRA generally attenuate or filter out high-frequency spikes, reducing the influence of these spikes on site response. Where amplification ratios are used to estimate peak accelerations, engineering judgment should be used as to which bedrock accelerations should be amplified. Generally, however, high-frequency spikes in bedrock records can be safely ignored for evaluation of liquefaction resistance.

References

Idriss, I.M. (1985). "Evaluating Seismic Risk in Engineering Practice." Proceedings, 11th International Conference on Soil Mechanics and Foundation Engineering, San Francisco, Vol. 1, p. 255-320.

Idriss, I.M. (1990). "Response of Soft Soil Sites During Earthquakes." Proceedings, H. Bolton Seed Memorial Symposium, Vol. 2, BiTech Publishers, LTD, Vancouver, B.C. Canada, p. 273-90.

Heaton, T.H., Tajima, F., and Mori, A.W., 1986, "Estimating Ground Motions Using Recorded Accelerograms." Surveys in Geophysics, Vol. 8, p. 25-83.

Idriss, I.M. (1991). "Earthquake Ground Motions at Soft Soil Sites." Proceedings, 2nd International Conference on Recent Advances in Geotechnical Earthquake Engineering and Soil Dynamics, Vol 3, p. 2265-71.

Seed, H.B., Idriss, I.M., Makdisi, F. and Banerjee, N., 1975, "Representation of Irregular Stress Time Histories by Equivalent Uniform Stress Series in Liquefaction Analyses." Report No. EERC 75-29, Earthquake Engineering Research Center, University of California, Berkeley, Calif.

Seed, H.B., Tokimatsu, K, Harder, L.F., and Chung, R.F., 1984, "The Influence of SPT Procedures in Soil Liquefaction Resistance Evaluations, Report No. UBC/EERC-84/15, Earthquake Engineering Research Center, University of California, Berkeley, California.

Seed, H.B., and Idriss, I.M. (1982). Ground Motions and Soil Liquefaction During Earthquakes. Earthquake Engineering Research Institute Monograph.

Seed, R.B., Dickenson, S.E., Rau, G.A., White, R.K., and Mok, C.M., (1994) "Site Effects on Strong Shaking and Seismic Risk: Recent Developments and Their Impact on Seismic Design Codes and Practice." Proceedings, Structural Congress II, ASCE, (1):573-78.

LIQUEFACTION CRITERIA BASED ON STATISTICAL AND PROBABILISTIC ANALYSES

T. Leslie Youd

Professor of Civil Engineering
Brigham Young University
Provo, Utah, 84602-4081

Steven K. Noble

Project Engineer
DOWL Engineers, Inc.
Anchorage, Alaska, 99503-5999

Abstract

Probabilistic procedures for evaluating liquefaction resistance have the advantage of allowing an acceptable level of risk to be specified by the user. Liao and his colleagues used a logistic procedure to develop probabilistic CRR curves. The original Seed and Idriss magnitude scaling factors, however, were used to correct for magnitude. Youd and Noble (herein) use the logistic procedure to analyze liquefaction resistance with a magnitude added as an independent variable. New case history data and $(N_1)_{60cs}$ (corrected for fines content) were added to enlarge the case history data set. Primary conclusions from the study are:

- The probabilistic procedure allows direct incorporation of an appropriate probability, or risk factor in liquefaction hazard analyses. The procedure also provides a more scientifically rigorous method of analysis of the data than the hand-shaped curves used in the simplified procedure.

- The analyses by Liao and his colleagues indicate, for clean sands, that the standard criteria from the simplified procedure provide a probability of occurrence of about 20% for corrected blow counts $(N_1)_{60}$ between 11 and 28. Below an $(N_1)_{60}$ of 11, the original simplified base curve is characterized by a probability of liquefaction smaller than 20%. Above an $(N_1)_{60}$ of 28, the curves of Liao et al. indicate a probability of liquefaction greater than 20%. The curves in the upper par of the range, however, are near the limit of liquefaction occurrences and are not well constrained by empirical data.

- The analyses by Youd and Noble include magnitude as an independent variable eliminating the need for magnitude scaling factors in the analysis. The Youd and Nobel results are more conservative than those of Liao et al. for $(N_1)_{60cs}$ less than 20 and characterize the simplified base curve by probabilities ranging from 20% to 50%.

Introduction

Liao et al. (1988) reviewed several studies involving statistical or probabilistic analyses of cyclic stress ratio, standard penetration resistance, and field performance data that have been reported in the geotechnical literature. Although useful for estimating probable error in evaluating liquefaction resistance at field sites, these methods do not provide adequate quantification of conditional probability for use in risk-type analyses. To provide a more quantitative and direct model for risk-type analyses, Liao et al. used a logistic function along with statistical regression to quantify the probability of liquefaction as a function of cyclic resistance ratio (CRR) and $(N_1)_{60}$.

As part of their study, Liao et al. reevaluated all known liquefaction case-history data as of 1988, using data contained in several catalogues, including the 125 case histories compiled by Seed et al. (1985). Because many case study sites are characterized by incomplete or uncertain information, Liao et al. disregarded some site data. They finally selected 278 sites that they classified as "reliable" case studies that could be used for statistical regression analyses. Even so, the data from many of these sites were imperfect, requiring engineering judgment in selecting some property values. In their reanalysis of borehole data, Liao et al. generally used the minimal standard-penetration blow-count measured in granular layers as the critical blow count for their analyses.

Loertscher and Youd (1994) and Youd and Noble (this paper) extended the analyses of Liao et al. to include magnitude as an additional independent variable and added several new case histories to the data set. The work of Youd and Noble was specifically conducted for this workshop to evaluate the use of probabilistic and statistical procedures both directly for evaluation of liquefaction resistance (this paper), and as a method for evaluating magnitude scaling factors for use with the simplified procedure (Magnitude Scaling Factors, this report). The analyses and results reported herein were developed after the formal workshop event, and hence were not discussed or approved during the workshop discussions.

Logistic Analysis by Liao and His Colleagues

Clean Sands

Liao et al. (1988) conducted statistical regression analyses using data from sites underlain by clean sands (fines content equal to or less than 12%) and sites underlain by silty sands (fines content greater than 12%). Probabilistic regression curves from the analysis on clean sand sites are reproduced in Figure 1. The regression equation for these curves, which could be applied directly in practice, follows:

$$Q_L = 16.477 + 6.4603\ln(CSRN) - 0.39760(N_1)_{60} \quad (1)$$

where $Q_L = \text{logit}(P_L) = \ln[(P_L/(1-P_L)]$. P_L is defined as the probability that liquefaction will occur, $1-P_L$ is the probability that liquefaction will not occur, and CSRN is the cyclic stress ratio generated at the site normalized to a magnitude of 7.5. The magnitude scaling factors published by Seed and

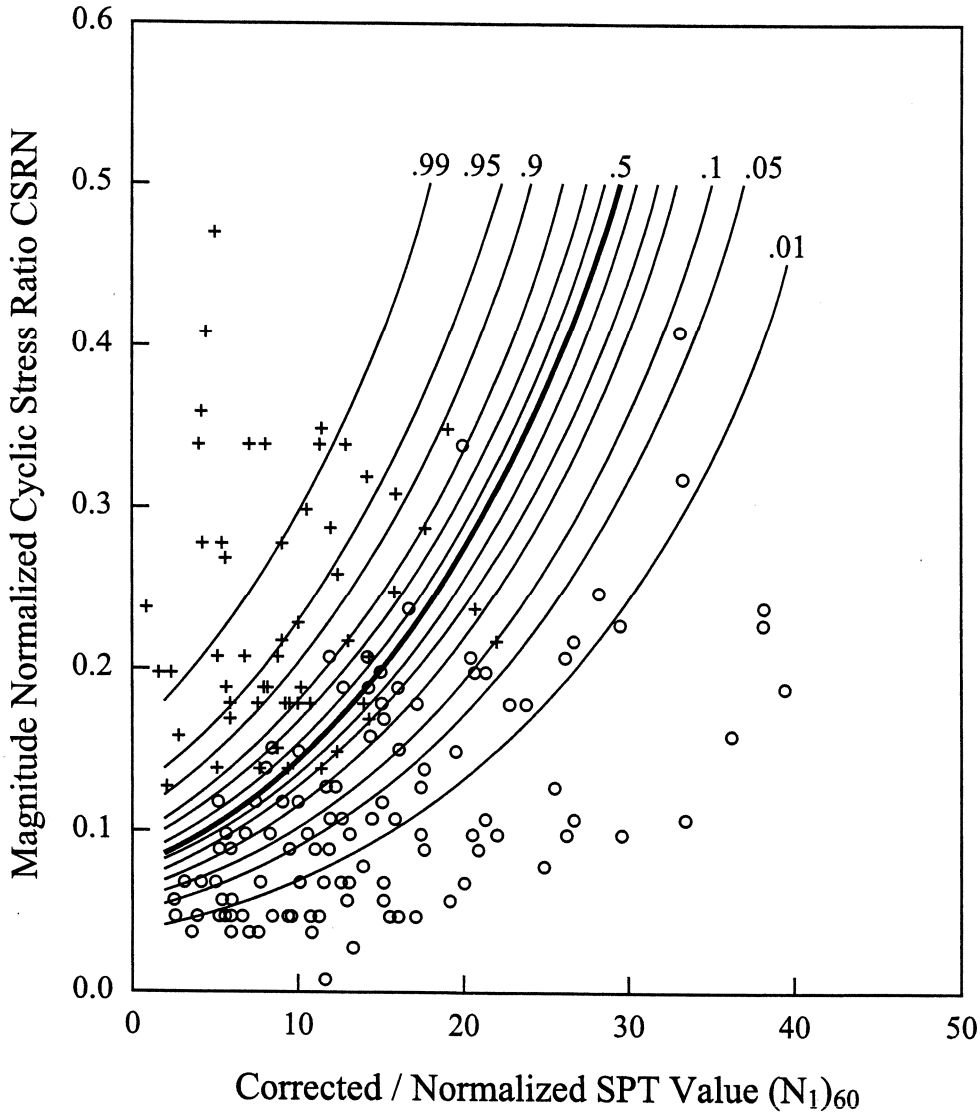

Figure 1 Contours of Equal Probability of Liquefaction, P_L, for Clean Sand (Fines Content Less than 12%); Plus Symbols Indicate Data from Sites where Liquefaction Occurred; Circles Indicate Data where Surface Evidence of Liquefaction Did Not Occur (modified from Liao, 1996)

Idriss (1982), which have been conventionally used in liquefaction hazard analyses, were applied by Liao et al. to normalize CSR to CSRN. P_L can be explicitly calculated as

$$P_L = 1/[1 + \exp(-Q_L)] \quad (2)$$

The primary advantage of Equation 1 for engineering applications is that the user can select an appropriate probability of exceedance or risk of occurrence for analyzing liquefaction hazard. For example, for noncritical sites, a probability of liquefaction of 20% to 30% might be appropriate.

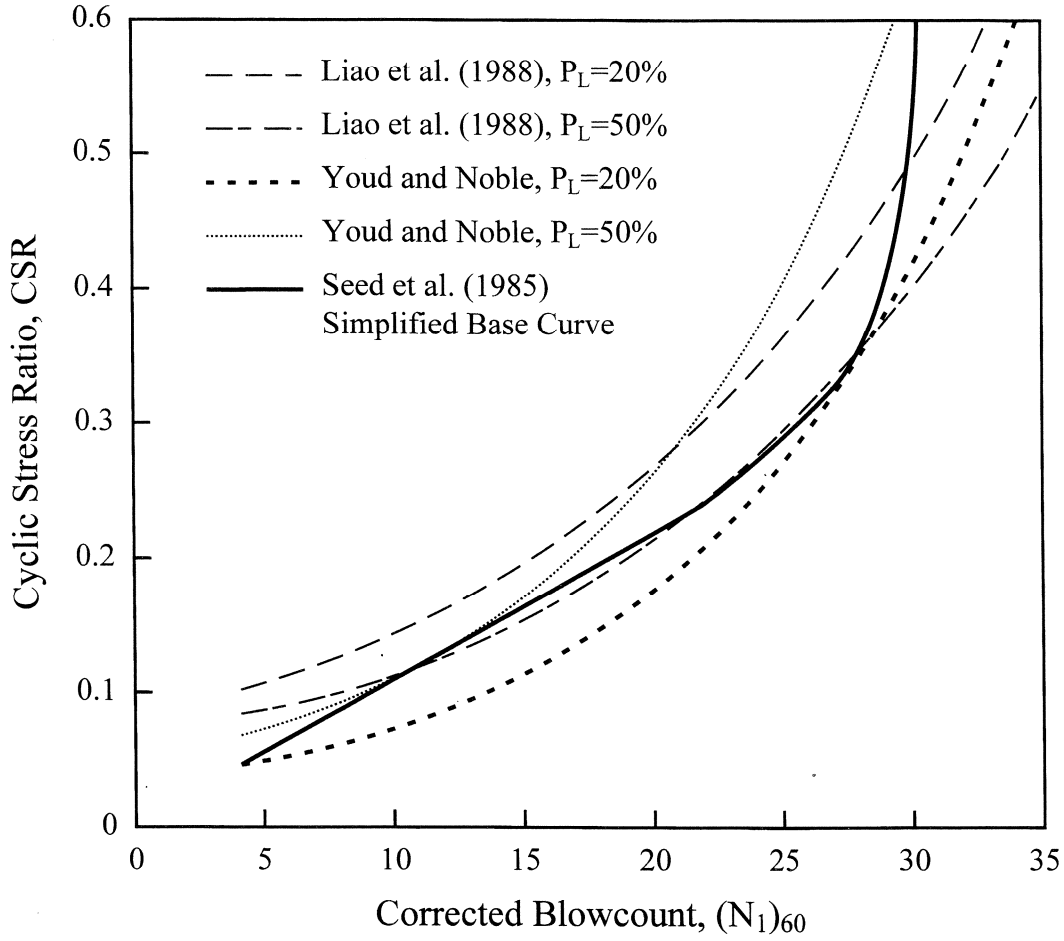

Figure 2 Comparison of Probabilistic Results from Equation 1 (Liao et al., 1988), Equation 6, and the Simplified Base Curve

If more conservative criteria are being applied in other aspects of the seismic analysis, such as earthquake selection, a probability on the order of 5% to 10% might be appropriate.

Because the cyclic resistance ratio versus $(N_1)_{60}$ curves developed by Seed et al. (1985) for the simplified procedure were conservatively drawn by hand, the probability of liquefaction was not determined, nor was the probability of occurrence constant across the trajectory of the curves. Figure 2 shows clean sand curves developed by Liao et al. (1988) for magnitude 7.5 earthquakes along with the base curve for clean sands from the simplified procedure, hereafter called the simplified base curve. (Probabilistic curves from Youd and Noble are also included on this diagram.) Between corrected blow counts, $(N_1)_{60}$, of 11 and 28, the simplified base curve lies near the 20% probability curve of Liao et al. Below an $(N_1)_{60}$ of 11, the original simplified base curve becomes very conservative compared to the curves of Liao et al. The primary reason for this divergence is that Seed et al. (1985) projected their curve through the origin of the plot, whereas Liao et al. let the regression analysis shape the trajectories of the probabilistic curves. As a consequence, the trajectories of probabilistic curves flatten to meet the $(N_1)_{60} = 0$ ordinate at cyclic stress ratios of

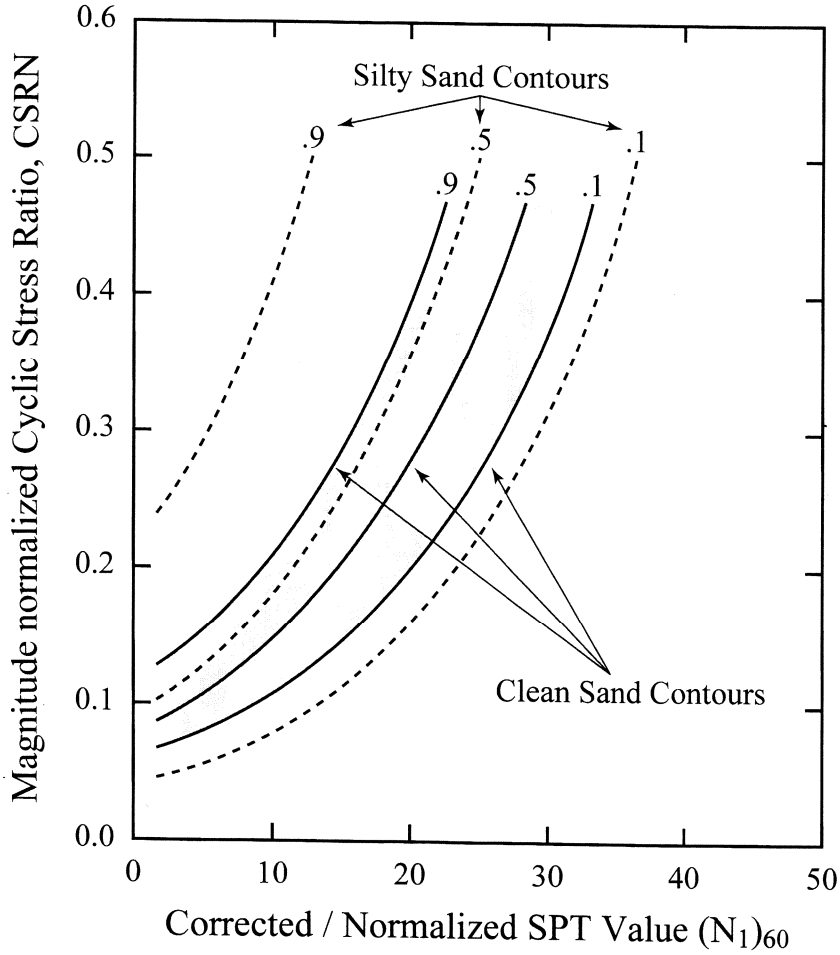

Figure 3 Comparison of Probabilistic CRR Curves from Clean and Silty Sands (modified from Liao, 1996)

0.055 and 0.078, respectively. Above an $(N_1)_{60}$ of 28, the curves diverge with the simplified base curve rising steeply to become asymptotic with the $(N_1)_{60}$=30 ordinate, while the 20% probability curve continues to curve gently upward. There is very little case history data to constrain the curves in either the lower or upper regions where they diverge.

Silty Sands

The analysis of silty sands (fines contents greater than 12%) by Liao et al. are plotted on Figure 3 along with the previously reported curves for clean sands. In this instance, the 50% curve lies significantly to the left of the equivalent clean sand curve, indicating that silty sands are generally more resistant to liquefaction than clean sands based on $(N_1)_{60}$ criteria. The curves for silty sand are reproduced on Figure 4 along with CRR curves for various fines contents developed by Seed et al. (1985). The 50% probability curve for silty sands from Liao et al. lies between the 15% and 35% fines content curves of Seed et al. Thus the mean or 50% curve from Liao et al. is in reasonable agreement with the higher fines content curves of Seed et al.

The width of the band of probabilistic curves between 10% and 90% probability, however, is very wide for silty sands. These curves extend well beyond the equivalent clean sand curves on either side of the plot (Figure 3). The latter relationship indicates that at the 10% probability level, greater $(N_1)_{60}$ is required to prevent silty sands from liquefying than is required for clean sands. This relation is opposite to the relationship suggested by Seed et al. and the relationship at the 50% probability level.

The wide range of the probabilistic curves for silty sands is largely a consequence of the large amount of scatter in the observational data. Possible contributors to this scatter include imprecisions in reported fines contents and the possible influence of soil plasticity. Fines contents at many investigated sites may be too variable within soil layers to be easily or adequately characterized by a single number. The plasticity of the fines may also have a significant influence on liquefaction resistance that is not accounted for in the present criterion. The scatter may also indicate large variances in the liquefaction behavior of silty sands and sandy silts. In any event, the uncertainty, as demonstrated by the curves for silty sands in Figure 3, is so large that the use of the probabilistic

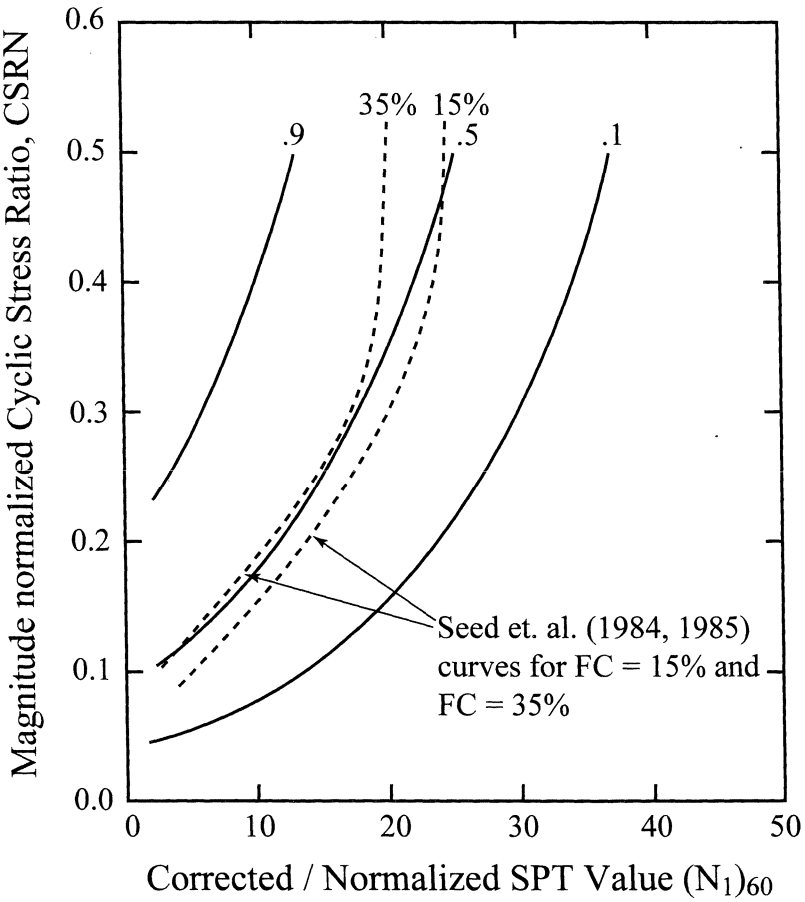

Figure 4 Comparison of Probabilistic CRR Curves for Silty Sands (Fines Contents Greater Than 12%) with Deterministic CRR Curves from Seed et al., (1985) for Sands with Fines Contents of 15% and 35% (modified from Liao, 1996)

curves is questionable for silty materials, at least at low- or high-probability levels. This scatter also raises doubts concerning the reliability of simple correction factors for fines content as presently applied in evaluations of liquefaction resistance of silty soils.

Applications

Following the workshop, S.S.C. Liao submitted the following information: There have been many applications where a probabilistic evaluation of liquefaction has been incorporated as part of a risk analysis framework. Projects include tailings and earth dams (Vick, 1994) and regional hazard studies (Budhu et al., 1987; Hashash, 1987). In these studies, liquefaction probability was based on the logistic regression equations derived by Liao et al. (1988). Ostadan et al. (1991) incorporated the equations of Liao et al. (1988) into a computer program combined with earthquake hazard models, which were used in risk analyses for a nuclear material storage facility (Arango et al., 1996). Similarly, the Liao et al. (1988) model formed the basis of the liquefaction probability calculations (RMS, 1997) in a project to develop a standardized earthquake loss estimation methodology embodied in computer program HAZUS. This program was funded by the Federal Emergency Management Agency (FEMA) and managed by the National Institute of Building Sciences (NIBS). This program has been used in earthquake economic loss studies for Portland, Oregon (Dames and Moore, 1996) and Boston, Massachusetts (EQE/PB, 1997). In general, however, application of probabilistic analysis is beyond the normal practice of most geotechnical engineers. Hence the workshop participants did not approve recommendations for engineering practice, but did encourage continued development of these concepts.

Probabilistic Analyses by Loertscher and Youd and by Youd and Noble

Loertscher and Youd (1994) extended the analyses of Liao et al. to include earthquake magnitude as an independent variable and added new case histories to the data base from earthquakes with magnitudes less than 7. Most of the data analyzed by Loertscher and Youd were taken from previous compilations of case history data, including Seed et al. (1985), Liao (1986), Ambraseys (1988), and Bartlett and Youd (1992). Loertscher and Youd added new case histories from the Marina District of San Francisco, where abundant liquefaction effects developed in response to the 1989 Loma Prieta earthquake ($M_w = 6.8$), but where liquefaction effects were not reported following the 1957 Daly City earthquake ($M_w = 5.3$). The Loma Prieta event generated peak accelerations estimated at about 0.15 g to 0.25 g in the Marina District (Bardet et al., 1992). Peak accelerations during the Daly City event were estimated at about 0.20 g (Loertscher and Youd, 1994). Data were also added from sites where liquefaction effects were observed or were not observed after several Imperial Valley, California earthquakes: 1979 Imperial Valley ($M_w = 6.6$), 1981 Westmorland ($M_w = 6.0$), 1987 Elmore Ranch ($M_w = 6.2$), and 1987 Superstition Hills ($M_w = 6.6$). New data were also added from several sites underlain by saturated granular materials that were strongly shaken by the 1987 Whittier Narrows event ($M_w = 5.9$), but liquefaction effects were not reported.

Loertscher and Youd (1994) analyzed the compiled data set using a logistic regression analysis similar to that used by Liao et al. (1988). The analyses, however, yielded unexpected differences

with results published by Liao et al. (1988) and also conflicted with results embodied in the simplified procedure. Youd and Noble (herein) corrected some inconsistencies in the Loertscher and Youd data set, and reanalyzed the data to verify the results of Loertscher and Youd. They also expanded the analysis to more fully consider issues such as the form of the probabilistic equation.

Following the procedures of Liao et al., Youd and Noble (herein) analyzed data from sands with fines content less than 12%. Unfortunately, there were insufficient data in that set to constrain the analysis. To increase the amount of data, sands with fines contents up to 35% were used by correcting $(N_1)_{60}$ for fines content. Corrections were made by increasing $(N_1)_{60}$ to an equivalent clean-sand corrected blow count, $(N_1)_{60cs}$, using the fines content correction factor recommended by Idriss and Seed as noted in the Summary Report (this report).

$$(N_1)_{60cs} = \alpha + \beta(N_1)_{60} \tag{3}$$

where α and β are coefficients determined from the following equations:

$$\alpha = 0 \quad \text{for FC} \leq 5\% \tag{4a}$$
$$\alpha = \exp[1.76 - (190/FC^2)] \quad \text{for } 5\% < \text{FC} < 35\% \tag{4b}$$
$$\alpha = 5.0 \quad \text{for FC} \geq 35\% \tag{4c}$$

$$\beta = 1.0 \quad \text{for FC} \leq 5\% \tag{5a}$$
$$\beta = [0.99 + (FC^{1.5}/1000)] \quad \text{for } 5\% < \text{FC} < 35\% \tag{5b}$$
$$\beta = 1.2 \quad \text{for FC} \geq 35\% \tag{5c}$$

where FC is fines content measured from laboratory gradation tests on retrieved soil samples. The final data set is available at http://www.et.byu.edu/~cewww/faculty/youd/papers/liqdata.xls.

The addition of the fines-content corrected penetration resistances, $(N_1)_{60cs}$, provided sufficient data to adequately constrain the analyses for magnitudes between 5.75 and 7.75 to yield meaningful results. At lower magnitudes, between 5.25 and 5.75, constraint is provided by approximately 25 sites where effects of liquefaction were not observed, but only one site where effects were observed. Case history data are not available for magnitudes smaller than 5.25, which is approximately the threshold magnitude for generation of liquefaction.

The results of the Youd and Noble reanalysis are incorporated in the following equation, which is similar in form to the equation developed by Liao et al. (Equation 1), except that magnitude, M_w, is added as an independent variable.

$$Q_L = \text{Logit}(P_L) = \ln[P_L/(1-P_L)] = -7.633 + 2.256\, M_w - 0.258\, (N_1)_{60cs} + 3.095 \ln \text{CRR} \tag{6}$$

$(N_1)_{60cs}$ is the corrected blow count, including a correction for fines content. Equation 6 can be rewritten for calculation of CRR as follows:

Table 1 Case History Data from Liquefied Sites Predicted as Nonliquefiable by the Simplified Base Curve for Magnitude 7.5 Earthquakes

Year	Locality/Site or Hole No.	Data Set	M_w	Depth (m)	Fines Content	$(N_1)_{60}$	$(N_1)_{60cs}$	CSR
1964	Niigata/G10-22	B-Y[1]	7.5	4	12	13.5	15.1	0.165
1964	Niigata/H10-45	B-Y[1]	7.5	3	8	12.6	13.3	0.140
1976	Tangshan/Luan Nan	Seed[2]	7.6	5.4	3	22.2	22.2	0.169
1976	Tangshan/Coastal Region	Seed[2]	7.6	3	10	11.4	12.5	0.124
1978	Miyagiken-Oki/Yurlag Br. 2	Seed[2]	7.7	3.3	7	22.5	22.9	0.229

[1]Data from Bartlett and Youd (1992) compilation of case histories
[2]Data from Seed et al. (1984) compilation of case histories

$$\ln CRR = 2.466 - 0.7289M_w + 0.0834(N_1)_{60cs} + 0.3231 \ln[P_L/(1-P_L)] \quad (7)$$

This form is useful for routine engineering calculations of liquefaction resistance where M_w, $(N_1)_{60cs}$, and P_L are determined from seismic, site, and risk evaluations, respectively. Curves derived from Equation 6 for magnitude 7.5 earthquakes are plotted on Figure 5. In this instance, the abscissa for the plot is the fines-content corrected blow count, $(N_1)_{60cs}$, rather than $(N_1)_{60}$. Case history data, in terms of CSR and $(N_1)_{60cs}$, for earthquakes with magnitudes between 7.25 and 7.75 are also shown on the plot. The simplified base curve is plotted on Figure 5 for reference.

Unexpected results from this analysis are that the probabilistic curves of Youd and Noble generally plot much lower on the diagram than those of Liao et al. for clean sands and $(N_1)_{60cs}$ less than 25 (Figure 2), and that the simplified base curve is enveloped between the 20% and 50% probability curves for $(N_1)_{60}$ between 4 and 25 (Figure 5). The latter result indicates that the simplified base curve may be characterized by higher probabilities of liquefaction than previously thought for $(N_1)_{60cs}$ between 5 and 25. The argument that the simplified base curve is characterized by probabilities of liquefaction between 20% and 50% in this $(N_1)_{60cs}$ range is supported by several data points indicative of liquefaction that are misclassified by the simplified base curve. Information on the misclassified data are listed in Table 1. Three of these data are from case histories compiled by Seed et al. (1984) but are characterized by fines contents greater than 5%, and hence were not plotted on diagrams such as Figure 1. These data most likely had strong influence on the results of the logistic analyses as well as similar data from other magnitude ranges in the data base. As noted, the implication of this result is that the simplified curve may not be as conservative as previously thought and perhaps not as conservative as generally desired for engineering practice.

Probabilistic CRR curves derived from Equation 6 are also plotted on Figure 2 for comparison with the clean-sand curves of Liao et al. The curves of Youd and Noble have the same general shape, but

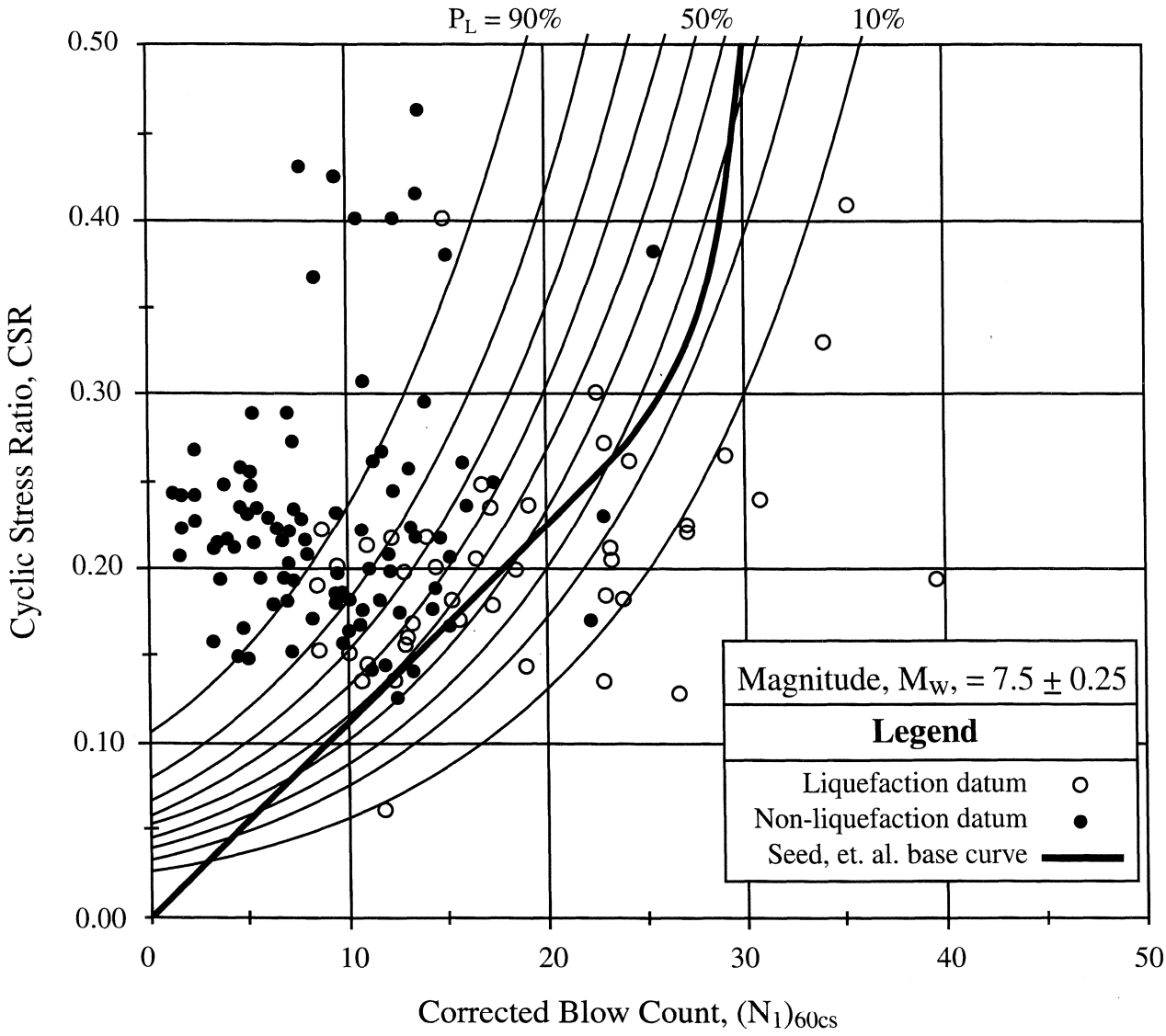

Figure 5 Probabilistic CRR Curves Derived from Equation 6 with Simplified Base Curve and History Data Plotted for Reference

are generally steeper in aspect and intersect the origin [$(N_1)_{60}$=0 ordinate] at lower CSR than those of Liao et al. For $(N_1)_{60}$ less than 20 and 27, respectively, the 50% and 20% curves of Youd and Noble lie below and are more conservative than the equivalent curves of Liao et al. Conversely, above blow counts of 20 and 27, respectively, the curves of Youd and Noble lie above, are less conservative, and are much steeper in aspect than the equivalent curves of Liao et al. Also, the spread between the 20% and 50% curves of Youd and Noble is greater across the plot than those of Liao et al. The increased spread may be due in part to the wider range of fines contents incorporated in the Youd and Noble data set. Other factors that could have caused differences between results of the two probabilistic investigations include the additional case history data used by Youd and Noble

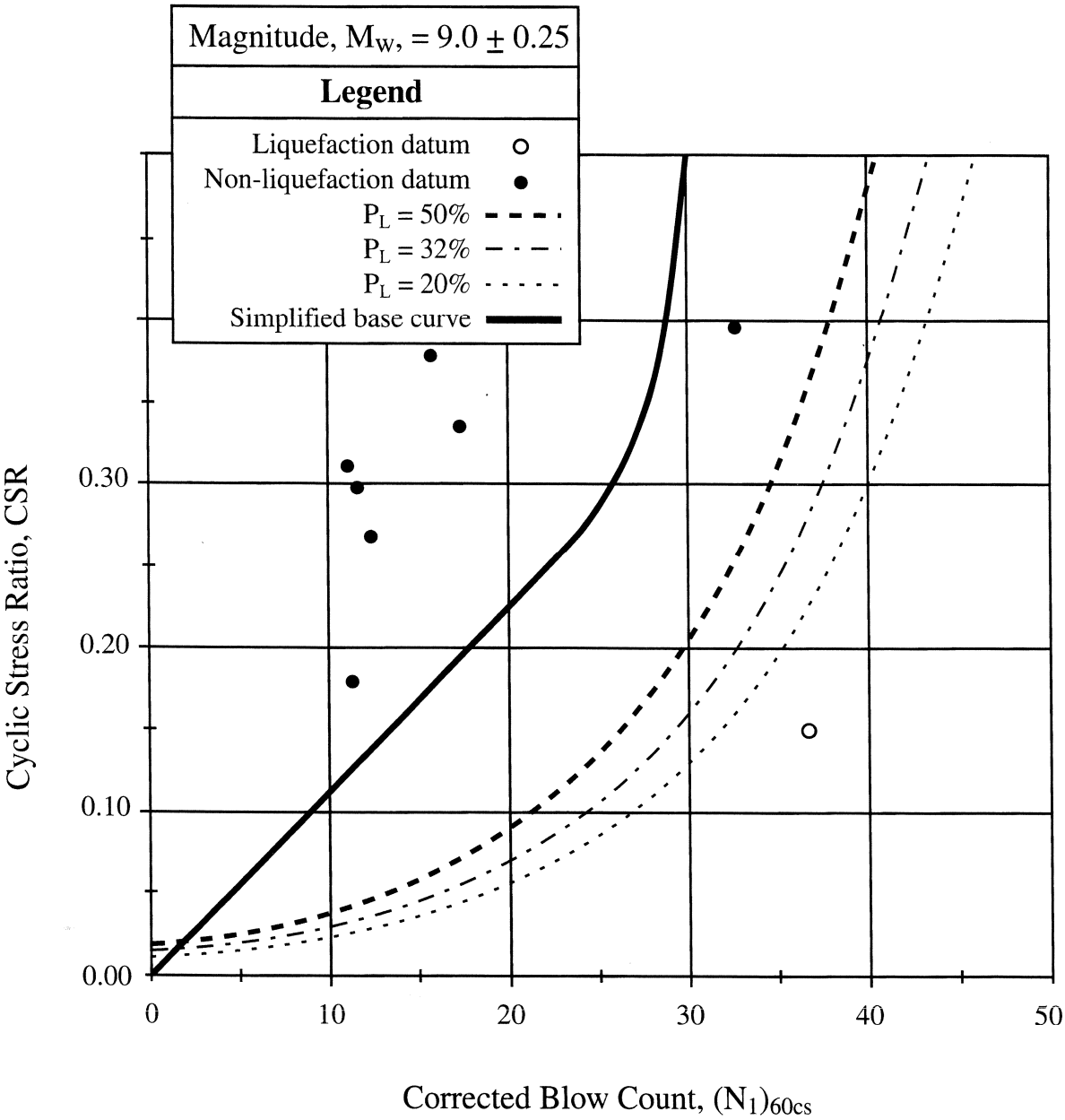

Figure 6 Probabilistic CRR Curves Developed from Equation 6 for M_w = 9.0 with Empirical Data from the 1964 Great Alaska Earthquake (M_w = 9.2)

and the incorporation of magnitude as an independent variable. Youd and Noble incorporated 369 data points into their analysis compared to 278 points by Liao et al. Most of the additional points are from earthquakes with magnitudes less than 7.

The lack of agreement with the results of Liao et al. and the indication that the simplified base curve is characterized by probabilities of liquefaction as great as 50% was the primary reason for the reanalysis of the Loertscher and Youd data by Youd and Noble (herein). In the reanalysis, the form

of the logit equation was simplified (cross terms removed) and a few errors in the data set were corrected. The results of the reanalysis, however, are in rather close agreement with results of Loertscher and Youd (1994). That is, for a given P_L, M_w, and $(N_1)_{60}$, CRR calculated from Equations 5 or 6 are consistently larger than those estimated by Loertscher and Youd, but by no more than a few percent for P_L between 20% and 80%, $(N_1)_{60cs}$ less than 30, and M_w between 5.5 and 7.5. Based on this reevaluation, Youd and Noble conclude that Equation 6 is a correct probabilistic assessment of the case history data set, assuming the forms of Equations 1 and 6 are properly formulated.

Equation 6 is sufficiently constrained by data to be valid for assessing liquefaction resistance (CRR) for magnitudes between 5.75 and 7.75 and CRR less than 0.4. Extrapolation to magnitudes less than 5.75 is justified by case history data from sites that did not liquefy and from the fact that the threshold magnitude for generation of liquefaction is about magnitude 5.

Insufficient case history data are available to adequately constrain the probabilistic regression analysis for magnitudes greater than 7.75. For example, Figure 6 shows probabilistic curves for magnitude 9 earthquakes along with empirical data for earthquakes with magnitudes between 8.75 and 9.25. The empirical data for this magnitude range is sparse, with data from only a few sites where liquefaction effects were observed following the 1964 great Alaska earthquake (M_w = 9.2). The data are even more sparse for magnitudes between 8.25 to 8.75 where no case histories are included in present data bases. The observational data for magnitude 7.75 to 8.25 earthquakes are also rather weak with data coming primarily from three pre-1925 earthquakes: the 1991 Mino-Owari, Japan (M = 7.8), 1906 San Francisco, California (M_w = 7.9), and 1923 Kwanto, Japan (M_w = 7.9).

The probabilistic curves shown on Figure 5 appear overly conservative with respect to the limited data plotted on the figure. Similarly conservative results are estimated for all magnitudes greater than 8. Because the probabilistic estimates are not adequately constrained by empirical data at these higher magnitudes, Equation 6 should not be used for magnitudes larger than 7.75. For magnitudes greater than 7.75, the workshop participants recommend use of the simplified procedure with the magnitude scaling factors (MSF) proposed by Idriss (Summary Report, this report).

Based on the above arguments, Youd and Noble (herein) recommend that Equations 6 and 7 with P_L of 20% to 30% should be used for evaluation of liquefaction resistance for earthquakes with magnitudes less than 7.75. This conservatism yields P_L with less than mean minus one standard deviation (32%) probabilities that liquefaction will occur. That level of conservatism is generally acceptable in engineering practice for noncritical structures.

Conclusions

The probabilistic analyses reviewed and conducted herein lead to the following conclusions:

1. The probabilistic procedure allows direct incorporation of probability of liquefaction occurrence or acceptable risk into liquefaction hazard analyses. Thus the engineer is given the option of specifying a level of risk as part of the analysis of liquefaction hazard.

2. Liao et al. (1988) conducted probabilistic regression analyses for clean sands (fines contents less than or equal 12%) and silty sands (fines contents greater than 12%). These investigators normalized cyclic stress ratios to magnitude 7.5 earthquakes by multiplying calculated cyclic stress ratios by magnitude scaling factor (MSF) published by Seed and Idriss (1982). Equation 1 embodies the results of Liao et al. for clean sands. This equation allows calculation of probability of liquefaction occurrence, P_L, for given input values of $(N_1)_{60}$ and magnitude, assuming the Seed and Idriss (1982) MSF. The Liao et al. analysis indicates that the simplified base curve for clean sands is characterized by a probability of liquefaction about 20% for $(N_1)_{60}$ between 12 and 28.

3. The 50% probability curve for silty sands determined by Liao et al. lies to the left of the 50% probability curve for clean sands, indicating that on average, silty sands are more resistant to liquefaction than clean sands based on $(N_1)_{60}$ criteria. This result is consistent with fines content criteria incorporated into the simplified procedure. The band for probabilities between 10% and 90% is very wide, however, for silty sands, indicating considerable scatter in the data. This width is so large that use of the probabilistic curves for silty sands is questionable, at least at low- and high-probability levels.

4. Youd and Noble (herein) used the probabilistic regression technique of Liao et al., but with magnitude, M_w, added as an independent variable. They also used an enlarged case history data set in order to provide sufficient data to constrain the analysis. Sands with fines contents as high as 35% were used by correcting $(N_1)_{60}$ for fines content. Equation 6 is the primary result from the latter analysis. CRR predicted from Equation 6, however, vary from those of Liao et al. (Equation 1) in several key respects. The curves by Liao et al. have the same general shape as those by Youd and Noble but are flatter in aspect and intersect the origin at a higher CRR. Also, the spread between the 20% and 50% curves of Youd and Noble is greater.

5. The Youd and Noble analyses indicate that the simplified base curve for magnitude 7.5 earthquakes is characterized by probabilities ranging from 20% to 50% for $(N_1)_{60}$ ranging between 5 and 25. This result indicates that the simplified base curve may not be as conservative as previously thought, and might not be sufficiently conservative for many engineering applications. Youd and Noble recommend use of Equations 6, with P_L of 20% to 30%, for general engineering practice for earthquakes with magnitudes less than 7.75. The case history data are insufficient to constrain the probabilistic regression procedure for magnitudes greater than 7.75.

6. Probabilistic procedures provide more statistically rigorous criteria for defining liquefaction resistance than was used in the original development of the simplified procedure. As with all empirical methods, however, the quality of the results are strongly dependent on the quantity and quality of the compiled input data. Between magnitudes of 5.75 and 7.75, and up to cyclic resistance ratios of 0.4, the probabilistic curves appear to be well constrained. Extrapolation beyond these limits leads to uncertain and perhaps erroneous results.

References

Ambraseys, N.N., 1988, "Engineering Seismology," *Earthquake Engineering and Structural Dynamics*, Vol. 17, p. 1-105.

Arango I., Ostadan, F., Lewis, M.R., and Gutierrez, 1996, "Quantification of Seismic Liquefaction Risk", *Proceedings, ASME Pressure Vessel and Piping Conference*, Montreal, Canada, 1996.

Bardet, J.P., Kapuskar, M., Martin, G.R., and Proubet, J., 1992, "Site Response Analysis," The Loma Prieta, California, Earthquake of October 17, 1989--Marina District (T.D. O'Rourke, ed.): U.S. Geological Survey *Professional Paper* 1551-F, p. 84-140.

Bartlett, S.F., and Youd, T.L., 1992, *Empirical Analysis of Horizontal Ground Displacement Generated by Liquefaction-Induced Lateral Spread*, National Center for Earthquake Engineering Research, Technical Report NCEER-92-0021.

Budhu, M. Vijayakumar, V. Giese, R. F., Baumgras, L., 1987, *Liquefaction Potential For New York State: A Preliminary Report on Sites in Manhattan and Buffalo*, Technical Report NCEER-87-0009, August 1987), National Center for Earthquake Engineering Research (NCEER), State University of New York, Buffalo, NY.

Dames and Moore, 1996, *Summary Results, Earthquake Loss Estimation Pilot Study for the Portland Metropolitan Region*, Report prepared by Dames & Moore, Inc. (D&M), for the National Institute of Building Sciences, under the sponsorship of the Federal Emergency Management Agency, December 1996.

EQE/PB, 1997, *Summary Results, Earthquake Loss Estimation Pilot Study for the City of Boston*, Report prepared by EQE International, Inc. and Parsons Brinckerhoff (PB), for the National Institute of Building Sciences, *for* Federal Emergency Management Agency, in press.

Hashash, Y.M.A., 1987, "Liquefaction Probability Mapping in Greater Boston" unpublished M.S. Thesis, Department of Civil Engineering, Massachusetts Institute of Technology Cambridge, Massachusetts, 1987.

Liao, S.S.C., 1986, Statistical Modeling in Earthquake-Induced Liquefaction, unpublished PhD Dissertation, Massachusetts Institute of Technology, Cambridge, Massachusetts.

Liao, S.S.C., 1996, Discussion of "Reconsideration of Initiation of Liquefaction in Sandy Soils" by C.E. Fear and E.C. McRoberts, *Journal of Geotechnical Engineering*, Vol. 122, No. 11, p. 957-959.

Liao, S.S.C., Veneziano, D., and Whitman, R.V., 1988, "Regression Models for Evaluating Liquefaction Probability," *Journal of Geotechnical Engineering*, Vol. 114, No. 4, p. 389-411.

Loertscher, T.W., and Youd, T.L., 1994, Magnitude Scaling Factors for Analysis of Liquefaction Hazard, unpublished Research Report No. CEG.94-02, Department of Civil and Environmental Engineering, Brigham Young University, Provo, Utah.

Ostadan, F., Marrone, J., Liteheiser, J.J., Arango, I., 1991, "Liquefaction Hazard Evaluation: Methodology and Application," *Proceedings, Third U.S. Conference on Lifeline Earthquake Engineering*, Los Angeles, CA, ASCE, pp. 591-600.

RMS, 1996, *Development of a Standardized Earthquake Loss Estimation Methodology, Draft Technical Manual*, Prepared for National Institute of Building Sciences, under the sponsorship of Federal Emergency Management Agency, 1996.

Seed, H.B., and Idriss, I.M., 1982, *Ground Motions and Soil Liquefaction During Earthquakes*, Earthquake Engineering Research Institute Monograph.

Seed, H.B., Tokimatsu, K, Harder, L.F., and Chung, R.F., 1984, "*The Influence of SPT Procedures in Soil Liquefaction Resistance Evaluations*," Report No. UBC/EERC-84/15, Earthquake Engineering Research Center, University of California, Berkeley, California.

Seed, H.B., Tokimatsu, K., Harder, L.F., and Chung, R.M., 1985, "The Influence of SPT Procedures in Soil Liquefaction Resistance Evaluations," *Journal of Geotechnical Engineering*, ASCE, Vol. 111, No. 12, p. 1425-45.

Vick, S.G., 1995, "Geotechnical Risk and Reliability--From Theory To Practice in Dam Safety," *Proceedings, The Earth, Engineers, and Education--A Symposium in Honor of Robert V. Whitman*, October 7 and 8, 1994, Dept. Of Civil Engineering, Massachusetts Institute of Technology, Cambridge, Massachusetts, pp. 45-58.

Liquefaction Criteria Based on Energy Content of Seismograms

T. Leslie Youd
Professor of Civil Engineering
Brigham Young University
Provo, Utah 84602-4081

Robert E. Kayen
Research Civil Engineer
U.S. Geological Survey
Menlo Park, California 94025

James K. Mitchell
University Distinguished Professor
Virginia Tech
Blacksburg, Virginia 24061-0105

Abstract

Because energy is a more fundamental property or measure of earthquake excitation than peak acceleration and magnitude, several investigators have suggested that the amount of energy generated at specific points in a soil layer in response to earthquake shaking may correlate better with the development of liquefaction than with cyclic stress ratio. Kayen (1993) reviewed the literature on this topic and investigated the use of accelerogram energy, expressed in terms of Arias intensity, as a parameter for use in evaluating liquefaction resistance of soils. The use of Arias intensity as a measure of seismic excitation has the advantage of eliminating other seismic parameters from the analysis, including peak acceleration, magnitude, and a magnitude scaling factor. Although the workshop agreed that use of accelerogram energy presents an important new direction in analysis of liquefaction resistance, the procedure is not yet sufficiently verified to be recommended for use in engineering practice. The following questions need to be addressed: What procedures should be used, and how accurately can Arias intensity be estimated for application at field sites where strong motion records are not available? Has sufficient case history data and experience been compiled and analyzed to provide adequate verification of the procedure? The workshop encourages continued research to answer these questions and further develop energy procedures for use in engineering practice.

Introduction

Several investigators have proposed the use of energy content of accelerograms as a measure of the excitation or demand placed on a liquefiable soil by earthquake shaking (Davis and Berrill, 1978; Figueroa and Dahisaria, 1991). Use of energy input at specific points in a soil layer obviates the need for other seismic parameters, such as peak acceleration, earthquake magnitude, and magnitude scaling factors as presently used in the simplified procedure. These investigators claim that energy is a more fundamental measure of earthquake excitation and should correlate better with insitu generation of pore pressures than the presently used cyclic stress ratio. In a Ph.D. dissertation, Kayen (1993) reviews the literature on this topic and investigated the use of accelerogram energy, expressed in terms of Arias intensity, as a tool for evaluating liquefaction resistance of soils. The workshop participants briefly considered the use of energy content of accelerogram records in evaluating liquefaction resistance, but concurred that the present state of development and verification is insufficient to recommend the procedure for general use in engineering practice. Nevertheless, the workshop encourages further research and development of the procedure for possible future implementation.

The following text, largely summarized from Kayen's Ph.D. dissertation (Kayen, 1993), provided the basis for the workshop discussion. Kayen and Mitchell (1997) further summarize these analyses and propose procedures for engineering application.

Energy Approach

Rather than using cyclic stress ratio, Kayen (1993) correlated liquefaction resistance with Arias intensity as a measure of the energy content of accelerograms recorded at several localities where surface effects of liquefaction were or were not observed following major earthquakes. Arias intensity is defined as the total energy per unit weight absorbed by single-degree-of-freedom-undamped oscillators evenly spaced in frequency from 0 to ∞ when excited by a time history (accelerogram) of earthquake motions. The total horizontal Arias intensity is calculated from the following equation:

$$I_h = I_{xx} + I_{yy} = \frac{\pi}{2g}\int_0^t .a_x^2(t)\ dt + \frac{\pi}{2g}\int_0^t .a_y^2(t)\ dt \qquad (1)$$

where I_h is total two-component horizontal Arias intensity, I_{xx} and I_{yy} are horizontal components of Arias intensity in the x and y directions, respectively, $a_x(t)$ and $a_y(t)$ are acceleration time histories from strong motion accelerograms in the x and y directions, and g is the acceleration of gravity. The parameter I_h represents the sum of intensities contributed by the two horizontal components of motion. Because the time integral of the squares of the accelerations are normalized by the acceleration of gravity, the dimensional units of Arias intensity are length divided by time, or velocity (Kayen, 1993, p. 29). The general practice is to use the metric system of units to define Arias intensity, yielding intensities in units of meters-per-second. Intensity values should be calculated from corrected accelerograms by the trapezoidal integration method.

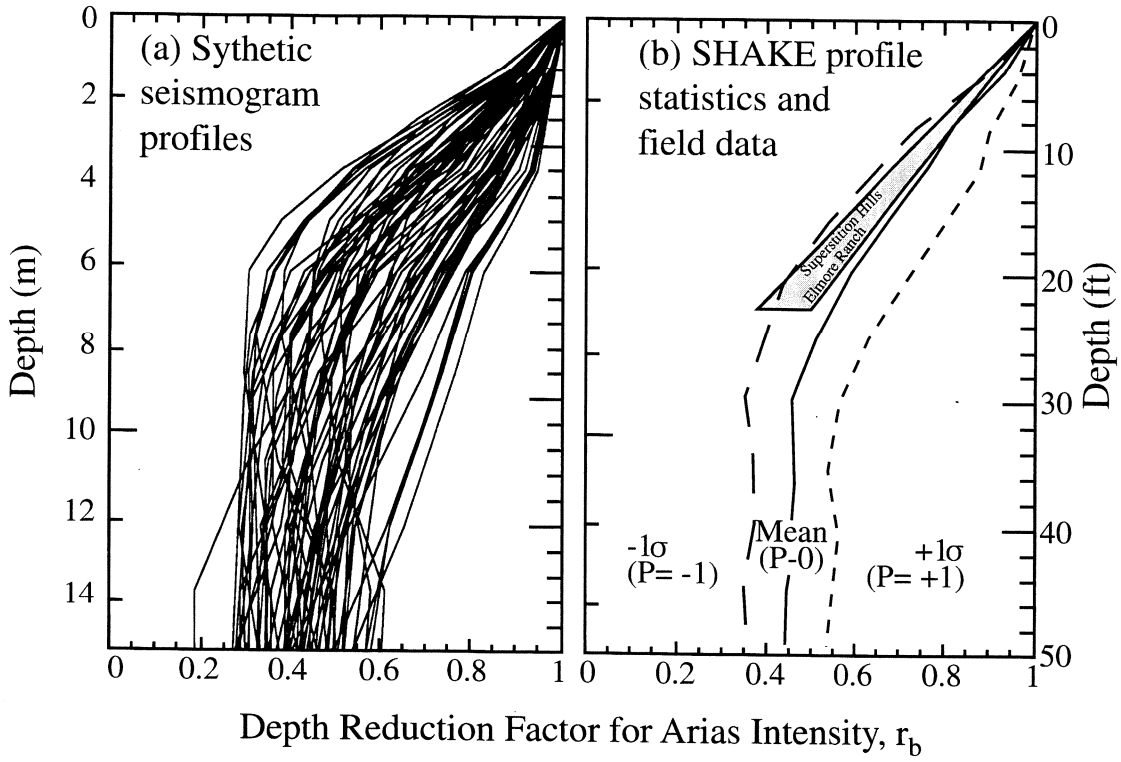

Figure 1 Normalized Arias Intensity versus Depth-Reduction Profiles Modeled Using SHAKE: (a) Profiles from Several Synthetic Seismograms; (b) Synthesis of Seismogram Profiles (modified from Kayen and Mitchell, 1997)

Kayen calculated Arias intensity values for a number of localities where strong motions were recorded and where surface effects of liquefaction were or were not reported. From these calculations, a data set was compiled that included Arias intensities, site soil profiles with measured penetration resistances, soil types, grain size properties, etc. To estimate the severity of earthquake motions within the soil column, a depth-reduction factor for Arias intensity, r_b, which is analogous to r_d, was developed with the ground response program SHAKE (Kayen and Mitchell, 1997). This analysis showed that r_b on average diminishes from 1.0 at ground surface to 0.58 at a depth of 6 m, and further diminishes to a value of 0.46 at depths of 10 m or below (Figure 1). The Arias intensity at depth in the soil column, I_{hb}, can be calculated as follows:

$$I_{hb} = I_h x r_b$$

From analyses of the compiled data set, Kayen and Mitchell (1997, p. 1169) reported the following:

> Based on these case studies of known field-behavior during earthquakes, a relation was developed between the measured liquefaction resistance of the soil and the Arias intensity characteristics of nearby strong motion recordings. The data included in this study are limited to sites where a direct measure or reasonably well-constrained estimate of the Arias intensity could be made. ... The resultant association finds excellent segregation of liquefaction and non-liquefaction points on a plot of the

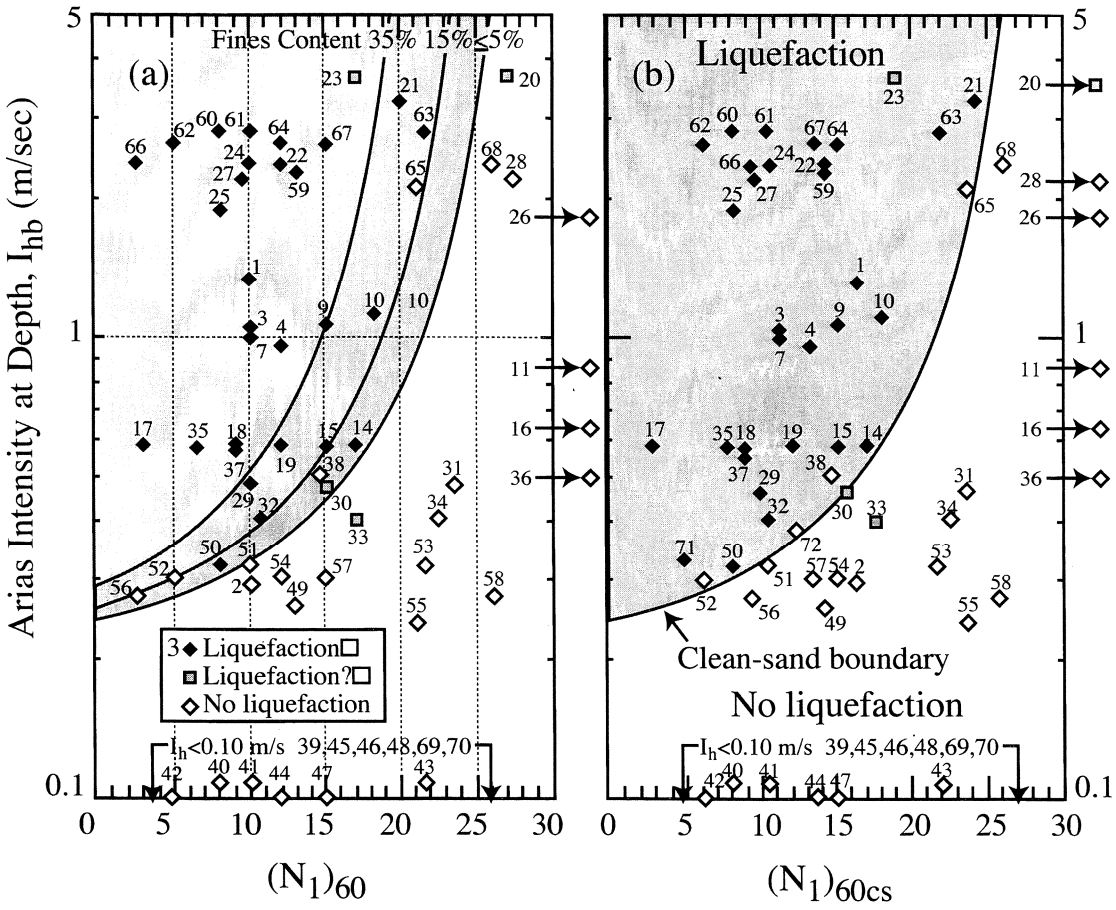

Figure 2 I_{hb} versus $(N_1)_{60}$ from Compiled Case Histories: (a) Plot Without Fines Content Correction; (b) Plot with Fines Content Correction (modified from Kayen and Mitchell, 1997)

estimated Arias intensity at depth (I_{hb}) versus values of $(N_1)_{60}$ [Figure 2a]. A boundary separating the liquefaction and non-liquefaction fields has an ordinate intercept $(N_1)_{60}$=0, of approximately I_h=0.22 meters/second. The lower-bound threshold indicates that a minimum Arias intensity is needed to trigger liquefaction even in extremely loose soil.

Kayen (1993, p.195) notes the following regarding the boundary curves presented in Figure 2:

> From the plot presented in Figure 2, it can be seen that the field penetration resistance used as a measure of soil resistance to liquefaction correlates with accelerogram energy in a similar way as it does with cyclic stress ratio. That is, the liquefaction boundary in I_{hb}-$(N_1)_{60}$ space has an upwardly concave curvature similar to that of the familiar CSR-$(N_1)_{60}$ and CSR-q_{c1} correlation. This curvature indicates that there is a limiting upper-bound penetration resistance above which liquefaction cannot occur, regardless of the strong motion input.

In Figure 2b, fines content correction factors for silty-sand were applied to the SPT data set following the guidelines given in the Summary Report (this report). Kayen and Mitchell (1997) report the following conclusions from this study:

> The correction factors for silty sands were used to convert the SPT data set ... to equivalent 'clean sand' SPT values. The clean-sand boundary curve presented in Figure 2b is a singular earthquake magnitude-independent boundary curve that delineates the threshold condition of initial liquefaction in I_{hb}-$(N_1)_{60}$ space. We found that the application of the (NCEER Workshop) fines-content correction factor above, segregates our data set almost entirely into distinct zones of liquefaction and non-liquefaction occurrence, such that the boundary clearly envelopes the liquefaction frontier.

The q_{c1} relation of Robertson and Campanella (1985) and CPT data collected during post-earthquake investigations of Loma Prieta liquefaction test sites allowed for the development of normalized-cone penetration resistance-Arias Intensity-space boundary curves as shown in Figure 3 (Kayen and Mitchell, 1997). To address the need for predictive models for Arias intensity at sites where strong motion records are not available, or for design-basis earthquakes, Kayen and Mitchell (1997) present equations describing surface-measured Arias intensity in terms of moment magnitude, M_w, and the Pythagorean source distance, r*, from the investigation site to the closest point to the fault rupture plane at the focal depth:

> ... earthquake motion and site characteristics data were tabulated for 66 earthquake records in the western United States, primarily from California (Kayen, 1993) and segregated the sites into three representative profiles--rock, alluvium, and soft soil--to regress the following relations between (average) two-component Arias intensity, moment magnitude, and source distance.

$$\text{Log } I_h = \mathbf{M_w} - 4.0 - 2 \text{ Log } r^* \quad \text{[rock sites]} \tag{3}$$

$$\text{Log } I_h = \mathbf{M_w} - 3.8 - 2 \text{ Log } r^* \quad \text{[alluvial sites]} \tag{4}$$

$$\text{Log } I_h = \mathbf{M_w} - 3.4 - 2 \text{ Log } r^* \quad \text{[soft sites]} \tag{5}$$

> For alluvium and soft soil sites, the regressed value of Arias intensity is higher than for rock sites owing to the effect of local soil amplification. ...Figure 4 presents the predicted mean intensity for rock, alluvium, and soft soil sites versus the horizontal (surface) distance to the fault rupture plane in kilometers, based on an earthquake focal depth of 10 kilometers.

Procedures used to develop these equations for attenuation of Arias intensity as a function of earthquake magnitude, distance from a seismic energy source, and local site condition (rock, alluvium, and soft soil sites) are similar to those of other investigators (e.g., Joyner and Boore, 1988) to develop relations between peak acceleration, peak velocity, etc., as a function of these same parameters.

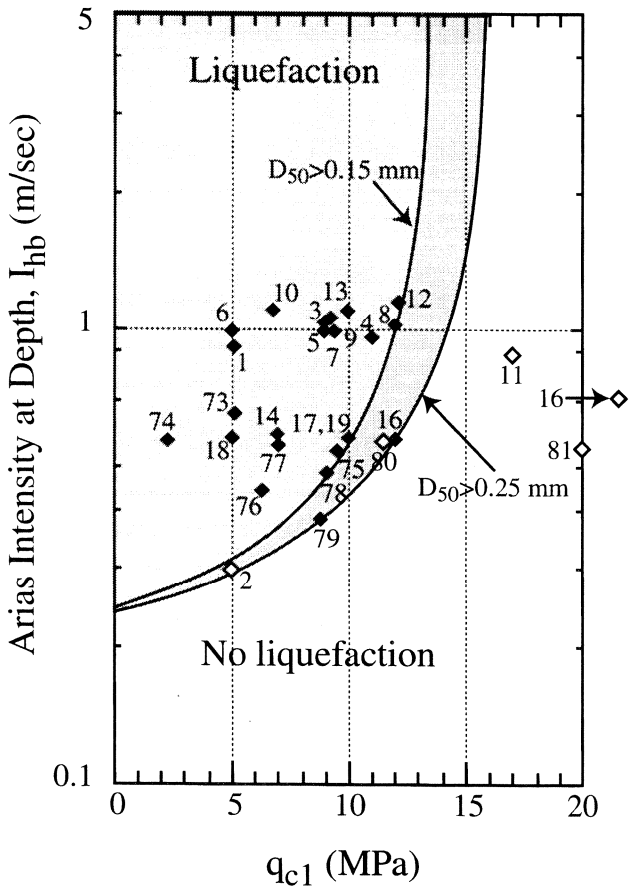

Figure 3 I_{hb} versus q_{c1} for Case History Sites (modified from Kayen and Mitchell, 1997)

Conclusions

Kayen (1993, p. 200) gives the following conclusions to this work:

> In conclusion, ... we have collected and evaluated a data set of points from which a boundary in I_{hb}-$(N_1)_{60}$ space was established, separating liquefaction occurrence from non-liquefaction occurrence. This boundary is based on the field performance of sites during moderate to large earthquakes. The most notable aspects of this boundary are that it is magnitude independent, and is constructed from an earthquake intensity parameter that is calculated directly from strong motion data measurable at a site, has a clear physical meaning, and contains no arbitrary elements.

The use of Arias intensity as a measure of seismic excitation for evaluating liquefaction resistance has the advantage of eliminating the need for other seismic parameters including peak acceleration, magnitude, and a magnitude scaling factor. Thus, use of Arias intensity could simplify the incorporation of seismic factors into the simplified procedure. Use of Arias intensity also has the advantage of using the more physically fundamental parameter of energy in the analysis.

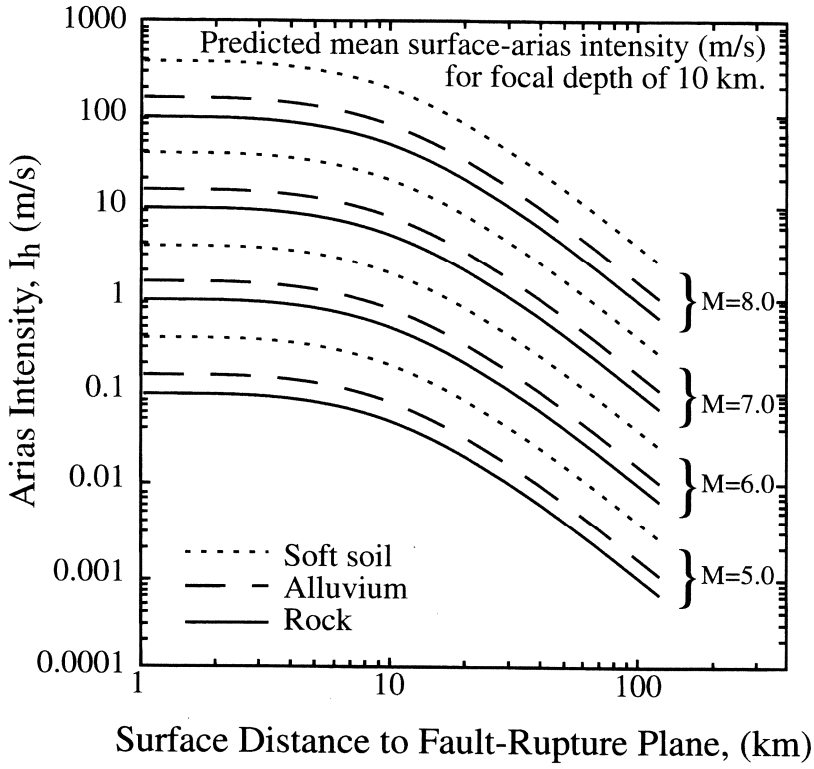

Figure 4 I_h for 50th percentile (P = 0) Earthquake response Plotted as a Function of Surface Distance to Fault Rupture (modified from Kayen and Mitchell, 1997)

Although the workshop agreed that the work by Kayen introduces an important new direction in analysis of liquefaction resistance, the procedure is not yet sufficiently verified to be recommended for immediate use in engineering practice. The following questions introduce primary issues that need to be addressed: What procedures should be used, and how accurately can Arias intensity be calculated for application at field sites where strong motion records are not available? Has sufficient case history data and experience been compiled and analyzed to provide verification of the procedure? Kayen and Mitchell (1997) have partially addressed the above questions by developing the attenuation relations above and compiling and comparing results from many case histories to further verify the applicability of the procedure. The workshop encouraged further research to answer these questions.

References

Davis, R.O., and Berrill, J.B., 1978, "Energy Dissipation and Seismic Liquefaction in Sands," *Earthquake Engineering and Structural Dynamics*, Vol. 10, p. 69-68.

Figueroa, J.L., and Dahisaria, N, 1991, "An Energy Approach in Defining Soil Liquefaction," *Proceedings*, 2nd International Conference on Recent Advances in Geotechnical Earthquake Engineering and Soil Dynamics, St. Louis, Missouri, Vol. 1. p. 407-410.

Joyner, W.B., and Boore, D.M., 1988, "Measurement, Characterization, and Prediction of Strong Ground Motion," *Earthquake Engineering and Soil Dynamics II--Recent Advances in Ground Motion Evaluation*, Geotechnical Special Publication 20, ASCE, New York, p. 43-102.

Kayen, R.E., 1993, "Accelerogram-Energy Approach for Prediction of Earthquake-Induced Ground Liquefaction," unpublished Ph.D. dissertation, University of California at Berkeley, Berkeley, California.

Kayen, R.E., and Mitchell, J.K., 1997, Assessment of Liquefaction Potential During Earthquakes by Arias Intensity: *Journal of Geotechnical Engineering*, ASCE, Vol 123, No. 12, p. 1162-1174.

Robertson, P.K, and Campanella, R.G., 1985, "Liquefaction Potential of Sands Using the CPT," *Journal of Geotechnical Engineering*, ASCE, Vol. 111, No. 3, p. 384-403.

Cyclic Liquefaction based on the Cone Penetrometer Test

Richard S. Olsen

Research Civil Engineer
Earthquake Engineering and Geophysics Branch
Geotechnical Laboratory
USAE Waterways Experiment Station
Vicksburg, MS

Abstract

This paper describes suggested recommendations for CPT-based estimation of liquefaction potential. Basically there are two approaches, those techniques based singularly on cone resistance and the CPT soil characterization chart technique. Selecting the optimum technique is dependent on the encountered soil type and if soil index tests are measured. Background information and limitations are described for each technique. Stress normalization is also fully described because its importance is not well known.

Introduction

The Cone Penetrometer Test (CPT) can now be considered the primary field test for assessing liquefaction resistance. The CPT became more accepted in the 1990's because it is a more accurate and repeatable test when compared with the Standard Penetration Test (SPT) and is less expensive and provides a continuous record. CPT-based techniques for estimating liquefaction resistance, which were developed and refined in the 1980's, have been verified in the 1990's. In concept, the SPT was an excellent tool for estimating liquefaction potential. However, performing repeatable and accurate SPT measurements is very difficult. The CPT has more potential for accurate estimation of liquefaction potential because it provides two accurate independent measurements; the cone resistance and sleeve resistance. However, unlike the SPT, soil samples are not retrieved during CPT soundings. Consequently, for CPT-based evaluations, some effort should be expended toward soil sampling, preferably using the SPT, for confirmation of soil type and for soil index testing.

This paper will fully describe the cone resistance based and the CPT soil characterization chart based techniques for estimating liquefaction resistance. Various techniques for stress normalization of the CPT cone resistance will also be fully described. Examples and a procedural cookbook are described at the end of the paper.

CPT Measurements and Relevance to Estimating Liquefaction Potential

The CPT independently measures tip stress (cone resistance) and side friction (sleeve friction resistance) which in combination can be used to estimate SPT blow count or liquefaction potential. CPT cone resistance is a bearing stress influenced by many factors, of which the drained friction angle is the most dominant. The CPT sleeve friction resistance is an index of remolded strength after breakage of the soil structure and after the soil has undergone large strain. Historically, CPT cone resistance singularly has been used to estimate liquefaction potential, but this is a limiting approach. Many factors influence liquefaction resistance such as confining stress, residual strength, density, soil type, fabric, etc. Using both CPT measurements to estimate liquefaction potential has more promise than using only cone resistance.

Stress Normalization for the CPT Cone Resistance

Stress normalization is required for all CPT-based techniques for estimating normalized liquefaction Cyclic Resistance Ratio (CRR_1). Stress normalization is very important for low confining stresses (depths less than 2 meters) and very high confining stresses (depths greater than 25 meters). For vertical effective stresses greater than one atmosphere (atm), an approximating linear stress normalization technique produces resultants which are increasingly overconservative. Always use the best available stress normalization technique when estimating liquefaction potential, regardless of the stress normalization technique used to develop the predictive technique.

CPT-based Techniques for Estimating Liquefaction CRR_1

Techniques for CPT-based estimation of liquefaction potential can be divided into two different approaches: 1) techniques based on the cone resistance and 2) the CPT soil characterization chart-based technique. If soil indices, such as fines content, are measured then they are used either 1) as an ingredient for estimating CRR_1 using the cone resistance-based technique, or 2) to verify the CPT soil characterization chart-based technique. Table 1 shows the decision process for selecting the CPT-based technique. Technique selection is based on the encountered soil type and the purpose of measured soil indices (if soil indices are measured). For clean sand, either technique can be used. For non clean sands, the cone resistance-based technique requires nearby soil samples for soil index tests. The CPT soil characterization technique can be used with any soil type and if soil indices are measured, then the indices are used to confirm the technique. Each of these three approaches will be fully described in the proceeding sections.

Table 1 Criterion for selecting the CPT-based technique for estimation of the normalized liquefaction cyclic resistance ratio (CRR_1)

General soil type	Are soil index tests measured?	CPT-based technique for estimating liquefaction potential	
		Cone resistance based techniques	CPT soil characterization chart based technique
Clean sands	No	✔ Easy to use procedure	✔
Non clean sands (fines < 40%)	Yes	✔ Soil index tests are part of the estimating process	✔ Soil index tests are used to confirm the technique
	No		✔
Other soil types (sandy silts to clay)	Yes		✔ Soil index tests are used to confirm the technique
	No		✔

Definitions of Cyclic Shear Stress and Calculating the Liquefaction Factor of Safety

Resistance to cyclic loading is generally represented in terms of the liquefaction cyclic resistance ratio (CRR). The earthquake load is now defined as the average induced cyclic shear stress ratio (CSR). CSR can be calculated using the r_d factor or computed with computer software such as SHAKE. The factor of safety against liquefaction is defined as

$$FS_{liq} = \frac{CRR}{CSR} \quad \textbf{(1)}$$

CPT and SPT-based techniques can estimate a normalized cyclic resistance ratio, CRR_1 (also referenced as $CRR_{7.5}$ in other publications). The CRR at the in situ vertical effective stress and design earthquake magnitude can be determined from CRR_1 with the following equation:

$$CRR = CRR_1 \; MSF \; K_\sigma \; K_\alpha \quad \textbf{(2)}$$

where
MSF = Earthquake magnitude scaling factor
K_σ = Confining stress scaling factor
K_α = Initial shear stress scaling factor

The earthquake magnitude scaling factor (MSF) can be estimated with the following equation (Idriss 1998):

$$MSF = \frac{10^{2.24}}{M^{2.56}} \quad \textbf{(3)}$$

where
M = Earthquake magnitude

This equation is an update to the Seed and Idriss (1982) formulation. An earthquake with a magnitude 7.5 represents approximately 15 cycles of shear (Seed and Idriss 1982). CPT and SPT-based techniques for estimating CRR_1 assume that the soil will experience 15 cycles of shear. For earthquakes with lower magnitudes, the soil experiences a lessor number of applied cycles of shear. Consequently, for the same earthquake applied shear stress level, the soil will have a higher apparent strength for lower magnitude earthquakes. The MSF in Equation 3 is equal to 1 for a earthquake magnitude 7.5 and is greater than 1 for smaller magnitude earthquakes.

For the laboratory cyclic triaxial test, CRR is given as the a ratio of maximum cyclic shear stress

to cause liquefaction to the initial effective confining stress, $\sigma_{dc}/2\sigma'_3$, times an correction factor of approximately 0.57. The 0.57 factor converts triaxial result to equivalent horizontal field results. The state-of-practice is to define liquefaction in laboratory cyclic tests as 5% double-amplitude axial strain. The laboratory CRR_1 is defined as the CRR for liquefaction at 15 cycles of uniform loading (to represent an earthquake magnitude (M) of 7.5) at a vertical effective stress of 1 atm (1 atm = 100 kPa) and using a 5% double-amplitude failure criterion.

The K_σ scaling factor corrects for failure envelope curvature of the liquefaction resistance to vertical effective stress envelope (Harder and Boulanger 1998; Olsen 1996). The resultant is that CRR decreases with increased vertical effective stress. For a vertical effective stress range of 0.5 to 2 atm, the K_σ scaling factor ranges from 1.05 to 0.9. Therefore for most non critical structures K_σ can be assumed equal to 1 for vertical effective stresses near 1 atm. The K_α scaling factor is for conditions near earth slopes. For level ground, K_α is equal to one.

Stress Normalization for CPT and SPT Measurements

The best means of estimating a geotechnical property with CPT data is to start by normalizing the CPT cone resistance to a standard vertical effective stress of 1 atmosphere (atm). The next step is to estimate the normalized geotechnical property (such as liquefaction resistance) using the normalized CPT data. All techniques for estimating liquefaction resistance do so for a condition representing a vertical effective stress of one atm. Thus the task of determining liquefaction resistance is greatly simplified because we only estimate liquefaction resistance for a single vertical stress level. The liquefaction resistance for other overburden stress levels is calculated using the inverse of the stress normalization technique. In all cases, using the best available stress normalization technique produces the most accurate predicted value.

There are numerous techniques for stress normalization of CPT and SPT measurements and liquefaction resistance. Approximating linear techniques are easy to use, while the stress focus-based technique uses a nonlinear stress exponent and requires computer-based processing. In most situations, a technique between these two extremes will provide results of sufficient accuracy.

To illustrate the difference between approximating and sophisticated stress normalization techniques, let's assume a uniform thick sand deposit having an equivalent friction angle of 35°. A sophisticated stress normalization technique would predict, using CPT data, an equivalent friction angle of 35° for all depths in this soil deposit. However, an approximating linear stress normalization technique would predict an equivalent value less than 35° (say 32°) for the bottom of the deposit and values greater than 35° (say 40°) for the top of the deposit. To estimate the most realistic equivalent value requires using the best stress normalization technique.

Techniques for estimating soil properties are not married to a particular stress normalization technique. Stated another way, the better the stress normalization technique the more accurate

the estimated equivalent value. The best possible stress normalization technique will enhance the accuracy of any predictive technique (which was developed using an approximating stress normalization technique).

Two general factors dictate the selection of the stress normalization technique: 1) the criticalness of the structure, and 2) overburden stress range. Any stress normalization technique gives the correct equivalent value for a soil element having a vertical effective stress of one atm. Similarly, linear and exponent techniques provide approximately the same result (within a few percent) for soil elements having a vertical effective stress between 0.8 and 1.2 atm. The need for the most accurate stress normalization technique is more critical for estimation of liquefaction resistance compared to estimating soil classification. The stress focus-based technique, using an iterative nonlinear stress exponent for stress normalization, should be required for estimating liquefaction resistance at overburden stress extremes (i.e., shallow offshore sediments or foundations for large earth dams) and for critical structures. Generally, start with the approximating linear-based stress normalization technique and progress to more sophisticated techniques, if required. While the stress focus based technique is technically the most accurate, the other techniques can be justified because a higher level of sophistication is only needed for shallow and deep conditions, and critical structures.

Stress normalization can be divided into the following categories (from the least sophisticated (and less accurate) to the most sophisticated (and more accurate):

1) linear relationship
   (Douglas and Olsen, 1981; Robertson 1981, 1986, 1988, 1996),
2) Constant exponent (i.e., 0.5 or 0.61) (Robertson 1994, 1995, 1996),
3) Variable stress exponent (i.e., 0.1 to 1) (Olsen 1984, 1986, 1988, 1990),
4) Stress focus technique (variable stress exponent based on soil type and relative strength)
   (Olsen 1994a, 1994b, 1995a, 1995b, 1996)

Each of these stress normalization techniques will be described using the CPT cone resistance. The same stress normalization factor determined for the CPT can be used for the SPT.

Approximating Linear Stress Normalization Technique

The approximating linear stress normalization technique shown in Equation 4 (Douglas and Olsen 1981; Robertson 1982, 1984, 1996) should only be used for general estimating purposes or when the overburden vertical effective stress is near one atm. The "linear relationship" technique is rarely justified except for quick field "back of the envelope" estimations. A linear stress normalization technique can be justified only for clay because clays exhibit little if any failure envelope curvature (Olsen 1994).

$$q_{c1L} = \frac{q_c}{\sigma_v'} \quad \textbf{(4)}$$

where

q_{c1L} = normalized cone resistance (q_{c1}) using the approximating linear technique (equivalent value at a vertical effective stress of 1 atm)

q_c = measured cone resistance (in atm units) (1 atm ≈ 100 KPa ≈ 0.1 MPa ≈ 1 ton/ft^2 ≈ 14.7 psi)

σ_v' = vertical effective stress (in atm units)

Constant Stress Exponent Technique for Stress Normalization

The constant stress exponent equation for stress normalization is shown in Equation 5, using a stress exponent of 0.7. This technique dates back to the early 1980's when Professor Schmertmann (1978) observed that the CPT cone resistance for a given relative density in large scale chambers, at differing confinement stresses, could be related using a constant stress exponent. This constant stress exponent is now sometimes published as 0.5. A stress exponent of 0.5 is incorrect because the trend of CPT chamber data with vertical effective stress for normally consolidated medium dense sand shows a stress exponent of approximately 0.7. The SPT chamber data trends show a general stress exponent of 0.5 which is inaccurate because of the short column of drilling mud (Olsen 1994). Many researchers would rather report the SPT chamber-based stress exponent of 0.5 rather than the CPT chamber-based stress exponent of 0.7. Recent research (Olsen 1994) indicates that a stress exponent of 0.7 represents a typical sand at a medium dense to loose consistency.

$$q_{c1c} = \frac{q_c}{\left(\sigma_v'\right)^{0.7}} \quad \textbf{(5)}$$

where

q_{c1c} = Normalized cone resistance (q_{c1}) based on a contact stress exponent (equivalent value at a vertical effective stress of 1 atm)

A well-published alternative (Skempton 1986; Kayen et al. 1992) to Equation 5 that also matches the combined scatter of field data is shown below;

$$q_{c1c} = \frac{q_c}{\left(\frac{0.7 + \sigma_v'}{1.7}\right)} \quad \textbf{(6)}$$

The only potential problem with this equation is at very low and very high stress conditions. The equation was designed to match data from 0.8 to 2 atm (80 KPa to 200 KPa) and will deviate from the constant stress exponent at extreme overburden stresses. However, the constant stress exponent technique in Equation 6 is easy to perform on a scientific calculator. This category of stress normalization should only be reserved for the most basic calculator or quick check calculations.

Stress Normalization using a Stress Exponent Dependent on Soil Type

The stress normalization technique using a stress exponent dependent on soil type is shown in Equation 7.

$$q_{c1s} = \frac{q_c}{\left(\sigma_v'\right)^c} \tag{7}$$

where

q_{c1s} = normalized cone resistance (q_{c1}) using a stress exponent based on soil type
c = stress exponent based on soil type

This technique requires an approximate knowledge of the soil type (Olsen 1984, 1988a, 1988b). For sands, the stress exponent is given a value of approximately 0.6. For clays, field data trends suggest a stress exponent of one. More specifically, the CPT estimated soil type can be used to directly estimate the stress exponent. A several step iterative solution is required when using software but one or two steps are sufficient if solved by hand. This technique has been superseded by the stress focus-based stress normalization technique.

CPT Stress Normalization Using the Stress Focus Based Variable Stress Exponent Technique

Recent research on the influence of confining stress on CPT and SPT measurements has resulted in a new theory - The stress focus theory (Olsen 1994; Olsen and Mitchell 1995). The stress focus theory uses a variable stress exponent for stress normalization as shown in Equation 8.

$$q_{c1e} = \frac{q_c - \sigma_{total}}{\left(\sigma_v'\right)^c} \tag{8}$$

where

q_{c1e} = normalized cone resistance (q_{c1}) using a nonlinear variable stress exponent (equivalent value at a vertical effective stress of 1 atm)

σ_{total} = total vertical stress in atm units

c = stress exponent dependent on soil type sand relative strength level (see contours of stress exponent in Figure 1)

The stress exponent, c, shown in Figure 1, is dependent on soil type and relative strength level. For sands, it defines the log-log slope for a constant relative density trend as shown in Figure 2. The cone resistance stress exponent, c, decreases as sand relative density increases and can be approximated (for sand) as shown below using relative density, D_r (Olsen and Mitchell 1995):

$$c = 1 - \left(D_r - 10\%\right) 0.007 \qquad \textbf{(9)}$$

The stress focus theory explains why the stress exponent for sands is dependent on initial relative density. For all overburden stress conditions, this "variable stress exponent" provides the most accurate CPT cone resistance normalization.

SPT Stress Normalization

The SPT blow count (N) is normalized to the equivalent value (N_1) at a vertical effective stress of 1 atm using Equation 10.

$$(N_1)_{60} = \frac{N_{60}}{\left(\sigma_v'\right)^n} \qquad \textbf{(10)}$$

The n stress exponent in Equation 10 was suggested by Seed and Idriss (1984) to equal 0.45 for sands having relative densities of 60 to 80% and equal to 0.55 for sands having relative densities of 40 to 60%. These recommendations were established based on data from SPT chamber tests reported by Marcuson and Bieganousky (1977). Recent research by Olsen (1994) suggests that the constant low mud pressure in the SPT chamber boreholes, at all confining stress levels, reduces the confining stress at the SPT sampler. This reduced stress causes the inferred stress exponents for sands to be too low by a value of 0.15. Stress focus theory explains why the SPT chamber-based stress exponents are lower than the CPT chamber values. The consequence is that the CPT determined stress exponent from Figure 1 or Equation 9 should also be used for SPT normalization. The 1997 draft ASTM SPT standard for SPT stress normalization references Olsen (1994) as an alternative technique where a higher level of sophistication is required. The CPT determined CPT stress exponent should be used with the SPT stress exponent and in general ranges from 0.6 for medium dense sand, 0.7 for loose sand, to 1 for clay.

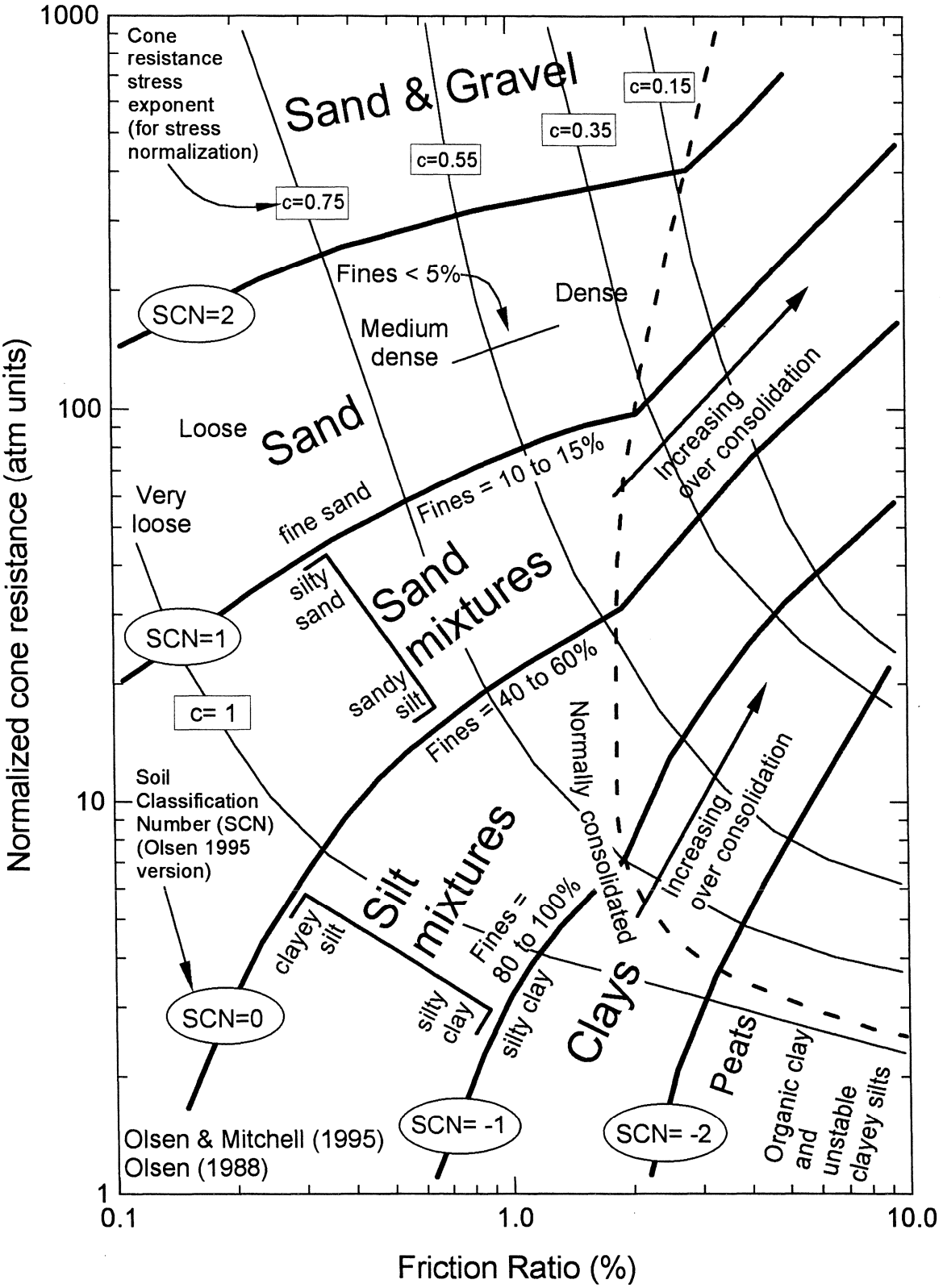

Figure 1 Stress exponents for cone resistance on the CPT soil characterization chart (Olsen and Mitchell 1995).

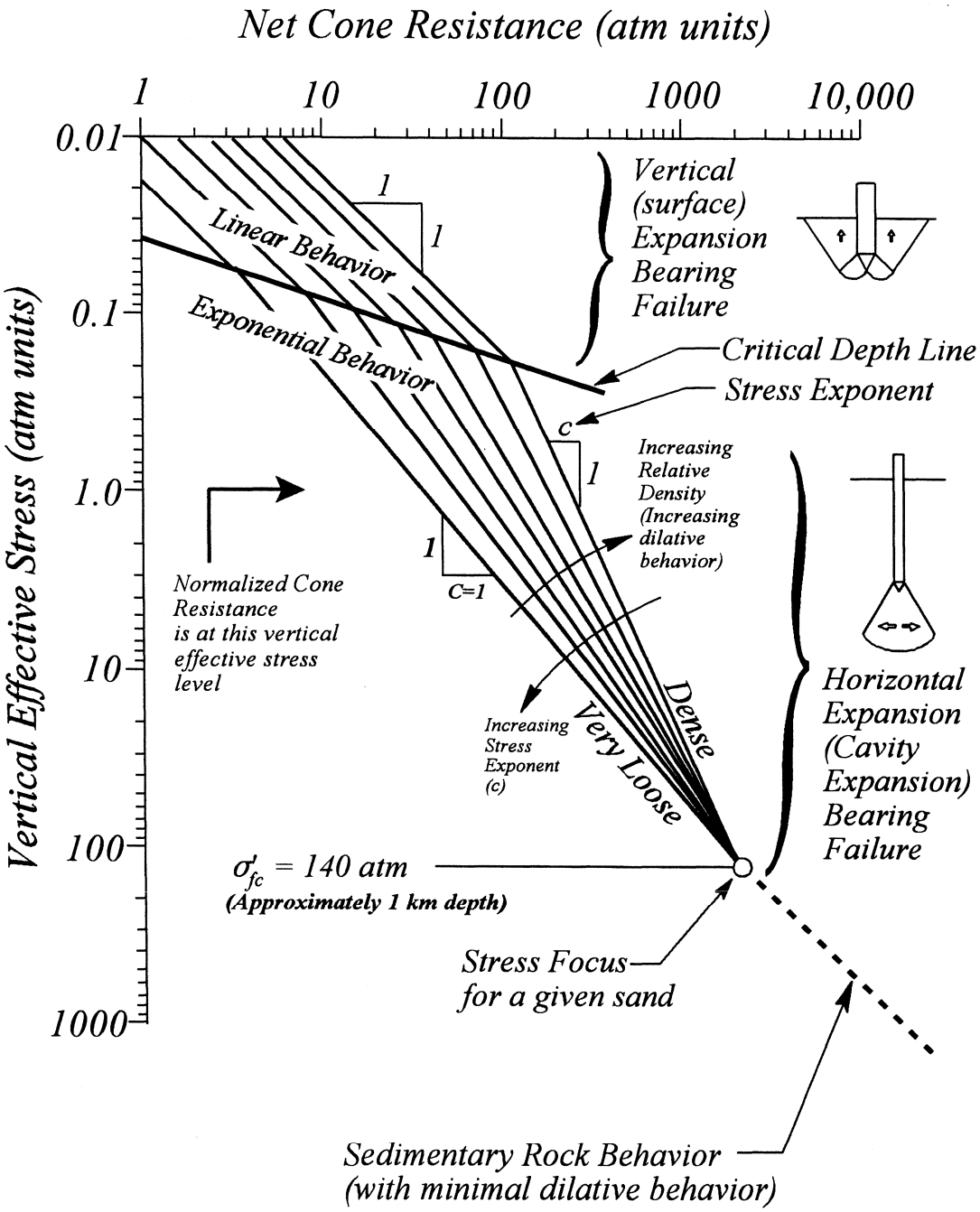

Figure 2 Description of how cone resistance trends toward the stress focus for any relative density (Olsen 1994).

CPT-based Estimation of Soil Classification

Knowing the soil classification of soils penetrated by the CPT is as important as estimating the liquefaction resistance. The soil type and relative strength infers how the soil reacts if liquefaction is triggered. In the past, soil type could be estimated from a CPT soil classification chart either manually or with non-linear chart lookup software. Robertson (1998) recently converted soil classification contours into an equation form (soil index, I_c) using a modification of the Olsen soil characterization chart (Olsen 1988). However, Robertson's I_c is an arbitrary value requiring memorization of the soil type for each I_c range. The most recent CPT-based chart for estimating soil type is shown in Figure 3 (Olsen and Mitchell 1995). The CPT Soil Characterization Number (SCN), shown on the soil classification contours, represents unique and definable soil types. The SCN has been part of all the CPT soil characterization charts (Olsen 1984, 1986, 1988, 1990, 1994; Olsen and Mitchell 1995). The CPT SCN can be approximated (for normally consolidted soils) by the following equation:

$$SCN = -3.58 + 2.08\sqrt{(0.76 * (1.3 - Log_{10}R_f)^2) + (Log_{10}\, q_{c1})^2} \qquad \textbf{(11)}$$

where

SCN = Soil Classification Number (SCN) (normally consolidated soil) (see Figure 3)

- +1 = boundary between a silty sand and fine sand (where the silt is effecting the strength behavior of sand, i.e., 10 to 15% fines content)
- 0 = behavior of a pure silt (ML behavior with fines content = 50 to 60%)
- -1 = boundary between a silty clay (CL or CH) and clayey silt (ML) (fines content = 80% to 100%)
- -2 = boundary to organic peats and unstable soils

q_{c1} = Normalized cone resistance (in atm units) (using the best possible technique)

R_f = Calculated friction ratio (percentage)

The calculated friction ratio (R_f) is defined as:

$$R_f = \frac{f_s}{q_c} 100 \qquad \textbf{(12)}$$

where

f_s = Measured CPT sleeve friction resistance in atm units (1 atm = 100KPa)

The SCN, from Equation 11, is only for normally consolidated soils. It produces SCN values too high for overconsolidated conditions. The following equation estimates the SCN for overconsolidated conditions which occur at friction ratios (R_f) generally greater than 1.9 %.

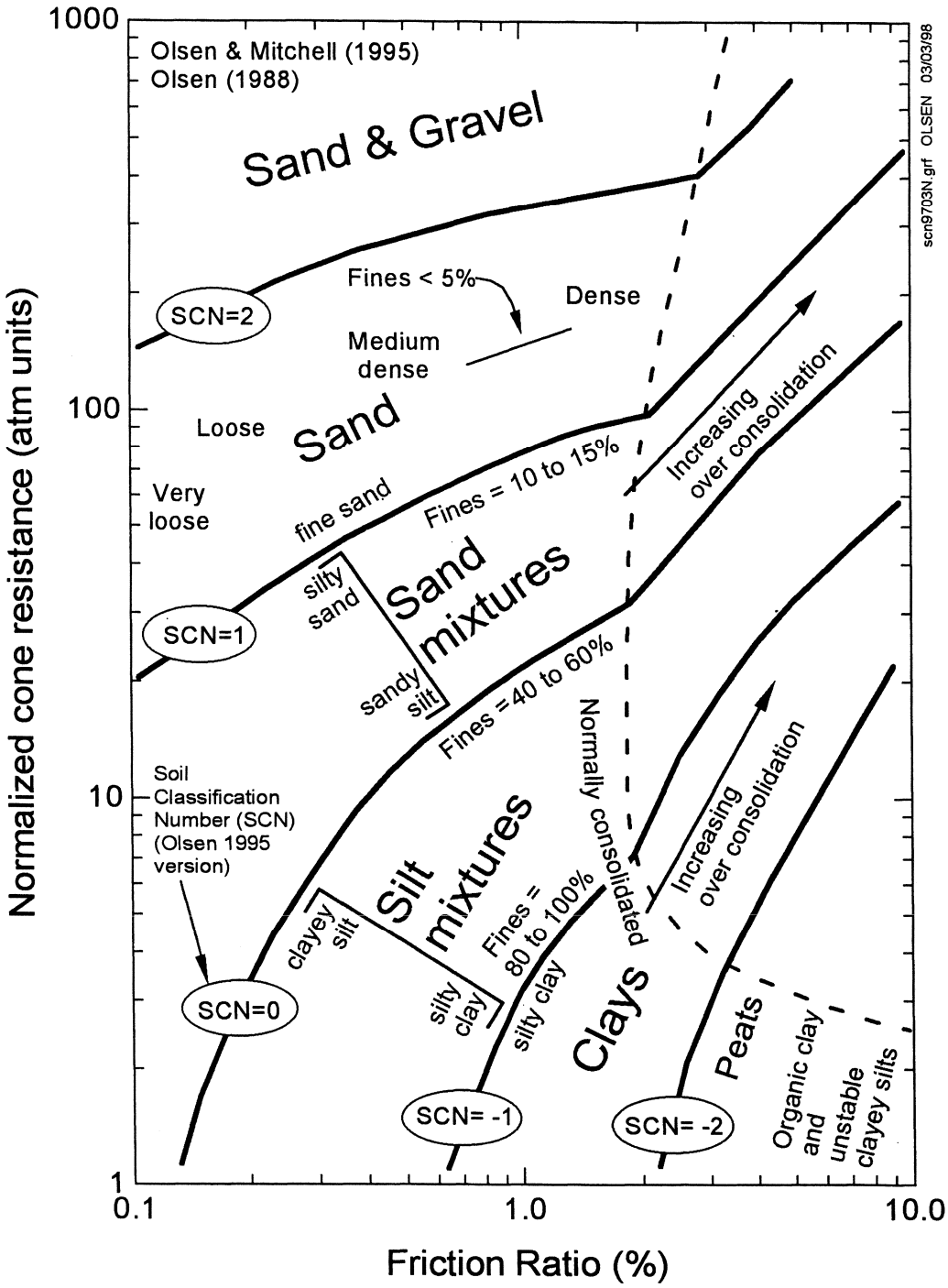

Figure 3 CPT soil characterization chart (Olsen and Mitchell 1995).

$$SCN^* = ((\log_{10} q_c)^{1.5} - 1.1\,(\log_{10} R_f - 0.27))\,1.34 - 1.87 \quad (For\ R_f > 1.9\%) \quad \textbf{(13)}$$

where

SCN^* = Soil Classification Number for over consolidation conditions (for $R_f > 1.9\%$)

The CPT Soil SCN was designed to represent unique properties at integer values (i.e. -1, 0 and 1) (Olsen 1984, 1986, 1988, 1994, 1995). At SCN equal to -1, the soil should have a classification and strength behavior between that of a silty clay and clayey silt. More specifically, SCN equal to -1 represents a Unified Soil Classification System (USCS) classification between CL (or CH or MH) and a ML. At SCN equal to 0, the soil behavior should be that of pure silt and the USCS equal to ML. At SCN equal to 1, the soil should have a classification and behavior between that of a fine sand (or slightly silty sand) and silty sand where the silt is starting to influence the strength level of the sand. The USCS for SCN equal to 1 is between a classification of SP/SM and SM. By USCS definitions, the boundary between an SP and SM is 5% fines, the boundary between SP/SM and SM is 12% fines, and the boundary between ML and SM is 50% fines. Therefore, an SCN equal to 1 (between SM/SP and SM) represents a fines content of approximately 12% and a SCN equal to 0 (pure silt) represents a fines content of approximately 70%. Over the last 15 years the location of these SCN boundaries have been adjusted as new field CPT data were included into the database.

Estimating Liquefaction Resistance of Clean Sand Using only the Cone Resistance

The CPT cone resistance-based technique for estimating liquefaction potential originated in the early 1980s as simple conversions from SPT-based techniques. The original correlation by Robertson (1982) and Robertson and Campanella (1985) for clean sands, shown in Figure 4, has been shown to be historically correct based on accumulated cyclic laboratory data and historical field performance data. A critical point for any cone resistance-based technique is the intersection of the liquefaction boundary line for a normalized cone resistance at CRR_1=0.2. Robertson (1982) established a normalized cone resistance of 118 atm for this intersection point and this value has been proven over the last 15 years. Figure 5 illustrates various cone resistance-based techniques for determining liquefaction potential of clean sand together with recent field performance data and the NCEER recommended relationship. Figure 6 is a simplification of Figure 5 showing only the NCEER recommended correlation and field performance data.

Field performance data points from Suzuki, et al. (1985) together with the NCEER-recommended correlations are shown in Figure 7. Three of Suzuki's field performance data points plot beyond the proposed liquefaction resistance relationship for clean sand. These data points represent 9% of the field performance data where liquefaction was observed but where the CPT-based technique estimates non liquefaction. The Suzuki database has not been scrutinized and the source of these four outlying data points are unknown. The NCEER recommended correlation in

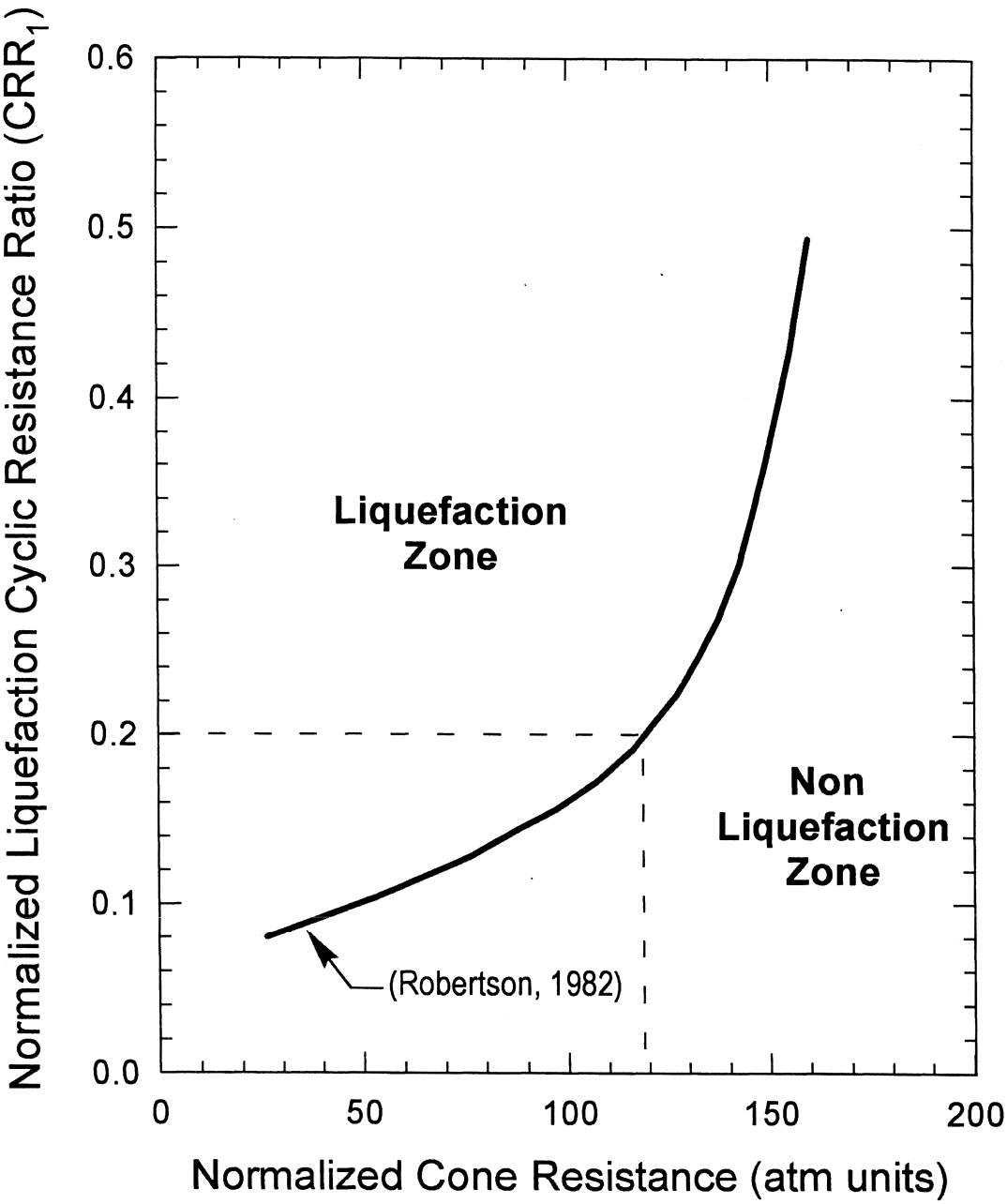

Figure 4 Relationship between normalized liquefaction cyclic resistance ratio (CRR_1) and normalized cone resistance by Robertson (1982).

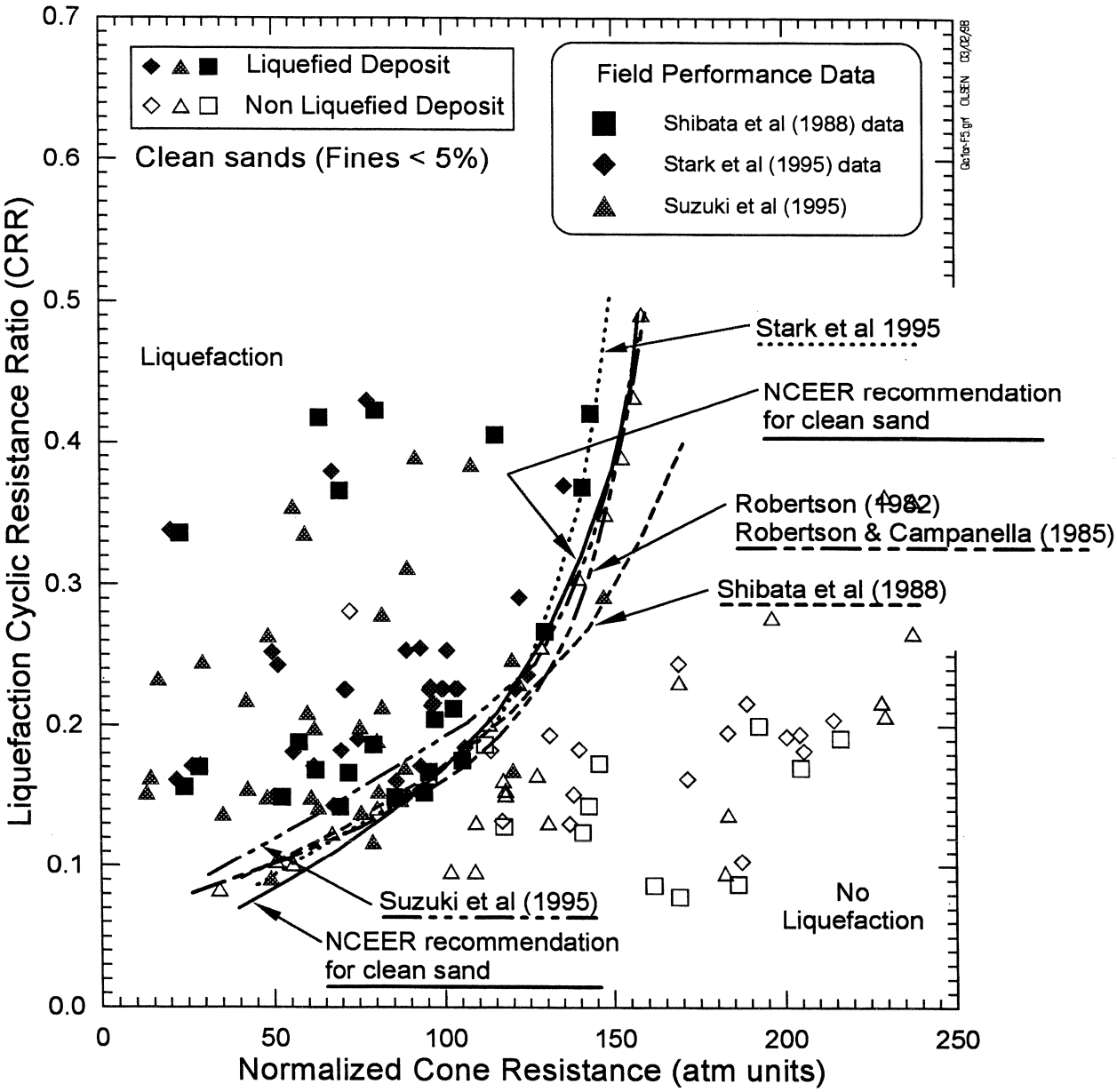

Figure 5 Comparison between CPT cone resistance-based methods to determine the normalized liquefaction cyclic resistance ratio (CRR_1) and recent field performance data.

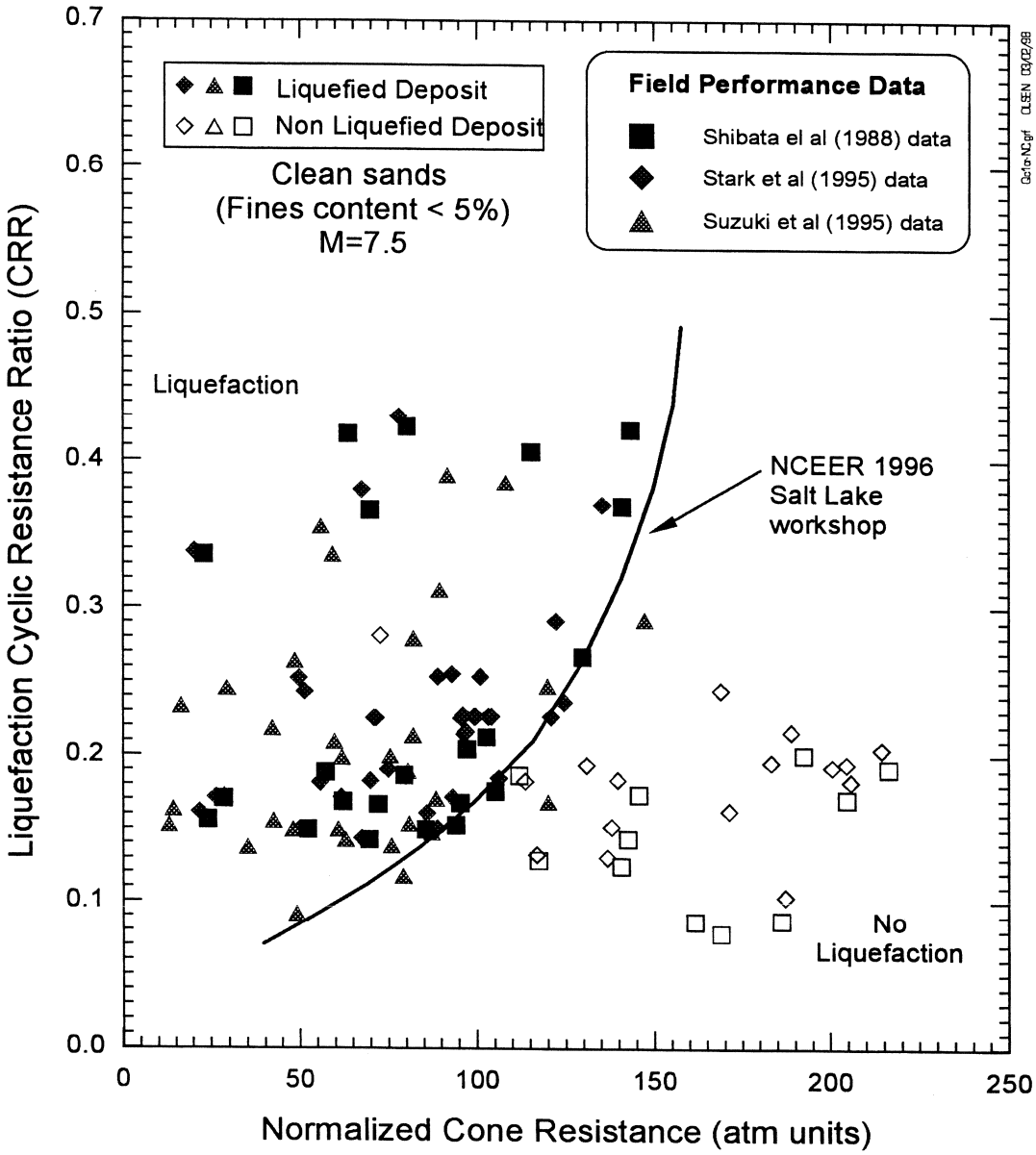

Figure 6 Comparison between the NCEER recommended cone resistance-based technique for determining the normalized liquefaction cyclic resistance ratio (CRR_1) and recent field performance data.

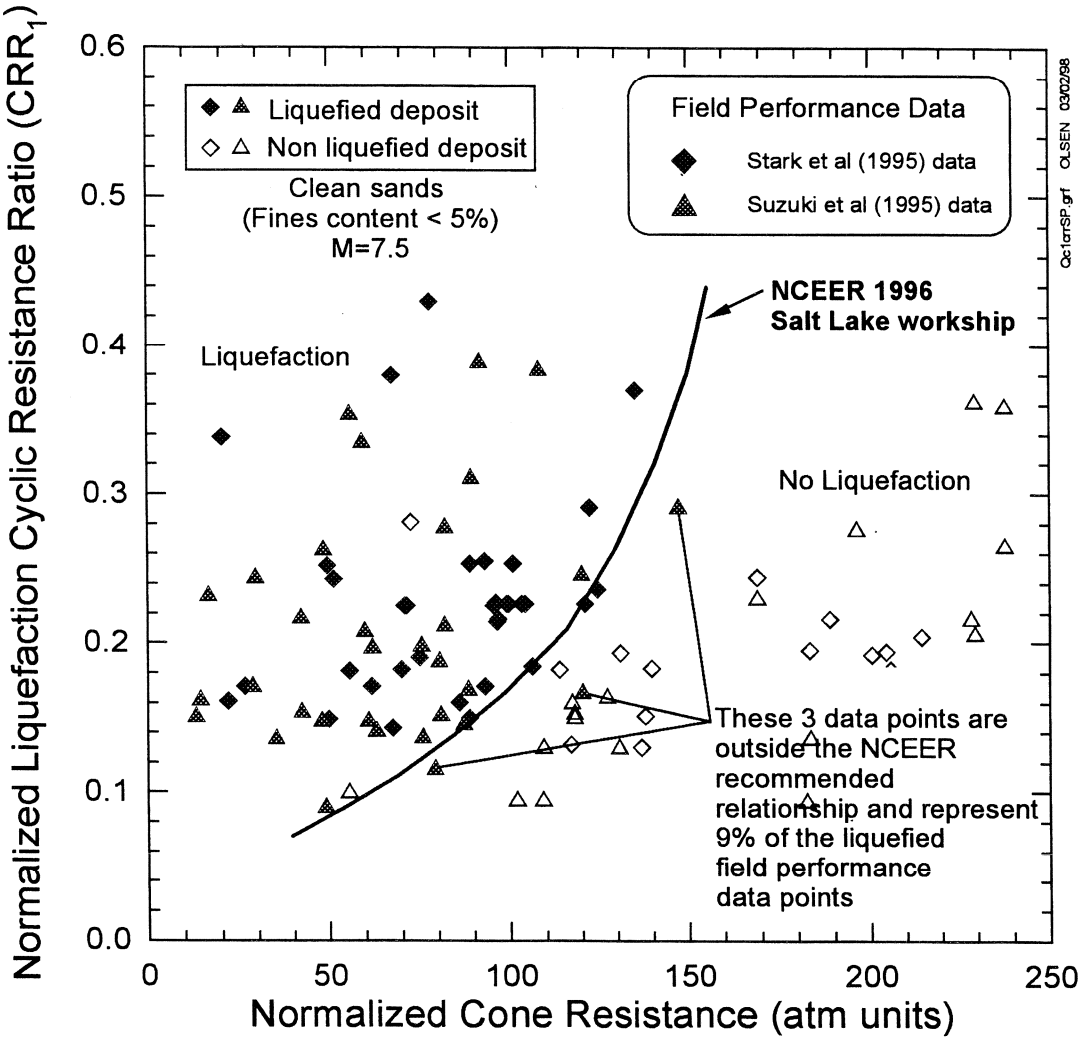

Figure 7 Comparison for clean sand between the NCEER-based CPT cone resistance technique to determine the normalized liquefaction cyclic resistance ratio (CRR_1) and recent field performance data.

Figure 5 represents the best available correlation for CPT cone resistance-based estimation of liquefaction resistance of clean sands.

Estimating Liquefaction Resistance of Non Clean Sands using the Cone Resistance

Inclusion of silt within a sand matrix decreases cone resistance and may decrease liquefaction resistance. Estimating the liquefaction resistance of non clean sands using cone resistance-based techniques can be accomplished by two means, either 1) the calculated equivalent clean sand (silt corrected) cone resistance, or 2) the chart-based solution in terms of a measured soil index. Limitations of the silt correction concept will be discussed in the next section.

The chart-based solution in Figure 8 is the most viable approach for cone resistance-based estimation of liquefaction resistance for non clean sands. This figure is based on fines content and/or mean grain size. There are only two fines content trends in Figure 8, namely 5% and 35%. The influence of fines content on SPT-based liquefaction resistance was observed by Seed, et al. (1983) to be non linear and it is likely that the CPT relationship is also non linear. At least three fines content trends are required for non linear interpolation purposes. Therefore, at present, there are insufficient fines content trends to establish a non linear relationship.

The relationship of mean grain size to liquefaction resistance represents a good correlation because of the large number of independently developed mean grain size trends in Figure 8. However, mean grain size is a less desirable index because a full gradation test is more expensive than a fines content test. Also, for a given soil composition, it is likely that the CPT estimated liquefaction CRR_1 value will be different when using a fines content or mean grain size criteria in Figure 8.

Equivalent Clean Sand Cone Resistance, $(q_{c1})_{cs}$

The equivalent clean sand cone resistance, $(q_{c1})_{cs}$, is the same concept as the SPT equivalent clean sand cone resistance, $((N_1)_{60})_{cs}$. One means of defining $(q_{c1})_{cs}$ is shown below (Robertson and Wride 1998):

$$(q_{c1})_{cs} = K_c \; q_{c1} \qquad \textbf{(14)}$$

where
K_c = correction factor that is a function of grain characteristics

CRR_1 then estimated using clean sand relationships of CRR_1 versus $(q_{c1})_{cs}$ such as Figure 6. There is no physical or theoretical meaning for $(q_{c1})_{cs}$ or $((N_1)_{60})_{cs}$. They do not represent the equivalent value a sand if the silt content was removed. They are only a convenience for calculating CRR_1.

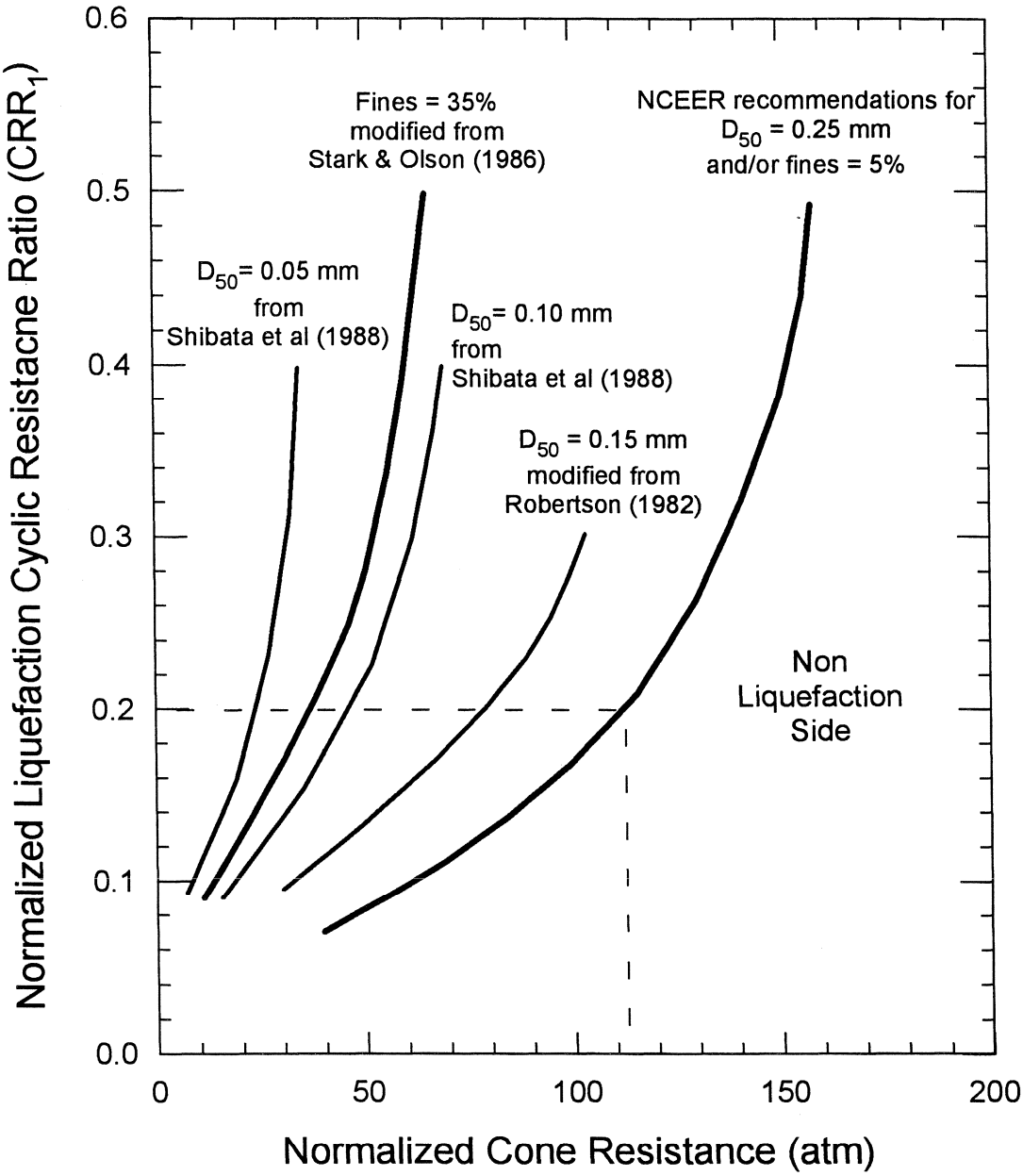

Figure 8 Comparison between various CPT-based techniques for estimating the normalized liquefaction cyclic resistance ratio (CRR_1).

The equivalent clean sand concept was originally developed for the SPT as a correction for grain size differences by the late Prof. H. Bolton Seed (1984). He then introduced a chart solution, in terms of fines content, which removed the need to determine the equivalent clean sand value. Olsen (1988) then reintroduced equivalent clean sand technique with the SPT silt correction chart (Figure 9) based on Seed's 1986 SPT liquefaction determination chart. The purpose for this silt correction chart was only to simplify development of the CPT soil characterization chart-based technique for estimating liquefaction potential (to be introduced in the next section). Ironically, this SPT silt correction chart has been widely referenced and copied, and has now been extended to the CPT equivalent clean sand cone resistance. It is important to repeat that there is no physical meaning for the equivalent clean sand cone resistance or SPT blow count. It is therefore recommended that cone resistance-based liquefaction potential should be determined using chart-based solutions rather than by means of equivalent clean sand cone resistance.

CPT Estimation of Fines Content

The fines content of non clean sands is an important ingredient for cone resistance-based techniques for estimating liquefaction resistance. Fines content can be either 1) measured from samples taken from nearby boreholes or 2) estimated using CPT-based techniques. Fines content can be estimated based on the CPT estimated soil type as shown in Figure 3 (Olsen and Mitchell 1995; Olsen and Koester 1995; Olsen 1988). However, techniques for estimating liquefaction resistance based on the equivalent clean sand normalized cone resistance are an over generalization of the CPT soil characterization-based chart technique (to be discussed in the next section). Estimating fines content using CPT measurements must be considered a crude prediction having a high standard deviation. Liquefaction resistance is also more complex than can be generalized with a simplistic correlation of CPT estimated soil classification to CPT estimated fines content. The CPT is a strength measurement test which is influenced rather than dominated by fines content.

Problems with Geologically Complex Sites

Unlike the SPT where the sampler recovers a soil sample of the tested soil, the CPT does not provide a soil sample. The CPT cone resistance-based technique for non clean sands however requires a soil sample, typically from a nearby boring several meters away. The disadvantages of measuring soil index tests are the economics of requiring nearby boreholes and the additional costs of laboratory testing. Also, soil conditions at geologically complex sites can quickly change over short lateral distances. Consequently, measured soil indices from a nearby borehole may not match the soils penetrated with the CPT a short distance away. Measured soil indices should only be used when the potentially critical soil layers are thick and uniform. The calculated liquefaction potential will be conservative if the sampled soil is finer than the soil probed; similarly, the calculated value will be unconservative if the sampled soil is coarser than the soil probed. CPT-based techniques for estimating liquefaction potential that require soil samples should not be used at geologically complex sites.

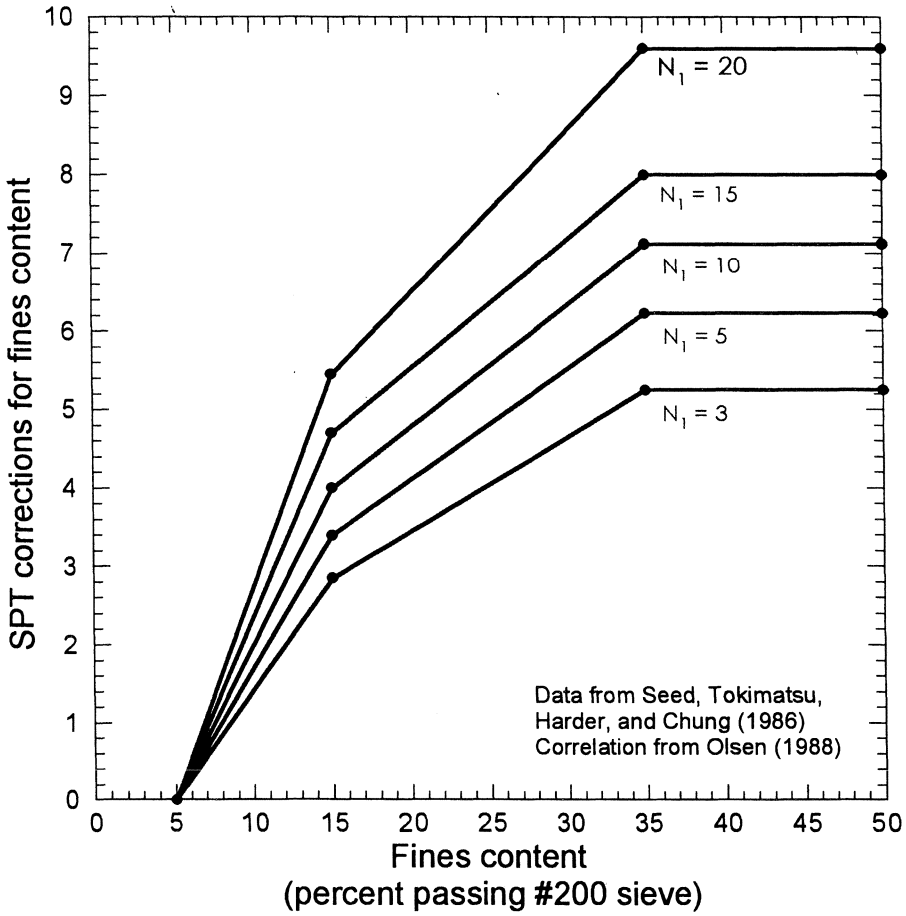

Figure 9 Estimating the SPT silt correction based on fines content (Olsen 1988) (data from Seed, Tokimatsu, Harder, and Chung 1986).

Estimating Liquefaction Resistance for All Soil Types using the CPT Soil Characterization Chart Technique

The CPT soil characterization chart technique for estimating liquefaction resistance is shown in Figure 10 (Olsen and Koester 1995). The normalized liquefaction cyclic resistance ratio (CRR_1) is determined for any depth and any soil type based on the combination of normalized cone resistance and friction ratio. This technique does not require laboratory measured soil index tests to estimate liquefaction resistance, unlike other SPT and CPT-based techniques.

Historical Development of the CPT Soil Characterization Chart Technique

The CPT soil characterization chart technique for estimating liquefaction potential originated in the early 1980s (Olsen 1984) and has been constantly refined and improved since then (Olsen 1988; Olsen and Farr 1986; Olsen and Koester 1995; Olsen, Koester, and Hynes 1996). This technique indirectly includes the effects of soil type, fines content influence, peak strength, high strain strength, and lateral stress influence. Specifically, it was developed based on: 1) correlations to cyclic laboratory tests, 2) trends of CPT estimated normalized SPT values, 3) trends of SPT silt corrections using CPT estimated silt content, 4) the Seed, et al. (1984, 1986) SPT to CRR_1 correlations, and finally 5) field performance data (Tokimatsu, et al. 1990; Kayen, et al. 1992; Suzuki, et al. 1995, 1995b; file data; project data; etc.).

Estimating SPT Blow Count Using the CPT Soil Characterization Chart Technique

The critical starting point for this chart technique was to using an accurate technique for CPT-based estimation of SPT blow count. Contours of CPT-estimated SPT-normalized blow counts, N_1, can be established on the CPT soil characterization chart as shown in Figure 11. These SPT contours were developed using both CPT measurements (Olsen 1984, 1988, 1994) and are more accurate than if based on the q_c/N ratio (Robertson 1983; Seed, et al. 1986). Seed, et al. (1986) used the q_c/N technique to establish a cone resistance-based technique for estimating CRR_1; we now know that this approach results in unconservative estimates of CRR_1. The next step, after establishing SPT contours (Figure 11), was establishing contours of CPT-estimated equivalent clean sand normalized blow counts, $(N_1)_{cs}$, using the procedure shown in Figure 12 (Olsen 1988). Equivalent clean sand SPT contours were calculated based on the combination of SPT N_1 contours and CPT estimated fines content together with the SPT-based silt correction relationship shown in Figure 9. CRR_1 contours were then approximated by converting the $(N_1)_{cs}$ contours to CRR_1 contours based on the Seed $(N_1)_{cs}$ to CRR_1 relationship (Figure 13). These SPT-estimated CRR_1 contours are the framework for further refinements based on cyclic laboratory and field performance data.

CPT-based Cyclic Laboratory Data Trends of Liquefaction Resistance

The cyclic laboratory data (also shown Figure 12) were used to refine the position of SPT-developed CRR_1 contours on the CPT soil characterization chart. The cyclic laboratory

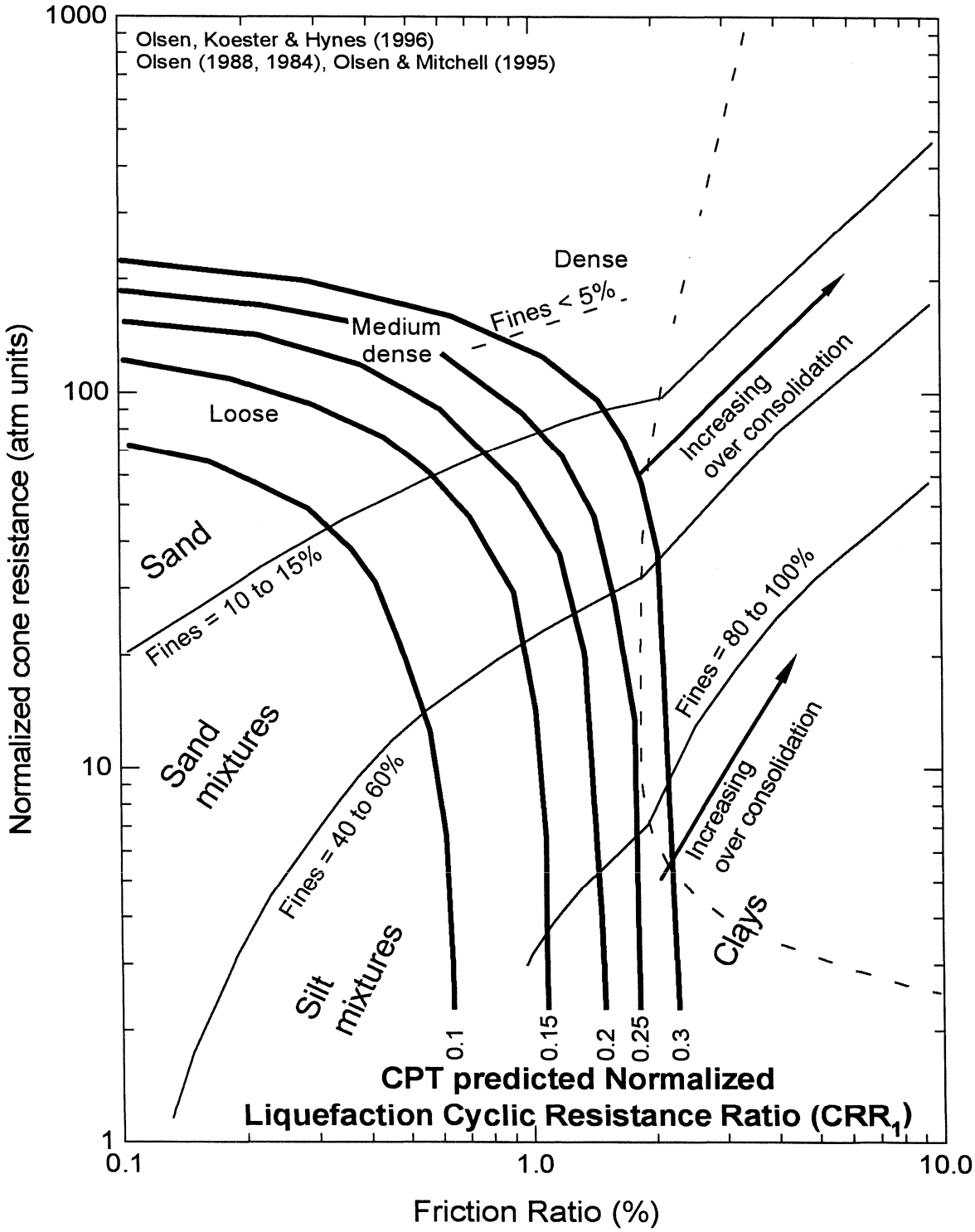

Figure 10 Estimation of the normalized liquefaction cyclic resistance ratio (CRR_1) using the CPT soil characterization techniques (Olsen, Koester, & Hynes 1996).

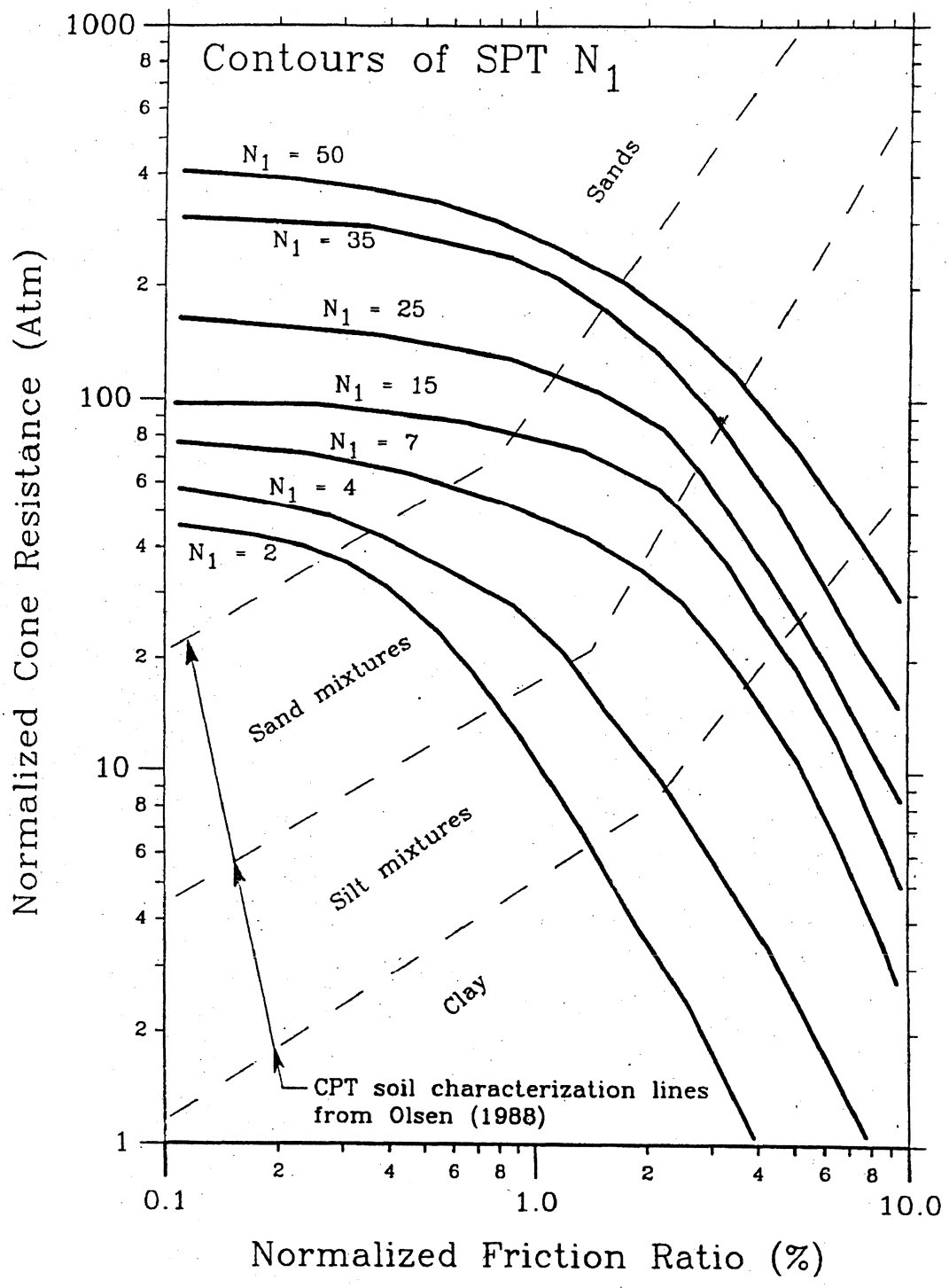

Figure 11 CPT estimation of SPT N_1 using both CPT measurements (Olsen 1994, 1988, 1986, 1984).

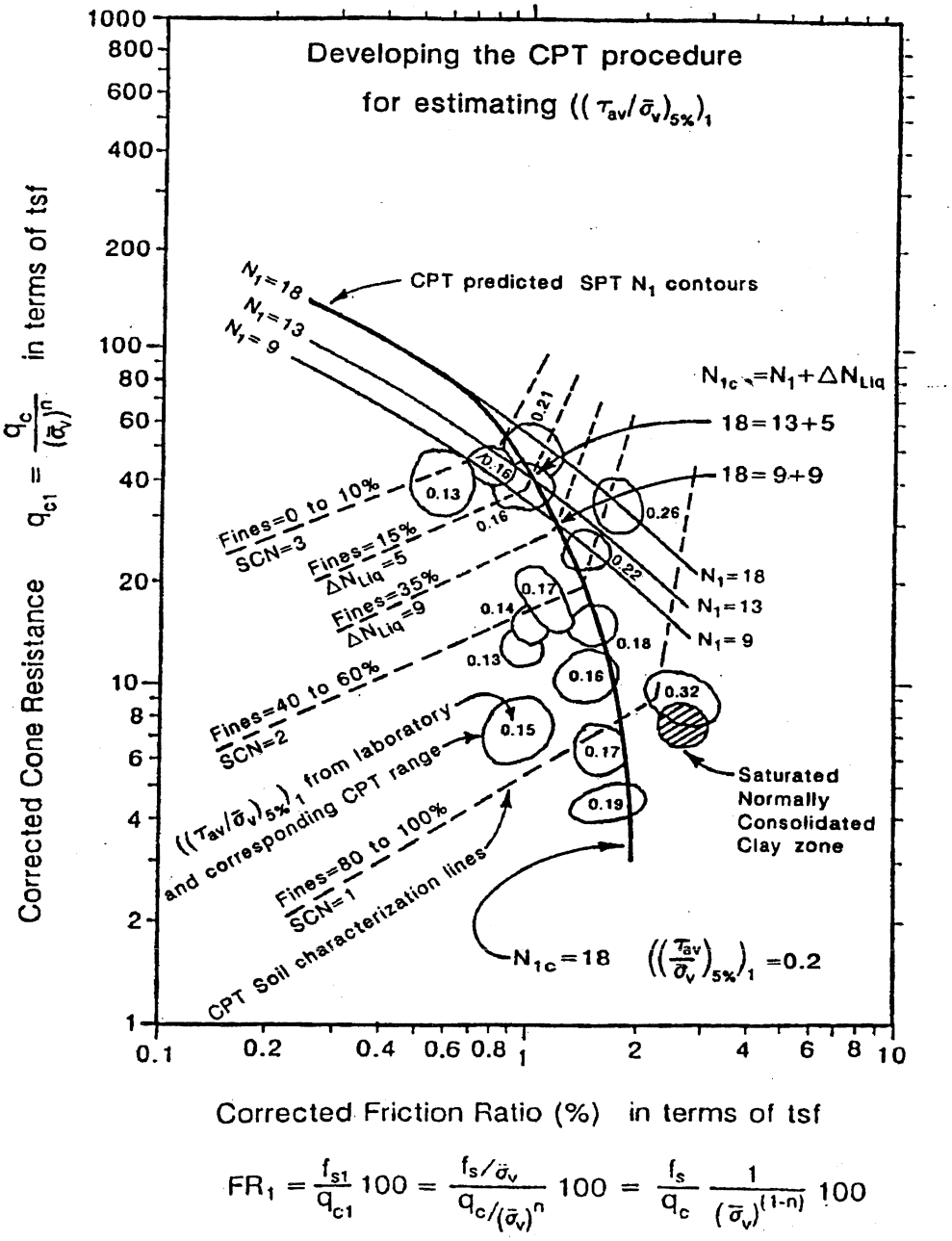

Figure 12 Graphical procedural steps for CPT-based determination of the SPT blow count, fines content, equivalent clean sand SPT blow count, and normalized liquefaction cyclic resistance ratio (CRR_1) (Olsen 1988).

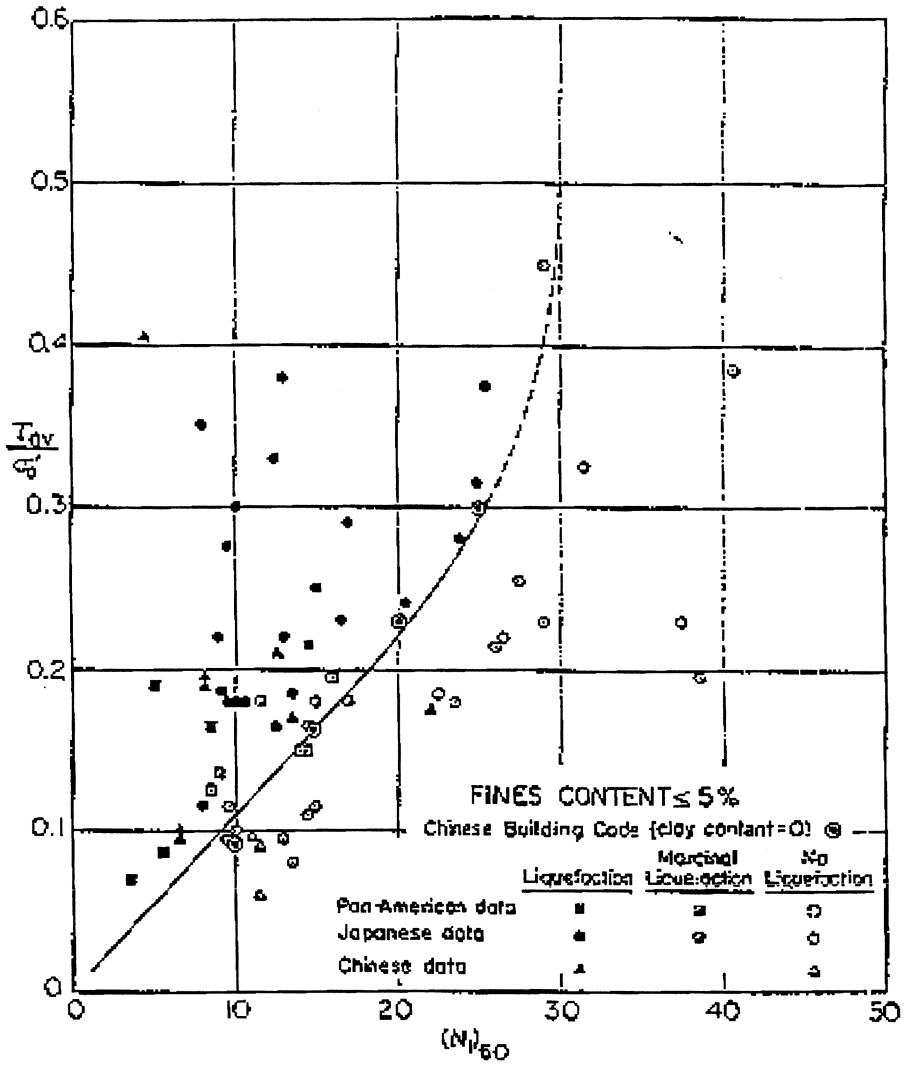

Figure 13 Relationship between normalized liquefaction cyclic resistance ratio (CRR_1) and N_1 for clean sand (Seed et al. 1984).

database contains soil types from clean sand to silty clay and CRR_1 levels from 0.12 to 0.32. Each laboratory-based data point represents a normalized cyclic resistance ratio value (CRR_1) and was typically determined from a series of laboratory cyclic tests. The cyclic laboratory data confirm that the CRR_1 contours curve down into the clay region of the CPT soil characterization chart.

Strain Potential of Clays

This technique uses a strain based criterion for liquefaction designation rather than a pore pressure generation criterion. Clays can strain during earthquakes and expressing cyclic mobility. Normally consolidated soft clays can accumulate 5% cyclic strain during an earthquake if the average earthquake induced shear stresses approach the static strength. Consequently, if earthquake induced stresses are greater than the clay undrained strength, the clay will deform and meet the liquefaction criterion. The static clay undrained strength is best expressed as the undrained strength divided by vertical effective stress, designated as the strength ratio, and signified as the c/p ratio; for normally consolidated clay, the c/p is approximately 0.31. An earthquake-induced CSR of 0.3 represents a large nearby earthquake and if applied to a normally consolidated clay deposit will induce dynamic deformation. Normally consolidated soft clays therefore can have an equivalent liquefaction resistance CRR_1 of at least 0.28 as is reflected in Figure 10.

This CPT soil characterization technique also includes estimates CRR_1 contours for sensitive clay and sensitive soil mixture in Figure 10. For increasing soil sensitivity, the CPT estimated CRR_1 contour change from CRR_1=0.28 (for normally consolidated clays and silts) down to CRR_1= 0.1 (highly sensitive clays and silts). The CRR_1 contours for sensitive soils were developed primarily based on laboratory cyclic tests.

If a clay or silt mixture and is flagged as liquefiable (based on this technique) than the soil layer should be sampled for further evaluation. An excellent index is the liquidity index (LI), defined as:

$$LI = \frac{w_n - PL}{LL - PL} \qquad \textbf{(15)}$$

where
LL = Liquid limit (in percentage)
PL = Plastic limit (in percentage)
w_n = In situ water content (in percentage)

The LI is a relative strength index because the LL and PL represent the water contents for two strength levels. The "China Criterion" specifies that soils are potentially liquefiable if LI is greater than 0.9. Alternatively, for clays and clayey silts, if in situ or laboratory-based vane shear tests

indicate a sensitivity greater than 4 than the soil should be labeled suspect. The purpose of these index tests are to flag non sands that may experience severe softening and strength loss during an earthquake. The MSF should not be applied to clays and silt mixtures for earthquake magnitude less than 7.5. The MSF factor may not apply to clays and silt mixtures because MSF applies to cyclic induced pore pressure generation in sands; the sensitive behavior of weak clays and soil mixtures developed primarily by over straining.

Limitations of Field Performance Data

Field performance data is defined as are soil deposits having in situ measurements together with observations on whether liquefaction effects occurred during an earthquake. For the last 20 years, the preferred means of correlating SPT to liquefaction potential was with field performance data. This procedure has been extended to cone resistance-based technique (Stark and Olson 1995) for sands. It is also possible to use CPT field performance data to establish the CPT soil characterization chart. However, this task is more difficult than collecting a statistically significant number of data points. The data that actually defines the correlations are based only on field performance data that have a liquefaction factor of safety near one. Soil deposits with obvious liquefaction (i.e., factor of safety <0.7) do not contribute toward establishing the liquefaction resistance contour lines. Sand boil expression at ground surface during an earthquake signifies that a sandy soil layer is densifying due to liquefaction; the problem is identifying which soil layer(s) liquefied. Also, not all liquefied deposits express sand boils at the ground surface. Establishing a useable field performance database that contains marginal liquefaction data is difficult. A good field performance database must represent all soil types and all relative strength levels and have a sufficient number of data points representing marginal liquefaction. However, only part of the worldwide field performance database represents marginal liquefaction. The required field performance database to establish a CPT based correlation of liquefaction potential is not likely to exist for the foreseeable future.

Using Field Performance Data to Prove the CPT Soil Characterization Chart Technique

The best use for field performance data is to confirm the CPT soil characterization chart technique because the quantity of field performance data to establish a CPT soil chart technique is not likely to exist for the foreseeable future. On the other hand, cyclic laboratory data represents a factor of safety of one and can be used directly to establish contours of liquefaction CRR_1. Cyclic laboratory data should only be considered an indicator of liquefaction potential while field performance data should be considered direct data. Figures 14 and 15 show the field performance data from Suzuki, et al. (1995) together with the CPT soil characterization chart-based contours for CRR_1 equal to 0.25 and 0.15, respectively. The field performance data for CRR_1=0.25 matches the CPT soil characterization chart CRR_1=0.25 contour in Figure 14. A few of the field performance data are beyond the CPT soil characterization chart CRR_1=0.15 contour in Figure 15.

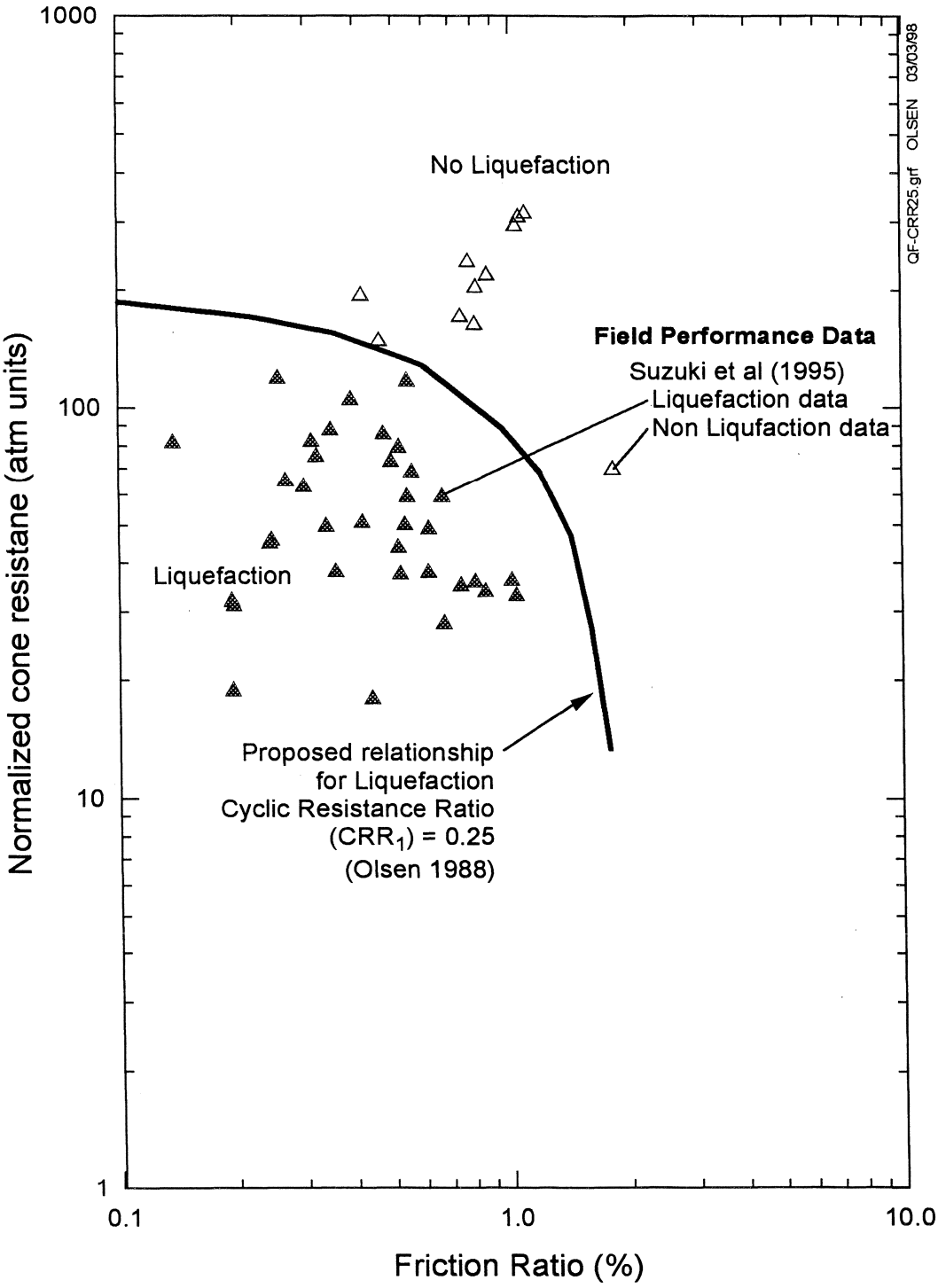

Figure 14 Comparison of CPT soil characterization chart technique (Olsen 1988) to field performance data (Suzuki, et al.. (1995) for a normalized liquefaction cyclic resistance ratio (CRR_1) equal to 0.25.

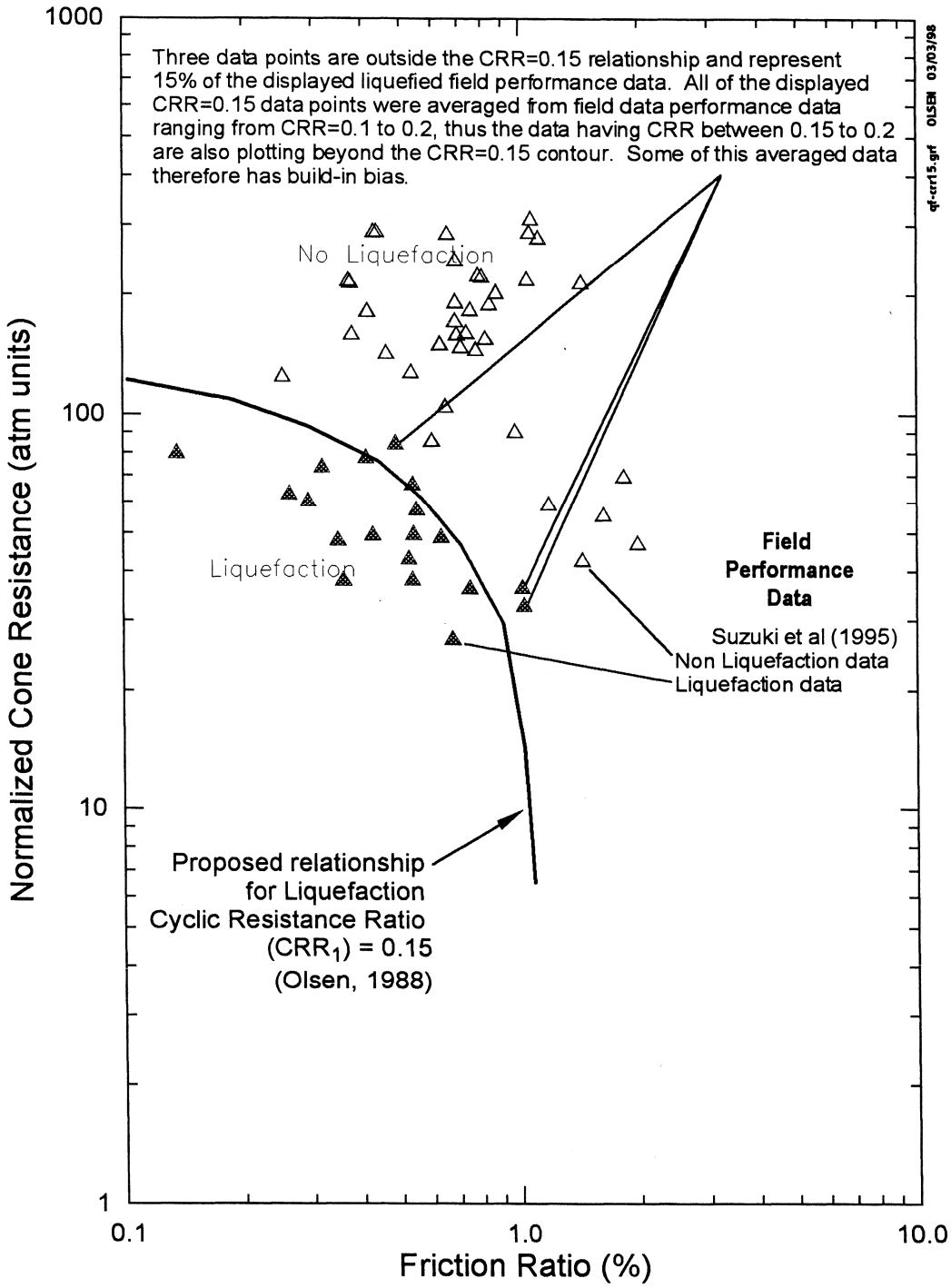

Figure 15 Comparison of CPT soil characterization chart technique (Olsen 1988) to field performance data (Suzuki, et al.. 1995) for a normalized liquefaction cyclic resistance ratio (CRR_1) equal to 0.15. Three of the data points fall outside of the CRR_1=0.15 bounds, most likely because the field performance data is averaged.

Suzuki Field Performance Data to Prove the CPT Soil Characterization Chart Technique

Three of the Suzuki et al (1995) field performance data points plot beyond the CPT soil characterization chart-based CRR_1=0.15 contour in Figure 15. These three data points represent 15% of the 19 liquefied field performance data for CRR_1=0.15. These three points may not represent the critical data point such as from Niigata or San Fernando Dam on the H. Bolton Seed SPT liquefaction potential chart. The CRR_1=0.15 field performance designation represents an average corresponding to data within the range of 0.1 to 0.2. Figure 16 graphically illustrates the probable width of the CRR_1=0.15 designation. The upper end of this CRR_1=0.15 contour has CRR_1 levels from 0.15 to 0.2. It is therefore logical that some of the CRR=0.15 field performance data should plot between the 0.15 and 0.20 contours in Figure 15. The same number of data points from Suzuki also fall outside of the normalized cone resistance versus CRR_1 relationship for clean sand in Figure 7. It therefore appears that these outlying data from Suzuki in Figure 7, Figure 15, and Figure 14 may have built-in conservatism.

New Graphic Format for the CPT Soil Characterization Chart Technique

The CPT soil characterization chart technique for determining liquefaction potential is an unfamiliar format to many geotechnical engineers. A more familiar format might enhance the acceptance of this technique. The CPT soil characterization chart-based technique can be translated to the same graphic format as the standard plot of normalized cone resistance versus CRR_1. Contours of CRR_1 from the CPT soil characterization chart (Figure 10) were transformed into R_f contours on a chart of q_{c1} versus CRR_1 as shown in Figure 17 (Olsen, Koester, and Hynes 1995). This is an exact transformation, either chart (Figure 10 or Figure 17) will estimate the same CRR_1. Liquefaction CRR_1 is estimated (from the vertical axis in Figure 17) by scaling the CPT q_{c1} on the horizontal axis and intersecting the corresponding CPT R_f contour.

Soil classification contours (Olsen and Mitchell 1995) and corresponding CPT estimated fines content (from Figure 3) are shown in Figure 18. The CPT characterization chart technique can be confirmed on a project basis by comparing measured soil classification to the contours of soil classification in Figure 18. Remember, soil samples retrieved several meters from a CPT sounding may not reflect the probed soil.

Figure 19 displays the various cone resistance-based techniques for estimating liquefaction resistance of clean and non clean sands together with the soil characterization chart technique. Measured soil indices are used with the cone resistance-based techniques for estimating liquefaction resistance. Measured soil indices now have a double purpose: 1) to estimate liquefaction resistance using the cone resistance technique (using Figure 19), and/or 2) to confirm the CPT soil characterization chart technique (in Figure 18). These charts allow the results of both techniques to be compared when soil indices are measured.

Figure 20 is a complex compilation including the cone resistance-based technique for estimating liquefaction resistance, the CPT estimated soil types, inferred fines contents trends, and finally

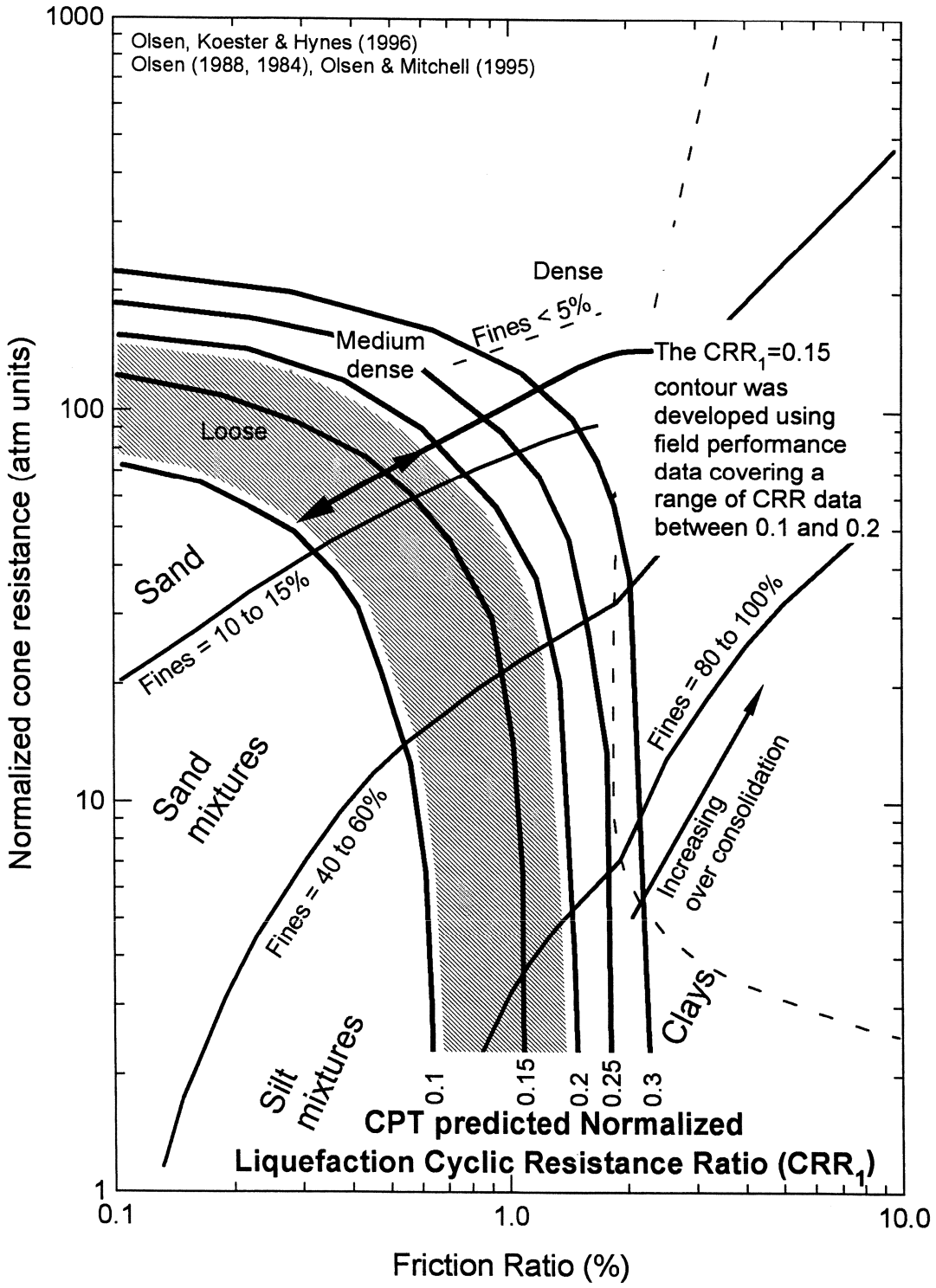

Figure 16 The data range for the CRR_1=0.15 contour which Suzuki, et al (1995) used to establish the CRR_1=0.15 designation.

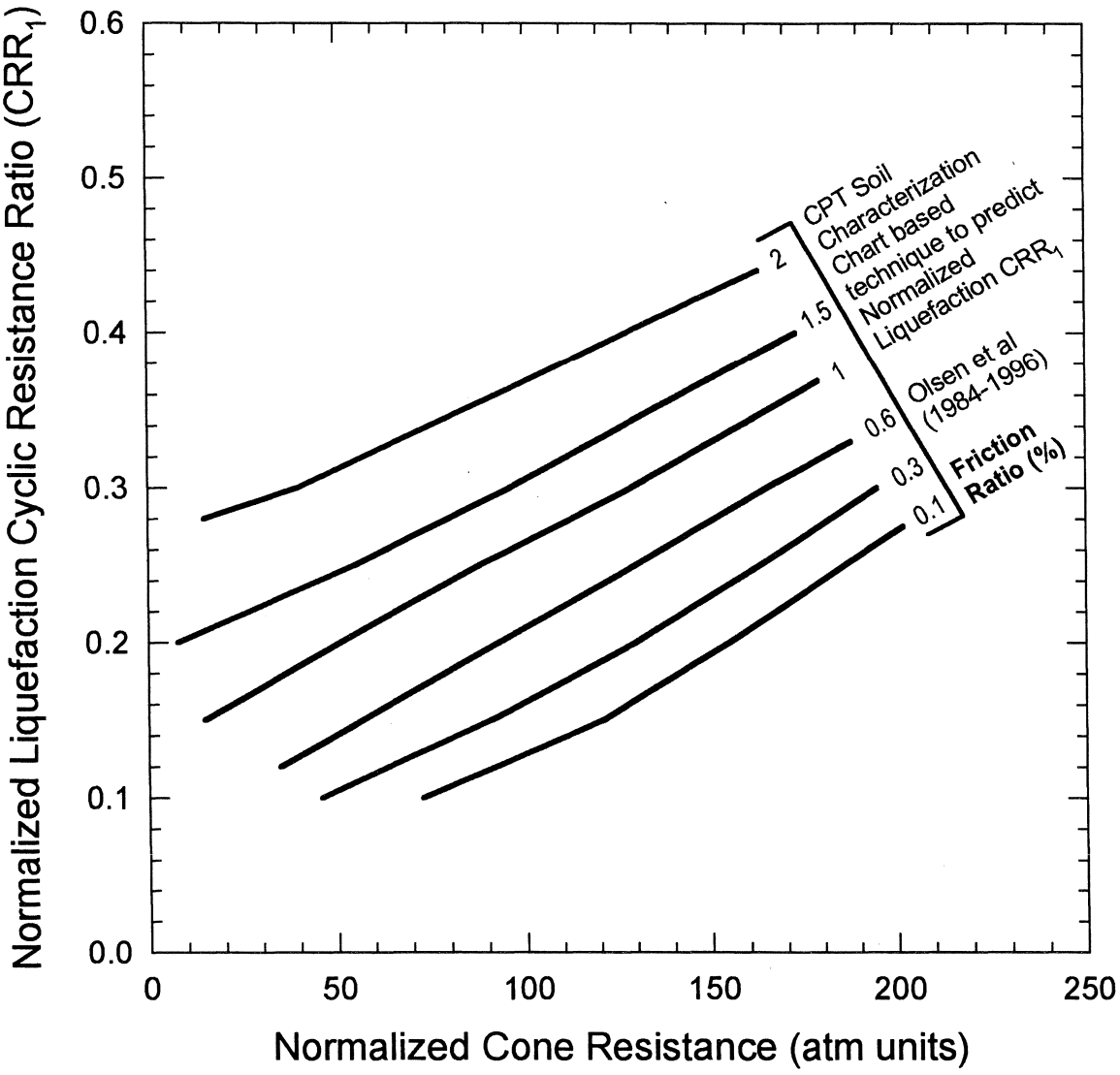

Figure 17 Relationship between the normalized liquefaction cyclic resistance ratio (CRR_1) and normalized cone resistance in terms of the CPT friction ratio contours proposed by Olsen, Koester, and Hynes (1996)..

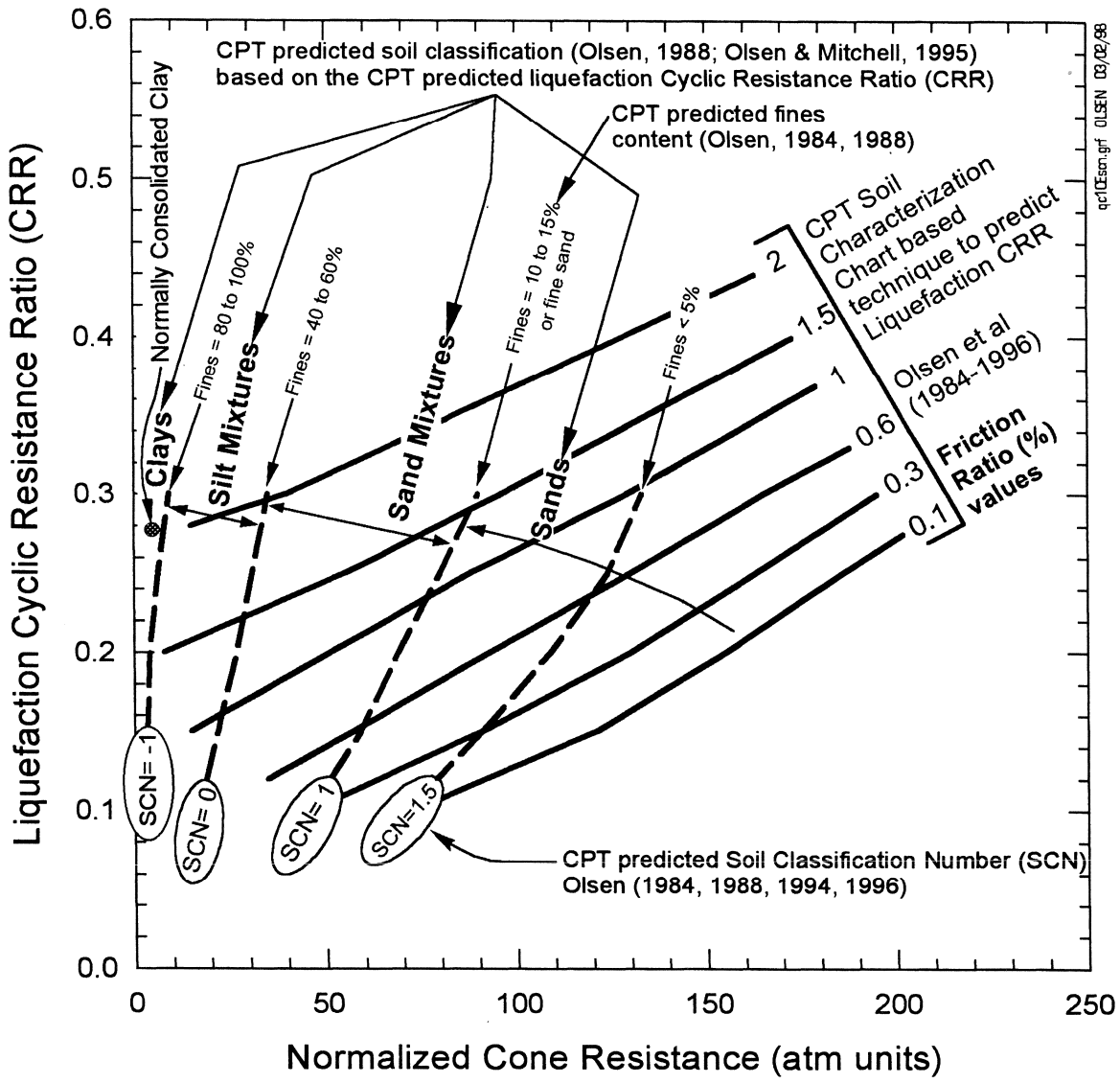

Figure 18 Inclusion of CPT estimated soil classification on the cone resistance versus CRR_1 chart using the CPT soil characterization technique for estimating liquefaction CRR_1

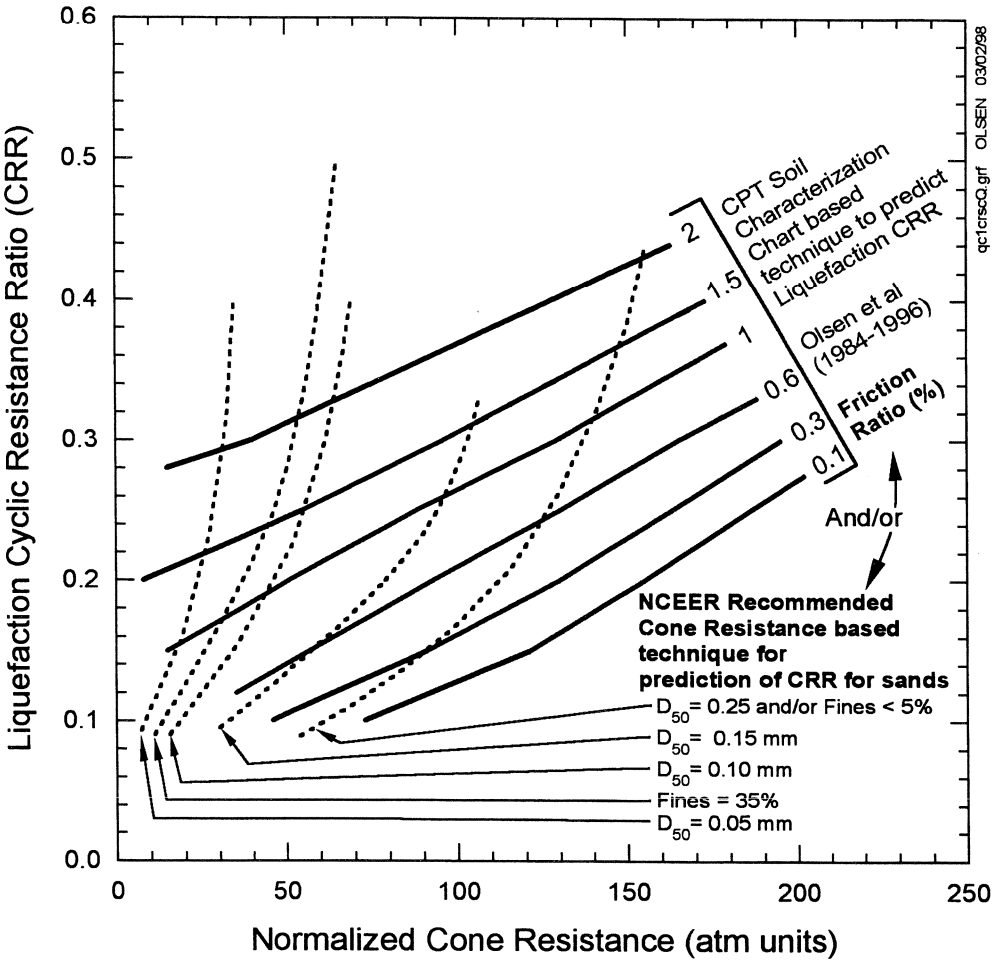

Figure 19 Comparison of the cone resistance based technique and the CPT soil characterization chart based technique on the cone resistance versus CRR_1 chart

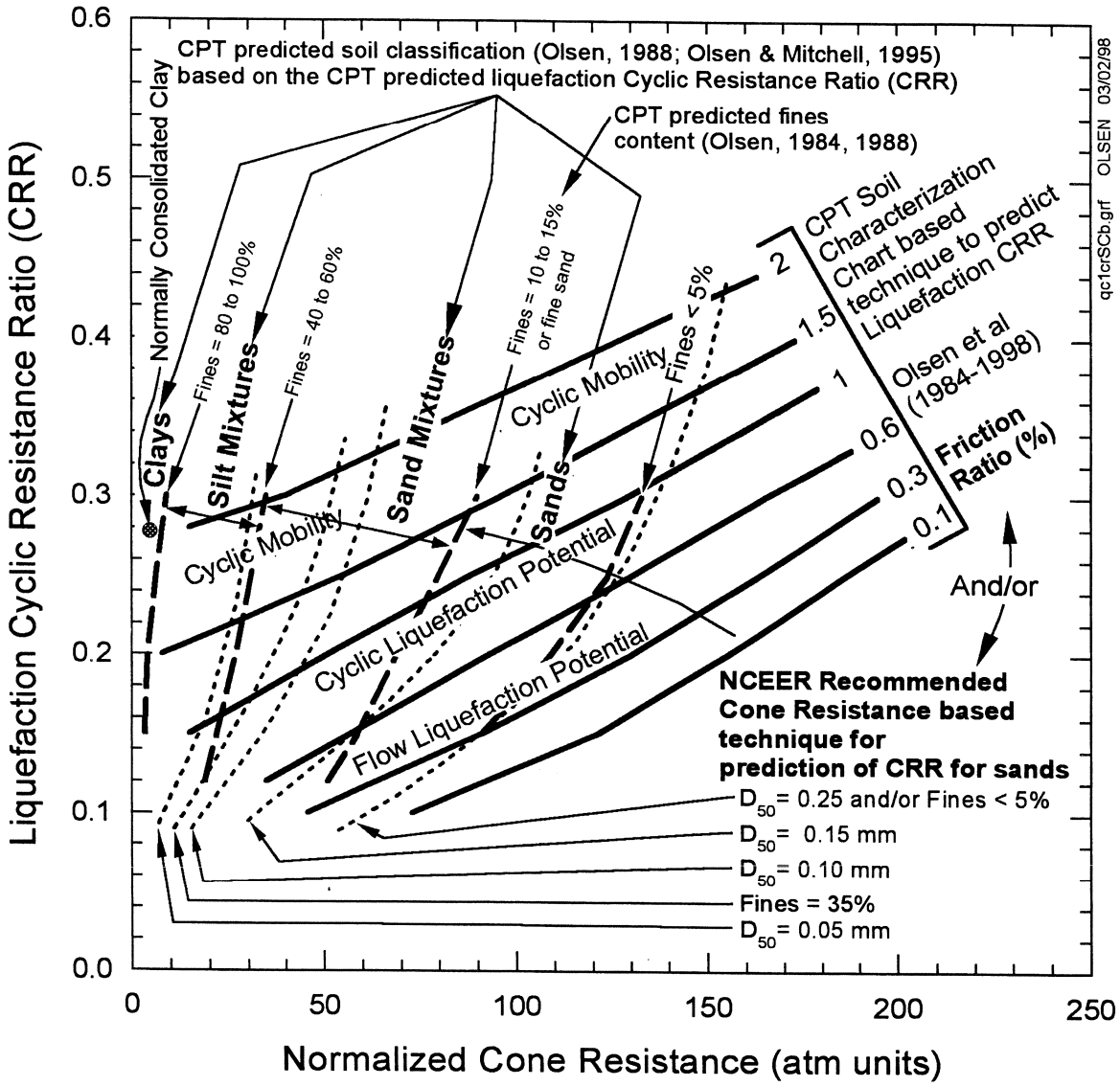

Figure 20 Inclusion of 1) CPT estimated soil type, 2) CPT soil characterization based technique for predicting CRR_1, and 3) the cone resistance technique for estimating CRR_1 on the cone resistance versus CRR_1 chart

friction ratio contours for estimating liquefaction potential using the CPT soil characterization chart technique. Note how the CPT estimated fines contents from the soil classification contours match the contours at different fines contents for the cone resistance-based technique. For example, the soil characterization technique estimated liquefaction resistance contour for "fines < 5%" matches the cone resistance-based contour labeled "D_{50}=0.25 mm or Fines<5%". Also, the cone resistance-based technique contour labeled "Fines=35%" is between the CPT soil characterization contours labeled "Fines= 40 to 60%" and "Fines= 10 to 15%" at high CRR_1 levels. Figure 20 illustrates that the fines content trends with the soil characterization chart technique match the trends from the cone resistance-based technique.

CPT-Based Estimation of Liquefaction CRR_1 Using a Single Equation

Specialized software is required to effectively estimate liquefaction CRR_1 for all data points in a CPT sounding using Figure 10. A single equation was therefore developed which matches all the non-linear contours in Figure 10 and is applicable to all soil types. CPT based estimation of CRR_1 in Figure 10 (or Figure 17) can be approximated and simplified with the following equation:

$$CRR_1 = \left(0.00128 \frac{q_c}{(\sigma_v')^{0.7}} \right) - 0.025 + (0.17 R_f) - (0.028 R_f^2) + (0.0016 R_f^3) \qquad \textbf{(16)}$$

Where

$\frac{q_c}{(\sigma_v')^{0.7}}$ = Generalized normalized cone resistance (q_{c1}) (see Equations 7 and 8)

CRR_1 = Normalized liquefaction cyclic resistance ratio
R_f = Calculated friction ratio (percentage)
q_c = CPT measured cone resistance (in atm units) (1 atm = 100 kPa)
σ_v = Vertical effective stress (in atm units)

Equation 16 is a simplification of Figure 10 because normalization of the CPT cone resistance can be simplified and the CRR_1 curves have been generalized. These assumptions are adequate for non critical conditions and for depths between 5 and 13 meters. The estimated CRR_1 from Equation 16 for clays and clayey silts is more conservative than from Figure 10. This conservatism may flag soil mixture and clay layers as liquefiable and therefore necessitate soil sampling (to determine the liquidity indices or for vane shear testing to determine sensitivity). For deep deposits of clay, the stress normalization portion of this equation generates CRR_1 values too high. The equation is also conservative for overconsolidated conditions. The uniqueness of this technique is that it can estimate CRR_1 for all soil types and now is in an equation form.

Consequence of Liquefaction Resistance as Estimated by the CPT

The consequence of liquefaction can be divided into three broad categories: 1) flow slides, 2) deformation/cracking, and 3) sand boil expression. These categories can be differentiated if they all represent a soil near the bottom toe of a slope. A liquefaction-induced flow slide typically represents 100% pore pressure generation, large strain softening, a dramatic drop in shear strength, and large slope movements. Deformation and cracking of a slope without massive movement suggests that 1) slope movement causes the soil to dilate which increased the soil resistance to movement, or 2) slope movement stopped when the earthquake motions stopped (i.e., Newmark sliding). Sand boil expression on level ground surface reflects grain matrix densification, resulting in water expulsion. Sand boil expression at the bottom of a slope without slope cracking/movement indicates that an isolated liquefied sand zone generated excess pore fluid.

Consequences of liquefaction can be depicted on the CPT soil characterization chart, as shown in Figure 21, based on relative density (for sand) and soil type. Specifically, liquefaction flow potential with large slope movement can occur with very loose sands. Cyclic liquefaction potential (having low slope movement potential) can occur with medium dense sand. Dense sand can experience cyclic mobility where a slight slope movement causes the sand to dilate, resulting in a dramatic strength gain and decrease of slope movement. Finally, cyclic mobility potential with little potential for post earthquake sliding can occur for normally consolidated clays. These trends from cyclic mobility to liquefaction flow potential depicted in Figure 21 are inversely proportional to the CPT friction ratio. The potential for slope movement is low to moderate for R_f=1% and increases to major for R_f=0.2%. This R_f trend to liquefaction flow potential is not dependent on soil type. If a soil layer has a calculated liquefaction factor of safety near or less than 1 then the next step is to check for liquefaction flow potential using the CPT friction ratio. If a soil layer is estimated to liquefy and the friction ratio is low (such as lower than 0.6%), and ground geometry is not level, then there may be potential for slope movement.

Examples of CPT Estimated Liquefaction CRR_1

Examples of the CPT soil characterization technique for estimating liquefaction resistance are shown in the next several figures for sites which have experienced earthquakes. Each chart presents raw CPT data (cone resistance, sleeve friction resistance, and calculated friction ratio) and CPT estimated geotechnical properties (soil classification, liquefaction CRR, and fines content). Also shown are estimates of the average induced-earthquake cyclic stress ratio (CSR) from a recent earthquake for comparison to estimated liquefaction resistance CRR.

The first two examples are for the Moss Land site that experienced liquefaction during the 1989 Loma Prieta earthquake. The first example, in Figure 22, is from Sandholdt Road next to Moss Landing Harbor at CPT sounding UC-4 (data from Boulanger, et al. 1997, Boulanger 1998). Slope inclinometer measurements show that 26 cm of lateral deformations occurred between a

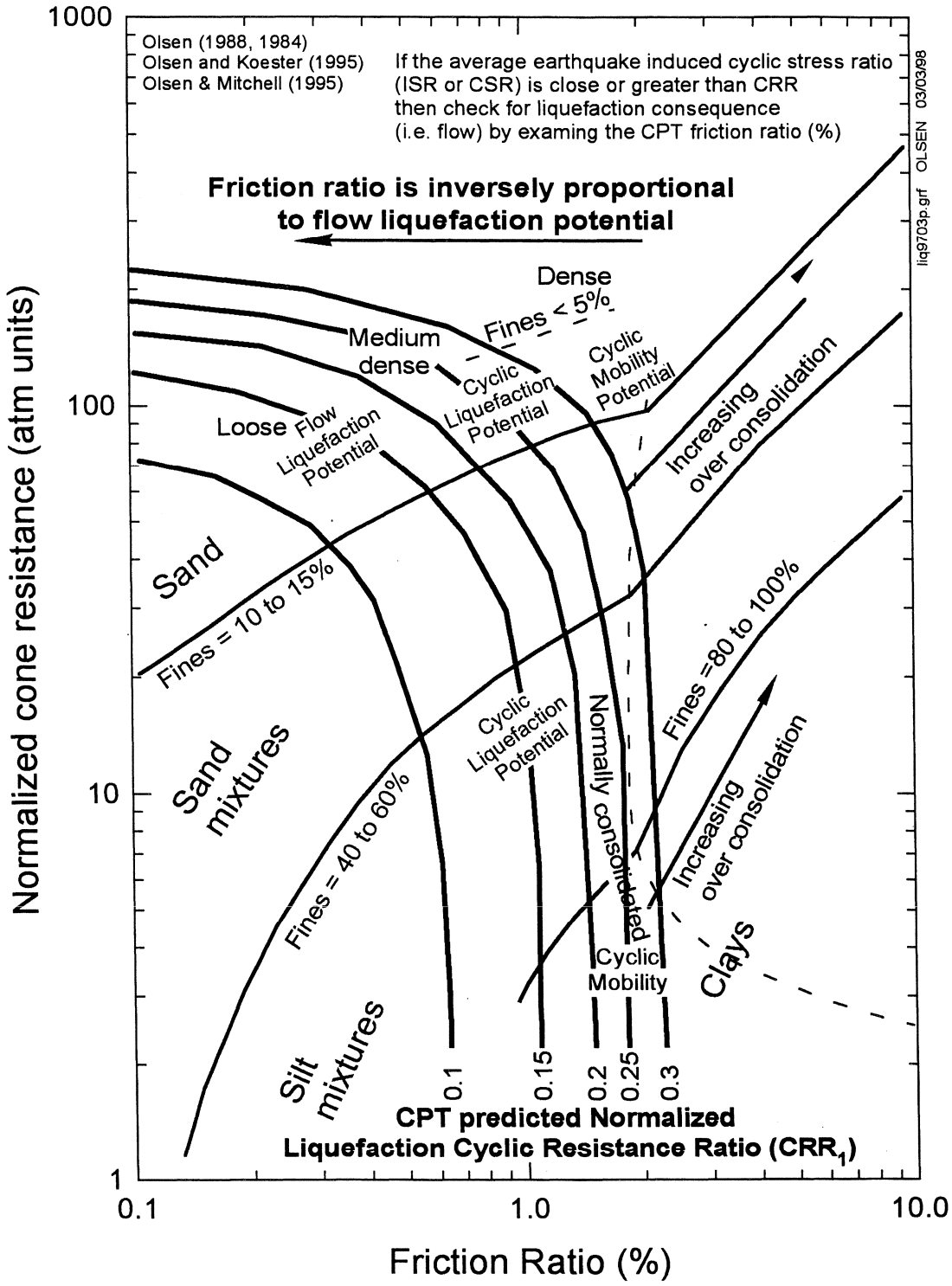

Figure 21 Fully annotated chart for estimating normalized liquefaction cyclic resistance ratio (CRR_1) using the CPT soil characterization chart technique.

depth of 2 and 4.5 meters. Between a depth of 3.5 and 6 meters the earthquake induced CSR is at the low extreme of the CPT estimated CRR range, i.e., marginal liquefaction. This zone is composed of soil mixtures and sand. A relatively clean sand layer at a depth of 4 to 4.5 meters has a friction ratio of 0.2% but a CRR>0.3. It appears that slope movement occurred within this soil mixture soil zone between a depth of 3.5 and 4 meters.

The second example for Moss Landing are three CPT soundings near the Marine laboratory building (adjacent to a volleyball court) as shown in Figure 23 (data from Boulanger, et al. 1997; Boulanger 1998; Youd 1997). Silt was observed in the sand boil expressions next to the volleyball court (Boulanger, et al. 1997). The CPT-estimated data infers extensive liquefaction at numerous depth zones composed of sands and soil mixtures. The excess pore fluid for the sand boil expressions probably originated from the clean sands at a depth of 1.5 to 10+ meters. The soil mixture layer composed of silts to dirty sand located at a depth between 1.5 and 4 meter, were probably liquefied during the earthquake and "dragged" to the ground surface with flow of excess pore fluid from all the liquefied sand layers.

The next example, in Figure 24, is from the USGS Wildlife site, CPT sounding c3g, which experienced sand boil expression on the ground surface and minor lateral spreading (data from Youd 1997). Based on the CPT-estimated data, three soil zones appear to have experienced liquefaction: a thin soil mixture zone layer at 2 meters, a dirty sand zone from 2.5 to 3.6 meters, and clean sand to dirty sand from 5.8 to 6.2 meters. The soil zone at 2.5 to 3.6 meters has a friction ratio less than 0.5% and therefore a high potential for slope movement. Sand boil expression on the ground surface probably originated from a depth of 5 to 6.5 meters because of the low fines content.

Cross Sections of CPT-Estimated Liquefaction resistance

Cross sections of CPT-estimated liquefaction resistance are the ultimate means of evaluating liquefaction potential. Individual depth plots of CPT-based estimation of liquefaction resistance have been the state-of-the-art for some time (Olsen 1988), but individually provide no spatial information. However, cross sections of CPT-estimated liquefaction are the best means of geotechnical site characterization for the purpose of evaluating sand boil expression potential, building foundation instability, and sliding potential. Isolated liquefiable soil lenses at different elevations can be identified with cross sections and are generally not a problem. Continuous liquefiable lenses or layers can be a major stability problem. If a continuous soil layer or zone is estimated to experience liquefaction, then CPT-estimated soil classification (or friction ratio) can be used to estimate the potential for slope movement.

A cross section of CPT-estimated liquefaction resistance for Moss Landing is shown in Figure 25. This cross section was developed using the soil layer tracing technique. Note how continuous soil layers of low liquefaction resistance can be tracked across the site.

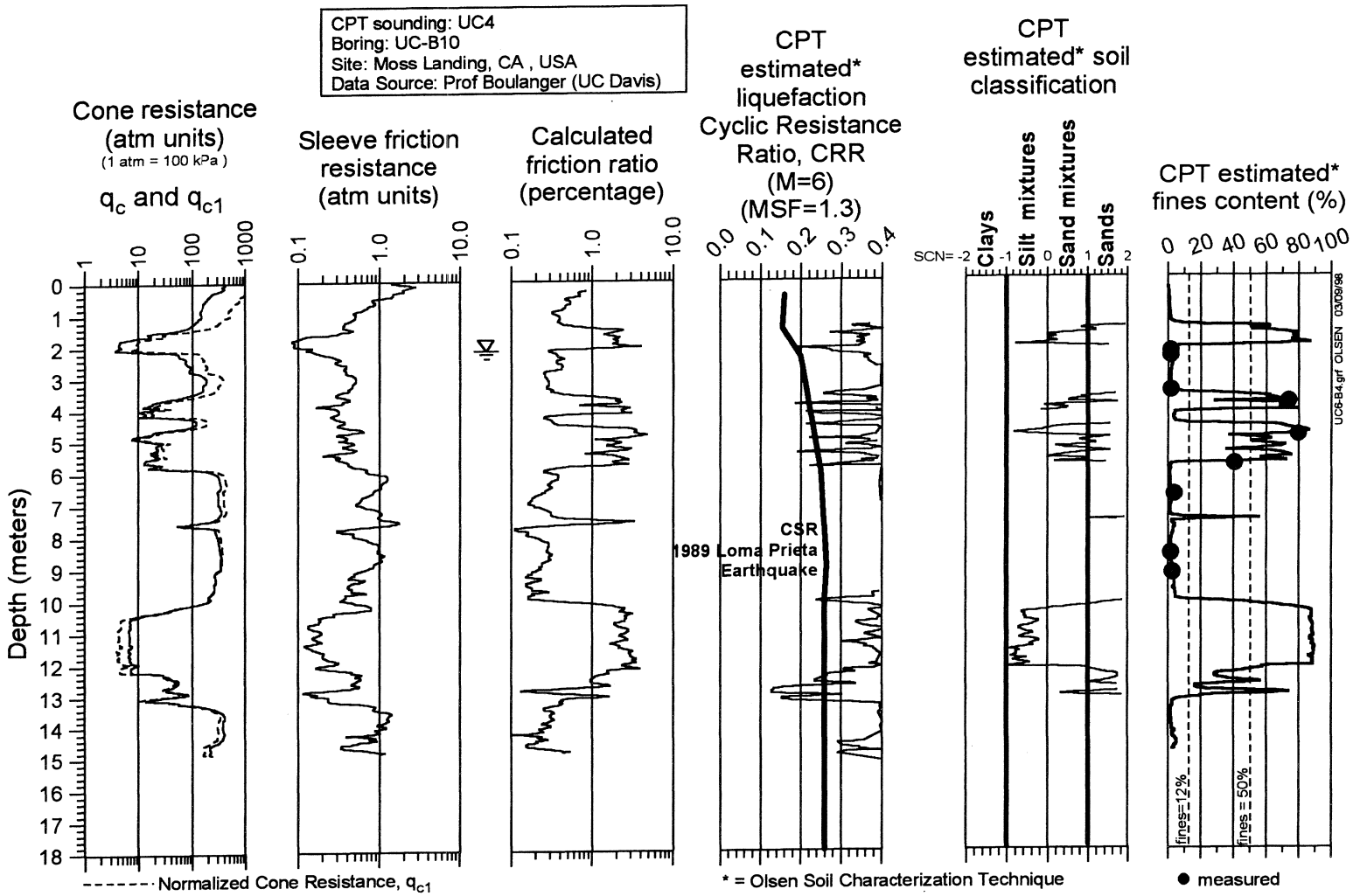

Figure 22 Use of the CPT soil characterization technique for estimating normalized liquefaction cyclic resistance ratio (CRR_1) for CPT soundings UC-4 at Moss Landing which experienced liquefaction and lateral spreading during the 1989 Loma Prieta Earthquake (Data from Boulanger, 1998).

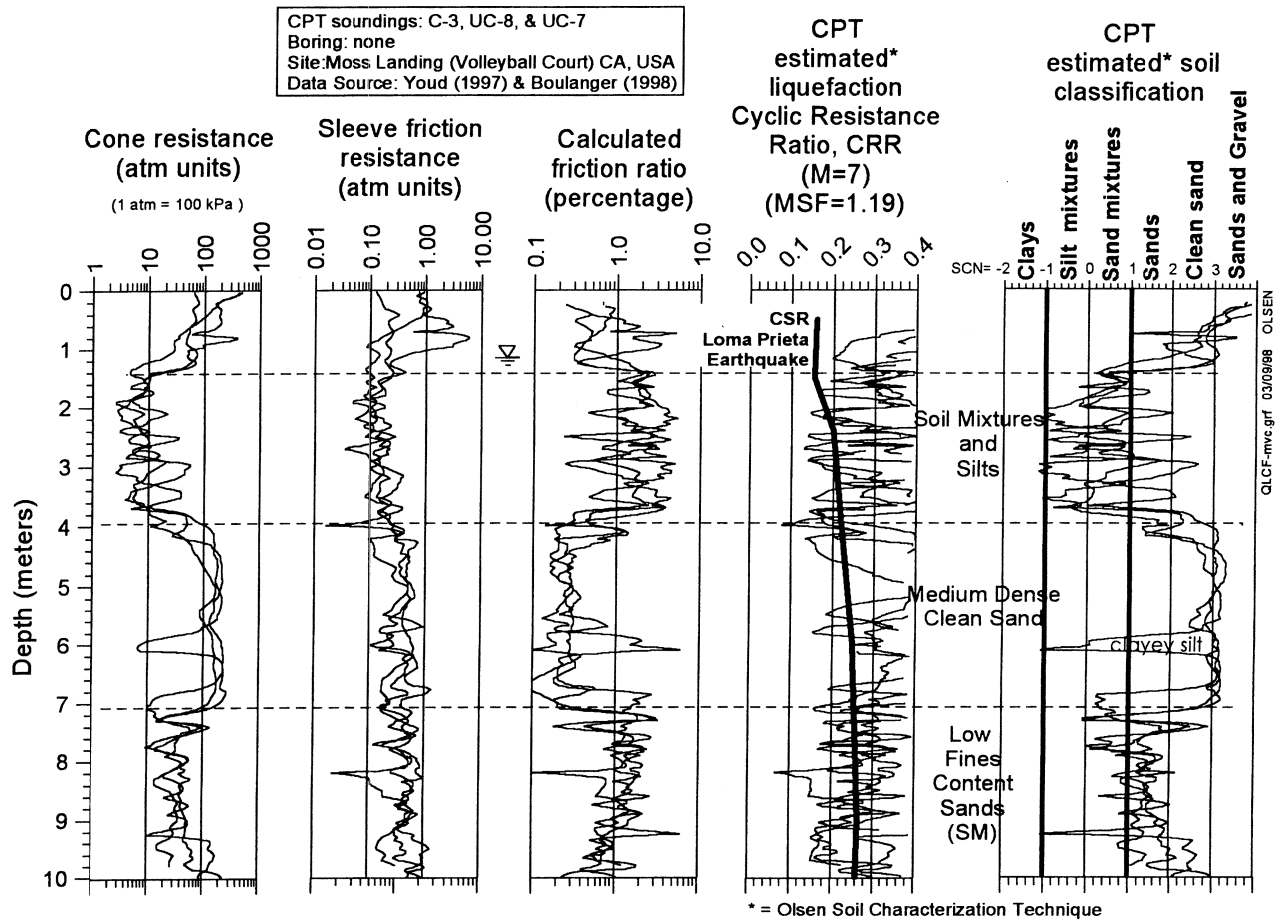

Figure 23 Use of the CPT soil characterization technique for estimating normalized liquefaction cyclic resistance ratio (CRR_1) for three CPT soundings at volleyball court next to the Moss Landing Marine Laboratory where "silt" boil expressions were observed (next to the volleyball court) during the 1989 Loma Prieta Earthquake (Data from Youd 1997 and Boulanger 1998).

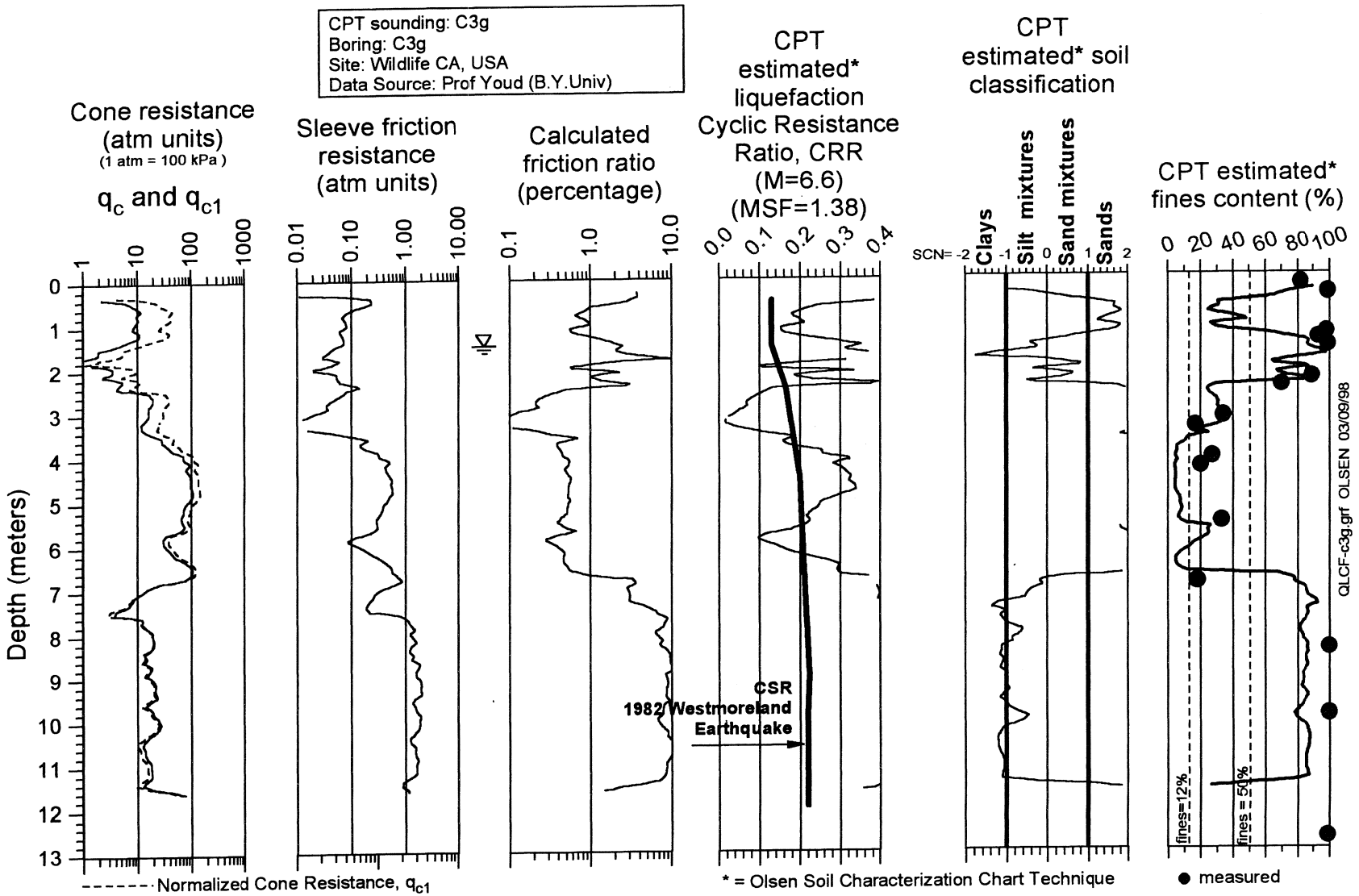

Figure 24 Use of the CPT soil characterization technique for estimating normalized liquefaction cyclic resistance ratio (CRR_1) for CPT soundings c3g at the USGS Wildlife research site which experienced liquefaction (Data from Youd 1997).

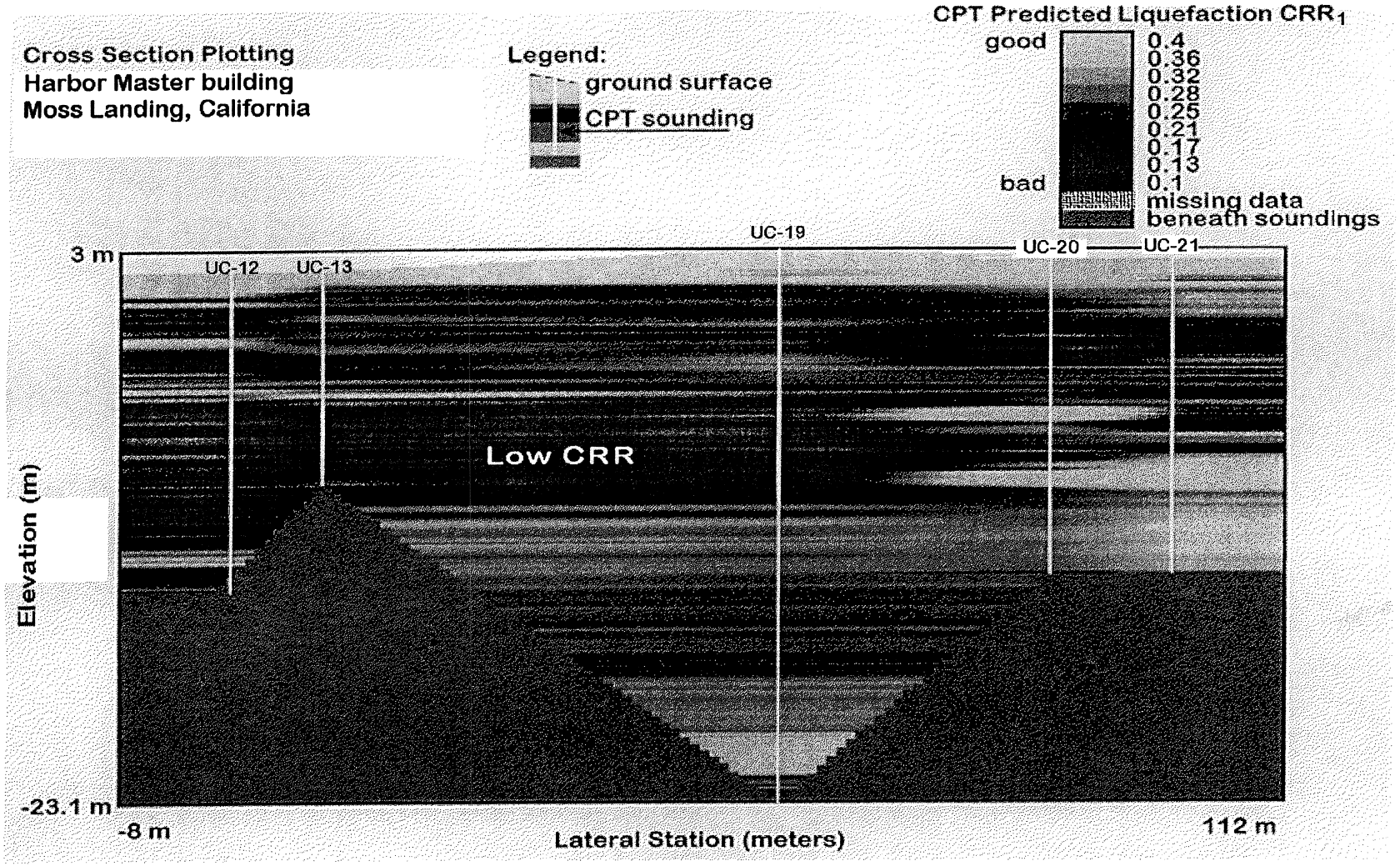

Figure 25 Cross section example (using the soil trace method) of CPT estimated liquefaction resistance for the Harbor Master building area at Moss Landing, California (CPT data from Boulanger 1998).

A Procedure for CPT-Based Estimation of Liquefaction Resistance

This section describes the step by step procedure for using the CPT soil characterization technique to estimate liquefaction potential. Details of this technique are described in the body of this paper.

The two critical parts of this procedure are 1) calculating the normalized CPT cone resistance and 2) estimating the liquefaction resistance using the CPT soil characterization technique. The procedure starts by normalizing the CPT cone resistance to a standard vertical effective stress of 1 atmosphere (atm) (1 atm = 100 kPa ≈ bar ≈ tsf). The next step is CPT-based estimation of normalized liquefaction cyclic resistance ratio (CRR_1) using normalized CPT data for all data in each CPT sounding. The CPT soil characterization technique does not use a silt correction factor to determine an equivalent clean sand cone resistance for the purpose of estimating liquefaction resistance because there is no physical meaning for an equivalent clean value. CRR_1 is then converted to an equivalent liquefaction resistance ratio (CRR) representing the in situ vertical effective stress and for the design earthquake. CRR is then compared to the earthquake induced cyclic shear stress ratio (CSR) to calculate the liquefaction factor of safety and to evaluate soil behavior if liquefaction is predicted to occur.

The seven step procedure is:

1) Determine the earthquake induced cyclic stress ratio (CSR) with the following steps:
   a) Establish the earthquake magnitude (M)
   b) Determine the surface ground acceleration (a_g)
   c) Establish the CSR versus depth profile, by one of two methods:
      i) with software evaluation (such as with SHAKE software), or
      ii) with the r_d technique

2) Estimate CRR_1 using the CPT soil characterization technique.
   This step requires normalizing the CPT cone resistance which is used to estimate the CRR_1 for all data points in a CPT sounding. Using the best available stress normalization technique produces the most accurate predicted value. For many geotechnical situations, an approximating stress normalization techniques will achieve good results. There are numerous techniques for stress normalization of the CPT cone resistance, ranging from constant exponent techniques to the soil characterization chart technique requiring specialized software. The CPT estimated CRR_1 can be accomplished by one of the three following procedures (from a single equation procedure to a technique requiring computer software):

a) CPT-based procedure for estimation of CRR_1 using a generalized equation.
This procedure shown in Equation 16 is a generalization and conservative representation of the CPT soil characterization chart technique shown in Figure 10 (or Figure 17) (and described in item c below). This simplified procedure uses a constant stress exponent of 0.7 (for all soil types) to normalize the cone resistance in Equation 16. This approach can be justified for most non critical liquefaction evaluations and for a vertical effective stress range of 0.8 to 1.3 atm (80 to 130 kPa). This formulation was designed to produce conservative CRR_1 values for clays and silt mixtures when compared to the chart solution in Figure 10. For deep deposits of clay this formulation generates CRR_1 values close to the chart solution.

b) Modification of the simplified equation.
The above procedure can be improved by using more accurate estimates of the stress exponent. For example, the 0.7 stress exponent in Equation 16 can be replaced with soil type dependent exponents, such as 0.6 for sand and 1 for clay. Alternatively, the stress exponent for sands can be estimated using Equation 9 based on the estimated relative density.

c) The CPT soil characterization chart technique for estimating liquefaction resistance.
The CPT soil characterization chart based technique for stress normalization is described by Olsen (1994, 1998, 1995) and Olsen & Mitchell (1995) and requires a software program because it's an iterative technique. This technique is usable for all soil types, strength levels, and confining stress levels.

3) Calculate the CPT soil classification number (SCN) using Equation 11 (see Figure 3). Estimating soil type is as important as estimating liquefaction resistance because soil type controls soil behavior if liquefaction is triggered. The CPT estimated soil classification number (SCN) shown in Figure 3 is an index of soil classification (Olsen and Mitchell 1995) and can be estimated by Equation 11. The SCN was developed to represent unique soil behavior at integer values (i.e., -1, 0, and 1) and is important for liquefaction evaluation. At SCN equal to -1, the soil should have a behavior between that of a silty clay and clayey silt. At SCN equal to 1, the soil should have a classification and behavior between that fine sand and silty sand.

4) Calculate CRR (in situ value) from CRR_1 (normalized value) based on Equation 2 using the Earthquake magnitude scale factor (MSF) (see Equation 3) and K_σ

5) Calculate liquefaction factor of safety ($_{Fsliq}$) using Equation 1.

6) If the FS_{liq} is less than 1.2 then sand boil and slope movement potential should be evaluated using the procedure in Figure 21. If the friction ratio is less than 0.8% and $FS_{liq} < 1.2$ than there is potential for slope movement. If the CPT friction ratio is less than 0.5% and $FS_{liq} < 1.2$ then there is major potential for movement. The potential for sand

boil expression is high when the SCN is high, such as SCN>1. If the SCN is low, such as SCN<0 (i.e. silt to clay), the soil layer should be sampled and evaluated using Liquidity Index criterion (Equation 15) or the strength sensitive determined, such as with the vane shear device. If the earthquake induced stress is greater than the static strength of a normally consolidated soft clay (i.e. large nearby earthquake with CSR=0.28) then the soil can dynamically deform to meet the liquefaction criterion. Any continuous low FS_{liq} soil layer should be independently sampled, using SPT procedures, to at least verify CPT predicted SPT values and gradation characteristics.

7) The CPT estimated data should then be displayed in a depth or elevation format such as shown in Figure 24. CPT soundings should be positioned along strings (Olsen and Farr, 1986) with the CPT estimated CRR_1 shown in cross sections such as shown in Figure 25.

Conclusions

The CPT soil characterization-based chart technique for estimating liquefaction resistance of any soil type is shown in Figure 10 (or Figure 17) and can be expressed by Equation 16. This technique is comprehensive, technically mature, and well published and was developed based on many contributing factors. Numerous stress normalization techniques were described in this paper for calculating the normalized CPT cone resistance. The criticalness of the structure should dictate which stress normalization technique is required. Estimated liquefaction resistance based on the CPT characterization chart technique can be confirmed on a project basis by comparing measured fines content to the CPT-estimated fines contents from the CPT soil characterization chart in Figure 3. The best means of verifying the CPT soil characterization chart approach is if CPT-predicted SPT (using Figure 11) matches field measured values. The uniqueness of this technique is that both CPT measurements are used to estimate liquefaction resistance for all soil types, all strength levels, and for all overburden stresses. All other techniques require estimating the soil fines content, calculating a silt correction factor in order to determine the equivalent clean sand value which is then used to estimate liquefaction resistance using equivalent clean relationships. There is no physical or theoretical meaning for the equivalent clean sand value; it's just a convenience for determining liquefaction resistance of non clean sands. The CPT soil characterization technique directly estimates liquefaction resistance using both CPT strength measurements because these measurements are unique.

References

Boulanger, R.W., Mejia, L.H., and Idriss, I.M. (1997) "Liquefaction at Moss Landing during Loma Prieta Earthquake," Journal of Geotechnical and Geoenvironmental Engineering, ASCE, May 1997, 123 (5), pg 454-467

Boulanger, R.W. (1998). Personal communication to R.S.Olsen (CPT and SPT data for Moss Landing).

Casagrande, Arthur. (1932) "The structure of clay and its importance in foundation engineering," Contributions to Soil Mechanics 1925-1940, Boston Society of Civil Engineers, pg 257-276.

Campanella, R. G. and Robertson, P. K. (1984). "A seismic cone penetrometer to measure engineering properties of soil," 54th Annual International Meeting and Exposition of the Society of Exploration Geophysicists, Atlanta, GA, pg 138-141.

Douglas, B.J., Olsen R.S., and Martin, G.R. (1981). "Evaluation of the cone penetrometer test for SPT liquefaction assessment." *Proceedings of in situ testing to evaluate liquefaction susceptibility*, ASCE: New York.

Douglas, B. J., and Olsen, R. S. (1981). "Soil classification using the electric cone penetrometer," *Proceedings of a Session Entitled Cone Penetration Testing and Experience* - ASCE Fall Convention, ASCE, New York, 209-227.

Douglas, B. J., Olsen R. S., and Martin, G. R. (1981). "Evaluation of the Cone Penetrometer Test for SPT Liquefaction Assessment," *Proceedings of In Situ Testing to Evaluate Liquefaction Susceptibility*, ASCE, New York.

Marcuson, S.F. III and Bieganousky, W.A. (1977), "SPT and Relative Density in Coarse Sands," Journal of Geotechnical Engineering Division, ASCE, Vol. 103, No. GT11, pp. 1295-1309.

Martin, G. R., and Douglas, B. J. (1980). "Evaluation of the Cone Penetrometer for Liquefaction Hazard Assessment," for U.S. Geological Survey, Contract No. 14-08-0001-17790, October, Project No. 79-153, Long Beach, CA.

Olsen, R.S. (1996) "The influence of confining stress on Liquefaction Resistance", US-Japan workshop on Advanced Research on Earthquake Engineering for Dams, at Waterways Experiment Station, Vicksburg, MS, Nov 12-14, 1996.

Olsen, R.S., Koester, J.P., and Hynes, M.E. (1996) "Evaluation of Liquefaction Potential using the CPT", Proceedings of the 28th Joint meeting of the US-Japan Cooperative Program in Natural Resources - Panel on Wind and Seismic Effects, U.S. National Institute of Standards and Technology, Gaithersburg, Maryland, May 1996

Olsen, R.S. and Mitchell, J.K. (1995) "CPT Stress Normalization and Prediction of Soil Classification", Proceedings of the International Symposium on Cone Penetrometer Testing - CPT'95, Linkoping, Sweden, October 1995

Olsen, R.S. and Koester, J.P. (1995) "Prediction of Liquefaction Resistance using the CPT", Proceedings of the International Symposium on Cone Penetrometer Testing - CPT'95, Linkoping, Sweden, October 1995

Olsen, R.S. (1994) "Normalization and Prediction of Geotechnical Properties using the Cone

Penetrometer Test", Technical Report GL-94-29, USAE Waterways Experiment Station, Vicksburg, MS 39180, August 1994

Olsen, R.S. (1994) "Normalization and Prediction of Geotechnical Properties using the Cone Penetrometer Test (CPT)", Ph.D. Dissertation submitted to the University of California, Berkeley, May 1994

Olsen, R.S. (1988) "Using the CPT for dynamic site response characterization". *Proceedings of the Earthquake Engineering and Soil Dynamic II Conference*, Geotechnical Special Publication Number 2, ed. J. Lawrence Von Thun, 374-388. ASCE: New York.

Olsen, R.S. (1988) "Soil classification and site characterization using the cone penetrometer test" *Proceedings of the First International Symposium on Penetration Testing (ISOPT-1)*, ed. J. de Ruiter, 887-893. A. A. Balkema: Rotterdam, Netherlands.

Olsen, R. S. and Farr, J. V. (1986) "Site Characterization using the Cone Penetrometer Test," Proceedings of In Situ 86 - Use of In Situ Tests in Geotechnical Engineering, Geotechnical Special Publication Number 6, S. P. Clemence, ed., ASCE, New York, pg 854-868.

Olsen, R.S. (1984) "Liquefaction analysis using the cone penetrometer test" *Proceedings of the Eighth World Conference on Earthquake Engineering*, Volume III, 247-254. Prentice-Hall Inc.: Englewood Cliffs, NJ.

Robertson, P. K. (1982) "In-Situ Testing of Soil with Emphasis on its application to Liquefaction Assessment," Ph.D. Dissertation submitted to the University of British Columbia, December, 1982

Robertson, P. K., Campanella, R. G., Gillespie D., and Greig, J. (1986). "Use of Piezometer Cone Data," Proceedings of In Situ 86 - Use of In Situ Tests in Geotechnical Engineering, Geotechnical Special Publication Number 6, S. P. Clemence, ed., ASCE, New York, 1263-1280.

Robertson, P. K. and Campanella, R. G. (1983). "Interpretation of Cone Penetration Tests - Part I (Sand)," Canadian Geotechnical Journal, Vol. 20, No. 4, pp. 734-745.

Robertson, P. K. and Campanella, R. G. (1983). "Interpretation of Cone Penetration Tests - Part 11 (Clay)," Canadian Geotechnical Journal, Vol. 20, No. 4.

Robertson, P. K., Campanella, R. G., and Wightman, A. (1983). "SPT-CPT Correlations," Journal of the Geotechnical Division, ASCE, Vol. 109, November.

Schmertmann, J. H. (1976). "Predicting the q_c/N Ratio," Final Report D-636, Engineering and Industrial Experiment Station, Department of Civil Engineering, University of Florida, Gainesville.

Schmertmann, J. H. (1978a). "Guidelines for Cone Penetration Test, Performance and Design," U.S. Department of Transportation, Federal Highway Administration, Report FHWA-TS-78-209, Washington, July 1978, 145 pgs.

Schmertmann, J. H. (1978b). "Study of Feasibility of Using Wissa-Type Piezometer Probe to Identify Liquefaction Potential of Saturated Sands," U.S. Army Engineer Waterways Experiment Station, Report S-78-2.

Schmertmann, J. H. (1979a). "Statics of SPT," Journal of the Geotechnical Engineering Division, ASCE, Vol. 105, No. GT5, May.

Schmertmann, J. H. (1979b). "Energy Dynamics of SPT," Journal of the Geotechnical Engineering Division, ASCE, Vol. 105, No. GT8, August.

Seed, H. B. (1976). "Evaluation of Soil Liquefaction Effects on Level Ground During Earthquakes," Liquefaction Problems in Geotechnical Engineering, ASCE Preprint 2752, Philadelphia, PA.

Seed, H. B. and De Alba, P. (1986). "Use of SPT and CPT tests for evaluating the liquefaction resistance of soils," Proceedings of the Specialty Conference on the Use of In Situ Tests in Geotechnical Engineering, Blacksburg, VA, ASCE Geotechnical Special Publication No. 6, pp. 120-134.

Seed, H. B. and Idriss, I. M. (1970). "Soil Moduli and Damping Factors for Dynamics Response Analysis," Report No. EERC 70-10, Univ. of California, Berkeley, December.

Seed, H. B. and Idriss, I. M. (1981). "Evaluation of Liquefaction Potential of Sand Deposits Based on Observations of Performance in Previous Earthquakes," Geotechnical Engineering Division, ASCE National Convention, St. Louis, Session No. 24.

Seed, H. B. and Idriss, I. M. (1982). *Ground Motions and Soil Liquefaction during Earthquakes*, Earthquake Engineering Research Institute, Berkeley, CA.

Seed, H. B., Idriss, I. M. and Arango, T. (1983). "Evaluation of Liquefaction Potential Using Field Performance Data," Journal of Geotechnical Engineering Division, ASCE, Vol. 109, No. 3, March 1983, pp. 458-492.

Seed, H. B., Seed, R. B., Harder, L. F., and Jong, H. L. (1988). "Re-Evaluation of the Slide in the Lower San Fernando Dam in the Earthquake of February 9, 1971," Report No. UCB/EERC-88/04, April, Earthquake Engineering Research Center, University of California at Berkeley, Berkeley, CA.

Seed, H. B., Seed, R. B., Harder, L. F., and Jong, H. L. (1989). "Re-Evaluation of the Lower San Fernando Dam - Report 2 - Examination of the Post-Earthquake Slide of February 9, 1971,"

Contract Report GL-89-2, U.S. Army Engineer Waterways Experiment Station, Vicksburg, MS.

Skempton, A.W. (1986) "Standard Penetration Test Procedures and the Effects in Sands of Overburden Pressure, Relative Density, Particle Size, Aging, and Over consolidation," Geotechnique, Vol. 36, No. 3, pp 425-447.

Suzuki, Y., Tokimatsu, K., Koyamada K., Taya, Y., Kurbota, Y. (1995) "Field Correlation of Soil Liquefaction based on CPT Data," Proceedings of the International Symposium on Cone Penetrometer Testing - CPT'95", Linkoping, Sweden, October 1995.

Suzuki, Y., Koyamada K., Tokimatsu, K., Taya, Y., Kurbota, Y. (1995) "Empirical Correlations of Soil Liquefaction based on Cone Penetrometer Test," First International Conference on Earthquake Geotechnical Engineering", K. Ishihara Editor, 1985.

Youd, T.L. and Idriss, I. M. editors. (1998) "Workshop on Evaluation of Liquefaction Resistance," Proceedings of a 4-5 January 1996 workshop, sponsored by FHWA, NSF and WES, to be published by the National Center for Earthquake Engineering Research, Salt Lake City.

Youd, T.L. (1997). Personal communications to R.S. Olsen (CPT data for several sites)

Appendix A
List of Participants

Chair of Workshop
T. Leslie Youd
368 CB
Brigham Young University
Provo, UT 84602

Co-Chair of Workshop
Izzat M. Idriss
P.O. Box 330
Davis, CA 95617-0330

Participants
Ronald D. Andrus
Research Civil Engineer
NIST
Bldg and Fire Rsrch Lab
Bldg 226, Room B158
Gaithersburg, MD 20899

Ignacio Arango
22 Bowling Drive
Oakland, CA 94618

Gonzalo Castro
GEI Consultants, Inc.
1021 Main Street
Winchester, MA 01890

John T. Christian
Consulting Engineer
23 Fredana Road
Waban, MA 02168-1103

Ricardo Dobry
Rensselaer Polytechnic Institute
Civil & Environmental Engineering
JEC 4040
Troy, NY 12180-3590

W.D. Liam Finn
University of British Columbia
Civil Engineering Department
2324 Main Mall
Vancouver, BC
CANADA V6T 1Z4

Leslie F. Harder
California Dept. of Water Res.
P.O. Box 942836
Sacramento, CA 94236-0001

Mary Ellen Hynes
Earthquake Engr. and Geo. Div.
Waterways Experiment Station
3909 Halls Ferry Road
Vicksburg, MS 39180-6199

Kenji Ishihara
2415-123 Nara-cho
Aoba-ku, Yokohama 123
JAPAN

Sam Liao
Parsons Brinkerhoff
One South Station
Boston, MA 02110

William F. Marcuson, III
Geotech Lab
USAE Waterways Experimental Station
3909 Halls Ferry Road
Vicksburg, MS 39180-6199

Geoffrey R. Martin
University of Southern California
Civil Engineering Department
Los Angeles, CA 90089-2531

James K. Mitchell
Virginia Tech
Civil Engineering Department
Patton Hall
Blacksburg, VA 24061

Yoshiharu Moriwaki
Woodward-Clyde Consultants
2020 E. First Street, Suite 400
Santa Ana, CA 92705

Maurice S. Power
Geomatrix Consultants
100 Pine St., Suite 1000
San Francisco, CA 94111

P.K. Robertson
University of Alberta
Department of Civil Engineering
Edmonton
CANADA T6G 2G7

Raymond Seed
University of California
Department of Civil Engineering
434C Davis Hall
Berkeley, CA 94720

Kenneth H. Stokoe
University of Texas
Civil Engineering Department
Austin, TX 78712

Appendix B
Workshop Agenda

WORKSHOP ON EVALUATION OF LIQUEFACTION RESISTANCE
The Inn at Temple Square
Salt Lake City, Utah, January 4 and 5, 1996
Chair: T.L. Youd, Co-Chair: I.M. Idriss

FINAL AGENDA

January 4, 1996

8:00 am	Opening Ceremonies	East Brunswick Room
	Conducting:	Les Youd, Brigham Young University
	Opening Remarks:	Geoff Martin, USC
	Keynote Remarks:	I.M. Idriss, University of Calif. at Davis
	Keynote Remarks:	Les Youd
8:20 am	Special Lecture	Liquefaction Lessons Learned from Recent Earthquakes In Japan - Kenji Ishihara, Science University of Tokyo
8:50 am	Topic 1: Liquefaction Resistance Criteria Based on Cone Penetration Measurements	
	Session Moderator:	John Christian
	Presenter:	Peter Robertson, University of Alberta
	Discussion:	James Mitchell, Virginia Tech
	Discussion:	Mary Ellen Hynes, Corps of Engineers
	Discussion:	Yoshi Moriwaki, Woodward-Clyde Consultants
	Open Discussion:	
	Consensus Building:	Maury Power, Geomatrix
10:40 am	Break	
10:50 am	Topic 2: Liquefaction Resistance Criteria Based on Standard Penetration (SPT) Measurements, Including the Influence of Fines Content	
	Session Moderator:	I.M. Idriss
	Presenter:	Peter Robertson, University of Alberta
	Discussion:	Ricardo Dobry, Rensselaer Polytechnic Institute
	Discussion:	John Christian, Private Consultant
	Discussion:	Gonzalo Castro, GEI, Inc.
	Open Discussion:	
	Consensus Building:	Bill Marcuson

12:30 pm Lunch

1:15 pm Topic 3: Criteria Based on Probabilistic Evaluation of SPT Measurements

Session Moderator:	Ricardo Dobry
Presenter:	Les Youd, BYU
Discussion:	Sam Liao, Parsons Brinkerhoff
Discussion:	I.M. Idriss, University of Calif. at Davis
Discussion:	Bill Marcuson, Corps of Engineers
Open Discussion:	

3:15 Break

3:40 pm Topic 4: Magnitude Scaling Factors

Session Moderator	Ricardo Dobry
Presenter:	Les Youd, BYU
Discussion:	Ignacio Arango, Bechtel
Discussion:	I.M. Idriss, UCD
Discussion:	Liam Finn, UBC
Open Discussion:	
Consensus Building: (Topics 3 and 4)	John Christian

5:30 pm End Day-1 Discussions

6:30 pm Dinner at a local restaurant
Informal after-dinner group discussions at various localities in hotel

January 5

8:00 am Opening Remarks Day-2: Les Youd

8:05 am Topic 5: Criteria Based on Measured Shear Wave Velocity

Session Moderator	Liam Finn
Presenter:	Ron Andrus, NIST
Discussion:	Ken Stokoe, Univ. of Texas at Austin
Discussion:	Peter Robertson
Discussion:	Yoshi Moriwaki
Open Discussion:	
Consensus Building:	Ricardo Dobry

10:00 am Break

10:20 am Topic 6: Criteria Based on Becker Hammer Measurements

Session Moderator:	Jim Mitchell
Presenter:	Les Harder, Calif. Division of Water Resources
Discussion:	Mary Ellen Hynes
Discussion:	Ron Andrus
Discussion:	I.M. Idriss
Open Discussion:	
Consensus Building:	Liam Finn

12:00 pm Lunch

12:45 pm Topic 7: Correction Factors, K_α, K_σ, age of deposit, etc.

Session Moderator	Yoshi Moriwaki
Presenter:	Les Harder
Discussion:	Ignacio Arango
Discussion:	Ray Seed
Discussion:	Maury Power
Open Discussion:	
Consensus Building:	Jim Mitchell

2:10 pm Break

2:30 pm Topic 8: Estimates of Peak Acceleration and Magnitude

Session Moderator:	Maury Power
Presenter:	Les Youd
Discussion:	Bill Marcuson
Discussion:	Liam Finn
Discussion:	Ignacio Arango
Open Discussion:	
Consensus Building:	Yoshi Moriwaki

3:45 pm Closing Remarks:

Summary and Research Needs Identified:	Geoff Martin
Summary and Guidance for Final Report:	Sam Liao
Summary and Guidance for Final Report:	I.M. Idriss
Final Comments and Appreciation:	Les Youd

4:30 pm Workshop Adjourns

Appendix C
Definitions of Terms

Definitions

Although definitions were not a major topic at the workshop, clarification of a few terms is necessary for communication and for incorporation of new information and methods into the simplified procedure. Three definitions widely used in the report are listed below. Other definitions are listed by authors of various sections to clarify their use of terms.

Liquefaction: The term liquefaction as used in this report refers to a change of state from a solid granular material to a dense viscous-like liquid without consideration of possible deformation or instability of the liquefied material. Thus, evaluation of liquefaction resistance as used herein refers to the determination of the capacity of a soil to resist this change of state, or in other words triggering of the liquefied condition.

Cyclic Stress Ratio (CSR): As used in the original development of the simplified procedure, the term cyclic stress ratio (CSR) refers to both the cyclic stress ratio generated by the earthquake and the cyclic stress ratio required to generate a change of state in the soil to a liquefied condition. To avoid confusion between these two uses, cyclic stress ratio in this report refers only to the cyclic stress ratios generated by the earthquake.

Cyclic Resistance Ratio (CRR): The stress ratio required to cause a change of state of the soil to a liquefied condition is referred to throughout this report as the cyclic resistance ratio (CRR). This change of terminology is recommended for standard use in engineering practice.

NATIONAL CENTER FOR EARTHQUAKE ENGINEERING RESEARCH
LIST OF TECHNICAL REPORTS

The National Center for Earthquake Engineering Research (NCEER) publishes technical reports on a variety of subjects related to earthquake engineering written by authors funded through NCEER. These reports are available from both NCEER Publications and the National Technical Information Service (NTIS). Requests for reports should be directed to NCEER Publications, National Center for Earthquake Engineering Research, State University of New York at Buffalo, Red Jacket Quadrangle, Buffalo, New York 14261. Reports can also be requested through NTIS, 5285 Port Royal Road, Springfield, Virginia 22161. NTIS accession numbers are shown in parenthesis, if available.

NCEER-87-0001 "First-Year Program in Research, Education and Technology Transfer," 3/5/87, (PB88-134275, A04, MF-A01).

NCEER-87-0002 "Experimental Evaluation of Instantaneous Optimal Algorithms for Structural Control," by R.C. Lin, T.T. Soong and A.M. Reinhorn, 4/20/87, (PB88-134341, A04, MF-A01).

NCEER-87-0003 "Experimentation Using the Earthquake Simulation Facilities at University at Buffalo," by A.M. Reinhorn and R.L. Ketter, to be published.

NCEER-87-0004 "The System Characteristics and Performance of a Shaking Table," by J.S. Hwang, K.C. Chang and G.C. Lee, 6/1/87, (PB88-134259, A03, MF-A01). This report is available only through NTIS (see address given above).

NCEER-87-0005 "A Finite Element Formulation for Nonlinear Viscoplastic Material Using a Q Model," by O. Gyebi and G. Dasgupta, 11/2/87, (PB88-213764, A08, MF-A01).

NCEER-87-0006 "Symbolic Manipulation Program (SMP) - Algebraic Codes for Two and Three Dimensional Finite Element Formulations," by X. Lee and G. Dasgupta, 11/9/87, (PB88-218522, A05, MF-A01).

NCEER-87-0007 "Instantaneous Optimal Control Laws for Tall Buildings Under Seismic Excitations," by J.N. Yang, A. Akbarpour and P. Ghaemmaghami, 6/10/87, (PB88-134333, A06, MF-A01). This report is only available through NTIS (see address given above).

NCEER-87-0008 "IDARC: Inelastic Damage Analysis of Reinforced Concrete Frame - Shear-Wall Structures," by Y.J. Park, A.M. Reinhorn and S.K. Kunnath, 7/20/87, (PB88-134325, A09, MF-A01). This report is only available through NTIS (see address given above).

NCEER-87-0009 "Liquefaction Potential for New York State: A Preliminary Report on Sites in Manhattan and Buffalo," by M. Budhu, V. Vijayakumar, R.F. Giese and L. Baumgras, 8/31/87, (PB88-163704, A03, MF-A01). This report is available only through NTIS (see address given above).

NCEER-87-0010 "Vertical and Torsional Vibration of Foundations in Inhomogeneous Media," by A.S. Veletsos and K.W. Dotson, 6/1/87, (PB88-134291, A03, MF-A01). This report is only available through NTIS (see address given above).

NCEER-87-0011 "Seismic Probabilistic Risk Assessment and Seismic Margins Studies for Nuclear Power Plants," by Howard H.M. Hwang, 6/15/87, (PB88-134267, A03, MF-A01). This report is only available through NTIS (see address given above).

NCEER-87-0012 "Parametric Studies of Frequency Response of Secondary Systems Under Ground-Acceleration Excitations," by Y. Yong and Y.K. Lin, 6/10/87, (PB88-134309, A03, MF-A01). This report is only available through NTIS (see address given above).

NCEER-87-0013 "Frequency Response of Secondary Systems Under Seismic Excitation," by J.A. HoLung, J. Cai and Y.K. Lin, 7/31/87, (PB88-134317, A05, MF-A01). This report is only available through NTIS (see address given above).

NCEER-87-0014 "Modelling Earthquake Ground Motions in Seismically Active Regions Using Parametric Time Series Methods," by G.W. Ellis and A.S. Cakmak, 8/25/87, (PB88-134283, A08, MF-A01). This report is only available through NTIS (see address given above).

NCEER-87-0015 "Detection and Assessment of Seismic Structural Damage," by E. DiPasquale and A.S. Cakmak, 8/25/87, (PB88-163712, A05, MF-A01). This report is only available through NTIS (see address given above).

NCEER-87-0016 "Pipeline Experiment at Parkfield, California," by J. Isenberg and E. Richardson, 9/15/87, (PB88-163720, A03, MF-A01). This report is available only through NTIS (see address given above).

NCEER-87-0017 "Digital Simulation of Seismic Ground Motion," by M. Shinozuka, G. Deodatis and T. Harada, 8/31/87, (PB88-155197, A04, MF-A01). This report is available only through NTIS (see address given above).

NCEER-87-0018 "Practical Considerations for Structural Control: System Uncertainty, System Time Delay and Truncation of Small Control Forces," J.N. Yang and A. Akbarpour, 8/10/87, (PB88-163738, A08, MF-A01). This report is only available through NTIS (see address given above).

NCEER-87-0019 "Modal Analysis of Nonclassically Damped Structural Systems Using Canonical Transformation," by J.N. Yang, S. Sarkani and F.X. Long, 9/27/87, (PB88-187851, A04, MF-A01).

NCEER-87-0020 "A Nonstationary Solution in Random Vibration Theory," by J.R. Red-Horse and P.D. Spanos, 11/3/87, (PB88-163746, A03, MF-A01).

NCEER-87-0021 "Horizontal Impedances for Radially Inhomogeneous Viscoelastic Soil Layers," by A.S. Veletsos and K.W. Dotson, 10/15/87, (PB88-150859, A04, MF-A01).

NCEER-87-0022 "Seismic Damage Assessment of Reinforced Concrete Members," by Y.S. Chung, C. Meyer and M. Shinozuka, 10/9/87, (PB88-150867, A05, MF-A01). This report is available only through NTIS (see address given above).

NCEER-87-0023 "Active Structural Control in Civil Engineering," by T.T. Soong, 11/11/87, (PB88-187778, A03, MF-A01).

NCEER-87-0024 "Vertical and Torsional Impedances for Radially Inhomogeneous Viscoelastic Soil Layers," by K.W. Dotson and A.S. Veletsos, 12/87, (PB88-187786, A03, MF-A01).

NCEER-87-0025 "Proceedings from the Symposium on Seismic Hazards, Ground Motions, Soil-Liquefaction and Engineering Practice in Eastern North America," October 20-22, 1987, edited by K.H. Jacob, 12/87, (PB88-188115, A23, MF-A01).

NCEER-87-0026 "Report on the Whittier-Narrows, California, Earthquake of October 1, 1987," by J. Pantelic and A. Reinhorn, 11/87, (PB88-187752, A03, MF-A01). This report is available only through NTIS (see address given above).

NCEER-87-0027 "Design of a Modular Program for Transient Nonlinear Analysis of Large 3-D Building Structures," by S. Srivastav and J.F. Abel, 12/30/87, (PB88-187950, A05, MF-A01). This report is only available through NTIS (see address given above).

NCEER-87-0028 "Second-Year Program in Research, Education and Technology Transfer," 3/8/88, (PB88-219480, A04, MF-A01).

NCEER-88-0001 "Workshop on Seismic Computer Analysis and Design of Buildings With Interactive Graphics," by W. McGuire, J.F. Abel and C.H. Conley, 1/18/88, (PB88-187760, A03, MF-A01). This report is only available through NTIS (see address given above).

NCEER-88-0002 "Optimal Control of Nonlinear Flexible Structures," by J.N. Yang, F.X. Long and D. Wong, 1/22/88, (PB88-213772, A06, MF-A01).

NCEER-88-0003 "Substructuring Techniques in the Time Domain for Primary-Secondary Structural Systems," by G.D. Manolis and G. Juhn, 2/10/88, (PB88-213780, A04, MF-A01).

NCEER-88-0004 "Iterative Seismic Analysis of Primary-Secondary Systems," by A. Singhal, L.D. Lutes and P.D. Spanos, 2/23/88, (PB88-213798, A04, MF-A01).

NCEER-88-0005 "Stochastic Finite Element Expansion for Random Media," by P.D. Spanos and R. Ghanem, 3/14/88, (PB88-213806, A03, MF-A01).

NCEER-88-0006 "Combining Structural Optimization and Structural Control," by F.Y. Cheng and C.P. Pantelides, 1/10/88, (PB88-213814, A05, MF-A01).

NCEER-88-0007 "Seismic Performance Assessment of Code-Designed Structures," by H.H-M. Hwang, J-W. Jaw and H-J. Shau, 3/20/88, (PB88-219423, A04, MF-A01). This report is only available through NTIS (see address given above).

NCEER-88-0008 "Reliability Analysis of Code-Designed Structures Under Natural Hazards," by H.H-M. Hwang, H. Ushiba and M. Shinozuka, 2/29/88, (PB88-229471, A07, MF-A01). This report is only available through NTIS (see address given above).

NCEER-88-0009 "Seismic Fragility Analysis of Shear Wall Structures," by J-W Jaw and H.H-M. Hwang, 4/30/88, (PB89-102867, A04, MF-A01).

NCEER-88-0010 "Base Isolation of a Multi-Story Building Under a Harmonic Ground Motion - A Comparison of Performances of Various Systems," by F-G Fan, G. Ahmadi and I.G. Tadjbakhsh, 5/18/88, (PB89-122238, A06, MF-A01). This report is only available through NTIS (see address given above).

NCEER-88-0011 "Seismic Floor Response Spectra for a Combined System by Green's Functions," by F.M. Lavelle, L.A. Bergman and P.D. Spanos, 5/1/88, (PB89-102875, A03, MF-A01).

NCEER-88-0012 "A New Solution Technique for Randomly Excited Hysteretic Structures," by G.Q. Cai and Y.K. Lin, 5/16/88, (PB89-102883, A03, MF-A01).

NCEER-88-0013 "A Study of Radiation Damping and Soil-Structure Interaction Effects in the Centrifuge," by K. Weissman, supervised by J.H. Prevost, 5/24/88, (PB89-144703, A06, MF-A01).

NCEER-88-0014 "Parameter Identification and Implementation of a Kinematic Plasticity Model for Frictional Soils," by J.H. Prevost and D.V. Griffiths, to be published.

NCEER-88-0015 "Two- and Three- Dimensional Dynamic Finite Element Analyses of the Long Valley Dam," by D.V. Griffiths and J.H. Prevost, 6/17/88, (PB89-144711, A04, MF-A01).

NCEER-88-0016 "Damage Assessment of Reinforced Concrete Structures in Eastern United States," by A.M. Reinhorn, M.J. Seidel, S.K. Kunnath and Y.J. Park, 6/15/88, (PB89-122220, A04, MF-A01). This report is only available through NTIS (see address given above).

NCEER-88-0017 "Dynamic Compliance of Vertically Loaded Strip Foundations in Multilayered Viscoelastic Soils," by S. Ahmad and A.S.M. Israil, 6/17/88, (PB89-102891, A04, MF-A01).

NCEER-88-0018 "An Experimental Study of Seismic Structural Response With Added Viscoelastic Dampers," by R.C. Lin, Z. Liang, T.T. Soong and R.H. Zhang, 6/30/88, (PB89-122212, A05, MF-A01). This report is available only through NTIS (see address given above).

NCEER-88-0019 "Experimental Investigation of Primary - Secondary System Interaction," by G.D. Manolis, G. Juhn and A.M. Reinhorn, 5/27/88, (PB89-122204, A04, MF-A01).

NCEER-88-0020 "A Response Spectrum Approach For Analysis of Nonclassically Damped Structures," by J.N. Yang, S. Sarkani and F.X. Long, 4/22/88, (PB89-102909, A04, MF-A01).

NCEER-88-0021 "Seismic Interaction of Structures and Soils: Stochastic Approach," by A.S. Veletsos and A.M. Prasad, 7/21/88, (PB89-122196, A04, MF-A01). This report is only available through NTIS (see address given above).

NCEER-88-0022 "Identification of the Serviceability Limit State and Detection of Seismic Structural Damage," by E. DiPasquale and A.S. Cakmak, 6/15/88, (PB89-122188, A05, MF-A01). This report is available only through NTIS (see address given above).

NCEER-88-0023 "Multi-Hazard Risk Analysis: Case of a Simple Offshore Structure," by B.K. Bhartia and E.H. Vanmarcke, 7/21/88, (PB89-145213, A05, MF-A01).

NCEER-88-0024 "Automated Seismic Design of Reinforced Concrete Buildings," by Y.S. Chung, C. Meyer and M. Shinozuka, 7/5/88, (PB89-122170, A06, MF-A01). This report is available only through NTIS (see address given above).

NCEER-88-0025 "Experimental Study of Active Control of MDOF Structures Under Seismic Excitations," by L.L. Chung, R.C. Lin, T.T. Soong and A.M. Reinhorn, 7/10/88, (PB89-122600, A04, MF-A01).

NCEER-88-0026 "Earthquake Simulation Tests of a Low-Rise Metal Structure," by J.S. Hwang, K.C. Chang, G.C. Lee and R.L. Ketter, 8/1/88, (PB89-102917, A04, MF-A01).

NCEER-88-0027 "Systems Study of Urban Response and Reconstruction Due to Catastrophic Earthquakes," by F. Kozin and H.K. Zhou, 9/22/88, (PB90-162348, A04, MF-A01).

NCEER-88-0028 "Seismic Fragility Analysis of Plane Frame Structures," by H.H-M. Hwang and Y.K. Low, 7/31/88, (PB89-131445, A06, MF-A01).

NCEER-88-0029 "Response Analysis of Stochastic Structures," by A. Kardara, C. Bucher and M. Shinozuka, 9/22/88, (PB89-174429, A04, MF-A01).

NCEER-88-0030 "Nonnormal Accelerations Due to Yielding in a Primary Structure," by D.C.K. Chen and L.D. Lutes, 9/19/88, (PB89-131437, A04, MF-A01).

NCEER-88-0031 "Design Approaches for Soil-Structure Interaction," by A.S. Veletsos, A.M. Prasad and Y. Tang, 12/30/88, (PB89-174437, A03, MF-A01). This report is available only through NTIS (see address given above).

NCEER-88-0032 "A Re-evaluation of Design Spectra for Seismic Damage Control," by C.J. Turkstra and A.G. Tallin, 11/7/88, (PB89-145221, A05, MF-A01).

NCEER-88-0033 "The Behavior and Design of Noncontact Lap Splices Subjected to Repeated Inelastic Tensile Loading," by V.E. Sagan, P. Gergely and R.N. White, 12/8/88, (PB89-163737, A08, MF-A01).

NCEER-88-0034 "Seismic Response of Pile Foundations," by S.M. Mamoon, P.K. Banerjee and S. Ahmad, 11/1/88, (PB89-145239, A04, MF-A01).

NCEER-88-0035 "Modeling of R/C Building Structures With Flexible Floor Diaphragms (IDARC2)," by A.M. Reinhorn, S.K. Kunnath and N. Panahshahi, 9/7/88, (PB89-207153, A07, MF-A01).

NCEER-88-0036 "Solution of the Dam-Reservoir Interaction Problem Using a Combination of FEM, BEM with Particular Integrals, Modal Analysis, and Substructuring," by C-S. Tsai, G.C. Lee and R.L. Ketter, 12/31/88, (PB89-207146, A04, MF-A01).

NCEER-88-0037 "Optimal Placement of Actuators for Structural Control," by F.Y. Cheng and C.P. Pantelides, 8/15/88, (PB89-162846, A05, MF-A01).

NCEER-88-0038 "Teflon Bearings in Aseismic Base Isolation: Experimental Studies and Mathematical Modeling," by A. Mokha, M.C. Constantinou and A.M. Reinhorn, 12/5/88, (PB89-218457, A10, MF-A01). This report is available only through NTIS (see address given above).

NCEER-88-0039 "Seismic Behavior of Flat Slab High-Rise Buildings in the New York City Area," by P. Weidlinger and M. Ettouney, 10/15/88, (PB90-145681, A04, MF-A01).

NCEER-88-0040 "Evaluation of the Earthquake Resistance of Existing Buildings in New York City," by P. Weidlinger and M. Ettouney, 10/15/88, to be published.

NCEER-88-0041 "Small-Scale Modeling Techniques for Reinforced Concrete Structures Subjected to Seismic Loads," by W. Kim, A. El-Attar and R.N. White, 11/22/88, (PB89-189625, A05, MF-A01).

NCEER-88-0042 "Modeling Strong Ground Motion from Multiple Event Earthquakes," by G.W. Ellis and A.S. Cakmak, 10/15/88, (PB89-174445, A03, MF-A01).

NCEER-88-0043 "Nonstationary Models of Seismic Ground Acceleration," by M. Grigoriu, S.E. Ruiz and E. Rosenblueth, 7/15/88, (PB89-189617, A04, MF-A01).

NCEER-88-0044 "SARCF User's Guide: Seismic Analysis of Reinforced Concrete Frames," by Y.S. Chung, C. Meyer and M. Shinozuka, 11/9/88, (PB89-174452, A08, MF-A01).

NCEER-88-0045 "First Expert Panel Meeting on Disaster Research and Planning," edited by J. Pantelic and J. Stoyle, 9/15/88, (PB89-174460, A05, MF-A01). This report is only available through NTIS (see address given above).

NCEER-88-0046 "Preliminary Studies of the Effect of Degrading Infill Walls on the Nonlinear Seismic Response of Steel Frames," by C.Z. Chrysostomou, P. Gergely and J.F. Abel, 12/19/88, (PB89-208383, A05, MF-A01).

NCEER-88-0047 "Reinforced Concrete Frame Component Testing Facility - Design, Construction, Instrumentation and Operation," by S.P. Pessiki, C. Conley, T. Bond, P. Gergely and R.N. White, 12/16/88, (PB89-174478, A04, MF-A01).

NCEER-89-0001 "Effects of Protective Cushion and Soil Compliancy on the Response of Equipment Within a Seismically Excited Building," by J.A. HoLung, 2/16/89, (PB89-207179, A04, MF-A01).

NCEER-89-0002 "Statistical Evaluation of Response Modification Factors for Reinforced Concrete Structures," by H.H-M. Hwang and J-W. Jaw, 2/17/89, (PB89-207187, A05, MF-A01).

NCEER-89-0003 "Hysteretic Columns Under Random Excitation," by G-Q. Cai and Y.K. Lin, 1/9/89, (PB89-196513, A03, MF-A01).

NCEER-89-0004 "Experimental Study of `Elephant Foot Bulge' Instability of Thin-Walled Metal Tanks," by Z-H. Jia and R.L. Ketter, 2/22/89, (PB89-207195, A03, MF-A01).

NCEER-89-0005 "Experiment on Performance of Buried Pipelines Across San Andreas Fault," by J. Isenberg, E. Richardson and T.D. O'Rourke, 3/10/89, (PB89-218440, A04, MF-A01). This report is available only through NTIS (see address given above).

NCEER-89-0006 "A Knowledge-Based Approach to Structural Design of Earthquake-Resistant Buildings," by M. Subramani, P. Gergely, C.H. Conley, J.F. Abel and A.H. Zaghw, 1/15/89, (PB89-218465, A06, MF-A01).

NCEER-89-0007 "Liquefaction Hazards and Their Effects on Buried Pipelines," by T.D. O'Rourke and P.A. Lane, 2/1/89, (PB89-218481, A09, MF-A01).

NCEER-89-0008 "Fundamentals of System Identification in Structural Dynamics," by H. Imai, C-B. Yun, O. Maruyama and M. Shinozuka, 1/26/89, (PB89-207211, A04, MF-A01).

NCEER-89-0009 "Effects of the 1985 Michoacan Earthquake on Water Systems and Other Buried Lifelines in Mexico," by A.G. Ayala and M.J. O'Rourke, 3/8/89, (PB89-207229, A06, MF-A01).

NCEER-89-R010 "NCEER Bibliography of Earthquake Education Materials," by K.E.K. Ross, Second Revision, 9/1/89, (PB90-125352, A05, MF-A01). This report is replaced by NCEER-92-0018.

NCEER-89-0011 "Inelastic Three-Dimensional Response Analysis of Reinforced Concrete Building Structures (IDARC-3D), Part I - Modeling," by S.K. Kunnath and A.M. Reinhorn, 4/17/89, (PB90-114612, A07, MF-A01).

NCEER-89-0012 "Recommended Modifications to ATC-14," by C.D. Poland and J.O. Malley, 4/12/89, (PB90-108648, A15, MF-A01).

NCEER-89-0013 "Repair and Strengthening of Beam-to-Column Connections Subjected to Earthquake Loading," by M. Corazao and A.J. Durrani, 2/28/89, (PB90-109885, A06, MF-A01).

NCEER-89-0014 "Program EXKAL2 for Identification of Structural Dynamic Systems," by O. Maruyama, C-B. Yun, M. Hoshiya and M. Shinozuka, 5/19/89, (PB90-109877, A09, MF-A01).

NCEER-89-0015 "Response of Frames With Bolted Semi-Rigid Connections, Part I - Experimental Study and Analytical Predictions," by P.J. DiCorso, A.M. Reinhorn, J.R. Dickerson, J.B. Radziminski and W.L. Harper, 6/1/89, to be published.

NCEER-89-0016 "ARMA Monte Carlo Simulation in Probabilistic Structural Analysis," by P.D. Spanos and M.P. Mignolet, 7/10/89, (PB90-109893, A03, MF-A01).

NCEER-89-P017 "Preliminary Proceedings from the Conference on Disaster Preparedness - The Place of Earthquake Education in Our Schools," Edited by K.E.K. Ross, 6/23/89, (PB90-108606, A03, MF-A01).

NCEER-89-0017 "Proceedings from the Conference on Disaster Preparedness - The Place of Earthquake Education in Our Schools," Edited by K.E.K. Ross, 12/31/89, (PB90-207895, A012, MF-A02). This report is available only through NTIS (see address given above).

NCEER-89-0018 "Multidimensional Models of Hysteretic Material Behavior for Vibration Analysis of Shape Memory Energy Absorbing Devices, by E.J. Graesser and F.A. Cozzarelli, 6/7/89, (PB90-164146, A04, MF-A01).

NCEER-89-0019 "Nonlinear Dynamic Analysis of Three-Dimensional Base Isolated Structures (3D-BASIS)," by S. Nagarajaiah, A.M. Reinhorn and M.C. Constantinou, 8/3/89, (PB90-161936, A06, MF-A01). This report has been replaced by NCEER-93-0011.

NCEER-89-0020 "Structural Control Considering Time-Rate of Control Forces and Control Rate Constraints," by F.Y. Cheng and C.P. Pantelides, 8/3/89, (PB90-120445, A04, MF-A01).

NCEER-89-0021 "Subsurface Conditions of Memphis and Shelby County," by K.W. Ng, T-S. Chang and H-H.M. Hwang, 7/26/89, (PB90-120437, A03, MF-A01).

NCEER-89-0022 "Seismic Wave Propagation Effects on Straight Jointed Buried Pipelines," by K. Elhmadi and M.J. O'Rourke, 8/24/89, (PB90-162322, A10, MF-A02).

NCEER-89-0023 "Workshop on Serviceability Analysis of Water Delivery Systems," edited by M. Grigoriu, 3/6/89, (PB90-127424, A03, MF-A01).

NCEER-89-0024 "Shaking Table Study of a 1/5 Scale Steel Frame Composed of Tapered Members," by K.C. Chang, J.S. Hwang and G.C. Lee, 9/18/89, (PB90-160169, A04, MF-A01).

NCEER-89-0025 "DYNA1D: A Computer Program for Nonlinear Seismic Site Response Analysis - Technical Documentation," by Jean H. Prevost, 9/14/89, (PB90-161944, A07, MF-A01). This report is available only through NTIS (see address given above).

NCEER-89-0026 "1:4 Scale Model Studies of Active Tendon Systems and Active Mass Dampers for Aseismic Protection," by A.M. Reinhorn, T.T. Soong, R.C. Lin, Y.P. Yang, Y. Fukao, H. Abe and M. Nakai, 9/15/89, (PB90-173246, A10, MF-A02).

NCEER-89-0027 "Scattering of Waves by Inclusions in a Nonhomogeneous Elastic Half Space Solved by Boundary Element Methods," by P.K. Hadley, A. Askar and A.S. Cakmak, 6/15/89, (PB90-145699, A07, MF-A01).

NCEER-89-0028 "Statistical Evaluation of Deflection Amplification Factors for Reinforced Concrete Structures," by H.H.M. Hwang, J-W. Jaw and A.L. Ch'ng, 8/31/89, (PB90-164633, A05, MF-A01).

NCEER-89-0029 "Bedrock Accelerations in Memphis Area Due to Large New Madrid Earthquakes," by H.H.M. Hwang, C.H.S. Chen and G. Yu, 11/7/89, (PB90-162330, A04, MF-A01).

NCEER-89-0030 "Seismic Behavior and Response Sensitivity of Secondary Structural Systems," by Y.Q. Chen and T.T. Soong, 10/23/89, (PB90-164658, A08, MF-A01).

NCEER-89-0031 "Random Vibration and Reliability Analysis of Primary-Secondary Structural Systems," by Y. Ibrahim, M. Grigoriu and T.T. Soong, 11/10/89, (PB90-161951, A04, MF-A01).

NCEER-89-0032 "Proceedings from the Second U.S. - Japan Workshop on Liquefaction, Large Ground Deformation and Their Effects on Lifelines, September 26-29, 1989," Edited by T.D. O'Rourke and M. Hamada, 12/1/89, (PB90-209388, A22, MF-A03).

NCEER-89-0033 "Deterministic Model for Seismic Damage Evaluation of Reinforced Concrete Structures," by J.M. Bracci, A.M. Reinhorn, J.B. Mander and S.K. Kunnath, 9/27/89, (PB91-108803, A06, MF-A01).

NCEER-89-0034 "On the Relation Between Local and Global Damage Indices," by E. DiPasquale and A.S. Cakmak, 8/15/89, (PB90-173865, A05, MF-A01).

NCEER-89-0035 "Cyclic Undrained Behavior of Nonplastic and Low Plasticity Silts," by A.J. Walker and H.E. Stewart, 7/26/89, (PB90-183518, A10, MF-A01).

NCEER-89-0036 "Liquefaction Potential of Surficial Deposits in the City of Buffalo, New York," by M. Budhu, R. Giese and L. Baumgrass, 1/17/89, (PB90-208455, A04, MF-A01).

NCEER-89-0037 "A Deterministic Assessment of Effects of Ground Motion Incoherence," by A.S. Veletsos and Y. Tang, 7/15/89, (PB90-164294, A03, MF-A01).

NCEER-89-0038 "Workshop on Ground Motion Parameters for Seismic Hazard Mapping," July 17-18, 1989, edited by R.V. Whitman, 12/1/89, (PB90-173923, A04, MF-A01).

NCEER-89-0039 "Seismic Effects on Elevated Transit Lines of the New York City Transit Authority," by C.J. Costantino, C.A. Miller and E. Heymsfield, 12/26/89, (PB90-207887, A06, MF-A01).

NCEER-89-0040 "Centrifugal Modeling of Dynamic Soil-Structure Interaction," by K. Weissman, Supervised by J.H. Prevost, 5/10/89, (PB90-207879, A07, MF-A01).

NCEER-89-0041 "Linearized Identification of Buildings With Cores for Seismic Vulnerability Assessment," by I-K. Ho and A.E. Aktan, 11/1/89, (PB90-251943, A07, MF-A01).

NCEER-90-0001 "Geotechnical and Lifeline Aspects of the October 17, 1989 Loma Prieta Earthquake in San Francisco," by T.D. O'Rourke, H.E. Stewart, F.T. Blackburn and T.S. Dickerman, 1/90, (PB90-208596, A05, MF-A01).

NCEER-90-0002 "Nonnormal Secondary Response Due to Yielding in a Primary Structure," by D.C.K. Chen and L.D. Lutes, 2/28/90, (PB90-251976, A07, MF-A01).

NCEER-90-0003 "Earthquake Education Materials for Grades K-12," by K.E.K. Ross, 4/16/90, (PB91-251984, A05, MF-A05). This report has been replaced by NCEER-92-0018.

NCEER-90-0004 "Catalog of Strong Motion Stations in Eastern North America," by R.W. Busby, 4/3/90, (PB90-251984, A05, MF-A01).

NCEER-90-0005 "NCEER Strong-Motion Data Base: A User Manual for the GeoBase Release (Version 1.0 for the Sun3)," by P. Friberg and K. Jacob, 3/31/90 (PB90-258062, A04, MF-A01).

NCEER-90-0006 "Seismic Hazard Along a Crude Oil Pipeline in the Event of an 1811-1812 Type New Madrid Earthquake," by H.H.M. Hwang and C-H.S. Chen, 4/16/90, (PB90-258054, A04, MF-A01).

NCEER-90-0007 "Site-Specific Response Spectra for Memphis Sheahan Pumping Station," by H.H.M. Hwang and C.S. Lee, 5/15/90, (PB91-108811, A05, MF-A01).

NCEER-90-0008 "Pilot Study on Seismic Vulnerability of Crude Oil Transmission Systems," by T. Ariman, R. Dobry, M. Grigoriu, F. Kozin, M. O'Rourke, T. O'Rourke and M. Shinozuka, 5/25/90, (PB91-108837, A06, MF-A01).

NCEER-90-0009 "A Program to Generate Site Dependent Time Histories: EQGEN," by G.W. Ellis, M. Srinivasan and A.S. Cakmak, 1/30/90, (PB91-108829, A04, MF-A01).

NCEER-90-0010 "Active Isolation for Seismic Protection of Operating Rooms," by M.E. Talbott, Supervised by M. Shinozuka, 6/8/9, (PB91-110205, A05, MF-A01).

NCEER-90-0011 "Program LINEARID for Identification of Linear Structural Dynamic Systems," by C-B. Yun and M. Shinozuka, 6/25/90, (PB91-110312, A08, MF-A01).

NCEER-90-0012 "Two-Dimensional Two-Phase Elasto-Plastic Seismic Response of Earth Dams," by A.N. Yiagos, Supervised by J.H. Prevost, 6/20/90, (PB91-110197, A13, MF-A02).

NCEER-90-0013 "Secondary Systems in Base-Isolated Structures: Experimental Investigation, Stochastic Response and Stochastic Sensitivity," by G.D. Manolis, G. Juhn, M.C. Constantinou and A.M. Reinhorn, 7/1/90, (PB91-110320, A08, MF-A01).

NCEER-90-0014 "Seismic Behavior of Lightly-Reinforced Concrete Column and Beam-Column Joint Details," by S.P. Pessiki, C.H. Conley, P. Gergely and R.N. White, 8/22/90, (PB91-108795, A11, MF-A02).

NCEER-90-0015 "Two Hybrid Control Systems for Building Structures Under Strong Earthquakes," by J.N. Yang and A. Danielians, 6/29/90, (PB91-125393, A04, MF-A01).

NCEER-90-0016 "Instantaneous Optimal Control with Acceleration and Velocity Feedback," by J.N. Yang and Z. Li, 6/29/90, (PB91-125401, A03, MF-A01).

NCEER-90-0017 "Reconnaissance Report on the Northern Iran Earthquake of June 21, 1990," by M. Mehrain, 10/4/90, (PB91-125377, A03, MF-A01).

NCEER-90-0018 "Evaluation of Liquefaction Potential in Memphis and Shelby County," by T.S. Chang, P.S. Tang, C.S. Lee and H. Hwang, 8/10/90, (PB91-125427, A09, MF-A01).

NCEER-90-0019 "Experimental and Analytical Study of a Combined Sliding Disc Bearing and Helical Steel Spring Isolation System," by M.C. Constantinou, A.S. Mokha and A.M. Reinhorn, 10/4/90, (PB91-125385, A06, MF-A01). This report is available only through NTIS (see address given above).

NCEER-90-0020 "Experimental Study and Analytical Prediction of Earthquake Response of a Sliding Isolation System with a Spherical Surface," by A.S. Mokha, M.C. Constantinou and A.M. Reinhorn, 10/11/90, (PB91-125419, A05, MF-A01).

NCEER-90-0021 "Dynamic Interaction Factors for Floating Pile Groups," by G. Gazetas, K. Fan, A. Kaynia and E. Kausel, 9/10/90, (PB91-170381, A05, MF-A01).

NCEER-90-0022 "Evaluation of Seismic Damage Indices for Reinforced Concrete Structures," by S. Rodriguez-Gomez and A.S. Cakmak, 9/30/90, PB91-171322, A06, MF-A01).

NCEER-90-0023 "Study of Site Response at a Selected Memphis Site," by H. Desai, S. Ahmad, E.S. Gazetas and M.R. Oh, 10/11/90, (PB91-196857, A03, MF-A01).

NCEER-90-0024 "A User's Guide to Strongmo: Version 1.0 of NCEER's Strong-Motion Data Access Tool for PCs and Terminals," by P.A. Friberg and C.A.T. Susch, 11/15/90, (PB91-171272, A03, MF-A01).

NCEER-90-0025 "A Three-Dimensional Analytical Study of Spatial Variability of Seismic Ground Motions," by L-L. Hong and A.H.-S. Ang, 10/30/90, (PB91-170399, A09, MF-A01).

NCEER-90-0026 "MUMOID User's Guide - A Program for the Identification of Modal Parameters," by S. Rodriguez-Gomez and E. DiPasquale, 9/30/90, (PB91-171298, A04, MF-A01).

NCEER-90-0027 "SARCF-II User's Guide - Seismic Analysis of Reinforced Concrete Frames," by S. Rodriguez-Gomez, Y.S. Chung and C. Meyer, 9/30/90, (PB91-171280, A05, MF-A01).

NCEER-90-0028 "Viscous Dampers: Testing, Modeling and Application in Vibration and Seismic Isolation," by N. Makris and M.C. Constantinou, 12/20/90 (PB91-190561, A06, MF-A01).

NCEER-90-0029 "Soil Effects on Earthquake Ground Motions in the Memphis Area," by H. Hwang, C.S. Lee, K.W. Ng and T.S. Chang, 8/2/90, (PB91-190751, A05, MF-A01).

NCEER-91-0001 "Proceedings from the Third Japan-U.S. Workshop on Earthquake Resistant Design of Lifeline Facilities and Countermeasures for Soil Liquefaction, December 17-19, 1990," edited by T.D. O'Rourke and M. Hamada, 2/1/91, (PB91-179259, A99, MF-A04).

NCEER-91-0002 "Physical Space Solutions of Non-Proportionally Damped Systems," by M. Tong, Z. Liang and G.C. Lee, 1/15/91, (PB91-179242, A04, MF-A01).

NCEER-91-0003 "Seismic Response of Single Piles and Pile Groups," by K. Fan and G. Gazetas, 1/10/91, (PB92-174994, A04, MF-A01).

NCEER-91-0004 "Damping of Structures: Part 1 - Theory of Complex Damping," by Z. Liang and G. Lee, 10/10/91, (PB92-197235, A12, MF-A03).

NCEER-91-0005 "3D-BASIS - Nonlinear Dynamic Analysis of Three Dimensional Base Isolated Structures: Part II," by S. Nagarajaiah, A.M. Reinhorn and M.C. Constantinou, 2/28/91, (PB91-190553, A07, MF-A01). This report has been replaced by NCEER-93-0011.

NCEER-91-0006 "A Multidimensional Hysteretic Model for Plasticity Deforming Metals in Energy Absorbing Devices," by E.J. Graesser and F.A. Cozzarelli, 4/9/91, (PB92-108364, A04, MF-A01).

NCEER-91-0007 "A Framework for Customizable Knowledge-Based Expert Systems with an Application to a KBES for Evaluating the Seismic Resistance of Existing Buildings," by E.G. Ibarra-Anaya and S.J. Fenves, 4/9/91, (PB91-210930, A08, MF-A01).

NCEER-91-0008 "Nonlinear Analysis of Steel Frames with Semi-Rigid Connections Using the Capacity Spectrum Method," by G.G. Deierlein, S-H. Hsieh, Y-J. Shen and J.F. Abel, 7/2/91, (PB92-113828, A05, MF-A01).

NCEER-91-0009 "Earthquake Education Materials for Grades K-12," by K.E.K. Ross, 4/30/91, (PB91-212142, A06, MF-A01). This report has been replaced by NCEER-92-0018.

NCEER-91-0010 "Phase Wave Velocities and Displacement Phase Differences in a Harmonically Oscillating Pile," by N. Makris and G. Gazetas, 7/8/91, (PB92-108356, A04, MF-A01).

NCEER-91-0011 "Dynamic Characteristics of a Full-Size Five-Story Steel Structure and a 2/5 Scale Model," by K.C. Chang, G.C. Yao, G.C. Lee, D.S. Hao and Y.C. Yeh," 7/2/91, (PB93-116648, A06, MF-A02).

NCEER-91-0012 "Seismic Response of a 2/5 Scale Steel Structure with Added Viscoelastic Dampers," by K.C. Chang, T.T. Soong, S-T. Oh and M.L. Lai, 5/17/91, (PB92-110816, A05, MF-A01).

NCEER-91-0013 "Earthquake Response of Retaining Walls; Full-Scale Testing and Computational Modeling," by S. Alampalli and A-W.M. Elgamal, 6/20/91, to be published.

NCEER-91-0014 "3D-BASIS-M: Nonlinear Dynamic Analysis of Multiple Building Base Isolated Structures," by P.C. Tsopelas, S. Nagarajaiah, M.C. Constantinou and A.M. Reinhorn, 5/28/91, (PB92-113885, A09, MF-A02).

NCEER-91-0015 "Evaluation of SEAOC Design Requirements for Sliding Isolated Structures," by D. Theodossiou and M.C. Constantinou, 6/10/91, (PB92-114602, A11, MF-A03).

NCEER-91-0016 "Closed-Loop Modal Testing of a 27-Story Reinforced Concrete Flat Plate-Core Building," by H.R. Somaprasad, T. Toksoy, H. Yoshiyuki and A.E. Aktan, 7/15/91, (PB92-129980, A07, MF-A02).

NCEER-91-0017 "Shake Table Test of a 1/6 Scale Two-Story Lightly Reinforced Concrete Building," by A.G. El-Attar, R.N. White and P. Gergely, 2/28/91, (PB92-222447, A06, MF-A02).

NCEER-91-0018 "Shake Table Test of a 1/8 Scale Three-Story Lightly Reinforced Concrete Building," by A.G. El-Attar, R.N. White and P. Gergely, 2/28/91, (PB93-116630, A08, MF-A02).

NCEER-91-0019 "Transfer Functions for Rigid Rectangular Foundations," by A.S. Veletsos, A.M. Prasad and W.H. Wu, 7/31/91, to be published.

NCEER-91-0020 "Hybrid Control of Seismic-Excited Nonlinear and Inelastic Structural Systems," by J.N. Yang, Z. Li and A. Danielians, 8/1/91, (PB92-143171, A06, MF-A02).

NCEER-91-0021 "The NCEER-91 Earthquake Catalog: Improved Intensity-Based Magnitudes and Recurrence Relations for U.S. Earthquakes East of New Madrid," by L. Seeber and J.G. Armbruster, 8/28/91, (PB92-176742, A06, MF-A02).

NCEER-91-0022 "Proceedings from the Implementation of Earthquake Planning and Education in Schools: The Need for Change - The Roles of the Changemakers," by K.E.K. Ross and F. Winslow, 7/23/91, (PB92-129998, A12, MF-A03).

NCEER-91-0023 "A Study of Reliability-Based Criteria for Seismic Design of Reinforced Concrete Frame Buildings," by H.H.M. Hwang and H-M. Hsu, 8/10/91, (PB92-140235, A09, MF-A02).

NCEER-91-0024 "Experimental Verification of a Number of Structural System Identification Algorithms," by R.G. Ghanem, H. Gavin and M. Shinozuka, 9/18/91, (PB92-176577, A18, MF-A04).

NCEER-91-0025 "Probabilistic Evaluation of Liquefaction Potential," by H.H.M. Hwang and C.S. Lee," 11/25/91, (PB92-143429, A05, MF-A01).

NCEER-91-0026 "Instantaneous Optimal Control for Linear, Nonlinear and Hysteretic Structures - Stable Controllers," by J.N. Yang and Z. Li, 11/15/91, (PB92-163807, A04, MF-A01).

NCEER-91-0027 "Experimental and Theoretical Study of a Sliding Isolation System for Bridges," by M.C. Constantinou, A. Kartoum, A.M. Reinhorn and P. Bradford, 11/15/91, (PB92-176973, A10, MF-A03).

NCEER-92-0001 "Case Studies of Liquefaction and Lifeline Performance During Past Earthquakes, Volume 1: Japanese Case Studies," Edited by M. Hamada and T. O'Rourke, 2/17/92, (PB92-197243, A18, MF-A04).

NCEER-92-0002 "Case Studies of Liquefaction and Lifeline Performance During Past Earthquakes, Volume 2: United States Case Studies," Edited by T. O'Rourke and M. Hamada, 2/17/92, (PB92-197250, A20, MF-A04).

NCEER-92-0003 "Issues in Earthquake Education," Edited by K. Ross, 2/3/92, (PB92-222389, A07, MF-A02).

NCEER-92-0004 "Proceedings from the First U.S. - Japan Workshop on Earthquake Protective Systems for Bridges," Edited by I.G. Buckle, 2/4/92, (PB94-142239, A99, MF-A06).

NCEER-92-0005 "Seismic Ground Motion from a Haskell-Type Source in a Multiple-Layered Half-Space," A.P. Theoharis, G. Deodatis and M. Shinozuka, 1/2/92, to be published.

NCEER-92-0006 "Proceedings from the Site Effects Workshop," Edited by R. Whitman, 2/29/92, (PB92-197201, A04, MF-A01).

NCEER-92-0007 "Engineering Evaluation of Permanent Ground Deformations Due to Seismically-Induced Liquefaction," by M.H. Baziar, R. Dobry and A-W.M. Elgamal, 3/24/92, (PB92-222421, A13, MF-A03).

NCEER-92-0008 "A Procedure for the Seismic Evaluation of Buildings in the Central and Eastern United States," by C.D. Poland and J.O. Malley, 4/2/92, (PB92-222439, A20, MF-A04).

NCEER-92-0009 "Experimental and Analytical Study of a Hybrid Isolation System Using Friction Controllable Sliding Bearings," by M.Q. Feng, S. Fujii and M. Shinozuka, 5/15/92, (PB93-150282, A06, MF-A02).

NCEER-92-0010 "Seismic Resistance of Slab-Column Connections in Existing Non-Ductile Flat-Plate Buildings," by A.J. Durrani and Y. Du, 5/18/92, (PB93-116812, A06, MF-A02).

NCEER-92-0011 "The Hysteretic and Dynamic Behavior of Brick Masonry Walls Upgraded by Ferrocement Coatings Under Cyclic Loading and Strong Simulated Ground Motion," by H. Lee and S.P. Prawel, 5/11/92, to be published.

NCEER-92-0012 "Study of Wire Rope Systems for Seismic Protection of Equipment in Buildings," by G.F. Demetriades, M.C. Constantinou and A.M. Reinhorn, 5/20/92, (PB93-116655, A08, MF-A02).

NCEER-92-0013 "Shape Memory Structural Dampers: Material Properties, Design and Seismic Testing," by P.R. Witting and F.A. Cozzarelli, 5/26/92, (PB93-116663, A05, MF-A01).

NCEER-92-0014 "Longitudinal Permanent Ground Deformation Effects on Buried Continuous Pipelines," by M.J. O'Rourke, and C. Nordberg, 6/15/92, (PB93-116671, A08, MF-A02).

NCEER-92-0015 "A Simulation Method for Stationary Gaussian Random Functions Based on the Sampling Theorem," by M. Grigoriu and S. Balopoulou, 6/11/92, (PB93-127496, A05, MF-A01).

NCEER-92-0016 "Gravity-Load-Designed Reinforced Concrete Buildings: Seismic Evaluation of Existing Construction and Detailing Strategies for Improved Seismic Resistance," by G.W. Hoffmann, S.K. Kunnath, A.M. Reinhorn and J.B. Mander, 7/15/92, (PB94-142007, A08, MF-A02).

NCEER-92-0017 "Observations on Water System and Pipeline Performance in the Limón Area of Costa Rica Due to the April 22, 1991 Earthquake," by M. O'Rourke and D. Ballantyne, 6/30/92, (PB93-126811, A06, MF-A02).

NCEER-92-0018 "Fourth Edition of Earthquake Education Materials for Grades K-12," Edited by K.E.K. Ross, 8/10/92, (PB93-114023, A07, MF-A02).

NCEER-92-0019 "Proceedings from the Fourth Japan-U.S. Workshop on Earthquake Resistant Design of Lifeline Facilities and Countermeasures for Soil Liquefaction," Edited by M. Hamada and T.D. O'Rourke, 8/12/92, (PB93-163939, A99, MF-E11).

NCEER-92-0020 "Active Bracing System: A Full Scale Implementation of Active Control," by A.M. Reinhorn, T.T. Soong, R.C. Lin, M.A. Riley, Y.P. Wang, S. Aizawa and M. Higashino, 8/14/92, (PB93-127512, A06, MF-A02).

NCEER-92-0021 "Empirical Analysis of Horizontal Ground Displacement Generated by Liquefaction-Induced Lateral Spreads," by S.F. Bartlett and T.L. Youd, 8/17/92, (PB93-188241, A06, MF-A02).

NCEER-92-0022 "IDARC Version 3.0: Inelastic Damage Analysis of Reinforced Concrete Structures," by S.K. Kunnath, A.M. Reinhorn and R.F. Lobo, 8/31/92, (PB93-227502, A07, MF-A02).

NCEER-92-0023 "A Semi-Empirical Analysis of Strong-Motion Peaks in Terms of Seismic Source, Propagation Path and Local Site Conditions, by M. Kamiyama, M.J. O'Rourke and R. Flores-Berrones, 9/9/92, (PB93-150266, A08, MF-A02).

NCEER-92-0024 "Seismic Behavior of Reinforced Concrete Frame Structures with Nonductile Details, Part I: Summary of Experimental Findings of Full Scale Beam-Column Joint Tests," by A. Beres, R.N. White and P. Gergely, 9/30/92, (PB93-227783, A05, MF-A01).

NCEER-92-0025 "Experimental Results of Repaired and Retrofitted Beam-Column Joint Tests in Lightly Reinforced Concrete Frame Buildings," by A. Beres, S. El-Borgi, R.N. White and P. Gergely, 10/29/92, (PB93-227791, A05, MF-A01).

NCEER-92-0026 "A Generalization of Optimal Control Theory: Linear and Nonlinear Structures," by J.N. Yang, Z. Li and S. Vongchavalitkul, 11/2/92, (PB93-188621, A05, MF-A01).

NCEER-92-0027 "Seismic Resistance of Reinforced Concrete Frame Structures Designed Only for Gravity Loads: Part I - Design and Properties of a One-Third Scale Model Structure," by J.M. Bracci, A.M. Reinhorn and J.B. Mander, 12/1/92, (PB94-104502, A08, MF-A02).

NCEER-92-0028 "Seismic Resistance of Reinforced Concrete Frame Structures Designed Only for Gravity Loads: Part II - Experimental Performance of Subassemblages," by L.E. Aycardi, J.B. Mander and A.M. Reinhorn, 12/1/92, (PB94-104510, A08, MF-A02).

NCEER-92-0029 "Seismic Resistance of Reinforced Concrete Frame Structures Designed Only for Gravity Loads: Part III - Experimental Performance and Analytical Study of a Structural Model," by J.M. Bracci, A.M. Reinhorn and J.B. Mander, 12/1/92, (PB93-227528, A09, MF-A01).

NCEER-92-0030 "Evaluation of Seismic Retrofit of Reinforced Concrete Frame Structures: Part I - Experimental Performance of Retrofitted Subassemblages," by D. Choudhuri, J.B. Mander and A.M. Reinhorn, 12/8/92, (PB93-198307, A07, MF-A02).

NCEER-92-0031 "Evaluation of Seismic Retrofit of Reinforced Concrete Frame Structures: Part II - Experimental Performance and Analytical Study of a Retrofitted Structural Model," by J.M. Bracci, A.M. Reinhorn and J.B. Mander, 12/8/92, (PB93-198315, A09, MF-A03).

NCEER-92-0032 "Experimental and Analytical Investigation of Seismic Response of Structures with Supplemental Fluid Viscous Dampers," by M.C. Constantinou and M.D. Symans, 12/21/92, (PB93-191435, A10, MF-A03).

NCEER-92-0033 "Reconnaissance Report on the Cairo, Egypt Earthquake of October 12, 1992," by M. Khater, 12/23/92, (PB93-188621, A03, MF-A01).

NCEER-92-0034 "Low-Level Dynamic Characteristics of Four Tall Flat-Plate Buildings in New York City," by H. Gavin, S. Yuan, J. Grossman, E. Pekelis and K. Jacob, 12/28/92, (PB93-188217, A07, MF-A02).

NCEER-93-0001 "An Experimental Study on the Seismic Performance of Brick-Infilled Steel Frames With and Without Retrofit," by J.B. Mander, B. Nair, K. Wojtkowski and J. Ma, 1/29/93, (PB93-227510, A07, MF-A02).

NCEER-93-0002 "Social Accounting for Disaster Preparedness and Recovery Planning," by S. Cole, E. Pantoja and V. Razak, 2/22/93, (PB94-142114, A12, MF-A03).

NCEER-93-0003 "Assessment of 1991 NEHRP Provisions for Nonstructural Components and Recommended Revisions," by T.T. Soong, G. Chen, Z. Wu, R-H. Zhang and M. Grigoriu, 3/1/93, (PB93-188639, A06, MF-A02).

NCEER-93-0004 "Evaluation of Static and Response Spectrum Analysis Procedures of SEAOC/UBC for Seismic Isolated Structures," by C.W. Winters and M.C. Constantinou, 3/23/93, (PB93-198299, A10, MF-A03).

NCEER-93-0005 "Earthquakes in the Northeast - Are We Ignoring the Hazard? A Workshop on Earthquake Science and Safety for Educators," edited by K.E.K. Ross, 4/2/93, (PB94-103066, A09, MF-A02).

NCEER-93-0006 "Inelastic Response of Reinforced Concrete Structures with Viscoelastic Braces," by R.F. Lobo, J.M. Bracci, K.L. Shen, A.M. Reinhorn and T.T. Soong, 4/5/93, (PB93-227486, A05, MF-A02).

NCEER-93-0007 "Seismic Testing of Installation Methods for Computers and Data Processing Equipment," by K. Kosar, T.T. Soong, K.L. Shen, J.A. HoLung and Y.K. Lin, 4/12/93, (PB93-198299, A07, MF-A02).

NCEER-93-0008 "Retrofit of Reinforced Concrete Frames Using Added Dampers," by A. Reinhorn, M. Constantinou and C. Li, to be published.

NCEER-93-0009 "Seismic Behavior and Design Guidelines for Steel Frame Structures with Added Viscoelastic Dampers," by K.C. Chang, M.L. Lai, T.T. Soong, D.S. Hao and Y.C. Yeh, 5/1/93, (PB94-141959, A07, MF-A02).

NCEER-93-0010 "Seismic Performance of Shear-Critical Reinforced Concrete Bridge Piers," by J.B. Mander, S.M. Waheed, M.T.A. Chaudhary and S.S. Chen, 5/12/93, (PB93-227494, A08, MF-A02).

NCEER-93-0011 "3D-BASIS-TABS: Computer Program for Nonlinear Dynamic Analysis of Three Dimensional Base Isolated Structures," by S. Nagarajaiah, C. Li, A.M. Reinhorn and M.C. Constantinou, 8/2/93, (PB94-141819, A09, MF-A02).

NCEER-93-0012 "Effects of Hydrocarbon Spills from an Oil Pipeline Break on Ground Water," by O.J. Helweg and H.H.M. Hwang, 8/3/93, (PB94-141942, A06, MF-A02).

NCEER-93-0013 "Simplified Procedures for Seismic Design of Nonstructural Components and Assessment of Current Code Provisions," by M.P. Singh, L.E. Suarez, E.E. Matheu and G.O. Maldonado, 8/4/93, (PB94-141827, A09, MF-A02).

NCEER-93-0014 "An Energy Approach to Seismic Analysis and Design of Secondary Systems," by G. Chen and T.T. Soong, 8/6/93, (PB94-142767, A11, MF-A03).

NCEER-93-0015 "Proceedings from School Sites: Becoming Prepared for Earthquakes - Commemorating the Third Anniversary of the Loma Prieta Earthquake," Edited by F.E. Winslow and K.E.K. Ross, 8/16/93, (PB94-154275, A16, MF-A02).

NCEER-93-0016 "Reconnaissance Report of Damage to Historic Monuments in Cairo, Egypt Following the October 12, 1992 Dahshur Earthquake," by D. Sykora, D. Look, G. Croci, E. Karaesmen and E. Karaesmen, 8/19/93, (PB94-142221, A08, MF-A02).

NCEER-93-0017 "The Island of Guam Earthquake of August 8, 1993," by S.W. Swan and S.K. Harris, 9/30/93, (PB94-141843, A04, MF-A01).

NCEER-93-0018 "Engineering Aspects of the October 12, 1992 Egyptian Earthquake," by A.W. Elgamal, M. Amer, K. Adalier and A. Abul-Fadl, 10/7/93, (PB94-141983, A05, MF-A01).

NCEER-93-0019 "Development of an Earthquake Motion Simulator and its Application in Dynamic Centrifuge Testing," by I. Krstelj, Supervised by J.H. Prevost, 10/23/93, (PB94-181773, A-10, MF-A03).

NCEER-93-0020 "NCEER-Taisei Corporation Research Program on Sliding Seismic Isolation Systems for Bridges: Experimental and Analytical Study of a Friction Pendulum System (FPS)," by M.C. Constantinou, P. Tsopelas, Y-S. Kim and S. Okamoto, 11/1/93, (PB94-142775, A08, MF-A02).

NCEER-93-0021 "Finite Element Modeling of Elastomeric Seismic Isolation Bearings," by L.J. Billings, Supervised by R. Shepherd, 11/8/93, to be published.

NCEER-93-0022 "Seismic Vulnerability of Equipment in Critical Facilities: Life-Safety and Operational Consequences," by K. Porter, G.S. Johnson, M.M. Zadeh, C. Scawthorn and S. Eder, 11/24/93, (PB94-181765, A16, MF-A03).

NCEER-93-0023 "Hokkaido Nansei-oki, Japan Earthquake of July 12, 1993, by P.I. Yanev and C.R. Scawthorn, 12/23/93, (PB94-181500, A07, MF-A01).

NCEER-94-0001 "An Evaluation of Seismic Serviceability of Water Supply Networks with Application to the San Francisco Auxiliary Water Supply System," by I. Markov, Supervised by M. Grigoriu and T. O'Rourke, 1/21/94, (PB94-204013, A07, MF-A02).

NCEER-94-0002 "NCEER-Taisei Corporation Research Program on Sliding Seismic Isolation Systems for Bridges: Experimental and Analytical Study of Systems Consisting of Sliding Bearings, Rubber Restoring Force Devices and Fluid Dampers," Volumes I and II, by P. Tsopelas, S. Okamoto, M.C. Constantinou, D. Ozaki and S. Fujii, 2/4/94, (PB94-181740, A09, MF-A02 and PB94-181757, A12, MF-A03).

NCEER-94-0003 "A Markov Model for Local and Global Damage Indices in Seismic Analysis," by S. Rahman and M. Grigoriu, 2/18/94, (PB94-206000, A12, MF-A03).

NCEER-94-0004 "Proceedings from the NCEER Workshop on Seismic Response of Masonry Infills," edited by D.P. Abrams, 3/1/94, (PB94-180783, A07, MF-A02).

NCEER-94-0005 "The Northridge, California Earthquake of January 17, 1994: General Reconnaissance Report," edited by J.D. Goltz, 3/11/94, (PB193943, A10, MF-A03).

NCEER-94-0006 "Seismic Energy Based Fatigue Damage Analysis of Bridge Columns: Part I - Evaluation of Seismic Capacity," by G.A. Chang and J.B. Mander, 3/14/94, (PB94-219185, A11, MF-A03).

NCEER-94-0007 "Seismic Isolation of Multi-Story Frame Structures Using Spherical Sliding Isolation Systems," by T.M. Al-Hussaini, V.A. Zayas and M.C. Constantinou, 3/17/94, (PB193745, A09, MF-A02).

NCEER-94-0008 "The Northridge, California Earthquake of January 17, 1994: Performance of Highway Bridges," edited by I.G. Buckle, 3/24/94, (PB94-193851, A06, MF-A02).

NCEER-94-0009 "Proceedings of the Third U.S.-Japan Workshop on Earthquake Protective Systems for Bridges," edited by I.G. Buckle and I. Friedland, 3/31/94, (PB94-195815, A99, MF-A06).

NCEER-94-0010 "3D-BASIS-ME: Computer Program for Nonlinear Dynamic Analysis of Seismically Isolated Single and Multiple Structures and Liquid Storage Tanks," by P.C. Tsopelas, M.C. Constantinou and A.M. Reinhorn, 4/12/94, (PB94-204922, A09, MF-A02).

NCEER-94-0011 "The Northridge, California Earthquake of January 17, 1994: Performance of Gas Transmission Pipelines," by T.D. O'Rourke and M.C. Palmer, 5/16/94, (PB94-204989, A05, MF-A01).

NCEER-94-0012 "Feasibility Study of Replacement Procedures and Earthquake Performance Related to Gas Transmission Pipelines," by T.D. O'Rourke and M.C. Palmer, 5/25/94, (PB94-206638, A09, MF-A02).

NCEER-94-0013 "Seismic Energy Based Fatigue Damage Analysis of Bridge Columns: Part II - Evaluation of Seismic Demand," by G.A. Chang and J.B. Mander, 6/1/94, (PB95-18106, A08, MF-A02).

NCEER-94-0014 "NCEER-Taisei Corporation Research Program on Sliding Seismic Isolation Systems for Bridges: Experimental and Analytical Study of a System Consisting of Sliding Bearings and Fluid Restoring Force/Damping Devices," by P. Tsopelas and M.C. Constantinou, 6/13/94, (PB94-219144, A10, MF-A03).

NCEER-94-0015 "Generation of Hazard-Consistent Fragility Curves for Seismic Loss Estimation Studies," by H. Hwang and J-R. Huo, 6/14/94, (PB95-181996, A09, MF-A02).

NCEER-94-0016 "Seismic Study of Building Frames with Added Energy-Absorbing Devices," by W.S. Pong, C.S. Tsai and G.C. Lee, 6/20/94, (PB94-219136, A10, A03).

NCEER-94-0017 "Sliding Mode Control for Seismic-Excited Linear and Nonlinear Civil Engineering Structures," by J. Yang, J. Wu, A. Agrawal and Z. Li, 6/21/94, (PB95-138483, A06, MF-A02).

NCEER-94-0018 "3D-BASIS-TABS Version 2.0: Computer Program for Nonlinear Dynamic Analysis of Three Dimensional Base Isolated Structures," by A.M. Reinhorn, S. Nagarajaiah, M.C. Constantinou, P. Tsopelas and R. Li, 6/22/94, (PB95-182176, A08, MF-A02).

NCEER-94-0019 "Proceedings of the International Workshop on Civil Infrastructure Systems: Application of Intelligent Systems and Advanced Materials on Bridge Systems," Edited by G.C. Lee and K.C. Chang, 7/18/94, (PB95-252474, A20, MF-A04).

NCEER-94-0020 "Study of Seismic Isolation Systems for Computer Floors," by V. Lambrou and M.C. Constantinou, 7/19/94, (PB95-138533, A10, MF-A03).

NCEER-94-0021 "Proceedings of the U.S.-Italian Workshop on Guidelines for Seismic Evaluation and Rehabilitation of Unreinforced Masonry Buildings," Edited by D.P. Abrams and G.M. Calvi, 7/20/94, (PB95-138749, A13, MF-A03).

NCEER-94-0022 "NCEER-Taisei Corporation Research Program on Sliding Seismic Isolation Systems for Bridges: Experimental and Analytical Study of a System Consisting of Lubricated PTFE Sliding Bearings and Mild Steel Dampers," by P. Tsopelas and M.C. Constantinou, 7/22/94, (PB95-182184, A08, MF-A02).

NCEER-94-0023 "Development of Reliability-Based Design Criteria for Buildings Under Seismic Load," by Y.K. Wen, H. Hwang and M. Shinozuka, 8/1/94, (PB95-211934, A08, MF-A02).

NCEER-94-0024 "Experimental Verification of Acceleration Feedback Control Strategies for an Active Tendon System," by S.J. Dyke, B.F. Spencer, Jr., P. Quast, M.K. Sain, D.C. Kaspari, Jr. and T.T. Soong, 8/29/94, (PB95-212320, A05, MF-A01).

NCEER-94-0025 "Seismic Retrofitting Manual for Highway Bridges," Edited by I.G. Buckle and I.F. Friedland, published by the Federal Highway Administration (PB95-212676, A15, MF-A03).

NCEER-94-0026 "Proceedings from the Fifth U.S.-Japan Workshop on Earthquake Resistant Design of Lifeline Facilities and Countermeasures Against Soil Liquefaction," Edited by T.D. O'Rourke and M. Hamada, 11/7/94, (PB95-220802, A99, MF-E08).

NCEER-95-0001 "Experimental and Analytical Investigation of Seismic Retrofit of Structures with Supplemental Damping: Part 1 - Fluid Viscous Damping Devices," by A.M. Reinhorn, C. Li and M.C. Constantinou, 1/3/95, (PB95-266599, A09, MF-A02).

NCEER-95-0002 "Experimental and Analytical Study of Low-Cycle Fatigue Behavior of Semi-Rigid Top-And-Seat Angle Connections," by G. Pekcan, J.B. Mander and S.S. Chen, 1/5/95, (PB95-220042, A07, MF-A02).

NCEER-95-0003 "NCEER-ATC Joint Study on Fragility of Buildings," by T. Anagnos, C. Rojahn and A.S. Kiremidjian, 1/20/95, (PB95-220026, A06, MF-A02).

NCEER-95-0004 "Nonlinear Control Algorithms for Peak Response Reduction," by Z. Wu, T.T. Soong, V. Gattulli and R.C. Lin, 2/16/95, (PB95-220349, A05, MF-A01).

NCEER-95-0005 "Pipeline Replacement Feasibility Study: A Methodology for Minimizing Seismic and Corrosion Risks to Underground Natural Gas Pipelines," by R.T. Eguchi, H.A. Seligson and D.G. Honegger, 3/2/95, (PB95-252326, A06, MF-A02).

NCEER-95-0006 "Evaluation of Seismic Performance of an 11-Story Frame Building During the 1994 Northridge Earthquake," by F. Naeim, R. DiSulio, K. Benuska, A. Reinhorn and C. Li, to be published.

NCEER-95-0007 "Prioritization of Bridges for Seismic Retrofitting," by N. Basöz and A.S. Kiremidjian, 4/24/95, (PB95-252300, A08, MF-A02).

NCEER-95-0008 "Method for Developing Motion Damage Relationships for Reinforced Concrete Frames," by A. Singhal and A.S. Kiremidjian, 5/11/95, (PB95-266607, A06, MF-A02).

NCEER-95-0009 "Experimental and Analytical Investigation of Seismic Retrofit of Structures with Supplemental Damping: Part II - Friction Devices," by C. Li and A.M. Reinhorn, 7/6/95, (PB96-128087, A11, MF-A03).

NCEER-95-0010 "Experimental Performance and Analytical Study of a Non-Ductile Reinforced Concrete Frame Structure Retrofitted with Elastomeric Spring Dampers," by G. Pekcan, J.B. Mander and S.S. Chen, 7/14/95, (PB96-137161, A08, MF-A02).

NCEER-95-0011 "Development and Experimental Study of Semi-Active Fluid Damping Devices for Seismic Protection of Structures," by M.D. Symans and M.C. Constantinou, 8/3/95, (PB96-136940, A23, MF-A04).

NCEER-95-0012 "Real-Time Structural Parameter Modification (RSPM): Development of Innervated Structures," by Z. Liang, M. Tong and G.C. Lee, 4/11/95, (PB96-137153, A06, MF-A01).

NCEER-95-0013 "Experimental and Analytical Investigation of Seismic Retrofit of Structures with Supplemental Damping: Part III - Viscous Damping Walls," by A.M. Reinhorn and C. Li, 10/1/95, (PB96-176409, A11, MF-A03).

NCEER-95-0014 "Seismic Fragility Analysis of Equipment and Structures in a Memphis Electric Substation," by J-R. Huo and H.H.M. Hwang, (PB96-128087, A09, MF-A02), 8/10/95.

NCEER-95-0015 "The Hanshin-Awaji Earthquake of January 17, 1995: Performance of Lifelines," Edited by M. Shinozuka, 11/3/95, (PB96-176383, A15, MF-A03).

NCEER-95-0016 "Highway Culvert Performance During Earthquakes," by T.L. Youd and C.J. Beckman, available as NCEER-96-0015.

NCEER-95-0017 "The Hanshin-Awaji Earthquake of January 17, 1995: Performance of Highway Bridges," Edited by I.G. Buckle, 12/1/95, to be published.

NCEER-95-0018 "Modeling of Masonry Infill Panels for Structural Analysis," by A.M. Reinhorn, A. Madan, R.E. Valles, Y. Reichmann and J.B. Mander, 12/8/95.

NCEER-95-0019 "Optimal Polynomial Control for Linear and Nonlinear Structures," by A.K. Agrawal and J.N. Yang, 12/11/95, (PB96-168737, A07, MF-A02).

NCEER-95-0020 "Retrofit of Non-Ductile Reinforced Concrete Frames Using Friction Dampers," by R.S. Rao, P. Gergely and R.N. White, 12/22/95, (PB97-133508, A10, MF-A02).

NCEER-95-0021 "Parametric Results for Seismic Response of Pile-Supported Bridge Bents," by G. Mylonakis, A. Nikolaou and G. Gazetas, 12/22/95, (PB97-100242, A12, MF-A03).

NCEER-95-0022 "Kinematic Bending Moments in Seismically Stressed Piles," by A. Nikolaou, G. Mylonakis and G. Gazetas, 12/23/95.

NCEER-96-0001 "Dynamic Response of Unreinforced Masonry Buildings with Flexible Diaphragms," by A.C. Costley and D.P. Abrams," 10/10/96.

NCEER-96-0002 "State of the Art Review: Foundations and Retaining Structures," by I. Po Lam, to be published.

NCEER-96-0003 "Ductility of Rectangular Reinforced Concrete Bridge Columns with Moderate Confinement," by N. Wehbe, M. Saiidi, D. Sanders and B. Douglas, 11/7/96, (PB97-133557, A06, MF-A02).

NCEER-96-0004 "Proceedings of the Long-Span Bridge Seismic Research Workshop," edited by I.G. Buckle and I.M. Friedland, to be published.

NCEER-96-0005 "Establish Representative Pier Types for Comprehensive Study: Eastern United States," by J. Kulicki and Z. Prucz, 5/28/96.

NCEER-96-0006 "Establish Representative Pier Types for Comprehensive Study: Western United States," by R. Imbsen, R.A. Schamber and T.A. Osterkamp, 5/28/96.

NCEER-96-0007 "Nonlinear Control Techniques for Dynamical Systems with Uncertain Parameters," by R.G. Ghanem and M.I. Bujakov, 5/27/96, (PB97-100259, A17, MF-A03).

NCEER-96-0008 "Seismic Evaluation of a 30-Year Old Non-Ductile Highway Bridge Pier and Its Retrofit," by J.B. Mander, B. Mahmoodzadegan, S. Bhadra and S.S. Chen, 5/31/96.

NCEER-96-0009 "Seismic Performance of a Model Reinforced Concrete Bridge Pier Before and After Retrofit," by J.B. Mander, J.H. Kim and C.A. Ligozio, 5/31/96.

NCEER-96-0010 "IDARC2D Version 4.0: A Computer Program for the Inelastic Damage Analysis of Buildings," by R.E. Valles, A.M. Reinhorn, S.K. Kunnath, C. Li and A. Madan, 6/3/96, (PB97-100234, A17, MF-A03).

NCEER-96-0011 "Estimation of the Economic Impact of Multiple Lifeline Disruption: Memphis Light, Gas and Water Division Case Study," by S.E. Chang, H.A. Seligson and R.T. Eguchi, 8/16/96, (PB97-133490, A11, MF-A03).

NCEER-96-0012 "Proceedings from the Sixth Japan-U.S. Workshop on Earthquake Resistant Design of Lifeline Facilities and Countermeasures Against Soil Liquefaction, Edited by M. Hamada and T. O'Rourke, 9/11/96, (PB97-133581, A99, MF-A06).

NCEER-96-0013 "Chemical Hazards, Mitigation and Preparedness in Areas of High Seismic Risk: A Methodology for Estimating the Risk of Post-Earthquake Hazardous Materials Release," by H.A. Seligson, R.T. Eguchi, K.J. Tierney and K. Richmond, 11/7/96.

NCEER-96-0014 "Response of Steel Bridge Bearings to Reversed Cyclic Loading," by J.B. Mander, D-K. Kim, S.S. Chen and G.J. Premus, 11/13/96, (PB97-140735, A12, MF-A03).

NCEER-96-0015 "Highway Culvert Performance During Past Earthquakes," by T.L. Youd and C.J. Beckman, 11/25/96, (PB97-133532, A06, MF-A01).

NCEER-97-0001 "Evaluation, Prevention and Mitigation of Pounding Effects in Building Structures," by R.E. Valles and A.M. Reinhorn, 2/20/97, (PB97-159552, A14, MF-A03).

NCEER-97-0002 "Seismic Design Criteria for Bridges and Other Highway Structures," by C. Rojahn, R. Mayes, D.G. Anderson, J. Clark, J.H. Hom, R.V. Nutt and M.J. O'Rourke, 4/30/97, (PB97-194658, A06, MF-A03).

NCEER-97-0003 "Proceedings of the U.S.-Italian Workshop on Seismic Evaluation and Retrofit," Edited by D.P. Abrams and G.M. Calvi, 3/19/97, (PB97-194666, A13, MF-A03).

NCEER-97-0004 "Investigation of Seismic Response of Buildings with Linear and Nonlinear Fluid Viscous Dampers," by A.A. Seleemah and M.C. Constantinou, 5/21/97, (PB98-109002, A15, MF-A03).

NCEER-97-0005 "Proceedings of the Workshop on Earthquake Engineering Frontiers in Transportation Facilities," edited by G.C. Lee and I.M. Friedland, 8/29/97, (PB98-128911, A25, MR-A04).

NCEER-97-0006 "Cumulative Seismic Damage of Reinforced Concrete Bridge Piers," by S.K. Kunnath, A. El-Bahy, A. Taylor and W. Stone, 9/2/97, (PB98-108814, A11, MF-A03).

NCEER-97-0007 "Structural Details to Accommodate Seismic Movements of Highway Bridges and Retaining Walls," by R.A. Imbsen, R.A. Schamber, E. Thorkildsen, A. Kartoum, B.T. Martin, T.N. Rosser and J.M. Kulicki, 9/3/97.

NCEER-97-0008 "A Method for Earthquake Motion-Damage Relationships with Application to Reinforced Concrete Frames," by A. Singhal and A.S. Kiremidjian, 9/10/97, (PB98-108988, A13, MF-A03).

NCEER-97-0009 "Seismic Analysis and Design of Bridge Abutments Considering Sliding and Rotation," by K. Fishman and R. Richards, Jr., 9/15/97, (PB98-108897, A06, MF-A02).

NCEER-97-0010 "Proceedings of the FHWA/NCEER Workshop on the National Representation of Seismic Ground Motion for New and Existing Highway Facilities," edited by I.M. Friedland, M.S. Power and R.L. Mayes, 9/22/97.

NCEER-97-0011 "Seismic Analysis for Design or Retrofit of Gravity Bridge Abutments," by K.L. Fishman, R. Richards, Jr. and R.C. Divito, 10/2/97, (PB98-128937, A08, MF-A02).

NCEER-97-0012 "Evaluation of Simplified Methods of Analysis for Yielding Structures," by P. Tsopelas, M.C. Constantinou, C.A. Kircher and A.S. Whittaker, 10/31/97, (PB98-128929, A10, MF-A03).

NCEER-97-0013 "Seismic Design of Bridge Columns Based on Control and Repairability of Damage," by C-T. Cheng and J.B. Mander, 12/8/97.

NCEER-97-0014 "Seismic Resistance of Bridge Piers Based on Damage Avoidance Design," by J.B. Mander and C-T. Cheng, 12/10/97.

NCEER-97-0015 "Seismic Response of Nominally Symmetric Systems with Strength Uncertainty," by S. Balopoulou and M. Grigoriu, 12/23/97.

NCEER-97-0016 "Evaluation of Seismic Retrofit Methods for Reinforced Concrete Bridge Columns," by T.J. Wipf, F.W. Klaiber and F.M. Russo, 12/28/97.

NCEER-97-0017 "Seismic Fragility of Existing Conventional Reinforced Concrete Highway Bridges," by C.L. Mullen and A.S. Cakmak, 12/30/97.

NCEER-97-0018 "Loss Asssessment of Memphis Buildings," edited by D.P. Abrams and M. Shinozuka, 12/31/97.

NCEER-97-0019 "Seismic Evaluation of Frames with Infill Walls Using Quasi-static Experiments," by K.M. Mosalam, R.N. White and P. Gergely, 12/31/97.

NCEER-97-0020 "Seismic Evaluation of Frames with Infill Walls Using Pseudo-dynamic Experiments," by K.M. Mosalam, R.N. White and P. Gergely, 12/31/97.

NCEER-97-0021 "Computational Strategies for Frames with Infill Walls: Discrete and Smeared Crack Analyses and Seismic Fragility," by K.M. Mosalam, R.N. White and P. Gergely, 12/31/97.

NCEER-97-0022 "Proceedings of the NCEER Workshop on Evaluation of Liquefaction Resistance of Soils," edited by T.L. Youd and I.M. Idriss, 12/31/97.

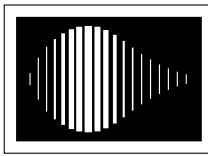

NATIONAL CENTER FOR EARTHQUAKE ENGINEERING RESEARCH

Headquartered at the State University of New York at Buffalo

State University of New York at Buffalo
Red Jacket Quadrangle
Buffalo, New York 14261
Telephone: 716/645-3391
FAX: 716/645-3399

ISSN 1088-3800